STRENGTH AND DEFORMATION CHARACTERISTICS OF ROCKFILL

A thesis submitted to the
University of London
(Imperial College of Science and Technology)

for the degree of

Doctor of Philosophy in the Faculty of Engineering

by

Stanley Graham Tombs, B.Sc. (Hons.) Salford.

January 1969

ABSTRACT

In this thesis the techniques used for determining the shear strength of rockfill, both in the field and in the laboratory, are reviewed.

Very little research has been carried out to date to predict the shear strength of rockfill from laboratory investigations.

It was thought that if geometrically similar gradings of a material were tested under similar conditions a similar behaviour might be expected.

A large scale triaxial apparatus was designed and constructed and a series of experiments were then carried out on geometrically similar gradings of silurian cleaved mudstone, granitic gneiss and chert.

From this investigation a number of conclusions have been reached on the behaviour of rockfill materials.

CONTENTS

SECTION		PAGE
Abstract		(ii)
Contents		(iii)
List of Figures		(ix)
List of Tables		(xv)
List of Plates		(xvi)
List of Symbols		(xvii)
Chapter 1.	Introduction	1
Chapter 2.	Field determinations of the shear strength of rockfill and associated materials.	9
2:1	Introduction	9
2:2	The determination of the angle of friction between bedrock and a rockfill	9
2:3	The determination of the angle of internal friction of rockfill by means of shear box tests.	10
2:4	Passive cone shear test.	12
Chapter 3	Some laboratory investigations of the shear strength of rockfill and associated materials	20
3:1	Introduction	20
3:2	The drained shear strength of rockfill under triaxial conditions.	20
3:3	The drained shear strength of associated materials under triaxial conditions.	26
3:4	The drained shear strength of rockfill under plane strain condition.	30
3:5	Other drained shear tests on rockfill and associated materials.	31
3:6	Undrained shear tests on associated materials.	35
3:7	Shear strength, dilatancy and interparticle friction.	35
3:8	Contact stresses in rockfill and other materials.	37
3:9	Particle breakdown and compressibility.	39
3:10	The effect of membranes on the measured shear strength of rockfill.	44

SECTION		PAGE
Chapter 4	The triaxial equipment for testing samples 12" in diameter and 24" high.	77
4:1	The design specification.	77
4:2	The loading frame.	77
4:2:1	The foundation.	78
4:2:2	The base.	78
4:2:3	The crosshead.	78
4:2:4	The stiffening column.	79
4:2:5	The mechanical jack.	79
4:2:6	The drive mechanism.	80
4:2:6:1	The Kopp Variator.	80
4:2:6:2	The rapid return motor	80
4:3	The triaxial cell.	81
4:3:1	The cell barrel.	81
4:3:2	The cell base.	81
4:3:3	The pedestal.	81
4:3:4	Lifting and handling.	82
4:3:5	The top cover and piston bushing.	82
4:3:6	The piston.	82
4:3:7	The top cap.	83
4:3:8	Anti-corrosive protection.	83
4:3:9	Porous stones.	84
4:4	Electric resistance straingauge loadcells.	84
4:4:1	Calibration.	84
4:5	Rubber membranes.	85
4:6	The compaction mould.	86
4:7	The compaction tool.	86
4:8	Permeability apparatus.	86
4:9	Cell pressure control systems.	87
4:9:1	The pneumatic system.	87
4:9:2	The hydraulic pressure control system.	88
4:9:3	Resonance.	90
4:10	Electrical control circuits.	90
4:11	The special lifting arm.	91
4:12	The sieving machine.	91
4:13	Modifications to small scale apparatus.	92
4:13:1	Modifications to the standard triaxial apparatus for testing 4" diameter samples.	92
4:13:2	Modifications to the standard triaxial apparatus for testing $1\frac{1}{2}$" diameter samples.	92

SECTION		PAGE
Chapter 5	The Material	119
5:1	The material tested.	119
5:2	The silurian cleaved mudstone.	119
5:2:1	Mineral composition.	119
5:2:2	Average composition in thin section.	119
5:2:3	Unconfined compressive strength.	120
5:2:4	Particle shape.	120
5:2:5	Material treatment prior to testing.	121
5:3	The granitic gneiss.	122
5:3:1	Average composition in thin section.	122
5:3:2	Unconfined compression strength.	123
5:3:3	Particle shape.	123
5:3:4	Material treatment prior to testing.	123
5:4	The chert gravel.	124
5:5	Scaling of gradings.	125
5:5:1	Chert scaling.	126
5:6	Gradings used in the tests.	126
5:7	Interparticle friction.	127
5:7:1	Measurement of the coefficient of interparticle friction for silurian cleaved mudstone.	127
5:7:2	Measurement of the coefficient of interparticle friction for chert.	128
5:8	Relative density determinations.	129
5:8:1	Minimum density.	131
5:8:2	Maximum density.	131
5:9	Specific gravity.	132
Chapter 6	Testing Procedure	140
6:1	Preparation of 12" diameter samples.	140
6:1:1	Grading preparation.	140
6:1:2	Membrane sealing.	140
6:1:3	Sample building.	141
6:1:4	Orientated samples.	142
6:1:5	Positioning the top cap.	142
6:1:6	Sample stability.	142
6:1:7	Sample measurement.	143
6:1:8	Membrane inspection.	143
6:1:9	Sample consolidation.	143
6:1:10	Sample saturation.	144

SECTION		PAGE
6:1:11	Permeability determination.	145
6:2	Drained tests.	145
6:3	Tests with zero lateral strain.	145
6:4	Tests causing failure by reduction of effective stresses.	146
6:5	Test to determine the pore pressure parameter B.	147
6:6	Undrained shear tests.	147
6:7	Strain rate.	147
6:8	Total strain.	148
6:9	Sample dismantling.	148
6:10	Small scale samples.	148
6:11	Calculation of stresses and corrections.	149
6:12	Membrane corrections.	150
6:13	Ram friction.	151
Chapter 7	The results of the tests on silurian cleaved mudstone	161
7:1	Compaction and sample density.	161
7:2	Isotropic consolidation.	162
7:3	Shear strength.	165
7:3:1	Shear strength of 12" dia.samples (drained shear tests).	165
7:3:2	Shear strength of 12" dia.samples with orientated particles.	166
7:3:3	Shear strength of 12" dia.samples with special gradings.	167
7:3:4	Shear strength of 12" dia.samples subjected to anisotropic consolidation.	167
7:3:5	Shear strength of 4" dia.samples (drained shear tests).	168
7:3:6	Shear strength of 1½" dia.samples (drained shear tests).	169
7:3:7	Shear strength of samples sheared under undrained conditions.	170
7:4	Deformation.	172
7:4:1	Deformation of 12" dia.samples (drained shear tests).	172
7:4:2	Deformation of 12" dia.samples with orientated particles.	173

SECTION		PAGE
7:4:3	Deformation of 12" dia.samples with special gradings.	173
7:4:4	Deformation of 12" dia. samples subjected to anisotropic consolidation.	173
7:4:5	Deformation of 4" dia.samples (drained shear tests).	174
7:4:6	Deformation of 1½" dia.samples (drained shear tests).	175
7:4:7	Axial deformation of samples sheared under undrained conditions.	175
7:4:8	Volumetric strain and deviator stress.	176
7:4:9	Creep.	176
7:4:10	One dimensional compressibility.	177
7:4:11	Particle breakdown.	178
Chapter 8	The results of tests on granitic gneiss.	219
8:1	Compaction and sample density.	219
8:2	Isotropic consolidation.	220
8:3	Shear strength	221
8:3:1	Shear strength of 12" dia.samples (drained shear tests).	221
8:3:2	Shear strength of 12" dia.samples subjected to anisotropic consolidation.	222
8:3:3	Shear strength of 4" dia.samples (drained shear tests).	222
8:3:4	Shear strength of 1½" dia.samples (drained shear tests).	223
8:3:5	Shear strength of samples sheared under undrained conditions.	225
8:4	Deformation.	226
8:4:1	Deformation of 12" dia.samples (drained shear tests).	226
8:4:2	Deformation of 12" dia.samples subjected to anisotropic consolidation.	227
8:4:3	Deformation of 4" dia.samples (drained shear tests).	227
8:4:4	Deformation of 1½" dia.samples (drained shear tests).	228
8:4:5	Axial deformation of samples sheared under undrained conditions.	228

SECTION		PAGE
8:4:6	Volumetric strain and deviator stress.	229
8:4:7	Creep.	229
8:4:8	One dimensional compressibility.	230
8:4:9	Particle breakdown.	230
Chapter 9	The results of the tests on chert	258
9:1	Compaction and sample density.	258
9:2	Isotropic consolidation.	258
9:3	Shear strength.	258
9:4	Deformation.	260
9:4:1	Volumetric strain and deviator stress.	260
9:4:2	Creep.	260
9:4:3	One dimensional compressibility.	260
9:4:4	Particle breakdown.	261
Chapter 10	Conclusions	272
10:1	Consolidation.	272
10:2	Shear strength.	272
10:3	Deformation.	274
10:4	Particle breakdown.	275
10:5	Sample size.	276
10:6	Recommendations for future research.	276.
Acknowledgements.		287
Bibliography.		288

FIGURES

Fig.No.	Title	Page
1:1	Cross-section of Mattmark Dam (1965)	6
1:2a	Reconstruction of Tunhovd Dam (1965)	7
1:2b	Cross-section of Relief Dam (1910)	7
1:3	Cross-section of Djatiluhur Dam (1958)	8
2:2:1	T.V.A. Rockfill Friction Test Apparatus.	14
2:3:2	Field shear tests on rockfill.	15
2:3:3	Field shear box tests for Rama Dam.	16
2:3:4	Insitu shear box tests on Bwlch-y-Gle weathered shale.	17
2:4:1	Passive cone shear test on rockfill.	18
2:4:2	Passive cone shear test on rockfill	19
3:2:1	Vacuum triaxial tests for the heightening of Schwammenauel Dam.	45
3:2:2	Vacuum triaxial tests on loose greywacke.	46
3:2:3	Cross-section of triaxial cell for testing rockfill samples (after Marsal).	47
3:2:4	Large triaxial cell with plane strain apparatus (after Marsal).	48
3:2:5	Triaxial cell for testing samples 20cms.dia. by 50 cms. high at $\sigma_3' = 50 kg/cm^2$ (after Marsal).	49
3:2:6	Grading and shear strength of El Infiernillo angular silicified conglomerate from insitu density tests (after Marsal).	50
3:2:7	Grading and shear strength of El Infiernillo Diorite from Quarry No.5 (after Marsal).	51
3:2:8	Grading and shear strength of Pinzandaran gravel.	52
3:2:9	Grading and shear strength of Malpaso conglomerate.	53
3:2:10	Variation of angle of internal friction with sample size (after Marsal).	54
3:2:11a	Structural void ratio (after Marsal)	55
b)	Triaxial tests on quartz sand mixture (after Marsal)	
c)	Triaxial tests with different diameters of samples on uniform moraine (after Idel).	
3:2:12	Angles of internal friction for basalt and metavolcanic (U.S.Army Engrs.Report 526).	56
3:3:1	Shear tests on moraine materials for the shoulders of Goeschenenalp Dam (after Zeller and Wullimann).	57

Fig.No.	Title	Page
3:3:2	Shear strength of talus material used in the Goeschenenalp Dam (after Huder and Fetz).	58
3:3:3	Angles of internal friction for gradings with varying maximum particle size (after Leslie).	59
3:3:4	Shear strength of crushed limestone and Nurek gravel (after Nichiporovitch)	60
3:4:1	Rigid boundary plane strain apparatus (after Marsal)	61
3:4:2	Plane strain test onEl Pedregal Basalt (after Marsal)	62
3:4:3	Plane strain test on Pinzandaran sand and gravel (after Marsal)	63
3:5:1	12" square shear box tests on sands and gravel (after Bishop)	64
3:5:2	Shear apparatus and tests results (after Kjellman)	65
3:5:3a	Angles of internal friction for loose tipped crushed granite rockfill (after Lewis).	66
3:5:3b	Shear box tests on disintegrated shale (after Dvorak).	
3:6:1	Stress paths for undrained tests on Ham River sand (after Skinner)	67
3:7:1	Variation of dilatancy throughout a sample (after Blight).	68
3:9:1	Correlation of the principal stress ratio at failure and particle breakage (after Marsal).	69
3:9:2	Pressure compression curves (after Kjaernsli)	70
3:9:3	Deformation time plots for syenite (after Kjaernsli) and silurian cleaved mudstone (after Howkins).	71
3:9:4	Compressibility of angular and subrounded granite (after Lee and Farhoomand).	72
3:9:5	Relative crushing of coarse soils at different stress conditions (after Lee and Farhoomand).	73
3:9:6	Comparison of crushing of soils with different initial gradings (after Lee and Farhoomand).	74
3:10:1	Effects of membrane sand jacket (after Hillis)	75
4:2:3	Half section of crosshead bush.	94
4:3	The triaxial cell.	95
4:3:1	The cell barrel (detail)	96
4:3:2	The cell base (detail)	97
4:3:3	Loading head, top cap and pedestal (cross-section)	98

Fig.No.	Title	Page
4:3:3:1	Pore water distributors	99
4:3:5	Cover plate (detail)	100
4:4	Load cell - diagramatic cross-section.	101
4:6	The compaction mould.	102
4:8:1	High pressure gradient permeability apparatus.	103
4:8:2	Low pressure gradient permeability apparatus.	104
4:9	The cell pressure control system.	105
4:9:1	Air-water interface vessel (end construction details).	106
4:10:1	Schematic diagram of 100 tons loadframe and cell pressure control.	107
4:10:2	Main drive and crosshead motors power circuit.	108
4:10:3	Crosshead control circuit.	109
4:10:4	Modified main drive motor control circuit.	110
4:10:5	Auto manual control circuit.	111
4:10:6	Rapid return motor circuit.	112
4:10:7	Additional control box circuit.	113
4:10:8	Auxiliary circuits.	114
4:13:1:1	4" diameter pedestal	115
4:13:1:2	4" diameter perforated end plates.	116
4:13:1:3	Loading head and top cap.	117
5:6:1	Silurian cleaved mudstone standard gradings.	133
5:6:2	Granitic gneiss standard gradings.	134
5:6:3	Chert gradings.	135
5:7:1	Direction of shearing with respect to the bedding.	136
5:7:2a, 5:7:2b, 5:7:2c	Load displacement curves for direct shear tests.	137
6:12:1	Membrane correction.	153
6:12:2	Membrane correction added to the minor principal effective stress when membranes containing a filter were used (R.F.Type)	154
6:13:1	The effect of piston friction on the value of ϕ_f'	155
7:2:1	Isotropic consolidation 12" dia.samples silurian cleaved mudstone.	186

Fig.No.	Title	Page
7:2:2	Isotropic consolidation 4" dia.samples silurian cleaved mudstone and granitic gneiss.	187
7:2:3	Isotropic consolidation 1½" dia.samples silurian cleaved mudstone.	188
7:3A	The relation between ϕ'_f and σ'_3 for silurian cleaved mudstone and chert samples at initial R_d = 50%.	189
7:3B	The relation between ϕ'_f and $(d\epsilon_v / d\epsilon_1)_f$ for silurian cleaved mudstone samples.	190
7:3C	The relation between $(d\epsilon_v / d\epsilon_1)_f$ an the minor principal stress for all the materials tested.	191
7:3D	Möhr failure circles, silurian cleaved mudstone 12" dia.samples.	192
7:3E	Möhr failure circles, silurian cleaved mudstone 4" dia.samples.	193
7:3F	Möhr failure circles, silurian cleaved mudstone 1½" dia.samples.	194
7:3:1	Stress strain curves,silurian cleaved mudstone grading A (12" dia.samples).	195
7:3:2	Stress strain curves, silurian cleaved mudstone orientated samples. (12" dia.samples).	196
7:3:3	Stress strain curves, silurian cleaved mudstone special gradings (12" dia.samples).	197
7:3:4	Stress strain curves, silurian cleaved mudstone K_o tests (12" dia.samples).	198
7:3:5a	Stress strain curves, silurian cleaved mudstone grading F (4" dia.samples).	199
b)	Stress strain curves, silurian cleaved mudstone grading F (4" dia. samples).	200
c)	Stress strain curves, silurian cleaved mudstone grading C (4" dia samples)	201
d)	Stress strain curves, silurian cleaved mudstone grading D (4" dia.samples).	202
7:3:6a	Stress strain curves, silurian cleaved mudstone, grading F (1½" dia. samples).	203
b)	Stress strain curves, silurian cleaved mudstone, grading E (1½" dia.samples).	204
7:3:7a	Undrained test, 30M/12.	205
b)	Undrained tests, 31M/12 and 32M/12	206
c)	Undrained tests, (4" dia.samples)	207

Fig.No.	Title	Page
7:4:10a	K_o consolidation stage, 14M/12	208
b)	K_o consolidation stage, 15M/12	209
c)	K_o consolidation stage, 16M/12	210
d)	K_o consolidation stage, 20M/12.	211
e)	K_o consolidation stage, 21M/12.	212
f)	K_o consolidation stage, 26M/12.	213
g)	K_o consolidation stage, 28M/12	214
h)	Secant values of λ_v for silurian cleaved mudstone.	215
8:2:1	Isotropic consolidation 12" samples granitic gneiss	22
8:2:2	Isotropic consolidation 1½" samples granitic gneiss	234
8:3A	The relation between ϕ_f' and σ_3' for granitic gneiss samples at initial R_d = 90%	235
B	The relation between ϕ_f' at failure to $d\epsilon_v/d\epsilon_1$ at failure for granitic gneiss.	236
C	Mohr failure circles, granitic gneiss, 12" dia. samples.	237
D	Mohr failure circles, granitic gneiss, 4" dia. samples.	238
E	Mohr failure circles, granitic gneiss, 1½" dia. samples.	239
8:3:1a	Stress strain curves, granitic gneiss, grading H. 12" dia.samples.	240
b)	Stress strain curves, granitic gneiss, grading J 12" dia.samples.	241
c)	Stress strain curve. , granitic gneiss, grading H 12" dia.samples.	242
8:3:2	Stress strain curves, granitic gneiss,12"dia. samples.	243
8:3:3a	Stress strain curves, granitic gneiss, grading K 4" dia.samples.	244
b)	Stress strain curves, granitic gneiss, grading L 4" dia.samples.	245
8:3:4a	Stress strain curves, granitic gneiss, grading O 1½" dia.samples.	246
b)	Stress strain curves, granitic gneiss, grading M 1½" dia.samples.	247
c)	Stress strain curves, granitic gneiss, grading Q 1½" dia.samples.	248

Fig.No.	Title	Page
8:3:5a	Undrained tests, 16V/12 and 17V/12	249
b)	Undrained tests, 4" dia.samples	250
8:4:8a	K_o consolidation stage, 13V/12	251
b)	K_o consolidation stage, 18V/12.	252
c)	K_o consolidation stage, 19V/12.	253
d)	Secant values of m_v for granitic gneiss and chert.	254
9:2	Isotropic consolidation.	263
9:3	The relation between ϕ_f' at failure to $(d\epsilon_v / d\epsilon_1)$ at failure for chert.	264
9:3A	Stress strain curves, chert, $\frac{3}{4}$" - $\frac{3}{8}$"	265
B	Stress strain curves, chert, $1\frac{1}{2}$" - $\frac{3}{4}$"	266
C	Möhr failure circles, chert, $\frac{3}{4}$" - $\frac{3}{8}$"	267
D	Möhr failure circles, chert, $1\frac{1}{2}$" - $\frac{3}{4}$"	268
9:4:3A	Stress strain curve, K_o test, $\frac{3}{4}$" - $\frac{3}{8}$"	269
B	K_o consolidation stage, $\frac{3}{4}$" - $\frac{3}{8}$"	270
10:2	The relation between the angle of internal friction and σ_3' for chert, mudstone and granite.	277
10:2:1	The relation between sample diameter and ϕ_f' for samples of silurian cleaved mudstone.	278
10:2:2	The relation between sample diameter and ϕ_f' for samples of granitic gneiss.	279
10:2:3	The relation between $\phi_{c\nu}$ and ϕ_μ	280
10:2:4	The relation between ϕ_f' and $(d\epsilon_v / d\epsilon_1)$ for all the samples tested compared with Ham River sand, Basalt and Metavolcanic rock.	281
10:2:5	The relation between ϕ_f' and n for samples of granitic gneiss.	282
10:2:6	The relation between ϕ_f' and n for samples of silurian cleaved mudstone.	283
10:2:7	The Möhr failure envelopes for various materials.	284
10:3:1	The relation between ϵ_{1f} and σ_3' for all sizes of granite samples.	285
10:3:2	The relation between ϵ_{1f} and σ_3' for all sizes of mudstone samples.	286

TABLES

No.	Title	Page
3:9:1	Compressibility of crushed syenite, gneiss and limestone.	76
5:6:1	Gradings used in 12" dia. samples of silurian cleaved mudstone.	138
7A	Triaxial tests on 12" dia. samples of silurian cleaved mudstone.	216
7B	Triaxial tests on 4" dia. samples of silurian cleaved mudstone.	217
7C	Triaxial tests on 1½" dia. samples of silurian cleaved mudstone.	218
8A	Triaxial tests on 12" dia. samples of granitic gneiss.	255
8B	Triaxial tests on 4" dia. samples of granitic gneiss.	256
8C	Triaxial tests on 1½" dia. samples of granitic gneiss.	257
9A	Triaxial tests on 12" dia. samples of chert.	271

PLATES

No.		Title	Page
4:2		The large scale triaxial apparatus	118
5:1		Grain shapes of the materials tested.	139
6:1:1A	a)	Initial grading of sample No. 31M/12 (silurian cleaved mudstone)	156
	b)	Initial grading of granitic gneiss (grading H).	
6:1:1B	a)	Granitic gneiss grading J before testing.	157
	b)	Granitic gneiss grading after a shear test with $\sigma_3' = 450$ p.s.i.	
6:1:3	a)	Granitic gneiss sample after failure.	158
	b)	Silurian cleaved mudstone sample after failure (11M/12).	
6:9	a)	Silurian cleaved mudstone sample No.22M/12 after failure (10% passing No.100 B.S.sieve)	159
	b)	Silurian cleaved mudstone sample No.23M/12 after failure (3% passing No.100 B.S.sieve).	
6:12	a)	Chert sample after failure.	160
	b)	Silurian cleaved mudstone sample after failure.	

List of Symbols

H_o = sample height at the end of isotropic consolidation.

V_o = sample volume at the end of isotropic consolidation.

σ_1' = major principal effective stress

σ_3' = minor principal effective stress

σ_{1f}' = major principal effective stress at failure

σ_{3f}' = minor principal effective stress at failure

σ_1 = major principal total stress

σ_3 = minor principal total stress

ϕ_f' = angle of internal friction at failure

ϕ_{cv} = angle of internal friction at constant volume

ϕ_μ = angle of friction between particle surfaces

$-\Delta H/H_o = \epsilon_1$ = strain in the direction of the major principal effective stress.

ϵ_{1f} = strain in the direction of the major principal effective stress at failure

$\Delta V/V_o = \epsilon_v$ = volumetric strain

ϵ_{vf} = volumetric strain at failure

γ_d = dry density of compacted rockfill

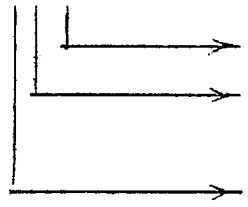
$(d\epsilon_v/d\epsilon_1)_f$ = rate of dilatancy at failure

K_o = coefficient of earth pressure at rest

m_v = secant value of the coefficient of volume decrease (compressibility in one-dimensional consolidation)

D/d = sample diameter (ins)/nominal particle size (ins).

12V/4



= sample diameter in inches

= material: C = chert, M = silurian cleaved mudstone and V = granitic gneiss

= sample number

CHAPTER I

Introduction

Civilisations have always been dependant on adequate supplies of fresh water. Water is essential for human life and regions of the world without it are devoid of habitation. Climatic changes were responsible for the migration of the centres of early civilisations.

Man slowly learned to control some of the gifts of nature and stored water in reservoirs many thousands of years ago. There is evidence that earth dams were built in China, Pakistan and the Middle East as many as 5000 years ago.

One of the earliest known dams, Sadd el Kafara Dam, was built in Egypt about 2500 years B.C. It comprised two rubble masonry walls enclosing an earth core and the dam failed soon after construction by overtopping because it was not provided with a spillway. A later dam though, of the rockfill type, built at Homs in Syria about 1300 years B.C. is still in use today. (Schnitter 1967). However, most of the early structures probably failed by internal erosion or overtopping.

With the development of quarrying techniques, mortars and concrete, subsequent structures were of masonry construction which was less easily eroded.

Within the last hundred years a number of minor dams have been constructed using wood or steel and, more recently, structures with a variable crest elevation have been constructed in the form of an inflatable PVC bag. They have not always met with complete success and, on one project, a rockfill bund was substituted.

In general, dams may be built for four functions, water storage, irrigation, flood control and the generation of power. Liquids other than water may be impounded and some major structures have been built for the storage of crude oil.

Positioning a dam across a river does not always have wholly beneficial results. Farmers in some parts of the world have relied, for thousands of years, on the annual flood depositing a thick coat of fertile mud on the land with which to grow the new years crops. A dam which impounds an enormous reservoir puts an end to this. Serious doubts about the economic viability of some projects may be raised because the substitution of electrical energy may not be worth the fertilising power of the silt.

There has always been a tendancy to solve problems along the lines of well established practice, with little added originality. A rock foundation was, for many years, regarded as the ideal upon which any

structure might safely be constructed. Masonry, concrete gravity and cupola arch dams were built in valleys where rock formations were stable and where there was little alluvium to be excavated before bed rock was reached. Arch dams have also been built for political prestige at sites where an earth or rockfill structure would have provided the better engineering solution, simply because a slender arch structure commands more admiration from the layman than a seemingly enormous pile of earth.

The reservoir sites where foundation problems existed were abandoned in favour of easier locations, even though they may have been further from the market for water or power.

We are now rapidly reaching the stage where all the easy foundation sites have been developed and future dams will have to be built in the more difficult regions previously abandoned.

The world is becoming progressively more cost conscious too so there is added incentive for originality in economic and safe dam design.

There are now more large dams being constructed of earth and rockfill than all other types put together. The reason for this is that they are as safe as concrete dams, they are much more durable, and they are cheaper. The main reasons for the reduced cost are several fold.

A minimum of foundation excavation is required and earth and rockfill structures may be built on hundreds of feet of alluvium as Serre Poncon, High Aswan and Mattmark Dams (Fig.1:1).

The material for construction is near at hand and needs a minimum of specialised processing and control. Specialised products, such as steel and cement, do not have to be shipped or hauled over great distances.

Perhaps the most significant factor is the change in relative costs of concrete and earth or rockfill. This has been achieved mainly by the efforts of American engineers in their development of enormous and very reliable and economic earth moving plant. The number of operatives is low and the unit cost of excavation and placing of fill has continually reduced as the unit cost of concrete has risen.

The excavated material from spillways, power house foundations and tunnel spoil may be used in its entirety instead of going to waste or to special processing for concrete aggregates.

One of the earliest rockfill dams in North America was English Dam, built on the Mid Fork Yuba River in 1856. It was essentially a planked timber crib 100' high with an upstream slope of I vertical on 0.87 horizontal and a downstream slope of I vertical on 0.60 horizontal. This is a smaller cross-section than many concrete gravity structures. This dam disappeared in 1883, supposedly after being blown up.

The more usual type of rockfill dam though was constructed as a dry-stone wall battered at a slope upstream of I vertically to 0.5 to 0.75

horizontally (Fig.1:2b). This was faced with wood, mortar, steel, bitumen or concrete and supported on the other side by loose rock placed at its angle of repose. This form of construction was followed for several dams around 200' high, built in Algeria in the late 1920's and early 1930's.

When railways using steam traction were the main medium of transport for constructing rockfill dams it was necessary to have almost level haul roads. As a result if a 300' high dam was to be constructed of rockfill a trestle, 100' high, was built across the valley and a quarry opened up with its floor at that level. All transport was then carried out at one elevation and the dam constructed by side tipping rock blocks up to a maximum of 25 tons in weight from the trestle. Compaction was by the kinetic energy of falling blocks. Further trestles were constructed and quarries opened up at the required elevations until the dam was complete.

An upstream facing "cushion" of derrick placed rock was constructed against the upstream face of the dumped rockfill. Finally, a facing of wood, gunite, concrete or asphalt was added.

Dams of this type were prone to excessive settlements which led to cracking of the upstream face.

Meanwhile, in Europe, similar dams were being constructed by placing the fill material in thin lifts and subjecting it to heavy compaction and sluicing to minimise deformations.

The problem of constructing earth dams throughout the year in Northern lattitudes was partially overcome by building the downstream shoulder of rockfill with the upstream slope at the angle of repose. This work, comprising the greater volume of fill, could continue for most of the year and then filter and core placing could be carried out at a great pace in more clement weather conditions. The resulting inclined core necessitates flattening the upstream slope. Such a core is probably less likely to crack as a result of differential settlements than a central vertical core of similar thickness.

The contact stresses between rockfill particles are very high and there is a growing awareness that this is potentially very dangerous in a saturated fill if subjected to shear from seismic shock. As a result, the highest dams under construction in the western world have well graded dense fills with maximum particle sizes of 6" to 8".

Materials of this size are being used for the 984' high Nurek Dam, in Russia, which, it is believed is being constructed by hydraulic fill, a process last used in the western world for large dams at Fort Peck, although part of the island for the Expo World Fair was constructed by this method.

Dump trucks now have carrying capacities in excess of 100 tons and 1000 horse power diesel electric drives but, on the larger projects, difficult hauls may be carried out by conveyer, as at Portage Mountain

Dam (600' high).

Here, the main conveyor was fed with the glacial moraine material by gathering conveyors which were fed by trap loaders loaded by D - 9 Caterpillar tractors fitted with extra large blades. At Oroville Dam (735'high) borrow pit excavation was carried out using a 5,700 tons per hour bucket wheel excavator. Even larger excavators of this type are at work in open cast lignite mines in Germany.

Many concrete dams have been replaced by earth or rockfill structures. The arch - gravity Exchequer Dam in California now forms the upstream toe of the new Exchequer Dam, a 480' high rockfill dam with an upstream membrane.

In Norway, the Tunhovd Dam had to be converted into an earth and rockfill structure because of grave deterioration of the concrete due to the action of acid water (Sande 1966). The rebuilding was effected without emptying the reservoir. A boulder clay core and filter and the downstream rockfill were constructed in the dry against the downstream face of the old dam and the upstream shoulder was added by dumping rockfill into the reservoir from the crest of the existing dam (Fig.1:2a)

A concrete dam begins to weather and deteriorate as soon as it is exposed to the elements whereas an earth dam is constructed of material which has withstood the ravages of time for thousands of years and is very likely to continue doing so for hundreds, if not thousands more.

The main disadvantage of an earth or rockfill dam lies in its poor resistance to erosion if overtopped. Floods of the magnitude that overtopped Kariba (2) or Aldeadavilla (3) dams during construction would cause considerable damage to an earth structure so that conservative and expensive diversion schemes are nearly always necessary.

The foundation conditions for an hydro-electric power station and the Djatiluhur Dam (Fig.1:3 on the Tjitarum River in Indonesia were so bad that a unique design was developed (Coyne 1958). The power station and overflow spillway were combined in a circular structure 315' in diameter and rather like a cooling tower. By keeping the elevation of the dam well ahead of the spillway large floods could be passed during construction with minimal diversion works. Several similar structures have since been constructed in Yugoslavia (1).

There are, however, several rockfill dams which have been over-topped during construction and with the impervious zones in place. The Brownlee Dam, on the Snake River in the U.S.A., was overtopped by a flood of 70,000 cusecs with little damage. In 1963 a flood of 457,000 cusecs was passed over part of the crest of the Akosombo Dam in Ghana and the core material was scoured out right down to bedrock.

Although a well designed and constructed earth dam is capable of absorbing energy from seismic activity it is very vulnerable to erosion

from overtopping by subsequent tidal waves and liberal freeboard should be allowed.

It has been suggested that rockfill underwater bunds across tidal estuaries would form an ideal foundation for hosts of tidal power turbines housed in individual caissons and sunk onto the rockfill foundation. Construction would be particularly cheap by comparison with conventional methods.

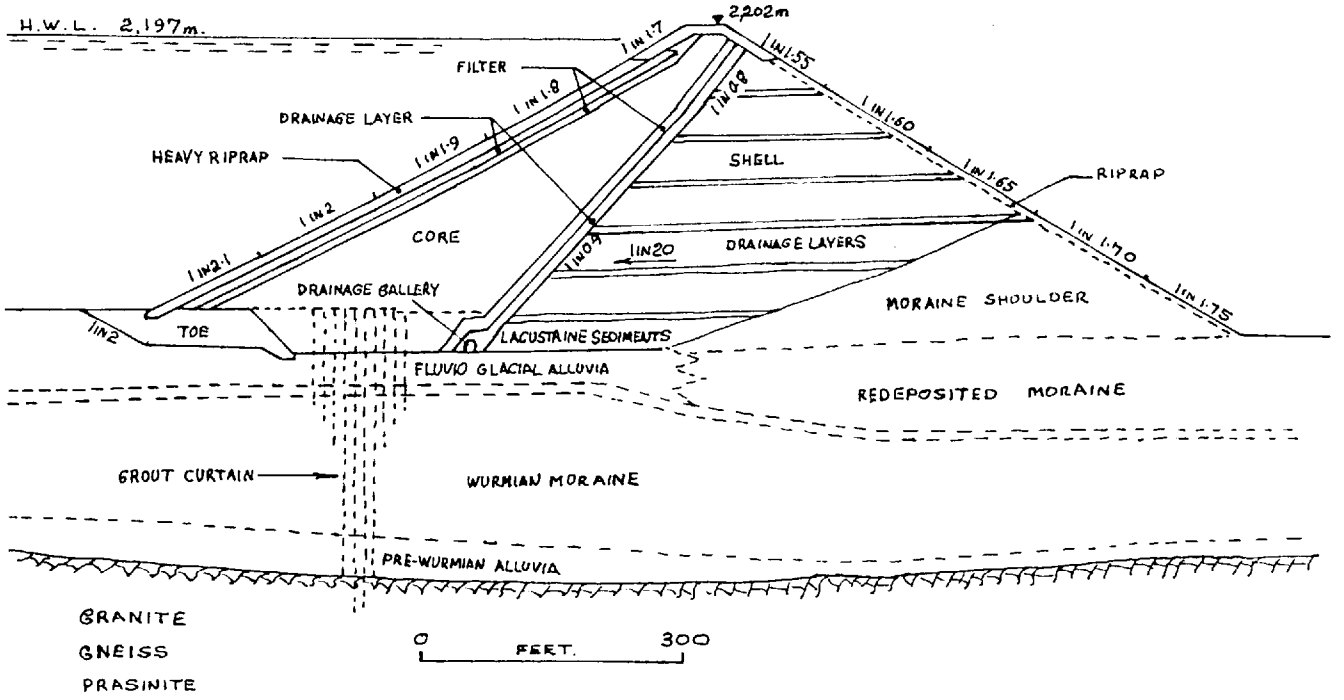
Meanwhile rockfill dams on dry land are rising to ever increasing heights and design parameters are becoming wider extrapolations of previous experience. Deformations are probably the more serious problem at present and most design is aimed at reducing differential settlements between rockfill and core to a minimum. At least in this field design parameters can be checked by the appropriate instrumentation.

As yet, no rockfill dam has failed catastrophically by a deep seated shear failure but cases have occurred where rigid concrete cores have been sheared off at the first reservoir filling because of excessive deformation of the downstream rockfill shoulder. At the same time, no one knows what the shear strength of a rockfill is under high stresses. The time is therefore ripe to attempt to find out.

In this thesis determinations of the shear strength of rockfill in the laboratory and in the field have been reviewed and investigations concerning one dimensional consolidation will be reported by Pigeon (1969). Investigations reported elsewhere have, in the main, either tested materials at non representative stresses or else non representative materials. Investigations with geometrically scaled gradings have been inconclusive because of other variables.

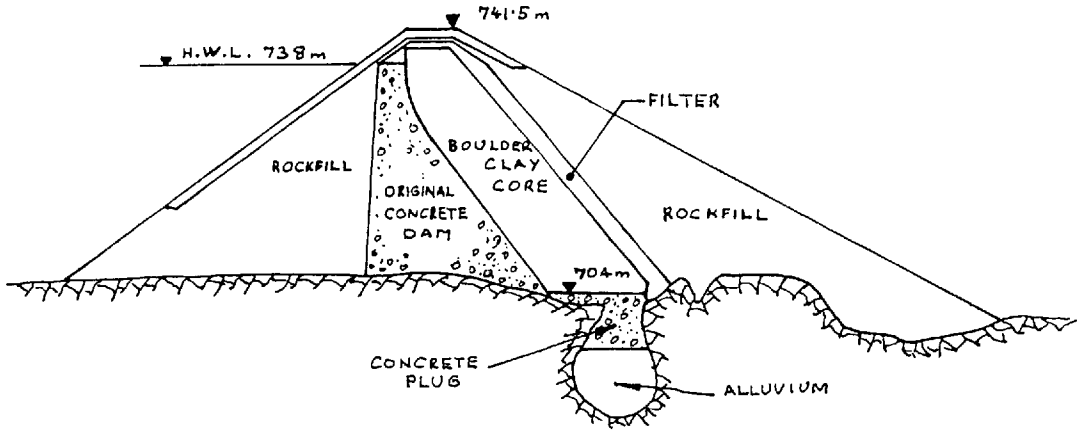
Many other investigations, however, have been carried out with a reduced number or variables but the results have not been made generally available.

This thesis also describes the design and construction of triaxial apparatus capable of applying to a sample of rockfill, one foot in diameter by two feet high, major and minor principal stresses of 2000 p.s.i. and 500 p.s.i. respectively. The results of a series of experiments on geometrically similar gradings are then reported and discussed in the light of our present knowledge on the behaviour of rockfill dams.

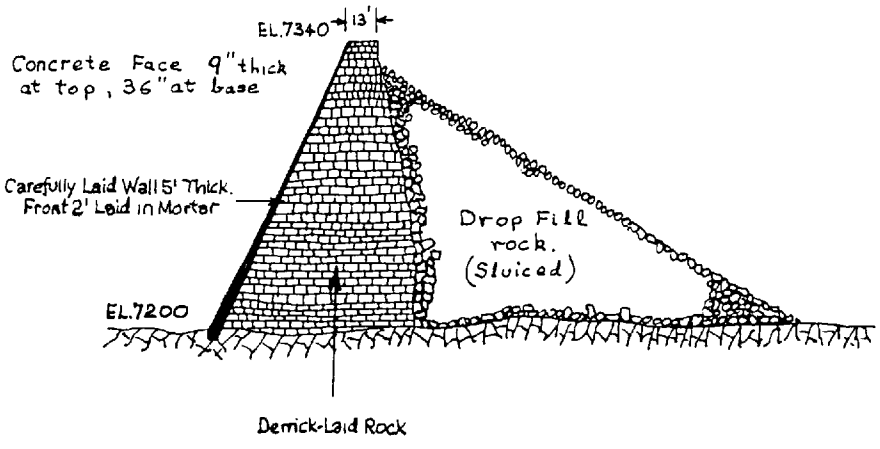


CROSS-SECTION OF MATTMARK DAM (1965).

FIG. 1:1.

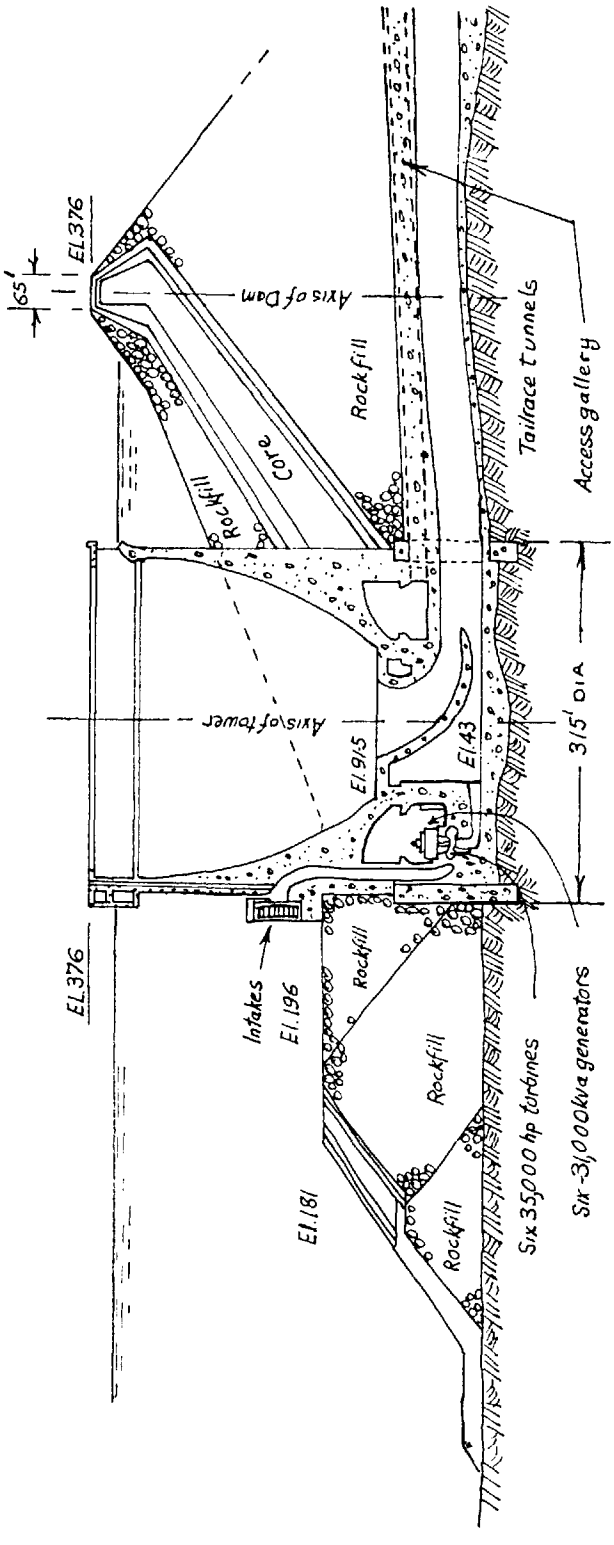


(A) RECONSTRUCTION OF TUNHOVD DAM (1965).



(B) CROSS-SECTION OF RELIEF DAM (1910).

FIG. 1:2.



CROSS-SECTION OF DJATILUHUR DAM (1958).

FIG. 1:3.

CHAPTER 2

Field determinations of the shear strength of rockfill and associated materials

(2:1) Introduction

Rules of thumb techniques for the design of earth and rockfill structures have slowly given way to more sophisticated theory and the scientific experimental approach as gross extrapolations of previous experience have been proved to be dangerous.

The volume, and hence the cost, of a rockfill dam is very dependant on the angle of internal friction of the rockfill. Although the cost of shear tests on rockfill is very high it is surprising that a more concerted effort has not been made to determine this parameter for the conditions actually experienced in the heart of very high rockfill structures. Without the relevant shear strength parameter not only is the safety of the structure always in doubt but, more important, the lives of all those persons living downstream are threatened.

(2:2) The determination of the angle of friction between bedrock and a rockfill.

To obtain design parameters for the angle of friction between bedrock and rockfill for the T.V.A's South Holston Dam large scale shear box tests were carried out with rockfill compacted against bedrock (Leonard 1958). It was stated that the rockfill must be made of sound rock having good compressive strength and durability against weathering. Quartzites, limestones and dolomites of the region were generally acceptable, whereas shales were not. At South Holston Dam a high grade sandstone was used and the characteristics of this material were uncertain. When the quarry was opened up appreciable quantities of shale and sandstone were found in which the cementing agent had disappeared. Large scale shear box tests were carried out on these materials. The shear box was supported just clear of the bedrock area and rock particles between 6" and 12" diameter were compacted in the box by vibration. A surcharge of six feet of concrete was added to produce the normal load. This though hardly seems to represent the stress condition prevailing at the foundation of a 285' high dam and the particle size used was probably excessive too for that size of shear box.

The shearing force was applied by hydraulic jacks (Fig.2:2:1) and it was observed that a certain amount of particle breakdown took place during shear.

The tests indicated an angle of friction of 45° between bedrock and the sound sandstone and 30° for the uncemented sandstone and shale.

It was concluded, therefore, that the tests effectively verified the use of the generally assumed value of 45° for the angle of friction of a good dumped rockfill.

A similar test to determine the angle of friction between rockfill and bedrock at the site of the Djatiluhur Dam was reported by Coyne (1958).

In Norway it is generally assumed that the angle of friction between a rockfill and bedrock polished by glaciation is 40° (Kjaernsli 1968).

(2:3) The determination of the angle of internal friction of rockfill by means of shear box tests

(2:3:1) Sowers 1961

For the design of the 300' high Lewis Smith Dam a series of shear tests was carried out on carboniferous sandstone. A shear box, with a cross-section measuring 6' by 6' and with a total depth of 3', was used for the tests. The box was placed on the fill of a trial embankment and further material was compacted in and around it using the normal compaction equipment. When compaction was completed the material around the box was excavated. The normal and shear loads were applied by hydraulic jacks. The reactions were taken in a similar manner to those in the shear box in Fig.2:3:2. In this case, however, the tie bars were anchored to the lower box and a set of rollers was inserted between the top cap and the hydraulic jack. Shearing was carried out by pushing the upper box over the lower box. The grading analysis of the material tested is shown in Table 2:3:1.

The normal stresses applied varied between 14.5 p.s.i. and 27.8 p.s.i. Once again, this hardly simulated the worst stress conditions in a 300' high dam. The value of ϕ_f' obtained, when testing a grading with particles up to 12" diameter was 45°. The unconfined compressive strengths of intact and weathered sandstone were 7,800 p.s.i. and 2,000 p.s.i. respectively.

Sieve size (mm)	% passing
300	100
150	93
100	88
30	52
10	31
3	22
1	17
0.3	14
0.2	13
0.1	8
0.03	2
0.01	1

Table 2:3:1 The grading analysis of carboniferous sandstone rockfill tested by Sowers

A complementary series of tests was carried out on the same material but with a maximum particle size of 5mm, in small scale triaxial apparatus. The angle of internal friction was found to be 42° but the grading, applied stresses and sample size were not stated.

(2:3:2) Nichiporovitch 1967

Shear box tests were carried out on sandstone and gravel to obtain shear strength parameters for the design of Nurek Dam in the U.S.S.R. The shear box is shown diagramatically in Fig.2:3:2. The normal and shear stresses were applied by hydraulic jacks and the displacements were measured with dial gauges. Shearing was carried out by pulling the lower box under the upper box. Each half of the shear box was 41 cms. deep and the sample cross section measured 150 cms by 150 cms. The maximum size of material tested was 20 cms. which seems somewhat on the large size for a shear box of these dimensions.

Although the proposed height of Nurek Dam is 984', the maximum normal stresses applied to samples in the shear box were about 150 p.s.i.

Both the shingle and the sandstone showed a straight line relationship at any given porosity between the normal pressure and the angle of internal friction for normal stresses up to 7 kg/cm^2. At higher stresses a reduction of ϕ_f' was noticed.

For the shingle, ϕ_f' varied from 40° to 47° for porosities from 29% to 21% respectively and for the sandstone 38° to 47° for porosities from

40% to 33% respectively.

With the field shear box a reduction of the cohesion intercept was noticed when the clearance between the upper and lower boxes was increased from 35mm to 160mm (Fig.2:3:2)

(2:3:3) Krsmanovic 1967

A very large shear apparatus, for testing rockfill to be used for three large dams in Yugoslavia, was described by Krsmanovic.

The cross-section of the shear box measured 290 cms. by 190 cms. and the total depth of the box was 150 cms.

In order to obtain the necessary reactions to apply normal stresses of up to 360 p.s.i. the apparatus was installed in an adit.

The lower box was made of steel and shearing was accomplished by pushing it over the lower one by means of eight 300 tons capacity jacks. The normal reaction, which was provided by eight 150 tons capacity jacks, was taken by the roof and floor of the adit (Fig.2:3:3)

Samples were compacted using a Vibromax plate compactor. The maximum particle size in the samples tested was 70 cms. There appeared to be no provision for reducing to a minimum the apparatus friction in the horizontal direction. These last two points may well be responsible for the shape of the Möhr failure envelopes shown in Fig.2:3:3.

(2:3:4) Bwlch-y-Gle shear test

Insitu shear box tests were carried out on the compacted fill of the Bwlch-y-Gle Dam.

The material was a weathered shale and the particles were flat and elongated. The fill was placed in layers 18" thick and compacted with a 5 tons vibrating roller operating at a frequency of 30 cycles per second.

A test pit was excavated in the fill, to a depth of about 5' and a stump of fill left which was then carefully trimmed to fit a 2' square shear box. Four shear tests were carried out on saturated samples.

The samples were loaded by hydraulic jacks and the loads were measured by electric loadcells. Displacements were determined using long travel dial gauges. The reaction for the normal load was provided by a bridge of rolled steel joists weighted with concrete blocks. The grading of the material and the results of four tests at various normal loads are given in Fig.2:3:4.

(2:4) Passive cone shear test.

A few passive wedge tests have been carried out by the Institute of Foundation Engineering of the Bayerishe Landesgewerbeanstatt, Nuremburg, to determine the shear strength of compacted rockfill.

One such test which relies on a passive cone theory developed by Steinfeld (1952) was reported by Kany (1967). The general arrangement of this test is shown in Fig.2:4:1.

An area, about 35 metres in diameter, was stripped of overburden and a circular pad, 5 metres in diameter, was constructed of concrete in the centre. On this area teflon sliding bearings were constructed for four concrete segments which were going to be used to push outwards on the fill to induce a passive failure cone. The four segments were cast on the bearings and then tests were carried out to determine the friction between the concrete and teflon.

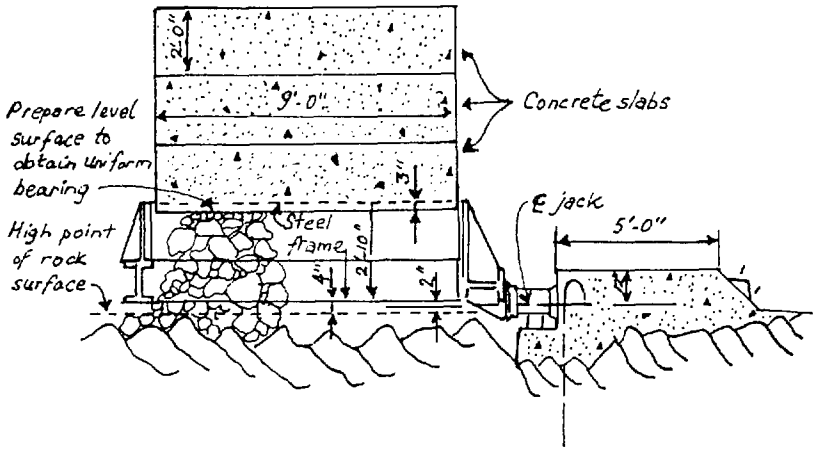
A circular embankment, 3 metres high, was then constructed around the segments, using normal construction equipment. The main compactor was an ABG SA 180 vibrating roller and fill adjacent to the segments was compacted with a Losenhausen AT 2000 plate vibrator. The normal grading is shown in Fig. 2:4:1 but the surface was levelled with fines and a skim of lean gypsum sand mortar was added to detect the failure surface.

The fill material was described as trap sandstone and had a bulk density, when placed, of 1.98 tons/metre^3.

The shearing force was applied to the concrete segments by hydraulic jacks with a total potential force of 2400 tons. Power was supplied by a mobile test vehicle fitted with equipment to monitor the readings of displacement transducers so that equal displacements could be given to each segment.

The load-displacement curves are shown in Fig.2:4:2 along with the failure diagram and the formula derived by Steinfeld for calculating ϕ'. Ep is the force applied to each segment and the angle of internal friction determined from this test was 48.5°.

The normal stresses in the test were about one tenth of those in the actual construction so one might expect a reduction of ϕ' to something less than 48.5°.

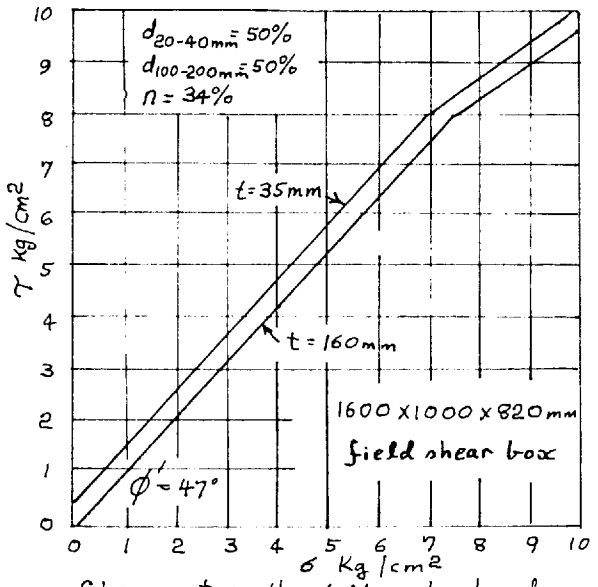


Condition	Angle of Friction
Sandstone on Sandstone Bedrock.	45°
Shale on Sandstone Bedrock.	30°

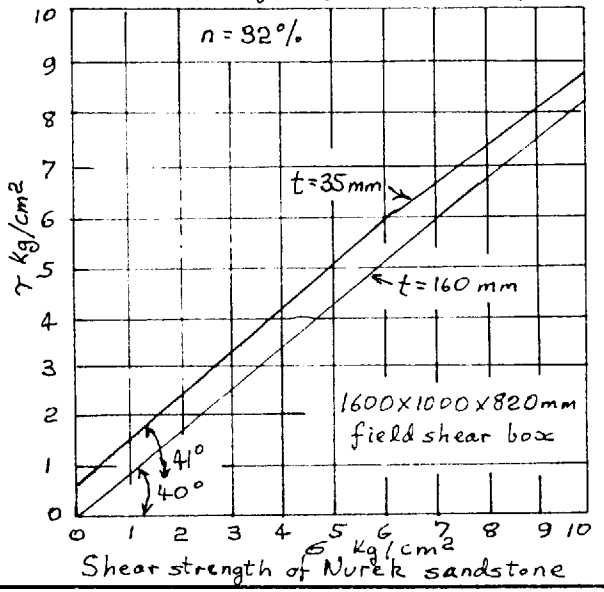
T.V.A. ROCKFILL FRICTION TEST APPARATUS.

FIG. 2:2:1

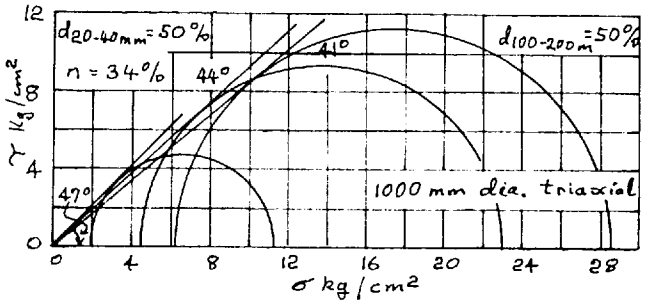
FIELD SHEAR TESTS ON ROCKFILL



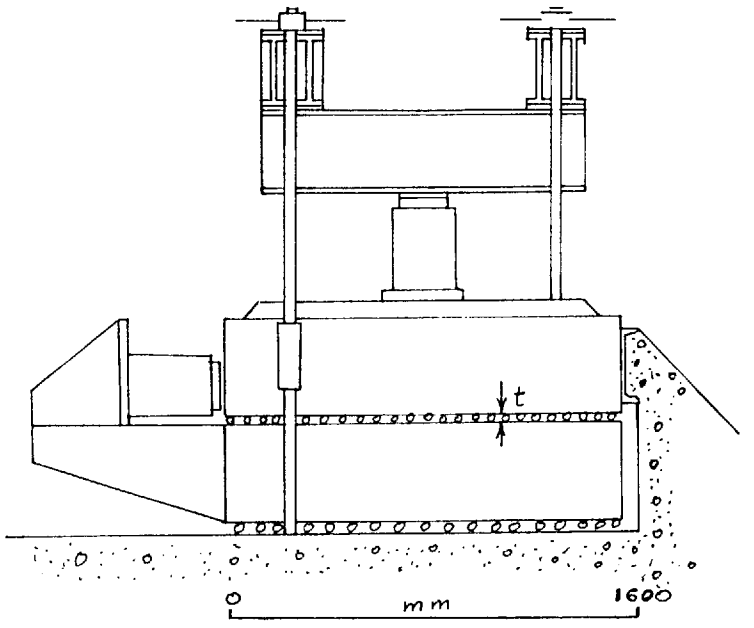
Shear strength of Nurek shingles



Shear strength of Nurek sandstone



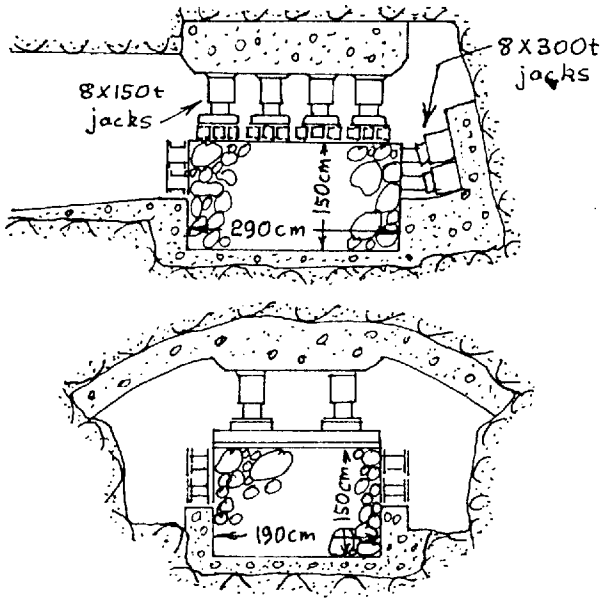
Shear strength of Nurek sandstone.

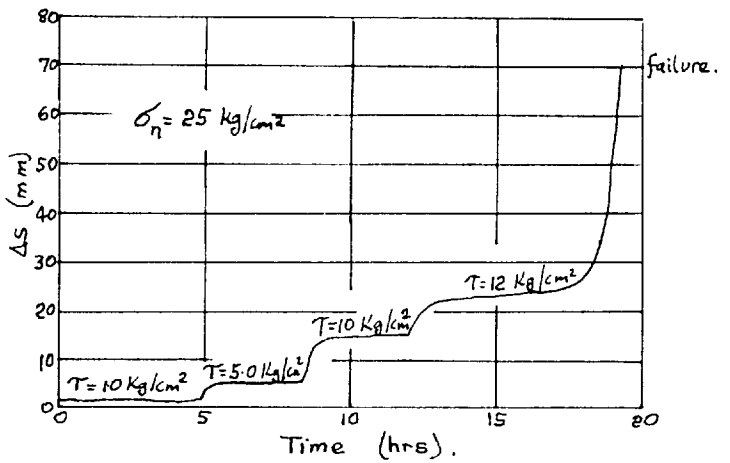


Schematic diagram of field shear apparatus.

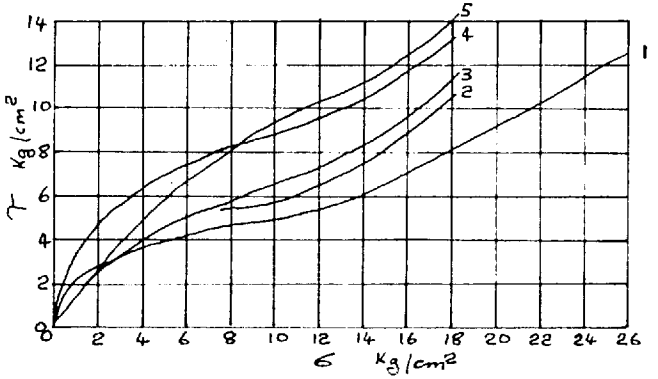
FIG. 2:3:2

Field Shear Box Tests for Rama Dam.

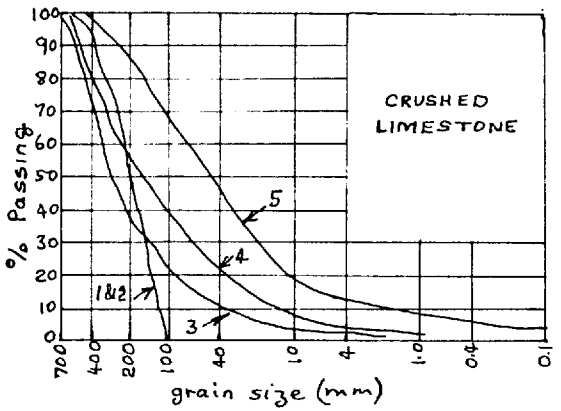




Time ~ displacement curve for various shear stresses at constant normal stress.

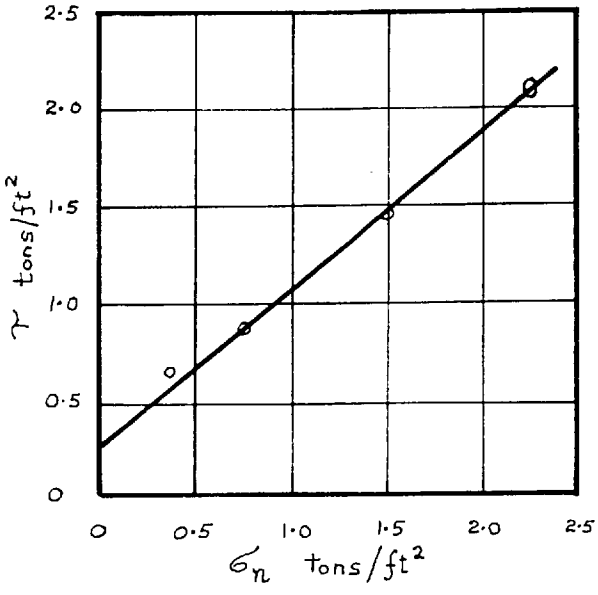


Möhr failure envelopes.



Grain size curves.

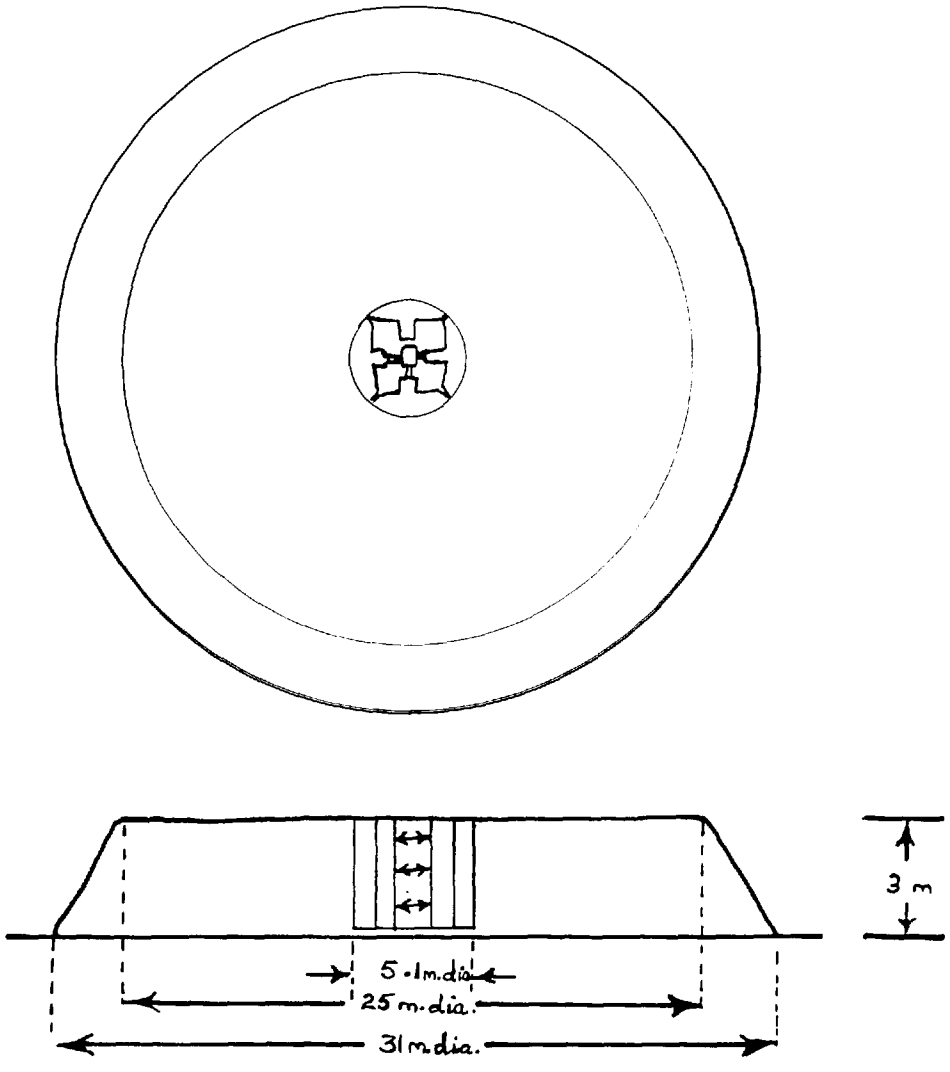
FIG. 2:3:3



GRAIN SIZE	% passing.
6"	100
3"	90
1½"	89
¾"	63
⅜"	40
3/16"	27
No. 7	17
14	11
25	8
52	4
100	2
200	1

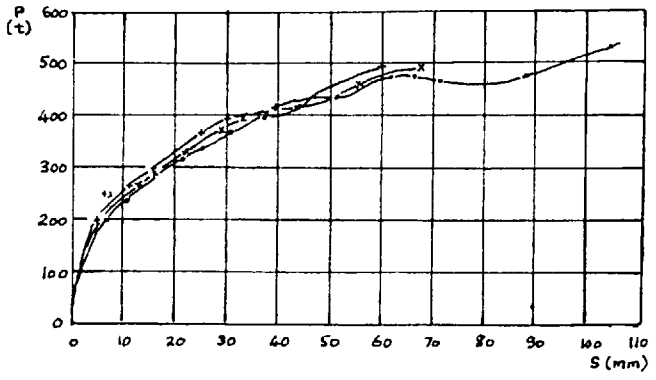
INSITU SHEAR BOX TESTS ON BWLCH-Y-GLE WEATHERED SHALE.

FIG. 2:3:4

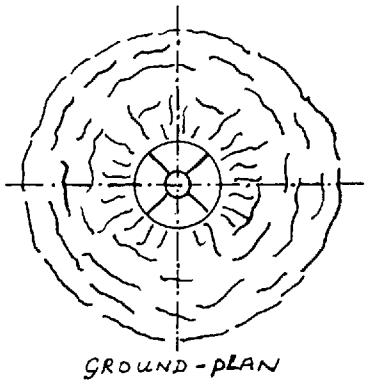


PASSIVE CONE SHEAR TEST ON ROCKFILL.

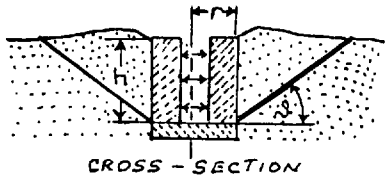
FIG. 2:4:1



LOAD DISPLACEMENT DIAGRAMS FOR PRESSURE SEGMENTS



GROUND - PLAN



CROSS - SECTION

SPATIAL EARTH RESISTANCE OF CONE ACCORDING TO STEINFELD.

$$\phi = \operatorname{arctg}\left\{\frac{\dfrac{E_p}{\left(\dfrac{r}{tg\vartheta}+\dfrac{h}{3\,tg^2\vartheta}\right)\cdot\pi\cdot\gamma\cdot h^2}\,tg\vartheta}{1+\dfrac{E_p}{\left(\dfrac{r}{tg\vartheta}+\dfrac{h}{3\cdot tg^2\vartheta}\right)\cdot\pi\cdot\gamma\cdot h^2}\cdot tg\vartheta}\right\}$$

PASSIVE CONE SHEAR TEST ON ROCKFILL.

FIG. 2:4:2

CHAPTER 3

Some laboratory investigations of the shear strength of rockfill and associated materials.

(3:1) Introduction

"Rockfill" was the term used by the Americans to describe a material consisting of very hard, durable rocks varying in size from about 40 pounds to 20 tons in weight. This material was used for harbour breakwaters and dams built in very high lifts dumped at the angle of repose.

It was impossible to determine the angle of internal friction of such a grading experimentally without inducing failure in a trial bank 100 or more feet high. This would have been a very costly experiment and, as numerous dams had been built to 300' high without any failures, there seemed little need to do other than copy previous experience.

The term "rockfill" is now more loosely used and, in general, incorporates all coarse grained aggregates, including quarried rock and tunnel spoil.

With the increasing height of rockfill dams and especially in the case of those in seismic areas a new appraisal of the significant design and construction procedures was called for.

(3:2) The drained shear strength of rockfill under triaxial conditions.

In 1948 the U.S.Army, South Pacific Division, carried out a series of triaxial tests using a vacuum apparatus. The sample size was 18" diameter by 37" high and a quarried granite, with a straight line grading from 4" to 28mm. was tested at confining pressures of 4.4, 8.8 and 13.8 p.s.i. The respective angles of internal friction were 47.2°, 43.8° and 44.8°. However, it is not clear whether the samples were tested dry or saturated or how the sample volume changes were measured.

A vacuum triaxial apparatus for testing samples 50 cms. diameter by 125 cms. high was used by Schultze (1957) to obtain shear parameters for a slatey greywacke which was to be used for heightening Schwammenauel Dam. The confining pressure was applied using a water ejector to evacuate the specimen and diameter changes were calculated from the extension of a circumferential belt at the sample mid height.

Six tests were carried out on dense samples at confining pressures of 0.25, 0.50 and 0.75 kg/cms^2. using material less than 10 cms. in diameter. A tangent drawn to the Möhr circles at the two lower pressures gave an angle of internal friction of 43° and a cohesion intercept of 0.45 Kg/cm^2 The third Möhr circle suggested a higher angle of internal friction.

(Fig.3:2:1)

Nine further tests on loose samples indicated an angle of internal friction of 42.2° and a cohesion intercept of 0.095 Kg/cm^2 . The dense samples reached a distinct peak but the loose ones did not and failure in the latter case was defined as the point at which the stress strain curve became a straight line (Fig.3:2:2). The points of failure for the three tests fell on a common straight line.

It was stated that field shear tests were carried out which confirmed the above results.

In a series of tests on a gravel, at a porosity of 25%, from a lignite waste tip, an angle of internal friction of 35° was obtained in the vacuum triaxial apparatus. Small tests, with the porosity of 29%, gave an angle of internal friction of 41° which was deemed an excessive result. Further tests in a Casagrande 10 cm. x 10 cm. shear box, with the porosity 28%, gave a value of ϕ' of 42°. In a 6 cm. x 6 cm. constant rate of strain shear box and with n equal to 29% the value of ϕ' was 45°. In the small tests particles retained on a 5mm sieve were discarded. It was stated "this could only reduce the angle of friction".

Vacuum tests on a further material gave a ϕ' value of 32°, whereas in the small triaxial, with n = 44.3%, ϕ' was 28°. With the Casagrande shear box, n = 45%, ϕ' = 34° and with the constant rate of strain shear box n = 44%, ϕ' = 31°.

Schultze drew the following conclusions from his series of tests:

1. Direct, as well as triaxial, large shear tests make it possible to investigate filling material with coarse particles for earth dams.
2. If the apparatus is to be simple to manufacture and handle, the maximum normal pressures are limited to 1.5 Kg/cm^2.
3. Whether the shear envelope up to 1.5 Kg/cm^2 is also accurate enough for higher normal stresses depends on the material tested. In general, the shear envelope is not so curved at the beginning, so that large errors do not appear. This question has to be cleared up by comparison tests with large and small apparatus. For this, only fine grained soil can be used in the small apparatus.
4. With slightly cohesive soils it is recommended that the actual lateral pressure be determined in the sample with pressure cells.
5. The coarse fraction of the soils tested produced a higher shear strength. Consequently, sieving out the remainder and testing it in small apparatus is unrealistic.
6. The density of the soils does not affect the internal angle of friction but it does affect the cohesion and compressibility.
7. Exact details of the relationship between the largest grain diameter

and the instrument diameter have not yet been determined. Up to now, when using a flaky, broken slate, the ratio of the grain size to apparatus diameter has not exceeded 1:5 . However, only a small proportion of the whole was made up of coarse particles.

A certain doubt exists as to the validity of some of the above statements.

Direct comparison between the results obtained for various sizes of sample is complicated by the use of different types of apparatus as well as various ratios of maximum particle size to sample size. This ratio may well vary for triaxial and shear box samples.

The initial design work for El Infiernillo Dam was carried out in 1960. However, no design parameters could be obtained for the rockfill with existing soils equipment. Casagrande, therefore, recommended a comprehensive investigation requiring the design of large scale and sophisticated rockfill testing apparatus. The design of the apparatus and the initial testing programme were reported by Marsal in 1965.

The main item of equipment was a triaxial cell capable of testing samples of rockfill 113 cms diameter by 250 cms high at confining pressures up to 25 Kg/cm^2. This apparatus had a dual function as a plane strain attachment to test samples 75 cm x 75 cm x 180 cms could be fitted into the cell in place of the normal triaxial sample (Figs.3:2:3, 3:2:4).

To initiate a testing programme as soon as possible and to train operatives a vacuum triaxial apparatus with the same sample size was built whilst the more sophisticated apparatus was under design and construction.

In addition, a further triaxial apparatus was designed to test samples of 20 cm diameter by 50 cm high at confining pressures up to 50Kg/cm^2 (Fig. 3:2:5)

Two oedometers were also designed, one to test samples 50 cms diameter x 50 cms high at normal stresses to 32Kg/cm^2 and another, samples 114 cms diameter x 60 cms high at normal stresses of 320 Kg/cm^2

A direct shear apparatus was designed to obtain the coefficients of friction of various materials so that a suitable material might be chosen to line the walls of the above mentioned plane strain apparatus.

The main apparatus, contained in a spherical pressure vessel 4.2 metres in diameter, required a laboratory building 33' high and a 22 tons capacity overhead travelling crane.

The deviator load was applied by numerous hydraulic retracting rams and the confining pressure was held constant at various set values by a standpipe from overflow tanks situated at various elevations on a hill adjacent to the laboratory.

Two membranes with a 5 cms thick sand or clay filling between them

were used for tests on samples containing material up to 20 cms. These membranes were made on site.

All the initial samples were tested dry and volume changes were calculated from deformation belts placed around the sample. The deviator load was determined from the pressure acting in the hydraulic rams.

Preliminary conclusions suggest that for the five materials tested the Möhr failure envelope curves considerably . Values of the angle of internal friction varying from about 50° to 35° at confining pressures of 0.5 Kg/cm^2 and 25Kg/cm^2 respectively. Samples of a natural mixture of sand, gravel and boulders showed the greatest shear strength.

The axial deformation required before the peak shear strength was mobilised increased with increasing confining pressure especially with the more uniformly graded materials.

Most samples consolidated initially under shear loading and then dilated, the dilatancy being less noticeable at high confining pressures.

Repetitive tests on Malpaso conglomerate showed that each successive test displayed a higher shear strength, a smaller axial strain to failure and a greater dilatancy.

Oedometer tests showed that particle breakdown was a function of particle strength and of intergranular stress which was dependant on the applied stresses, the grading and void ratio of the sample.

There were important secondary effects, such as the appreciable additional settlement on saturation of an initially dry sample which had already achieved a state of equilibrium under a given stress condition.

Measurements carried out in the fill of El Infiernillo Dam suggested that deformations were considerably smaller than those predicted in triaxial compression tests. It was, therefore, recommended that plane strain apparatus be used to test rockfill samples.

The Möhr failure circles for four materials tested in the dry state are shown in Figs. 3:2:6, 3:2:7, 3:2:8, 3:2:9.

Marsal (1965) reported a reduction in shear strength with increase in sample size when testing silicified conglomerate from El Infiernillo Dam and a granitic gneiss in samples 113 cms. diameter and 20 cms diameter. The results and gradings are given in Fig. 3:2:10. The densities were about the same for all samples of such material. The relative densities for the large and small samples were, therefore, probably quite different, especially as the gradings varied. However, the gradings tested were not geometrically similar and the ratio of sample diameter to maximum particle size was not the same for each case.

A distinction was drawn between the structural void ratio e' and the sample void ratio e for samples containing mixtures of two sizes of particle Fig. 3:2:11a.

Leussink (1965) found that the flatter the grading curve the smaller the angle of internal friction and suggested that as long as geometrically the same material was tested in various sizes of apparatus the result was similar (Fig.3:2:11b,c). The explanation for Marsal obtaining lower angles of internal friction in the large apparatus was that the gradings in that apparatus comprised 50% coarse material which performed a different function during shear. In the large specimen the load is mainly transmitted by the large grains because of their much higher modulus of deformability compared with that of the total assembly of grains. Particle breakage in the large tests was 46% to 130% greater than in the small tests. Very often one observed large particles with well developed shear planes through their mass after the completion of a shear test.

The results of further investigations on basalt and granitic gneiss were reported by Marsal in 1967. Material passing the 200 mm sieve was used for the tests and the membrane sand jacket was made up of that fraction of the material being tested which passed the No.4 sieve. These materials were tested in a saturated condition and the volume changes were measured both by burettes and circumferential extensometers. There was a large discrepancy between these two methods which was due to an error in determining the volume change with the circumferential extensometers (Marsal 1968). As usual, the materials showed a decrease in the angle of internal friction with increasing confining pressure. The actual values obtained though are suspect because it is not known which method of volume change measurement was used in determining the mean cross-section of the sample.

In 1967 a short report was published (4) of the investigations on the shear strength of rockfill carried out by the Snowy Mountains Authority for the design of their rockfill dams.

A triaxial apparatus was designed to test 22½" diameter by 45" high samples at confining pressures up to 200 p.s.i. The deviator load was applied and measured in a MÖHr and Federhoff 180 tons universal testing machine. The cell was fitted with a rotating bush and the sample was loaded via a spherical seating designed to rotate under load. Cell pressure was maintained by an air water system.

Tests were carried out on geometrically similar gradings on several smaller sizes of sample. Scaling the particle shape was the difficulty and small samples comprised particles which were hand picked and sorted. This sorting operation made the cost of a test on a 6" diameter sample about the same as that on a 22½" diameter sample. As yet no data has been published.

Unfortunately, this also applies to a vast amount of data accumulated

in the last ten years by the U.S.Army Corps of Engineers and many other bodies. However, a table of results of a recent study (5) on the shear strength of rockfill is given in Fig.3:2:12. Two materials were tested, crushed basalt and metavolcanic. Tests were carried out on samples of either 12" or 6" diameter, depending on the maximum grain size. The following straight line gradings were used

Grading	Cu
$\frac{1}{4}$" to No. 30	3.3
$\frac{1}{2}$" to No. 30	4.7
1" to No. 30	6.7
2" to No. 30	9.4
3" to No. 30	11.6

Table 3:2:1 Gradings used in the U.S.Army Engineers' Tests.

The dense samples were at a relative density of about 95% to 100% and the medium dense at about 70% to 75% relative density.

A certain number of conclusions were reached as a result of the study:

a) The metavolcanic rock and the basalt had equal shear strengths.

b) The shear strength increased with sample density.

c) The shear strength increased with increasing coefficient of uniformity.

d) The angle of internal friction decreased with increasing confining pressure.

e) There is a considerable increase in strength between the gradings with $\frac{1}{4}$" and 3" maximum particle sizes.

A certain number of tests were carried out at the Comision Federal De Electricidad Rockfill Laboratory at El Infiernillo on gradings from 3.5" to No.30 and 7" to No.30 and no difference in shear strength was detected between these gradings.

However, it is rather difficult to know just how c) and e) above are related in their contribution to the shear strength of a rockfill. Particle strength and shape are involved and the sample dilatancy characteristics vary with the geometry of the grading. The dilatancy is a function of confining pressure because it is a measure of volume change characteristics which themselves are affected by stress. The critical stress being a function of particle contact forces to the strength of the particle contacts. The contact forces are dependant not only on the grading but the principal stress ratio as well.

(3:3) The drained shear strength of associated materials under triaxial conditions

For the design of the Goeschenenalp Dam an attempt was made to predict the shear strength of the shell materials (Zeller and Wullimann 1957). Triaxial shear tests were carried out using four different sizes of apparatus and various gradings, such that the maximum particle size was always less than 1/5 the diameter of the sample. The gradings used were not geometrically similar but they all had a common minimum size particle. The four sets of triaxial apparatus were capable of testing samples 505 x 900 mm., 252.5 x 500 m., 160 x 250 mm. and 80 x 150 mm.

The dam was to be 155 metres high and, therefore, it was really necessary to test samples at lateral pressures up to about 250 p.s.i. The largest triaxial apparatus mentioned above was a vacuum type designed by Bjerrum in 1957 for the design of the Marmorera Dam. The apparatus was modified by adding an external cell. The maximum confining pressure was then 78 p.s.i. with a full vacuum also applied. The axial load was measured by three hydraulic loadcells at the base and the deviator was applied by pumping up an hydraulic jack by hand. The sample volume changes were not always measured and the deviator stress was assumed equal to:

$$\sigma_1' - \sigma_3' = \frac{P}{A_o}(1 - \epsilon_1)$$

where p was the applied deviator load, A_o the initial sample area and the axial strain. For all the tests carried out one half of the maximum deviator stress was plotted against the logarithm of the maximum particle size for each porosity at a given confining pressure.

From this plot it was concluded that the maximum shear strength for any given porosity was achieved with the grading containing the minimum particle size. (Fig. 3:3:1)

The reason for this is probably twofold. Firstly, the unit particle strength is probably greater with small particles because of the smaller incidence of flaws and hence a greater dilatancy takes place rather than breakdown. Secondly, the grading is more uniform and hence the rate of dilatancy is greater at failure. The contact stresses are much higher with uniform material but the mean applied stresses were quite low so that particle breakdown, in this case would not have had a predominant influence on the results.

Huder and Fetz (1967) reported a series of tests which were used to predict the shear strength of the talus material used for the shoulders of the Goeschenenalp Dam. They found that it was possible to extrapolate

from tests on material finer than 10mm when the grading curve had smaller exponents than the Fuller's curve (< 0.5), that is, a larger coefficient of uniformity and a coefficient of curvature less than 3. Moraine and talus material satisfy this requirement and for Alpine conditions, where these soil types are frequently used in the construction of embankments, it is possible to perform representative tests on small scale samples. Materials such as boulder rubble and boulder slope material exhibit a smaller coefficient of uniformity, that is an exponent greater than 0.5, and it is necessary to test as coarse a sample as possible. If the coarse grains are completely surrounded by finer material they are not in a position to contribute to the shear strength of the mass. Gradings with different maximum particle sizes were compared on the assumption that the same shear strength existed at the corresponding dry density. All the large triaxial shear tests were performed by Zeller and Wullimann (1957) in the vacuum triaxial apparatus. The gradings tested are shown in Fig. 3:3:2a and the initial results and corrected results in Fig. 3:3:2 b and c.

One half of the deviator stress is plotted against initial porosity for tests run at a minor principal stress of 0.9 Kg/cm^2. Each grading displays a different shear strength for any given porosity.

For converting the porosity (n) of a sample of Maximum particle diameter (d) to that of a larger maximum particle diameter (D) the following equations are used:

$$n_D = n_d \ (I - P) + P \ (I - Py)$$

or

$$\gamma d_D = \gamma d_d \ (I - P) + P_y \ G.P.$$

where γd_D denotes the corrected dry density in t/m^3

γd_d denotes the dry density of the sample with the smaller maximum particle diameter

P denotes the percentage of oversize grains.

G denotes the specific gravity of the grains.

P_y is the conversion factor in Fig.3:2:d.

As long as the grading curve fulfills the previous conditions a value of 0.9 for P_y is satisfactory.

Leslie (1963) reported a series of tests on alluvial soils with subrounded and subangular particles in which he used various gradings and sample sizes to determine the effect of large particles on the shear strength of a fill.

Two series of tests were performed and in all cases the confining pressure was 60 p.s.i. The gradings tested are set out overleaf:

	Straight Line Grading		Coefficient of Uniformity
First Test Series	2"	No. 30	9.4
	1"	No. 30	6.7
	$\frac{1}{2}$"	No. 30	4.7
	$\frac{1}{4}$"	No. 30	3.3
Second Test Series	2"	4.5 mm	3.3
	1"	2.3 mm	3.3
	$\frac{1}{2}$"	1.1 mm	3.3
	$\frac{1}{4}$"	0.6 mm	3.3
	No.10	0.18mm	3.3

Table 3:3:1 Gradings tested by Leslie.

The tests were carried out in apparatus using samples 5.9" diameter by 13 8" high, 6" x 12" and 12" x 24". This latter was later altered to 12" diameter by 27.6" high.

It was the usual practice to express the density of cohesionless material in terms of its relative density. When the limits for the different gradings were determined in the various sizes of apparatus various maximum and minimum values were obtained which were inconsistent. Density was therefore expressed in terms of porosity.

In the first test series the results for all the triaxial tests showed that the angle of internal friction, for a particular grading, increased with increasing initial dry density. The maximum density of the gradings increased as the maximum particle size increased. Hence, the maximum value of the angle of internal friction was obtained from the densest sample with the largest maximum size. However, extrapolating the plots in Fig. 3:3:3b it can be seen that for any given porosity the more uniform gradings of smaller maximum size have higher values of internal friction.

In the second test series there was again, an increase in the angle of internal friction with increasing density for each grading. All the gradings in this series were parallel lines and hence, if the particle shapes were exactly the same, the packings were geometrically similar at a given porosity.

Again, for any given porosity the finer gradings displayed higher angles of internal friction (Fig.3:3:3a). It was noticed that the maximum density obtainable from any grading increased with the sample size.

It was concluded that: (1) The angle of internal friction for gravelly soils would lie between 35° and 40°.

(2) Oversize particles did not have as great an effect on shear strength as initially thought.

(3) Particle breakdown was substantial and a thorough investigation was required for very large structures.

In 1963 Hall and Gordon reported a series of tests to obtain shear strength parameters for the design of Oroville Dam. Some of the materials were naturally occurring and others were gold dredging tailings from the late 1800's gold rush. Material up to 3" maximum size was tested at confining pressures up to 125 p.s.i in a sample 12" in diameter and 27.6" high and $1\frac{1}{2}$" material up to 650 p.s.i. in a 6" diameter by 13.8" high specimen. Two membranes were used on the samples with $2\frac{1}{2}$" wide strips of polythene placed vertically in between them.

Pervious materials were compacted to 100% relative density using vibration and a 1 to 3 p.s.i. surcharge.

For the pervious sandy and gravelly materials the reduction in slope of the Möhr envelope was 6° to 11° for major principal stresses from 90 p.s.i. to 1200 p.s.i.

This decrease in slope was assumed to be due to particle breakdown, most of which occurred during shear. The particle degredation was a function of the grading and was less for well graded soils which showed little segretation.

Within the range of pressure used no similar decrease in the slope of the Möhr envelope with increasing pressure was noticed for the clayey and silty materials.

Insley and Hillis (1963) carried out a series of triaxial tests on a compacted glacial till at about optimum moisture content to determine shear strength parameters for the core material of the 650' high Mica Creek Dam on the Columbia River. They used confining pressures of up to 450 p.s.i. on 6" diameter specimens containing particles up to $1\frac{1}{2}$" diameter. The reduction in slope of the Möhr envelope over this range was only 2 or 3 degrees.

For the design of the 360' high Shikmen Dam in Taiwan a series of scaled tests were carried out by Lowe (1964). The shoulder fill was to be well rounded gravel and cobble material passing a 12" sieve. A geometrically similar grading was made up with a maximum particle size of $1\frac{1}{2}$" and drained triaxial tests were carried out on samples 6" diameter. At dry densities of 130 and 137 lbs/ft^3 the respective angles of internal friction were 41° and 43°, the Möhr envelope being a straight line for confining pressures up to 200 p.s.i.

Nichiporovitch (1967) described the field and laboratory investigations for the design of several large dams in Russia, Nurek (300 meters high),

Charvak, Sarsang and V.Tobol. The field apparatus has been briefly described in Chapter 2.

Laboratory shear tests were carried out on uniform gradings of crushed limestone and Nurek gravel at normal stresses up to 6Kg/cm^2 in a shear box 20 cms x 20 cms x 10 cms. The results for various initial porosities of the samples are shown in Fig.3:3:4. In general, an increase in shear strength was noted with increase in density and maximum particle size.

Scaled gradings, which were geometrically similar to the field gradings, were tested in triaxial apparatus. The maximum confining pressures used were 6Kg/cm^2 which were hardly equivalent to the maximum stresses in Nurek Dam.

The results of tests in the shear box and the triaxial apparatus were compared at the normal stresses acting on the shear planes. Large differences were noted in the shear strengths obtained in the two types of apparatus. The Möhr failure circles for a series of triaxial tests on 1000 mm diameter samples of Nurek sandstone are shown with the field shear box test results on an identical grading and porosity of the same material (Fig.2:3:2)

(3:4) The drained shear strength of rockfill under plane strain conditions

Marsal (1967) further augmented his rockfill testing facilities by constructing a plane strain apparatus which applied all stresses through rigid boundaries. The maximum values of 6_1, and 6_3 were 140, 50 and 22Kg/cm^2 respectively. The sample was a prism 70 x 75 x 180 cms and the major principal stress was applied by a 600 tons capacity hydraulic jack.

The apparatus was basically very similar to that installed in the spherical pressure vessel at the El Infiernillo laboratory. The intermediate principal stress was measured via instrumented tie bars holding the platens together. The minor principal stress was measured via the hydraulic fluid pressure in the jacks controlling the platens. The major principal stress was measured via Freyssinet flat jacks, both in the base of the sample and under the top loading platen. In this way wall friction could be estimated. The displacements were measured by linear displacement transducers. The apparatus is shown diagramatically in Fig.3:4:1. The faces of the platens were lined with layers of various materials to reduce friction to a minimum. This treatment consisted of 3 layers of grease and polythene squares glued to paper. Friction losses were estimated at about 4% of the applied load.

Two materials were tested, an angular basalt from El Pedregal and a semi-rounded sand and gravel from Pinzandaran.

The samples were consolidated by applying equal increments of $6'_3$ and $6'_1$ until the desired value of $6'_3$ was reached. Considerable creep occurred at each stress increment. $6'_3$ was then held constant and $6'_1$ increased in steps until failure. Deformations were nearly as great as in the triaxial apparatus and with the tests at the higher stresses $6'_1$ and $6'_3$ had to be reduced to zero to reset the jack when its limit of travel was reached. The ratio of the major to the intermediate principal stress was almost constant in the range of stresses applied for both materials.

Material	Porosity (n)	$6'_3$ kg/cm^2	$6'_2 / 6'_1$	Coefficient of uniformity.
Pinzandaran semi rounded sand & gravel	25.9	5.1	0.260	
	25.4	10.1	0.262	12.5
	25.4	15.3	0.249	
El Pedregal basalt	33.8	5.1	0.329	
	32.4	10.3	0.321	7.3
	35.1	14.4	0.325	

Table 3:4:1. Plane strain test results (after Marsal)

The stress strain curves for the two materials are shown in Figs.3:4:2 and 3:4:3. It will be noted that the failure strains are very large compared with those obtained by Cornforth on Brasted sand.

A certain amount of yield must occur because of particle points bedding into the polythene plates and grease and hence a true plane strain condition is not achieved. The total thickness of the polythene sheets is 12 mm which may easily amount to 15 mm or more when the paper and grease layers are added. This would suggest that the intermediate principal stress should be higher than that recorded. A certain amount of the creep observed may also be due to these boundary conditions and the squeezing out of grease from under a particle point.

(3:5) Other drained shear tests on rockfill and associated materials

For thedesign of several rolled gravel fill dams for new reservoirs in the Thames Valley a range of shear tests was carried out on sands and gravels, using a shear box 1' square and 6" deep (Bishop 1948). Five materials were tested at various porosities so that a correlation could be obtained between field density and shear strength. Loose samples were

produced by rapid pouring. Dense samples were produced by hand tamping in a number of layers. The grading curves of the materials, together with a table of some of the results, is given in Fig.3:5:1. Also shown is the relationship between the initial porosity and the angle of internal friction for the various gradings. The uniform and graded materials seem to split into two different zones which converge at high porosities. It must be noted, however, that gradings 1 to 4 were tested at a normal stress of 2.0 tons/ft^2 and grading 5 at 0.5 tons/ft^2.

The lower porosities of the well graded, sandy gravel resulted in an angle of internal friction of about 50°. Dense graded sand gave a considerably lower value.

It is interesting to note that the two uniform materials (i.e. those having geometrically similar gradings) Chesil Bank pebbles and Ham River sand (rounded), had similar angles of internal friction for a given initial porosity within the stress range applied.

In 1955 Kjellman and Jakobson reported a comprehensive series of tests, which were carried out in an apparatus designed to take a sample of 50 cms. diameter and 100 cms in height. This apparatus could be used as an oedometer or a direct shear machine. The investigation covered uniform, fine and coarse gravel and macadam , in both the dense and loose states. The gravels were rounded, whereas the macadams were angular materials. The maximum particle size tested was 5 cms.

As the sample was high, compared with its diameter, the confining ring was split horizontally to minimise silo effects. This confining ring was made up of 20 mild steel rings, each 5 cm. deep and 0.7 cm. thick, spaced apart by 2 mm. Unless the rings touched during deformation all the normal load had to be transmitted thoughout the sample without any loss through the confining rings. However, a small variation, about 2%, in the normal stress occurred between particles at an elevation of mid-height of the rings and those at the gap between rings.

Axial deformation was measured by dial gauges, which were attached to rings in the central portion of the sample so that effects due to rigid end boundaries and bedding would be by-passed. Lateral stresses were calculated from the circumferential deformations of the rings, which were measured by three methods, mechanically, optically and electrically. The first method was insensitive and the second was very difficult because of all the other strains which were taking place, leaving the electrical method the most satisfactory

When shear tests were to be carried out the sample supporting rings were considerably stiffened, being 2 cm. deep by 6.5 cm. thick. Loads were applied to the sample by hydraulic jacks and the general arrangement

is shown schematically in Fig.3:5:2 together with the material composition and the shear test results.

In the oedometer tests it was noticed that the angular material compressed about 5 to 6 times as much as the rounded material at similar porosity and stresses. Considerable particle breakdown occurred and sample compaction induced a state of overconsolidation because Young's Modulus decreased during the first load increments and then increased. Very little rebound occurred on removal of the normal load from a sample of macadam but a more noticeable amount occurred with the pebbles. Because of creep the load increments had to be applied at about 2 hourly intervals.

It was concluded that Poisson's ratio for laterally confined coarse grained materials was constant during the first loading, irrespective of pressure, grain size or shape and sample density and corresponded to a value of K_o of 0.44

During shear the loose samples tended to consolidate, whereas dense samples consolidated and then dilated. The rounded material dilated more than the angular.

The grain size seemed to have little effect on volume changes in the applied stress range although grain shape was an important factor, angular grains deforming more than rounded ones. This though is to be expected even when the grains are made of the same mineral because the actual contact deformations are very different for the transmission of a given load from one particle to another. When two spherical surfaces are in contact the contact area is supported by the restraint of the surrounding material. In the case of an angular material the contact is probably conical or linear and the restraint from the body of the particle is thus ineffective. The point breaks down until sufficient contact area and restraint exist to transmit the load. This is probably why the creep rates of various materials are very similar at a given time after the initial deformation.

The range of particle sizes used in the testing programme was insufficient to detect effects due to grain size because the number of contacts and hence the contact forces were comparable and the stress range was also very limited.

However, the maximum size of particle which can be tested in any particular apparatus is not simply a function of size ratios but of particle shape and strength and also of the grading of the material of which it forms a part.

A series of drained shear tests on uniform gradings of granite, in 6 cm. x 6 cm. and 12" x 12" shear boxes, was reported by Lewis (1956).

All the gradings tested were geometrically similar and the particle shapes were also similar. The tests were run wet and all the initial densities were the same. The maximum normal load of these tests are shown in Fig.3:5:3a.

It was found that if the maximum particle size was less than 1/40 of the shear box width the angles of internal friction had a linear relation with the particle size, when plotted to a logarithmic scale. From the small scale tests extrapolations were made to predict the behaviour of much larger particles. The explanation was that there was more interference and interlocking with the larger particles. This was indicated by continuous dilation, despite the fact that the stone was loose tipped. The dilation was greater for the larger stone. Dilation has been discussed in several papers and an energy correction derived which must be subtracted to give a more fundamental value of inter particle friction In practice, however, this extra strength is available and should not be ignored.

A certain number of triaxial tests were also carried out and these gave values of ϕ' about 3° higher than the shear box. This was attributed to the more uniform distribution of stress in a triaxial test. Also, the actual state of stress is unknown in the shear box. The principal stresses are inclined and the usual planes of failure at $45^{\circ} - \phi'/2$ to the maximum principal stress do not coincide with the forced failure plane between the two halves of the shear box. During the test the outside edges of the sample fail before the centre and these two effects oppose each other. The actual area being sheared is constantly diminishing during the test and sheared material bears on the end of the shear box.

Dvorak (1961) found that, when using shear boxes to determine the peak shear strength of a disintegrated shale, the angle of internal friction increased as the area of the cross-section of the shear box was increased (Fig.3:5:3b).

In 1967 Bernaix briefly reported a series of tests using a circular shear box 55 cms internal diameter and 40 cms deep. The insitu grading of the material tested is given in the table overleaf. . The materials actually tested comprised that fraction passing 63 mm, 5 mm and 3.5 mm and the resulting values of the angle of internal friction are also recorded in the table.

Sieve size mm	% passing	Grading	Angle of internal friction
150	100	less than 63 mm	41.5°
63	92		
20	70	less than 5 mm	34.0°
5	40		
2	31		
0.2	20		
0.1	18	less than 3.5 mm	32.0°

Table. 3:5:1 Results of tests by Bernaix on an altered schist for the design of a 200m. high dam.

(3:6) Undrained shear tests on associated materials.

In a dry, or partly saturated, material the volume decrease may not be particularly important as long as adequate shear strength is available. Differential settlement though, particularly between the core and shoulders of an earth dam could be dangerous. However, if the material is saturated and subject to shear, say from seismic shock, a potentially dangerous situation arises as the resulting stress path becomes very similar to that of a quick clay. The stress paths for two undrained tests, by Skinner, on Ham River sand, one consolidated isotropically, the other anisotropically were reported by Bishop (1965) and are shown in Fig. 3:6:1.

The situation is likely to be particularly severe with a rockfill having high intergranular contact stresses.

Consolidated undrained tests by Lowe (1964) on material finer than the No.4 sieve indicated an angle of internal friction of 37°. This value reduced to 28° when full saturation was achieved using a back pressure of 100 p.s.i. There is, however, another factor which effects resultant pore pressure. This is a function of the membrane stiffness and its thickness relative to the sample particle size. If the application of the cell pressure causes considerable membrane penetration then subsequent sample consolidation during shear will build up the pore pressure in opposition to the cell pressure and the membrane penetration will be reduced. The flexibility of the boundary will, therefore, be equivalent to partial drainage with resulting error in the pore pressure determination.

(3:7) Shear strength dilatancy and interparticle friction.

In 1962 Rowe proposed that the dilatancy and strength of an assembly

of individual particles in contact and subjected to a deviatoric stress system were dependant on the angle of friction, ϕ'_μ between the particle surfaces, on the geometry of the packing and on the degree of energy loss during remoulding.

Hirschfeld and Paulos (1963) reported a series of tests on undisturbed Canonsville silt and on a compacted sand obtained by sieving out the material passing a No.10 sieve from a sandy gravel. Confining pressures up to about 600 p.s.i. were applied to samples 3.58 cms. diameter and 8.5 cms. high. The sand samples were compacted by vibrations to a dense state.

At a confining pressure of 60 p.s.i. the angles of internal friction for the silt and sand were both 36°. When the minor principal stress was increased to 600 p.s.i. the angle of internal friction dropped to 33° for the sand and to 26.7° for the silt. It was noticed that at the high stresses there was a tendancy for the samples to consolidate throughout the test and at low stresses an initial consolidation was followed by dilation. Because of this a correction was applied to the peak deviator stresses using the modified deviator stress obtained by Rowe (1962), i.e.

modified deviator stress $= \left[\sigma'_1 / \left(1 + \frac{d\upsilon}{d\epsilon}\right) \right] - \sigma'_3$

where σ'_1 = measured effective major principal stress.

σ'_3 = measured effective minor principal stress.

$d\upsilon$ = volumetric strain (increase + V E)

$d\epsilon$ = axial strain (compression + V E)

The Möhr envelopes were recalculated, the sand giving a straight line through the origin and the silt a slight curvature. The curvature of the modified envelope for the silt was attributed to it behaving as an overconsolidated soil below a confining pressure of 300 p.s.i. and normally consolidated above.

It was assumed that the initial curvature of the Möhr envelope was, therefore, caused by the volume changes during shear.

This is not exactly the same as saying that particle degradation is the cause.

Rowe (1963) suggested that the modified Möhr envelope for the silt was satisfactory as it yielded, according to the theory, an acceptable angle of interparticle friction of 30.2°.

The modified envelope for sand though suggested an unacceptably high value of interparticle friction of 37°. This was explained by membrane penetration and the affect of rigid end platens on the mean rate of dilatancy at failure.

Rigid end platens were also used though when testing the silt and the membrane penetration with a constant cell pressure is unlikely to affect the rate of volume change at failure.

The variation in the rate of dilatancy for various parts of a sample was shown by Blight (1963) Fig.3:7:1. Also data presented by Shockley and Ahlvin (1960) indicate that end restraint can cause an objectionable error in the measured rates of dilatancy.

Vesic and Barksdale (1963) tentatively concluded from very high pressure tests on Chatahoochee River sand that dilatancy was a low pressure phenomenon only and at high pressures the Mõhr envelope for dense rejoined that for loose sand.

Granular material, whether placed loose or dense, seems to behave at high pressures rather like a loose sand. Cornforth (1961 and 1964) found that there was little difference in strength between loose samples tested in triaxial and plane strain apparatus.

Leussink and Wittke (1963) carried out a theoretical study of the shear strength of a regular packing of spheres in triaxial and plane strain conditions. This was followed by a laboratory investigation using similar packings of steel balls and glass balls. For an hexagonal packing angles of internal friction of 40.7° and 51.4° respectively were obtained for triaxial and plane strain conditions. The coefficient of interparticle friction of the "grains" seemed to have little effect on the shear strength of the pack (Wittke 1963) as the same ultimate shear strength was obtained for steel and glass balls having very different coefficients of interparticle friction.

Borowicka (1963) was also of the opinion that the shear strength of a soil was a function of interlocking of the packing rather than interparticle friction.

Further evidence that the shear strength does not correlate with ϕ_μ is provided by Skinner (1969).

(3:8) Contact stresses in rockfill and other materials.

To understand the large deformations of rockfill structures it is useful to compare the contact forces between particles in different materials for a given mean applied effective stress.

Marsal (1963) approached this problem and determined the order of magnitude of contact stresses in various materials. He determined the number of contacts per particle and the number of particles cutting a plane. If the force normal to the plane was known then the force per contact could be established. This, of course, is assuming that the contacts are reacting normal to the plane which is unlikely to be true. If all the contacts are not reacting normal to the plane then the mean contact load is increased.

He suggested that $\frac{1}{1+e} = \frac{\pi}{6} n_v r_v d_m^3$ - - - - - - - - - (1)

Where n_v = number of particles in a given volume

$n_s = n_v^{2/3}$ = number of particles in a given plane.

$n_L = n_v^{1/3}$ = number of particles in a given unit length.

r_v = shape factor.

d_m^3 = mean particle dimension which is not equal to the nominal size, except for a sphere.

For gravels the above parameters were easily determined, though the process was very tedious. The number of particles in a given plane was determined by counting after photographing the plane. Similarly, for the number per unit length and those per unit volume simply by counting the particles in a given volume container. Particle lengths, widths and breadths were obtained by measuring and the surface areas by coating each in wax and determining the thickness weight and density of the wax film.

The number of contacts per particle was found by flooding a sample with paint, draining it and allowing the paint to go hard on the particles. The number of unpainted spots on each particle then determined the number of its contacts. In general, there were 6 contacts per particle for loose and 7 or 8 for dense samples.

From equation (1) above $n_s = n_v^{2/3} = \left[\frac{6}{\pi r_v (1+e)}\right]^{2/3} \frac{1}{d_m^2}$

From the analysis the following average contact forces were determined for a mean effective stress of 1 Kg/cm

Material	e	Dia cms.	Shape factor	grains per m^3	No.of contacts per grain	No.of contacts per m^2	Average contact force.Kg
Mexico City volcanic clay							$1x10^{-9}$
Sand	0.5	.02	0.5	$3.19x10^{1}$	6	97x10	$1.79x10^{-4}$
Rockfill	0.7	20	0.7	2x10	7	39.7	400

Table 3:8:1 Grain contact forces (after Marsal)

For the simple case of spheres in a cubical pack Bishop (1965) used Timoshenko's (1951) solution for the contact stresses between two equal spheres to predict the tensile failure of a quartz grain.

If P is the contact force between particles of diameter d and the mean effective stress is 6

Then: $P = 6\ d^2$

The contact pressure is:

$$6_m = 0.6 \left[4PE^2 / d^2\right]^{1/3}$$

where E = Youngs Modulus and Poisson's ratio is assumed equal to 0.3. For quartz E = 1 x 10^6 Kg/cm^2 and the approximate tensile and shear strengths are 830 Kg/cm^2 and 11,000 Kg/cm^2 respectively.

Substituting in the above equations, tensile failure and shear failure will occur at σ = 4 p.s.i and 600 p.s.i. respectively.

In practice, however, d in Timoshenko's equation refers to the diameter of the surface contact which for angular soil grains will be very much less than the mean diameter of the particle and hence, the contact stresses will be higher still and local tensile failure will occur at very low values of mean effective stress.

Later, in 1967, Marsal developed a statistical method of analysing intergranular stresses in certain ideal gradings and taking into account grain shape and void ratio. He then compared the results with a series of experiments by Weber (1966). Weber used a photoelastic method to determine contact stresses between perspex particles. The two analyses were not in agreement and differences in orders of magnitude were apparent.

An acoustic method is being developed for detecting the onset of fracture in metals (Brown 1965) but difficulties are immense, especially in relating acoustic output to local stress and in the elimination of extraneous sounds. This method, for the time being anyway, is probably an unsuitable approach to determining contact stresses in rockfill.

(3:9) Particle breakdown and compressibility

Marsal suggested that particle breakdown (B) would be related to the ratio of the particle contact force ($\bar{P}$) to the strength of the particle points Pa such that $B = \alpha \bar{P}/P_a$.

In brittle particles of spherical form tensile failure occurs as a result of normal tangential contact forces. From elastic theory one can show that the tangential force causes considerably higher tensile stresses than the normal component.

Brauns and Leussink (1967) assumed that the tensile strength of glass was 100 Kg/cm^2. From this they calculated that a cubic pack of spheres could withstand an all round applied stress of 1,200 Kg/cm^2 prior to fracture. If coefficient of interparticle friction of 0.3 was assumed and a stress ratio of 1.85 applied particle fractures would occur at a minor principal stress of only 9Kg/cm^2. This is in agreement with observations on particle breakdown by Vesic and Barksdale (1963) and Bishop (1965 and 1966).

Marsal (1967) also correlates the principal stress ratio at failure with particle breakdown (Fig.3:9:1). The shear strength of a sample decreases as the particle breakage increases and he suggests that this plot

defines a lower limit of principal stress ratio in terms of particle breakdown. However, it is not a simple plot of principal stress ratio against particle breakdown because the mean stress level is varying enormously.

The average contact force $\bar{P}$ for a given stress level was re-defined by Marsal (1968) such that

$$\bar{P} = 4.5\ p\ /\ n_s\ N_c$$

where N_c is the average number of contacts per particle.

n_s is the average number of particles per unit area.

p is the resultant external stress.

For a uniform granular material this becomes

$$\bar{P} = 4.5\ d^2\ p/N_c \left[r_v\ (1 + e) \right]^{\frac{2}{5}} \quad \text{where}$$

r_v is a particle shape factor

e is the void ratio of the sample.

When the grading is not uniform the mean value of contact forces for particles of fraction j is

$$\bar{P}\ j = \bar{P}\ dj\ /\ \bar{d} \quad \text{where}$$

$\bar{d}$ is the average grain diameter of the whole sample.

Kjaernsli (1963) reported on a series of compressibility tests on some coarse grained aggregates. Uniaxial compression tests were carried out on square samples of syenite, granite and limestone. Various strengths were obtained depending on the moisture content of the samples. For the syenite the ratio of the compressive strengths of oven dried, saturated and saturated submerged samples was 100, 94 and 85 respectively. More dramatic variations were found by Queiroz (1963) when testing sound quartzite in the dry and saturated states. This material was used in the shoulders of Furnas Dam and displayed a dry strength of 1720 Kg/cm^2 and 901 Kg/cm^2 after soaking in water for 48 hours. This strength reduction is a function of surface activity and is discussed later. In practice it can lead to sudden and substantial deformations of previously unwetted rockfills (Baumann 1941).

Kjaernsli designed an oedometer in which loads of up to 500 $tons/m^2$ were applied to samples with a maximum grain size of 128 mm. During the tests the wall friction was also measured and was found to vary between 12% and 40% of the total applied load.

This friction probably depends on the relative hardness of the oedometer ring and the rock material being tested. Mild steel is quite soft and granite will bed into it.

It was found that the compressibility of a rockfill varied with initial density and grading. A dense, broad grading being much less compressible than a loose, narrow grading. The compressibility is

decreased by an increase in hardness of the rock and is greater for angular, rough surface aggregates than for smooth, rounded aggregates. Some results of tests on crushed syenite, gneiss and limestone, together with moraine and gravel, are shown in Figs. 3:9:2 and 3:9:3

The result of one oedometer test carried out by Kjaernsli is shown in Fig.3:9:3. It will be seen that the syenite continued to creep for the duration of the test (330 days) and a sudden collapse of the sample was recorded when it was saturated without change in effective stress. The extra deformation was not as dramatic as that recorded by Hawkins (1966) in a similar test on silurian cleaved mudstone (Fig.3:9:3). However, for there to be no increase in deformation on saturation the initial moisture content of the mudstone had to be about 5%. It may, therefore, be that the syenite sample tested by Kjaernsli was not in fact oven dry prior to saturation and hence a much smaller increase in deformation was recorded. However, a 100% increase should not be expected for all rock types as this will be partly dependant on the mineralogy of the sample.

To obtain a fill of minimum compressibility it was suggested that a broadly graded gravel, with smooth surface rounded particles, be placed and compacted wet and in thin layers.

At the Goeschenenalp Dam the moraine shoulders were compacted solely by the construction traffic and settled three times as much as the core which was compacted using pneumatic rollers (Gilg 1963).

Janbu (1963) has shown that for principal stress ratios of 0.35 to 0.45 the deviator stress is responsible for 75% to 90% of the total compression.

One problem which has always existed with earth dams is the design of suitable filters to prevent internal erosion. Filter materials are often of a different rock type to the materials on either side of them and, to prevent segregation during construction, they may well be made up of a series of uniform gradings.

As dams have increased in height so filters have been subjected to increasing stresses with the attendant particle breakdown. The problem is to ensure that filter and drainage requirements are still met after breakdown has occurred in the filter and in the materials on either side of it.

This problem was investigated by Lee and Farhoomand (1967) by subjecting a granite aggregate to various stress ratios at different stress levels.

The basic soil used for the investigation was a very angular crushed granite. Subrounded material was produced by tumbling the angular granite for several weeks in a ball mill.

Tests on material passing the No.4 sieve were carried out in 1.4" diameter by 3.5" high samples and larger material in 2.8" by 6" samples. All samples were saturated by back pressure and then volume changes were measured by burette at atmospheric pressure. Stress ratios of 1.0 and 2.0 and 2.8 were used and all samples were vibrated to 100% relative density. The grading analyses of the materials are shown in Fig.3:9:4a.

A comparison between the compressibilities of the angular and subrounded materials is shown in Fig.3:9:4b. It should be noted that principal stress ratios of 1.0, 2.0, and 2.8 were used and the volume changes formed a unique curve when plotted against the major principal stress.

In contrast to Marsal's "B value" particle breakdown was measured by the change in the D_{15} size before and after test. This size was chosen because it is the commonly accepted size upon which filter designs are based.

The relative crushing of angular and subrounded material B when subjected to a principal stress ratio of 2.8 and at a minor principal stress of 80 Kg/cm^2 is shown in Fig.3:9:4c

The relative crushing of soils A and B under various stress ratios is shown in Fig.3:9:5 and a comparison of the crushing of various gradings of angular material at various stresses with the principal stress ratio equal to one is shown in Fig.3:9:6.

The following general conclusions were drawn:

a) Granular soil is quite compressible under an applied stress.

b) Compression is usually accompanied by a certain amount of particle breakage and the two phenomena seem to be somewhat related to each other.

c) Coarse soils compress more and show more particle crushing than fine soils.

d) Soils with angular particles compress more and show more particle crushing than soils with rounded particles.

e) Uniform soils compress and crush more than graded soils of the same maximum particle size.

f) Under any particular stress the compression and particle crushing continue to increase at an ever decreasing rate for an indefinite period of time.

g) For the soils tested there appeared to be a unique relationship between the volume change and the major principal stress which was completely independent of the principal stress ratio. No such relation was observed with respect to crushing. In the case of crushing the greater the principal stress ratio the greater greater the crushing.

h) Since all soils crushed and became finer under load the data indicated that for a soil which met the filter requirements for a certain foundation material before compression appeared also to meet the new filter requirements for the same foundation material after crushing.

Conclusion (h) may not be valid though where the particle strengths of the filter and adjoining material vary widely.

Ladanyi (1967) suggests that conclusion (g) should be limited to the stress paths used in the tests as no proof has yet been given that this statement is valid for all possible stress paths and particularly those involving anisotropic consolidation at the beginning of loading.

Broscoe (1967) stated that some of the greater compressibility of angular material may have been due to a difference in strength between the rounded and angular particles. This was simply because the rounded material was produced from the angular material by rolling in a ball mill and one would expect an affect on the mineralogical composition of the finer material. The uniformly graded material B could be substantially affected by the rounding process in the ball mill. The finer particles of such a soil would consist of quartz and feldspar particles. The quartz would withstand the weathering action of the ball mill but feldspar and mica would probably be eliminated from the material.

The suggestion that the volume change in a granular soil is a unique function of the major principal stress implies that the granular soil behaves elastically (Insley 1967). However, tests by Terzaghi and Peck (1948) and Menzenbach (1958) illustrated that granular soil exhibits a stress history which indicates that the change in principal stress ratio and, therefore, the minor principal stress affects the behaviour.

The unique relationship between volume change and major principal stress was also questioned by Holubec (1967) who suggested it may have been due to sample shape and the boundary conditions. It would be interesting to separate out the volume changes, reversible due to elastic compression and irreversible due to particle breakdown.

The Istituto Sperimentale Modelli e Strutture has very considerable experience of the physical properties of many hundreds of materials used in model tests on structures. Oberti (1968) suggested that this knowledge would be invaluable in testing large scale models of rockfill dams to minimise the number of unknown factors as these structures steadily increased in height.

At the above laboratory a unique oedometer has been developed for testing rockfill at high stresses (Fumagalli 1968). Instead of the usual solid oedometer confining ring alternate rings of steel and a highly

deformable material are glued together. This produces a test chamber which may be considered as a highly anisotropic material, having a radial stiffness 10 times that of its vertical stiffness. A recent modification was the replacement of the steel rings with plexiglas rings so that particle crushing and orientation could be observed during the test.

A number of gradings have been tested in oedometers 100 mm diameter by 200 mm high, 500 mm by 1000 mm and 1300 mm by 2600 mm in an investigation to predict rockfill behaviour in the field from small scale laboratory tests.

It is anticipated that the results will be published in the middle of 1969.

(3:10) The effect of membranes on the measured shear strength of rockfill.

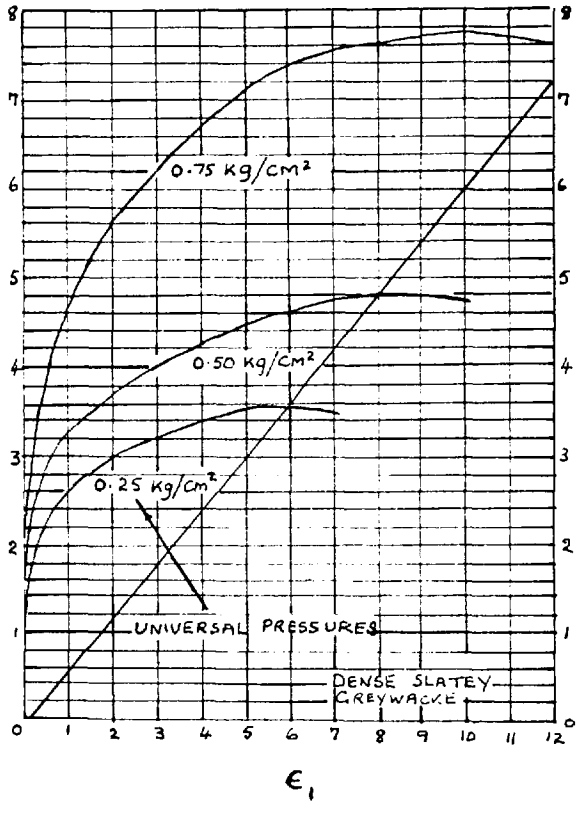
The effect of the rubber membrane on the measured shear strength of a soil sample has always been subject to doubt. In Marsal's case there is also a sand jacket with a cross-section equal to 17% of the entire sample. The characteristics of the sand, even if it is the fines of the rockfill being tested, are likely to vary from those of the rockfill. At any particular axial strain prior to failure the sand may be nearer to its peak strength and demonstrating far different dilatancy characteristics. External measurements of volume change are, therefore, probably deceiving.

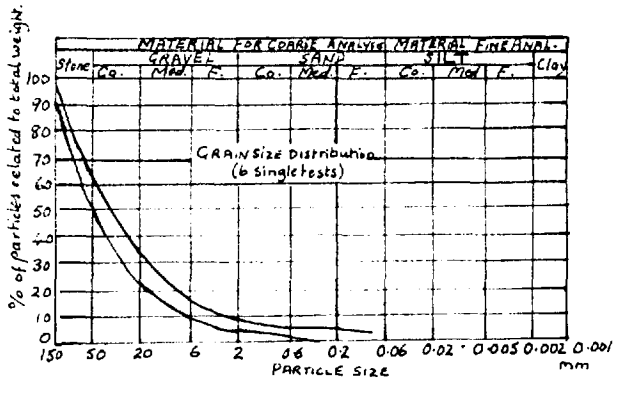
The action of the sand jacket was discussed by Hillis and Skermer in 1968. It was assumed that the confining pressure was fully transmitted across the sand jacket to the rockfill. If the sand was stiff it could conceivably form a stiff ring around the rockfill thus reducing the effective stresses on it. In this case the shear strength of the rockfill would be underestimated.

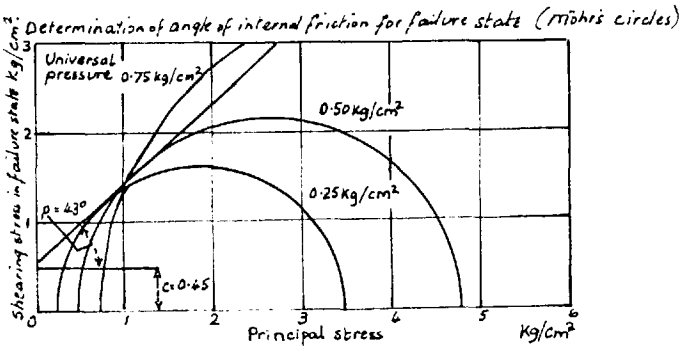
If the sand and rockfill reached peak strength at the same axial strain and the measured ϕ' for the whole was 30° and the sand was at such a density that its ϕ' value was 35° then the rockfill angle of internal friction w ould be 29%. If the sand ϕ' value was 45° then the true rockfill ϕ' value would be 25° for a measured value of 30°.

Triaxial tests were carried out on the sand jacket material used by Marsal and the stress strain curves, the initial grading of the rockfill and the Mohr envelopes for an axial strain of 12% are plotted in Fig.3:10:1

It was concluded that errors in measuring the peak shear strength of the rockfill were probably only 1° or 2° but at low axial strains the errors may be somewhat greater.

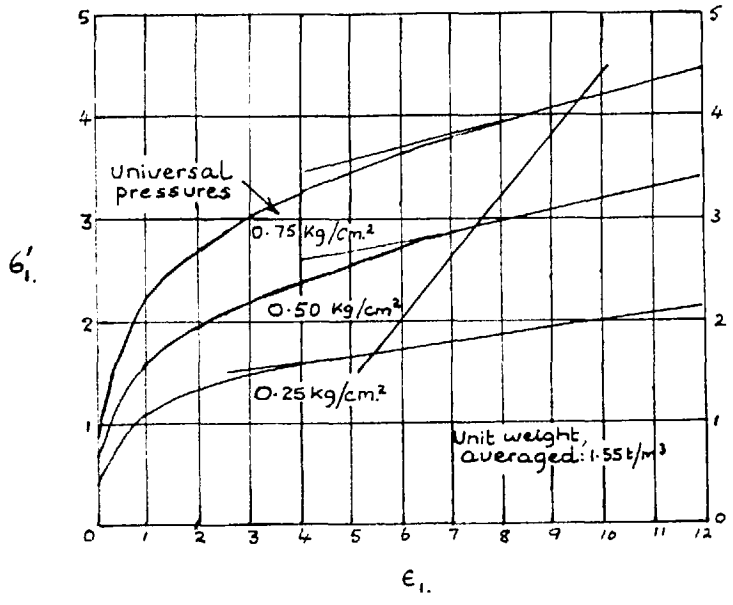


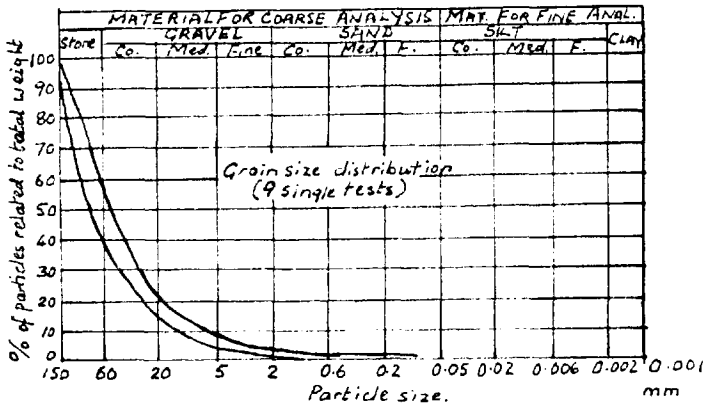


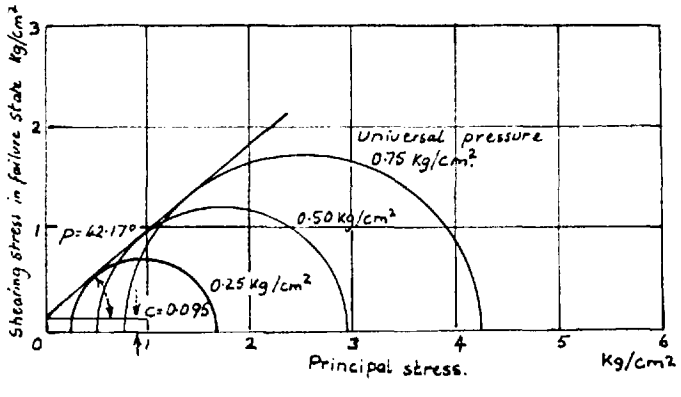


VACUUM TRIAXIAL TESTS FOR THE HEIGHTENING OF SCHWAMMENAUEL DAM.

FIG. 3:2:1

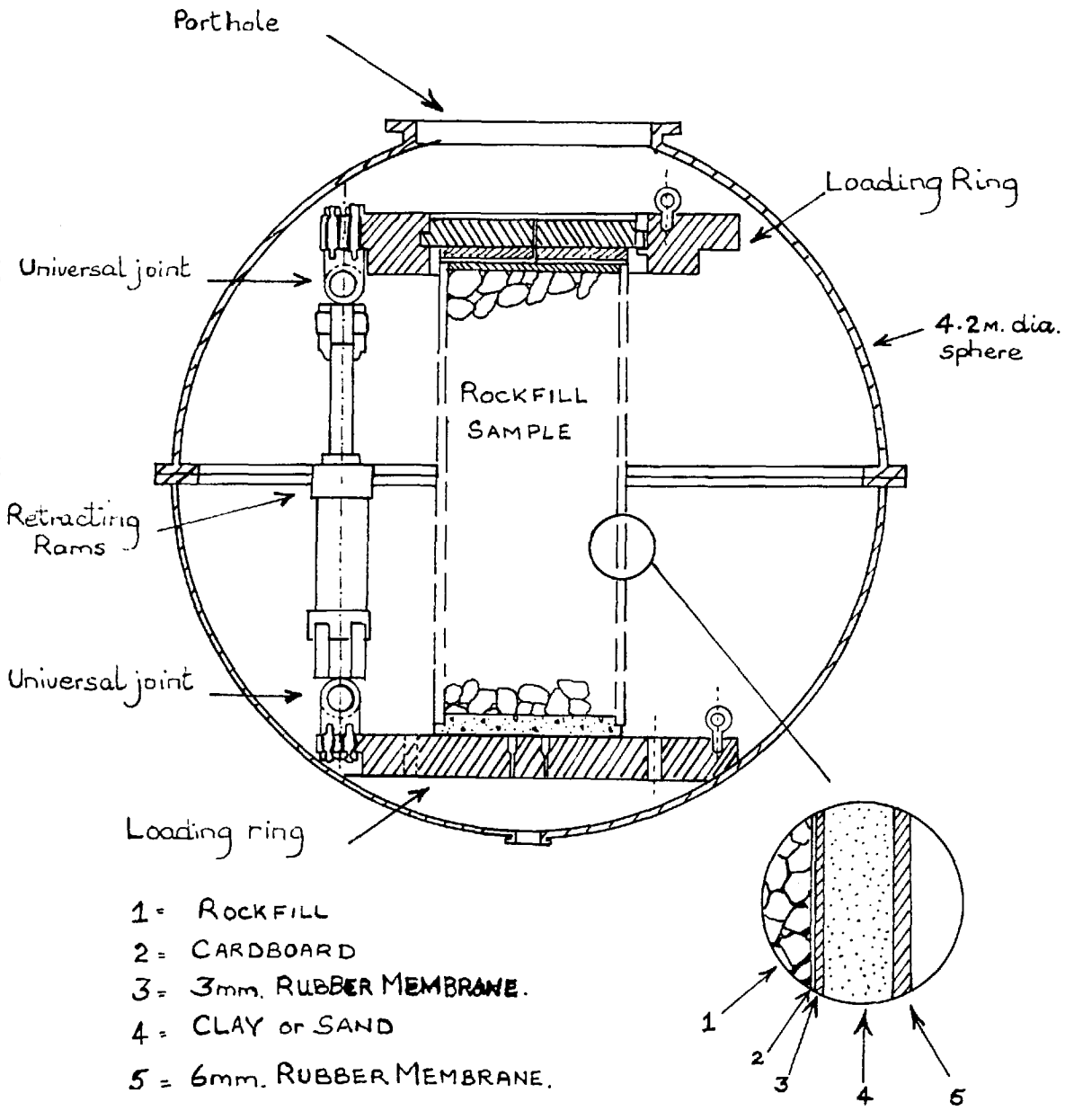






VACUUM TRIAXIAL TESTS ON GREYWACKE (LOOSE).

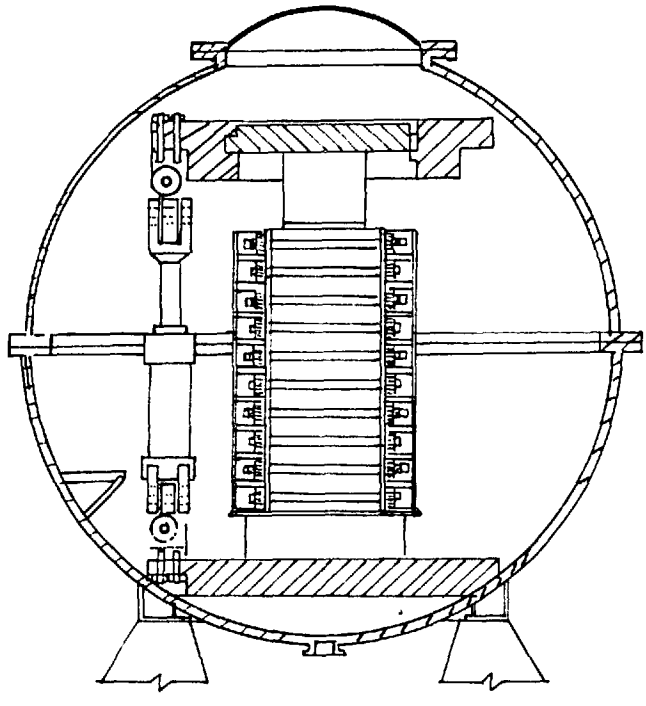
FIG. 3:2:2



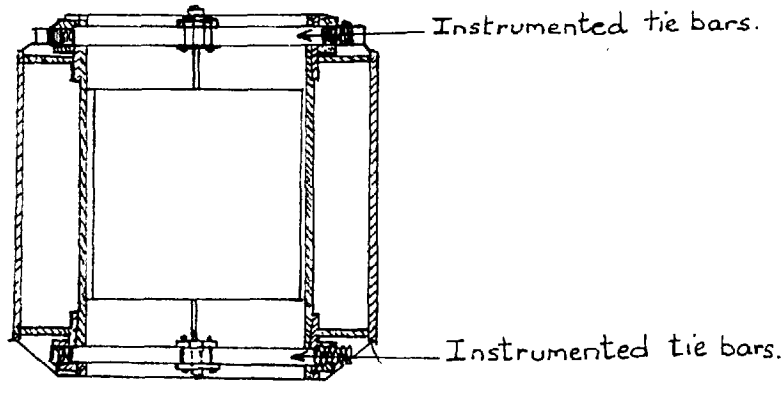
Cross-Section of Triaxial Cell For Testing Rockfill Samples

113 cms. dia. by 250 cms. high at confining pressures of 25 kg/cm^2.

FIG. 3:2:3



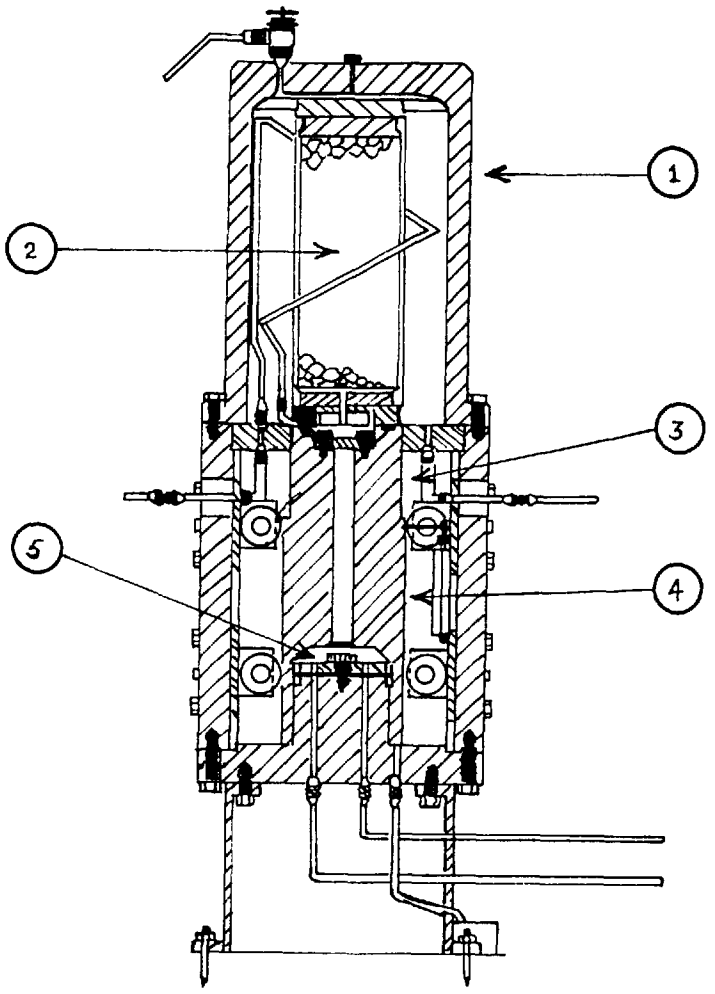
CROSS-SECTION OF CELL AND PLANE STRAIN APPARATUS.



PLAN OF PLANE STRAIN ATTACHMENT.

LARGE TRIAXIAL CELL WITH PLANE STRAIN APPARATUS IN POSITION.

FIG. 3:2:4



(1) = CELL

(2) = SAMPLE

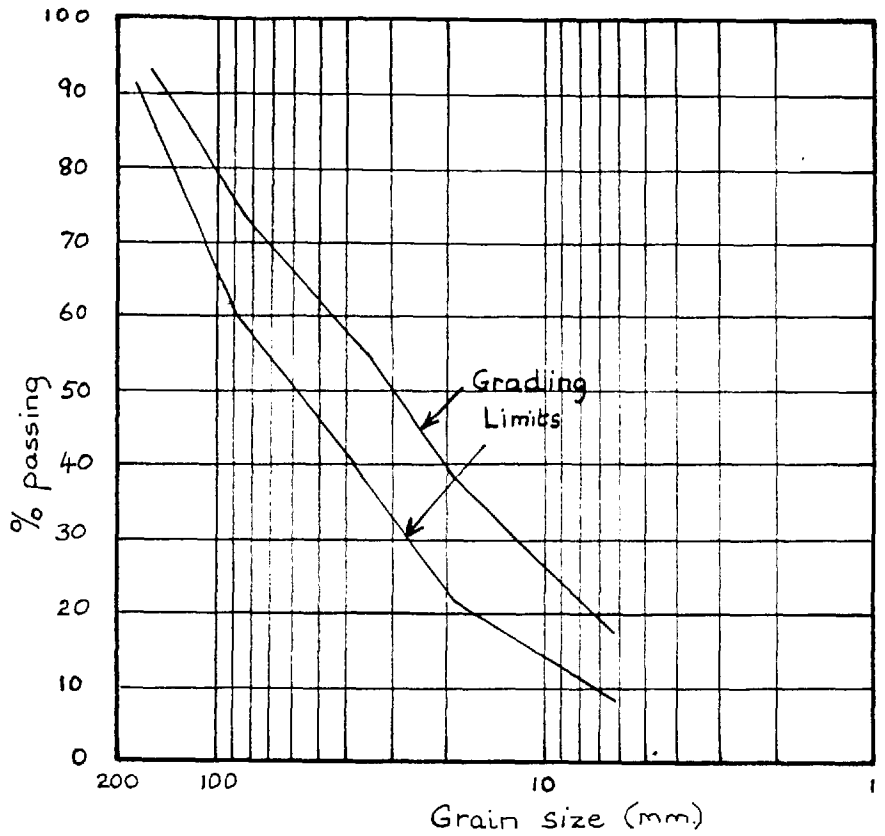
(3) = CIRCULAR PORTION OF PISTON

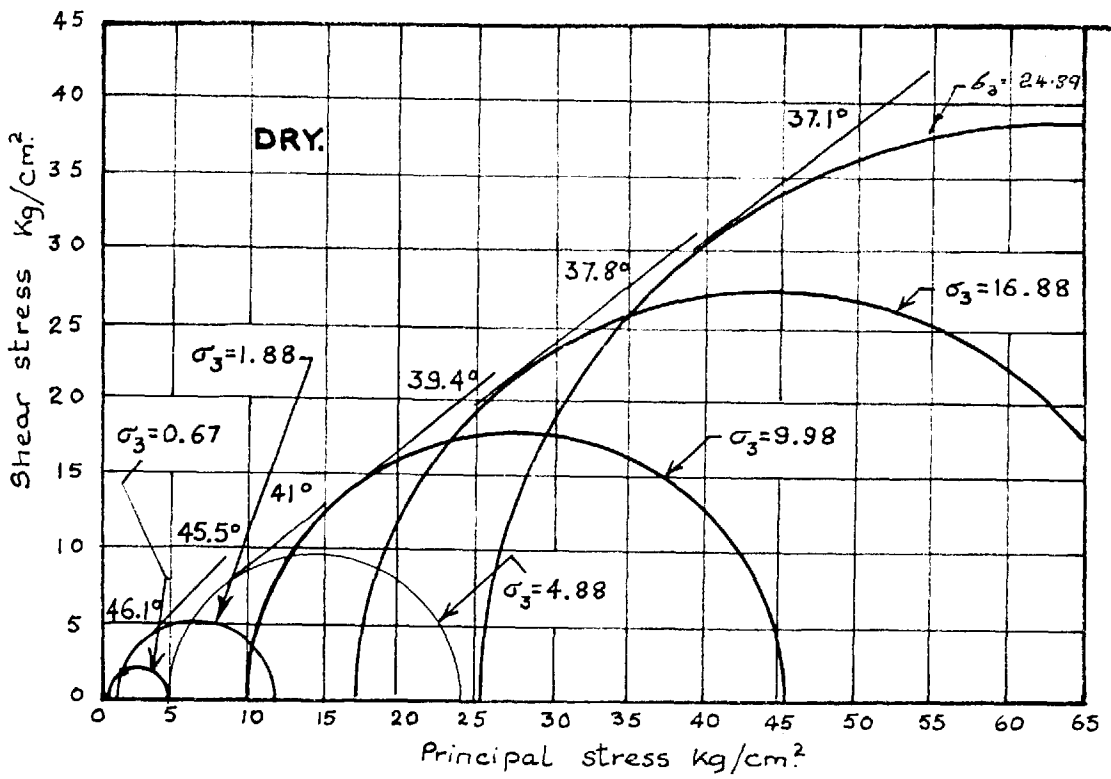
(4) = 12 SIDED PORTION OF PISTON, GUIDED BY 24 ROLLER BEARINGS

(5) = INSIDE OF PISTON HOLLOWED TO ACT AS HYDRAULIC JACK.

TRIAXIAL CELL FOR TESTING SAMPLES 20 CM DIAMETER BY 50 CM HIGH AT CONFINING PRESSURES OF 50 Kg/cm²

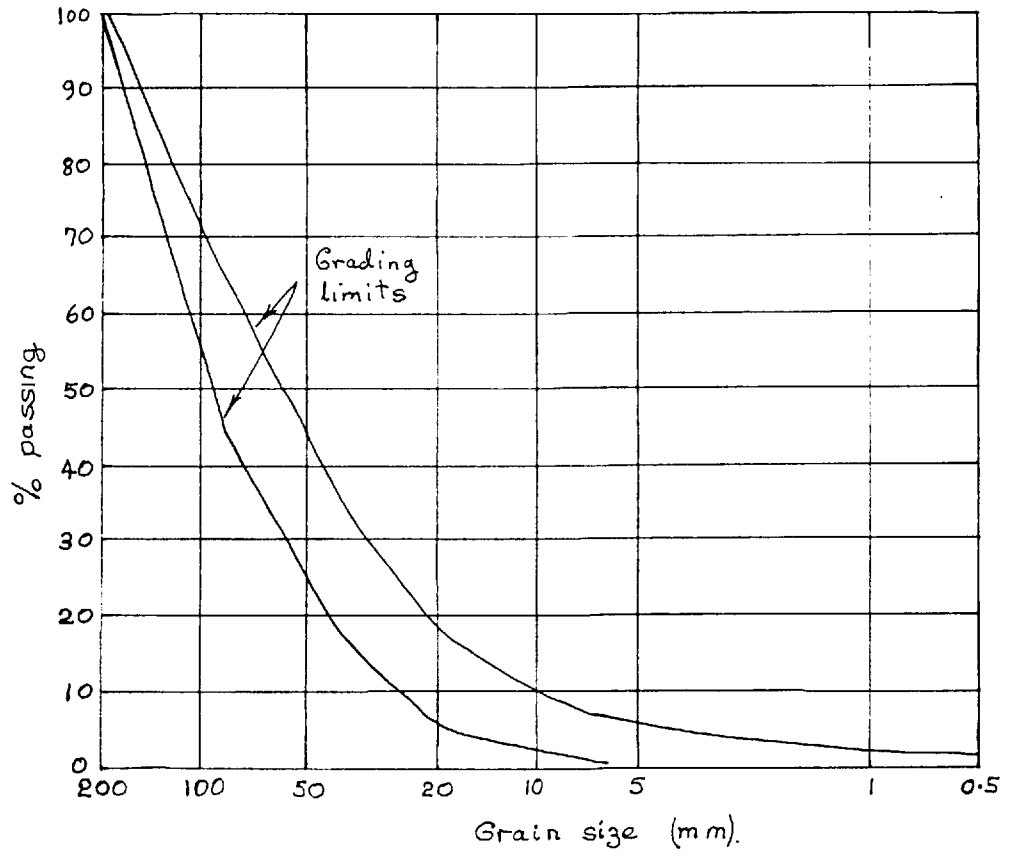
FIG. 3:2:5



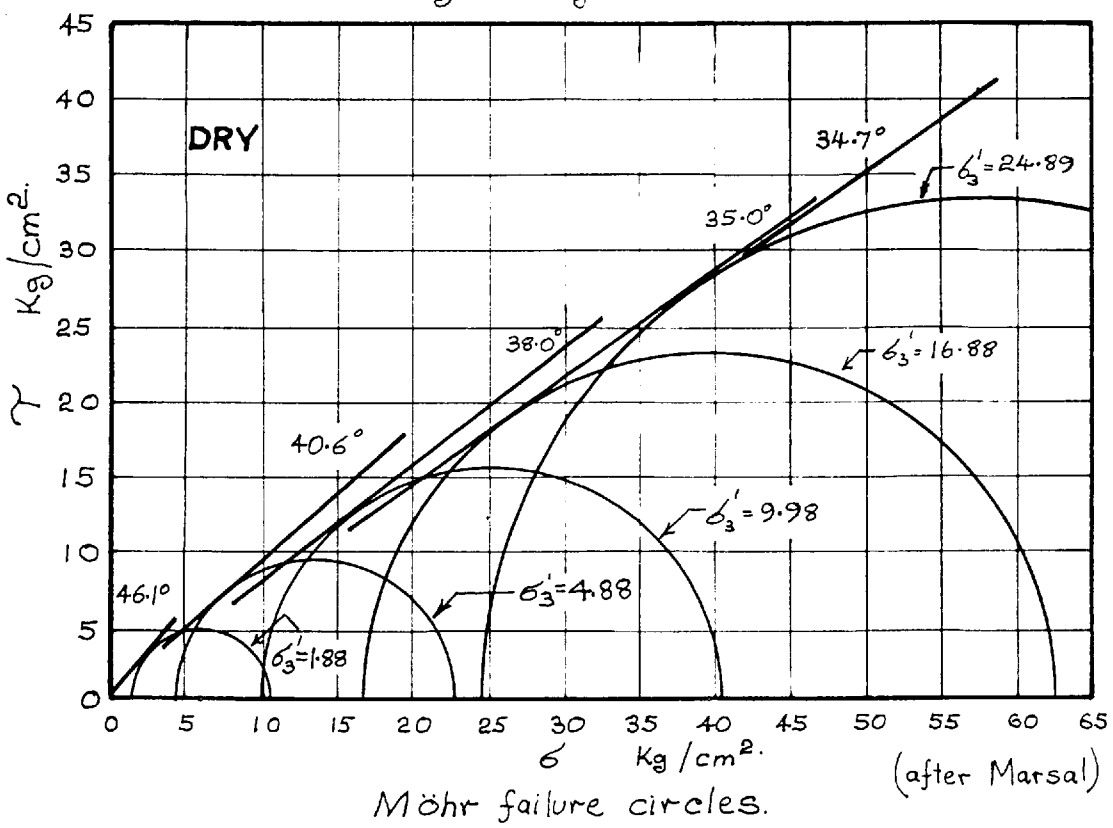


GRADING AND SHEAR STRENGTH OF EL INFIERNILLO ANGULAR SILICIFIED CONGLOMERATE FROM INSITU DENSITY TESTS.

FIG. 3:2:6



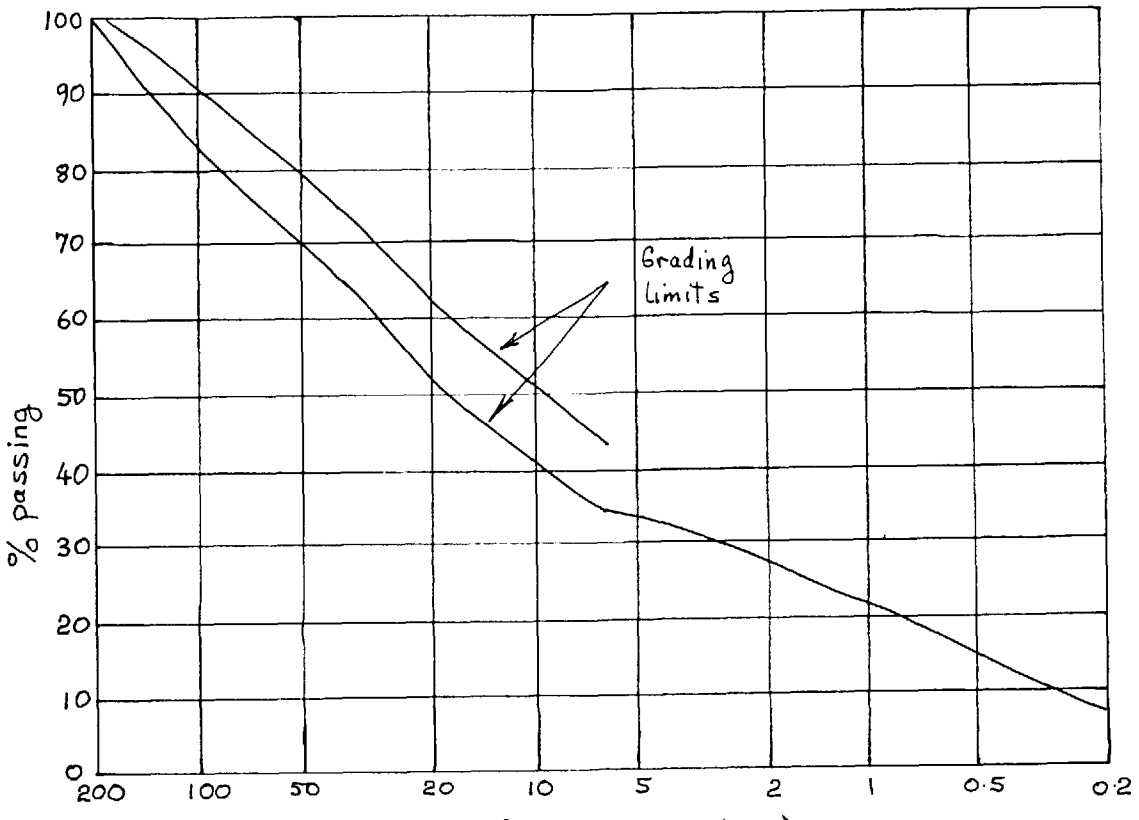
Grain size analysis.



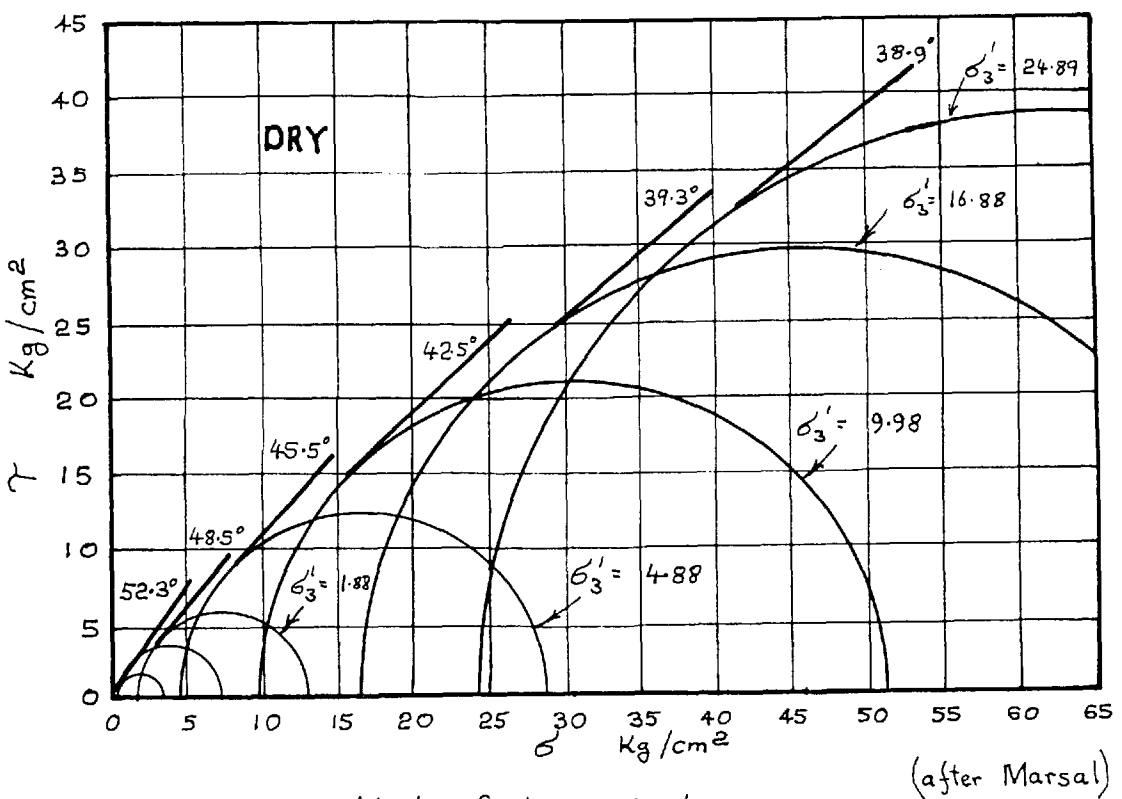
Möhr failure circles.

GRADING AND SHEAR STRENGTH OF EL INFIERNILLO DIORITE FROM QUARRY NO. 5.

FIG. 3:2:7



Grain size analysis.

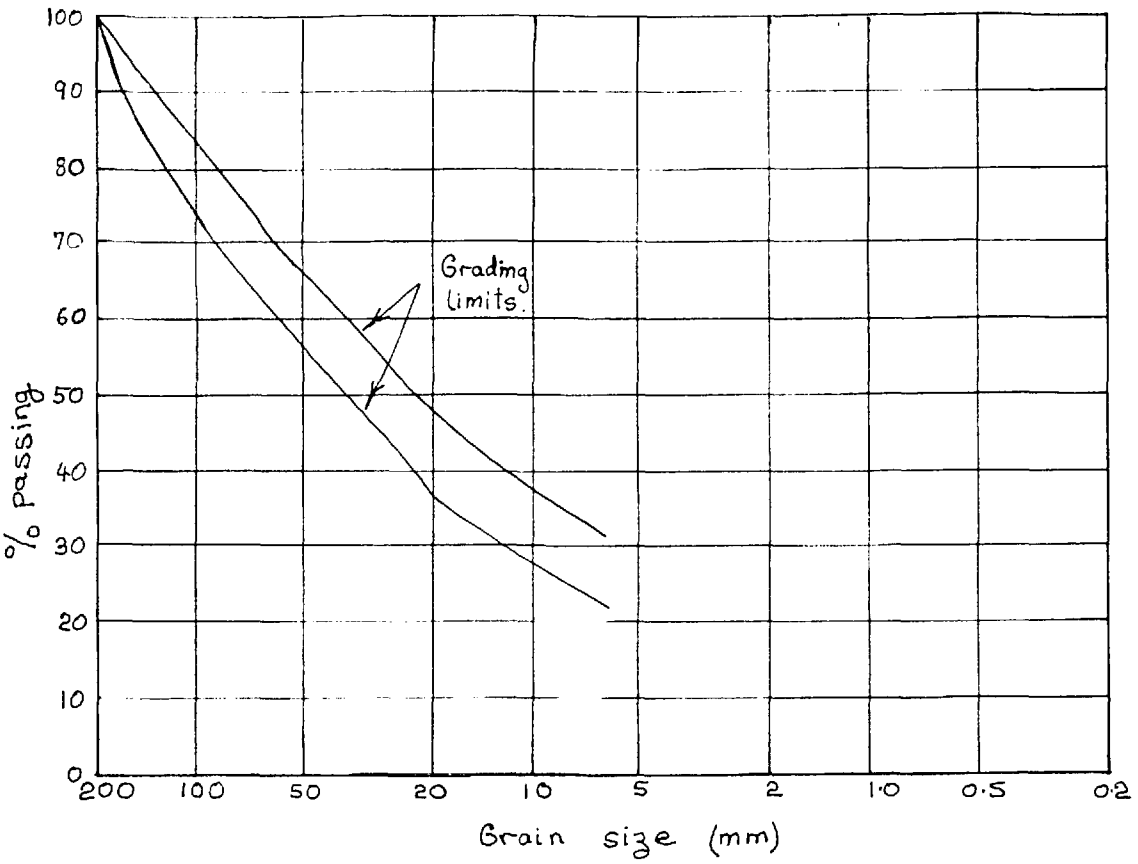


(after Marsal)

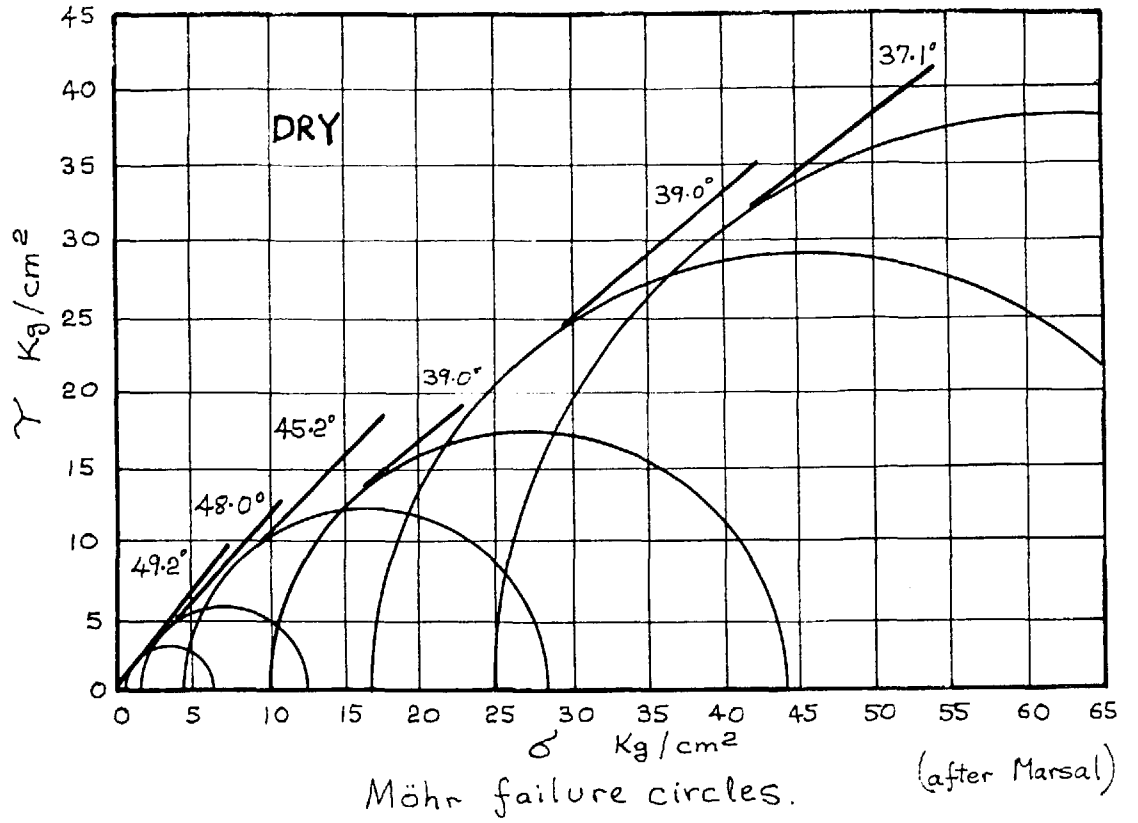
Möhr failure circles

GRADING AND SHEAR STRENGTH OF PINZANDARAN GRAVEL

FIG. 3:2:8



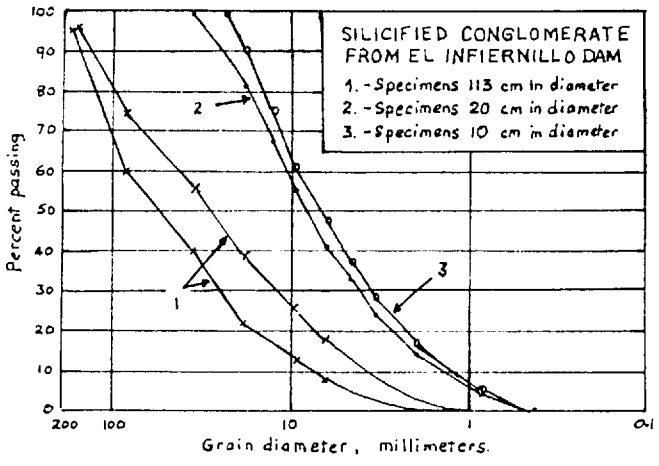
Grain size analysis.



Möhr failure circles. (after Marsal)

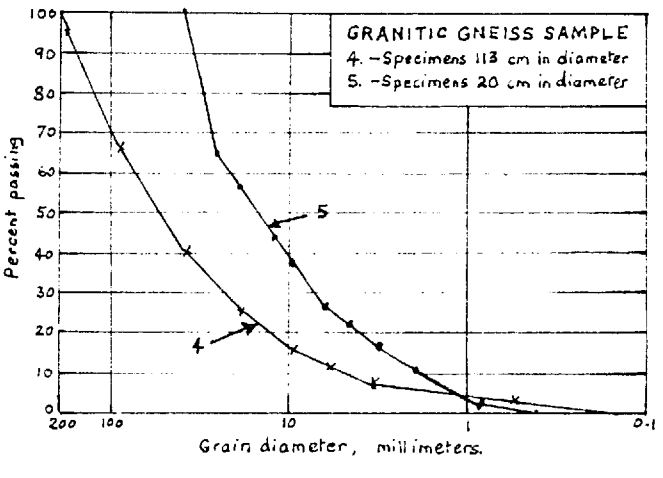
GRADING AND SHEAR STRENGTH OF MALPASO CONGLOMERATE.

FIG. 3:2:9



Approx. $6'_3$ Kg/cm^2	5	10	17	25
Sample 113cm.d	42.2°	39.5°	37.6°	36.3°
Sample 20cm.dia	47.3°	42.8°	43.3°	40.8°
Sample 10cm.dia	47.0°	45.6°	43.2°	40.4°

VALUES OF ϕ'_f FOR SILICIFIED CONGLOMERATE, EL INFIERNILLO DAM.



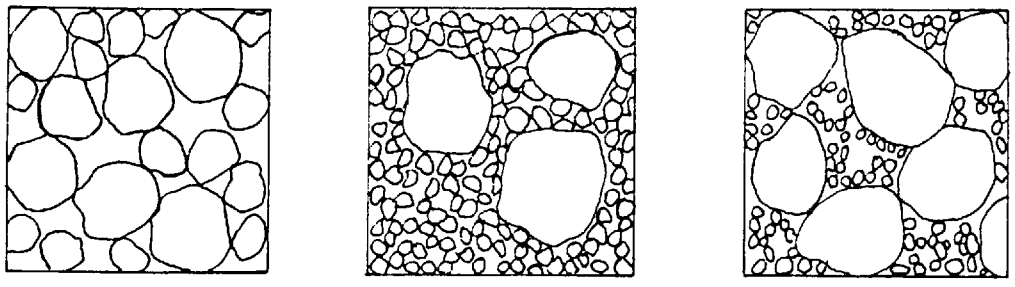
Approx. $6'_3$ Kg/cm.^{2}	5	10	17	25
Sample 113cm.dia.	37.1°	34.7°	32.8°	31.8°
Sample 20cm. dia.	44.5°	42.2°	41.3°	39.3°

VALUES OF ϕ'_f FOR GRANITIC GNEISS SAMPLES.

VARIATION OF THE ANGLE OF INTERNAL FRICTION WITH SAMPLE SIZE.

FIG. 3:2:10

(a)



$$e = \frac{V_t - V_s}{V_s} \qquad e = \frac{V_t - (V_1 + V_2)}{V_1 + V_2} \qquad e = \frac{V_t - (V_1 + V_2)}{V_1 + V_2}$$

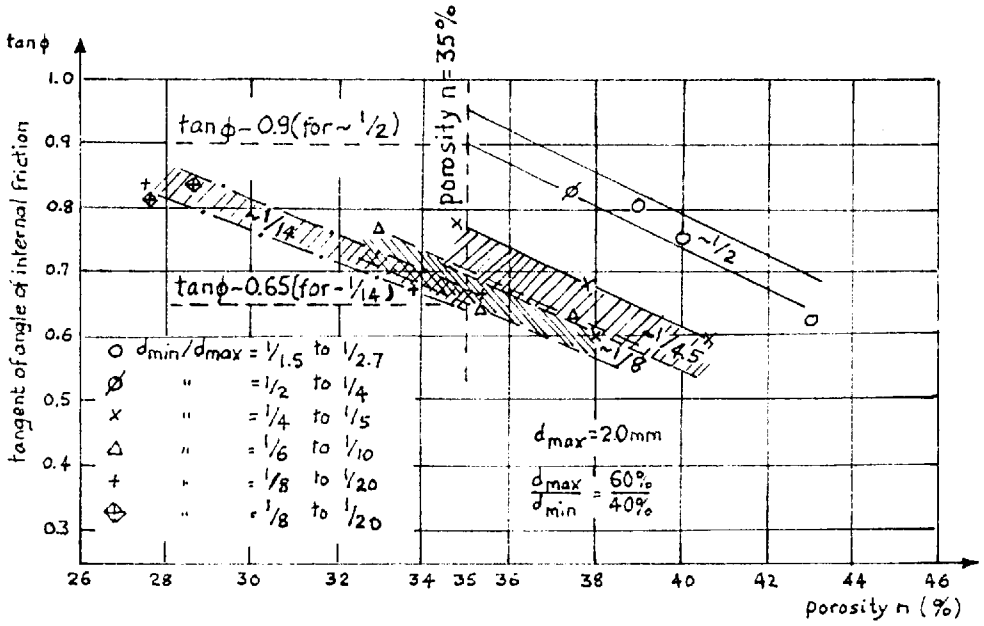
$$e' = e \qquad e' = \frac{(V_t - V_1) - V_2}{V_2} \qquad e' = \frac{V_t - V_1}{V_1}$$

Soil matrix for $d_{min}/d_{max} \sim 1/2$.

Soil matrix for $d_{min}/d_{max} \sim 1/14$.

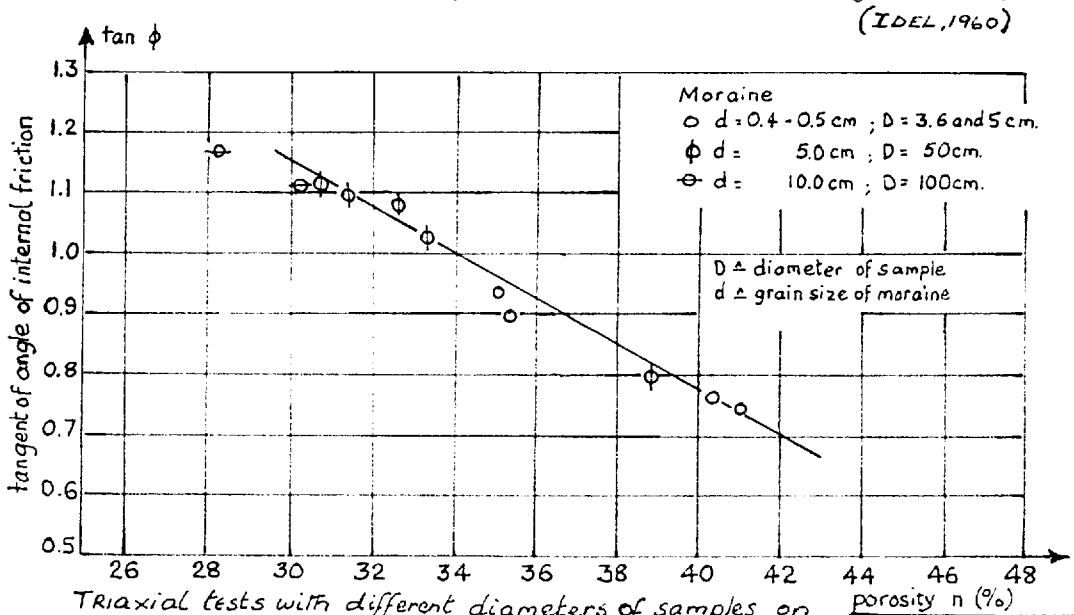
e = nominal void ratio
e' = structural void ratio
V_1 = volume of larger particles
V_2 = volume of smaller particles
$V_s = V_1 + V_2$ = volume of solids
V_t = total volume.

(b)



TRIAXIAL shear tests on quartz-sand mixtures of two different grain sizes (d_{min} and d_{max})
(IDEL, 1960)

(c)



TRIAXIAL tests with different diameters of samples on uniform moraine.
(IDEL, 1960)

FIG. 3:2:11

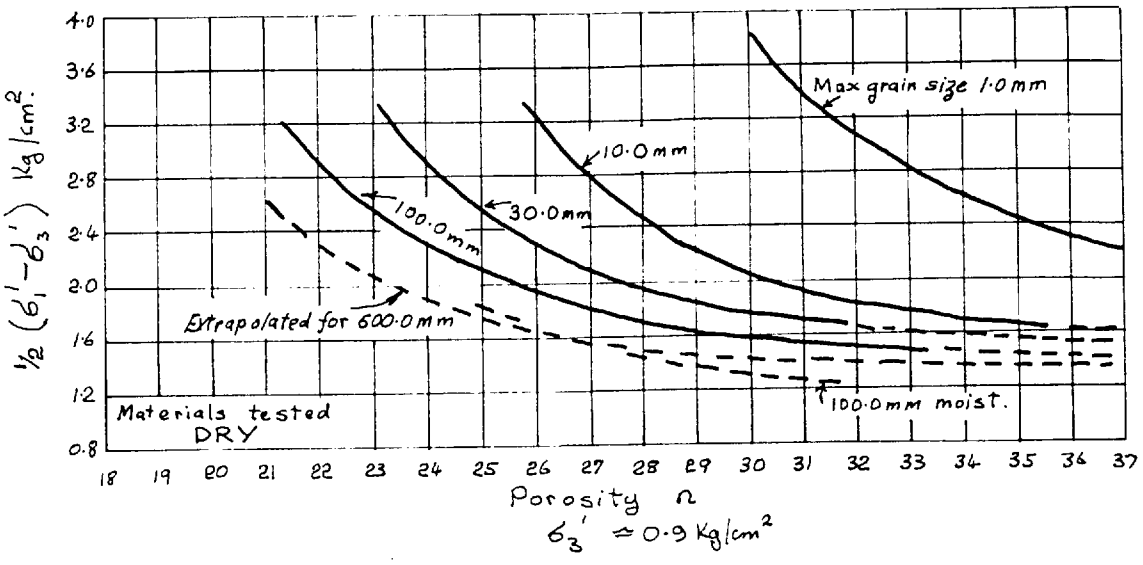
ANGLES OF INTERNAL FRICTION

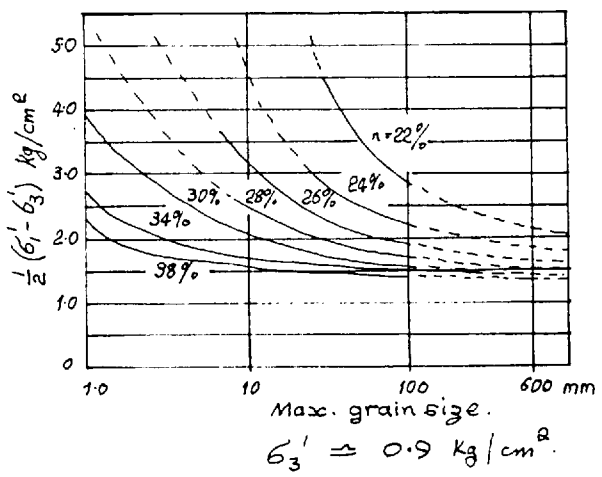
BASALT						METAVOLCANIC					
HIGH DENSITY						HIGH DENSITY					
D_{max}	1/4"	1/2"	1"	2"	3"	D_{max}	1/4"	1/2"	1"	2"	3"
C_U	3·3	4·7	6·7	9·4	11·6	C_U	3·3	4·7	6·7	9·4	11·6
σ_3 p.s.i		ϕ' degrees				σ_3		ϕ' degrees.			
60	45·3	46·7	49·5	50·6	51·5	60	43·7	45·1	47·1	49·9	51·2
125	42·0	43·1	45·6	46·5	48·4	125	40·5	41·9	44·6	45·6	47·3
300	37·8	39·6	40·4	41·3	42·2	300	37·3	39·3	40·3	41·0	41·7
425						425					39·5
450			38·1	38·6	39·2	450			38·2	39·2	
500	35·7	37·3				500	36·3	37·6			
MEDIUM DENSITY						MEDIUM DENSITY					
60	42·7	44·1	46·5	47·3	48·6	60	42·0	43·3	45·4	47·3	48·2
125	39·0	40·7	43·1	43·9	45·0	125	39·0	40·0	41·8	43·0	44·5
300	36·5	37·5	39·0	39·5	40·5	300	36·7	38·1	38·4	39·5	40·5
425						425					38·3
450			37·3	37·8	38·9	450			36·6	38·4	
500	35·0	36·0				500	35·0	36·0			

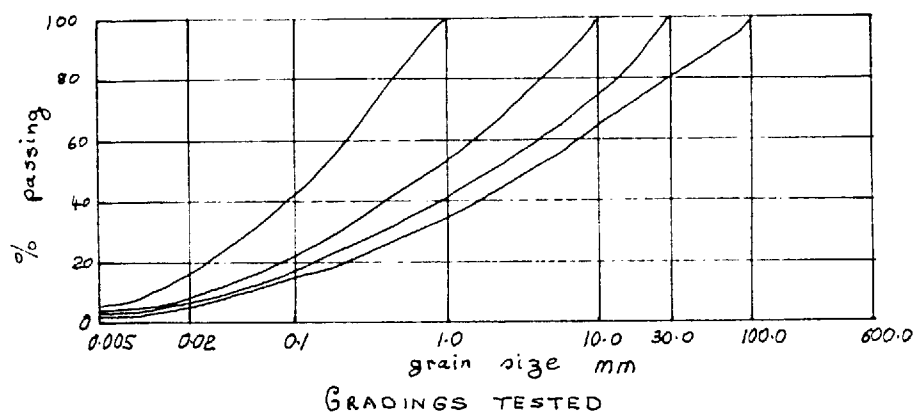
Note: ALL GRADINGS ARE STRAIGHT LINES TERMINATING AT U.S. STANDARD SIEVE No.30.

ANGLES OF INTERNAL FRICTION FOR BASALT AND METAVOLCANIC

FIG. 3:2:12



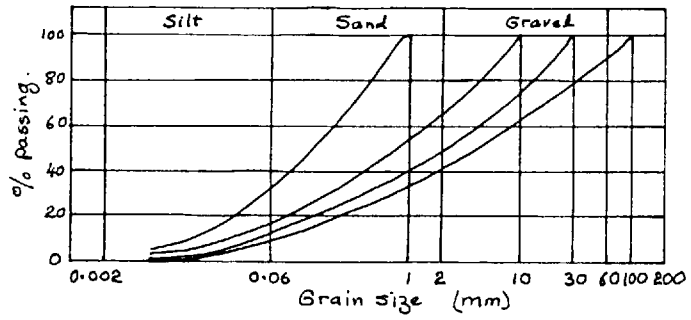


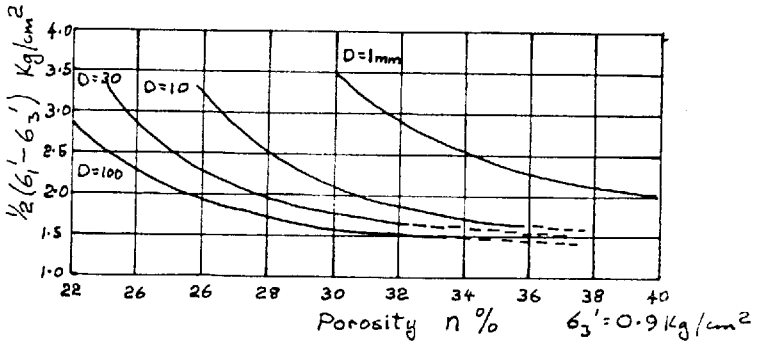


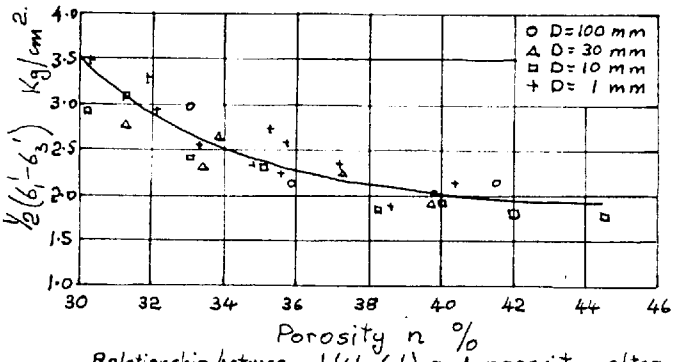
GRADINGS TESTED

SHEAR TESTS ON MORAINE MATERIALS FOR THE SHOULDERS OF GÖESCHENENALP DAM.

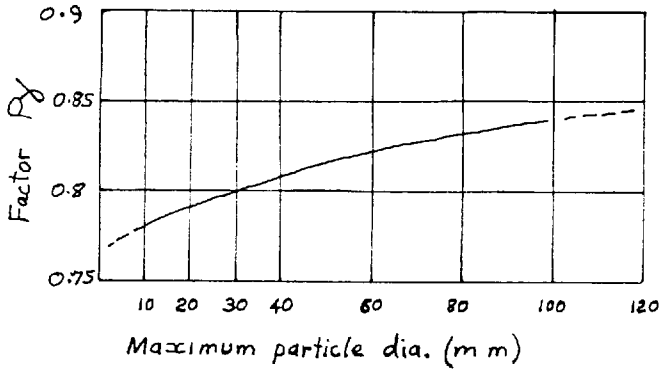
FIG. 3:3:1





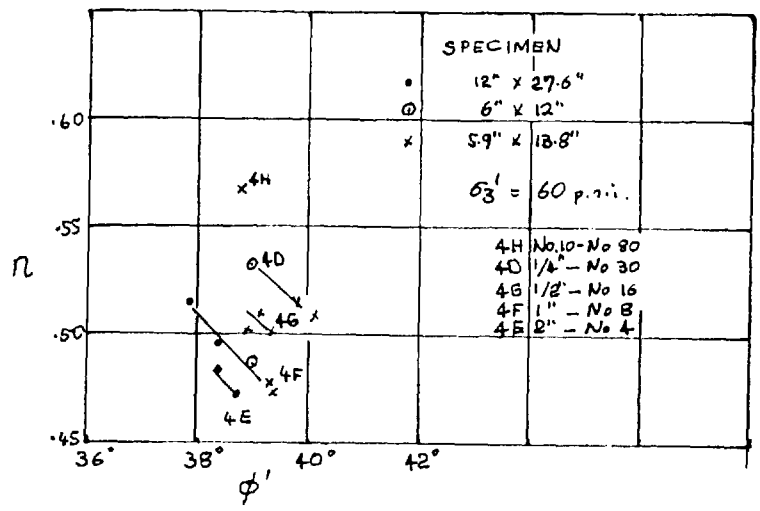


Relationship between $\frac{1}{2}(\sigma_1'-\sigma_3')$ and porosity after conversion with factor P_γ.

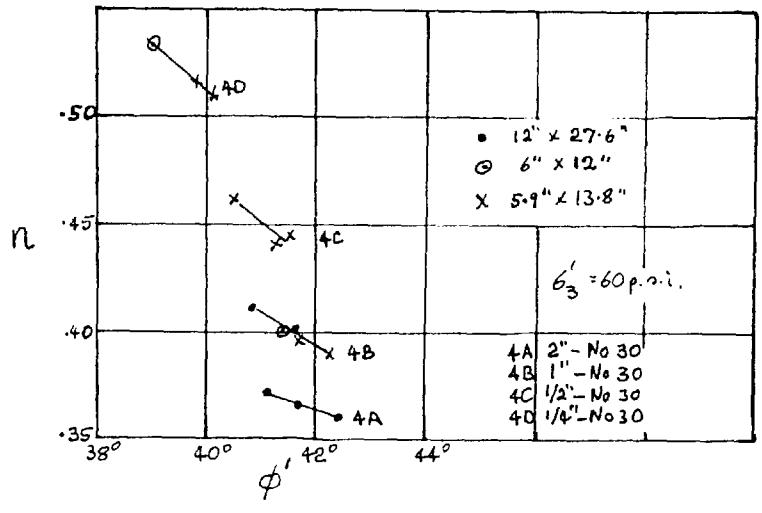


SHEAR STRENGTH OF TALUS MATERIAL USED IN THE GOESCHENENALP DAM.

FIG. 3:3:2



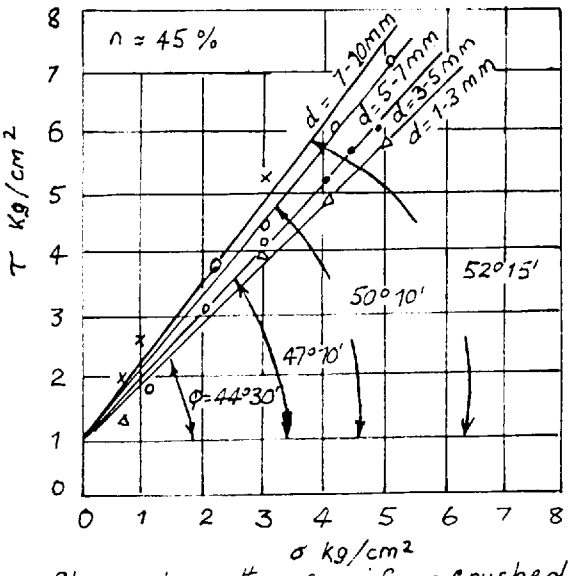
(A)



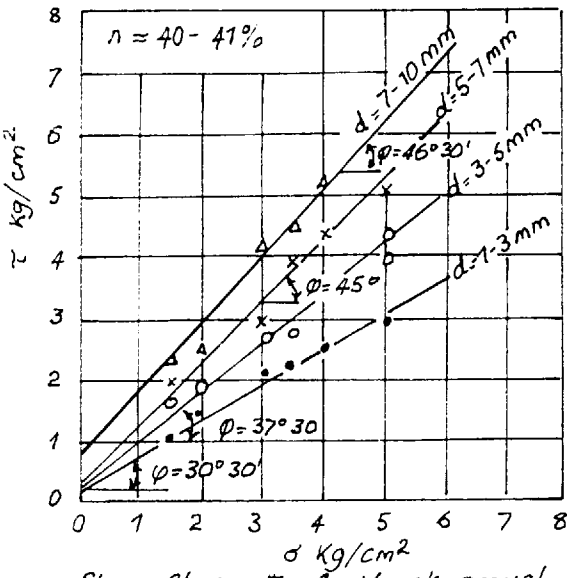
(B)

ANGLES OF INTERNAL FRICTION FOR GRADINGS WITH VARYING MAXIMUM PARTICLE SIZE.

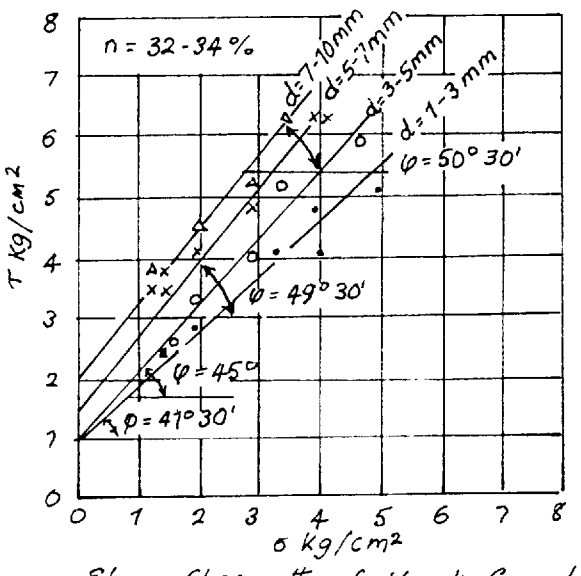
FIG. 3:3:3



Shear strength of uniform crushed limestone.

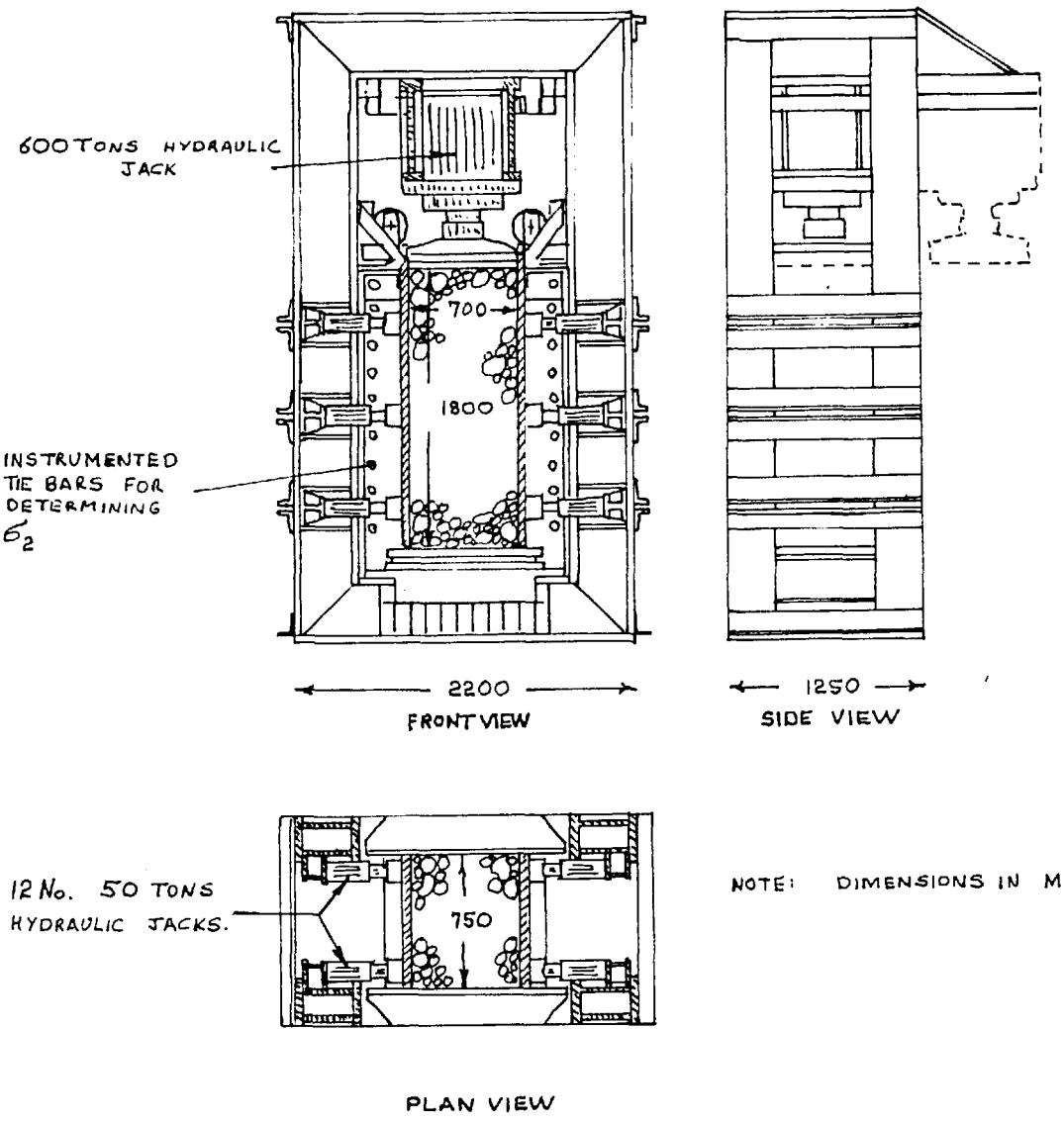


Shear Strength of Nurek gravel.



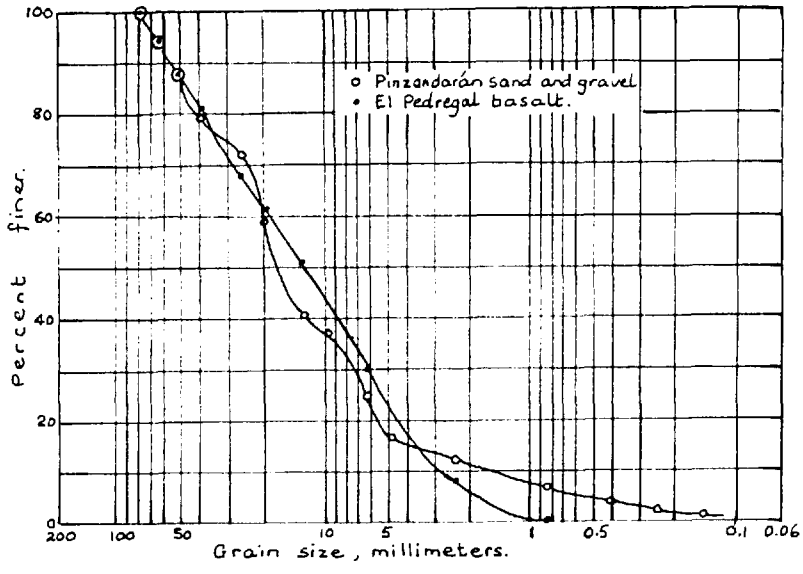
Shear Strength of Nurek Gravel.

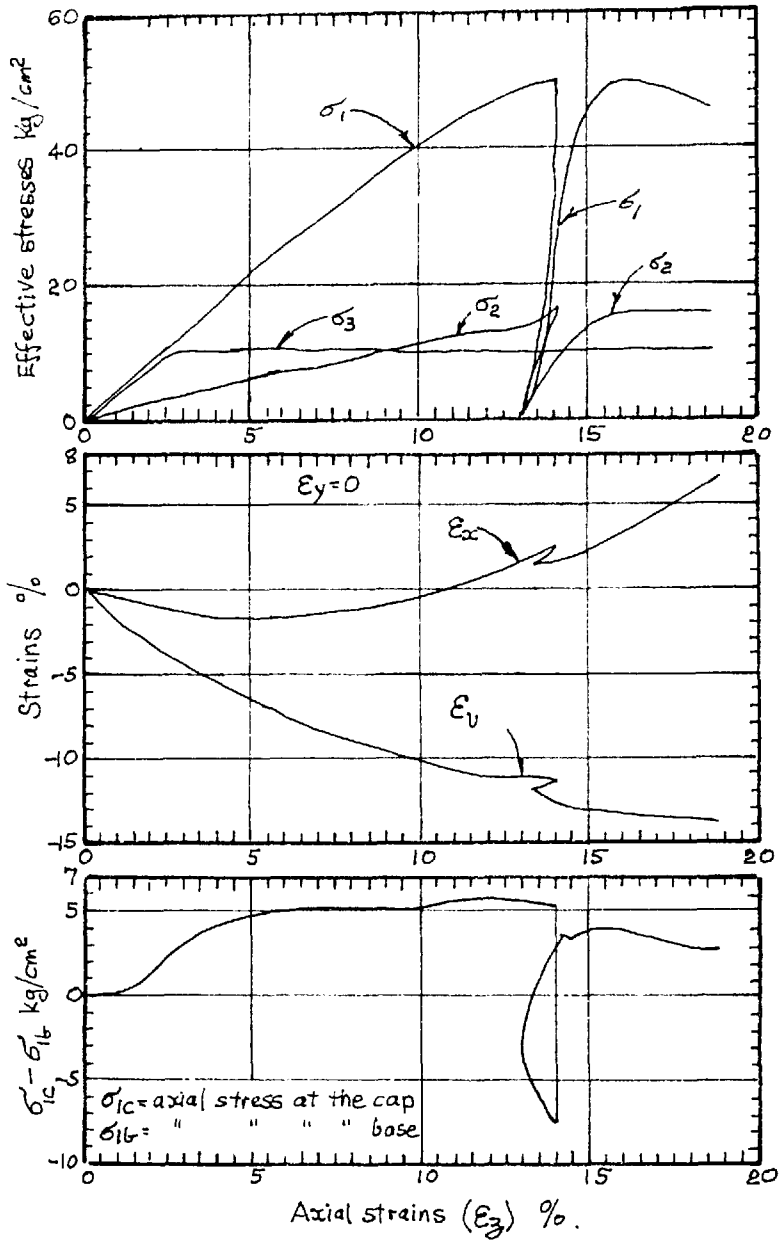
FIG. 3:3:4



RIGID BOUNDARY PLANE STRAIN APPARATUS

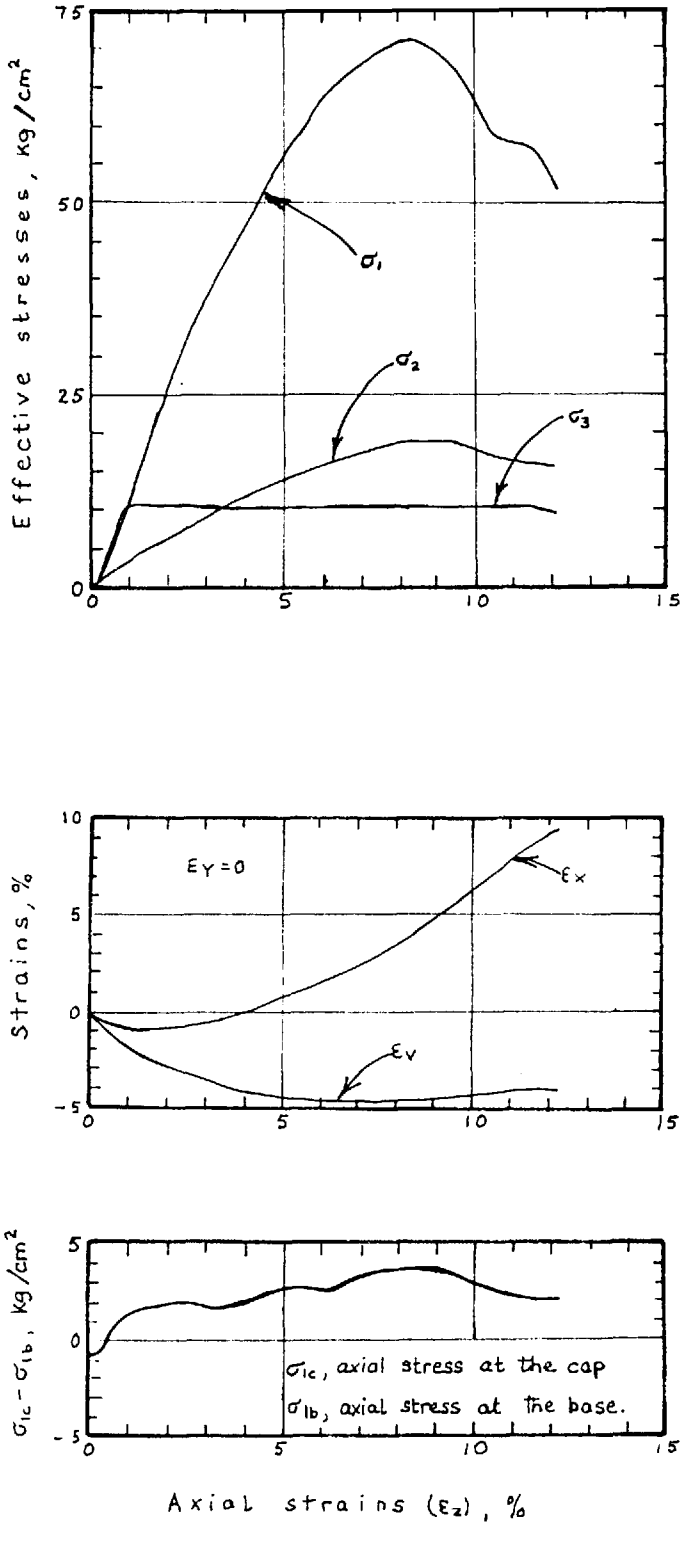
FIG. 3:4:1





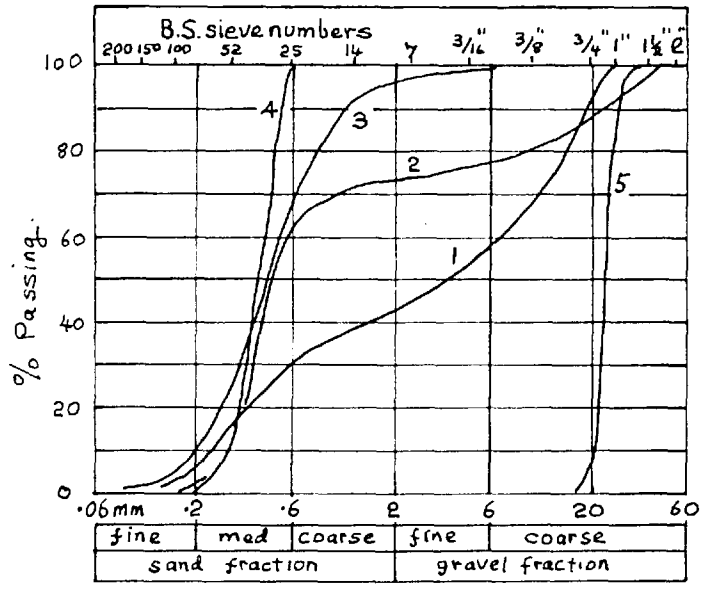
PLANE STRAIN TEST ON EL PEDREGAL BASALT.

FIG. 3:4:2



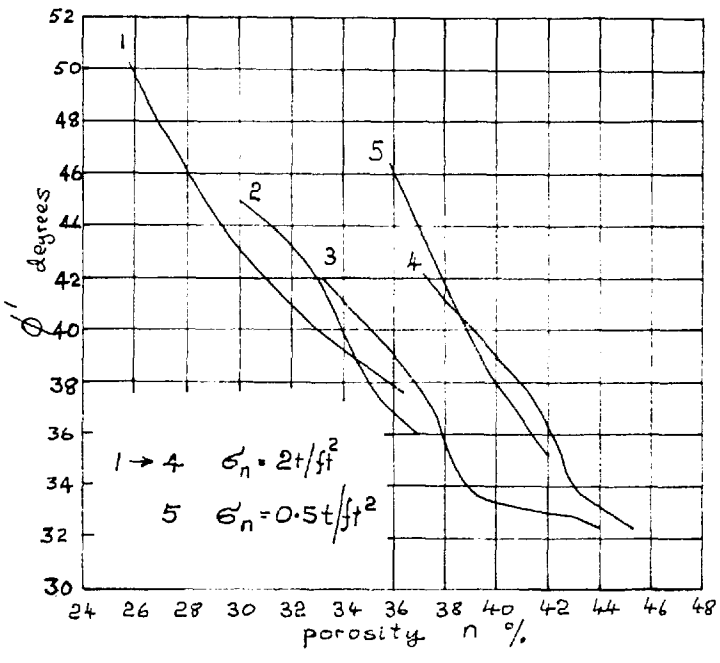
PLANE STRAIN TEST ON PINZANDARAN SAND AND GRAVEL.

FIG. 3:4:3



GRADING

1. Heathrow: Thames Valley gravel
2. Walton gravel.
3. Brasted sand.
4. Ham River sand.
5. Chesil Bank pebbles.



12" SQUARE SHEAR BOX TESTS ON SANDS AND GRAVELS

FIG. 3:5:1

SHEAR APPARATUS AND TEST RESULTS

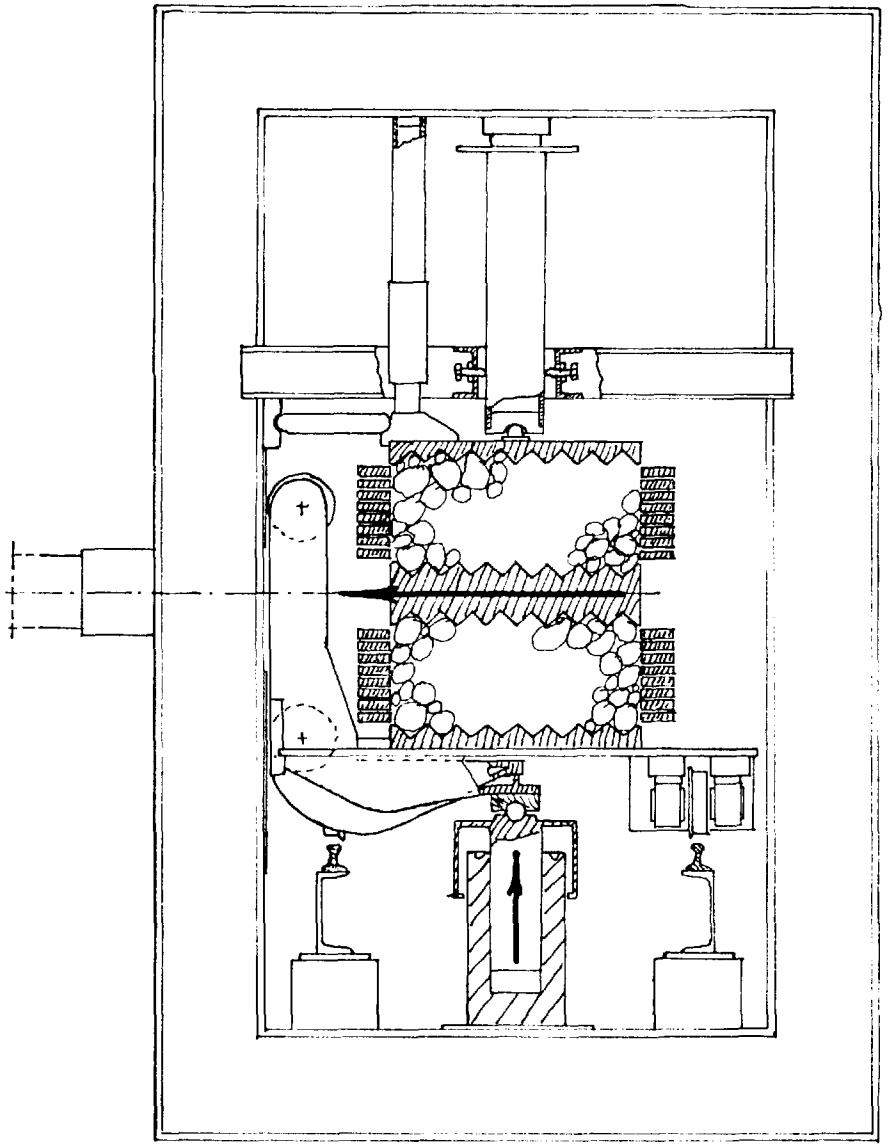


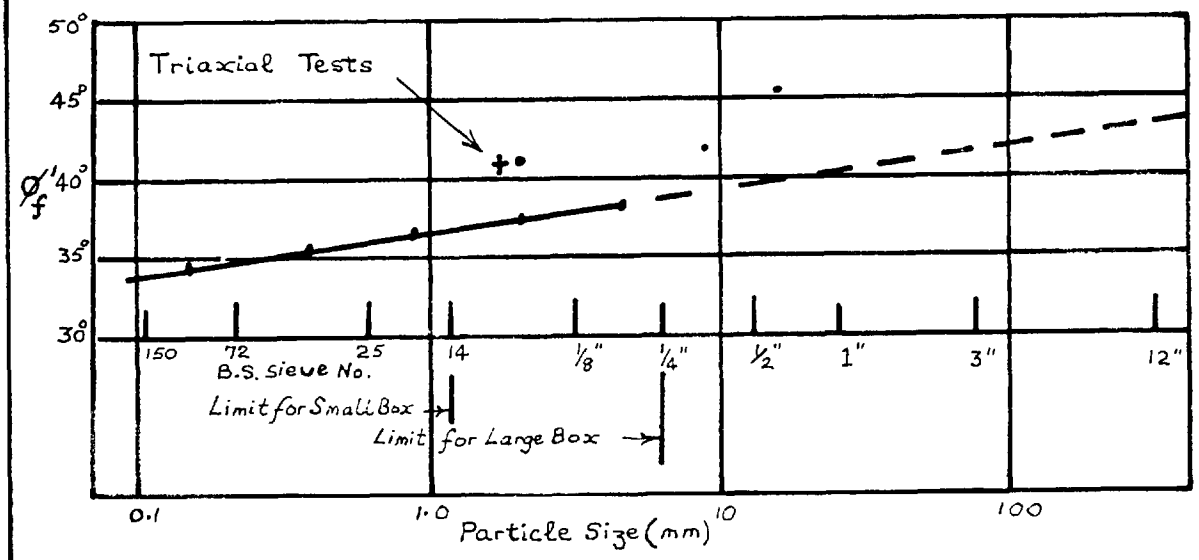
FIG. 3:5:2

The Materials Tested

Code	Grain		Type of Rock	Porosity %		Flakiness
	Shape	size mm		Loose	Dense	
Pebbles F	rounded	8–11	88% granite and gneiss-granite 12% petrosilex	41·8	34·3	1·36
Pebbles C	rounded	38–53	84% granite and gneiss 16% pegmatite	—	—	1·18
Macadam F	angular	8–11	68% granite and gneiss-granite 32% Pegmatite	51·5	41·3	1·61
Macadam C	angular	38–53	100% granite and gneiss	—	—	1·22

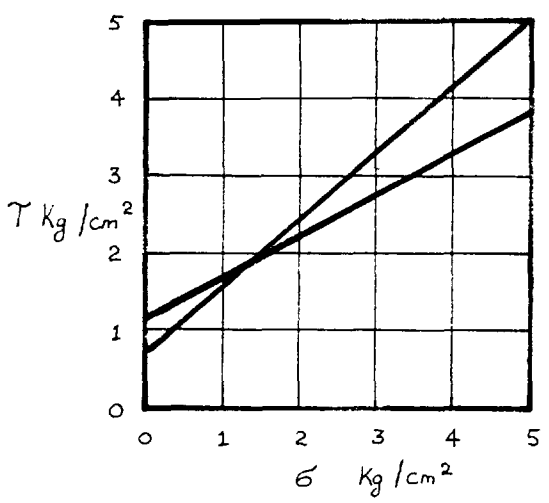
Shear Test Results

Material	State	ϕ'	Unit weight t/m³		R. Density	
			at start of test	at failure	at start of test	at failure
Pebbles F	Loose	36·2°	1·54	1·53	−0·01	−0·07
	Dense	42·9°	1·63	1·59	0·47	0·26
Pebbles C	Loose	37·1°	1·43	1·42		
	Dense	44·1°	1·53	1·50		
Macadam F	Loose	28·4°	1·29	1·33	0·02	0·15
	Dense	34·4°	1·42	1·44	0·55	0·62
Macadam C	Loose	31·3°	1·26	1·28		
	Dense	40·5	1·42	1·43		



ANGLES OF INTERNAL FRICTION FOR LOOSE TIPPED CRUSHED GRANITE ROCKFILL.

FIG. 3:5:3a

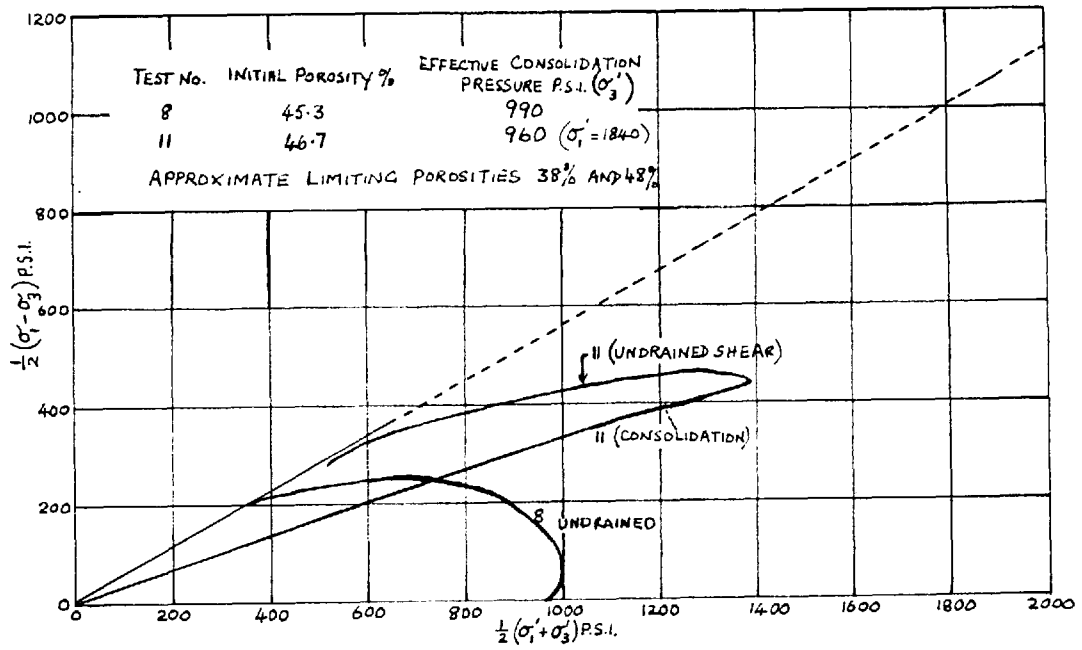


1.0 m² disintegrated shale.

0.25 m² disintegrated shale.

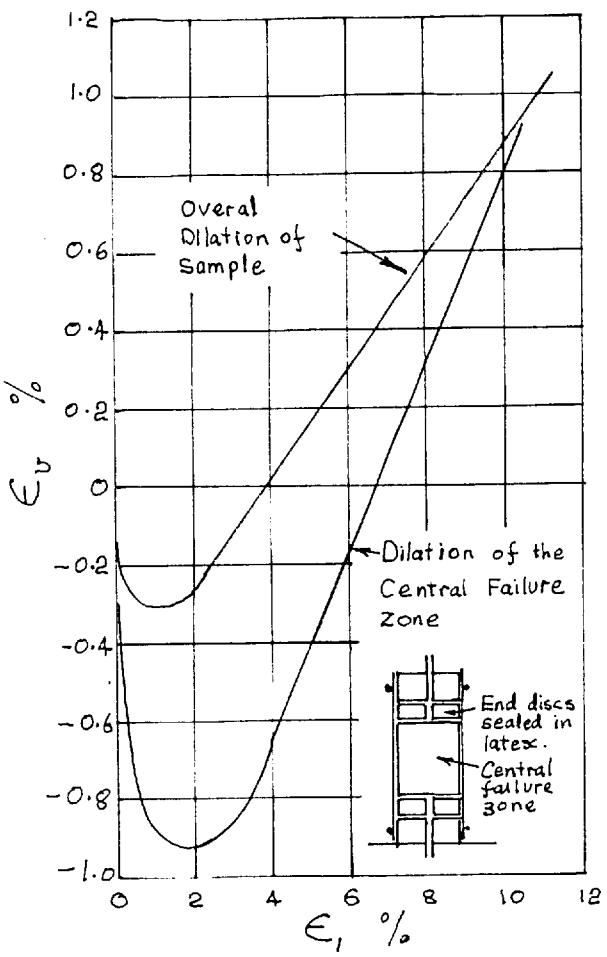
SHEAR BOX TESTS ON DISINTEGRATED SHALE.

FIG. 3:5:3b



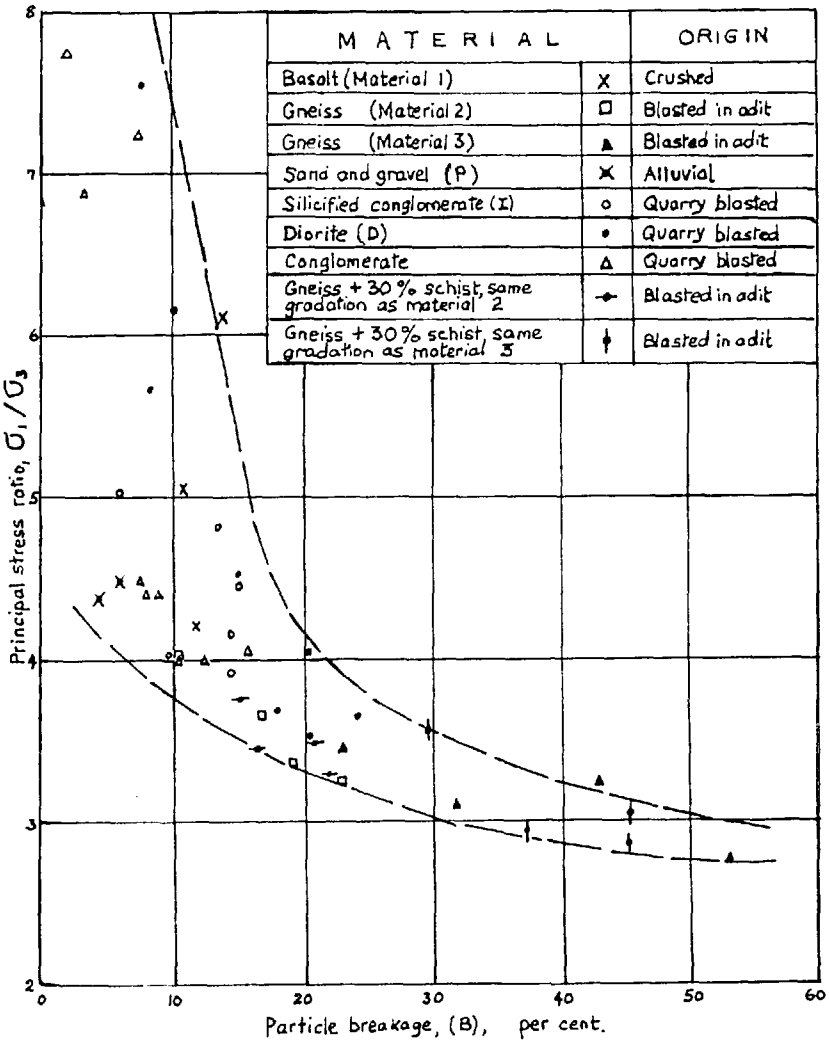
STRESS PATHS FOR UNDRAINED TESTS ON HAM RIVER SAND.

FIG. 3:611



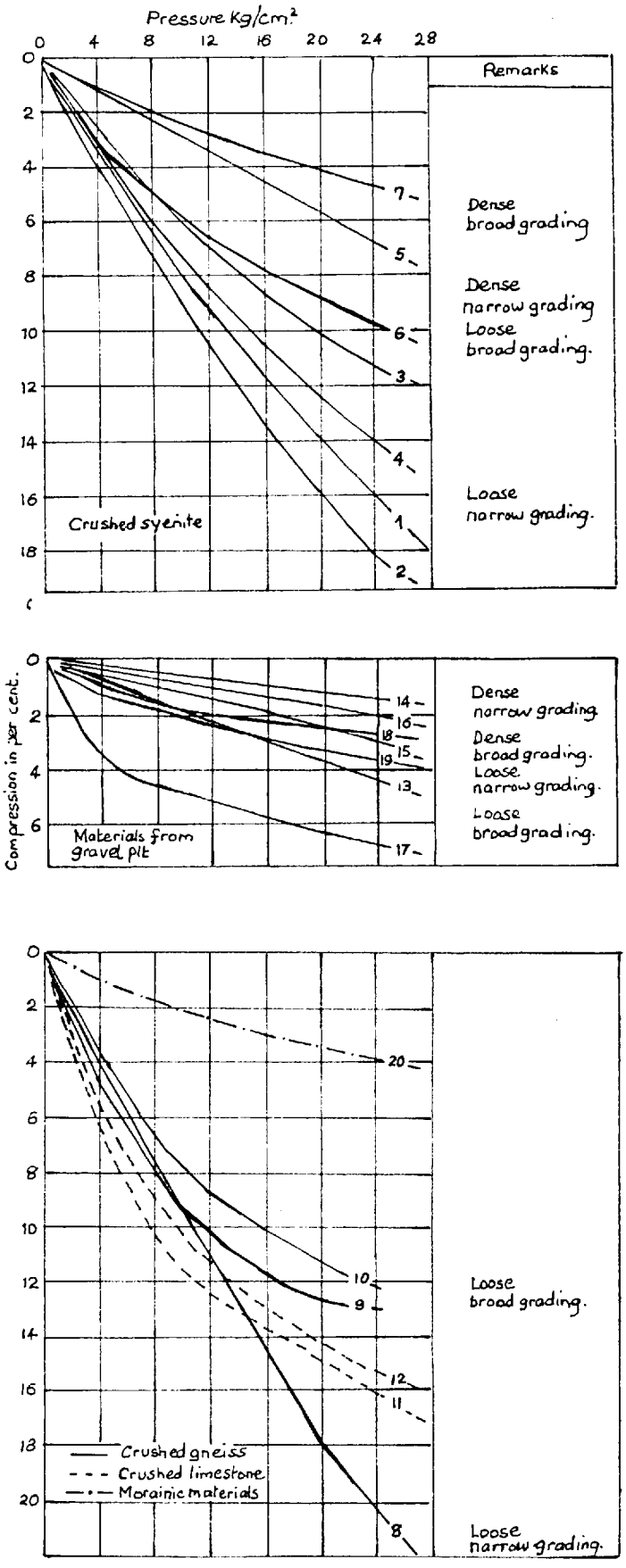
VARIATION OF DILATANCY THROUGHOUT A SAMPLE.

FIG. 3:7:1



CORRELATION OF THE PRINCIPAL STRESS RATIO AT FAILURE AND PARTICLE BREAKAGE.

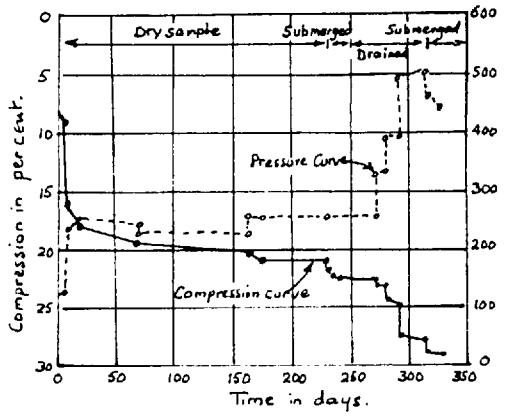
FIG. 3:9:1



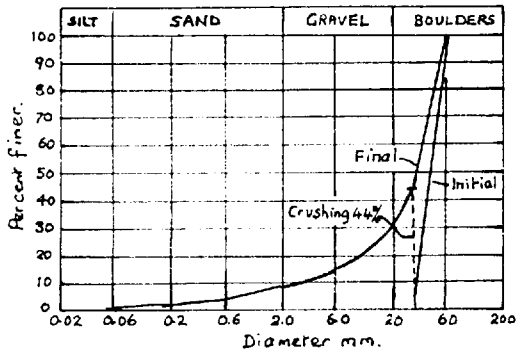
PRESSURE-COMPRESSION CURVES OF AGGREGATES FOR THE TESTS LISTED IN TABLE 3:9:1.

See also Fig. 3:9:3.

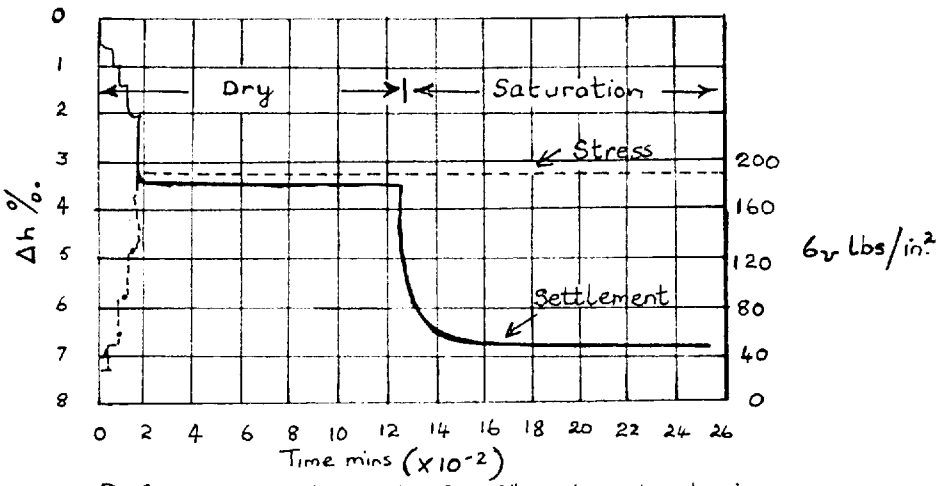
FIG. 3:9:2



Time – compression – pressure diagram for aggregates of crushed syenite with grain size $32 < d < 64$ mm.



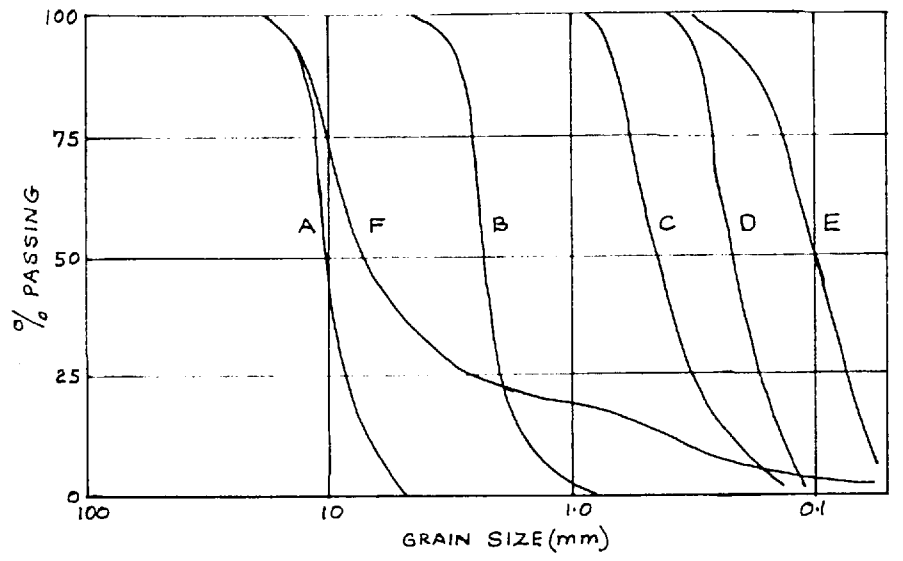
Grain size distribution curves for aggregate of crushed syenite ($32 < d < 64$) before and after compression test.



Deformation – time plot for 9" oedometer test on silurian cleaved mudstone. $n = 24{\cdot}8\%$

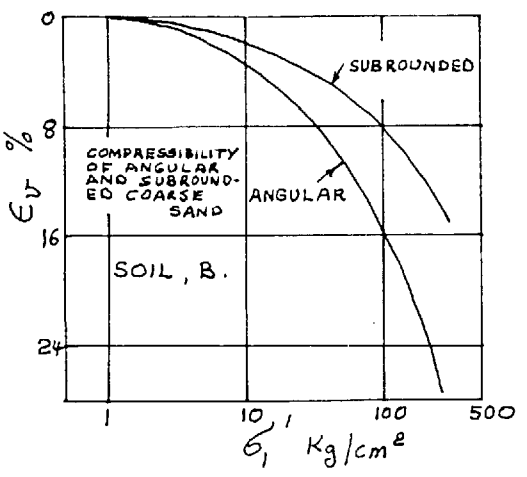
See also FIG. 3:9:2 and Table 3:9:1.

FIG. 3:9:3



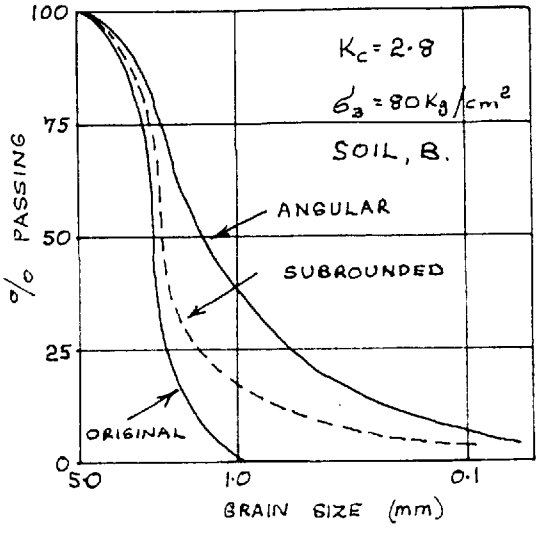
Original grain size distribution curves.

(A)



Compressibility of angular and subrounded coarse sand.

(B)

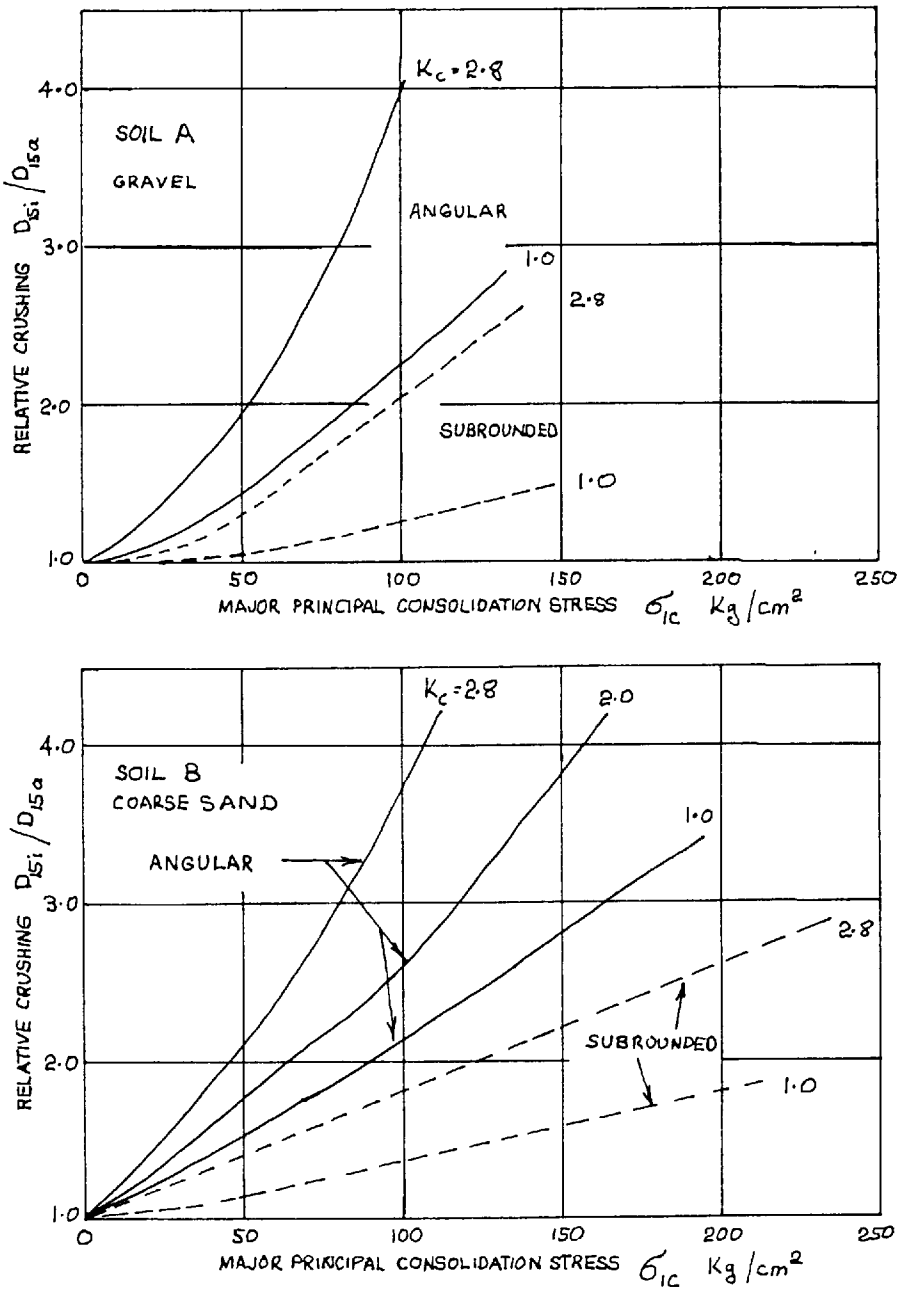


Crushing of angular and subrounded coarse sand.

(C)

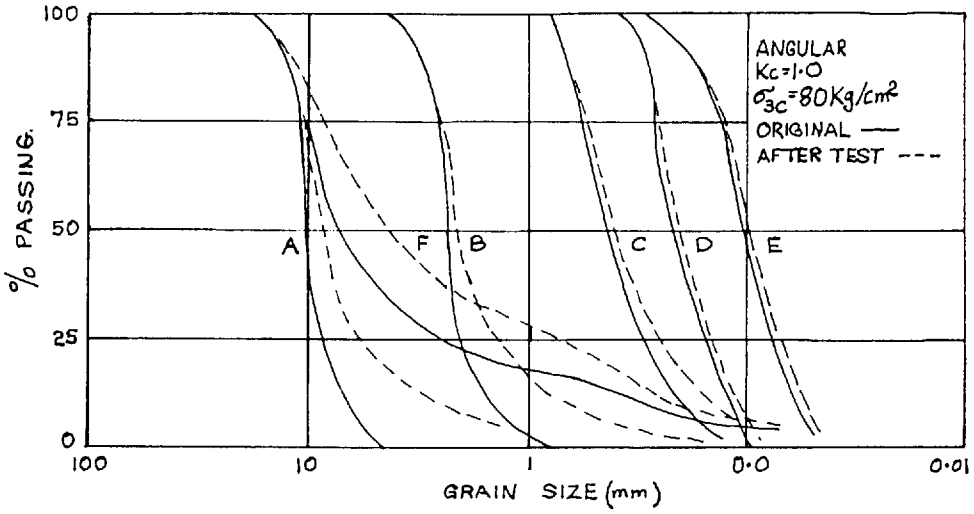
COMPRESSIBILITY OF ANGULAR AND SUBROUNDED GRANITE

FIG. 3:9:4

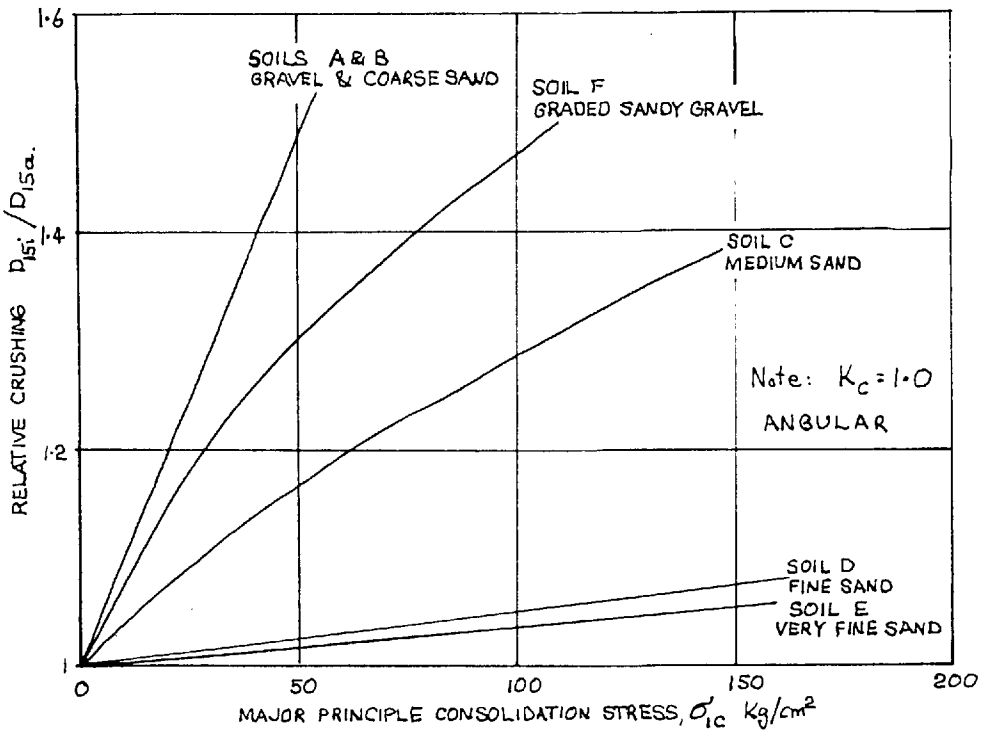


RELATIVE CRUSHING OF COARSE SOILS AT DIFFERENT STRESS CONDITIONS

FIG. 3:9:5



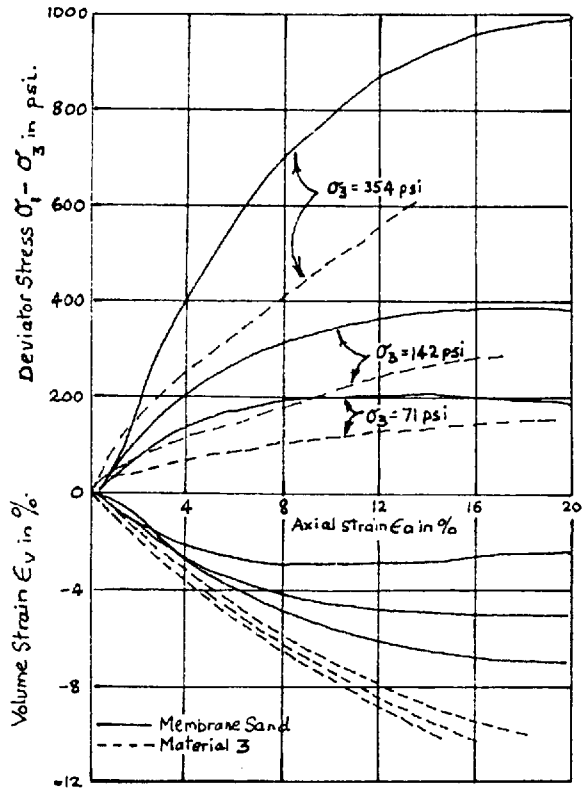
Comparison of crushing of soils with different initial grain sizes



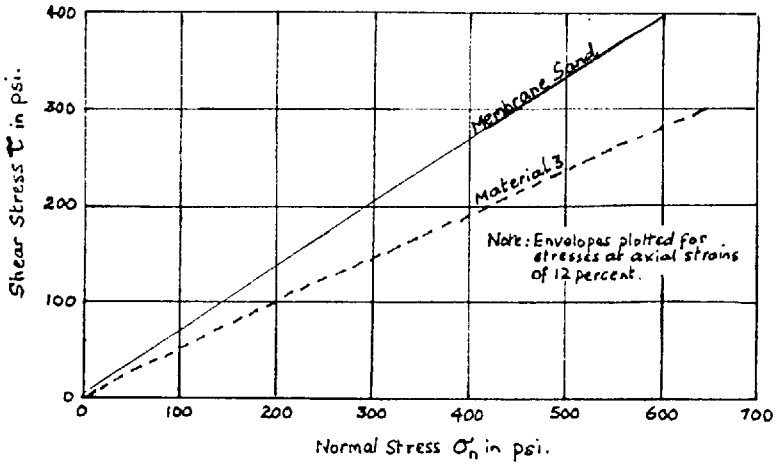
Comparison of relative crushing of different initial grain sizes.

COMPARISON OF CRUSHING OF SOILS WITH DIFFERENT INITIAL GRADINGS

FIG. 3:9:6



RESULTS OF TRIAXIAL TESTS ON MEMBRANE SAND.



MÖHR ENVELOPES OF STRESS.

EFFECTS OF MEMBRANE SAND JACKET.

FIG. 3:10:1

Materials	Test No.	Grain size D mm	Uniformity coefficient $U_o = \frac{D_{60}}{D_{10}}$	Crushing %	Porosity		Rel. density D_r %	Ultimate load kg/cm²	Specific gravity
					n_o	n_1			
Crushed angular particles of syenite	1	$32 < d < 64$	1.4	44	50.5	30.5	17	52.5	2.58
	2	$32 < d < 64$	1.4	22	51.2	39.3	7	27.0	—
	3	$32 < d < 64$	1.4	17	44.3	36.4	94	27.0	—
	4	$4 < d < 32$	2.8	8	47.5	37.5	18	27.0	—
	5	$4 < d < 32$	2.8	7	39.6	34.4	100	27.0	—
	6	$d < 64$	26	small	38.2	30.0	22	27.0	—
	7	$d < 64$	25	small	28.8	24.2	100	27.0	—
Crushed angular particles of gneiss (tunnel spoil)	8	$32 < d < 64$	1.4	42	46.7	30.4	35	31.2	2.64
	9	$d < 128$	56	small	39.7	30.8	1	24.1	—
	10	$d < 128$	56	small	34.0	25.0	41	25.1	—
Crushed angular particles of limestone (flaky shaped)	11	$32 < d < 64$	1.4	40	44.7	33.3	—	27.0	2.72
	12	$d < 128$	30	small	33.3	20.7	—	27.0	—
Gravel from a glacio-fluvial deposit (rounded particles)	13	$32 < d < 64$	1.4	10	42.8	39.7	4	27.0	2.67
	14	$32 < d < 64$	1.4	5	35.0	33.8	95	27.0	—
	15	$4 < d < 32$	2.8	3	34.0	31.3	40	27.0	—
	16	$4 < d < 32$	2.8	3	29.1	27.0	95	27.0	—
	17	$d < 64$	50	small	27.1	19.0	38	27.0	—
	18	$d < 64$	50	small	19.0	16.0	100	27.0	—
	19	$d < 64$	57	small	28.0	24.5	33	27.0	—
Morainic materials (subrounded particles)	20	$d < 64$	100	small	26.7	23.5	87	27.0	2.70

TABLE. 3:9:1

COMPRESSIBILITY OF CRUSHED SYENITE, GNEISS AND LIMESTONE.

See also Figs. 3:9:2 and 3:9:3.

CHAPTER 4

The Triaxial Equipment for Testing Samples 12" in Diameter and 24" High

(4:;) The Design Specification

For many years now dams have been built both in this country and abroad using dumped or rolled rockfill for shoulder material.

Dams of this type have now surpassed the highest concrete constructions and yet our knowledge of the behaviour of these materials under stress is sadly lacking.

The problem is simply the size and cost of suitable equipment and the time necessary to carry out the relevant investigations.

Many eminent engineers are worried about this problem and in recent years several investigators abroad have approached the problem but our information is still very sparse.

With the proposal to build a 300' high dam, using a cleaved mudstone for shoulder material, impetus was added to the drive for large scale research equipment in this country.

The size of this equipment was governed by the existing laboratory facilities, bearing in mind the weight of the equipment and the disruption of other research by the volume of materials to be processed and handled.

On these bases it was decided that the largest practical sample size was 12" in diameter by 24" high. It was assumed that one could test particles up to those passing a 3" square sieve.

In accordance with previous practice, tests were to be run at a constant rate of strain applied by a mechanical jack; the largest commercially available being 100 tons capacity. This limited the deviator load and set the maximum confining pressure at 500 p.s.i.

Load, volume, deformation and pressure measuring devices were to have an accuracy commensurate with the size of the samples and a system of electrical and mechanical interlocks was installed in the apparatus to prevent accidental damage.

It was intended that the apparatus should be able to perform all types of tests except tension.

(4:2) The Loading Frame

Mr.G.E.Green designed the 100 tons capacity load frame around a Duff Norton screw jack and two existing tie bars of 4" diameter and $\frac{3}{8}$" square thread. (Plate 4:2)

(4:2:1) The Foundation

The foundation comprised a 1" thick mild steel plate bedded on Plycolay on a hardwood block floor and anchored to the concrete slab with four internal expanding Rawlbolts. Levelling was accomplished with a set screw in each corner of the plate prior to the Plycolay setting.

(4:2:2) The Base

The loadframe base, a 6" thick mild steel slab, was then positioned above the foundation plate by four hollow mild steel cylindrical spacers to allow the jack ram to retract. Four 1" diameter bolts, passing through the spacers, hold the base and foundation plates together.

The jack was bolted down to the base by six bolts. $1\frac{1}{2}$" diameter clearance holes were provided in the jack body for this purpose because it is a push-pull type but, as we were only using it to push $\frac{1}{2}$" diameter bolts with $2\frac{1}{2}$" diameter washers were used and fixed into the top of $1\frac{1}{2}$" diameter locating studs.

The tie bars were lowered through clearance holes in the base and retained by large diameter nuts tightened by a tommy bar. As the loadframe was to be fitted with a motorised crosshead, the tie bars could not be positioned until the crosshead drive was connected and the crosshead itself horizontal. The tie bars were then locked against rotation by two grub screws.

(4:2:3) The Crosshead.

The crosshead was a solid piece of mild steel 12" wide and 9" thick. A suitable hole was bored in each end and bronze bushes were machined to fit the crosshead and tiebars (Fig.4:2:3). Pressure greasing nipples were provided on the face of the crosshead.

The crosshead is powered by a $\frac{1}{4}$" H.P. 3P.H. geared motor with an output speed of 30 r.p.m., which is further reduced by a 3:1 roller chain drive to the bushes giving a travel speed of 5" per minute. The position of the motor can be adjusted to tighten the drive chains and although the chain operates in a horizontal plane without support rollers, no trouble has been experienced because the drive chains are tight and the unsupported span between sprockets is small.

A solid type of chain guard should have been fitted as experience showed that chains from the chain blocks used for lifting the cell into and out of the frame tended to get entangled with this drive.

In the centre of the underside of the crosshead a platen was fixed and connected by a rod through the crosshead to two limit switches which were set such that a small movement halted the crosshead down drive and a further movement locked the crosshead against upward or downward movement.

This latter device was installed to prevent the crosshead being moved during a test, though it was impossible to move the crosshead when the load exceeded 3 tons, due to friction exceeding motor power.

However, by loading elsewhere than on this platen, the crosshead could be used as a very efficient clay sample extruder.

If necessary, these limit switches could be overridden.

Two further limit switches were fitted at the upper and lower extremes of travel.

(4:2:4) The Stiffening Column

A 9" x 9" square box column was bolted to the foundation plate and connected to the tops of the tie bars by a triangular steel plate with a section cut away to allow a hoist to be positioned above the machine centre line. This column should have been fixed to the base plate for greater stiffness because the second moment of area of the 1" thick plate was not compatible with that of itself.

The limit switches were mounted on this column and surrounded by a small box section for protection. They were operated by 1" square steel bars projecting from the jack ram and the crosshead.

Several operations concerned with setting the apparatus up for tests were aggravated by its size and non-slip rungs should have been fitted to this column to facilitate access to the top of the cell.

(4:2:5) The Jacuator

The load is applied via a Duff Norton 100 tons capacity Worm Gear Jacuator (Model F 75323 - 12 - 1B). The body is a very substantial steel casting and the jack is designed to push or pull. The worm wheel is bronze and is located top and bottom by very large deep groove ball thrust races. The steel ram is six inches in diameter and has a $\frac{1}{2}$" square thread and is keyed against rotation. Bronze bushes are provided to take any eccentric loads which may be applied.

After one year of operation, this jack had to be dismantled completely to investigate a knock at high loads. An F.A.G. thrust bearing on the worm shaft had a ball missing. Since replacement no further trouble has occurred.

The 14" diameter ram head is covered with an aluminium disc for locating the base of the cell and minimising damage to the machined faces when the cell is lowered onto the jack.

The ram thread was lubricated with Molycote and the worm wheel and bearings with Mobilgrease No.234.

(4:2:6) The Drive Mechanism

Mounted on a separate foundation plate, which was levelled and fixed in the same way as the first, were the main drive motor, Kopp Variator, reduction gearbox and worm gear reduction.

Between the worm gear reduction box and the jacuator is an Oldhams coupling, which can take up any small mis-alignment of the shafts and can be readily disconnected prior to operating the rapid return motor.

The worm gearbox is a Crofts 60 to 1 ratio, size $7\frac{1}{2}$. It is fitted with a bronze worm wheel and ball bearings are fitted throughout. Lubrication is with S.A.E. 150 oil.

Power is provided by a I.H.P. 3PH. motor driving a size 16 Kopp Variator followed by a spur gear reduction box giving an output speed infinitely variable between 6 r.p.m. and 54 r.p.m. This gear box drives the worm reduction via a duplex roller chain. Sprockets are fitted to give gear ratios of 2:1 up or down. Final jack travel can be varied between 2 and 0.06" per hour.

(4:2:6:1) The Kopp Variator

The Kopp variator is a friction drive mechanism and hence is placed in the position of minimum torque adjoingingthe motor. One friction plate drives another through 3 balls at their circumference. The axes of the balls can be orientated to alter the effective driving and driven radii and, hence, the output speed is variable. On the output shaft several steel balls, which transmit the torque, are sandwiched between inclined steel plates, as the torque increases, so the plates are forced harder apart; in turn forcing the friction plates harder against the three drive balls. Hence, the drive is completely positive and thoroughly reliable. Lubrication is by Mobilfluid 62.

(4:2:6:2) The Rapid Return Motor

A $\frac{1}{4}$ H.P. geared motor is fitted to the opposite end of the jack worm shaft and connected by a small Oldhams coupling for winding the jack back to the starting position in 4 or 5 minutes, instead of up to 6 hours required by the main drive. Before this can be accomplished, the drive pin must be removed from the main drive Oldhams coupling. The main drive and rapid return motors are electrically interlocked

Protection of the loadframe steelwork was provided by one coat of red oxide paint, followed by a coat of light grey to visually minimise the bulk of the apparatus.

(4:3) The Triaxial Cell (Fig.4:3)

There was a particular wish to commence large scale testing at the earliest possible date and, as a result, the triaxial cell was designed to fit into an existing 50 tons capacity loadframe manufactured by Clockhouse Engineering.

(4:3:1) The Cell Barrel

The cell barrel is an 18" o.d. mild steel tube, $\frac{1}{2}$" thick It already existed in the college but was particularly corroded and had to be shot blasted prior to machining. Two rings were rough machined and welded to either end of the tube, inside and out, both for strength and to prevent corrosion (Fig.4:3:1). Final machining of the rings was then carried out to true them to the axis of the tube. The top ring was machined to take an O-ring seal and both rings were then drilled and tapped, the base to take 20 No.$\frac{3}{4}$" B.S.F studs and the top to take a similar number of bolts. The end rings were coated with a hard stainless steel paint; the remainder with polyurethane paint.

(4:3:2) The Cell Base. (Fig.4:3:2)

The base is a mild steel disc 3" thick and 20.5" in diameter. The underside has a 6" diameter by $\frac{1}{8}$" deep recess for locating on the aluminium plate on the jack ram. Two O-ring grooves are machined in the top, one to seal the base to the cell, the other to seal the pedestal to the base. 20 No. 13/16" diameter clearance holes are drilled around the circumference to mate with the studs in the lower ring of the cell. To locate the cell on the base a $\frac{3}{8}$" deep recess is machined with a diametral clearance, before painting, of 50 thou.

(4:3:3) The Pedestal

The pedestal is a mild steel disc 12" in diameter and 3" thick. It is located on the base by a $\frac{3}{8}$" diameter spigot and fixed by 6 No.$\frac{1}{2}$" B.S.F. cap screws (Fig.4:3:3)

Two fine bore connections were originally provided to the half round circumferential groove on the pedestal using copper tube. This was connected to Erme to fittings on the underside of the pedestal and compressed by a rubber seal between an AB 10 Klinger valve and the base at the other end. This system was adopted to prevent air being trapped. One lead of $\frac{1}{8}$" bore was to provide a flow and the other, of 1/16" bore, was to be a null line for determining head loss or pore pressure. This system was subsequently found to be unsuitable and both connections were bored out to $\frac{1}{2}$", the copper

pipe and fittings being abandoned. Having disposed of the copper tube and fittings, an O-ring seal had to be fitted around the water passages at the interface of the base and pedestal. The null line was fitted with a Klinger AB 10 valve on the outside of the base, the other with a ½" bore Klinger valve. The ½" bore flow line was led to the centre of the pedestal, from where water was distributed radially under a perforated plate designed to withstand a load of 120 tons (Fig.4:3:3:1)

Two ½" bore connections were provided for filling and emptying the cell. A further ½" bore connection was provided to the top cap and also a 3/16" diameter connection.

A 1½" diameter gland was fitted in the base for passing electrical leads into the cell for future instrumentation or an internal loadcell.

(4:3:4) Lifting and Handling

Fittings were provided for lifting and handling all parts of the triaxial apparatus.

(4:3:5) The Top Cover and Piston Bushing. (Fig.4:3:5)

The top cover plate and bushing were made to take a 5" diameter ram. The cover plate is 2" thick and 18" in diameter. It is bored to take, and welded to,a very substantial mild steel tube lined with a press fit 12" long bronze bush, retained at both ends by a circlip. The bushing is not symmetrical about the cover plate because the cell was designed to be used with either an internal or external loadcell.

The bore of the bronze liner was honed to a fine finish and the stainless steel ram was also honed to produce a close tolerance sliding fit. O-ring grooves were provided at the top and bottom ends of the liner. Only one O-ring was in fact used and that was placed on the outside to keep dirt out of the bore.

The cover plate was fitted with a Klinger AB 10 valve for letting air out and three other connections were provided for future use. A larger air release vent should have been provided because the head loss of air rushing out when filling the cell caused a pressure rise in the cell, thus consolidating the sample. This also meant that a closed standpipe had to be provided for indicating the water level during filling.

18 No.¾" B.S.F. stainless steel bolts and 2 No.¾" B.S.F. studs, which are used for lifting the completed cell and sample, are used for fixing the cover plate to the cell.

(4:3:6) The Piston

The stainless steel piston is about 5" in diameter, being about 3 thou.

under the bore of the bronze liner, and is 21" long. To the lower end is fitted a 5" thick by 8" diameter loading head. The load face of the head is fitted with a hardened and ground $\frac{1}{4}$" thick plate, glued on with Twin-Bond epoxy resin adhesive. This plate fell off after a load of 85 tons had been applied to a sample, but subsequently, in excess of 100 tons has been applied without ill effect, which suggests that the adhesive was not applied properly in the first instance.

The top end of the piston is turned down to accommodate the cantilever clamp, which holds the dial gauge recording axial deformation. The dial gauge will measure 2" and reads in 1/1000", whereas sample deformation may exceed 6". To overcome this difficulty, a rod (adjustable in length) has its lower end slotted at 1.900" centres and supported by a forked plate on a bracket on the cell base.

At the top end of the piston is a groove for a circlip to prevent the piston falling through the bushing.

At the lower end, a further circlip bears against a large diameter washer (Fig.4:3). This enables the entire cell to be lifted vertically from an eye bolt, which can be fixed into the top of the piston.

(4:3:7) The Top Cap (Fig.4:3:3)

The sample top cap is 4" thick and fitted with $\frac{1}{2}$" bore and 3/16" bore connections, as is the pedestal. Pore water is collected by a perforated plate backed by radial channels, in the same way as distribution takes place at the base.

The top of the top cap is recessed 1" and a hardened and ground plate $\frac{1}{4}$" thick and 10" in diameter, is inlaid. On this plate sits a ring, 9" i.d. confining 600 $\frac{3}{8}$" diameter ball bearings, which transmit the deviator load to the sample from the piston loading head. This system allows an almost frictionless lateral movement of the sample top. The plates are hardened to 65 Rockwell and have been slightly indented by the balls with loads in excess of 100 tons. The confining ring is required because the lateral displacement of the top cap is twice that of the balls and, under load, the loading head would push balls away, instead of climbing over them.

When the pedestal and top cap were fitted with $\frac{1}{2}$" bore connections, the problem arose of finding a hose of this bore which would withstand 500 p.s.i. externally and still be very flexible. The hose eventually found was Bardex, a thick walled polythene, reinforced with spirally wound steel wire and designed for vacuum applications by Griflex Products,Ltd. Leakproof seals were produced at fittings using Jubilee Clips.

(4:3:8) Anti-Corrosive Protection

Anti-corrosive protection for the cell, base, pedestal and top cap was

by stainless steel paint. It was not very satisfactory and future apparatus will probably be cadmium plated.

It is probably impossible to protect the faces actually in contact with rock, as, under high stresses, the rock gouges out the steel. Also it is difficult to protect the insides of the connecting passages.

(4:3:9) Porous Stones

Before the special end platens (Fig.4:3:3:1) were produced for distributing water to the sample, porous stones from Aerox Ltd. were used. These were of Pyrolith, a vitreous bonded refractory ceramic aggregate. Three grades were obtained: G 16, G 27 and G 28, with pore sizes of 180, 95 and 55 microns respectively. The could be turned with a tipped tool to provide one flat face and drilled with a durium drill for fixing to the pedestal and top cap. Several grades and permeabilities were available but under high stresses they tended to crack.

(4:4) Electric Resistance Strain Gauge Loadcells

The deviator load was measured with an electric loadcell inserted between the crosshead load platen and the piston. Two capacities were used: 0 to 25 tons and 0 to 100 tons. The cells were commercially available and manufactured by W.H.Mayes & Son to a National Coal Board design. Their normal function was to measure pit prop loads and hence they were constructed very substantially and sealed against ingress of dirt,moisture and condensation.

The load element is a thin walled steel ring, sandwiched between end plates (Fig.4:4).16 paper backed strain gauges were spaced equally around the ring to form a full bridge circuit and they were protected against moisture with an epoxy resin cover. Further protection was provided by packing the completed cell with grease.

The input signal to the loadcell was provided by a Boulton Paul Aircraft Ltd C 61 Transducermeter, modified for use with resistive or inductive circuits. The instrument measures the ratio of input to output voltage and is brought to a null balance by introducing resistances. The sensitivity was such that one division on the meter was equivalent to 10-lbs in the case of the 25 tons capacity cell and 50 lbs in that of the 100-tons cell.

(4:4:1) Calibration

Prior to use, a calibration was carried out by loading the cells between parallel flat platens with an Amsler hydraulic loading machine. In

the case of the 25tons capacity cell a 35 tons capacity machine was used and a 300 tons capacity machine was used for the 100 tons capacity cell.

An initial calibration over the full range was carried out and then the cell was subjected to several hundred full load cycles and a further calibration carried out.

In the case of one cell, the zero shifted and the total range of output also varied, indicating that the gauges were slipping. The cell was re-strain gauged.

In general, the range of output remained constant within one or two parts in 4000 and the zero shift over two years hovered about the original output by a similar amount.

If the leads connecting the load cell to the transducermeter were altered in any way recalibration was necessary.

The cells were reliable and very convenient to use because of their light weight and small bulk and also their output was almost linear over the full working range.

The 25tons capacity loadcell had the same calibration curve for loading and unloading but the 100-tons capacity loadcell displayed histeresis. For 95% of the total load range of the latter loadcell the unloading calibration curve was parallel to the loading calibration curve and, on average, the equivalent of one ton away from it.

(4:5) Rubber Membranes

Providing membranes for rockfill samples proved to be a problem and for coarse grained, uniform material the problem has not been satisfactorily solved for high confining pressures. Fortunately, the usual cases in practice are graded, quarried materials or sand and gravel mixtures and the membranes designed have proved man enough for these materials at confining pressures up to 500 p.s.i.

Neoprene mouldings were considered but samples proved to be too stiff and the cost was also rather excessive.

The cost of setting up plant to make latex membranes was also excessive and experience with the 4" diameter by 12" long version, with thick walls, showed that the quality left much to be desired.

Eventually, a firm supplying gaskets to the motor industry produced a membrane of industrial quality rubber, having a kaolin filler and of Shore hardness 50-55. The rubber tube was formed by splicing a sheet. Two thicknesses were originally supplied, 1/16" and $\frac{1}{8}$".

Membranes 3/16" and $\frac{1}{4}$" thick were subsequently purchased for the tests at higher confining pressures.

Membranes 1/16" and $\frac{1}{8}$" thick and Shore hardness 30-35, almost natural

rubber, were also purchased. They were twice as expensive as the former type and offered no advantages, except on clay samples.

Membranes were only used once on rockfill samples.

(4:6) The Compaction Mould

The mould was manufactured from a $\frac{1}{2}$" thick mild steel tube of 13" internal diameter, which was fitted with three external steel bands of $\frac{1}{4}$" square section and three lugs, spaced at approximately 120 degrees. (Fig.4:6). The tube was finish bored and cut into three 120 degrees segments. Each segment was lined with $\frac{3}{8}$" thick carpet underlay felt. This lining was attached with Bostik 5 Adhesive.

Small lips were bolted to the top of the tube segments to prevent relative movement and the butting edges were covered with rubber, using Bostik 5 as adhesive. The thickness of the rubber made up for the loss of circumference due to the milling cutter width.

The mould was held together by 3 chain tighteners made of roller chain. The rollers ran on the three external steel bands and reduced friction to a minimum so that the tightening force would be almost evenly distributed around the mould. Holding down was accomplished by three $\frac{3}{4}$" diameter bolts passing through the holes already existing in the cell base.

(4:7) The Compaction Tool

Samples were compacted with a medium size Kango Electric Hammer, Type F, fitted with 2" diameter Swivel Head Vibrating Tool, Part No. 624.

(4:8) The Permeability Apparatus

It was considered important to be able to measure the permeability of rockfill under various stress conditions.

Permeability tests were usually carried out using mains tap water. Hydraulic gradients, varying from zero to 80, could be applied. High gradients were supplied by direct connection of the base of the sample to the water main. The input pressure was varied by altering the setting of the mains tap. The head loss across the sample was determined by pressure tappings at each end and the quantity of water passing in a given time was determined by weighing (Fig.4:8:1). The head loss, when using large hydraulic gradients, was measured by determining the water pressure at each end of the sample on the same Bourdon gauge.

Low hydraulic gradients were supplied by a constant head tank fed by tap water, the excess flow overflowing to waste. The pressure tapping points at the ends of the sample were connected to two $\frac{3}{8}$" bore polythene tubes clamped to the steadying column (Fig.4:8:2). The head loss across

the sample was then determined simply by measuring the difference in height between the two meniscae. Water leaving the top of the sample had to be led to an overflow tank placed at a higher elevation; otherwise anomolous conditions were occasionally set up producing a negative head loss for a wide range of flows.

(4:9) The Cell Pressure Control Systems

(4:9:1) The Pneumatic System

Maintaining a constant cell pressure, with the volume changes and pressures involved, ruled out the possibility of using the standard mercury pot system.

An all hydraulic system would have been ideal from a safety standpoint but, as a temporary measure, an air control system to give cell pressures up to 135 p.s.i. was designed to function until an hydraulic system could be installed.

Subsequent to the installation of the hydraulic system, the air system fulfils the back pressure function when the need arises.

The design of the air system centred around the Whittaker Hall hydro-vane compressor already existing and feeding the ring main in the laboratory. This was a 7 c.f.m. pump, driven by a 2 H.P. electric motor and capable of producing a pressure of 200 p.s.i.

The pump was set to cut in and out at given pressure limits but as the mean pressure setting increased, so the limits diverged and, when allowance had been made for line losses, the maximum pressure, which could be accurately sustained was 135 p.s.i.

Air, at varying pressures, was fed to an Associated Electrical Industries Ltd. air control valve, Model 40-200. This was a diaphragm valve arranged such that the controlled air pressure, plus a spring pressure, was balanced by the greater and varying input pressure, all excess air being bled off.

This valve was fairly stable and would hold a set pressure within a $\frac{1}{4}$ p.s.i. for several days. The relationship between spring pressure and controlled air pressure was constant.

To increase the cell pressure at a constant rate for carrying out Ko-tests, a servo motor was set up to drive a sprocket connected to the valve spring spindle via an extendable coupling.

The controlled air was led into the top of an air water interface vessel (Fig.4:9:1). This vessel was a mild steel tube 5' long, 6" bore and $\frac{1}{2}$" wall thickness. Onto the ends were welded $\frac{3}{4}$" thick rings to which 1" thick end plates were bolted. The ends of the tube and undersides of

the rings were machined square with the axis after welding. Both ends were sealed with O-rings.

At the base were connections for pressurising the triaxial cell, a pressure gauge, a filling lead, a water level indicator and a drain tap. All the tubes, except the drain, were terminated about 2" above the base of the vessel to prevent rust and other deposits entering them. Fittings throughout were either Ermeto Corporation or Simplifix type.

The interior of the vessel was coated with an hydraulic paint.

(4:9:2) The Hydraulic Pressure Control System

Several specialist firms in hydraulic engineering were approached to produce an hydraulic system in which the pressure would remain constant, irrespective of volume changes. No satisfactory solution was received.

The system eventually adopted relied on a pressure maintaining unit from an Amsler Loading Machine. This unit was very simple. Oil entered a cylinder and pressed against a spring loaded piston. When the force, due to oil pressure, exceeded the spring force the excess oil was bled off (Fig.4:9). To minimise friction the piston was oscillated at 60 times a minute by a Parvalux 1/100 H.P. capacitor start motor. Complete rotation would have been an easy modification but the valve performed so well that it was not altered. The piston had several concentric grooves along its length and three longitudinal flats at 120° to each other.

The valve would maintain any set pressure, irrespective of volume changes, in the range in which it was used, 0 to 500 p.s.i. to better than 1/10 p.s.i. indefinitely.

For the valve to operate properly it had to be fed with oil of constant viscosity. This, in effect, meant providing hydraulic oil at constant temperature and without air in the system.

An Oswalds and Ridgeway Ltd. positive displacement swashplate SWO/O pump was chosen for this application. This pump could deliver 0.15 gallons per minute at 10,000 p.s.i. when operated at 1450 r.p.m. This was far in excess of our requirements but was adopted so that the pressure system could be used for jacking and other high pressure apparatus, if required. For this reason, the pumping unit was mounted on a mobile trolley.

As the pressure system was to be used for many purposes, it was thought advisable to build in a certain amount of flexibility in the drive speed as it was unnecessary to run this pump at high speed when pumping against a dead end.

A 1 H.P. 3P.H. motor was flange mounted on a size 16 Kopp Variator, which was also flange mounted on a spur gearbox giving an overall output

infinitely variable between 80 and 720 r.p.m. The final drive to the pump was by a Uniroyal Power Grip Belt size L 100. This type of drive was chosen rather than a V-belt to eliminate slippage if any oil was spilt on the drive. Normally, a 40 tooth sprocket drove a 60 tooth sprocket but it was desirable, under certain conditions, to reverse these. The pump shaft was $\frac{5}{8}$" diameter and that of the gearbox $1\frac{1}{2}$" diameter. Taper grip bushes were used to secure the sprockets on the shafts and, as a result, either sprocket could easily be fitted to either shaft.

When properly aligned, this drive was perfectly silent at all speeds but it was the cause of considerable trouble. Although the pump was being used far below its rated output, two new shafts were fitted in two years. The reason appeared to be a circlip groove which reduced the shaft diameter and caused stress concentrations at the root of the cantilever. The Power Grip drive was replaced by a V - belt drive after the second shaft failure.

The pump itself was flange mounted in the forward compartment of a 2 cubic feet capacity oil tank. This tank was partitioned off so that all the oil which bled past the Amsler valve was passed through an oil filter and returned to the rear compartment and cooled. The pump compartment was also fitted with a cooling element. The cooling elements were $\frac{1}{2}$" bore copper tube formed into coils and connected to form a continuous hydraulic circuit. This was fed by tap water and only a very small flow was required to maintain the oil at ambient temperature.

The pump was fitted with a suction filter and also a full flow porous bronze high pressure delivery filter.

Very great care was taken to smooth off all pipe ends and remove all swarf and scale from the oil circuit pipes by blowing out each one with compressed air prior to final fitting and also after assembly.

The tank was fitted with a drain valve and an oil level indicator.

Although the cooling water system was tested for leaks before filling the tank with oil, it was found that a considerable volume of water accumulated under the oil in time and an observation window was fitted near the base of the tank to indicate the oil water interface, so that the water could be drained off before it reached the pump suction elevation.

When the oil left the high pressure delivery filter it was fed into the top of an oil water interchange vessel with a T connection to the Amsler load maintaining valve. Nylon 11-3/16" o.d. tubing was used from the pump to the T but $\frac{1}{2}$" bore copper tube had to be used between the valve and the oil water interchange and between this vessel and the triaxial cells if pressure variations throughout the system were to be avoided.

The oil water interface vessel was identical to the air water one, except that it was fitted with a Sectru spring operated valve set to lift

at 530 p.s.i. and close about 2 p.s.i. below this figure. Oil passing this valve was also returned to the main tank via a filter.

The bore of the nylon oil level indicator tube was increased to $\frac{1}{2}$" because meniscus effects and the small density difference between oil and water made the reaction time too long if small bore nylon tube was used.

There was always a considerable build up of static electricity on the nylon tubing leaving the high pressure filter.

Excess oil bleeding from the Amsler valve and also the oil lost by seepage past the piston was returned to the main tank, after passing through filters.

The cross-sectional area of the tank was such that only a small variation took place in oil level during a test and the pump remained fully submerged at all times.

Bourdon type pressure gauges were connected to the water side of each of the interchange vessels which could be conveniently filled directly from the de-aired water ring main in the laboratory (Fig.4:9).

A $\frac{1}{2}$" bore, high pressure flexible hose was used to connect the shut off valves on the triaxial cell and the oil water interchange vessel.

(4:9:3) Resonance

The hydraulic system was not particularly stiff because of the large volumes of fluid involved but, at certain pressures and pump speeds, unstable conditions did develop and these were easily overcome by altering the pump speed with the Kopp Variator.

(4:10) The Electrical Control Circuits

A system of interlocks and limits was devised to minimise the risk of accidental damage to the equipment. (Fig.4:10:1).

The design and installation of the electrical control circuits to perform these functions and the choice of electrical control gear was the responsibility of the Civil Engineering Dept. Electrician, Mr.P.Clifford.

All functions, except the control of the pressure pump motor, were controlled from a console which could be isolated from the mains.

All the circuits were protected by fuses.

Five outlet sockets were provided on the console, one 3 PH. for the pressure pump motor, two 1 PH. for the transducermeters, one 1PH for the oscillator motor for the Amsler pressure maintaining valve and one 1 PH for the servo motor for controlling the cell pressure during K_o tests.

The jack main drive, crosshead and rapid return motors could be stopped by an emergency stop button, located conveniently near the loadframe.

The jack main drive and rapid return motors were interlocked and

stopped by switches set at the limits of the jack travel.

Switches were set to control the limits of the crosshead travel and two further switches were set to prevent further downward travel after a small upward displacement (relative to the crosshead) of the loading platen and lock the crosshead altogether after a further upward displacement.

The crosshead motor was controlled by manual push buttons.

The jack main drive motor could either be controlled manually by push buttons or automatically, via an interlock, by a sensing transducer on a K_o belt. In this case though the operation was upwards or stop only to prevent hunting taking place.

Control of the rapid return motor was by push buttons, down and stop only.

The laboratory was wired on a dual system basis, in such a way that if a failure occurred a standby supply was automatically switched in.

This changeover took a few seconds and, as a result, delay relays had to be fitted to the jack main drive and pressure pump motor starters to prevent them switching off. Therefore, to stop these motors permanently the stop buttons must be depressed for at least four seconds.

Nearly all the switchgear used was manufactured by Allen West (Switchgear) Ltd.

(4:11) The Special Lifting Arm

A special lifting arm was designed to enable the cell to be placed under the crosshead. This arm was not counterbalanced and, as a result, the cell hung slightly out plumb from the crane. This was an advantage when locating the cell on the jack because the recess in the cell base was able to just engage with the aluminium plate on one side and then slowly hinge down as the cell was lowered into its final position. As a result the cell could be positioned without subjecting the sample to any excessive shock.

(4:12) The Sieving Machine

The machine, which was used for the sieve analysis of the material tested in 12" diameter samples, had a rectangular screen frame 2' wide and 4' long. The inclination of this screen frame was variable to obtain the optimum sieving condition for any given particle size.

Various mesh sizes were mounted in sub frames and held against the main frame by spring clips. Vibration was produced at the upper end of the main frame by a 1 PH. $\frac{1}{2}$ HP., 1450 r.p.m. motor fitted with eccentric weights.

This machine was very suitable for bulk sieving where the aim was

merely to obtain segregates. It was not so suitable, however, for the sieve analysis of individual small samples because, being an open system rather than totally enclosed, a certain proportion of fine material was lost to the dust extraction plant.

(4:13) Modifications to the Small Scale Triaxial Apparatus

In order to test samples of 1½", 4", and 12" diameter under similar conditions of loading and end restraint minor modifications were made to the standard small scale triaxial equipment.

(4:13:1) Modifications to the Standard Triaxial Apparatus for Testing 4" diameter Samples

A mild steel pedestal was machined so that pore water could be distributed to the sample via radial channels and a stainless steel perforated plate in a similar manner to that in the large scale apparatus (Figs.4:13:1:1, 4:13:1:2).

The top cap was machined, from mild steel, in a similar manner and its upper face was hardened to 65 Rockwell. Ball bearings ¼" diameter, were held in position on this face by a retaining ring and the load was transferred from the piston to the ball bearings by a hardened steel loading head (Fig.4:13:1:3)

When testing very fine gradings, a copper gauze had to be placed over the perforated plate to prevent fine material from blocking the perforations. The edges of the copper gauze had to be floated in solder to form a smooth edge, otherwise the ends of the wire were pushed through the membranes, causing punctures.

Nylon 11 leads were used and fixed into the 3/16" diameter holes in the pedestal and top cap using Loctite Retaining Compound.

Confining pressures in this apparatus were limited to 120 p.s.i.

(4:13:2) Modifications to the Standard Triaxial Apparatus for Testing 1½" diameter Samples

A 1½" diameter hard brass loading cap was fitted to the end of the ram.

The top cap was a plain perspex disc, fitted with two 3.5 mm saran drainage leads, retained by Loctite Retaining Compound.

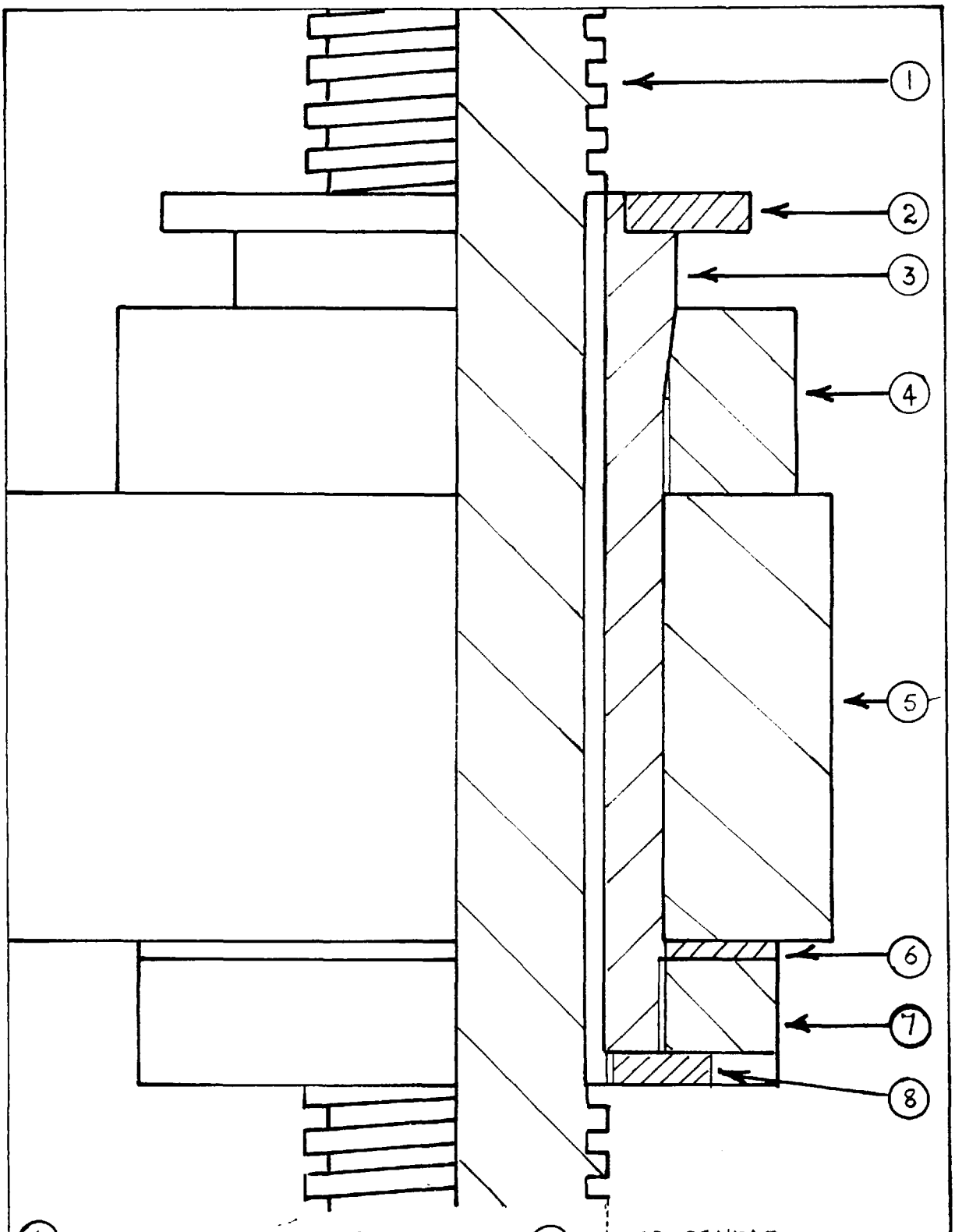
The upper face of the top cap was covered with 3/32" diameter ball bearings, held in place by Vaseline.

For the tests at cell pressures in excess of 80 p.s.i. steel discs were inserted, one above the perspex top cap and one below the brass loading cap with the ball bearings between them, to minimise bedding.

Cell pressures above 80 p.s.i. were generated by the hydraulic system designed for the large triaxial apparatus.

Porous stones, $\frac{1}{8}$" thick and cored from a carborundum wheel, were used to distribute pore water to the sample. The permeability of these stones was about 1×10^{-3} cms per second.

For pressures above 80 p.s.i. a steel cell was used.

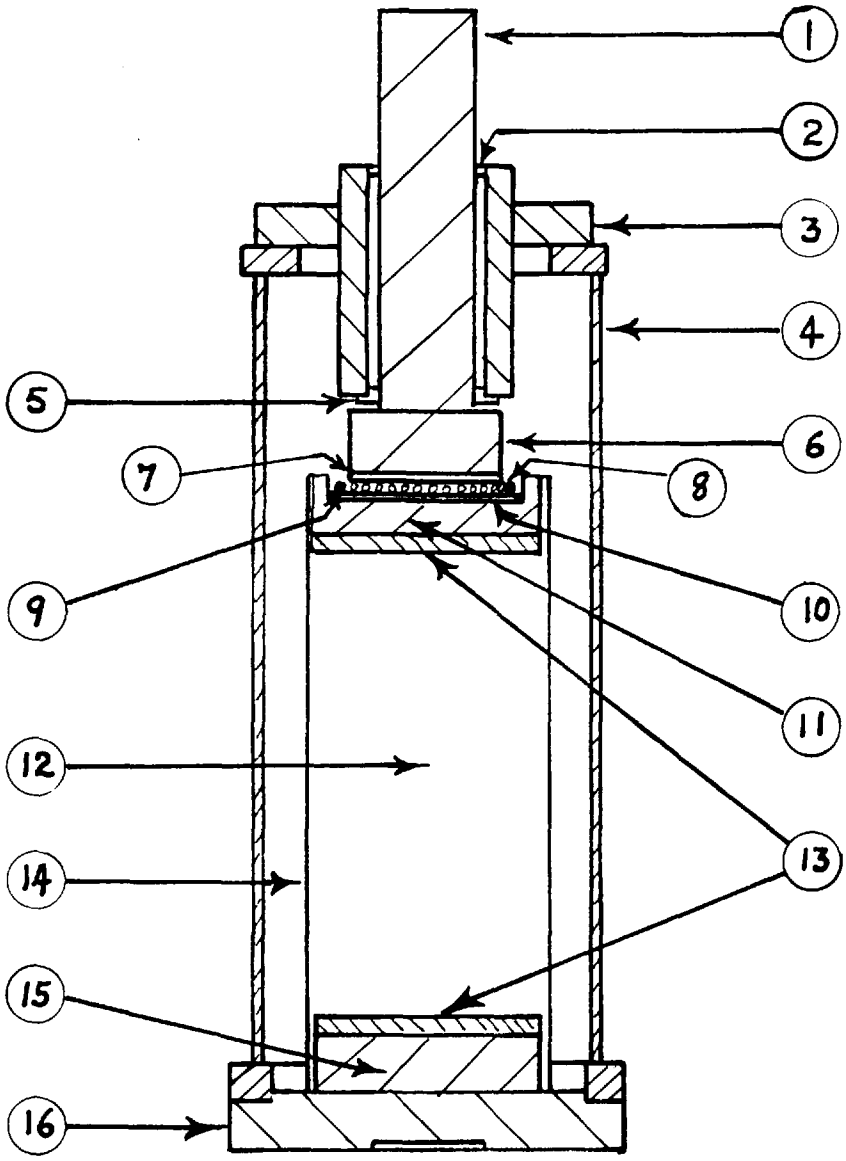


1. MILD STEEL TIE BAR
2. ROLLER CHAIN SPROCKET
3. BRONZE BUSH
4. MILD STEEL NUT
5. CROSSHEAD
6. BRASS RUBBING PLATE
7. MILD STEEL NUT
8. NUT LOCKING KEY.

SCALE : HALF FULL SIZE

HALF SECTION CROSSHEAD BUSH.

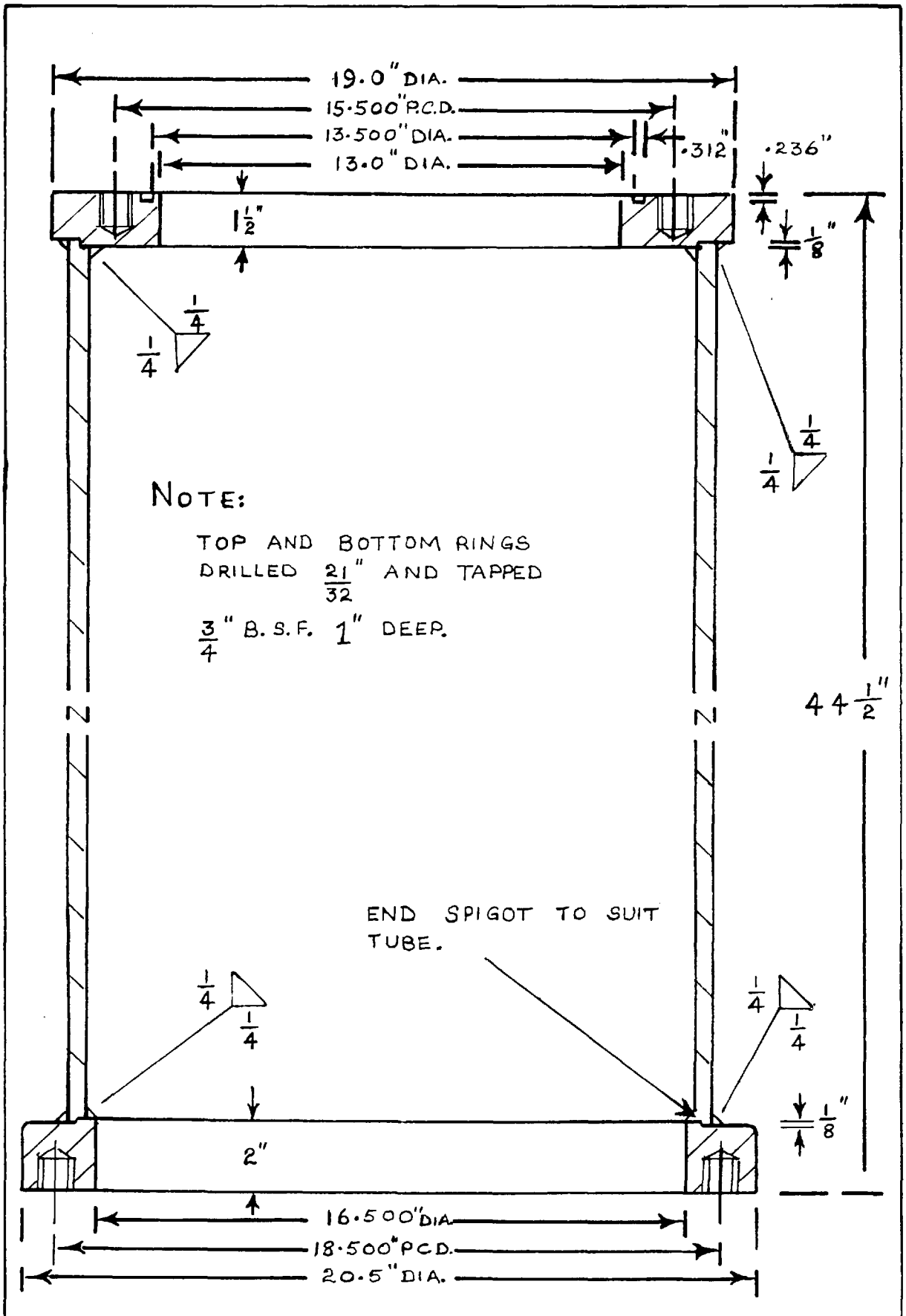
FIG. 4:2:3



1. STAINLESS STEEL PISTON
2. BRONZE BUSH
3. TOP PLATE
4. CELL BARREL
5. WASHER AND CIRCLIP
6. LOADING HEAD
7. HARDENED STEEL PLATE
8. BALL BEARINGS
9. RETAINING RING
10. HARDENED STEEL PLATE
11. TOP CAP
12. SAMPLE
13. PORE WATER DISTRIBUTORS
14. MEMBRANE
15. PEDESTAL
16. BASE

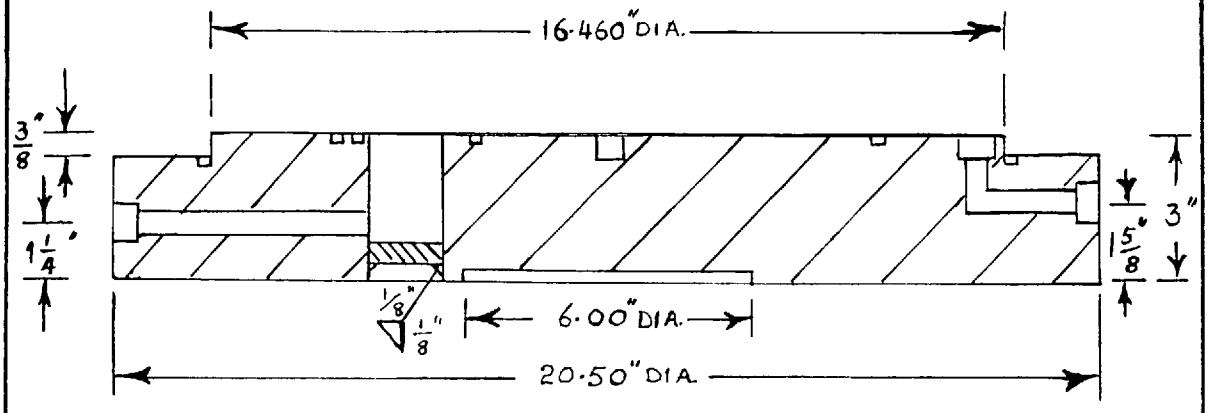
TRIAXIAL CELL GENERAL ASSEMBLY.

FIG. 4:3

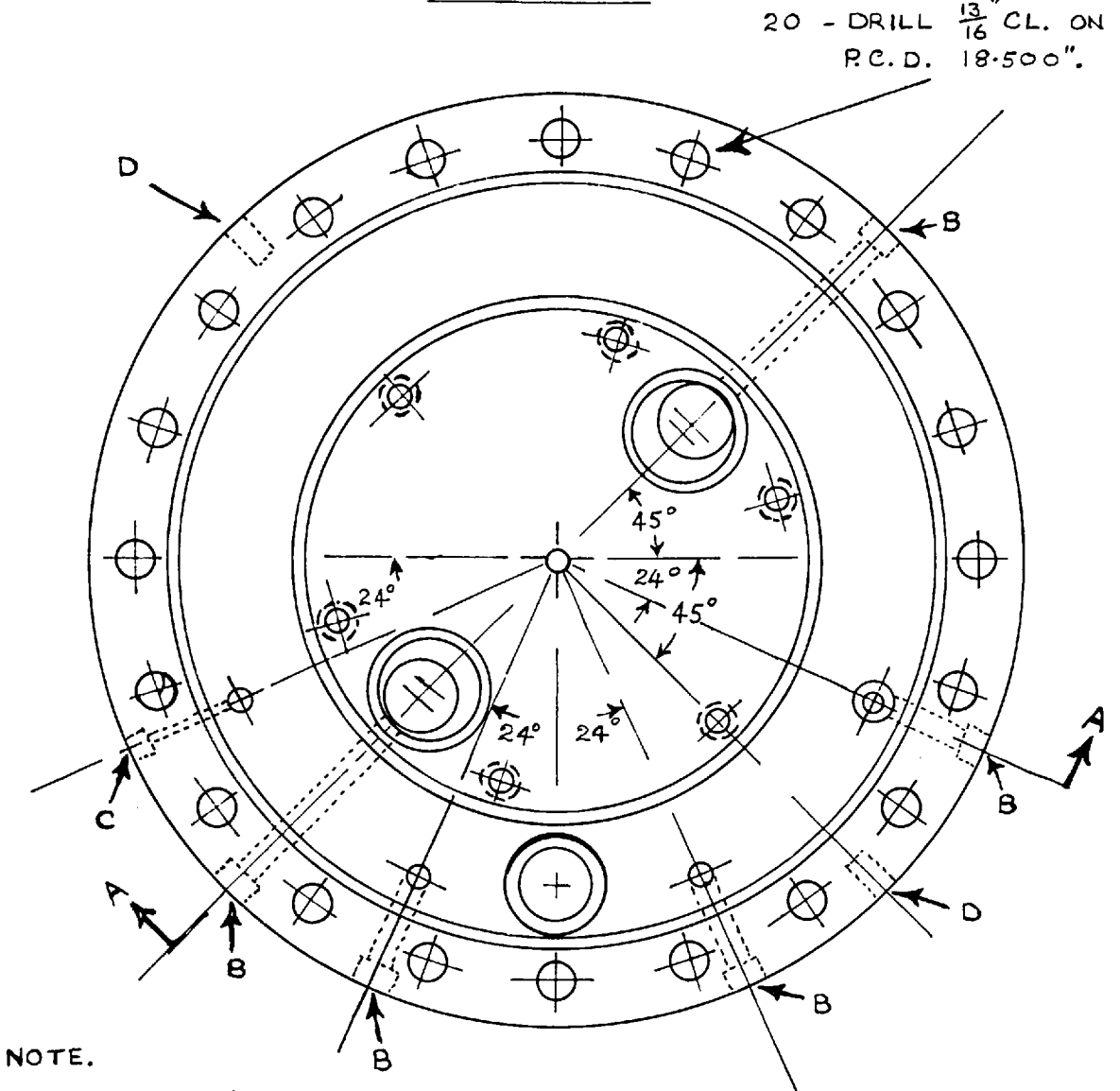


CELL BARREL DETAIL.

FIG. 4:3:1



SECTION A-A



NOTE.

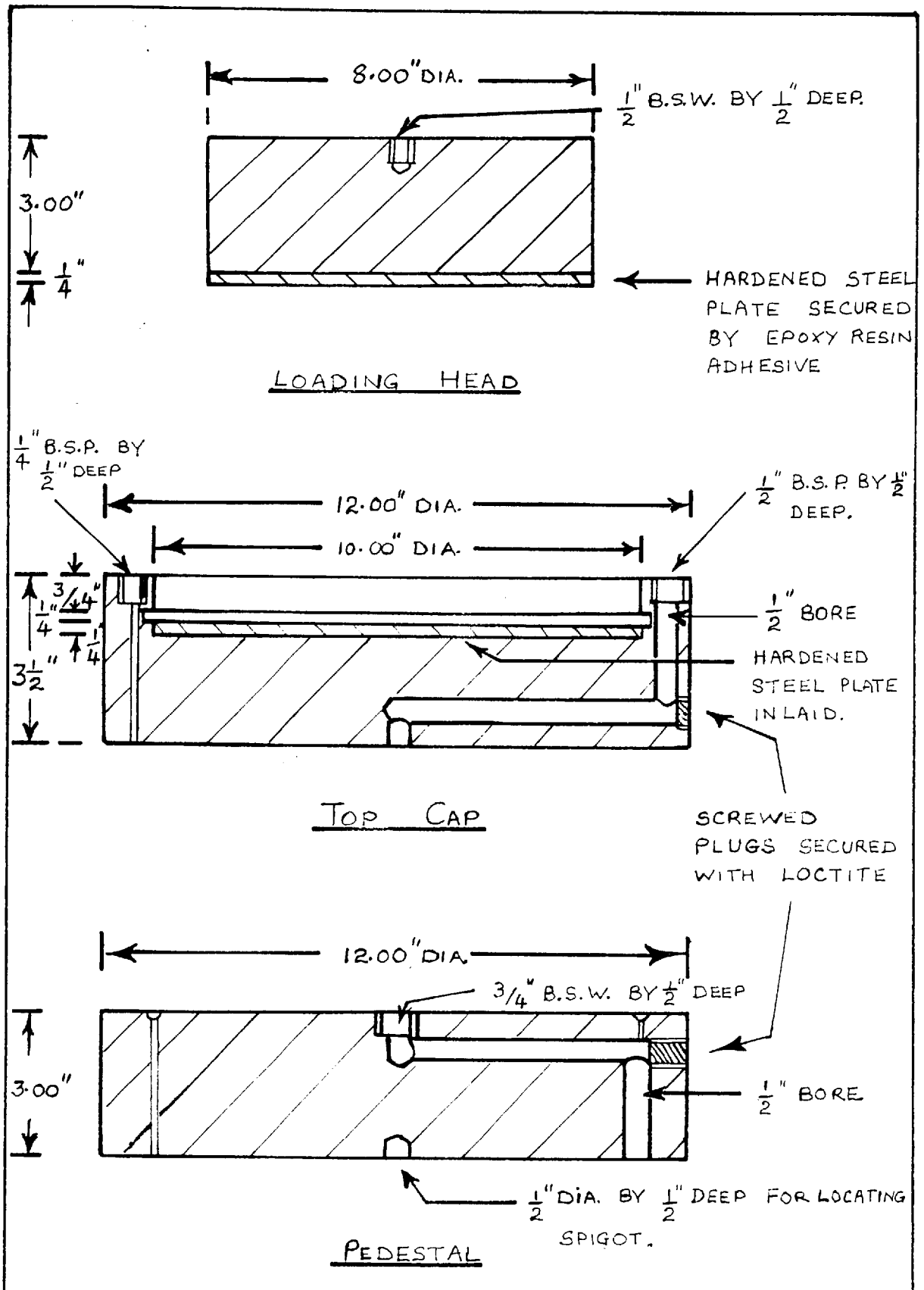
B: DRILL $\frac{1}{2}$" CL. SPOTFACE $1\frac{1}{2}$" DIA. C/BORE AND TAP $\frac{1}{2}$" B.S.P.

C: DRILL $\frac{3}{16}$" CL. SPOTFACE $1\frac{1}{2}$" DIA. C/BORE AND TAP $\frac{1}{4}$" B.S.P.

D: DRILL $\frac{7}{16}$" CL. SPOTFACE $1\frac{1}{2}$" DIA. TAP $\frac{1}{2}$" B.S.F.

CELL BASE DETAIL.

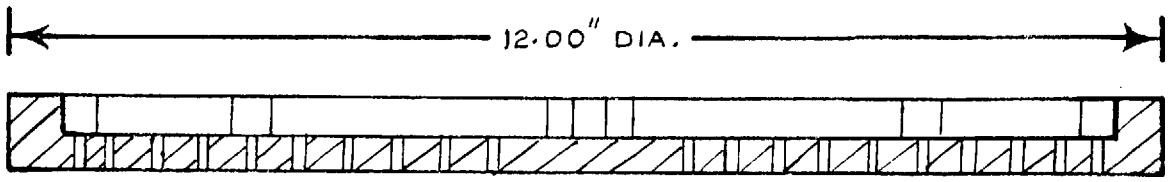
FIG. 4:3:2.



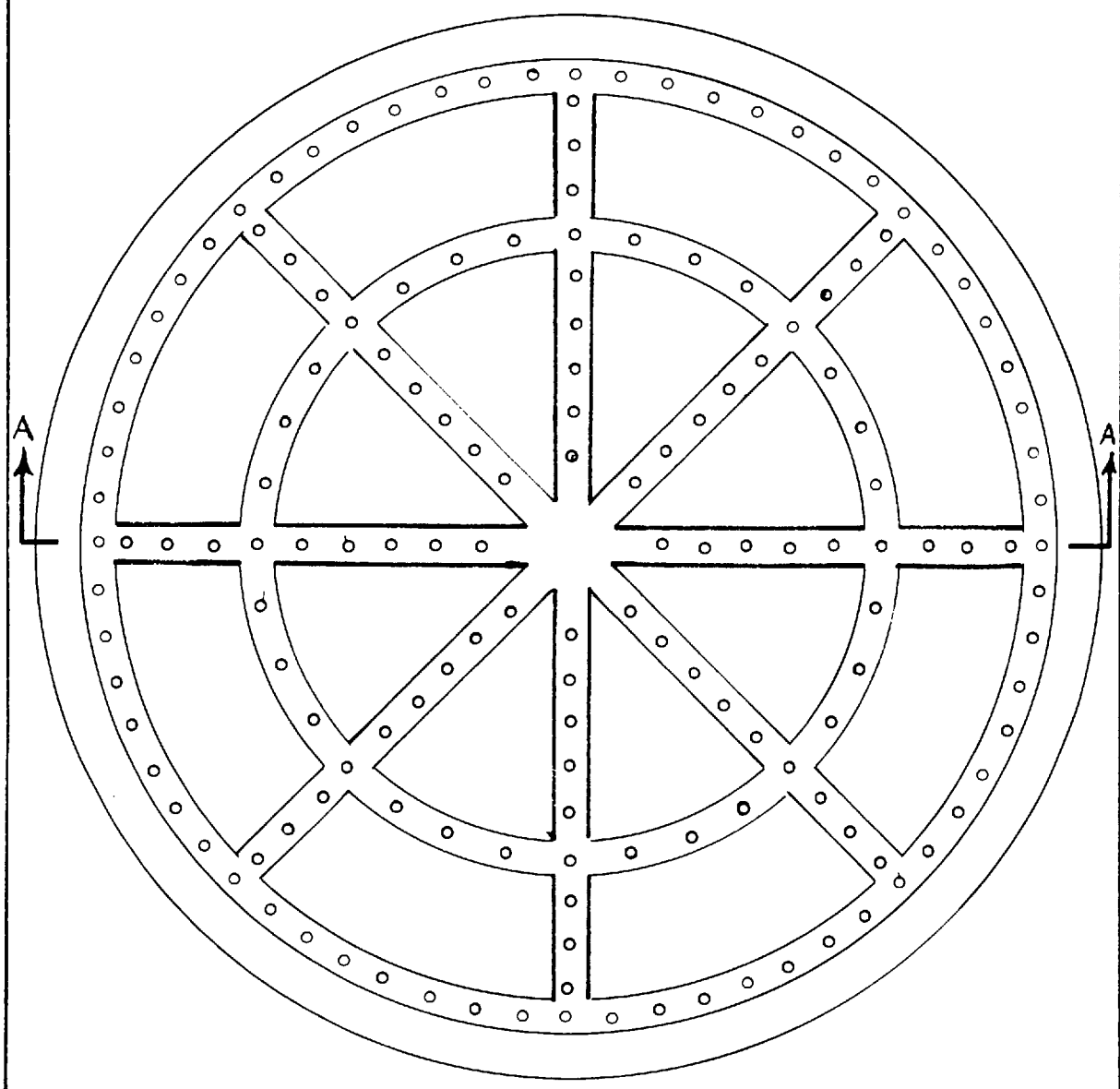
CROSS SECTIONS

LOADING HEAD, TOP CAP AND PEDESTAL

FIG. 4:3:3



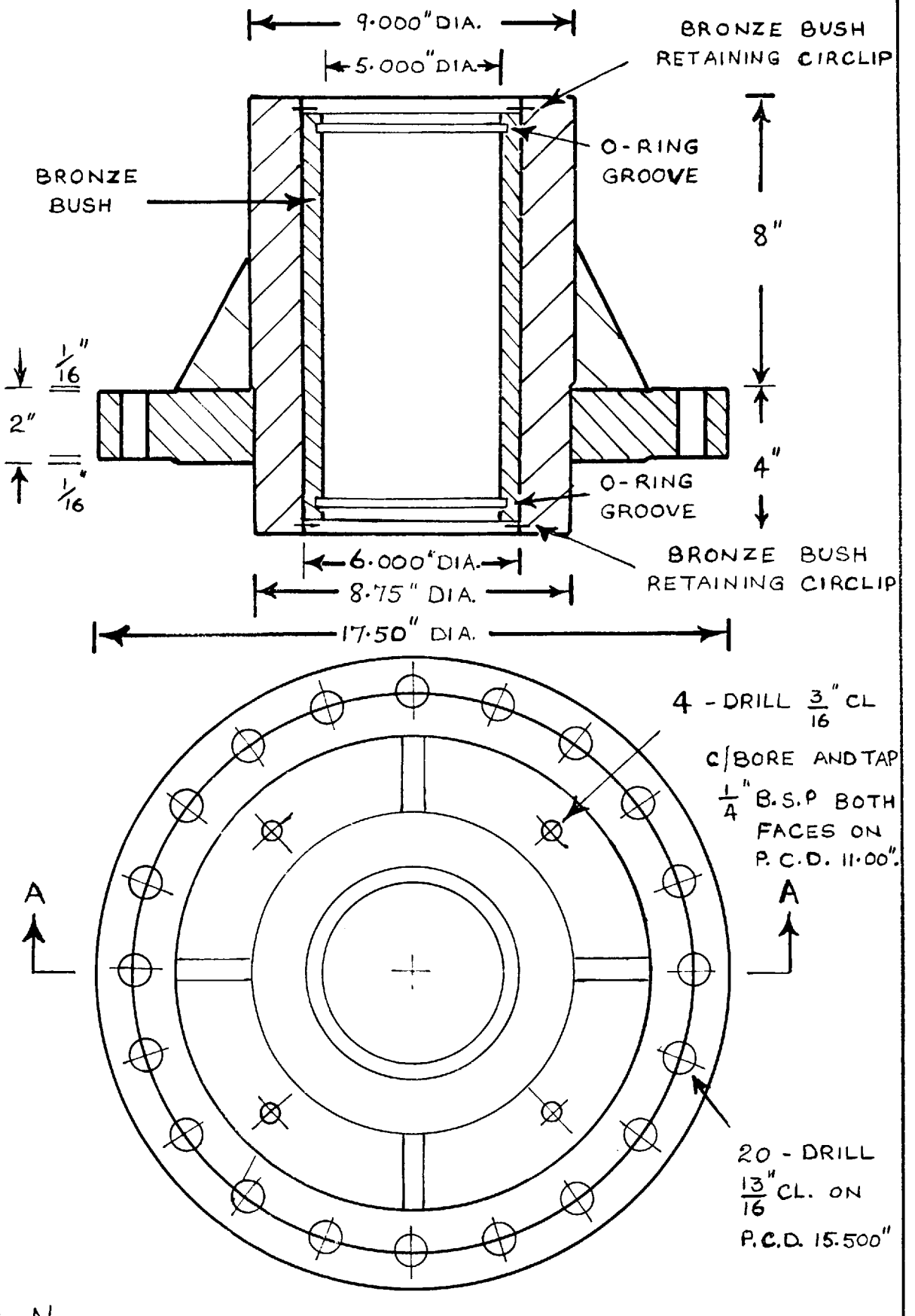
SECTION A-A.



NOTE: ALL HOLES $\frac{1}{8}$" DIA. ON P.C.D's 2", 3", 4", 5", 6", 7", 8", 9", 10" and 10·625"
RADIAL AND CONCENTRIC CHANNELS ARE $\frac{3}{8}$" × $\frac{3}{8}$"
NOMINAL PLATE THICKNESS $\frac{3}{4}$" MACHINED ALL FACES

PORE WATER DISTRIBUTORS

FIG. 4:3:3:1



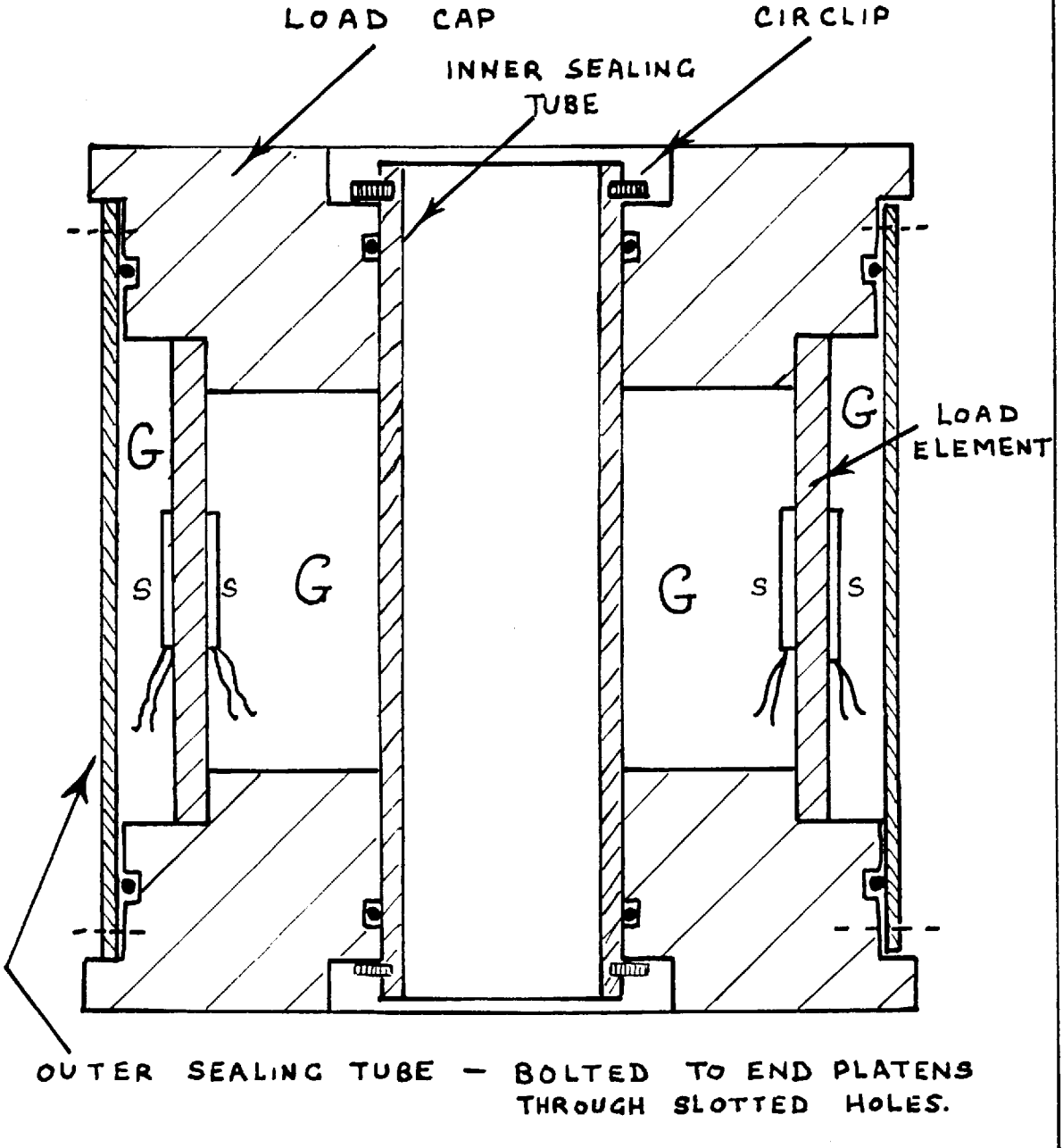
NOTE: BRONZE BUSH TO BE A PRESS FIT IN HOUSING

COVER PLATE DETAIL.

FIG. 4:3:5

G : THESE ANNULAR SPACES FILLED WITH GREASE.

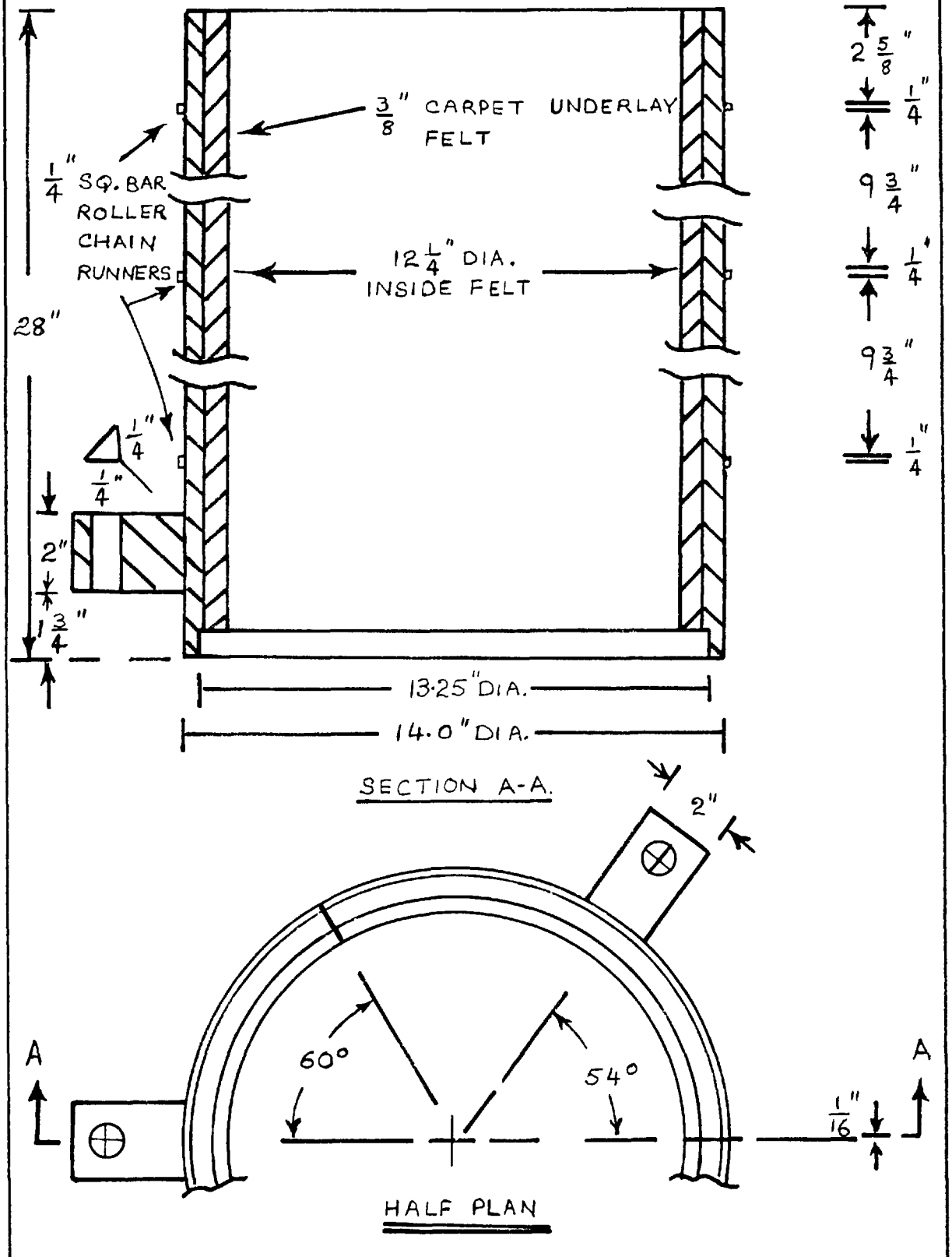
S : RESISTANCE STRAIN GAUGES.



LOAD CELL CROSS SECTION.

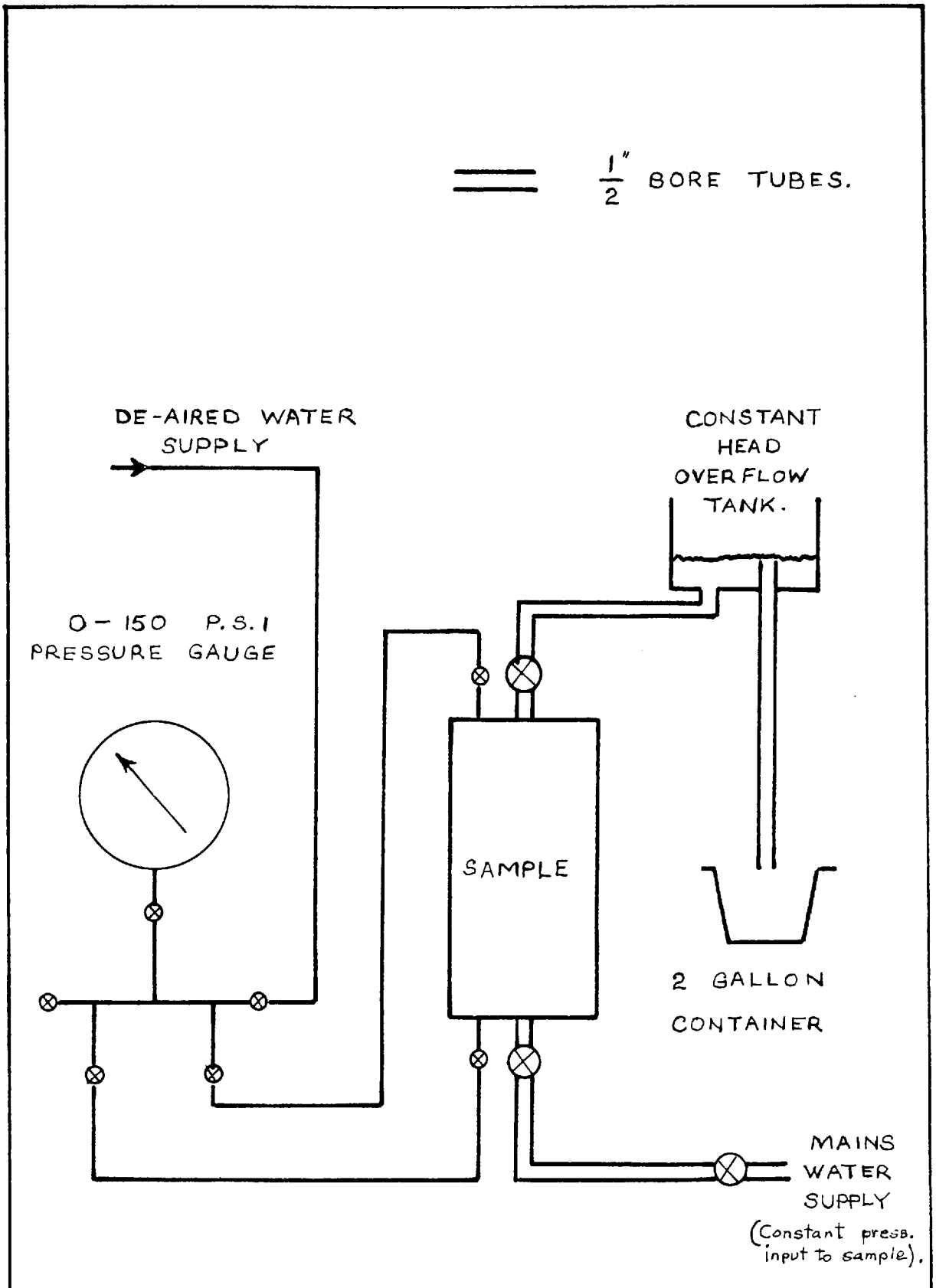
(TENSION-COMPRESSION TYPE)

FIG. 4:4.



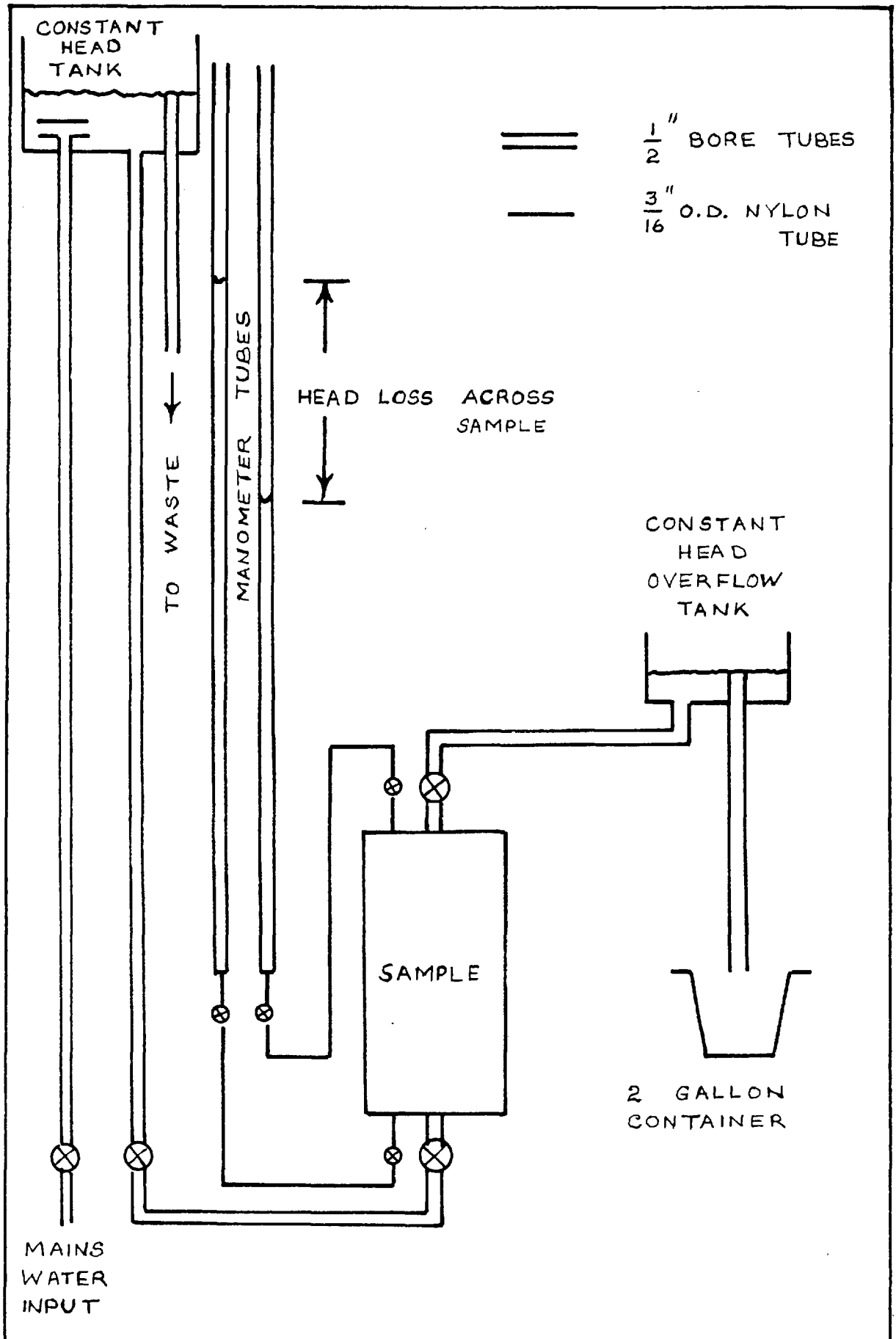
COMPACTION MOULD.

FIG. 4:6



HIGH HYDRAULIC GRADIENT PERMEABILITY APPARATUS.

FIG. 4:8:1



LOW HYDRAULIC GRADIENT PERMEABILITY APPARATUS.

FIG. 4:8:2

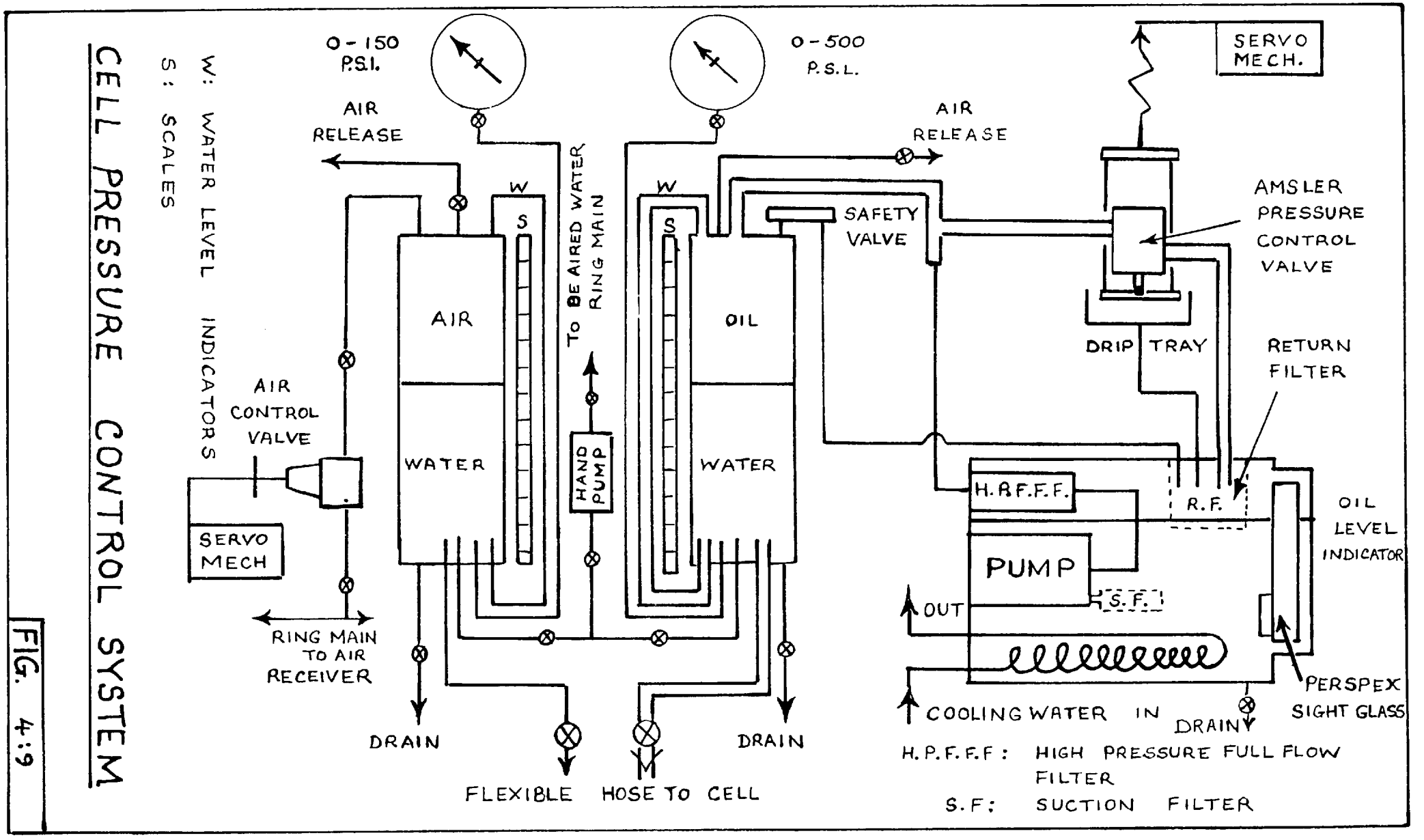
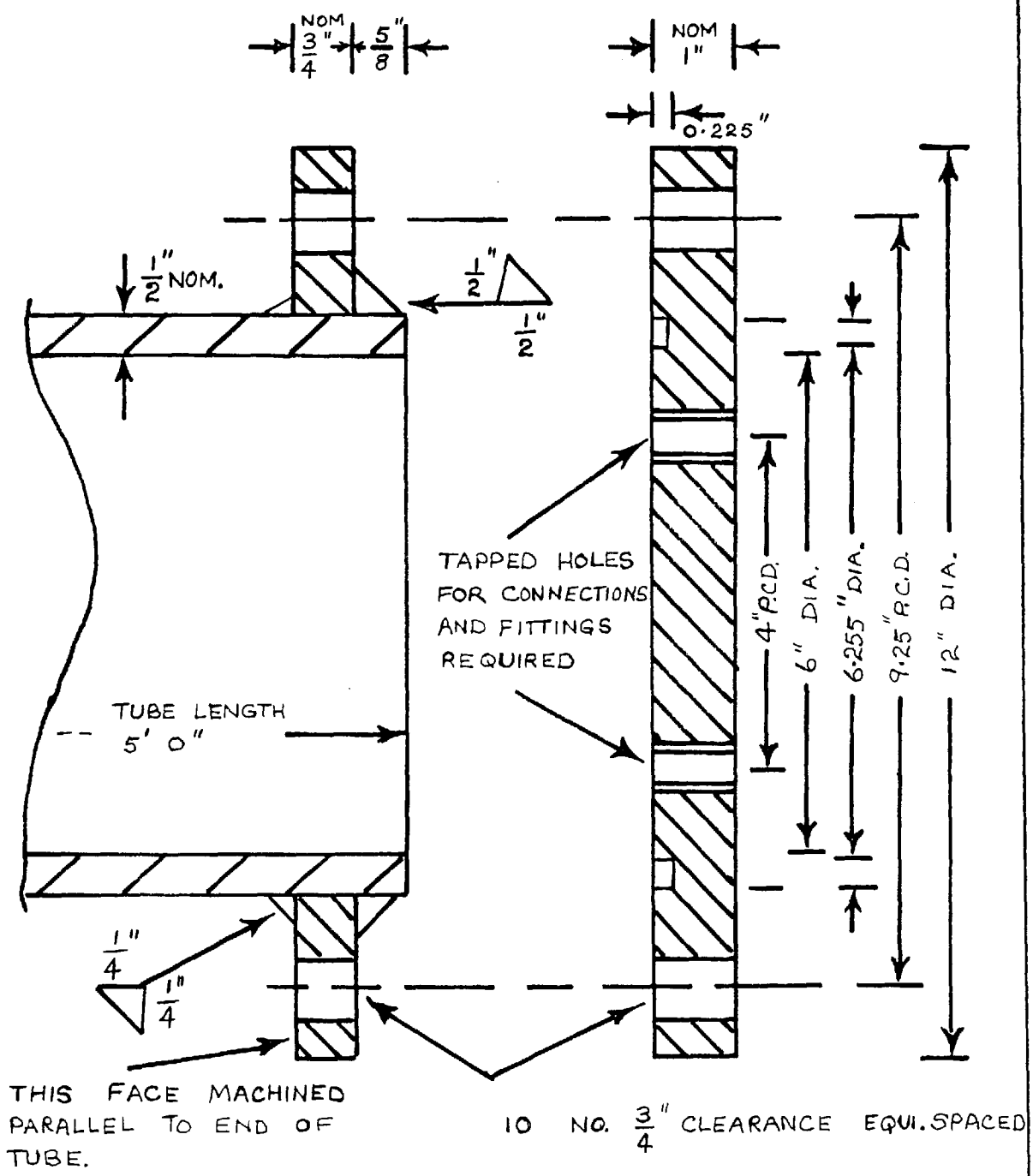

CELL PRESSURE CONTROL SYSTEM
W: WATER LEVEL INDICATORS
S: SCALES
0 - 150 P.S.I.
0 - 500 P.S.I.
AIR RELEASE
AIR RELEASE
W
S
W
S
AIR
WATER
OIL
WATER
TO BE AIRED WATER RING MAIN
HAND PUMP
SAFETY VALVE
SERVO MECH.
AMSLER PRESSURE CONTROL VALVE
DRIP TRAY
RETURN FILTER
AIR CONTROL VALVE
SERVO MECH
H.P.F.F.F.
R.F.
OIL LEVEL INDICATOR
PUMP
S.F.
OUT
RING MAIN TO AIR RECEIVER
DRAIN
DRAIN
FLEXIBLE HOSE TO CELL
COOLING WATER IN
DRAIN
PERSPEX SIGHT GLASS
H.P.F.F.F: HIGH PRESSURE FULL FLOW FILTER
S.F: SUCTION FILTER

FIG. 4:9



TUBE SECTION END CAP SECTION

NOTE: OIL WATER INTERFACE VESSEL IS IDENTICAL.

AIR-WATER INTERFACE VESSEL, END CONSTRUCTION DETAILS.

FIG. 4:9:1

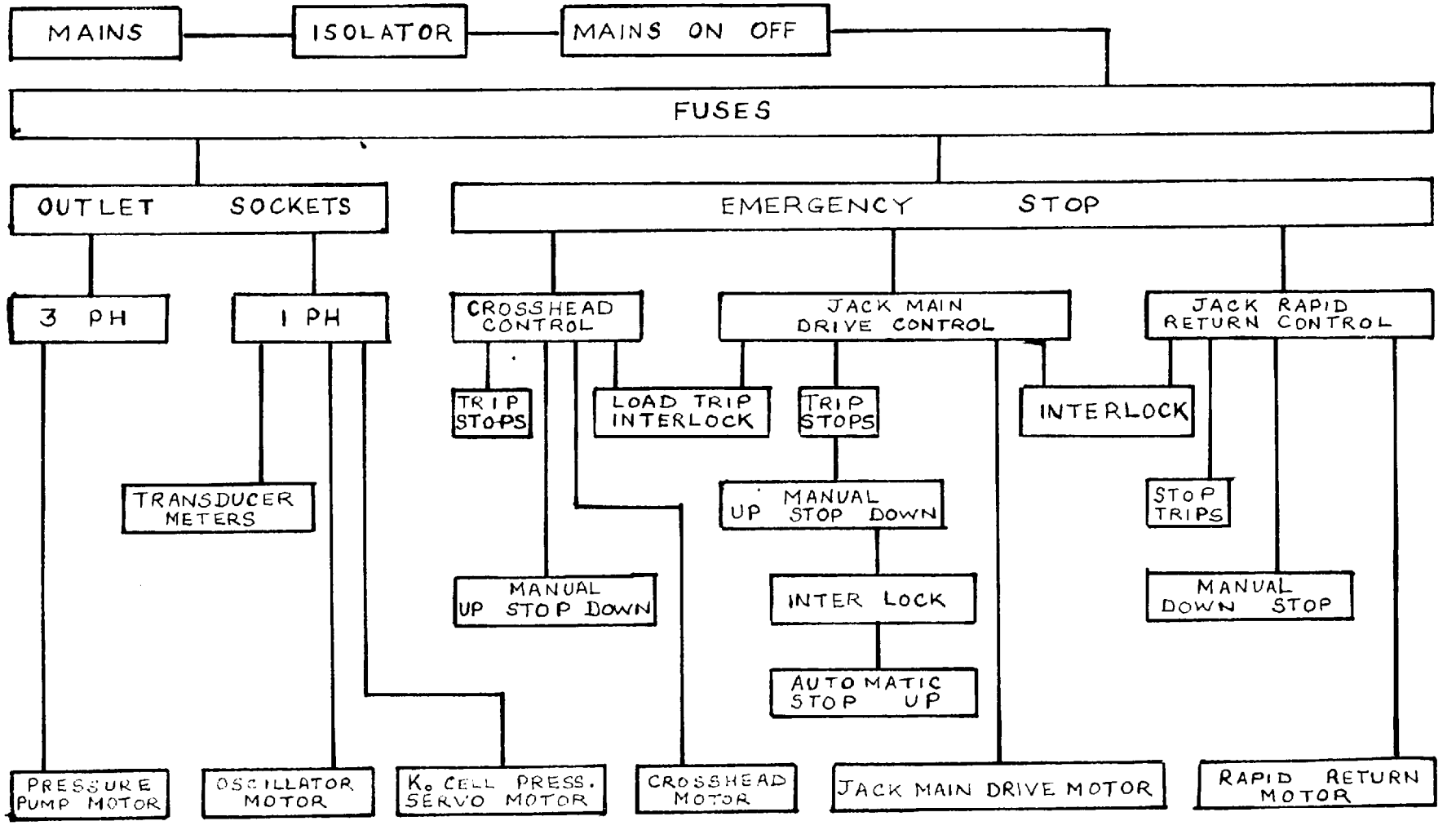
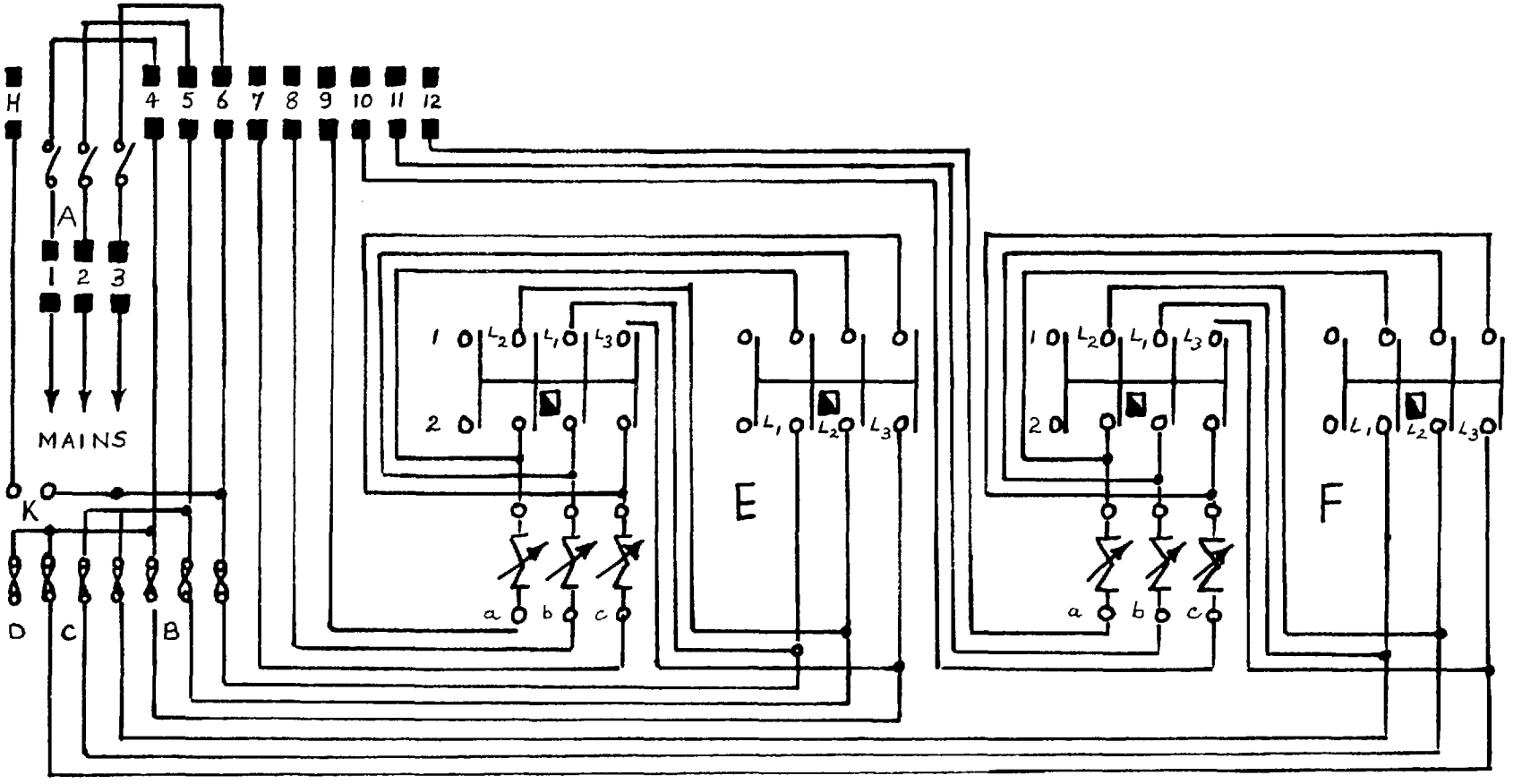


FIG. 4:10:1

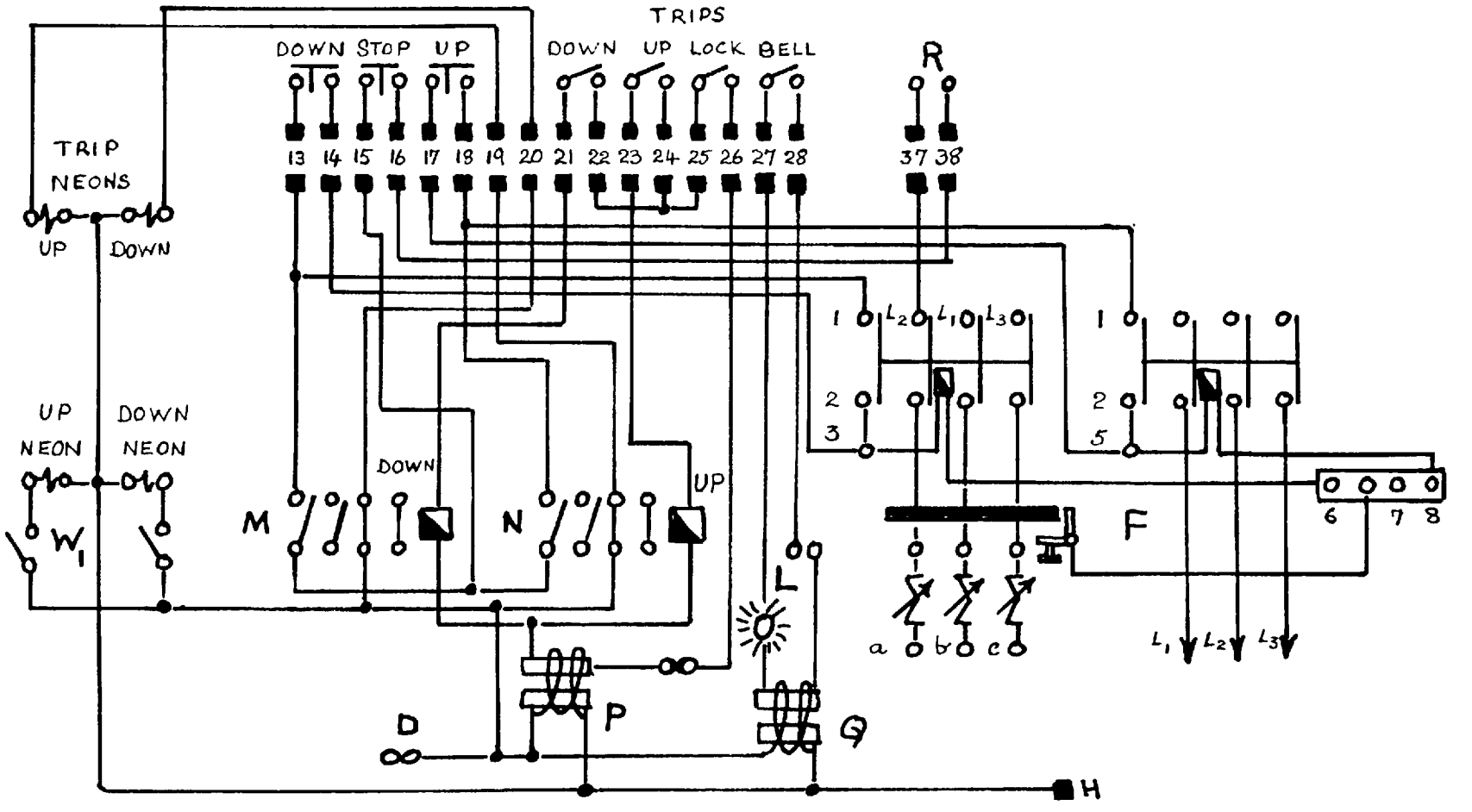
SCHEMATIC DIAGRAM OF 100 TONS LOADFRAME AND CELL PRESSURE CONTROL.

Main Drive and Crosshead Motors Power Circuit



A : MAIN ON~OFF 3PH SWITCH
B : MAIN DRIVE MOTOR 3PH FUSE
C : CROSSHEAD MOTOR 3PH FUSE
D : CONTROL CIRCUIT FUSE
E : 3 PH REVERSER STARTER FOR MAIN DRIVE MOTOR
F : 3 PH REVERSER STARTER FOR CROSSHEAD MOTOR
K : TWIN SOCKET OUTLET FOR TRANSDUCERMETERS.

FIG. 4:10:2

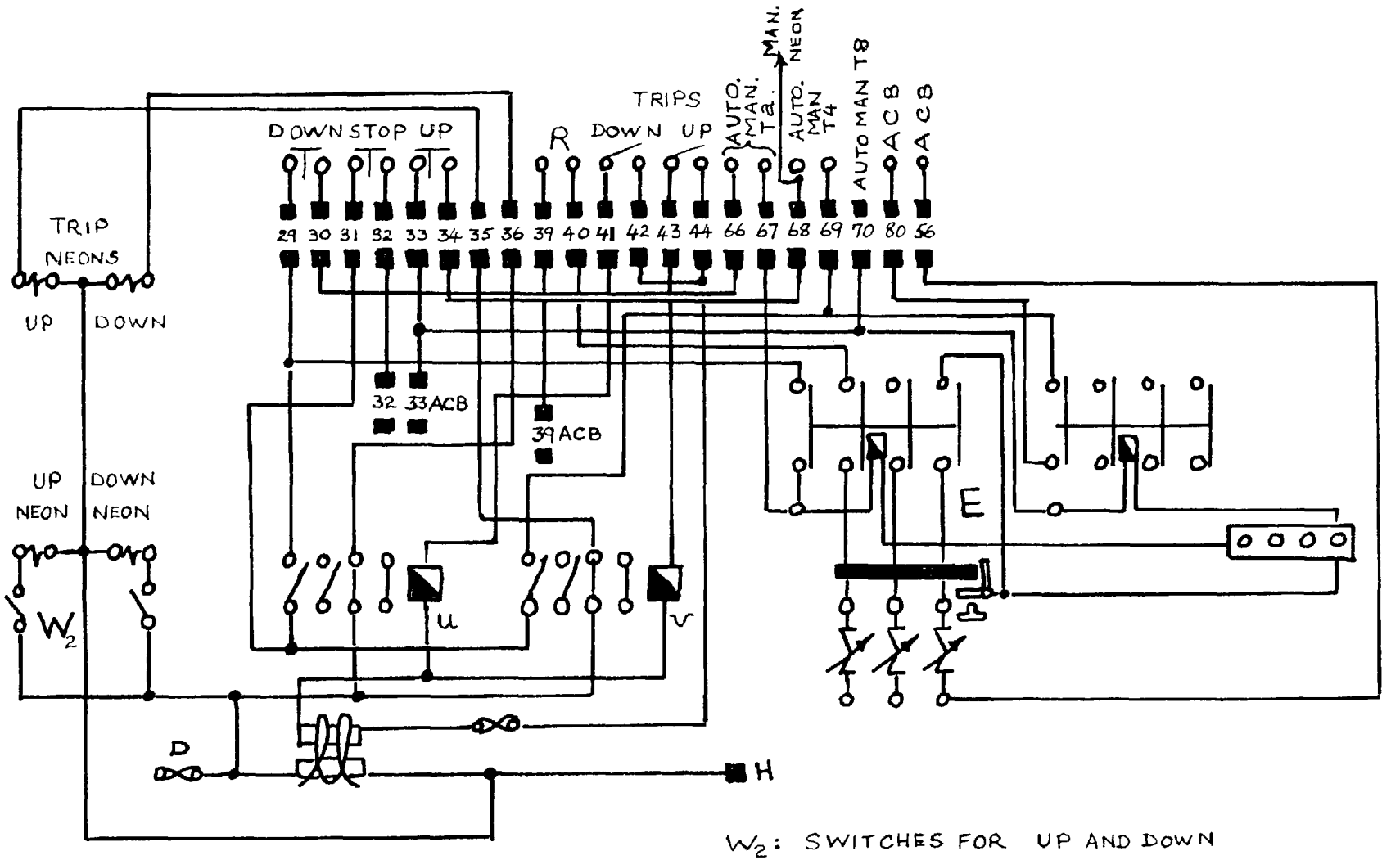


L : AXIAL DEFORMATION BELL
M : DOWN RELAYS
N : UP RELAYS
P : RELAY TRANSFORMER
Q : BELL TRANSFORMER
R : EMERGENCY STOP

W_1: SWITCHES FOR UP AND DOWN WARNING NEONS OPERATED BY REVERSER STARTER "F."

CROSSHEAD CONTROL CIRCUIT.

FIG. 4:10:3

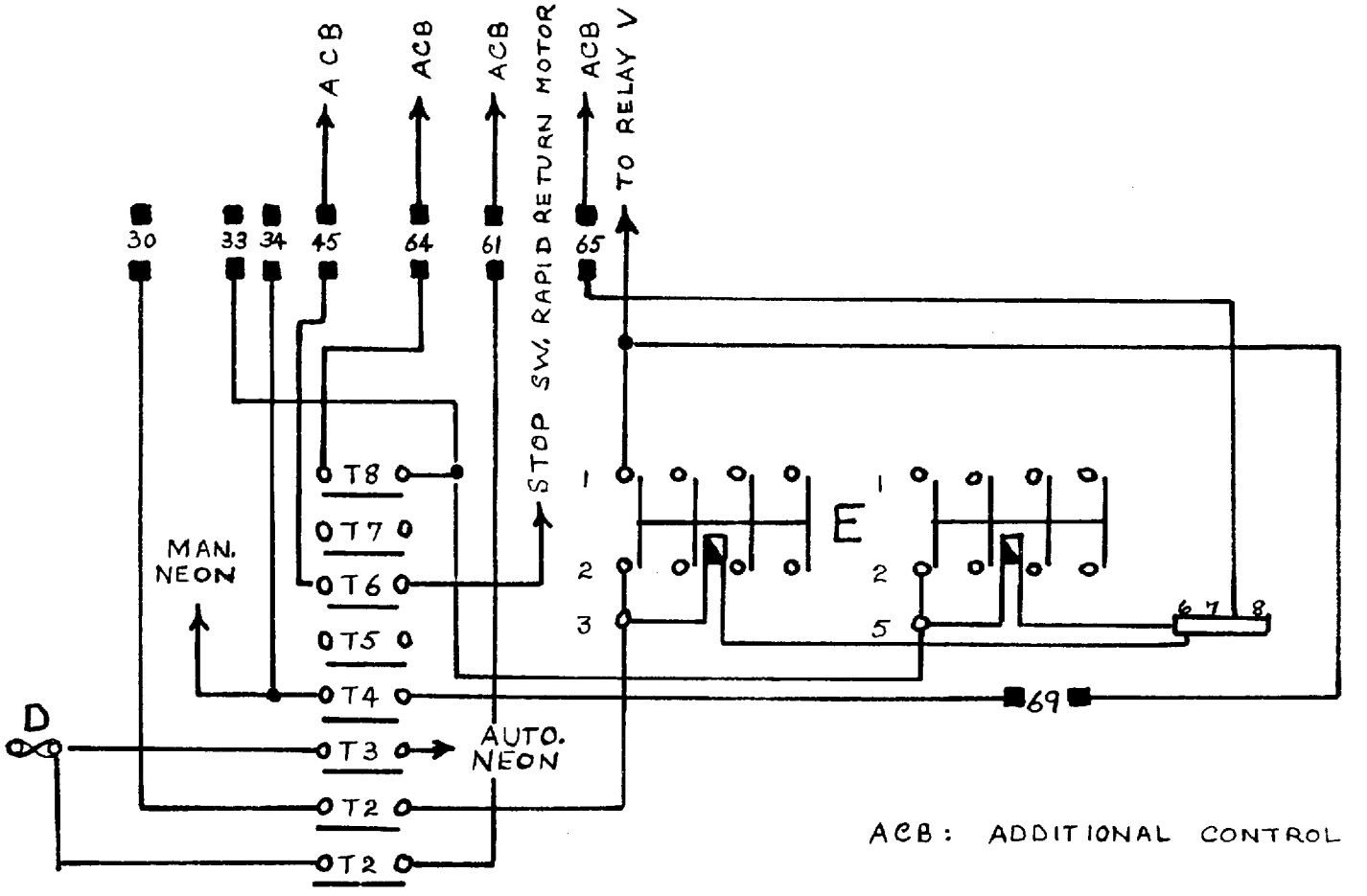


U: DOWN RELAYS
V: UP RELAYS

W_2: SWITCHES FOR UP AND DOWN WARNING NEONS OPERATED BY REVERSER STARTER "E"

FIG. 4:10:4

MODIFIED MAIN DRIVE MOTOR CONTROL CIRCUIT.



ACB : ADDITIONAL CONTROL BOX.

FIG. 4:10:5

AUTO-MANUAL CONTROL CIRCUIT.

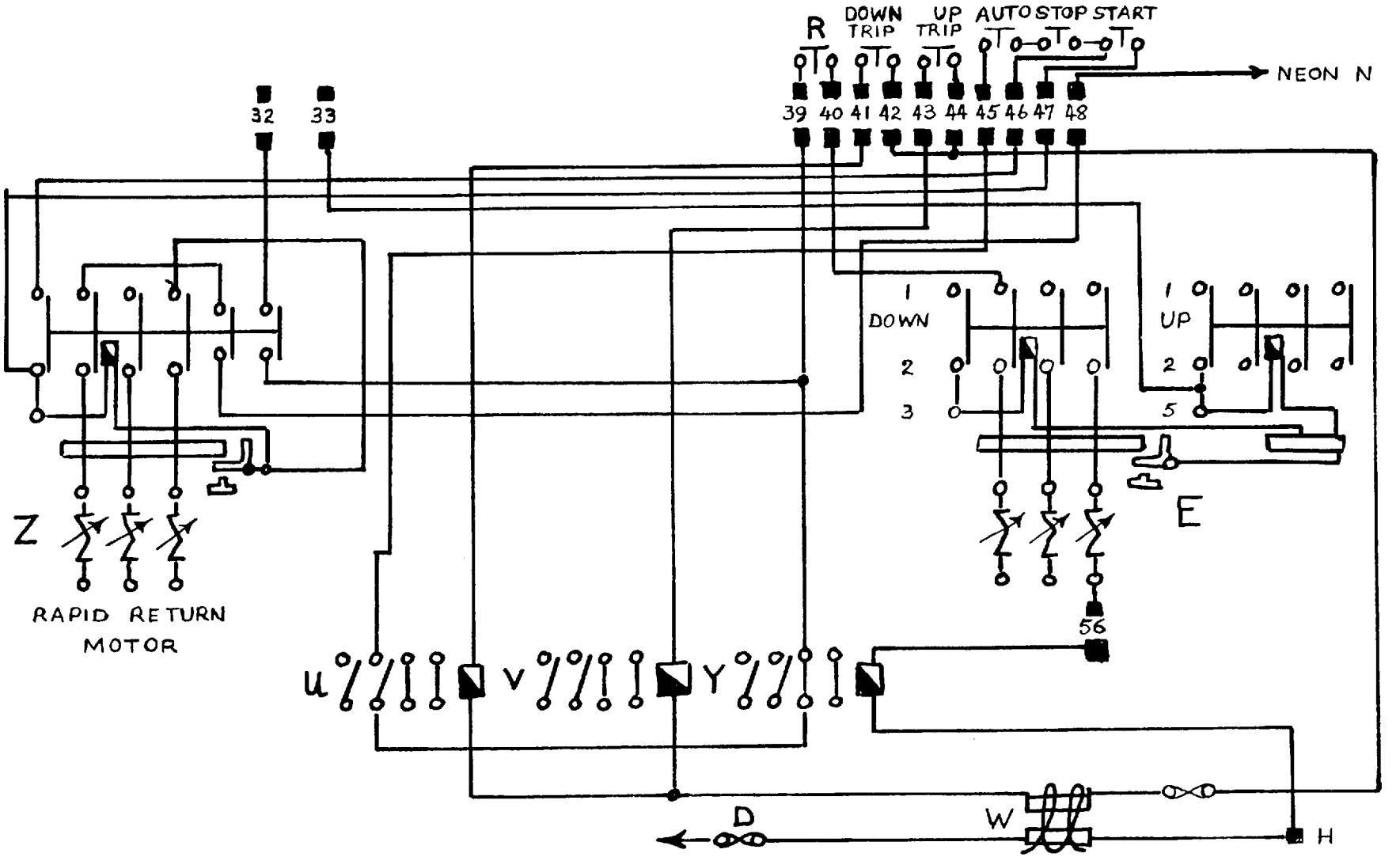
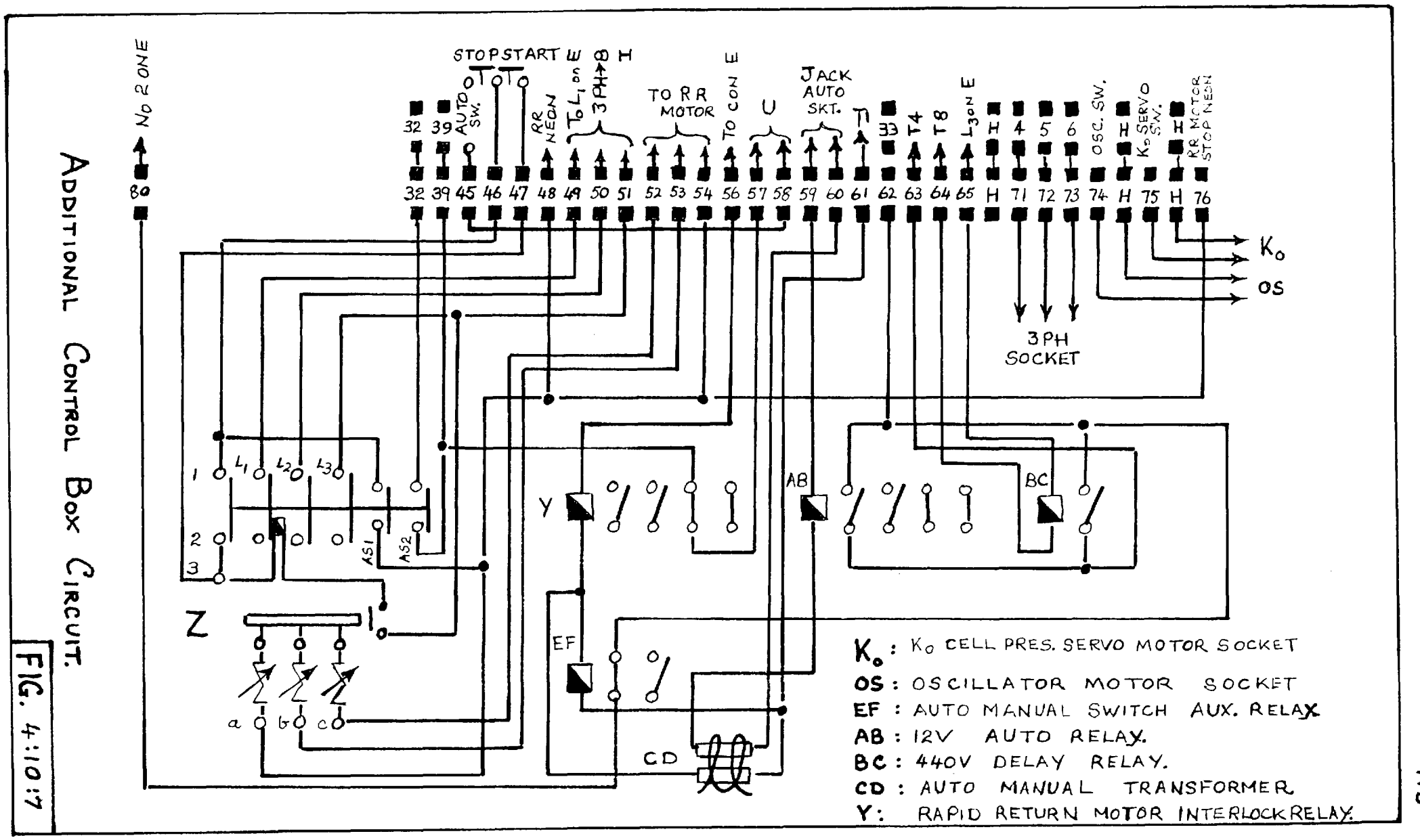


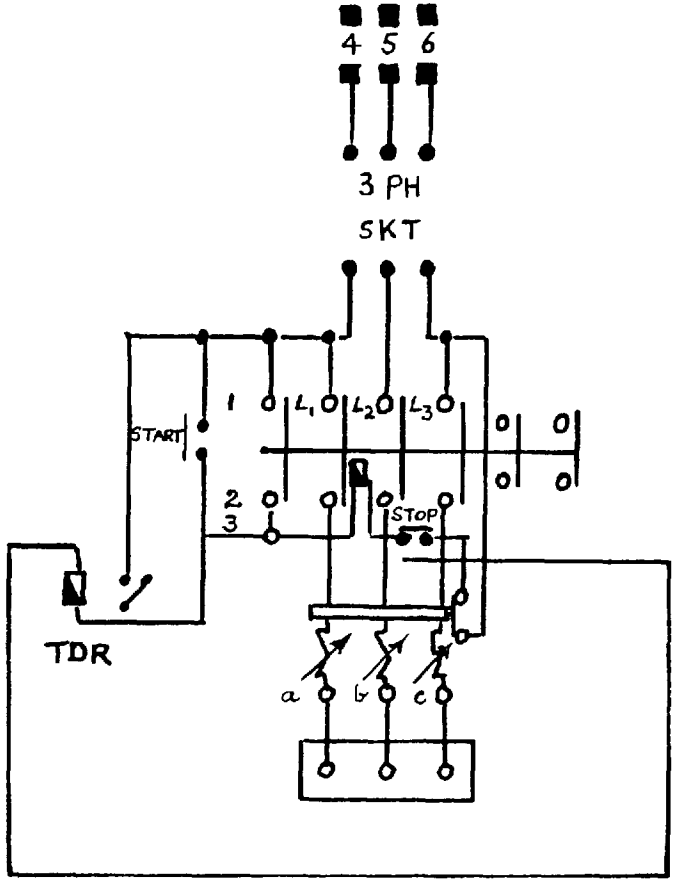
FIG. 4:10:6

RAPID RETURN MOTOR CIRCUIT.



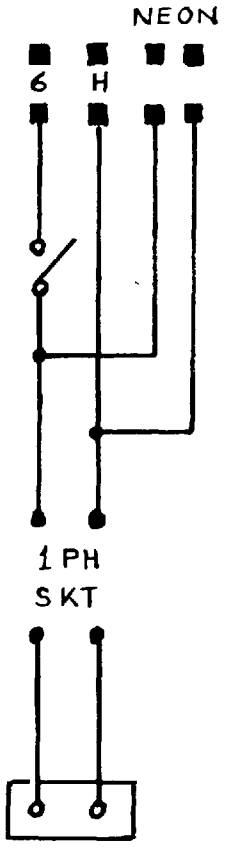
ADDITIONAL CONTROL BOX CIRCUIT.

FIG. 4:10:7

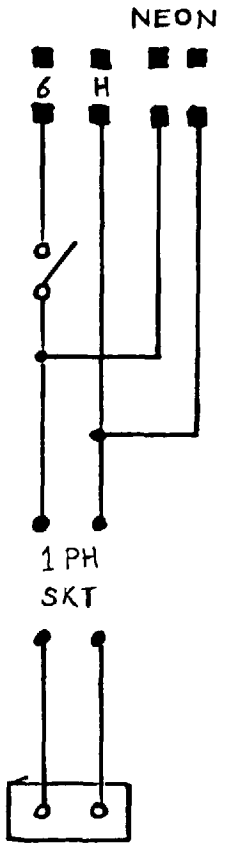


TDR: TIME DELAY RELAY

PRESSURE PUMP MOTOR CIRCUIT

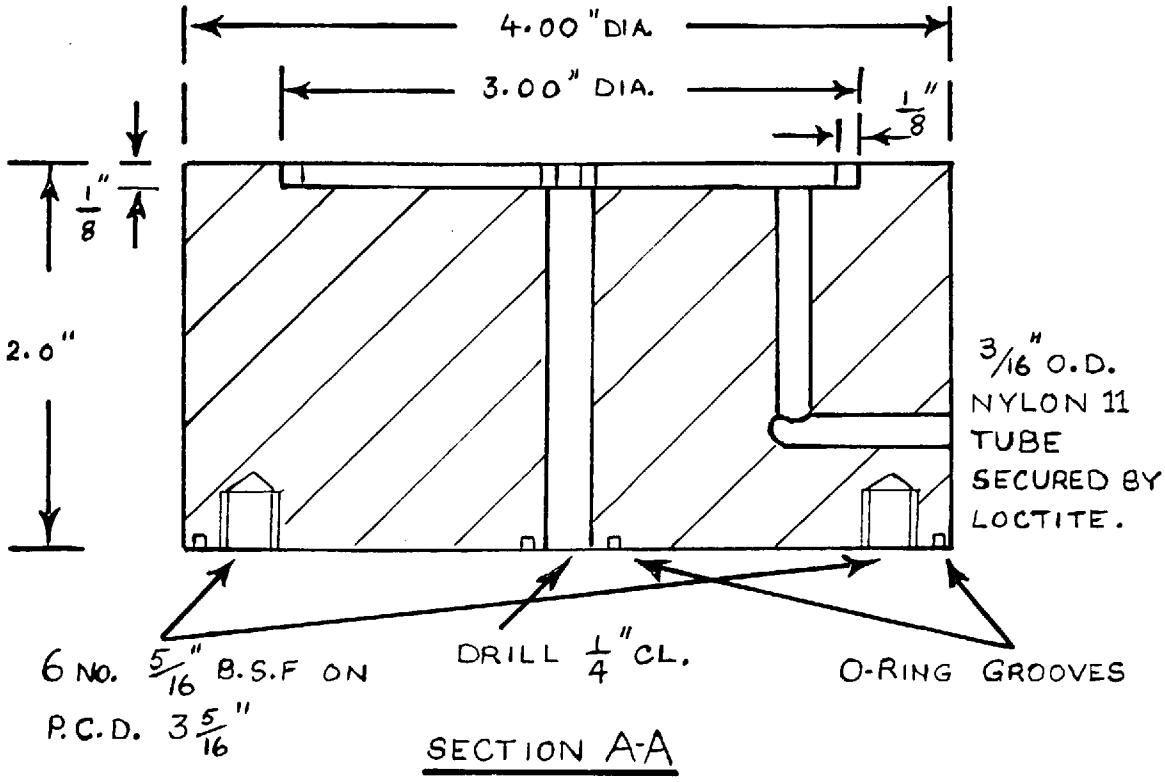


OSCILLATOR MOTOR CIRCUIT

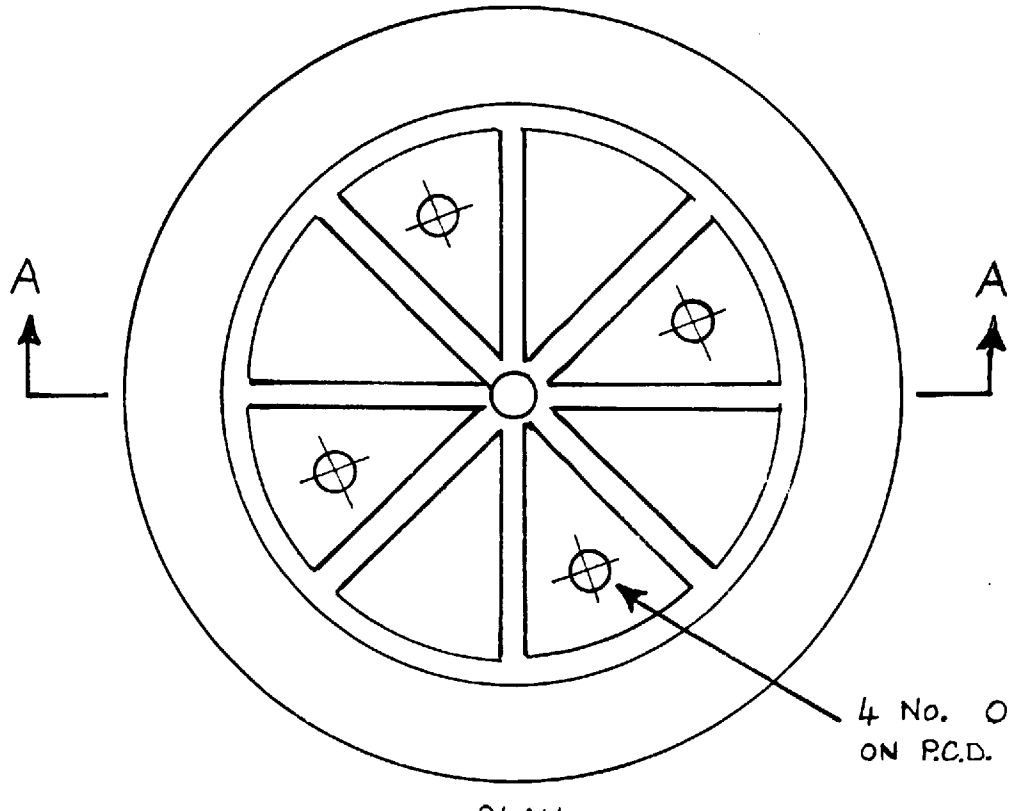


K_o CELL PRESSURE SERVO MOTOR CIRCUIT

FIG. 4:10:8



SECTION A-A

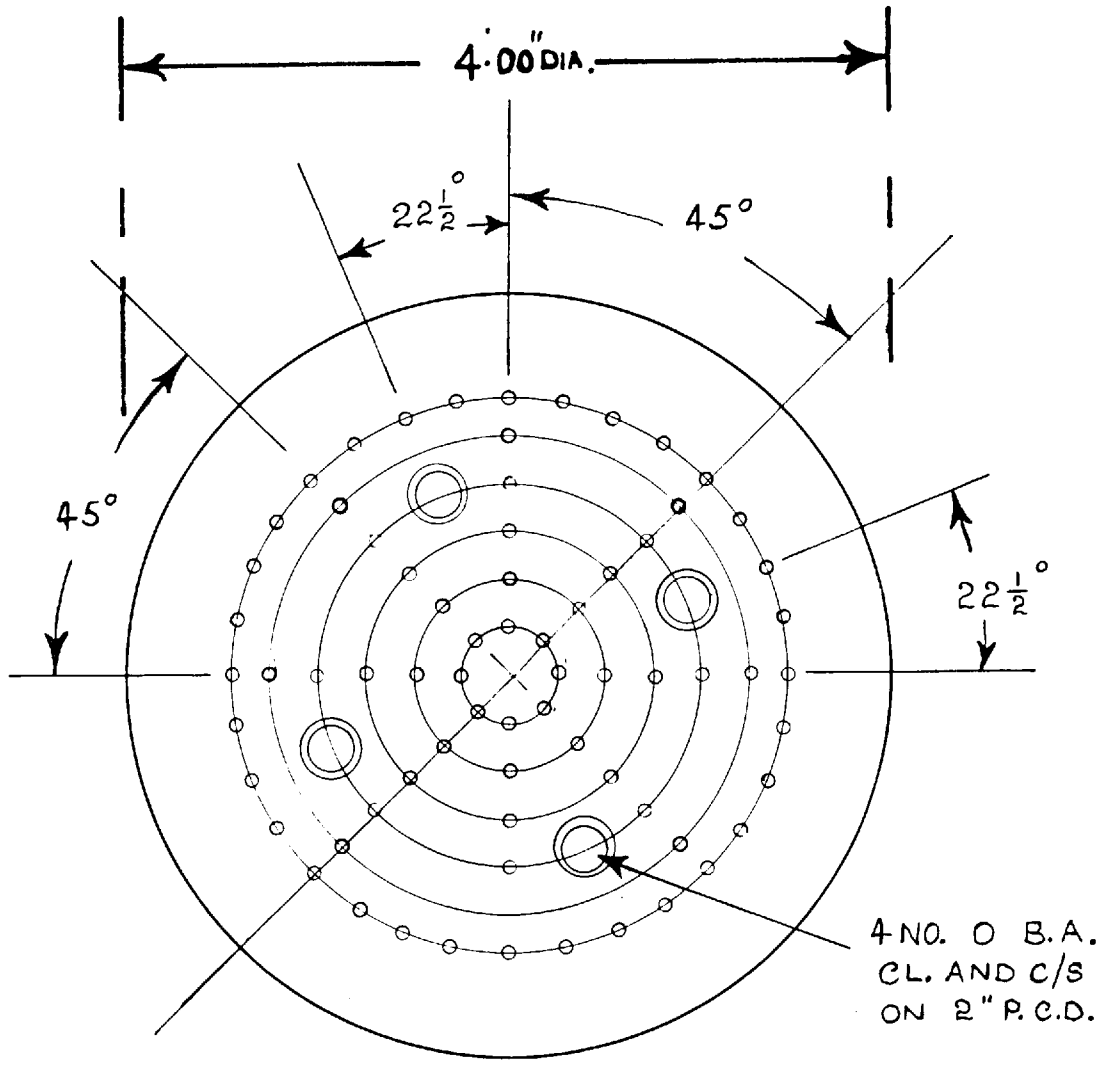


PLAN

MATERIAL : MILD STEEL CADMIUM PLATED.

4 INS. DIA. PEDESTAL

FIG. 4:13:1:1



NOTE.

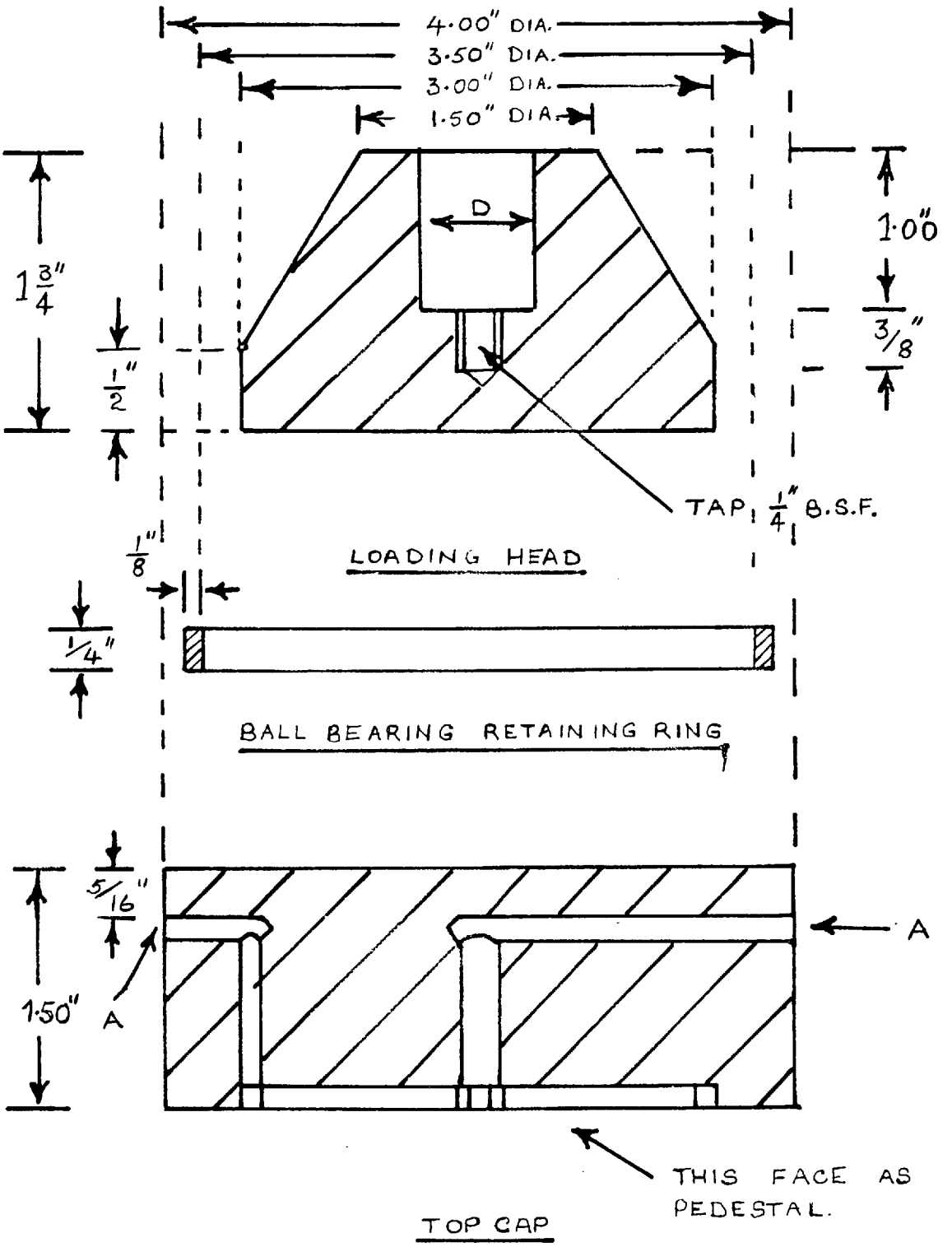
HOLES $\frac{1}{16}$" DIA.

P.C.D	$\frac{1}{2}$"	8 NO.
"	1"	8 "
"	1½"	8 "
"	2"	8 "
"	2½"	8 "
"	2 7/8"	32 "

2 OFF $\frac{1}{16}$" STAINLESS STEEL SHEET.

PERFORATED END PLATES

FIG. 4:13:1:2



NOTE: ALL PARTS MILD STEEL AND CADMIUM PLATED.

LOADING HEAD AND TOP CAP SURFACE HARDENED

D BORE TO SUIT EXISTING RAM.

A DRILL 3/16" CLEARANCE AND SECURE NYLON 11 LEADS WITH LOCTITE RETAINING COMPOUND.

FIG. 4:13:1:3



THE LARGE SCALE TRIAXIAL APPARATUS.

PLATE. 4:2

CHAPTER 5

THE MATERIAL

(5:1) The Materials Tested (Plate 5:1)

Five materials have been tested in the large scale triaxial apparatus.

Various triaxial tests have been performed on Silurian cleaved mudstone from Llyn Brianne Dam, granitic basic gneiss from Venemo Dam and two uniform gradings of chert gravel, which were used for an aircraft arresting investigation by The Royal Aircraft Establishment at Farnborough.

Undrained tests were carried out on 12" diameter by 24" high undisturbed samples of stiff, fissured, blue London clay. The results are reported by Agarwal (1967).

A dissipation test was performed on an isotropically consolidated 12" diameter by 12" high sample of Maesglas boulder clay for the core of Llyn Brianne Dam. The result is reported in an internal report of Binnie and Partners in 1967.

(5:2) The Silurian Cleaved Mudstone. (Plate 5:1)

The material is highly cleaved and jointed.

The bedding planes are at about 70° to the cleavage along which the material splits.

(5:2:1) Mineral Composition

The predominant mineral is chlorite, a complex, hydrated, alumina silicate, with variable amounts of iron, magnesium and other elements.

The chlorite is both fine and coarse. The coarse crystals appear orientated parallel to the bedding and the fine crystals are randomly orientated.

Sericite appears orientated parallel to the cleavage and as it has a similar chemical composition to chlorite may be due, in part, to low grade metamorphism.

(5:2:2) Average Composition in Thin Section

Sericite	20.0%
Fine Chlorite	63.2%
Coarse Chlorite	13.2%
Quartz	3.0%
Calcite	0.1%
Pyrite	0.5%

Table 5:2:2. Average composition of silurian cleaved mudstone.

The Calcite was originally detrital material which has, subsequently, been recrystallised. When very abundant, calcite can be leached out by acid waters, which may also lead to oxidation and expansion of pyrite.

However, the mudstone is very similar to the material used for the embankment dams of the Vianden pump storage scheme and whose durability is displayed inthe railway embankments in Luxembourg.

(5:2:3) Unconfined Compressive Strength

Difficulty was experienced in preparing cores for unconfined compression tests especially normal to the cleavage as the shear strength on the cleavage planes was exceeded by the torque of the coring tool.

Sample	Direction of sample w.r.t. cleavage	Dimensions height x dia.	Compression strength p.s.i.	Remarks
1	parallel	3" x 1.5"	4,118	All
2	parallel	3" x 1.5"	3,590	samples
3	normal	2.2" x 2"	15,650	kept
4	normal	1.9" x 2"	21,150	under
5	parallel	3" x 1.5"	3,390	water
6	45°	3" x 1.5"	12,750	until tested.

Table 5:2:3 Unconfined compressive strength of silurian cleaved mudstone.

(5:2:4) Particle Shape.

A random sample of particles retained on each size of sieve used in the grading analysis was photographed and the prints were then either reduced or enlarged so that all particles appeared about the same size.

The ratio of length to breadth was then measured for each particle and the mean ratio for material retained on various sieves is given below.

B.S.Sieves		Ratio Length/ Width
Passing	Retained	
3"	1½"	1.46
1½"	¾"	1.66
¾"	⅜"	1.23
⅜"	3/16"	1.62
3/16"	No.7	1.67
No.7	No.14	1.39
No.14	No.25	1.47
No.25	No.52	1.34

table continued:

B.S.Sieves		Ratio Length / Width
Passing -	Retained	
No.52	No.100	1.26
No.100	-	

Table 5:2:4 Particle shape of Silurian cleaved mudstone.

In general, the particles were flat and oblong, with coarse, jagged edges. There was a tendancy for the very fine material to adhere tightly to the surface of larger particles and, as a result, particles passing the No.14 B.S.sieve appeared to become more rounded with reduction in size.

The ratio of particle thickness to width was approximately four.

The fine material formed a cohesive paste on the addition of water.

(5:2:5) Material Treatment Prior to Testing

All the material used for the testing programme was obtained from a quarry which was opened up near to the proposed site of Llyn Brianne Dam.

Excavation was by blasting, using polar ammon gelignite, and all the material obtained came from within 30' of the original ground surface.

The majority of the material for the actual dam will be quarried at a greater depth.

After quarrying, the material was loaded into dump trucks by a front end loader, whence it was hauled to a trial embankment, dumped, levelled and tracked by bulldozer and compacted in layers varying from 18" to 6' by an $8\frac{1}{2}$ tons ABG vibrating roller.

Insitu density measurements were made in the trial embankment and the excavated material passing a 3" square mesh was sent to the laboratory for testing under triaxial stress conditions.

On arrival at the laboratory, the material was oven dried and a sieve analysis was carried out by hand. This proved to be excessively tedious and dusty. A few samples were treated in this manner and subsequently a bulk sample of about 5 tons was sieved by Soil Mechanics Ltd. at the Cement and Concrete Association's laboratory and the material was then delivered to the laboratory in individual sizes and in polythene bags.

Considerable breakdown of the larger particles was noticed, simply due to handling of the bags when loading and unloading the lorry on which they were transported. Further breakdown occurred every time a bag of material was moved.

Storage space presented a problem and the material was kept in polythene bags, inside dustbins, on the roof of the building.

(5:3) The Granite Gneiss. (Plate 5:1)

The rock is uniformly coarse grained and of mottled, white and black appearance and with a gneissose structure.

Mica, hornblende, quartz, and felspar are clearly visible.

(5:3:1) Average Composition in Thin Section

Orthoclase	27%	Felspar	57%
Albite	15%		
Microcline & Microperthite	15%		
Quartz	25%		
Biotite	12%		
Hornblende	4%		

Table 5:3:1 Average composition of granitic gneiss

The orthoclase is intimately interlocked with the quartz and occurs as anhedral crystals which all show slight decomposition to Kaolinite.

Quartz occurs entirely as anhedral crystals, forming an irregular mosaic with the felspathic minerals. Gas and liquid inclusions are common.

The plagioclase felspar is present as albite, which occurs in lath shaped crystals exhibiting typical polysynthetic twinning. This mineral has also undergone very slight kaolinisation.

Anhedral microcline and microperthite comprise the remaining felspar components and are found in intimate association with the other felspars.

Green and brown biotite are found as lath shaped crystals, occasionally containing zircons and the associated pleochroic haloes. It is found in well defined linear zones, separated by zones containing quartz and the above felspathic minerals. Within each zone the long axes of the biotite laths are orientated within a range of 45°.

Green hornblende, almost an accessary mineral, rarely exhibits good crystal form and is also confined to well defined linear zones, and always with biotite in association.

Traces of sphene, ilmenite and its alteration product, leucoscene, apatite and zircon occur in the granite.

The felspathic minerals are interlocked with quartz in a tight mosaic of typical grain size, approximately 1 mm. Clearly defined zones of orientated biotite and biotite and hornblende, alternating with more felspathic regions, give rise to the pronounced gneissose structure.

The zones of mica also give rise to planes of weakness.

(5:3:2) Unconfined Compression Strength

Several large lumps were cored to produce samples approximately 1½" diameter by 3" high.

The load axis was approximately 45° to schistosity. Some samples failed by vertical splitting and others along the schistosity.

The average uniaxial strength for dry samples was 23,900 p.s.i. and the shear wave velocity along the loading axis was 14,900 ft/sec.

The average uniaxial strength of samples tested in air after soaking in water for 4 days was 23,420 lbs. per square inch. This average value does not include one sample which failed along a joint at only 3,717 p.s.i.

(5:3:3) Particle Shape

The particles are highly angular and the proportions appear to remain fairly constant for all fractions.

Unlike the mudstone, the fine material does not adhere to the surface of the larger particles and does not form a cohesive paste.

B.S. Sieves Passing	-	Retained	Ratio Length / Width
-3"	+	1½"	1.26
-1½"	+	¾"	1.41
-¾"	+	⅜"	1.39
-⅜"	+	3/16"	1.44
-3/16"	+	No. 7	1.26
-No. 7	+	No.14	1.61
-No.14	+	No.25	1.43
-No.25	+	No.52	1.38
-No.52	+	No.100	1.42

Table 5:3:3. Particle shape of granitic gneiss.

A certain percentage of particles retained on the 1½" B.S.sieve had a length to width ratio of 4 or more and had to be discarded as they were far too large to be used in the testing apparatus.

(5:3:4) Material Treatment Prior to Testing

The Venemo Dam (Holestol, 1965) forms part of the Tokke Hydro-Electric Development in Norway (6)* The rockfill for the dam came from the Hyljelihyl - Venemo and Venemo - Totak tunnels, the surplus tunnel spoil being tipped to waste. Six tons of this surplus material (passing the 3" square sieve) was shipped in oil drums to the Cement and Concrete Association.

The total length of the tunnels was about 15 kilometers. As a result, varied rock types were encountered and several particles in our consignment were just quartz. However, the above mineral composition is considered to be a fair average for the material received.

A bulk sieve analysis of the material was carried out at the Cement and Concrete Association. The sample was slightly moist and the fines had to be dried by spreading them into thin layers on the floor and leaving them overnight prior to sieving. The floor was very clean and there was no visible contamination.

The segregates were transported to the laboratory where they were weighed to obtain the bulk grading. As the moisture content of the segregates varied there was a slight error in this grading, though probably no more than 1%.

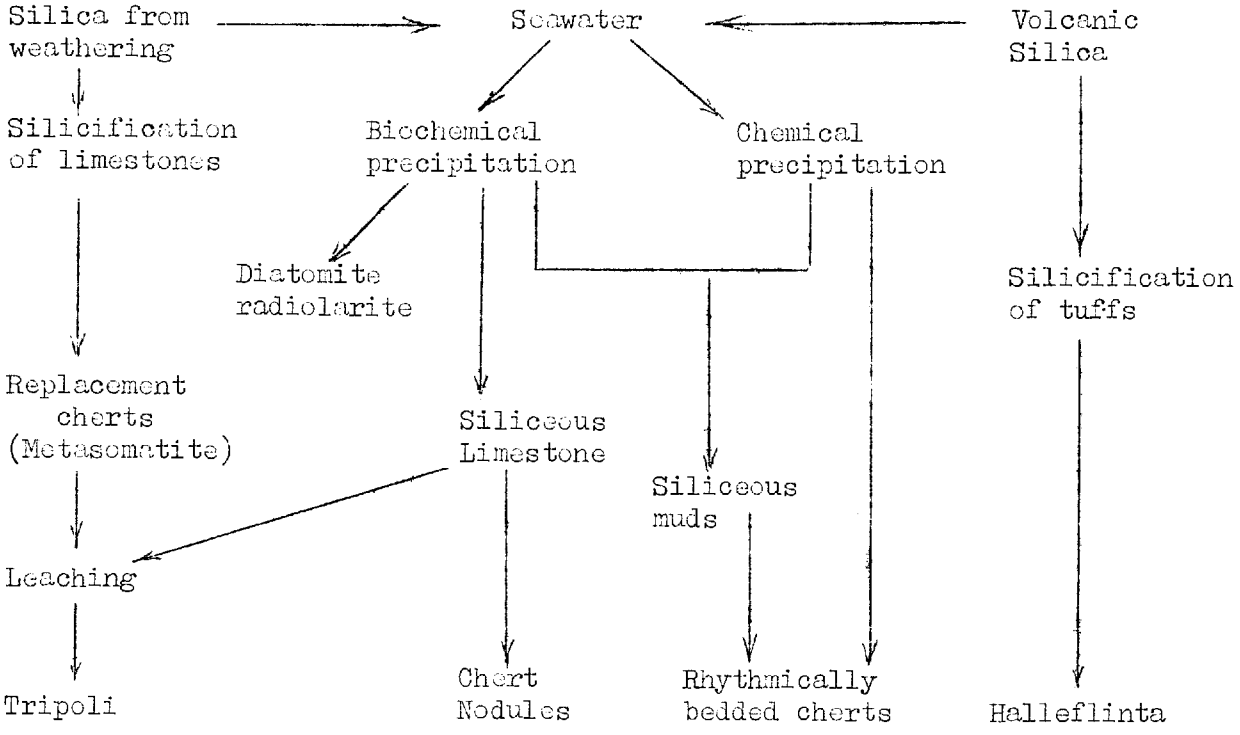
They were then stored in polythene bags in dustbins until required.

Although a dust extraction plant was functioning during the sieving operations, it was essential to wear a breathing mask as well.

(5:4) The Chert Gravel (Plate 5:1)

The formation of chert is still a controversial subject. Some authorities believe it was formed by replacement of limestone by percolating solutions and, therefore, of post depositional origin, whilst others believe it was formed by direct precipitation of masses of silica gel in sea water.

The various theories are set out in the cycle below:



(Pettijohn, 1957)

Chert is a dense, crystalline rock composed of chalcedony (microcrystalline fibrous silica and micro fibrous amorphous silica or opal and cryptocrystalline quartz).

In general the particles were cream, yellow, brown and black in colour and sometimes yellow or brown outside and black inside.

Some particles were smooth and rounded, like pebbles on a shingle whilst others were highly irregular, tuberous and rounded bodies.

A very few particles had a scariaceous texture and were cream in colour, with a porous, dry, earthy feel and appearance. A considerably higher value of ϕ_μ was recorded for these particles than for the dense rounded ones for the same normal load.

(5:5) Scaling of Gradings

The aim of the research programme was to compare the behaviour of various sizes of samples of rockfill under triaxial stress conditions, the ultimate goal being the prediction of field behaviour from small scale laboratory testing procedures.

In order to compare the various sizes of the samples tested the gradings used in each case had to be scaled.

However, for geometrically similar packings, in two different sample sizes with the same applied principal stresses, the contact forces between the grains are not equal.

If D is the Sample diameter and d is the nominal particle size:

The number of particles in any cross-section is proportioned to:	Force transmitted across the cross-section for any given pressure is proportioned to:
Small sample $\left(\frac{D_1}{d_1}\right)^2$ = constant	D_1^2
Large sample $\left(\frac{D_2}{d_2}\right)^2$ = constant	D_2^2

Where D_1 is the small sample diameter and D_2 is the large sample diameter.

Hence the average intergranular forces in the larger sample are $\left(\frac{D_2}{D_1}\right)^2$ times as great as in the smaller sample.

The stresses, though, are probably very similar as the material surface will yield until the product of contact area and compressive strength is equal to the applied load.

Furthermore the larger particles have a larger proportion of flaws and fissures than the smaller particles which, consequently, have a greater unit strength.

The distribution of the fissures is probably a function of the initial stress history and stress release and shattering due to blasting.

The compressive strength will not only vary according to the type of materials in contact but also with the shape of the surfaces in contact. A pyramid point contact will have a lower compressive strength than rounded or almost flat contacts because of the very different degrees of support afforded by the bulk of the surrounding material.

This will lead, in general, to greater deformation of angular material than of rounded material, for similar loading conditions.

In large and small samples with geometrically similar particle distribution and the same mean applied principal stresses, the greater inter-particle loading in the larger sample will lead to greater deformation. If, however, the unit shear strength of all the grains is similar the behaviour of the samples should also be very similar as the shear strength of the particles will be dependent on the square of their nominal size and, hence, proportional to the square of the sample diameter.

The effect of the increase in fines, in a large sample due to the increased breakdown because of the higher contact loading, will depend on the initial grading. In a grading particularly short of fines the additional particles may have little or no effect as they may just rest in the voids, leaving the larger particles to carry and transmit the applied loads.

Alternatively, if a large proportion of fines already exists, the dilatancy of the sample will be affected.

The effect on the sample dilatancy however, will be offset to a certain extent by the increased number of particles transmitting the load because there will be a threshold of load below which little contact point breakdown will occur.

A certain amount of breakdown was noticed during the bulk sieving as particles split when subjected to vibration.

(5:5:1) Chert Scaling

It was not possible to scale the chert particles because breakdown did not yield particles representative of the initial material.

In general, failure was explosive, giving a conchoidal and splintery fracture.

The resulting material lacerated membranes and could not be handled without protective gloves.

As a result no small scale tests were performed on chert.

(5:6) Gradings Used in the Tests

All the basic gradings are plotted in Figs.5:6:1, 5:6:2 and 5:6:3.

Grading A is the mean of all the gradings used for the drained shear

tests on the first nine 12" diameter samples of Silurian cleaved mudstone.

The testing programme on the Silurian cleaved mudstone was inconvenienced by numerous membrane punctures at the higher confining pressures and the particle breakdown reduced the permeability of the samples very considerably.

Many special gradings were therefore used and they are set out in Table 5:6:1.

(5:7) Interparticle Friction

It has been appreciated for many years that the angle of friction ϕ_μ between the surfaces of particles is less than the angle of internal friction ϕ_f' of a dense mixture of particles when measured in the drained triaxial test at normal stresses.

Caquot (1934) produced a theoretical expression for the relationship between ϕ_μ and the angle of internal friction at constant volume (ϕ_{cv}) under plane strain conditions by considering the forces on spherical particles.

$$\tan \phi_{cv} = \tfrac{1}{2}\pi \tan \phi_\mu$$

Bishop (1954) derived the following expression for triaxial conditions:

$$\sin \phi_{cv} = \frac{15 \tan \phi_\mu}{10 + 3 \tan \phi_\mu}$$

Rowe (1962) expanded the theory further to relate ϕ_f' with dilatancy.

An investigation by Horn and Deere (1962) showed that the coefficient of friction between mineral grains varied with the finish of the contact surfaces and the fluid present on those surfaces.

They found that if water was placed between polished surfaces of quartz or felspar it acted as an antilubricant and increased the coefficient of friction. If the surfaces were rough, the effect was considerably diminished. The rough surfaces, however, were produced by etching or polishing with No.240 carborundum grit and so could not be expected to be as rough as the interparticle contacts in a rockfill.

If a cohesionless material is sheared in the saturated drained condition it displays a lower angle of internal shearing resistance than when it is sheared in the dry condition. This may be due to several factors, one of which is the weakening of the surface of rocks due to the reduction in surface energy due to contact with water (Rehbinder and Lichtman,1957)

(5:7:1) Measurement of the Coefficient of Interparticle Friction of Silurian Cleaved Mudstone.

To determine the coefficient of interparticle friction of the Silurian cleaved mudstone individual particles were selected and mounted in a standard shear box.

One particle, with face dimensions about 1" by 2", was mounted in the lower half of the shear box using Polyfilla and such that the surface was in the plane of shearing. A second smaller matching particle was similarly positioned in the top box but, in this case, the interior faces of the box were lined with silicone grease prior to pouring the Polyfilla. Care was taken to see that no Polyfilla contaminated the shearing surfaces and it was also tapered away from the shear plane so that the only contacts during the shearing operation would be mudstone to mudstone.

The lower box was positioned in the shear apparatus and tap water was added until the shear plane was submerged. The top box was then carefully positioned and a normal load of 170 pounds was applied to the sample.

Shearing was carried out by pushing one particle over the other at 64×10^{-4} inches per minute before allowing for proving ring deformation.

Dilatancy was measured by a 1/10,000" dial gauge.

The bedding planes of the mudstone were at an angle of about 60° to the cleavage, along which it most easily broke. Shearing was, therefore, carried out on the cleavage surfaces and parallel to, normal to and across the bedding planes as shown in Fig.5:7:1.

Dilatancy was almost negligible in most cases but a polygon of forces was drawn in order to determine the coefficient of friction.

No special surface treatment was applied to the samples and they were sheared in their original state.

No stick slip motion was observed. This is often a function of the stiffness of the testing apparatus (Bowden and Tabor 1956).

Sample No.	Direction of shearing w.r.t. bedding	Condition	ϕ_μ
3	parallel	submerged	26.3°
7	normal	dry	29.7°
8	normal	submerged	24.9°
9	parallel	submerged	24.1°
2	across	submerged	23.6°
4	parallel	submerged	22.9°
1	normal	submerged	25.9°

Table. 5:7:1. Values of the angle of interparticle friction for Silurian cleaved mudstone. (See also Figs.5:7:1 and 5:7:2a)

(5:7:2) Measurement of the Coefficient of Interparticle Friction of Chert

To measure the coefficient of interparticle friction of chert a series of direct shear tests was carried out in a similar manner to that for the

silurian cleaved mudstone.

All the samples were tested submerged in tap water and the normal load was 100 pounds in each case.

A stick slip motion was observed after a rapid rise towards peak resistance.

One sample, with a soft, porous surface, displayed a considerably higher coefficient of interparticle friction than the remaining very hard smooth surfaced particles. (Table 5:7:2, Figs.5:7:2b amd 2c).

Sample No.	Description	ϕ_μ
1	Smooth, hard, yellow/brown	11.4°
2	Smooth, hard, grey	14.8°
3	Rounded, soft porous, yellow/grey	40.5°
4	Smooth, hard, shiny, yellow/brown	14.5°
5	Rounded, shiny black & smooth hard, flat & shiny yellow.	18.1°

Table.5:7:2 Values of the angle of interparticle friction for chert submerged.

Results of measurements of the coefficient of interparticle friction on granitic gneiss are given in Table 5:7:3 and are reported by Pigeon(1969) &

Normal load: 13.41 lbs.		
Test	Condition	ϕ_μ
1	submerged	35°
2	submerged	35.3°
3	submerged	35°
4	submerged	36.1°
5	air dry	36.4°
6	air dry	36.1°
7	air dry	37.7°
8	air dry	37.5

Table 5:7:3 Values of the angle of interparticle friction for granitic gneiss.

(5:8) Relative Density Determinations

In 1948 Kolbuszewski suggested that a reference property should be available for cohesionless soils in the same way that Atterberg Limits have become a useful guide to the behaviour of plastic soils.

He proposed an index relating the insitu porosity to the maximum and minimum porosities at which any particular insitu grading could exist.

This index he termed relative density.

As the peak shear strength of a sand or rockfill is to some extent, dependant on its dry density, it would appear that a suitable basis on which to compare various materials would be at a particular relative density.

After experimenting with numerous pouring techniques Kolbuszewski eventually obtained a consistent minimum dry density by placing 200 grms. of material in a 2,000 ccs corked measuring cylinder, inverting it and then righting it and measuring the volume displaced. The maximum dry density was achieved by vibration.

Several problems arise when determining the relative densities of a rockfill.

The wide range of maximum particle sizes demands a similar range of measuring container sizes. Inverting a measuring cylinder to obtain the minimum density limit becomes impractical and careful pouring methods are resorted to, using different sizes of pouring utensil, from a miniature scoop to a coal shovel, depending on the maximum grain size involved.

The maximum density limit is more difficult to achieve because of the more sophisticated machinery involved and the number of possible variables.

The maximum density limit may be determined by vibration of the mould and sample with or without a surcharge or by impact compaction. The amplitude, frequency and time of vibration may be varied to give varying results for any particular soil or rockfill. In fact, the amplitude, frequency surcharge and time must be varied to suit the soil type and its grading.

The attrition due to vibration or compaction causes breakdown which, in turn, alters the initial grading and, hence, the maximum density achievable.

The U.S.Dept.of the Interior, Bureau of Reclamation, has its own standards for maximum and minimum density determinations (7)* as do the U.S. Corps of Engineers, who use Density Ratio $D_r = \frac{D - Dmin}{Dmax - Dmin.}$

Many other State Authorities use these methods or adopt their own.

The exact significance of the maximum density limit is also arguable in the case of a grading having few fines which merely rest in the voids between large particles and play little part in the shear behaviour of the soil at low stresses.

The maximum density test is further discussed by Pettibone (1964), B.B.Gordon (1964), Winnitey (1964) and Burmister (1948 and 1964), who suggest that comprehensive investigations are urgently needed to improve compaction testing and establish adequate criteria for field control.

It was decided to determine the maximum and minimum dry densities of

the gradings which were used in the triaxial tests on 4" diameter and 1½" diameter samples of silurian cleaved mudstone and granitic gneiss.

(5:8:1) Minimum Density

The required gradings were made up by weighing out dry material and then the segregates were thoroughly mixed with a scoop.

A 4" internal diameter by 8" high split mould was fixed to a standard Procter base. This size of mould was chosen because it had the same proportions and size as the 4" diameter samples. It was also used for the gradings used in the 1½" diameter samples so that material could be placed by scoop at the base. If a 1½" diameter mould had been used pouring would have been necessary, leading to segregation of the graded material.

Material was placed slowly and carefully in layers in the mould. At the top an attempt was made to finish with the mould rim so that excess material would not have to be removed, thus disturbing the pack.

The material was weighed and the dry density calculated. The process was repeated several times with the same grading and material.

(5:8:2) Maximum Density

The required gradings were made up as for the minimum density determinations and the same mould was used. In this case though, new material was used for each maximum density determination on the same grading to limit the effects of particle breakdown.

The samples were compacted in 3 equal layers. A steel billet, 4" thick and a loose fit in the mould, was placed above each layer and the top of the billet was vibrated for one minute with a medium size Kango Electric Hammer, Type F, fitted with a 2" diameter Swivel Head Vibrating Tool, Part No. 624.

The gradings used and the results of the tests are given in Table 5:8a

Relative density limits for the 12" diameter samples were assumed from test results and field data. The assumed values are given in Table 5:8b.

Inconsistencies were noticed between the dry densities obtained in the 12" diameter by 24" high triaxial samples and the 24" diameter by 12" thick oedometer samples.

Compaction of the top two or three inches was always difficult because the material sheared or bounced about with the result that the top four inches were always looser than the rest. This, of course, had a larger effect on the oedometer samples because of the adverse sample height to diameter ratio. The boundary conditions also varied, the boundaries being steel, cast iron or bronze in oedometers and rubber, backed by felt, for

triaxial samples.

(5:9) Specific Gravity

The specific gravities of the particles of silurian cleaved mudstone granitic gneiss and chert were determined by the standard method.

The results are given in Table 5:9

Grading	Min. Density	Max.Density
K	91.7	125.3
L	94.2	128.2
N	95.2	129.8
C	98.9	142.0
D	104.0	143.2
E	98.1	138.6

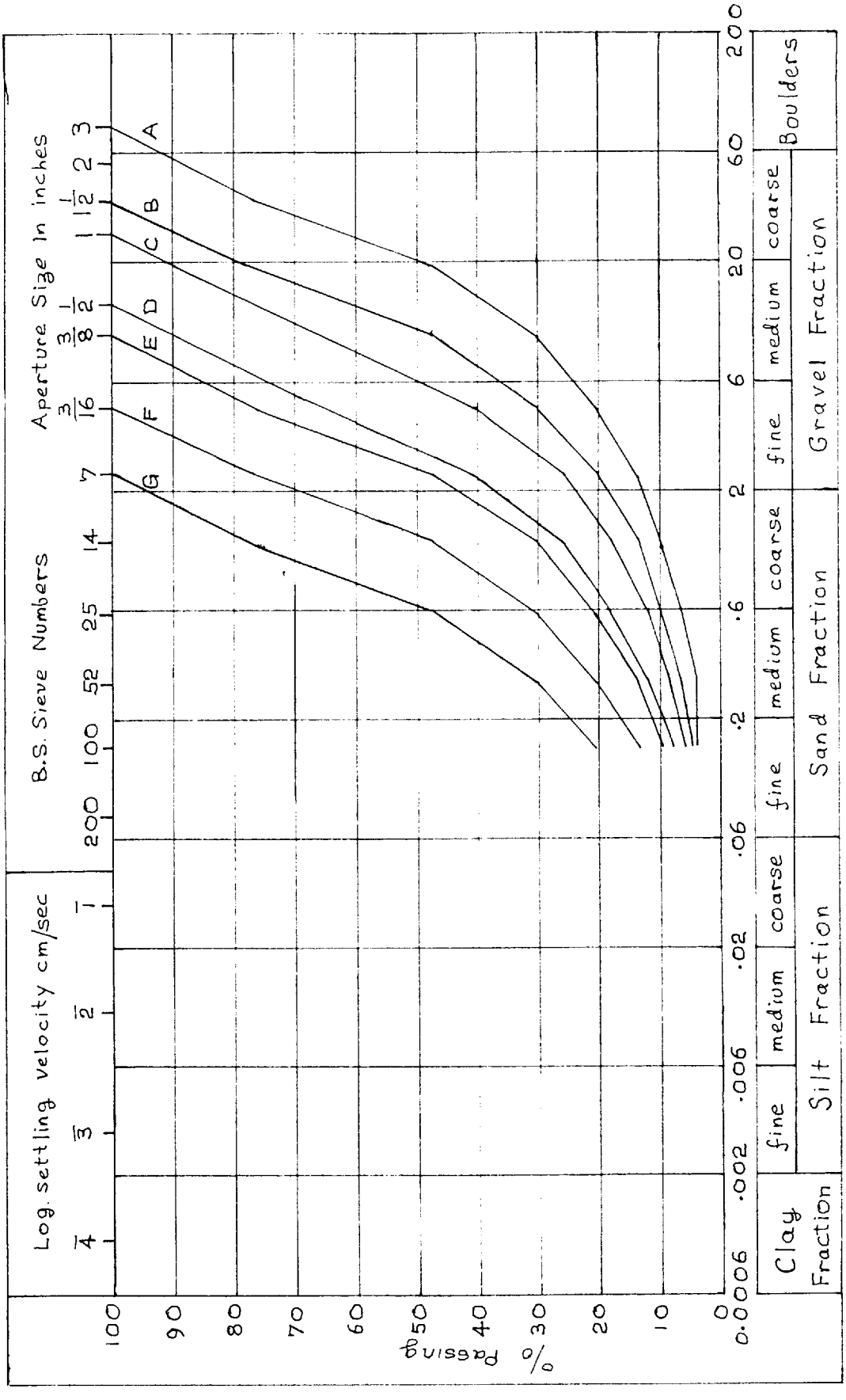
Table 5:8a: Maximum and Minimum Densities Obtained.

Grading	Min. Density	Max. Density
H	91.7	137.1
J	94.2	137.1
M	94.2	128.2
O	95.2	129.8
F	98.1	138.6
A	98.9	143.0
B	98.9	143.0
T	98.9	142.0
U	100.0	146.0

Table 5:8b: Assumed Maximum and Minimum Densities

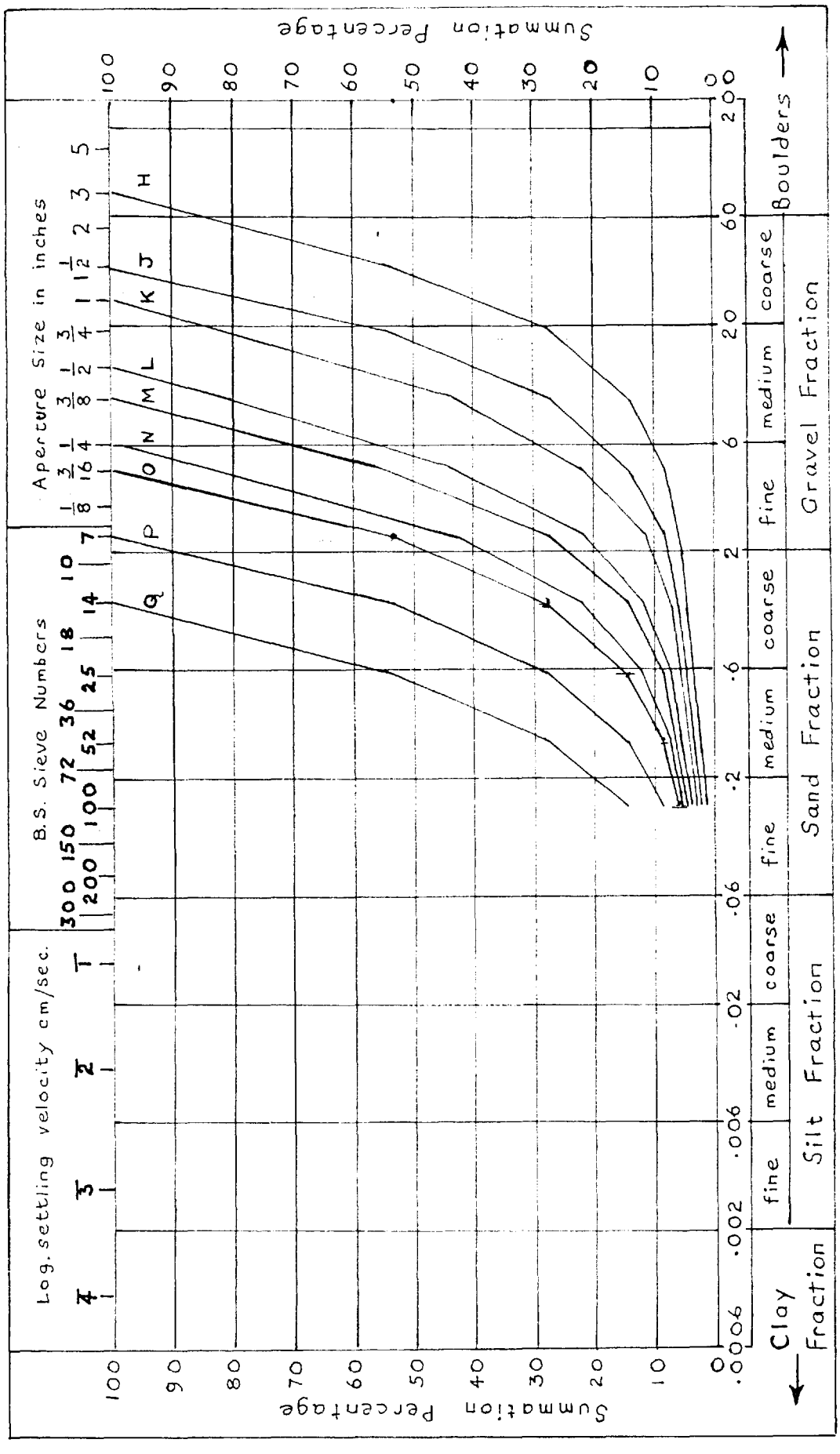
Particle size	Silurian cleaved mudstone	Granitic gneiss	Chert
< No.7	2.76	2.66	
> $1\frac{1}{2}$"	2.77		

Table 5:9 Specific Gravity.



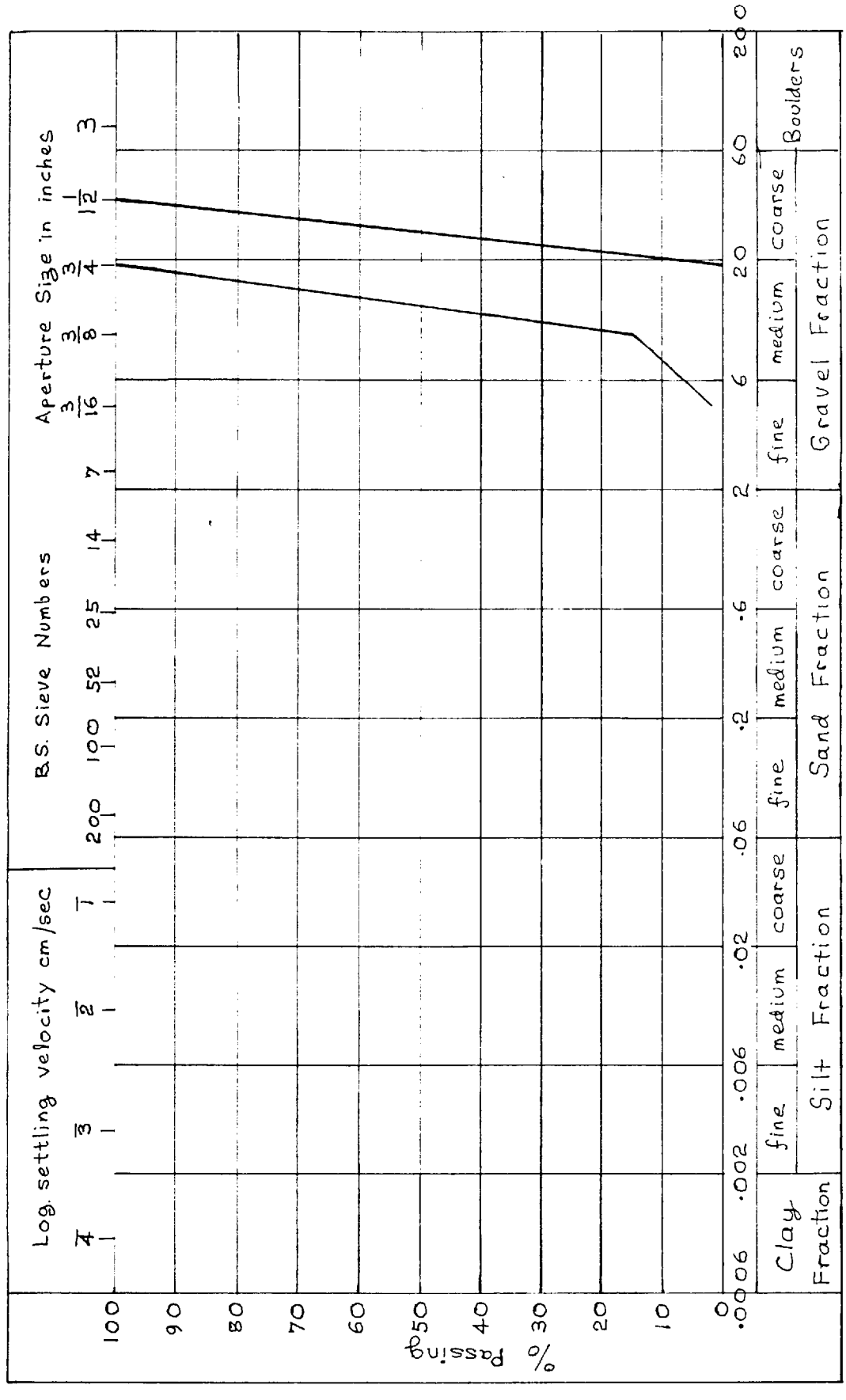
SILURIAN CLEAVED MUDSTONE STANDARD GRADINGS

FIG. 5:6:1



GRANITIC GNEISS STANDARD GRADINGS.

FIG. 5:6:2



CHERT GRADINGS.

FIG. 5:6:3

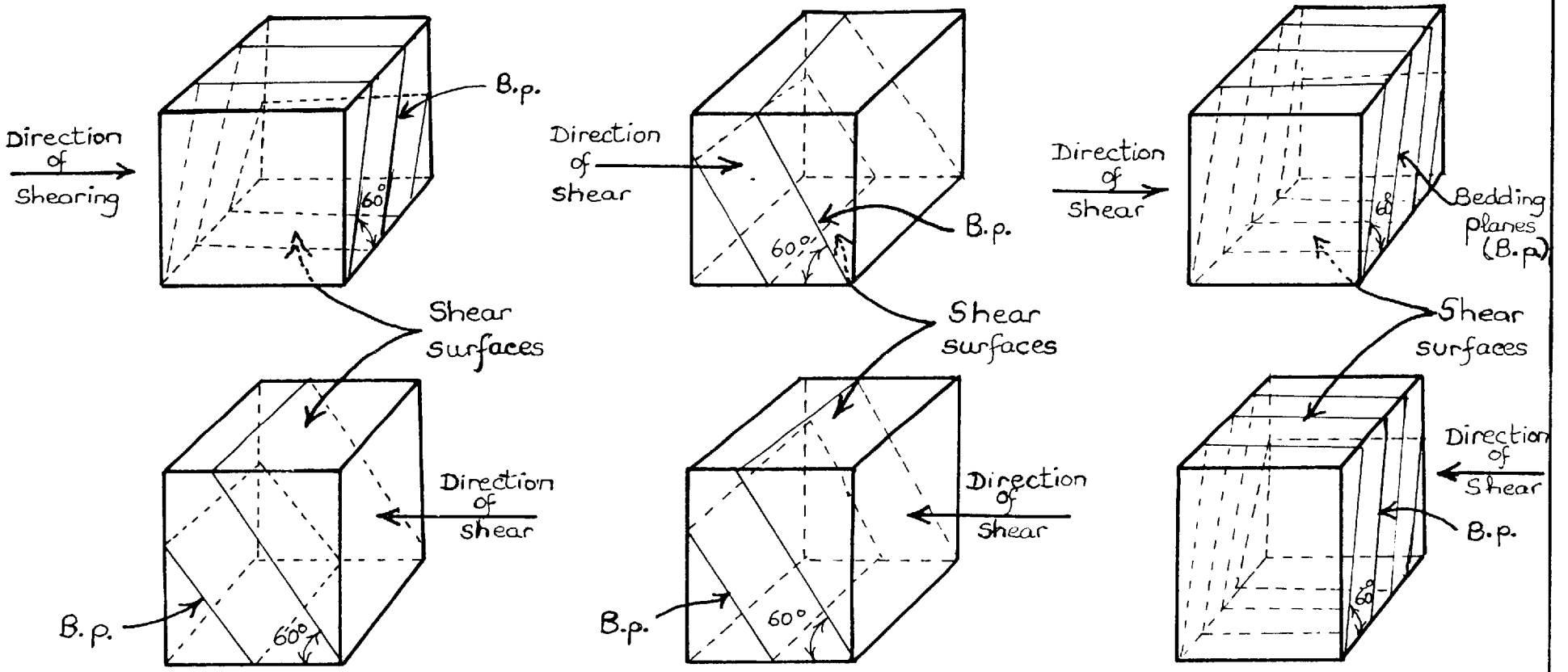
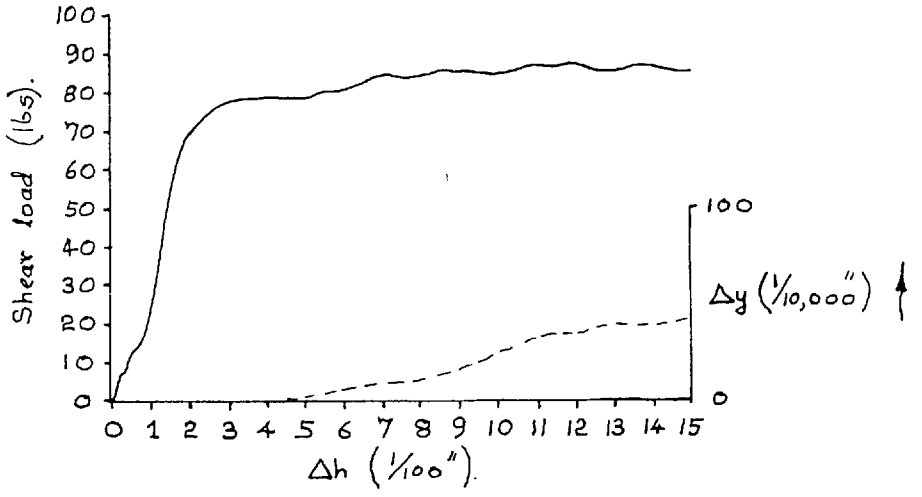
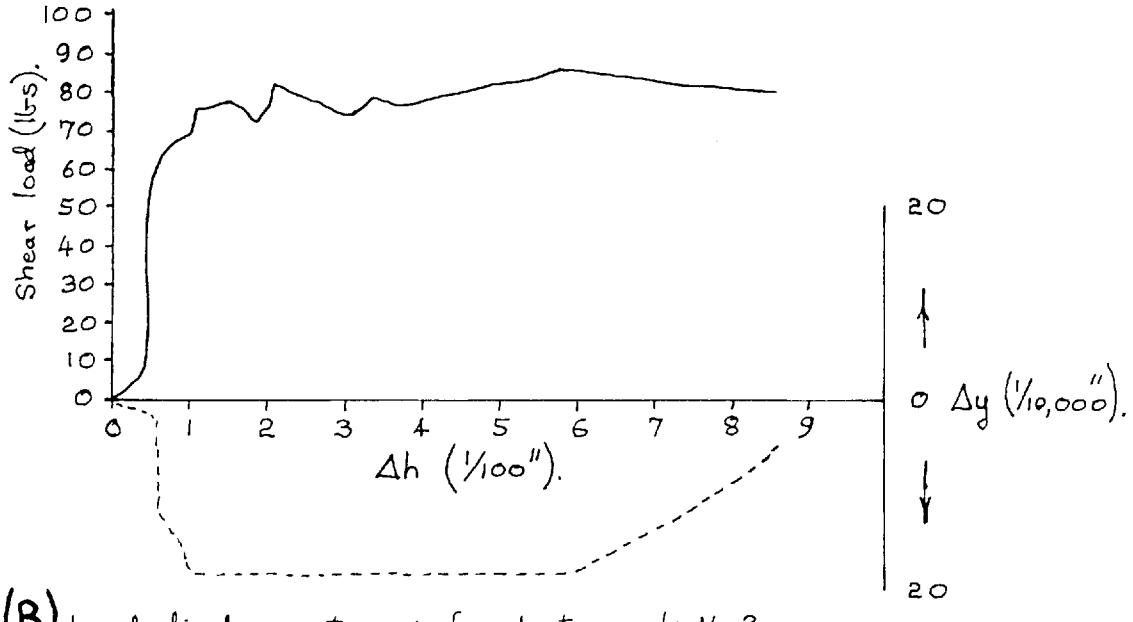


FIG: 5:7:1

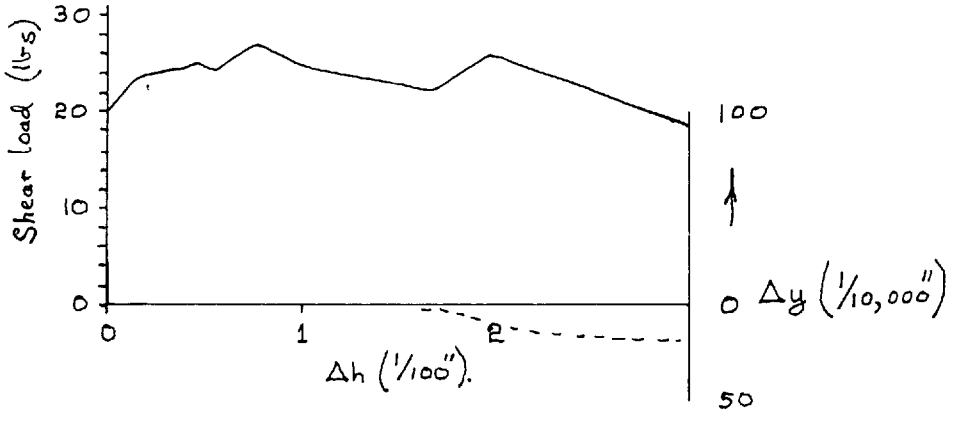
(C) SHEAR ACROSS THE BEDDING. (B) SHEAR NORMAL TO BEDDING. (A) SHEAR PARALLEL TO BEDDING



(A) Typical load displacement curve for silurian cleaved mudstone (Test No. 1 submerged, normal to the bedding).



(B) Load displacement curve for chert sample No. 3



(C) Load displacement curve for chert sample No. 2.

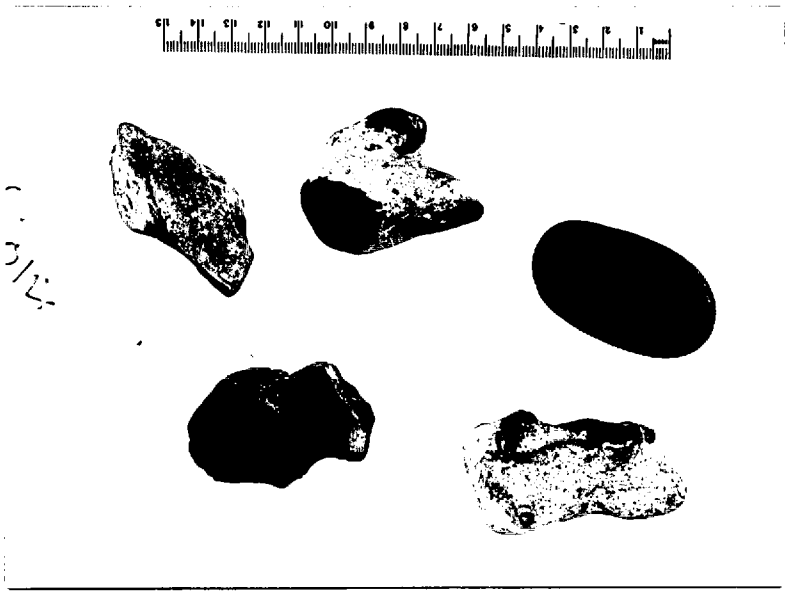
DIRECT SHEAR TESTS

FIG. 5:7:2.

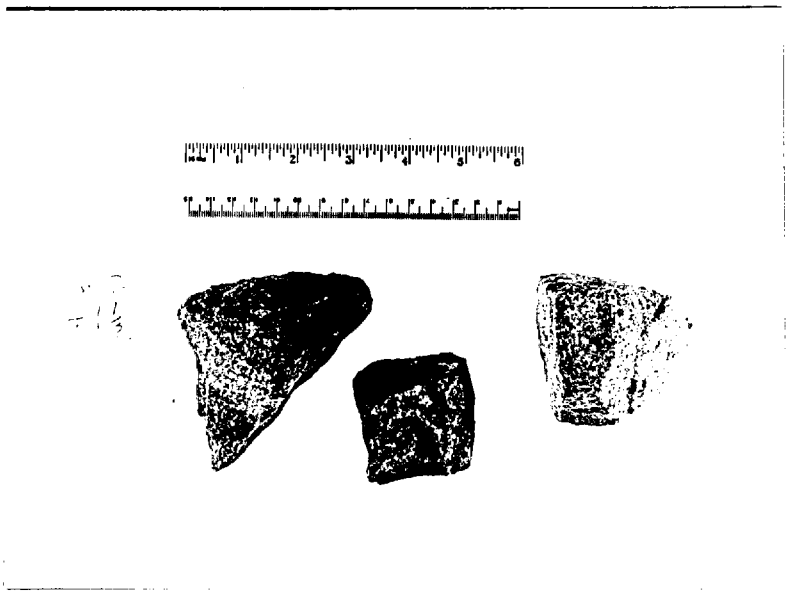
TABLE. 5:6:1

GRADINGS USED IN 12" DIA SAMPLES OF SILURIAN CLEAVED MUDSTONE.

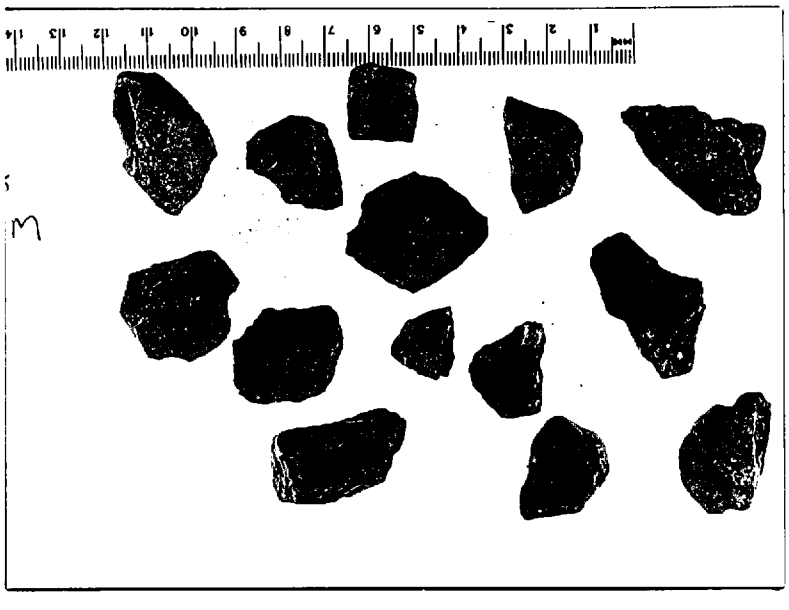
SAMPLE NO.	10	11	12	13	14	15	16	17	18	19	20 21 (T)	22	23 28	24	25 26 27 (U)	29 30 31 32
B.S. SIEVE																
+3"	100.0		100.0	100.0	100.0	100.0		100.0		100.0		100.0	100.0	100.0		100.0
+2½"	70.0		92.2	90.0	90.0	90.5		96.3		95.0		96.0	92.5	92.5		95.0
+2"	58.5		77.8	76.0	80.0	83.2		82.4	100.0	85.0		88.0	85.5	85.5	100.0	87.0
+1½"			57.4	60.0	72.2	73.8	100.0	68.4	88.0	77.5		83.0	76.0	76.0	90.0	76.0
+1"			38.2	38.0		54.9	84.0	56.3	68.0	58.0		77.0	66.0	66.0	77.0	58.0
+¾"	47.0		19.1	24.0	42.9			47.1	58.0	44.0	100.0	71.0	59.0	59.0	69.0	45.0
+½"		100.0														
+⅜"	35.0	95.0	0	0	23.5	27.7	55.0	32.1	40.0	27.0	75.0	55.0	42.5	42.5	49.0	27.0
+3/16"	23.5	77.0			15.3	21.7	40.0	19.0	27.0	17.0	50.0	37.0	28.0	28.0	32.5	17.5
+No.7.	0	63.0			9.2	15.8	30.0	12.0	17.5	12.0	25.0	28.0	17.5	17.5	21.5	12.0
+No.14		46.5			6.1	11.8	22.0	7.0	12.0	8.0	0	21.0	8.0	8.0	12.5	8.0
+No.25		30.0			4.0	7.8	14.5	4.0	5.0	5.0		16.0	0	4.0	4.0	6.0
+No.52		18.0			2.0	5.7	9.0	1.0	3.0	2.5		10.0		0	0	4.0
+No.100		10.0				3.6	6.0	0	1.5	1.0		7.0				2.0
+No 200												5.0				



CHERT



GRANITIC GNEISS



SILURIAN CLEAVED MUDSTONE

GRAIN SHAPES OF THE MATERIALS TESTED.

PLATE. 5:1

CHAPTER 6

TESTING PROCEDURE

(6:1) Preparation of 12" Diameter Samples

(6:1:1) Grading Preparation

The material retained on individual sieves was stored in polythene bags, inside dustbins, on the roof of the building.

Prior to making up a grading about one ton of the various segregates was oven dried and then stored in the laboratory.

The grading to be tested was then prepared by weighing out the various segregates on a 112 pounds capacity balance.

Initial mixing was achieved by placing the largest material first, followed by the finer, into a large tray placed on the floor, The mixing was completed by shovelling the grading into another tray and vice-versa until a condition of minimum segregation was achieved. Flat topped layers produced less segregation than conical piles. Initial gradings of silurian cleaved mudstone and granitic gneiss are shown in Plate 6:1:1.

Handling of the bags of material caused a certain amount of particle damage by breakage. This was very obvious with the larger material and undersize particles were removed. There was breakdown in the smaller sizes too because the bases of the bags were always covered in fine material.

With a uniform grading the fines could easily be removed but with a wide grading resieving would have been necessary.

As a result, all the gradings prepared probably had more fines than proposed.

(6:1:2) Membrane Sealing

For an effective seal between the steel pedestal and the rubber membrane a continuous line contact is required. The standard method with O-rings was ineffective because the membranes were too stiff and had a canvas texture finish. Several alternative methods were tried using Jubilee Clips, both on the membrane and on two O-rings around the membrane. Six 2" diameter Jubilee Clips were used so that an equal pull could be achieved all round the sample without scuffing. An alternative was to place P.T.F.E. tape around the membrane and under the Jubilee Clip.

Eventually, the most effective method found was to coat the pedestal with a layer of Revultex R, a self vulcanising rubber, and then to place the membrane over the pedestal and squeeze the Revultex into the surface

imperfections by rolling very tight O-rings down the outside of the membrane The Revultex would go off in about half the time required to make up a sample grading and produced a perfect seal.

One dry sample was tested by leaving it sealed for 60 hours under an initial partial vacuum of 28" of mercury. No reduction in the vacuum was recorded in that time.

This method of sealing was quite satisfactory as long as sample saturation was to take place after the application of a confining pressure, otherwise the pressure of the pore water at the base of a 2' high sample was sufficient to expand the membrane and O-rings and break the seal. Jubilee Clips, or the much superior stainless steel JCS Hi-Torque band, could be used to replace the O-rings and prevent the membrane expanding but the clearance inside the compaction mould was not really sufficient. The problem was solved more satisfactorily by binding the membrane tightly with dry string, which was subsequently wetted to shrink it tighter.

(6:1:3) Sample Building

All samples were built up in layers, each weighing about 30 pounds. The material in each layer was distributed as evenly as possible and then vibrated for one minute with a medium sized Kango Electric Hammer Type F, fitted with a Swivel Head Compaction Tool. Vibration was applied to the whole surface of the sample with particular care being taken adjoining the membrane, both to prevent damage and also to make certain there were no initial voids which might cause a membrane failure during testing. This operation required a dust extractor which probably removed a lot of the material passing the No.200 B.S. sieve.

The last layer was always difficult to compact, as mentioned earlier.

With some gradings, a certain amount of-3/16" + No.7 material had to be added to the circumference of the top of the sample to make a smoother transition between the sample and the top cap. This extra material was weighed out and allowed for in the average grading of the after test sieve analysis.

Levelling of the top surface was achieved by vibrating a 1" thick and 12" diameter plywood disc with the Kango Hammer. Alternatively, a heavy-weight was used.

The same amount of compaction was given to all samples but various densities resulted, although this would be expected for the various gradings.

It was felt that the samples were not always as homogeneous as they might have been, especially with the granitic gneiss and this was overcome, to a certain extent, by adding the fines after compacting the coarser material. The voids were sometimes quite large and one could hear fine

particles working their way down into the sample without the aid of vibration.

Non homogeneity was demonstrated by the after test sieve analyses on sample 16V/12 which failed by bulging in the upper half (Plate 6:1:3).

The testing of uniform and loose gradings was, in general, avoided because of the difficulties experienced with membranes puncturing.

One sample of silurian cleaved mudstone was compacted in a wet state but this practice was abandoned because of the safety aspect when using an electric compaction tool and also subsequent saturation proved to be excessively tedious.

The uniform gradings of chert, however, were compacted under water, using a hand tamper.

(6:1:4) Orientated Samples

The silurian cleaved mudstone comprised flat particles and it was therefore desirable to perform shear tests on samples in which the majority of the particles were orientated in a given direction.

It was hoped that the desired orientation would be produced by vibrating a whole sample in a mould inclined at the required angle. Experiments with geometrically similar gradings in a polythene beaker showed that the material just circulated, like concrete in a concrete mixer. The only alternative was to build up the samples by hand.

The first orientated sample was No.10M/12. This was constructed by hand with the mould in the vertical position. A wedge of material with a face slope of 30° was first built up on the pedestal. Compaction was by hand using a small weight. Further layers were built up with the larger material placed at 30° and infilled with fines. This resulted in quite a loose sample and a peculiar grading.

Further samples were constructed with the plane of orientation at 60° and 64° to the plane of the major principal stress. In these cases though the mould and pedestal were inclined at the required angle and the samples were built up in horizontal layers. Building a sample in this way required about one day's work.

(6:1:5) Positioning the Sample Top Cap

The top cap weighed 140 pounds and had therefore to be positioned by crane. The membrane was then sealed to the top cap, using Revultex R in the same manner as at the pedestal.

(6:1:6) Sample Stability

To afford stability to the sample whilst removing the mould and during

handling, a partial vacuum was applied. In samples with air as the pore fluid a vacuum of between $\frac{1}{2}$ p.s.i. and 1 p.s.i. was applied by a water ejector connected to the pedestal pore pressure connection. The vacuum was measured by a mercury monometer connected to the top cap pore pressure line. In samples which had been saturated whilst held by the compaction mould, the burette used for saturation was merely lowered and drained so as to produce a mean negative pressure of $\frac{1}{2}$ p.s.i.

(6:1:7) Sample Measurement

The sample diameter was measured, using calipers, at 5 elevations and in orthogonal directions. With a small vacuum applied the sample surface irregularities were not excessive. With a high vacuum applied, as in the first few cases, the irregularities were large and the mean diameter of the hollows was measured by calipers and the circumference over the peaks by tape measure and the mean sample cross-section was calculated from those measurements after allowance for membrane thickness.

The height of the sample was measured using a metre scale, which was "rocked" to obtain the correct height. If the height is measured at quarter points the mean of orthogonal measurements should coincide.

(6:1:8) Membrane Inspection

The membrane was now inspected to see if there were any signs of potential puncturing. If so, puncture repair patches were fixed at these locations.

At this stage the cell barrel was lowered over the sample and bolted to the cell base. The piston was then very carefully lowered to rest on the sample and the axial deformation apparatus was connected to give the initial zero.

The cell was then filled with mains tap water.

(6:1:9) Sample Consolidation

The applied vacuum was replaced in stages by an equal cell pressure. It was assumed that little or no volume change occurred during this change-over. Later, it was shown that the volume changes were between 0 and 10 ccs in a sample volume of about 44,000 ccs.

Cell pressure was applied initially by the pneumatic system and later by the hydraulic system. Cell pressure increments were applied in proportion to the confining pressure.

Initial volume changes of the sample were instantaneous, accompanied by the sound of fracturing particles. A certain amount of creep was

observed mainly with angular material, and the volume change usually reached a steady value for practical purposes after about ½ an hour.

Many samples were consolidated in the dry state when volume changes were measured by the volume of air expelled by the apparatus shown to the left in Plate 4:2. The level of the water surface in the burette was adjusted to that in the air water interface vessel so that the water manometer recorded an atmospheric pressure in the sample. It was essential to remove all moisture from the inside of the connecting leads by blowing compressed air through them prior to carrying out a test.

It was noticed that samples of silurian cleaved mudstone, though extremely permeable to air when dry, were rather impermeable to water when saturated.

Many samples were saturated after a consolidation in the dry state. Saturation took place under constant applied effective stress and the resultant volume change was measured by the water level change in the air water interface vessel of the pneumatic cell pressure control system.

It was noted that the volume change which took place on saturation was of the same order of magnitude as that during the previous dry consolidation. If the moisture content of the sample was above a certain threshold, about 5% for the silurian cleaved mudstone, no further volume change took place on saturation.

(6:1:10) Sample Saturation

Samples were saturated either before or after consolidation. Mains tap water was used for saturation and permeability determinations on all samples, except those used for consolidated undrained tests.

When saturating samples, which were still supported by the compaction mould, care had to be taken to avoid producing a pore pressure in excess of the minor principal effective stress. To remove air from all the connections the sample water was allowed to enter slowly from the base and was then circulated through the sample and attendant connections and leads until no further air bubbles were removed by the flow. This process would normally take several hours.

When saturating very impermeable samples, after consolidation it was possible to apply a back pressure of 40 p.s.i. by direct connection to the mains water tap. This though caused a large effective stress gradient between the top and bottom of the sample and could only be used, in any case, if the applied effective stresses on the sample were somewhat above 40 p.s.i. To prevent over consolidation of the sample the consolidation pressure can at no time exceed the minor principal effective stress at which it is to be tested. Further, to avoid sample disturbance and forcing

the membrane off the end platens the saturation pressure must be maintained below the consolidation pressure.

(6:1:11) Permeability Determination

The permeability of the samples could be measured under various stress conditions. Tap water, from a constant head tank, was allowed to enter the base of the sample through a $\frac{1}{2}$" bore connection and leave the top of the sample through a similar connection. The water was then led to an overflow tank, situated just above the top of the sample. If the outlet overflow tank was below the top of the sample an anomolous flow condition existed where the outlet pressure appeared to be greater than the inlet pressure. When a steady state of flow was reached, the head loss across the sample was measured by connecting a water manometer to each end platen. The volume of water passing through the sample, in a given time, was determined by weighing.

(6:2). Drained Tests

In general, drained shear tests were carried out at a strain rate of 8% per hour. The first six tests were carried out in a 50 tons capacity loadframe, where the maximum rate was 4% per hour. Test number 11 M/12 which had a grading with - $\frac{1}{2}$" + $\frac{3}{8}$" material as the maximum size, was very impermeable and the method described by Gibson and Henkel (1954) was used to determine a suitable testing rate.

Volume changes were measured by a 2,000 ml burette, open to atmospheric pressure. The burette was mounted so that the liquid surface was at the mid-height of the sample. It was recalibrated in cubic inches and also fitted with a base outlet tap. Volume changes in excess of 100 cubic ins were accommodated by adding, or subtracting a measured volume of water. The maximum volume change recorded was about 600 cubic ins.

To check that the test was, in fact, drained, the top cap pore pressure tapping was connected to a Bourdon pressure gauge (Volume change 1.3 ccs per 100 p.s.i.)

(6:3) Tests with Zero Lateral Strain (K_o - tests)

Several K_o - tests were carried out to determine the value of K_o (the coefficient of earth pressure at rest) and m_v (the coefficient of one dimensional compressibility).

Samples were compacted in the normal manner and were tested fully saturated and drained to atmosphere.

The condition of no-lateral strain was achieved by raising the minor principal effective stress at a constant rate and applying a strain in the

direction of the major principal effective stress to keep the area of cross section of the sample constant. The volume strain for a given axial strain was previously calculated and the axial strain rate varied to achieve the required volumetric strain.

This method had the disadvantage that, if the maximum particle size was large by comparison with the membrane thickness, an initial penetration would take place with increase in confining pressure. If the sample was isotropically consolidated, to say 20 p.s.i. then little further penetration was likely. On the other hand, breakdown which occurred on loading the sample caused fines, which had to go somewhere, and evidence from samples which were removed from the cell immediately after the K_o stage showed little sign of membrane penetration.

The alternative was to use a caliper or belt system to detect changes in diameter or circumference. These had the disadvantage of taking measurements of displacement at a point and if a large particle should break at that point, a non-representative picture of the sample behaviour as a whole would be given. The installation of several belts or calipers, to present an average picture of sample behaviour would mean a very sophisticated logic system to prevent the servo mechanism losing control of the situation.

The volume change method probably gave a reasonable average as long as the maximum particle size was kept below a nominal diameter of $1\frac{1}{2}$".

The determination of m_v in the triaxial cell, rather than the oedometer, is probably superior for materials such as sand because frictional effects are overcome. However, with rockfill the oedometer has distinct practical advantages. Any inaccuracies, due to the boundary conditions, will be acceptable in engineering practice and values of K_o may be determined by strain gauged rings.

No corrections were made for membrane effects on the K_o tests.

(6:4) Tests Causing Failure by Reduction of Effective Stresses

Failure of a rockfill embankment may occur through a reduction of the minor principal effective stress rather than an increase in the major principal effective stress.

Several tests were therefore carried out to study the behaviour of the rockfill under conditions of decreasing effective stress.

The samples were consolidated either under K_o conditions or isotropically. The cell pressure was held constant and the deviator load was varied to maintain at a constant value, as the area of cross section of the sample varied with the increasing pore pressure used to induce failure. Failure was defined by the maximum value of the ratio σ_1'/σ_3'. The pore

pressure was increased at a constant rate, using the pneumatic pressure control system. This was achieved by controlling the air pressure control valve with a simple servo system.

The volume change was measured by determining the volume of pore water entering the sample: this, in turn, was measured by the change in water level in the air water interface vessel. No corrections were made due to expansion of the air water interface vessel as its volume change, due to a pressure change of 100 p.s.i. was insignificant.

(6:5) Test to Determine the Pore Pressure Parameter B

A sample was compacted and saturated in the normal manner and a standard null indicator was fitted to the pedestal pore pressure connection. The cell pressure was increased and the pore pressure measured in the normal way (Bishop and Henkel, 1957). At first, the rise in pore pressure was considerably less than the applied increment of cell pressure, thus indicating incomplete saturation and the presence of air, though this was to be expected as the normal pore fluid was tap water. However, at cell pressures above 50 p.s.i. the rise in pore pressure was almost equal to the applied increment of cell pressure. Presumably, membrane penetration had accounted for the volume of trapped air.

(6:6) Undrained Shear Tests.

Undrained shear tests were carried out on loose and dense samples of silurian cleaved mudstone and granitic gneiss to determine the stress paths to failure under undrained conditions.

Stress conditions of this type could arise in the saturated upstream shoulder of a central core rockfill dam with a full reservoir and subjected to earthquake forces. With large contact forces between the particles of rockfill and the attendant breakdown, the compressibility of the rockfill skeleton is high and high pre pressures can, therefore, be developed.

The strain rate used for these tests was similar to that for drained tests and the pore pressure was measured at the base of the sample by connecting the pore pressure connection directly to a Bourdon gauge. The volume change of the gauge was 1.3 ccs per 100 p.s.i. and this was considered insignificant by comparison with the volume changes due to membrane penetration.

(6:7) Strain Rate

All the tests if possible, were carried out at a rate of axial strain of 8% per hour. This meant that the rate of axial displacement varied for each sample size though the rate of increase of stress was approximat-

ely constant.

However, one 12" diameter and numerous 4" diameter and 1½" diameter samples of silurian cleaved mudstone had to be tested at slower rates of strain because the permeabilities were very low.

(6:8) Total Strain

It was intended to take all the samples to 20% of axial strain so that particle breakdown could be compared at various confining pressures. Unfortunately, membrane punctures occurred in very many cases long before 20% of axial strain was reached. This applied especially in the case of 4" diameter specimens, where the quality of the membranes left much to be desired. Confining rockfill though provided a very severe test for the membranes. On consolidation the membranes would penetrate the voids and, as failure only occurred at large strains, even with dense samples, there was ample opportunity for rock particles adjoining the membrane, to reorientate themselves and pinch though the membranes.

(6:9) Sample Dismantling

To afford stability for handling the sample at the end of the test the drainage connection was closed off so that a negative pore pressure developed on removing the cell pressure. In the cases where membranes had been punctured the membrane stiffness was sufficient to confine the specimen but great care was necessary during subsequent handling.

After removing the top cap, a sling was fixed to the top of the membrane with G-clamps and the membrane seal on the pedestal was broken. It was then possible to lift the membrane and sample just clear of the pedestal and then rapidly position the lower end of the membrane above a tray, which was capable of holding the entire sample. By hitting the outside of the membrane the sample could usually be dislodged, after which the fines, still adhering to the membrane, were washed into the tray with tap water. Any material on the pedestal was also washed into the tray.

The sample was then oven dried and stored in the laboratory until the sieve analysis, which was carried out on the same sieves as the initial bulk sample.

Some samples were very cohesive after testing and could not be softened by adding water to the surface. Sample No. 11M/12 (Plate 6:9) had to be broken up using a hammer and cold chisel.

(6:10) Small Scale Samples

The material required for batching the initial small scale gradings was resieved from the initial bulk sample. Material for 4" diameter

samples was sieved on 12" diameter sieves and that for 1½" diameter samples on 8" diameter sieves. This had to be done so that before and after test sieve analyses could be carried out on exactly the same sieves. It also enabled the production of a more accurate grading because the segregates were considerably cleaner than in the bulk analysis and stayed so because the forces involved in handling the very small bags were so much less. To prevent overloading of the sieves silurian cleaved mudstone samples with nominal maximum particle sizes below ½" had to be sieved in two halves.

Compaction of the 1½" diameter samples was carried out using a ⅜" diameter steel rod, rounded off at the end and dipped in latex to form a thin rubber coating. The 4" diameter samples were compacted either with a larger steel rod or with the wooden shank of a 1 pound hammer.

Except for the minor modifications, already described, the small scale apparatus used was standard and as described in The Measurement of Soil Properties in the Triaxial Test (Bishop and Henkel,1962).

The permeability determinations before and after shearing the small scale samples were carried out using the falling head test. The results were somewhat affected by the head loss in the connecting tubes and, as a result the higher permeabilities recorded in Tables 8B and 8C only served as a general guide and a check that the tests were carried out fully drained.

(6:11) Calculation of Stresses and Corrections

In the large scale triaxial apparatus various corrections had to be applied to the measured stresses to obtain the mean stresses acting upon the sample.

All the pressure gauges which were used were calibrated using a Budenberg Dead Weight Tester.

All the stresses have been calculated referred to a datum at the mid-height of the sample.

The average cross-sectional area of the sample was calculated from the axial and volumetric strains. In general, failure was by bulging, followed by the formation of a shear plane or zone.

The confining pressure at the sample mid-height was calculated by allowing for the difference in elevation of the pressure gauge. During a shear test the cell could move vertically as much as 10", thus reducing the cell pressure by that head of water. The top of the sample always stayed at the same elevation though during the shear stage so the displacement of the mid point was never more than 5" and this pressure change was only taken into account with tests at very low confining pressures.

The pressure gradient between the base and the top of the sample was balanced by a similar gradient due to pore water pressure so the sample was subjected to a uniform value of $6\frac{1}{3}$ throughout its height.

There was also half the submerged sample weight and the submerged top cap weight to be allowed for.

(6:12) Membrane Corrections

A membrane correction for samples failing by symmetrical bulging and not on a single plane was determined directly (Henkel and Gilbert 1952) by comparing the undrained strengths of remoulded $1\frac{1}{2}$" diameter, clay samples when tested with and without membranes.

The analysis was extended to single plane failure by (Fraser 1958) and for the case of large strains to determine the residual strenght by (Petley 1966).

A comprehensive investigation of the effects of membranes and side drains on the measured strength of clay samples failing on a single plane was reported by (La Rochelle 1967).

Several assumptions were made on the behaviour of the membranes confining a sample of rockfill, based on visual evidence of samples after compaction and after failure. Also the confining effect of the membrane was apparent in Test No.30M/12 (Fig. 7:3:7a)

Assumed membrane behaviour

a) During and after compaction the membrane is unstressed.

b) On application of a confining pressure the membrane is folded around the particles and stretched.

c) The actual tension produced will depend on the ratio of the membrane thickness to particle diameter and the confining pressure.

d) The confining pressure produces tension on both x and y axes. (x and y axes are on the face of the membrane, y vertical and x horizontal).

e) Axial strain reduces tension on the y axis and sample barrelling increases tension on the x axis. This hoop action tends to produce a tension on the y axis.

f) ThePoisson's Ratio affects are small compared with the strains induced by folding around the particles.

With reference to Fig.6:12:1, let:

r = rock particle radius

t = membrane thickness

α = the angle between the intersection of the outer face of the membrane with the common tangent and the centre of a rock particle,

then $\sin\alpha = \dfrac{r}{r + t}$ --- (I)

the initial membrane length between mid points of the particles = 2r --(2)

the maximum possible length if t = 0 is πr -------(3)

the maximum centreline length if the membrane thickness is t is:

$$= 2\left(2\pi\left(r + \frac{t}{2}\right)\frac{\alpha}{360} + 2\pi\frac{t}{2}\frac{\alpha}{360}\right)$$

$$= \frac{\pi\alpha}{90}(r + t) \qquad \text{---------- (4)}$$

Maximum change in length due to the application of a confining pressure is:

$$\frac{\pi\alpha}{90}(r + t) - 2r \qquad \text{-------(5)}$$

Maximum percentage elongation is:

$$\left(\frac{\frac{\pi\alpha}{90}(r + t) - 2r}{2r}\right) \times 100$$

The approximate relationship betweenthe membrane stress condition and the sample axial strain and the r/t ratio is plotted in Fig.6:12:1.

Membrane distortions on samples of silurian cleaved mudstone, granitic gneiss and chert are shown in Plates 6:1:3 and 6:12.

Because of the very folded nature of the membrane it was assumed that it had negligible strength as a cylinder in axial compression. The main effect of the membrane was to increase the effective confining pressure due to a hoop tension effect as the average cross section of the sample increased. The hoop tension for any given sample area was determined experimentally for all the membranes used. This was achieved by measuring the force required to extend circumferentially a unit height hoop of the membrane by an amount equivalent to the increase in the mean sample circumference during a shear test.

However, it will be seen that the addition to $6_3'$ or subtraction from $6_1'$ of 1 or 2 p.s.i. at the failure stresses involved has little engineering significance because, at the low confining pressures where the membrane effects are most insignificant, the value of ϕ' is very much higher than acceptable design values. The correction to be added to σ_3' for a given membrane at various values of the average area of cross section of the sample is plotted in Fig.6:12:12.

(6:13) Ram Friction

If the ram and its bushing are correctly machined and lubricated the main sources of friction are eccentric leads, applied either internally by the sample or externally by misaligned loading apparatus.

A condition to be satisfied is that there should be a minimum leakage between the ram and bushing. This can be achieved by a complete seal or

by a fine tolerance with a viscous oil between the piston and bushing. The seal or viscous oil friction can easily be determined by pushing the ram into the cell at the required rate of strain and against the particular hydraulic pressure. The end force due to hydraulic pressure is easily calculated.

The friction due to eccentric loads is more difficult to determine. The problem may be avoided by internal load measuring devices, which must be unaffected by shear loading, or by rotation of the bushing. The latter is most expedient with small scale apparatus but a very major piece of engineering when testing a 12" diameter sample of dense rockfill at a confining pressure of 500 p.s.i. A rotating bush has been constructed for a somewhat larger piece of apparatus though (8).

Tests on small scale apparatus have shown that the friction increases with axial strain and may reach about 5% of the applied load. (Bishop and Henkel 1962).

As the bearing length in the bushing remains constant, so the forces on the side of the bushing increase for a given lateral force on the end of the piston as it is displaced from the bushing.

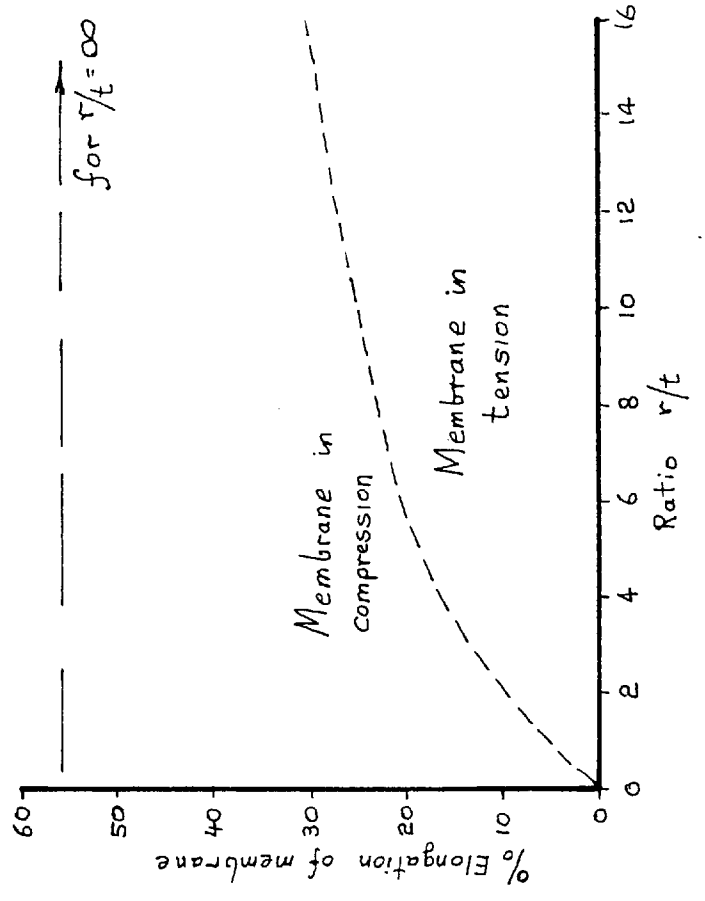
The frictional force will therefore be dependant on the failure characteristics of the rockfill, the degree of fixity of the sample loading arrangement and the relative dimensions of the piston overhang and the length of the bushing.

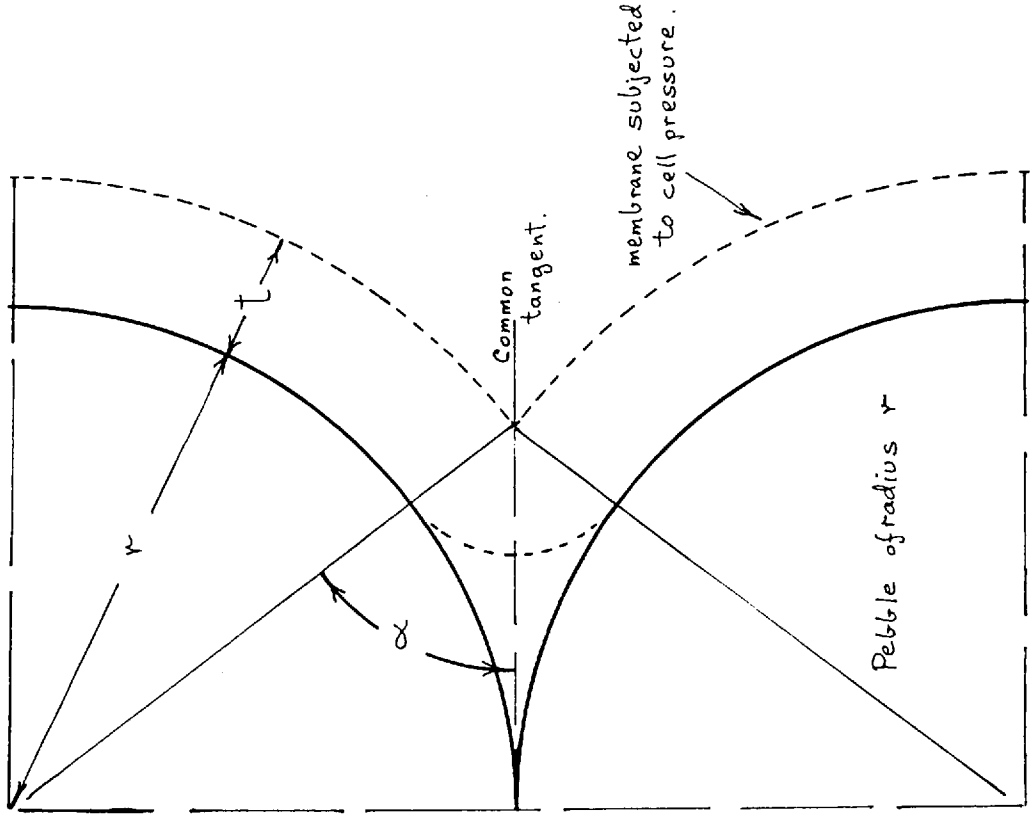
To minimise the lateral load transmitted from the sample to the piston a ball bearing head was used in all the apparatus and in all the tests.

Insley (1965) reported that the frictional force, developed in the bushing of a triaxial apparatus for testing moraine samples of 6" diameter and 12" high, was insignificant at confining pressures up to 450 p.s.i.

The value of ϕ' is fairly insensitive to errors in the measurement of the deviator stress. It can be seen from Fig.6:13:1 that an 18% error in determining the deviator stress causes an error in ϕ' of about 3.0° irrespective of the magnitude of ϕ'.

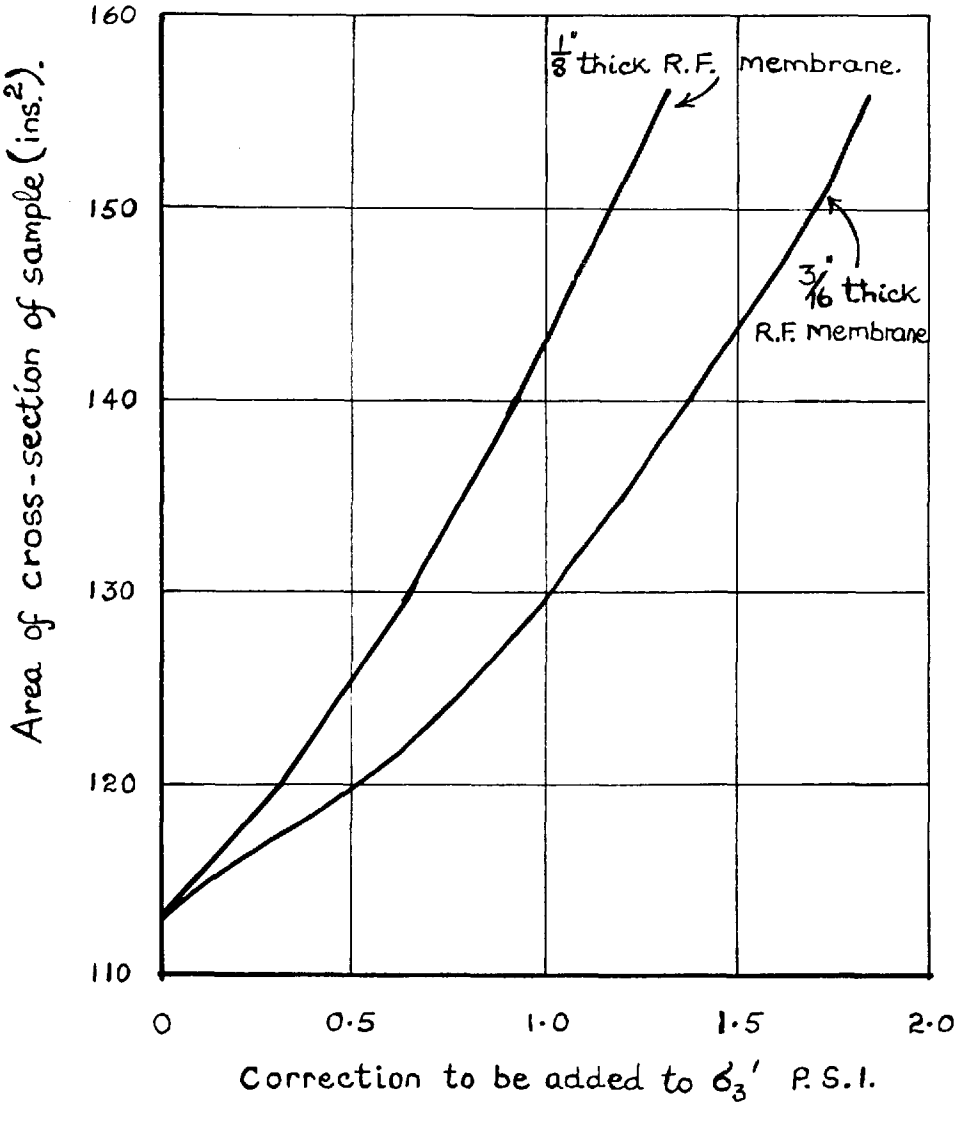
If a coefficient of friction of 0.25 is assumed between the piston and its bushing and a shear load of 20% of the measured deviator is applied to the head of the piston the error in the measurement of the deviator load is of the order of 18% at the failure strains involved. As ball bearings were placed between the piston head and the sample top cap it is unlikely that a shear load as great as 20% of the deviator could develop prior to peak. Although the error in ϕ' is still unknown it is unlikely to exceed 1° or 2° and no correction was made to the results of tests on 12" diameter samples.





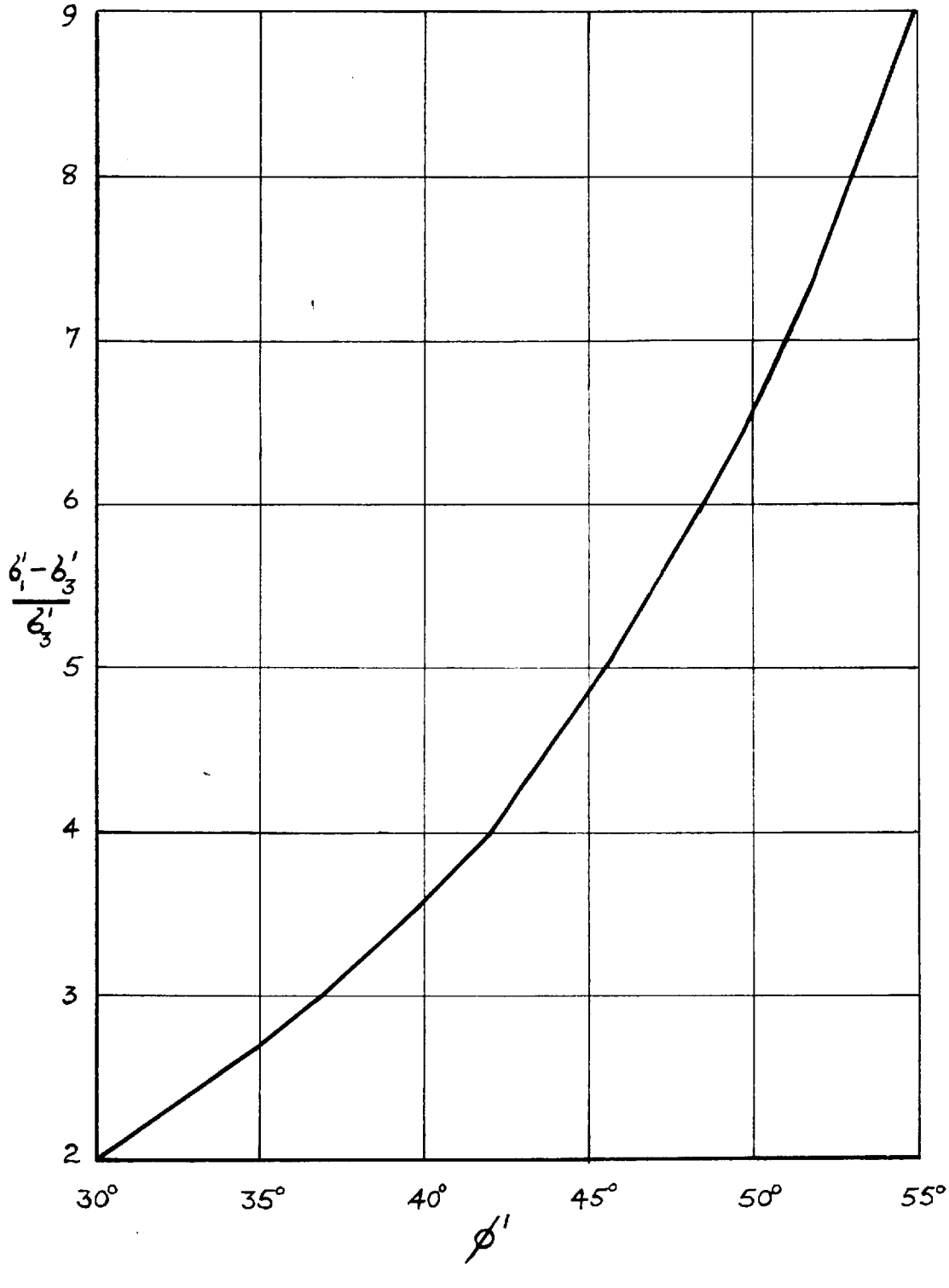
MEMBRANE CORRECTION.

FIG. 6:12:1



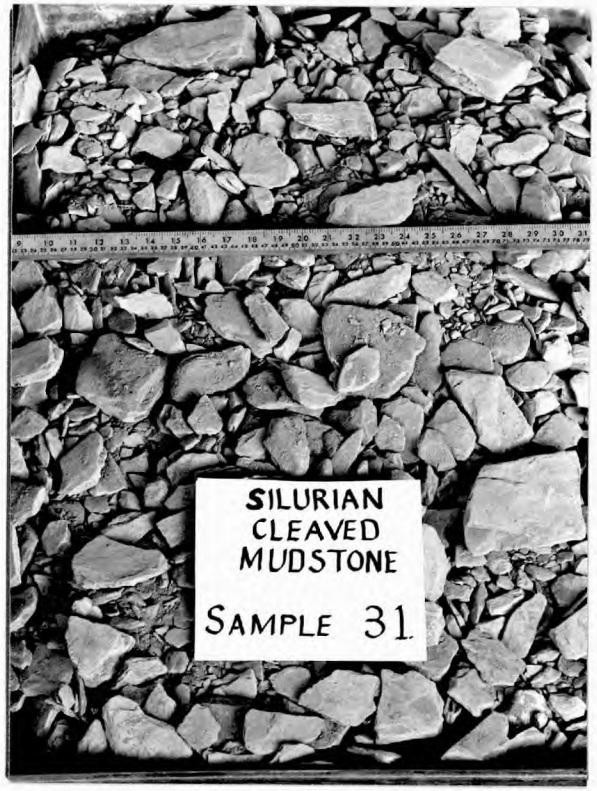
MEMBRANE CORRECTION ADDED TO THE MINOR PRINCIPAL EFFECTIVE STRESS WHEN MEMBRANES CONTAINING A FILLER WERE USED (R.F. TYPE).

FIG: 6:12:2

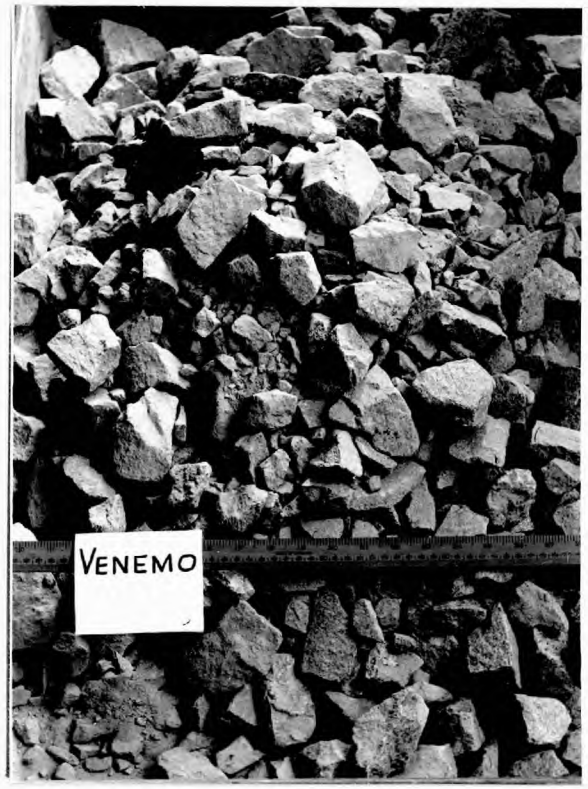


THE EFFECT OF PISTON FRICTION ON THE VALUE OF ϕ'.

FIG: 6:13:1.

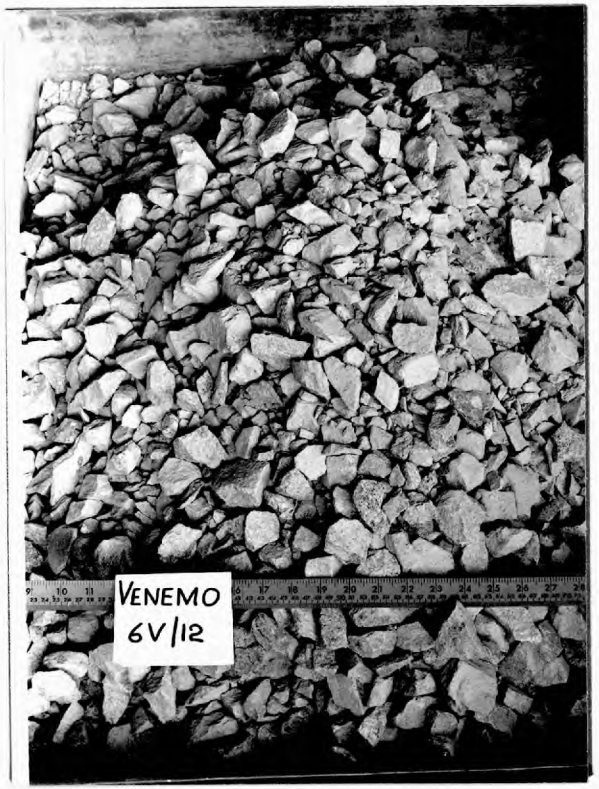


INITIAL GRADING OF SAMPLE No. 31M/12 (SILURIAN CLEAVED MUDSTONE).

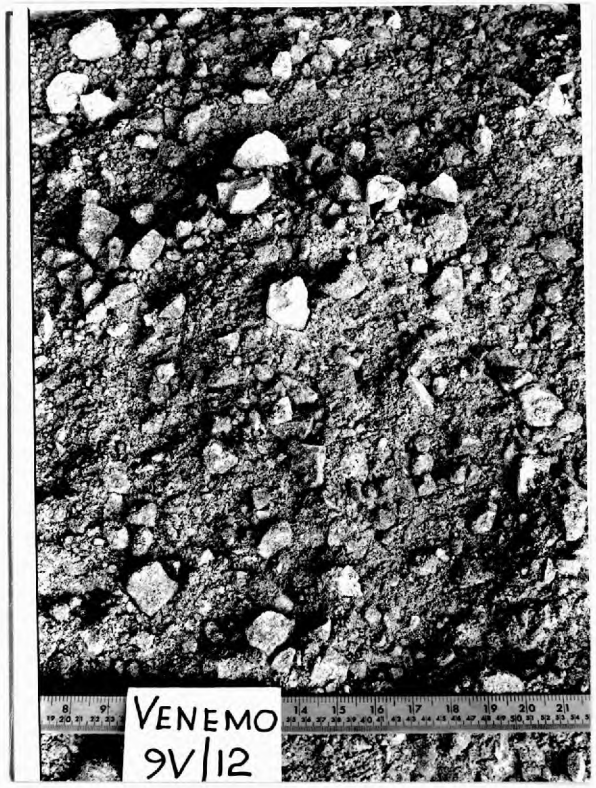


INITIAL GRADING OF GRANITIC GNEISS (GRADING H).

PLATE. 6:1:1A

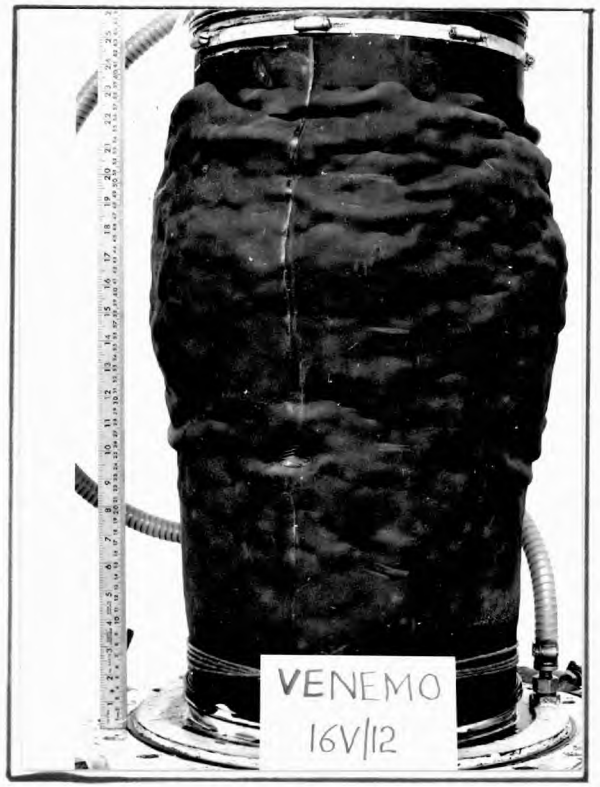


GRANITIC GNEISS GRADING J
BEFORE TESTING.

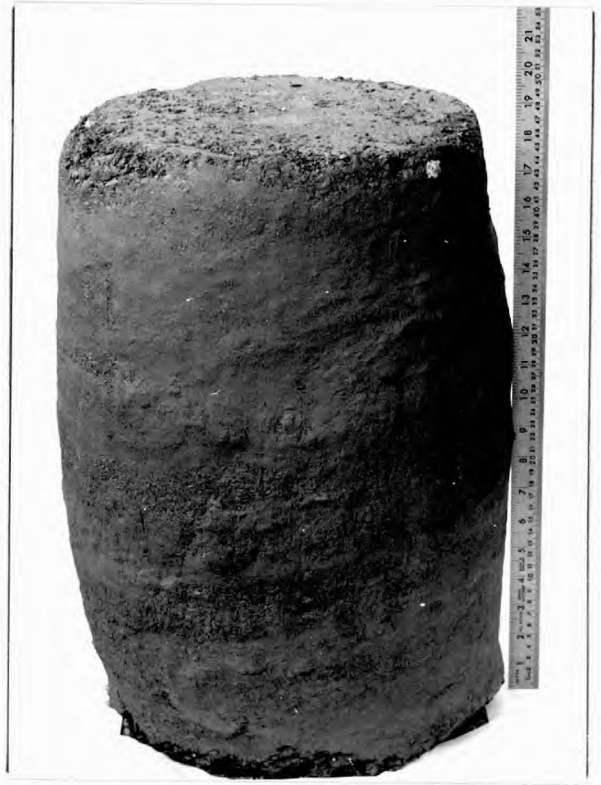


GRANITIC GNEISS GRADING J
AFTER A SHEAR TEST WITH
$\sigma_3' = 450$ LBS/IN.^{2}

PLATE. 6:1:18

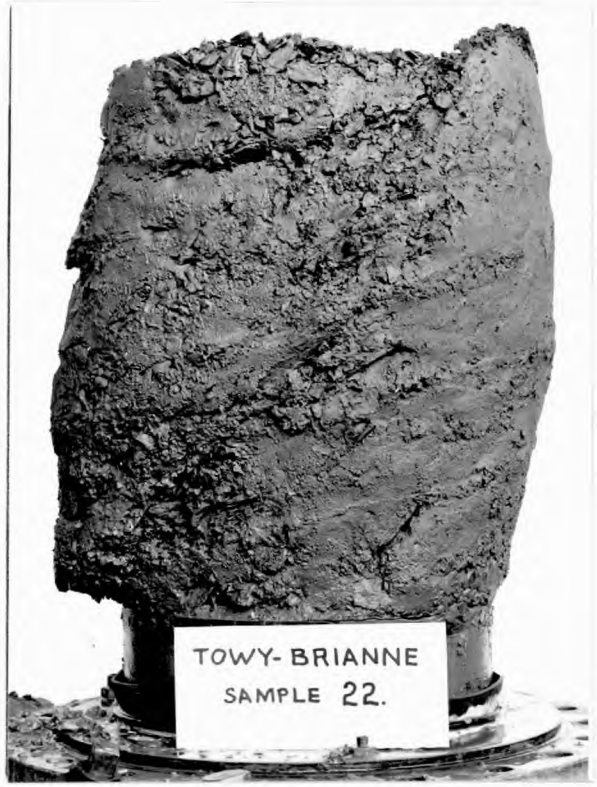


GRANITIC GNEISS SAMPLE
AFTER FAILURE



SILURIAN CLEAVED MUDSTONE
SAMPLE AFTER FAILURE
(SAMPLE No. 11M/12).

PLATE 6:1:3



SILURIAN CLEAVED MUDSTONE SAMPLE No. 22M/12 AFTER FAILURE (10% PASSING No.100 B.S. SIEVE).

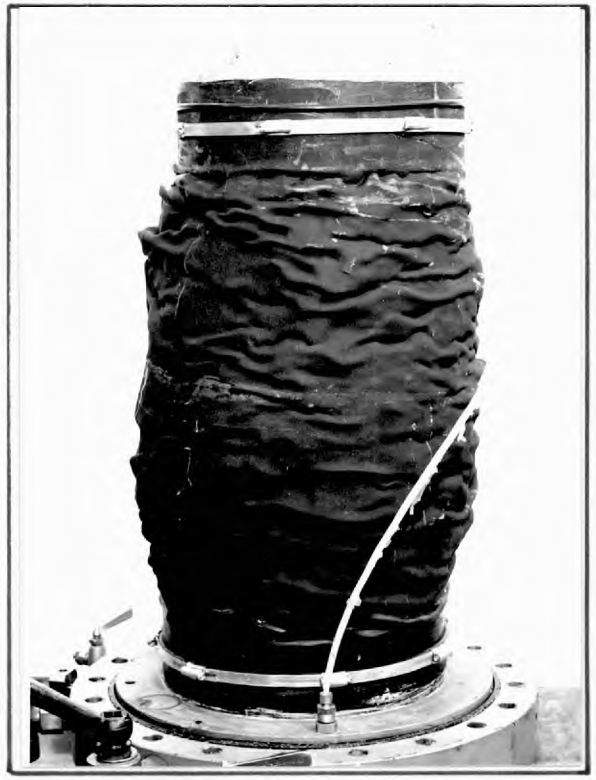


SILURIAN CLEAVED MUDSTONE SAMPLE No. 23M/12 AFTER FAILURE (3% PASSING No 100 B.S. SIEVE).

PLATE. 6:9



CHERT SAMPLE AFTER FAILURE



SILURIAN CLEAVED MUDSTONE SAMPLE AFTER FAILURE.

PLATE. 6:12

CHAPTER 7

THE RESULTS OF THE TESTS ON SILURIAN CLEAVED MUDSTONE

(7:1) Compaction and Sample Density

All of the 12" diameter samples which were to be used for drained shear tests were subjected to the same compactive effort but various dry densities resulted. Several factors may have contributed to this. Firstly, all the gradings were not exactly the same and for a given maximum particle size one would expect a lower density from a grading with a sparcity of fines. Secondly, it was very difficult to produce a perfectly homogeneous sample as segregation occurred during the mixing of the segregation and also whilst pouring the mixed material into the sample. During compaction there was a tendancy for the larger particles to "float" to the surface. This situation was partly overcome by adding the finer material after the coarse particles.

The samples were compacted by tamping rather than vibration because a sufficiently large vibrator was not available.

A sieve analysis was carried out on one sample of grading A immediately after compaction to determine the particle breakdown during sample building. Although one could see that some large particles were snapped in half during compaction the extent of this fracturing was obviously very small as it was not apparent from the grading curve. This grading though contained a good proportion of fines into which the larger particles could bed and one would expect a somewhat greater amount of particle breakage when compacting a uniform sample of large particles.

No particle breakdown was noticed during the compaction of samples having a maximum particle size of 1" or less.

It was noticed that densities achieved in triaxial samples were always higher than those in oedometer samples having the same grading and subjected to similar compactive efforts. The boundary conditions are different though, there being a rigid metal ring in the oedometer and a rubber membrane, backed by felt, in the triaxial apparatus. Also, the volume of the oedometer is more precisely known because of the regular boundaries. The most likely cause of the discrepancy though is in the compaction of the top two or three inches. This top layer was compacted to the same extent as lower layers but as the material bounced around it never achieved the same density. This layer forms a larger proportion of the sample in the oedometer and hence, a lower mean density is recorded.

Very high densities were achieved with grading A but the highest density was obtained with a grading with a maximum particle size of $-2"+1\frac{1}{2}"$.

In the latter case the material may have had a small moisture content, 3% would reduce the dry density by about 4.5 lbs/ft .

As would be expected, much lower densities were achieved with gradings having no fines and also in the cases of the orientated samples which were subjected to less compaction. (Table 7A and 5:6:1)

The dry densities of most of the 4" diameter samples were very similar. All samples were compacted by hand and subjected to similar compactive efforts.

Although the same densities were achieved the relative densities of the samples containing the larger particles were lower. This suggests that as the maximum particle size increases so a larger compactive effort is required to achieve the same relative density with a given weight of material (Table 7B).

No particle breakdown was noticed with 4" diameter samples during compaction except for a small amount of grading C.

The volume of material to be mixed for one sample was very much more convenient than in the case of the 12" diameter samples. As a result a more thorough mixing was achieved and a more homogeneous sample resulted.

The $1\frac{1}{2}$" diameter samples were compacted by hand and consistent densities were obtained. No particle breakdown was noticed during compaction. To make up an homogeneous sample with grading E the same procedure had to be adopted as with the large samples i.e. to add fine material after the coarse particles.

Similar densities were achieved with similar gradings in the 4" and $1\frac{1}{2}$" diameter samples. Higher densities were achieved in the 12" diameter samples. Presumably, the compactive energy per unit volume applied to these samples was higher than that applied to the two smaller sizes of sample. It is not known though just how much of the compactive energy is used in sample compaction and how much is lost by absorption of the mould and bouncing particles.

As the maximum particle size of a grading was reduced so the percentage of material passing the No.100 B.S. sieve increased. The shape of the grading curve beyond this point was not determined but it has been assumed that grading G is still similar to grading A.

There was no evidence of a predominantly horizontal particle orientation during compaction.

(7:2) Isotropic Consolidation.

All the volume changes measured during isotropic consolidation have an inherent error due to the membrane penetration. The extent of this penetration is unknown but dependant on confining pressure, membrane thick-

ness and the grading of the material. The maximum error will occur in samples with a uniform grading and containing the largest particle size. No uniform gradings were tested though because of the difficulties experienced with membranes puncturing. The mean penetration of the membrane must be 1/20" to cause a volume change error of 1½% of the sample volume and this produces a smaller error in the eventual determination of the major principal stress. Such an error in principal stresses is acceptable and a comprehensive investigation of the volume change caused by membrane penetration is not justified at this stage. It could probably be determined though by a series of tests on samples of different height to diameter ratios. The further complication of end effects is involved and lubricated end platens are not very suitable for rockfill. Marsal developed lubricated platens for his rigid boundary plane strain apparatus but rock points must penetrate the layers of PVC squares and the grease. Friction may be reduced but further volume change errors are introduced because of bedding.

The relation between volume change and consolidation pressure for several 12" diameter samples is shown in Fig: 7:2:1.

Sample No. 27M/12 (Fig.7:2:1) was initially consolidated anisotropically to a major principal stress of 52 p.s.i. and a minor principal stress of 29.5 p.s.i. The effective stresses on the sample were then reduced a almost to zero and the sample was re consolidated isotropically. The effect of over-consolidation is clearly shown in the initial part of the curve. Although this sample has a maximum particle size of 2" the volume change for unit increase in consolidation pressure is similar to that of sample No.11M/12 (Fig.7:2:1) with a maximum particle size of ½". The gradings are shown in Table 5:6:1: There is no strict comparison though because the density of sample No.27M/12 was 10 lbs/ft.^{3} higher than sample No.11M/12 and it was also saturated.

Samples 22M/12 and 23M/12 were quite loose and the particles were orientated, a larger volume change for a given consolidation pressure was therefore expected. Sample No.19M/12 was at a similar density with the particles orientated at 32°. A very much greater volume change was recorded.

Sample 13M/12 had a maximum particle size of 3" and no material passing ⅜". It was subjected to the usual compaction but, because all material below ⅜" was missing, the density was only 115.1 lbs/ft.^{3} A certain amount of membrane penetration would be expected with such a grading and the extent of penetration is evident with sample 9M/12 because of the marked initial curvature of the consolidation curve.

Further considerable volume changes took place during saturation with

the samples subjected to constant effective stresses. This extra volume change varied between 49% and 211% of the volume change which had already occurred. The smaller change occurred with sample No.13M/12, which had a grading between 3" and $\frac{3}{8}$", whereas the largest was with sample No.11M/12, which had a grading with $\frac{1}{2}$" as the maximum particle size and 10% passing the No.100 B.S. sieve. The greater volume change in the latter case is presumably due to the collapse of a much greater number of contact points. The contact forces between grains will vary but the contact stresses will probably always be the same for any given material and be equal to its yield strength in whatever medium it is surrounded.

It was noticed in 1928 (Rehbinder and Lichtman 1957) that the resistance of solids to strain and rupture varied according to the surrounding medium and temperature. This process was usually reversible and, hence, received considerable attention as it had potential uses in the metal forming and machining industries. Experiments were carried out on metals, glass and some rocks. Aslandova (1954) studied glass fibre in air, vacuum and water. In a vacuum or air ideal elastic behaviour was observed but in water the behaviour was non elastic and hysteresis and irreversible creep occurred. This was accompanied by a sharp decrease in strength especially with long term loading. Thus, because of absorption, (surface molecular interaction with the enveloping medium) solids become weakened. The most chemically resistant glasses exhibit strong effects of this nature.

The process is aided by a state of tensile stress which develops micro cracks. This is the case with rockfill where the contact stresses are high and micro fissures probably abound from blasting and excavation techniques and the different coefficients of expansion of the various minerals will also aid micro fissuring.

This weakening on wetting is a phenomenon of surface activity and has been observed by physical chemists in many materials. The weakening is not always observed though after treatment with an etching compound. Presumably, this is because spherical cavities are eroded at the roots of micro fissures thus reducing stress raising conditions.

The weakening on saturation is clearly demonstrated by the increase in the rate of volume change afterwards. It is even more noticeable as one would expect the rate of volume change to decrease with stress increase because of the increasing sample density.

The angle of internal friction is slightly lower for saturated than dry material and may be accounted for by the reduction in strength of the contact points and the particle surface asperities.

Overconsolidation effects, due to compaction, were not apparent during isotropic consolidation.

All the 4" and $1\frac{1}{2}$" diameter samples were consolidated after saturation.

With the 4" diameter samples, sample No.18M/4, with grading F, underwent considerably greater volume change than sample 14M/4 of similar initial density but with grading D. The former sample had about 20 times as many interparticle contacts as the latter but the load per contact is reduced accordingly.

Comparing samples 3M/1½ and 8M/1½ (Fig.7:2:3) with 14M/4 and 18M/4 (Fig.7:2:2) sample 3M/1½ had a larger maximum particle size and a higher density than 8M/1½ but a greater volume strain. Sample 14M/4 was slightly denser than 18M/4 and yet had a very much reduced volume strain.

(7:3) Shear strength

In the drained shear tests the angle of internal friction was defined as the angle at the origin between the principal stress axis and the tangent to the Möhr failure envelope and passing through the origin. The Möhr failure circle was drawn for the condition of maximum deviator stress.

(7:3:1) Shear strength of 12" diameter samples (drained shear tests)

The first seven drained shear tests on 12" diameter samples were carried out in a 50 tons capacity loadframe in which the axial displacement and the rate of displacement were somewhat limited. Later tests on small diameter samples indicated that the rate of axial strain had no effect on the shear strength or deformation characteristics of the sample as long as fully drained conditions existed.

The deviator stress had to be reduced to zero in test 2M/12 in order to reset the jack travel (Fig.7:3:1).

Several of the initial samples showed a 'premature' peak which was followed by a higher peak. This phenomenon may have been a function of the restraint of the sample top cap. If the sample failed along a shear surface the top of the sample could move horizontally by 1 inch, after which the inside rim of the top cap touched against the ram loading head. The effect of this was twofold, firstly, it set up extra shear stresses in the sample and it also forced the piston against the bushing thus increasing the friction. The maximum recorded deviator stress was used to calculate the angle of internal friction.

Although the initial sample densities and gradings varied there seemed to be only minor variations in the angle of internal friction for any given confining pressure. The smaller samples though seemed more sensitive to variations in initial density.

There was a linear relationship on a semi-log. plot between the angle of internal friction and the minor principal stress for the pressure range investigated.(Fig.7:3A).

For 12" diameter samples, with grading A (i.e. $\frac{D}{d} = 4$) compacted to a relative density of 90%, the angle of internal friction varied from about 51° to 40° at minor principal stresses of 10 p.s.i. and 150 p.s.i. respectively.

(7:3:2) Shear strength of 12" diameter samples with orientated particles (Fig.7:3:2)

Five tests were carried out to determine the effect of particle orientation on the value of ϕ'_f.

Sample No.10M/12 was constructed with the flat faces of the particles inclined at 30° to the horizontal. A rather peculiar grading resulted because of hand selection and placing and a very low density was obtained. The angle of internal friction was the same as the mean value for drained tests on samples with randomly orientated particles, though the axial strain required to reach peak strength was 22.5%.

Sample No.19M/12 was tested at a lower pressure and with the particles orientated at 32°. An improved dry density (126.8 lbs/ft.^{3}) and grading (Fig. 5:6:1) were achieved. The angle of internal friction at this density was about 3° below that for randomly orientated samples at a relative density of 90%. (Fig.7:3A)

Sample No.22M/12 had particles orientated at 60° to the horizontal, the initial density was 125.1 lbs/ft.^{3} and it was sheared at a confining pressure of 80 p.s.i. The angle of internal friction was about 3.6° below the average for normal samples compacted to a relative density of 90%.

Sample No.23M/12 had particles orientated at 64° to the horizontal, the initial density was 125.8 lbs/ft.^{3} and it was sheared at a confining pressure of 100 p.s.i. The angle of internal friction was about 4.0° below the average for normal samples.

In these samples only material above $\frac{3}{8}$" was definitely orientated at the stated angles as one had little or no control over the finer material. However, having all the larger material at the stated angle meant that the sample behaviour was predominantly governed by the orientation.

At a major principal stress of just over 400 p.s.i. the angle of internal friction was 37.6° with a sample of medium density and with particles orientated at 64°. It appeared, therefore, that orientation would not pose a significant problem with this material. This was especially so as there was little evidence of general orientation during the construction of a field trial embankment.

Observation of sample 23M/12, after shearing, showed that there had been a rotation of the plane of orientation from 64° to about 50° in the central section which was subject to the greatest amount of bulging.

(7:3:3) Shear strength of 12" diameter samples with special gradings.

Sample No.11M/12 was compacted to a density of 131.4 lbs/ft.^{3} and had a grading comprising material passing the $\frac{1}{2}$" B.S.sieve (Table 5:6:1). The angle of internal friction obtained was 39.4° at a confining pressure of 100 p.s.i. This was about 2.9° below the average for grading A at a relative density of 90% which corresponds to a density of about 137 lbs/ft.^{3}

Samples 12M/12 and 13M/12 contained only material retained on the $\frac{3}{8}$" B.S.sieve. Very low densities were achieved although the samples were subjected to the normal compaction. The ultimate shear strength was not reached by either sample due to membrane puncture.

(7:3:4) Shear Strength of 12" diameter samples subjected to anisotropic consolidation

(See Fig.7:3:4)

Sample No.14M/12 had a grading very similar to grading A and it was compacted to a density of 129.6 lbs/ft.^{3} The angle of internal friction was 39.8° at a confining pressure of 135 p.s.i. Sample 7M/12 was subjected to siotropic consolidation and the angle of internal friction was 39.9°. This sample though was somewhat denser than 14M/12 and the mean angle of internal friction for samples at 90% relative density was about 1° higher.

The angles of internal friction shown by samples 20M/12 and 21M/12, which were sheared at confining pressures of 300 lbs/in.^{2} and 500lbs/in.^{2} respectively, were about 1° below an extrapolation of the curve for isotropically consolidated samples. The gradings of these two samples were made up to prevent membrane punctures and preserve sufficient permeability at the higher stresses. However, differences of 1° in the value of ϕ'_f are of little significance and are within the variations obtained with supposedly identical samples.

Sample 26M/12 was failed by increasing the pore pressure and thus increasing the stress ratio. The angle of internal friction, at maximum stress ratio, was 48.3° which was about 2° above the mean for samples consolidated isotropically and sheared at the equivalent minor principal stress.

Sample 28M/12 was constructed with the particles orientated at 64°. After anisotropic consolidation it was failed by reducing the minor principal stress. The angle of internal friction obtained was about 2.5° below the mean for samples with random particle orientation and subjected to a normal shear test at an equivalent pressure. Thus there did not appear to be any significant difference in shear strength under drained conditions, between samples consolidated isotropically or anisotropically.

(7:3:5) Shear strength of 4" diameter samples (drained shear tests)

See Table 7B and Figs.7:3:5a, 7:3:5b, 7:3:5c and 7:3:5d.

Samples 4" in diameter, with grading C also $D/_d = 4$, compacted to a relative density of 90%, showed lower angles of internal friction than 12" diameter samples of grading A. However $1\frac{1}{2}$" diameter samples, at the same relative density, showed higher angles of internal friction with $D/_d = 4$ grading E (Fig.7:3A)

It might have been expected that a greater shear strength would be shown by samples with larger particles. Alternatively, as the particle size is reduced so the unit shear strength increases because of the lower proportion of flaws. The samples with smaller particles should, therefore exhibit greater dilatancy and, hence shear strength at any given minor principal effective stress.

The interparticle contact forces are very much lower in the smaller samples if geometrically similar gradings are used. Any horizontal plane in the three sizes of sample contains the same number of particles but the force to be transmitted is proportional to the square of the sample diameter. If the resultant particle fracture was simply the breaking off of contacts one would expect a much lower dilatancy from the larger sample and, hence, a lower value of ϕ'_f.

However, the plot of ϕ'_f against the rate of dilatancy at failure shows that, for any given ratio of sample diameter to nominal particle size there is a unique relationship for all sizes of sample. The shear strength of individual particles is proportional to their area of cross-section, which, in turn, is very approximately proportional to the square of the nominal size. Hence, the particle shear strength is roughly proportional to the forces to be transmitted in various sizes of sample when the gradings are scaled geometrically and all samples are subjected to the same principal effective stresses.

Samples 4" and $1\frac{1}{2}$" in diameter were also tested with the $\frac{D}{d}$ ratio equal to 8. Again, a unique relationship was found between $\phi'^{\frac{D}{d}}_f$ and the rate of dilatancy at failure (Fig.7:3B). The line lay below that for D/d = 4 and was rotated clockwise. The significance of the clockwise rotation is that a greater dilatancy is required for a given angle of internal friction. A maximum nominal particle size equal to $\frac{1}{4}$ of the sample diameter may be too large. Further tests with $D/_d \geq 16$ gave a unique line again rotated clockwise and below that for $D_d = \mathcal{C}$. It would suggest, therefore that the maximum particle size to be tested should be less than 1/16th of the sample diameter. The maximum particle size which may be used though is also dependant on the material grading and may also depend on the particular shape, surface texture and strength relative to

the applied stresses.

The greater the clockwise rotation the stronger is the material. The line does not become horizontal because the plot also reflects the relative density of the grading.

In general, very dense material which has high particle strength and or is subjected to low stresses plots in the upper right hand corner. Material which is weak and, or subjected to high stresses plots in the lower left hand corner. Dense and loose in this context refer to the relative densities and weak and strong to the relative strength of the particles compared with the forces applied to them. The material grading is important here because the loads will be transmitted more easily by a well graded than a uniform material.

The vertical position of the right hand end of the line will depend on the applied stresses and the particle shape rounded material below.

The silurian cleaved mudstone breaks down easily under stress and only a moderate dilatancy is achieved even at low stresses and in the dense state.

If the shear strength is produced solely by the friction between the particle surface and dilatancy all materials with different $\phi\mu$ values should give parallel lines. The alternative is an intersection of lines of two materials having different values of $\phi\mu$. An intersection infers that the $\phi\mu$ values are then equal.

When breakdown occurs at particle contacts they are separated by fine particles, which may act in a similar manner to rollers. A cubical box will usually roll rather than slide when pushed at the top edge, even on a surface with a low coefficient of friction. Few soil particles are cubical and all other shapes will roll more easily in at least one direction.

Samples of a given diameter, but with different maximum particle sizes, showed different strengths on a plot of the angle of internal friction against the minor principal stress (Fig.7:3A) The larger particles displayed the greater shear strength at low stresses. The rate of particle breakdown with increase in stress was also greater for the larger particles so that the two shear strengths coincided at some greater pressure.

(7:3:6) Shear strength of $1\frac{1}{2}$" diameter samples (drained shear tests)

(See Table 7C and Figs.7:3:6a and 7:3:6b)

The $1\frac{1}{2}$" diameter samples showed a greater shear strength than the 4" diameter samples having the same ratio of particle size to sample diameter.

The shear strength of grading A in the 12" diameter samples lay mainly between that for the two gradings tested in $1\frac{1}{2}$" diameter samples.

It has been estimated that the maximum ram friction in small scale apparatus amounts to about 5% of the deviator load which is equivalent to just under a 1° error in ϕ'. It is also only likely to take effect after the peak deviator stress has been passed as observation, of smaller samples showed that the deformation was predominantly by bulging until the peak deviator stress was reached. It is therefore unlikely that an error of more than 1° or 2° exists in the values of ϕ' obtained in the large triaxial apparatus.

One would expect that either progressively greater shear strengths would be shown by tests on $1\frac{1}{2}$, 4 and 12" diameter samples or else the reverse order. Similar angles of internal friction were obtained from tests on samples $1\frac{1}{2}$" and 12" in diameter and lower values from 4" diameter samples.

Grading F, when tested in 4" diameter samples, showed a lower shear strength than when tested in $1\frac{1}{2}$" diameter samples.

The Möhr failure circles are plotted in Figs 7:3D, 7:3E and 7:3F. The mean failure envelope for the $1\frac{1}{2}$" diameter samples is similar to that for the 12" diameter samples. The slope of the Möhr failure envelope reduces from about 50° at the low stresses to 30° at a normal effective stress of 850 p.s.i.

The average angles of internal friction for drained shear tests, on gradings E and F, tested in $1\frac{1}{2}$" diameter samples, were within 1° of the average values obtained with the various gradings tested in 12" diameter samples at confining pressures between 10 p.s.i. and 500 p.s.i.

The gradings tested in 4" diameter samples showed angles of internal friction about 3° below the 12" diameter samples, at confining pressures between 10 p.s.i. and 120 p.s.i. in drained shear tests.

It may be concluded that the silurian cleaved mudstone shows a very modest dilatancy because of the large amount of particle breakdown. It therefore behaves very much like a loose sand.

A greater dilatancy is shown with increasing maximum particle size but this would also be expected because of the change in the geometry of the gradings.

(7:3:7) Shear strength of samples sheared under undrained conditions

It has been shown that the stress paths to failure of some loose sands which are susceptible to flow slides, bear a close resemblance to those for sensitive clays (9).

Several 12" and 4" diameter samples were consolidated isotropically and then sheared under undrained conditions.

When testing a rockfill under undrained conditions a problem occurs

because of membrane penetration. During consolidation there is a certain amount of membrane penetration and as a pore pressure is built up during shear there is a change in the net stress across the membrane which subsequently yields, giving a small volume change. The volume change will depend on the membrane thickness, the grading of the material and the pore water and confining pressures. Errors due to membrane penetration would be a minimum with well graded material and a maximum with coarse, uniform gradings.

Sample 30M/12 was compacted to a dense state and the maximum particle size was 3". At the beginning of the shear stage the sample consolidated giving rise to an increase in pore pressure. The deviator stress rose sharply at first and then the curve flattened out.(Fig.7:3:7a). The stress path up to about 11% axial strain was very similar to that for a dense sand. At the peak deviator stress the angle of internal friction was about 5° above β'_f corresponding to zero dilatancy obtained from drained shear tests.

A puncture occurred in the membrane at about 11% axial strain and the pore pressure and confining pressure then equalised. The membrane was then responsible for applying the confining pressure. The value of $\phi' = 66.7^{\circ}$ was obtained by assuming that the membrane was applying a confining stress of 1.2 p.s.i. Extrapolating the plot on Fig.7:3A it appears that the membrane effect may have been about 2.2 p.s.i.

Sample 31M/12 had a similar grading to sample 30M/12 but it was compacted to a greater density. Again, the pore pressure built up rapidly with increasing deviator stress. The relationship between $\dot{\varepsilon}'_1$ and axial strain was very similar to that for a medium dense sand. The stress path to failure was also very similar to that for a medium dense sand.

Sample 32M/12 (Fig.7:3:7b) had a similar grading to the two previous samples and it was loosely compacted. A very high pore pressure built up and the sample had a stress path to failure similar to a loose sand.

Samples 31M/12 and 32M/12 also showed a greater peak value of ϕ' (Fig.7:3:7b) than that corresponding to zero rate of dilatancy for drained samples.

Two consolidated, undrained tests, on grading D in 4" diameter samples were carried out by Dr.B.Bros whilst on sabbatical leave from Poland. Both samples were compacted to medium relative density.

The first sample was consolidated isotropically to 75 p.s.i. The pore pressure built up slowly and the stress path was similar to that for a dense sand.

The second sample was consolidated isotropically to 25 p.s.i. The behaviour was somewhat similar to that in the first test (Fig.7:3:7c).

It showed a higher maximum stress ratio but this would be expected because of the lower effective stresses. The stress path showed that there was no tendancy to behave as a loose sand.

The value of ϕ' was again somewhat above that at zero rate of dilatancy for corresponding drained shear tests (Fig.7:3:7c)

De-aired water was passed through the large samples for 24 hours prior to testing. A back pressure was not used.

The differences in the stress paths between the 12" and 4" diameter samples showed that the smaller material was more resistant if subjected to undrained loading. The stresses involved were lower but the major difference probably arose because of the finer grading ($D/d = 4$ in 12" diameter samples and $D/d = 8$ in 4" diameter samples) and, hence, much lower interparticle forces. Particle breakdown would be less and hence the build up of pore pressure would also be less with the smaller material.

It would suggest that for maximum resistance to seismic shock under undrained loading the material should possess a wide grading and a small maximum particle size such that particle contact forces are a minimum.

(7:4) Deformation

Deformation occurs as a result of four major factors:

a) The breaking of particle contacts.
b) The destruction of particles by shearing or bending.
c) The reorientation of particles
d) The elastic deformation of particles
e) The sliding of particles.

The extent of the deformation depends on:

a) The particle strength.
b) The applied stress.
c) The grading of the material.
d) The initial state of packing

(7:4:1) Deformation of 12" diameter samples (drained shear tests)

The axial strain at failure of 12" diameter samples of grading A at similar densities tended to increase with increasing stress. Those samples which were initially loose also had a much greater axial strain before failure.

At low pressures the application of a deviator stress caused an initial consolidation, even with very dense samples, which was later followed by a small dilation (Fig.7:3:1) Samples subjected to higher pressures tended to consolidate and shear at approximately constant volume.

Sample No.1M/12awhich was somewhat looser than the remainder,under-

went a large axial strain to failure and consolidated throughout most of the test.

(7:4:2) Deformation of 12" diameter samples with orientated particles

The samples which were built up with the particles specially orientated had very large strains before the peak shear strength was reached and consolidation took place thoughout the tests.

The deviator stress built up particularly slowly in sample No10M/12. This was because the initial density was very low and also no material passing a No.7B.S.sieve was initially present. The total volume change for a deviator stress of 250 p.s.i. was more than double that for sample No.22M/12, which had a higher density, much wider grading and was tested at the same minor principal effective stress (Fig.7:3:2)

Failure strains for samples with randomly orientated particles were about half of those for samples with specially orientated particles.

Failure was along a shear plane with a slight amount of sample bulging.

(7:4:3) Deformation of 12" diameter samples with special gradings.

Samples 12M/12 and 13M/12 were compacted in the normal way but without any material passing the $\frac{3}{8}$" B.S.sieve (Table 5:6:1 and Fig.7:3:3). The peak deviator stresses were not reached with either sample because of the membrane difficulties when testing fairly uniform gradings of large particles even at low confining pressures. The axial and volume strains for a given deviator stress though are considerably greater than for a wide grading subjected to the same initial compactive effort as was sample 17M/12.

The effects of overconsolidation are apparent with sample 25M/12. This sample was consolidated isotropically to 300 p.s.i. and then failure was effected by increasing the pore pressure. The sample behaved in a very brittle manner without further volume change. It was initially very dense.

(7:4:4) Deformation of 12" diameter samples subjected to anisotropic consolidation.

Sample 16M/12 was a little denser than 15M/12 and had a grading with a smaller maximum particle size. Both samples were subjected to similar compactive efforts but the finer grading displayed much greater stiffness during anisotropic consolidation. Sample 14M/12 was slightly looser than 15M/12 and its axial strain was greater for a given deviator stress.

Samples 26M/12 and 28M/12 were consolidated anisotropically to a similar deviator stress. The latter sample had particles orientated at 64° and was also looser and had a greater maximum particle size. Its axial strain during consolidation was twice that of the former sample.

The strain required to achieve failure after the completion of consolidation was about the same for samples 14M/12 and 7M/12 but the isotropically consolidated sample had a somewhat higher initial density and the grading was not terminated at the No.100 B.S.sieve.

The volume strains to failure of samples 20M/12 and 21M/12 were very large but this is not surprising considering the very high stresses involved. Also the gradings of these two samples were without material passing the No.14 B.S.sieve and the maximum size of particle passed the $\frac{3}{4}$" B.S. sieve.

The axial strains to failure of these samples, after completion of anisotropic consolidation, were similar to those of samples tested at very much lower pressures.

(7:4:5) Deformation of 4" diameter samples (Drained shear tests)

Three different gradings were used in the shear tests on 4" diameter samples.

Samples 3M/4 and 4M/4 were made up with grading F and had very similar initial densities. The rate of axial strain applied to sample 4M/4 was 1/6th of that for sample 3M/4. Both samples had identical stress - strain curves and almost identical volume change characteristics. The axial strains at failure were 10.5% compared with 12% for a 12" diameter sample of grading A compacted to the same density.

In general the stress - strain curves for the drained shear tests were very similar for 12" and 4" diameter samples up to the peak deviator. Axial failure strains for 4" diameter samples varied between about 10% and 12.5% for minor principal effective stresses of 10 p.s.i. and 120 p.s.i. respectively.

Volume changes of the 4" and 12" diameter samples are very similar at any given applied effective stress, irrespective of the grading used.

At a confining pressure of 10 p.s.i. samples of each of the three gradings at similar initial densities had similar axial strains at failure.

This is surprising because of the very much greater number of particle contacts and the reduced particle contact forces of the grading having the smallest maximum size. Presumably, the greater number of points deforming account for the same volume change as occurs in the coarser grading due to particles snapping and point deformation.

Again, at a cell pressure of 120 p.s.i. samples of gradings D and F with the same initial density, had similar axial strains to failure,

With the 12" diameter samples the stress-strain curves tended to be flat topped after peak whereas the deviator stress reduced with the smaller samples. The sample top cap was allowed unlimited horizontal travel with

the smaller samples and rotating bushes were also used. It was after the peak that the samples started to shear along the plane. This set up shear forces producing extra piston friction in the largest apparatus, which was not fitted with a rotating bush and in which the top cap was only allowed a limited horizontal travel.

(7:4:6) Deformation of 1½" diameter samples (drained shear tests)

Drained shear tests were carried out on gradings E and F using 1½" diameter samples.

The axial strains at failure were of the same order of magnitude as those in 4" and 12" diameter samples.

In the tests on grading F there was a tendancy for the axial strain at failure to increase with stress but this trend was then reversed with the tests performed at confining pressures above 150 p.s.i. (Fig.7:3:6a).

The volume strains for a given deviator stress were very similar to those in 4" diameter samples in which similar gradings were tested at comparable densities. However, the volume strains of 12" diameter samples having gradings containing 3" particles were somewhat greater.

The volume strain of sample 11M/12 containing particles of ½" maximum size was very comparable with the strains of the smaller samples.

Samples tested at low pressures tended to have rather flat topped stress-strain curves after the peak whereas the deviator stress dropped off rapidly after the peak in tests performed at very high pressures.

It appeared, in general, that the volume and axial strains for dense samples with geometrically similar gradings were very comparable at a particular effective stress, irrespective of the sample size.

The failures of all the silurian cleaved mudstone samples were characterised by an initial bulging which was usually followed by shearing along a plane.

(7:4:7) Axial deformation of samples sheared under undrained conditions

Several undrained shear tests were performed on samples 4" and 12" in diameter. The results are plotted in Figs.7:3:7a, 7:3:7b, and 7:3:7c.

Sample 30M/12 was compacted to a dense state and consolidated isotropically to 80 p.s.i. Failure in terms of maximum stress ratio, occurred at about 7.5% of axial strain.

At 11% of axial strain a leak occurred and the pore pressure and cell pressure were equalised at 14% of axial strain.

Sample 31M/12 was compacted to a very dense state and consolidated isotropically to 120 p.s.i. Failure, in terms of maximum stress ratio, occurred at about 5% axial strain.

Sample 32M/12 was placed loose and consolidated isotropically to 80 p.s.i. Failure occurred at an axial strain of about 13%

During consolidation all the samples would have suffered a certain amount of membrane penetration because the maximum grain size was 3". The grading however, possessed a good proportion of fines (Table 5:6:1).

As the pore water pressure built up any initial penetration would be reduced and thus a truly undrained condition was probably not achieved.

Two medium, dense, 4" diameter samples, of grading D were tested at consolidation pressures of 25 p.s.i. and 75 p.s.i. The maximum stress ratios were reached at about 10% axial strain. The failure strains of all samples were, therefore, proportional to the relative densities.

(7:4:8) Volumetric strain and deviator stress

The volumetric strain was plotted against the deviator stress and it was found, for most samples, than an approximately linear relation existed. The higher the initial isotropic consolidation stress the greater the subsequent deviator stress for a given volume strain.

The effects of overconsolidation were apparent in sample 25M/12. This sample was consolidated isotropically to 300 p.s.i. and then failed by reduction of the minor principal stress. A deviator stress of about 250 p.s.i. was built up without any volume strain.

The volume strain-deviator stress curves for the K_o tests during anisotropic consolidation were not straight lines. After anisotropic consolidation there was an almost linear relationship between the deviator stress and the volume strain for the samples failed by increasing stresses. These lines were parallel for samples 20M/12 and 21M/12 and also for the latter parts of the anisotropic consolidation of samples 14M/12 and 16M/12. (Fig.7:3:4)

(7:4:9) Creep

Rockfill materials appear to creep at an ever decreasing rate almost indefinitely. Kjaernsli in a paper on the Venemo Dam in 1962 plotted the settlement of various layers as determined by cross arm measurements. At a large time after the initial deformation the rate of creep was very similar for all stress levels. This may suggest that contact stresses between grains of the same material are the same at any given time after loading and that creep is dependant on these stresses.
A certain amount of creep was noticed with all the samples tested.

During isotropic consolidation the major part of the volume change occurred almost instantaneously when a pressure increment was applied and it usually reached a steady value for practical purposes after about $\frac{1}{2}$ an hour.

When the applied axial strain ceased at the end of a shear test the deviator load reduced very rapidly with the 12" diameter samples. This was, to a certain extent, a function of the apparatus and the load measuring element. These being stiff, only a minute strain was required to record a great load reduction. In the small scale apparatus the deviator load was measured by a proving ring and, as a result, a small axial deformation of the sample made only a small reduction in the stresses applied to it.

(7:4:10) One dimensional compressibility

Several K_o tests were carried out to determine the values of K_o (the coefficient of earth pressure at rest) and m_v (the one dimensional compressibility).

All the curves (with one exception) of axial strain against major principal effective stress show an initial effect (Figs.7:4:10 A - G) which has been attributed to compaction and isotropic consolidation to about 25 p.s.i.

Samples 14M/12 and 15M/12 had a maximum particle size of 3" and they were compacted to a dense state. Sample 16M/12had a maximum particle size of $1\frac{1}{2}$" and was also compacted to a dense state. The finer grading shows no overconsolidation effects and also the plot of σ_3' against σ_1' shows that K_o remains constant throughout the stress range applied. This would suggest that membrane penetration has a large effect on K_o at low stresses. Part of this effect though may be due to the initial isotropic consolidation as extrapolations of the straight portions of the curves pass near to the origin.

The axial deformation of the finer grading was considerably less than that of the coarser gradings for a given major principal effective stress.

Samples 20M/12 and 21M/12 were subjected to the normal compaction but the density of the former sample was rather low. The initial stages of the consolidations were erratic. The looser sample showed a somewhat greater deformation for a given stress. Samples 21M/12 and 14M/12 had similar densities but the former, with a finer grading, had an axial strain about half that of the latter at a major principal effective stress of 250 p.s.i.

The large axial strains of samples 20M/12 and 21M/12 were to be expected because of the very high stresses.

Sample 28M/12 had particles orientated at 64° and this along with a larger maximum particle size and lower density accounted for the very much larger deformation than 26M/12 for similar stresses.

The values (secant) of m_v for a given major principal effective stress are plotted in Fig.7:4:10h.

It will be seen that dense, well graded materials with small maximum particle size show the lowest compressibilities.

After an initial effect which is presumed to be due mainly to the sample compaction there is a reduction of compressibility with increase in stress for all gradings.

Loose, uniform material shows the greatest compressibility.

The values of K_o are tabulated below and it will be noticed that all the values are very similar irrespective of the sample grading or its initial density.

Test No.	γ_d lbs/ft.	grading limits	K_o
14	129.6	3" to + 100	0.45 (1)
15	132.4	3" to - 100	0.43 (1)
16	136.2	$1\frac{1}{2}$" to - 100	0.51
20	120.9	$\frac{3}{4}$" to + 14	0.49
21	130.6	$\frac{3}{4}$" to + 14	0.44
26	138.0	2" to + 52	0.43
28 (2)	128.2	3" to + 25	0.39

(2) orientated particles (1) at higher stresses

Table 7:4:10 Average values of K_o.

The lowest value of K_o was shown by sample No.28M/12 in which the particles were orientated.

Very low values of K_o ($\simeq$ 0.25) were recorded in the initial stages of samples 14M/12 and 15M/12. This was attributed to membrane penetration, the effects of compaction and the initial isotropic consolication.

Except for the two tests mentioned above, the values obtained for K_o remained sensibly constant over the applied stress range (i.e. to a minor principal effective stress of 500 p.s.i.) The value of ϕ'_f decreased with increasing stress and the simple relation $K_o = 1 - \sin \phi'$, did not thereforehold (except for ϕ'_f obtained when shearing a sample at a minor principal effective stress of 500 p.s.i.) Further, the value obtained for K_o did not agree with that obtained by substituting ϕ' at constant volume (41°) in the above equation.

The membrane penetration at low stresses causes a greater initial compressibility and the mean area of cross-section of the sample increases. This leads to an error in calculating the deviator stress and subsequently to an underestimate of the value of K_o by 1 to 3%.

(7:4:11) Particle breakdown

The change in a grading due to particle breakdown under applied stress

depends on many factors. In the triaxial tests on silurian cleaved mudstone many gradings at various absolute and relative densities were tested. The stresses varied over a wide range and the stress ratios and resulting strains varied. The axial strain during a shear stage was often limited by membrane puncture. When all these factors are considered the comparison of gradings before and after stress application is particularly complex and will only be dealt with summarily here.

The change in grading also has an effect on permeability but again this also depends on the mineral composition of the material and the way the fines behave when wetted. When the mudstone was wetted material below a No.25 B.S. sieve formed a paste which considerably reduced the permeability to water.

Further complications arose during sieve analysis. The material would break downduring sieving and the longer it was sieved the more rounded and smooth it became. This, to a certain extent, may explain the lower angles of internal friction obtained with tests on 4" diameter samples. Most of the material was re-sieved after tests on 12" diameter samples and further sieved on 12" diameter sieves to remove adhering fine material before being used for 4" tests.

Material below the No.25 B.S.sieve tended to ball when sieving no matter how long it had been dried. Fine material also adhered to larger particles and it was particularly difficult to achieve an accurate grading analysis after testing. The sieving process could not be relied upon to clean the material in the time normally allowed. Sieving for a longer time produced more breakdown and fines as did hand cleaning of material.

Direct comparison of geometrically similar gradings in different sample sizes may be misleading. The breaking of particles point depends on the load being transmitted which is proportional to the square of the sample diameter. The strength of particles in shear is proportional to their cross-section, which is proportional to the square of the sample diameter. The bending strength of particles is dependant on their shape and for circular or cubical shapes proportional to the fourth power of their diameter or side. It is, therefore, likely that most breakdown occurs through shearing and at particle contacts and a smaller amount of bending perhaps at rigid boundaries.

When gradings were made up they probably contained a greater proportion of fine material than intended. This was especially so with the large samples where fine material adhered to larger particles and breakdown occurred due to handling bags of material. The dust extractor used during sample compaction then removed some fine material.

After test sieving recorded a greater proportion of fines than existed

immediately after the shear test because of breakdown during dismantling, drying and transport prior to sieve analysis which produced further breakdown.

When sieving out a bulk grading it is necessary to clean the sieves after each batch so that the correct proportion of various sizes of particle are maintained in any one sieve size interval.

In general, large particles broke into smaller ones having the same proportions.

Several methods have been used for describing breakdown determined by sieve analysis.

Marsal (1965) used the parameter $\bar{B}$ which he defined as the sum of the differences of a given sign between the percents retained in the original sample and in the specimen after testing.

Lee (1967) used the ratio of the D_{15} sizes in the original sample and after testing. This has an advantage in that it is the size on which filter designs are based.

Alternatively, the areas underthe original and final grading curves may be compared.

A further alternative is to take the mean of the increases in the percent of material retained on each sieve before and after testing.

If this last method is used to compare the breakdown of two $1\frac{1}{2}$" diameter samples with geometrically similar gradings, such that the interparticle forces are 4 times as great in the sample with the larger maximum particle size, it is noticed that the breakdown is also about 4 times as great (Table 7:4:11a).

Similar comparisons are made in Table 7:4:11b and c. In these cases balling of fine material was evident.

For one grading tested at several pressures the breakdown increased with pressure but was not directly proportional. This though is not surprising because of the stress history. The maximum stress ratio, which is probably most responsible for breakdown, reduces with increase in stress. Also the breakdown is a result of isotropic consolidation and shear.

Breakdown on $1\frac{1}{2}$" diameter samples of silurian cleaved mudstone.

$\sigma_3' = 10$ p.s.i. Tests: 2M/$1\frac{1}{2}$ and 7M/$1\frac{1}{2}$				each taken to $\epsilon_1 \approx 20\%$		
B.S.Sieve size	%passing before	after	diff.%	%passing before	after	diff.%
$\frac{3}{8}$"	100	100	0			

σ'_3 = 10 p.s.i.
Tests: 2M/1½ and 7M/1½ each taken to ϵ_1 = 20%

B.S.Sieve size	% passing before	% passing after	diff.%	% passing before	% passing after	diff.%
⅜"	100	100	0			
3/16"	77	84.9	7.9	100	100	0
No. 7	47.5	52.3	4.8	75	75.6	1.5
No.14	30.5	34.6	4.1	47.5	48.3	0.8
No.25	20.5	25.4	4.9	30.5	32.0	1.5
No.52	13.5	17.6	4.1	20.5	21.6	1.1
No.100	10.0	13.2	3.2	13.5	14.3	0.8
		Σ = 29.0				Σ = 5.7
		mean = 4.16				mean= 0.95

Table 7:4:11a.

σ'_3 = 40 p.s.i.
Tests: 1M/1½ and 4M/1½ each taken to ϵ_1 = 20%

B.S.Sieve size	%passing before	after	diff.%	% passing before	% passing after	diff.%
⅜"	100	100	0			
3/16"	77	85.5	8.5	100	100	0
No.7	47.5	55.6	8.1	75	76.6	1.6
No.14	30.5	37.5	7.0	47.5	48.8	1.3
No.25	20.5	28.1	7.5	30.5	31.8	1.3
No.52	13.5	20.5	7.0	20.5	19.3	-1.2
No.100	10.0	15.8	5.8	13.5	12.3	-1.2
		Σ = 44.0				Σ = 1.8
		mean = 6.29				mean = 0.3

Table 7:4:11b

σ'_3 = 147 p.s.i.
Tests: 3M/1½ and 5M/1½ each taken to ϵ_1 = 20%

B.S.Sieve six	% passing before	% passing after	diff%	% passing before	% passing after	diff.%
⅜"	100	100	0			
"	77	86.7	9.7	100	100	0
No.7	47.5	59.9	12.4	75	78.5	3.5
No.14	30.5	40.5	10.0	47.5	48.4	0.9
No.25	20.5	28.1	7.6	30.5	27.6	-2.9
No.52	13.5	18.7	5.2	20.5	15.4	-5.1
No.100	10.0	14.5	4.5	13.5	10.1	-3.4
		Σ = 49.4 mean = 7.06			Σ = 7.0 mean = 1.17	

Table 7:4:11c.

σ'_3 = 10 p.s.i.

Grading C Sample 8M/4 σ'_{1f} = 71.7 p.s.i		Grading D Sample 7M/4 σ'_{1f} = 64.3	Grading F Sample 8M/4 σ'_{1f} = 58.6	
B.S. Sieve	Diff in % passing after rest.	diff in % passing after test	B.S. Sieve	diff in % passing after test.
1"	0			
½"	1.5	0	3/16"	0
¼"	1.5	1.0	7	0.6
⅛"	1.5	0.8	14	0.8
No.8	1.0	1.0	25	1.3
No.18	-	1.5	52	1.9
No.36	-	1.0	100	0
No.72	-	0.3		
	Σ = 5.5 mean = 0.69	Σ = 5.6 mean = 0.80		Σ = 4.6 mean= 0.77

Table 7:4:11d

Sample 4M/12 Grading: A σ'_3 = 10 p.s.i.		Sample = 1M/12 Grading: A σ'_3 = 40 p.s.i	Sample:2M/12 Grading:A σ'_3 = 80 p.s.i.
B.S. Sieve	diff in % passing after test	diff.in % passing after test	diff. in % passing after test
3"	0	0	0
1½"	6.0	27.5	21.1
¾"	10.0	26.4	26.7
⅜"	3.5	17.8	25.1
3/16"	1.5	15.1	20.0
No.7	3.0	9.9	16.3
No.14	1.2	6.0	14.4
No.25	1.0	4.1	12.6
No.52	1.0		11.2
No.100	0.8		10.6
Σ = 28.0 mean = 2.8		Σ = 106.8 mean = 13.35	Σ = 158.0 mean = 15.8

Table 7:4:11e

Three tests on 4" diameter samples with different gradings, at a confining pressure of 10 p.s.i. showed almost identical breakdown. (Table 7:4:11d).

Three tests on 12" diameter samples at confining pressures of 10,40 and 80 p.s.i. showed a fourfold increase in breakdown between 10 and 40 p.s.i and a five or sixfold increase between 10 and 80 p.s.i.(Table 7:4:11e).

The increase in breakdown with maximum particle size for two 12" diameter samples sheared at a confining pressure of 100 p.s.i. is shown in Table 7:4:11f.

σ'_3 = 100 p.s.i. Sample 5M/12 ϵ_1 = 19.8%				σ'_3 = 100 p.s.i. Sample 11M/12 ϵ_1 = 12.5%		
B.S.Sieve	% passing before	% passing after	diff.%	% passing before	% passing after	diff.%
3"	100	100	0			
$1\frac{1}{2}$"	81	98	17			
$\frac{3}{4}$"	51	75	24			
$\frac{1}{2}$"				100	100	0
$\frac{3}{8}$"	31	51	20	95	96	1
3/16"	19	35	16	77	79	2
No.7	12	25	11	59	63	4
No.14	8	15	7	45	47	2
No.25	6	9	3	29	29	0
No.52	5	6	1	18	18	0
No.100	4	4	0	10	10	0
No.200	3	2	-1	4	4	0
		Σ = 98.0 mean = 8.9				Σ = 9.0 mean = 1.0

Table 7:4:11f

Samples 14M/12 and 15M/12 were subjected to anisotropic consolidation to a minor principal effective stress of 135 p.s.i. The former sample was sheared and the latter was not. The breakdown in the former sample was about 3 times that of the latter.

Sample 21M/12 was anisotropically consolidated to a minor principal effective stress of 500 p.s.i. and then sheared. A very large amount of breakdown was therefore to be expected even though the maximum particle size was $-\frac{3}{4}$" + $\frac{1}{2}$" and its extent is shown in Table 7:4:11g.

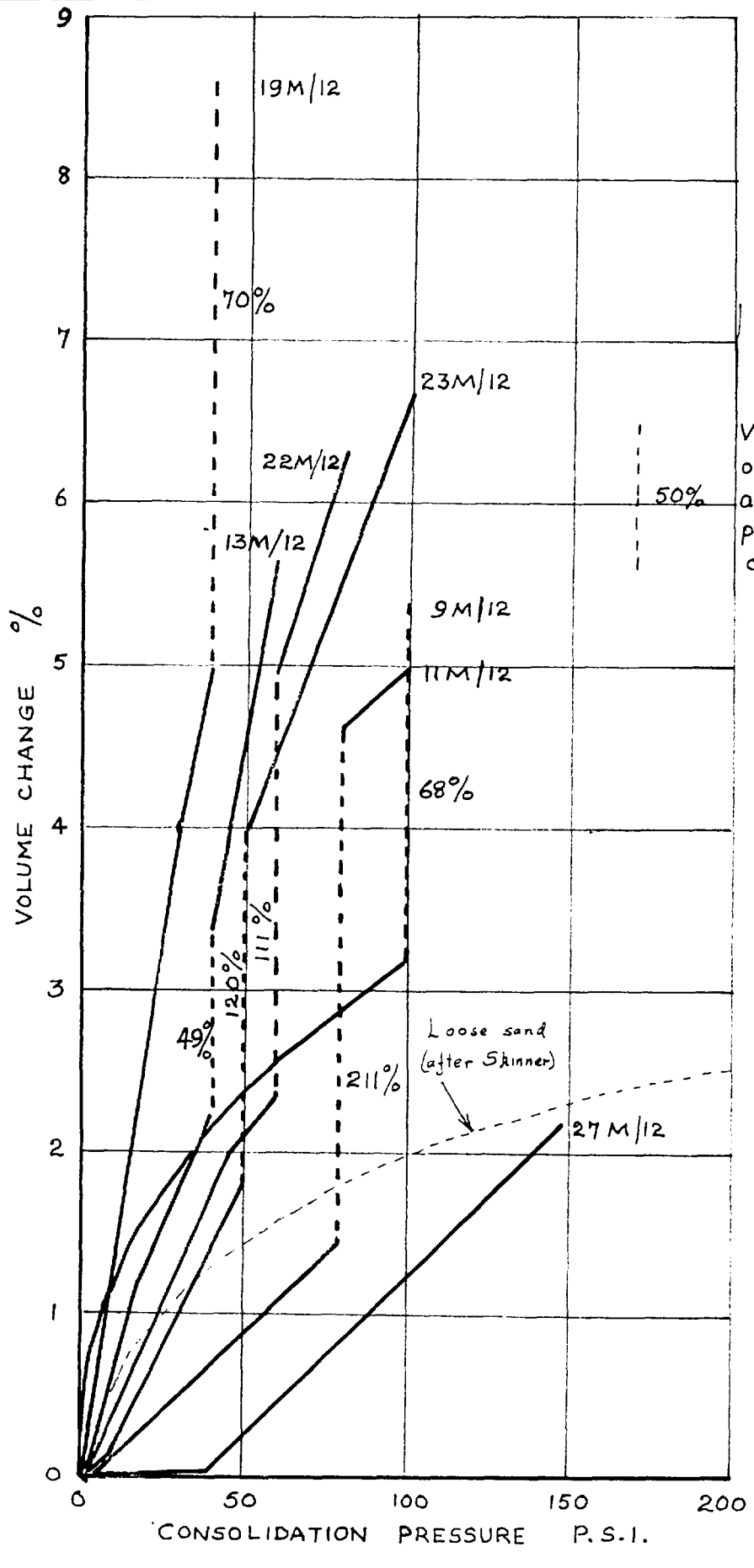
Sample No.21M/12			
B.S.Sieve	% passing before	% passing after	diff.%
$\frac{3}{4}$"	100	100	0
$\frac{3}{8}$"	74	89	15
$\frac{3}{16}$"	49	68	19
No.7	25	50	25
No.14	0	31	31
No.25	0	17.5	17.5
No.52	0	10.0	10.0
No.100	0	6.0	6.0
			Σ = 123.5 mean = 15.4

Table 7:4:11g

In general terms breakdown will increase with:

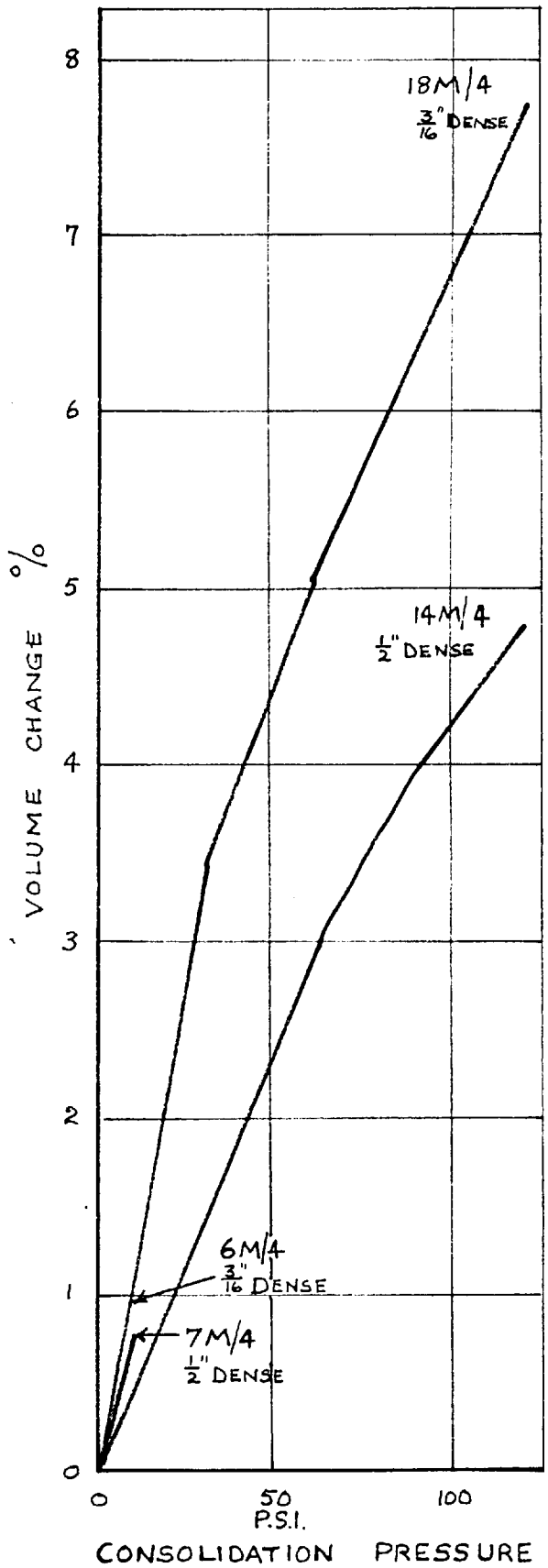
1) increase in maximum particle size.
2) increase in uniformity of grading.
3) increase in mean stress or stress ratio.
4) decrease in particle strength.
5) increase in angularity of particles.
6) increase in strain.
7) increase in time.
8) wetting.

The permeabilities of some of the samples before and after shearing are recorded in Tables 7A, 7B and 7C.



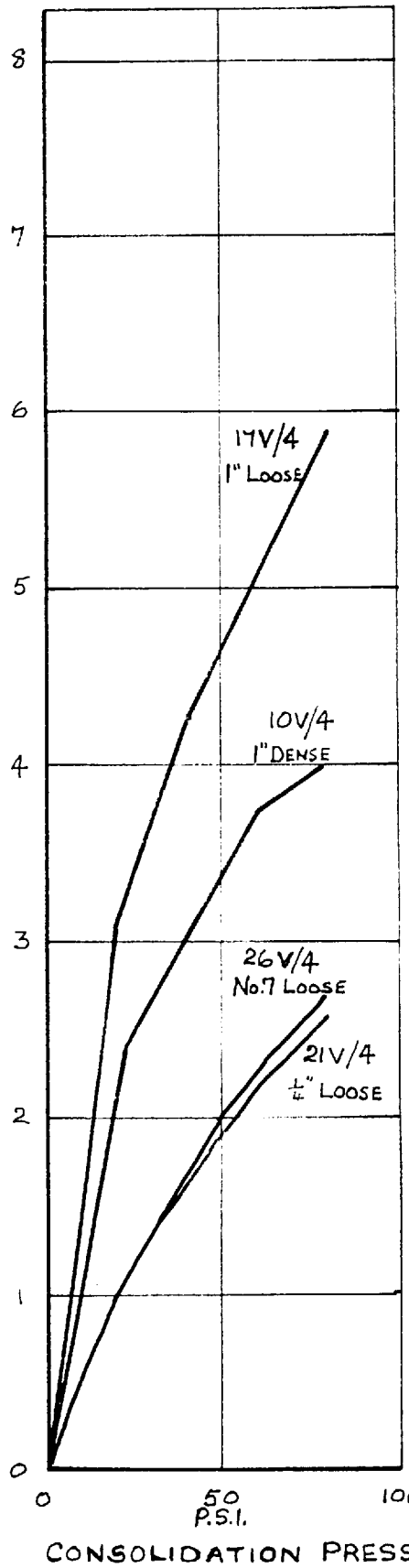
VOLUME CHANGE ON SATURATION DURING ISOTROPIC CONSOLIDATION. SILURIAN CLEAVED MUDSTONE 12" DIA. SAMPLES.

FIG. 7:2:1



CONSOLIDATION PRESSURE VOLUME CHANGE DURING ISOTROPIC CONSOLIDATION

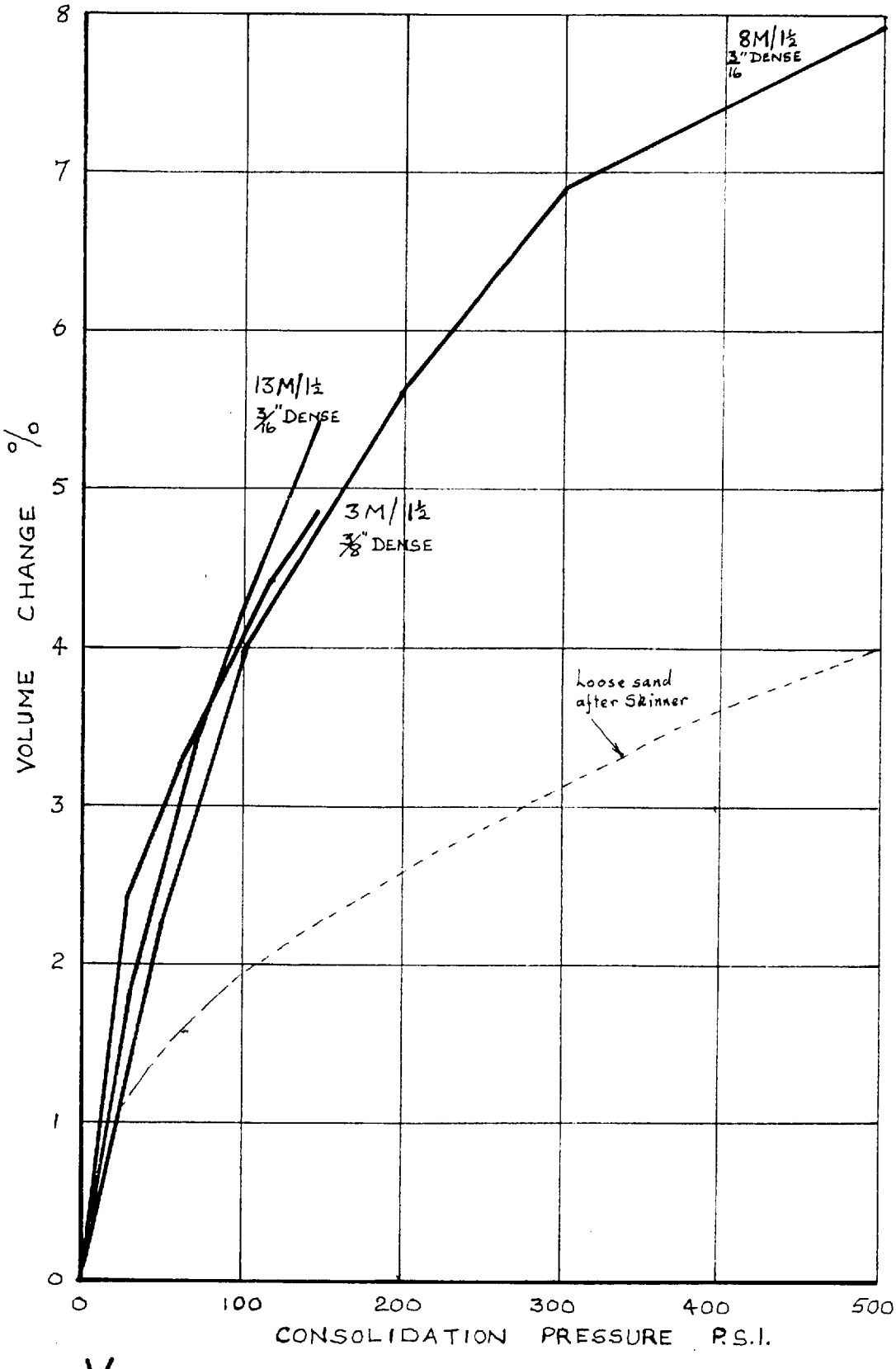
SILURIAN CLEAVED MUDSTONE 4" DIA. SATURATED SAMPLES.



CONSOLIDATION PRESSURE VOLUME CHANGE DURING ISOTROPIC CONSOLIDATION

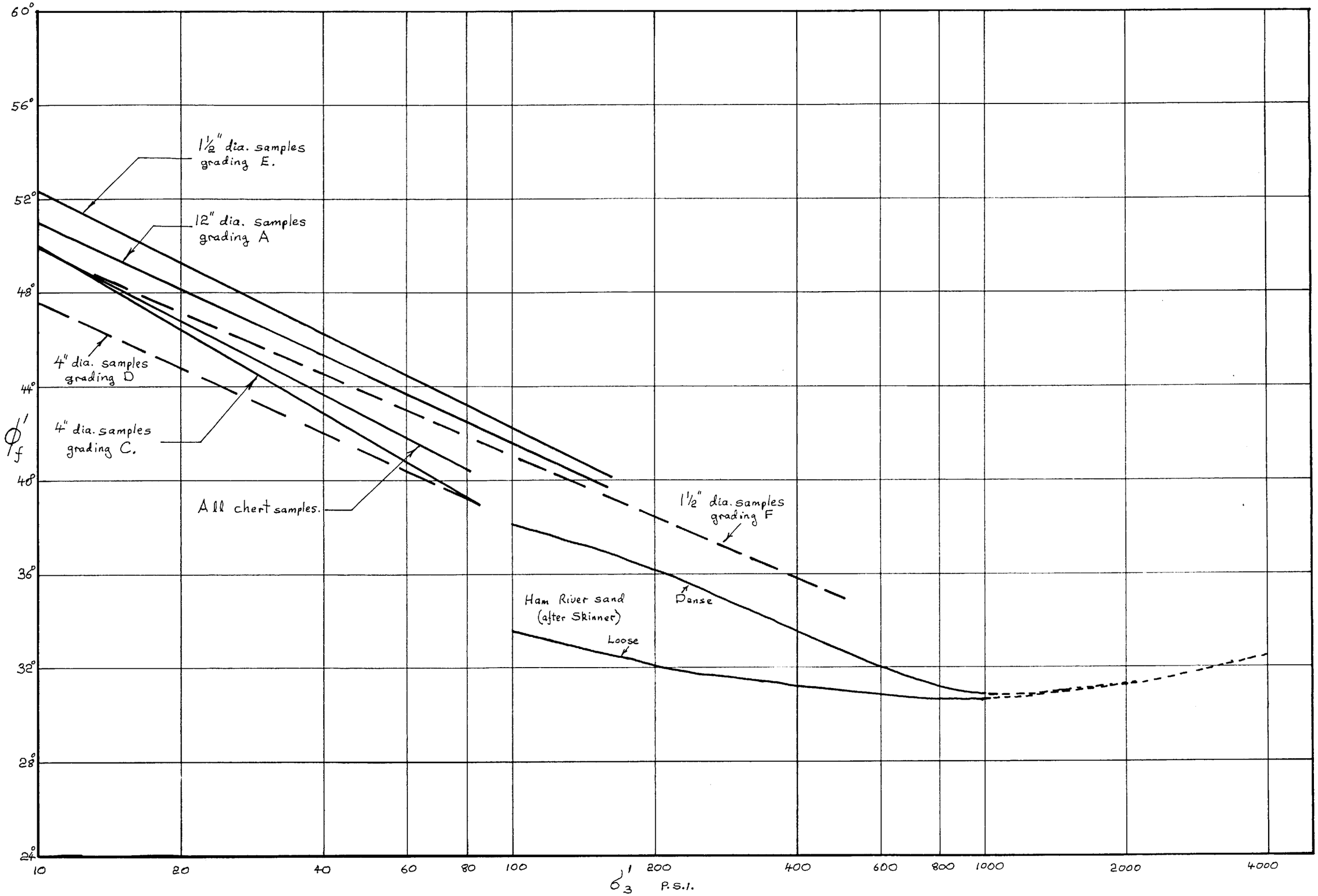
GRANITIC GNEISS 4" DIA. SATURATED SAMPLES.

FIG. 7:2:2



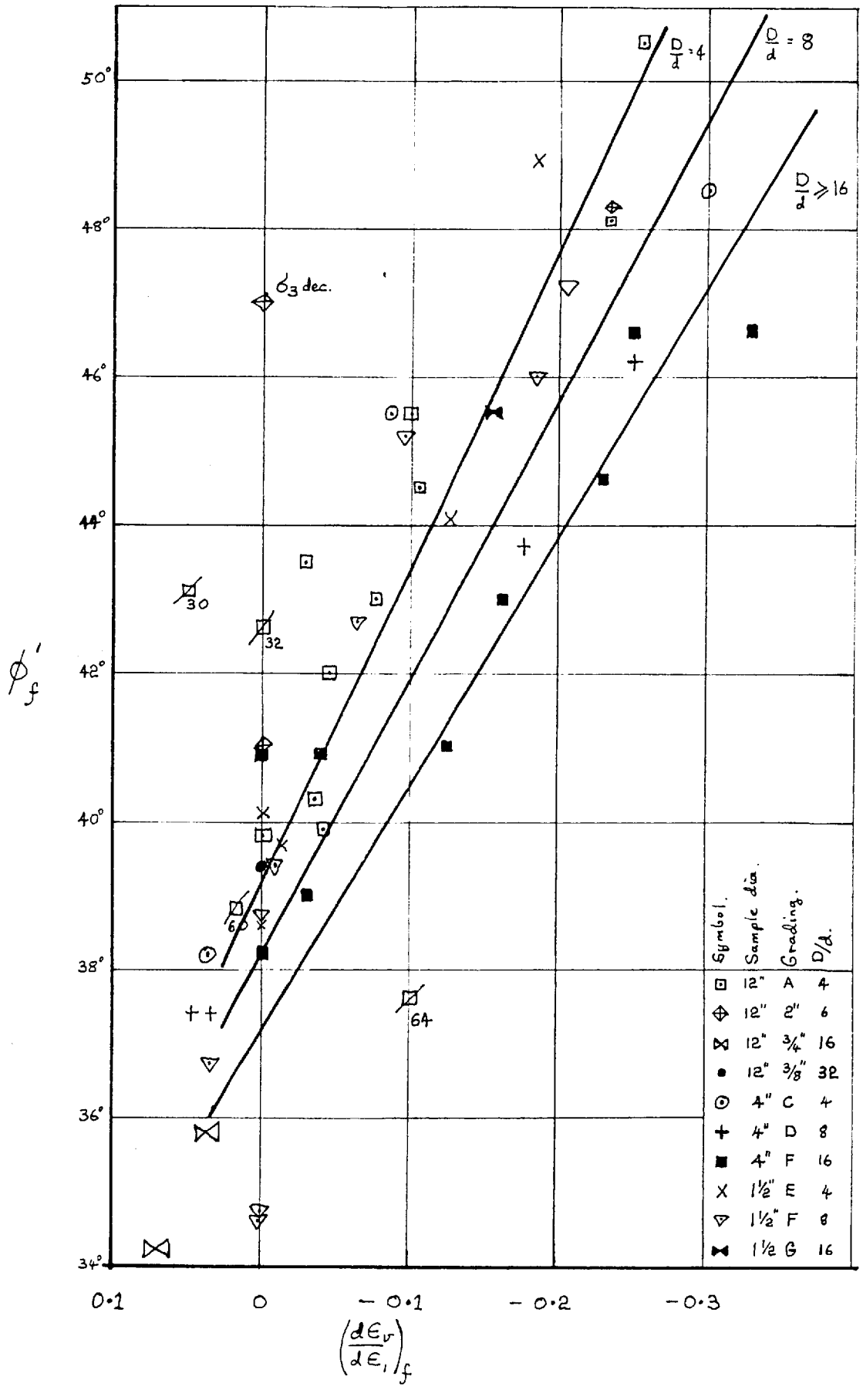
VOLUME CHANGES DURING ISOTROPIC CONSOLIDATION
SILURIAN CLEAVED MUDSTONE 1½" DIA. SATURATED SAMPLES.

FIG. 7:2:3



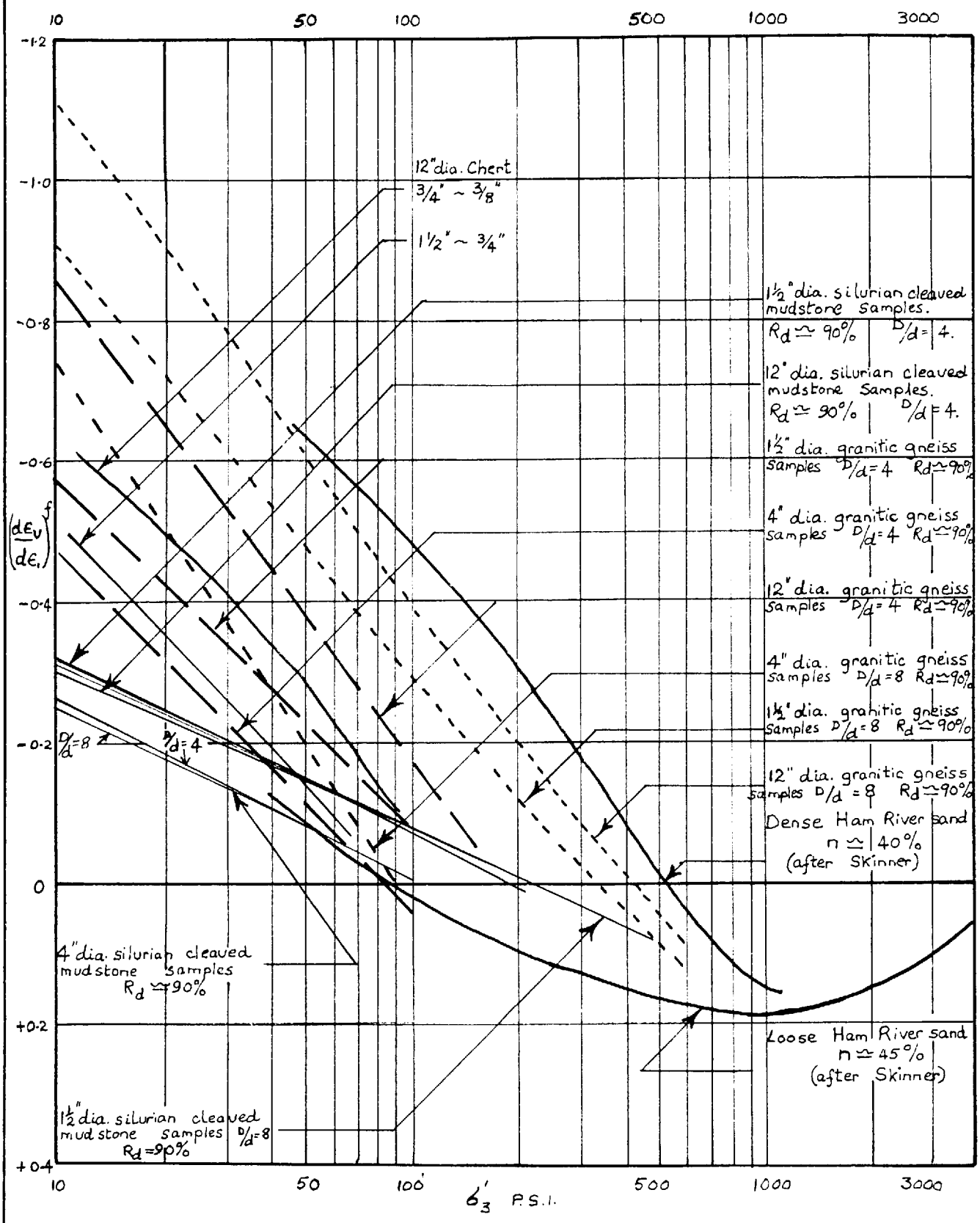
THE RELATION BETWEEN ϕ'_f AND σ'_3 FOR SILURIAN CLEAVED MUDSTONE SAMPLES AT INITIAL $R_d = 90\%$

FIG. 7:3A.



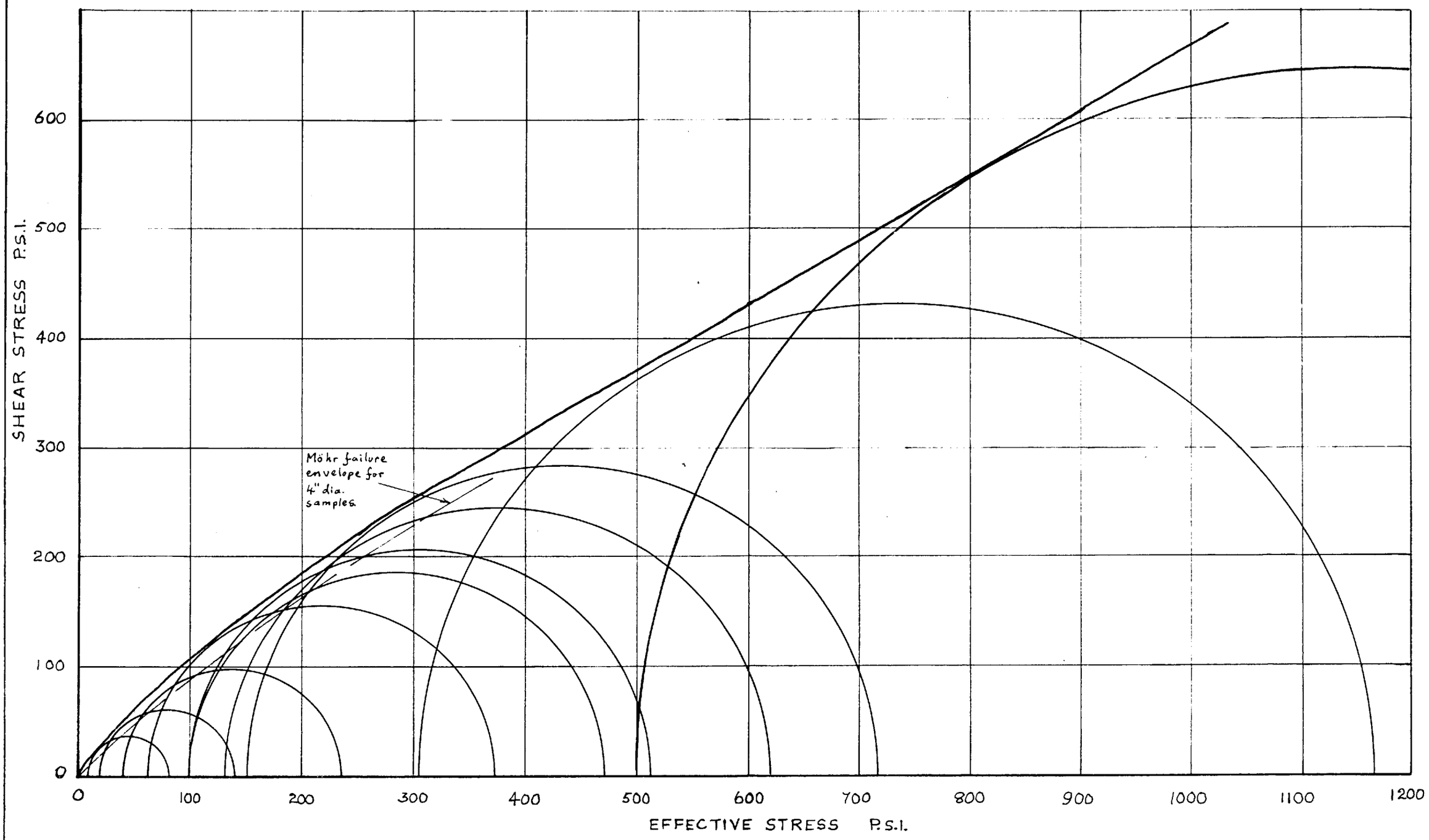
THE RELATION BETWEEN ϕ'_f AND $(d\epsilon_v/d\epsilon_1)_f$ FOR SILURIAN CLEAVED MUDSTONE SAMPLES.

FIG. 7:38



THE RELATION BETWEEN $\left(\frac{d\epsilon_v}{d\epsilon_1}\right)_f$ AND THE MINOR PRINCIPAL STRESS.

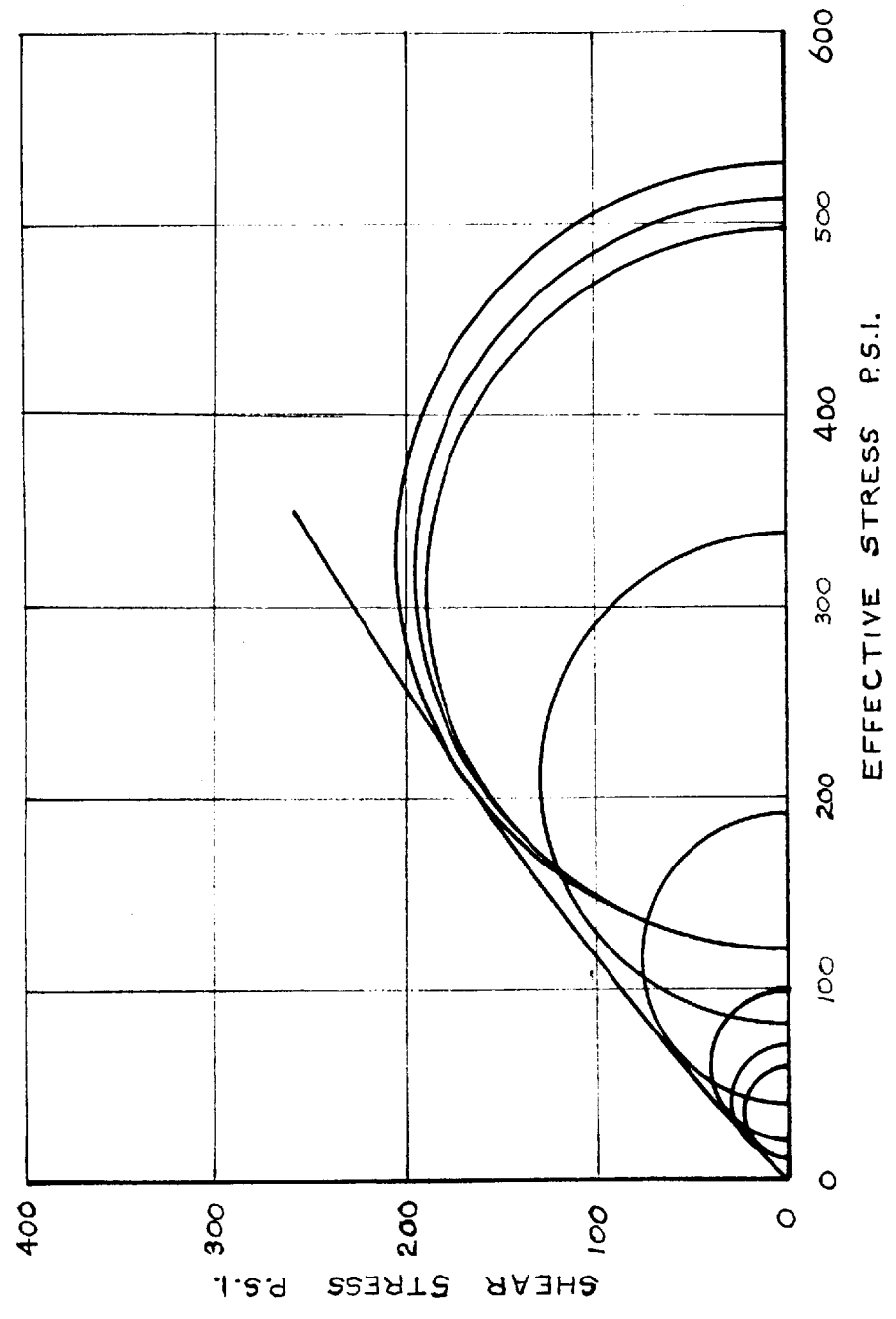
FIG: 7:3C



MÖHR FAILURE CIRCLES

SILURIAN CLEAVED MUDSTONE 12" DIA. SAMPLES.

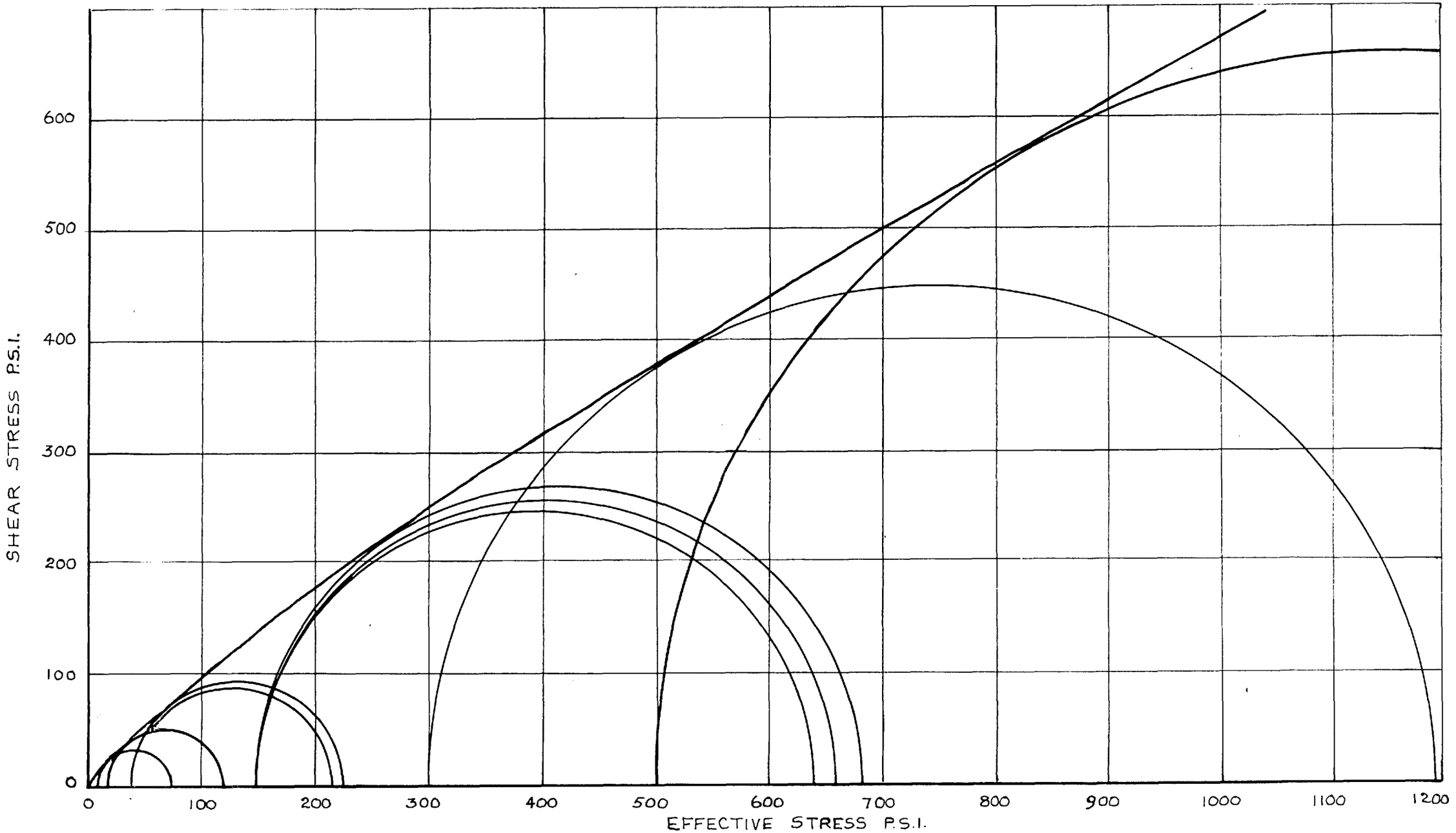
FIG. 7:3D



MÖHR FAILURE CIRCLES

SILURIAN CLEAVED MUDSTONE 4" DIA. SAMPLES.

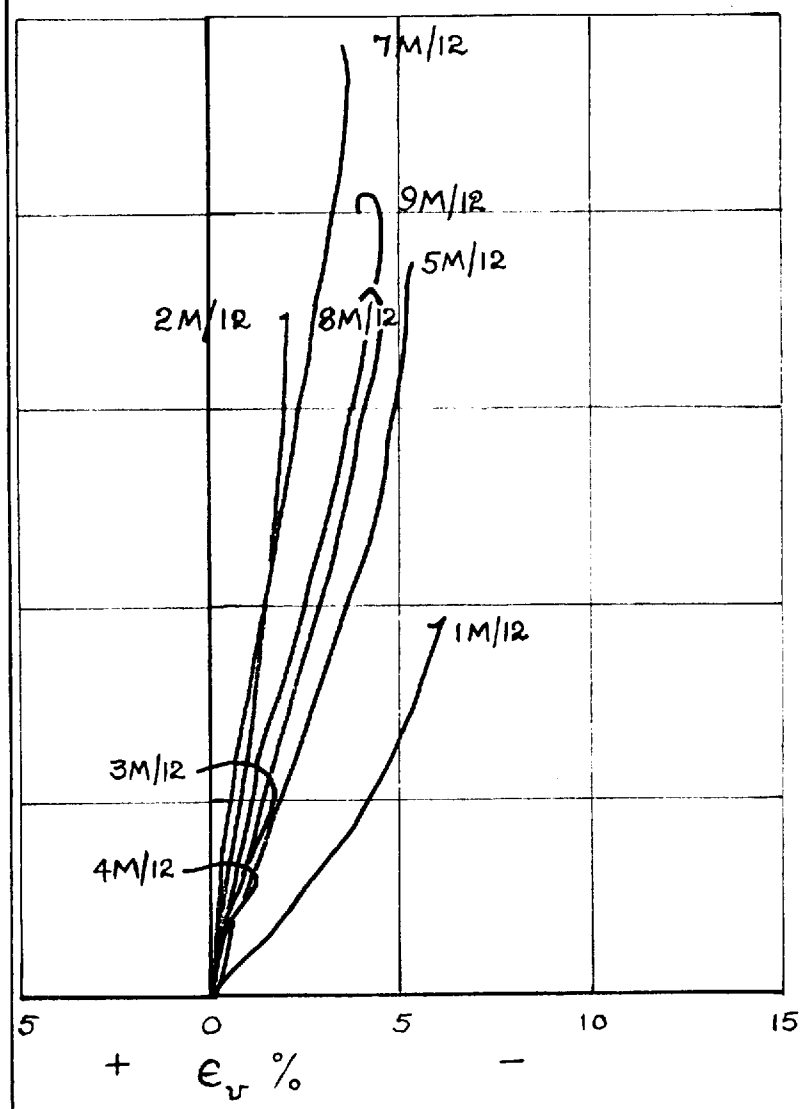
FIG. 7:3E

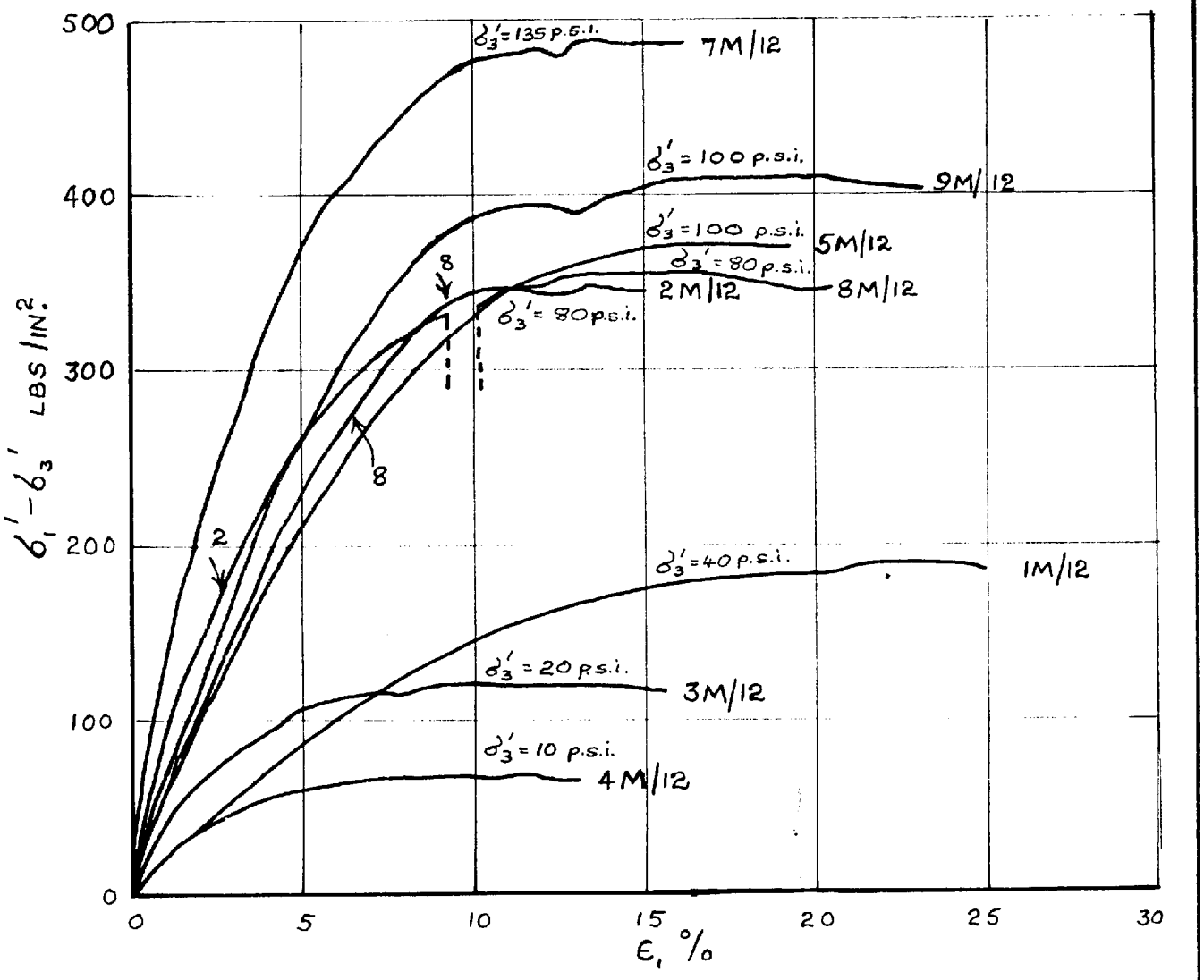


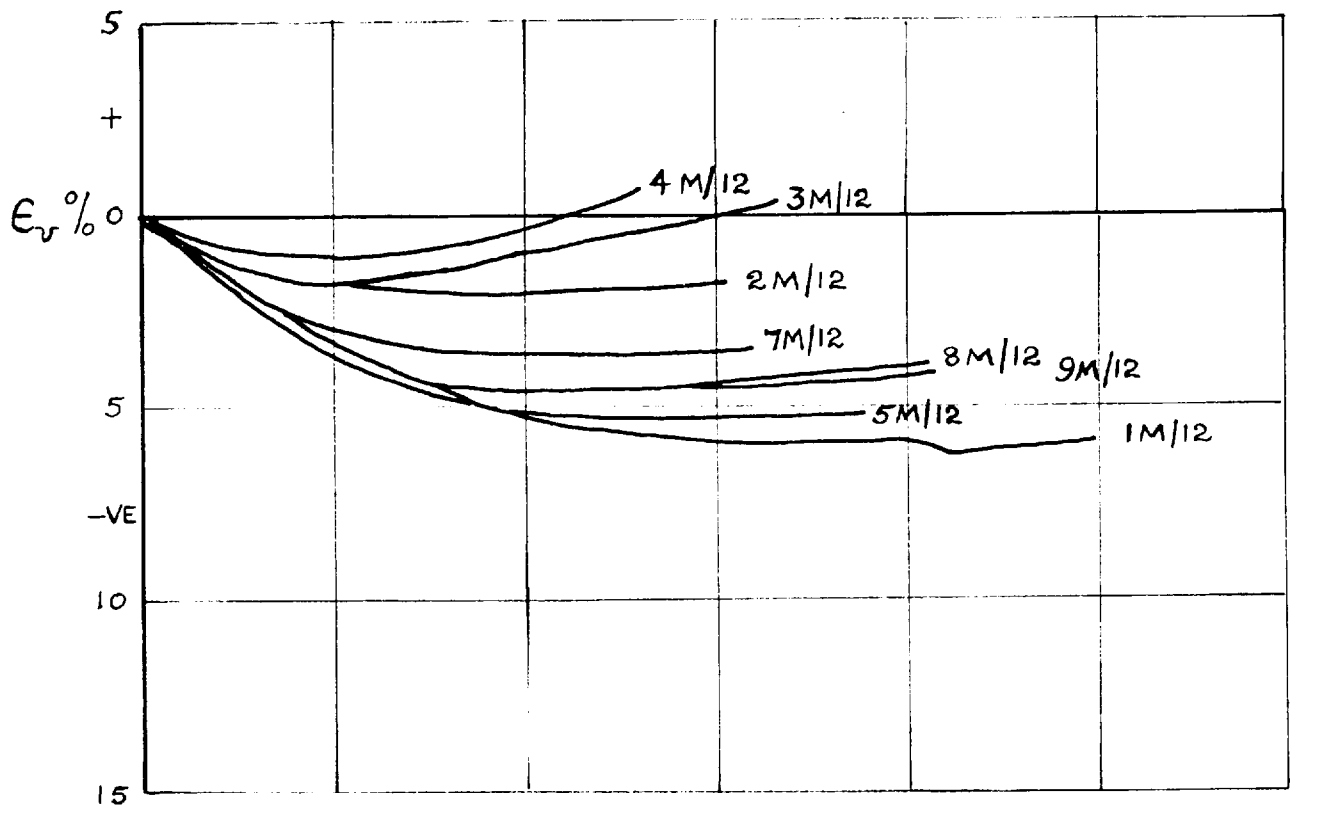
MÖHR FAILURE CIRCLES

SILURIAN CLEAVED MUDSTONE 1½" DIA. SAMPLES.

FIG. 7:3F



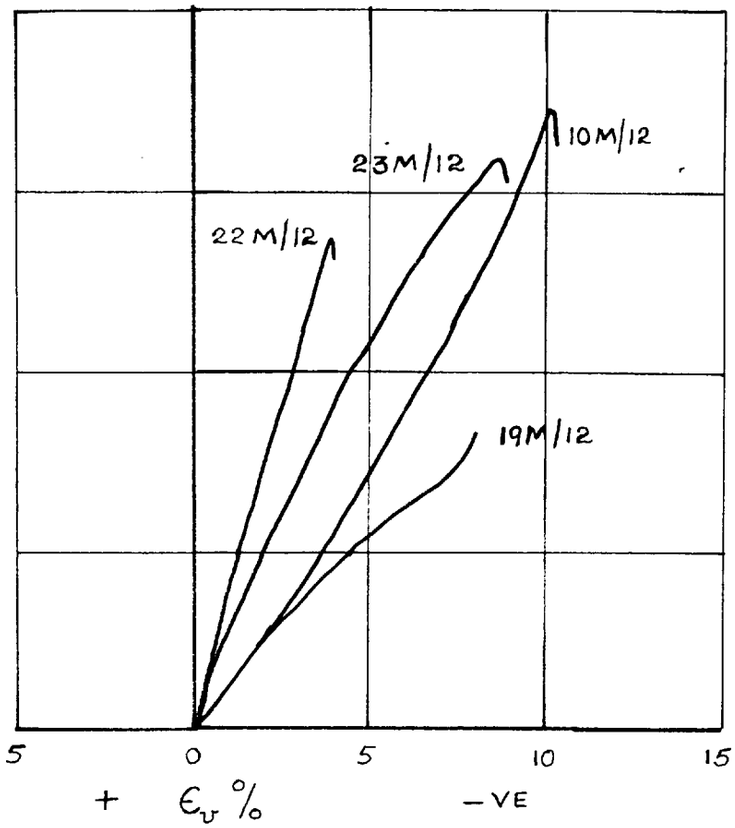


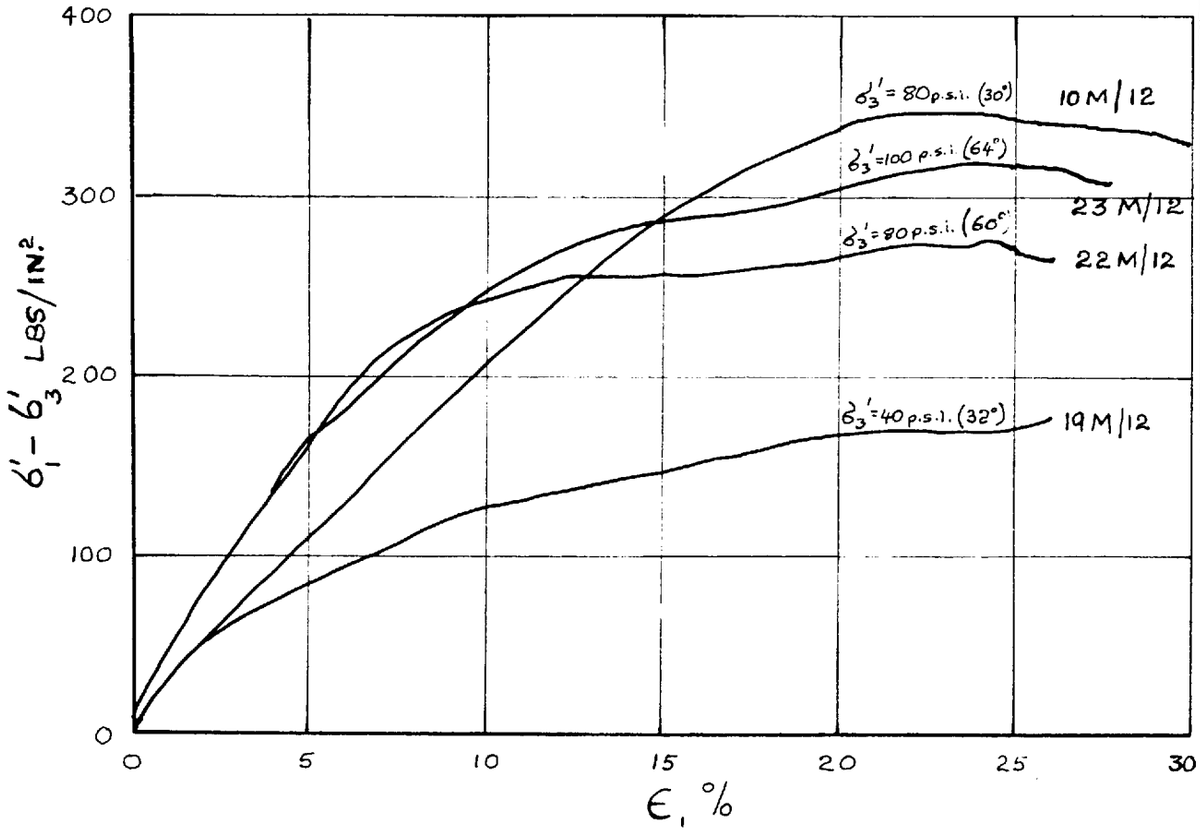


SILURIAN CLEAVED MUDSTONE ROCKFILL.

GRADING A

FIG. 7:3:1





SILURIAN CLEAVED MUDSTONE
ROCKFILL

ORIENTATED SAMPLES.

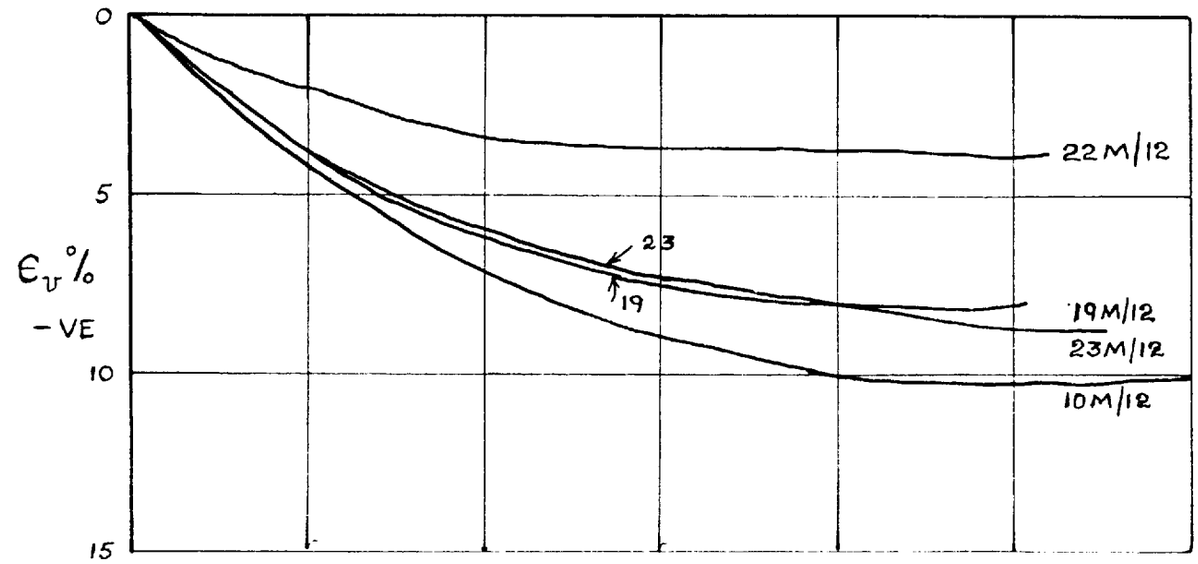
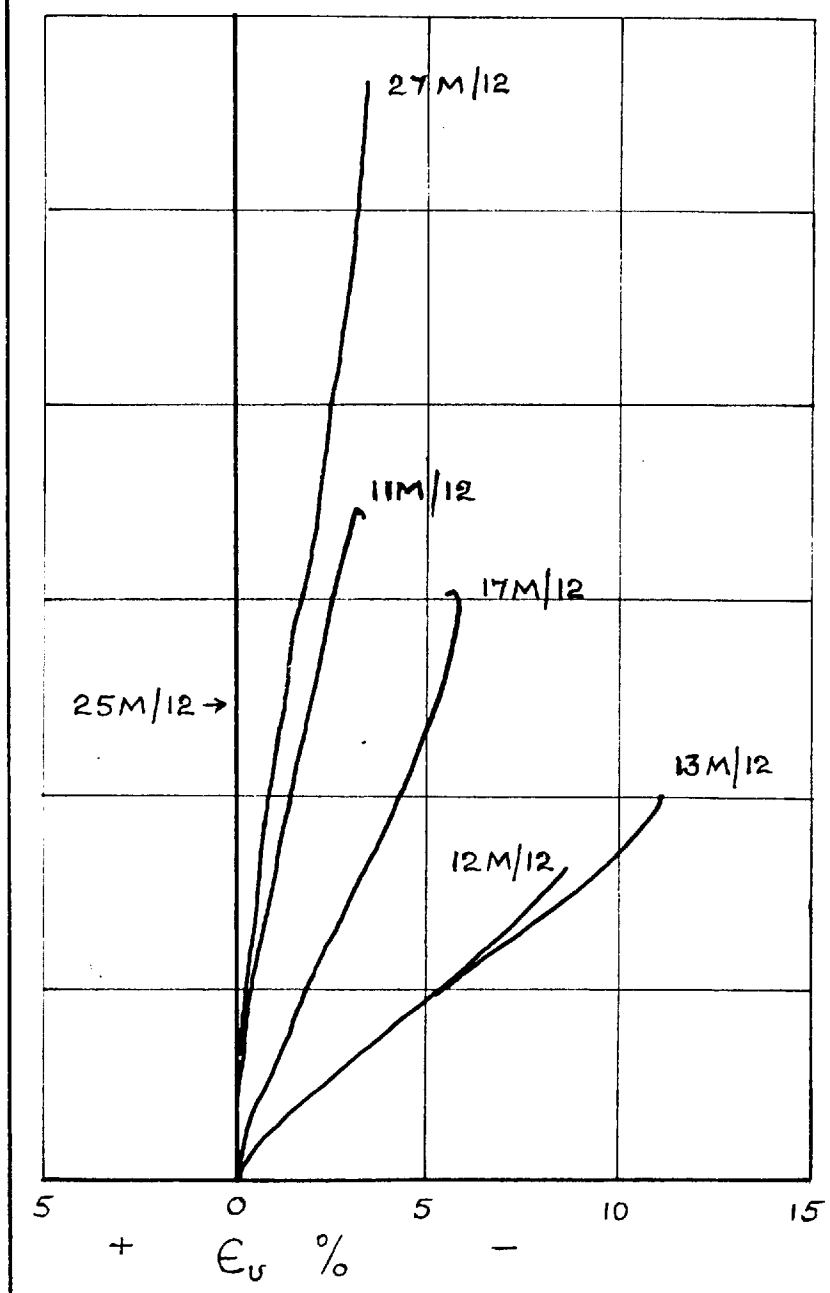
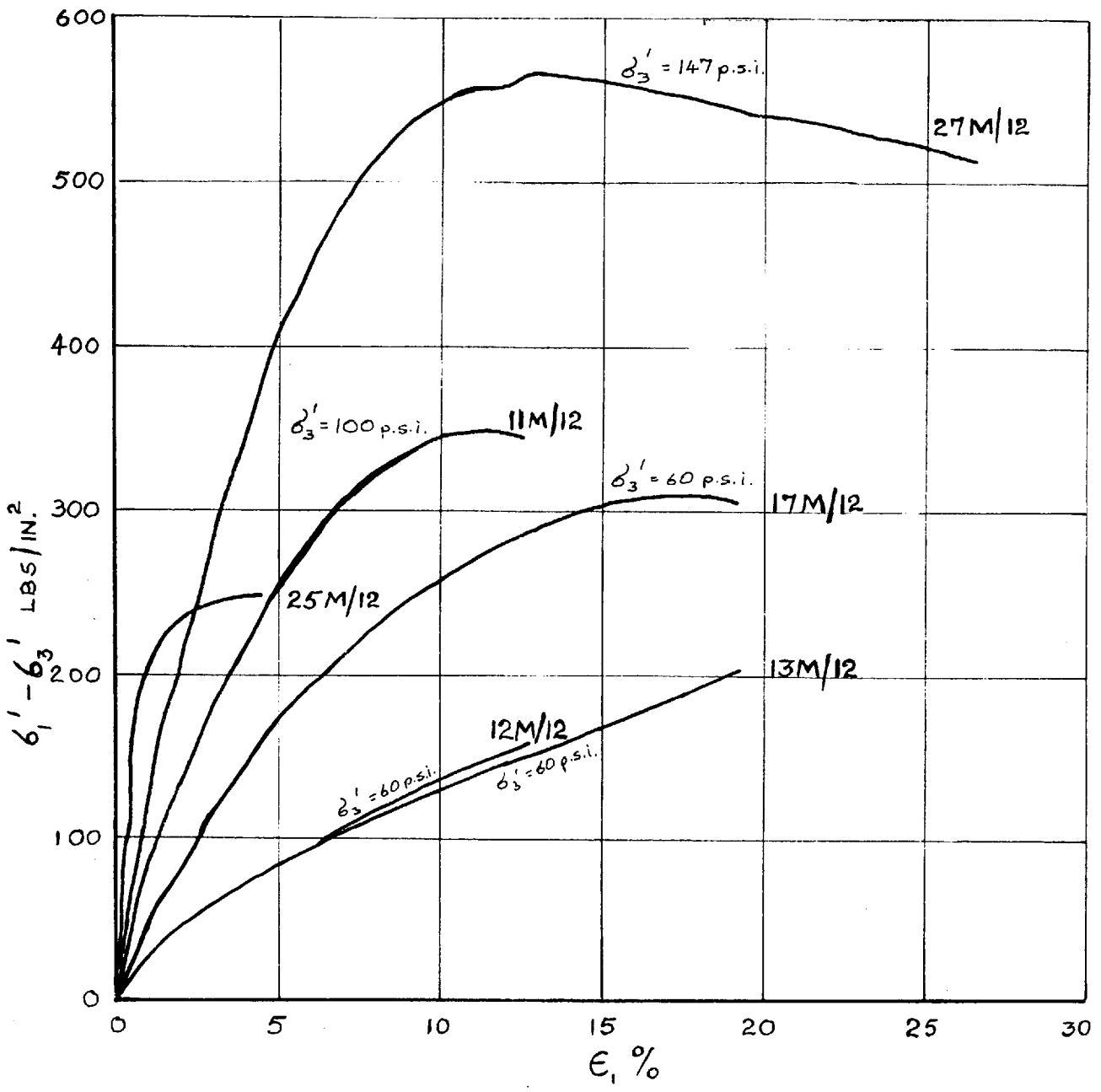
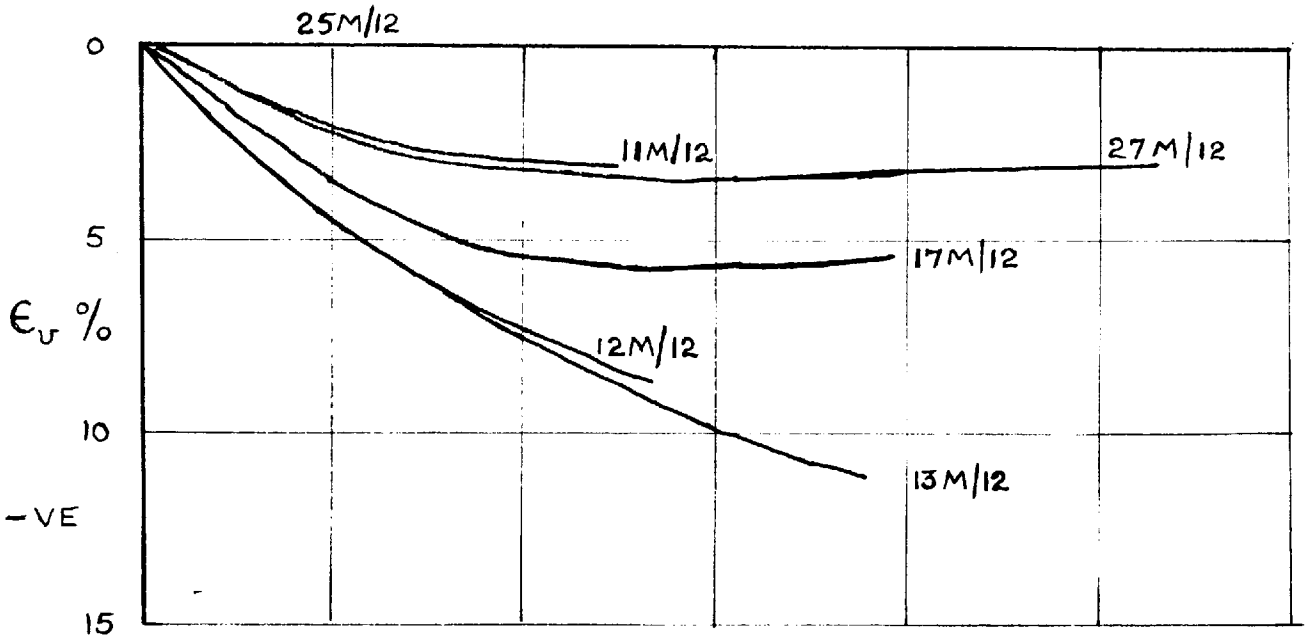


FIG. 7:3:2



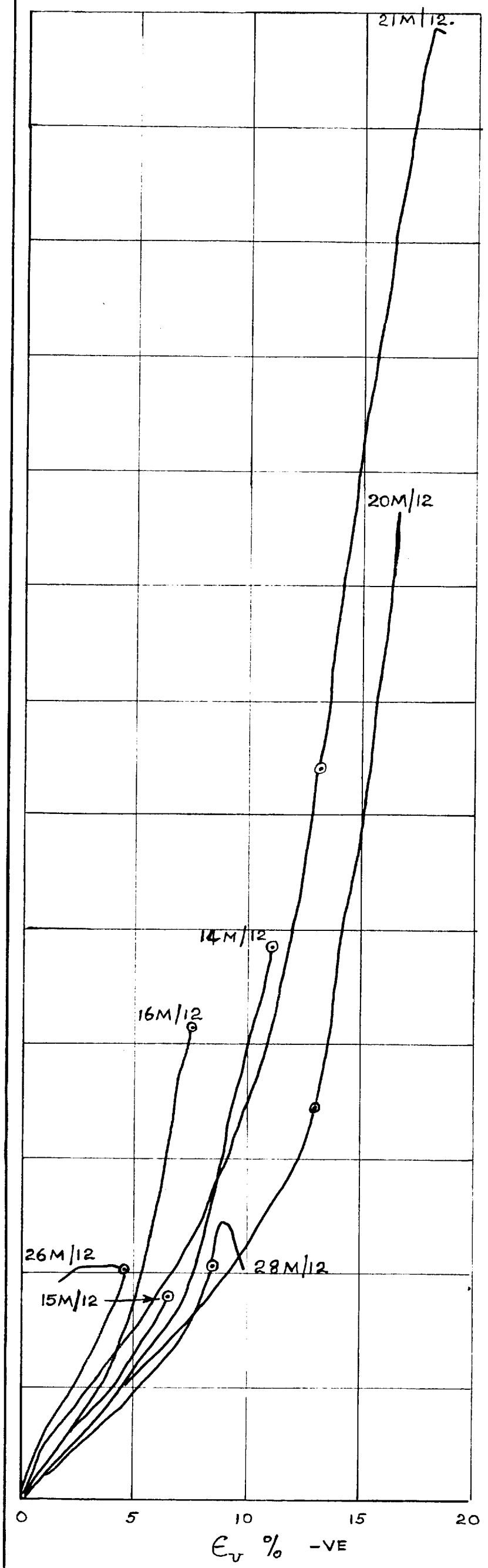


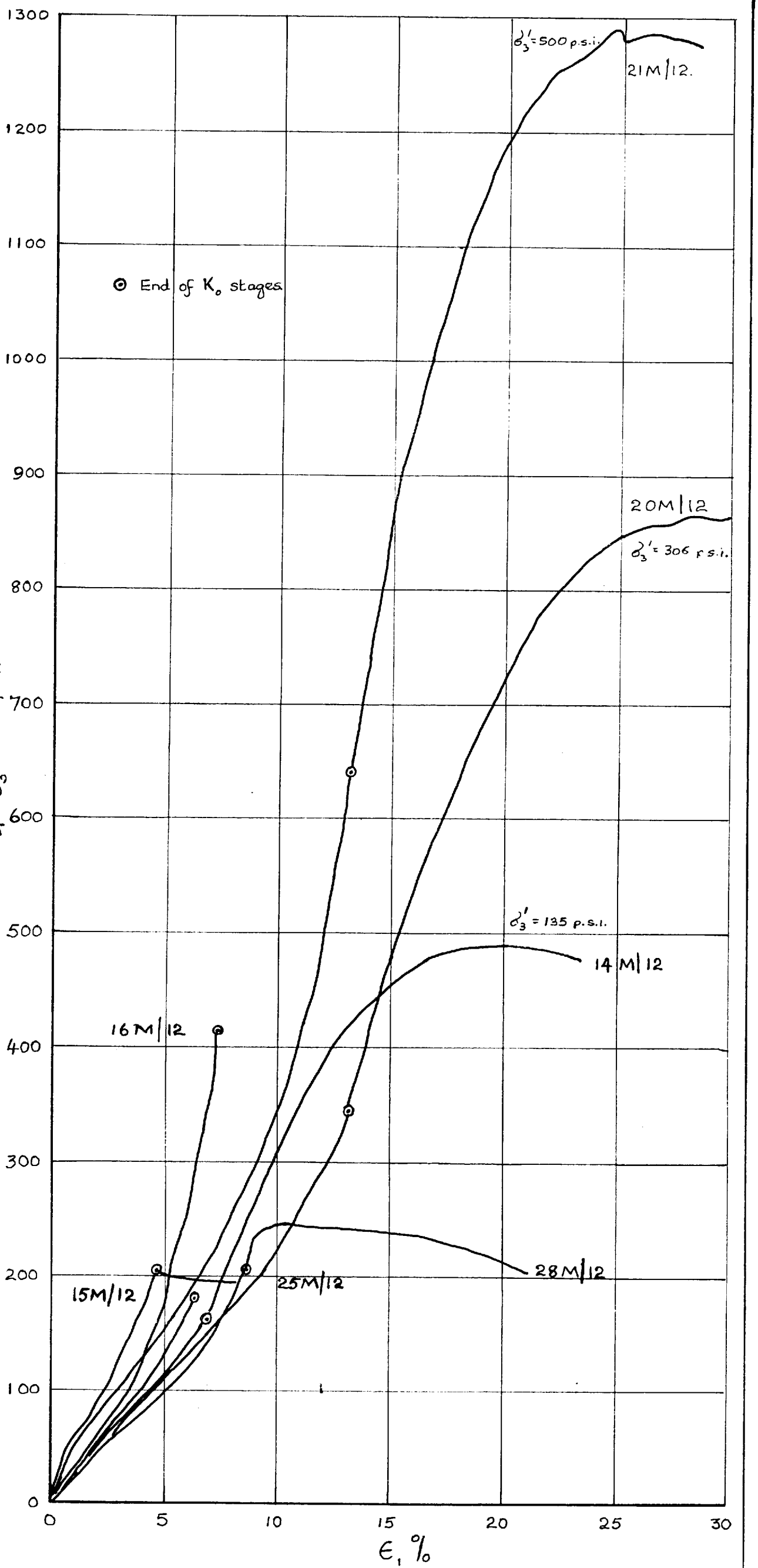


SILURIAN CLEAVED MUDSTONE
SPECIAL TESTS.

FIG. 7:3:3

1967





SILURIAN CLEAVED MUDSTONE

K_o TESTS.

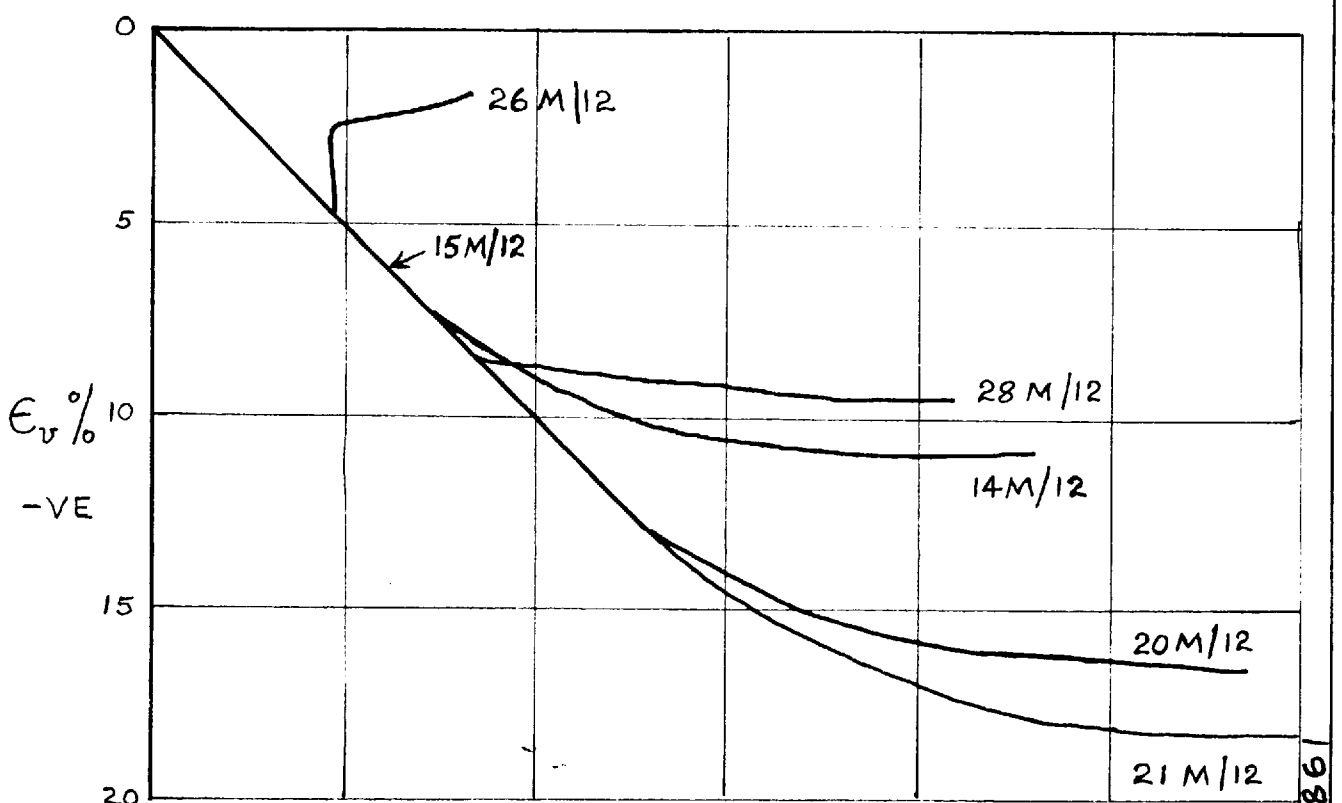
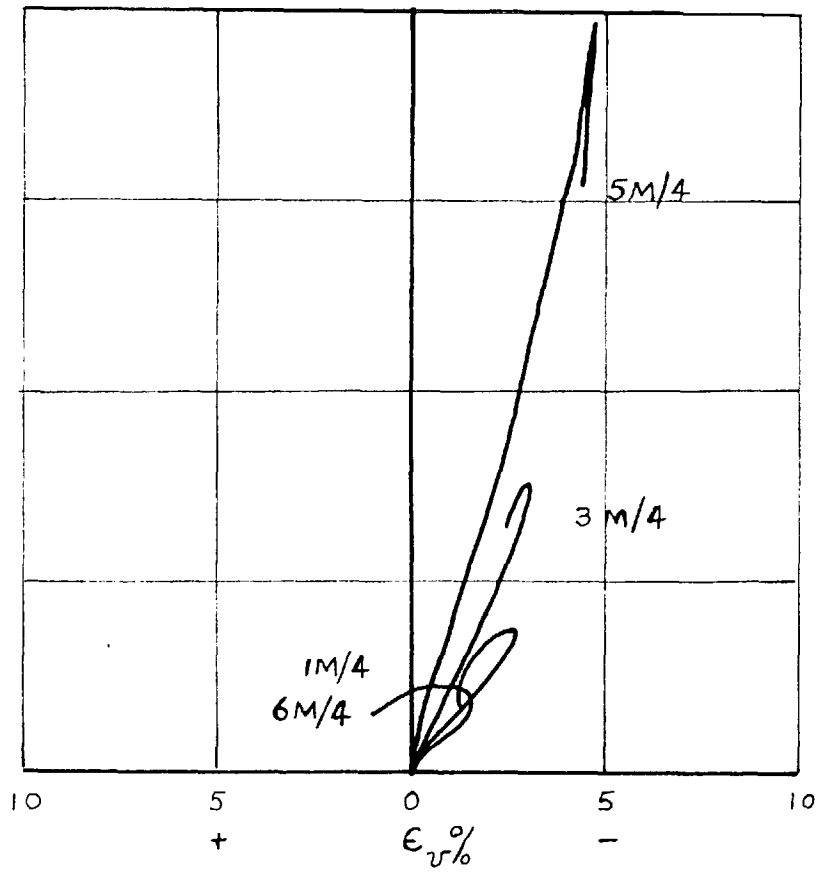
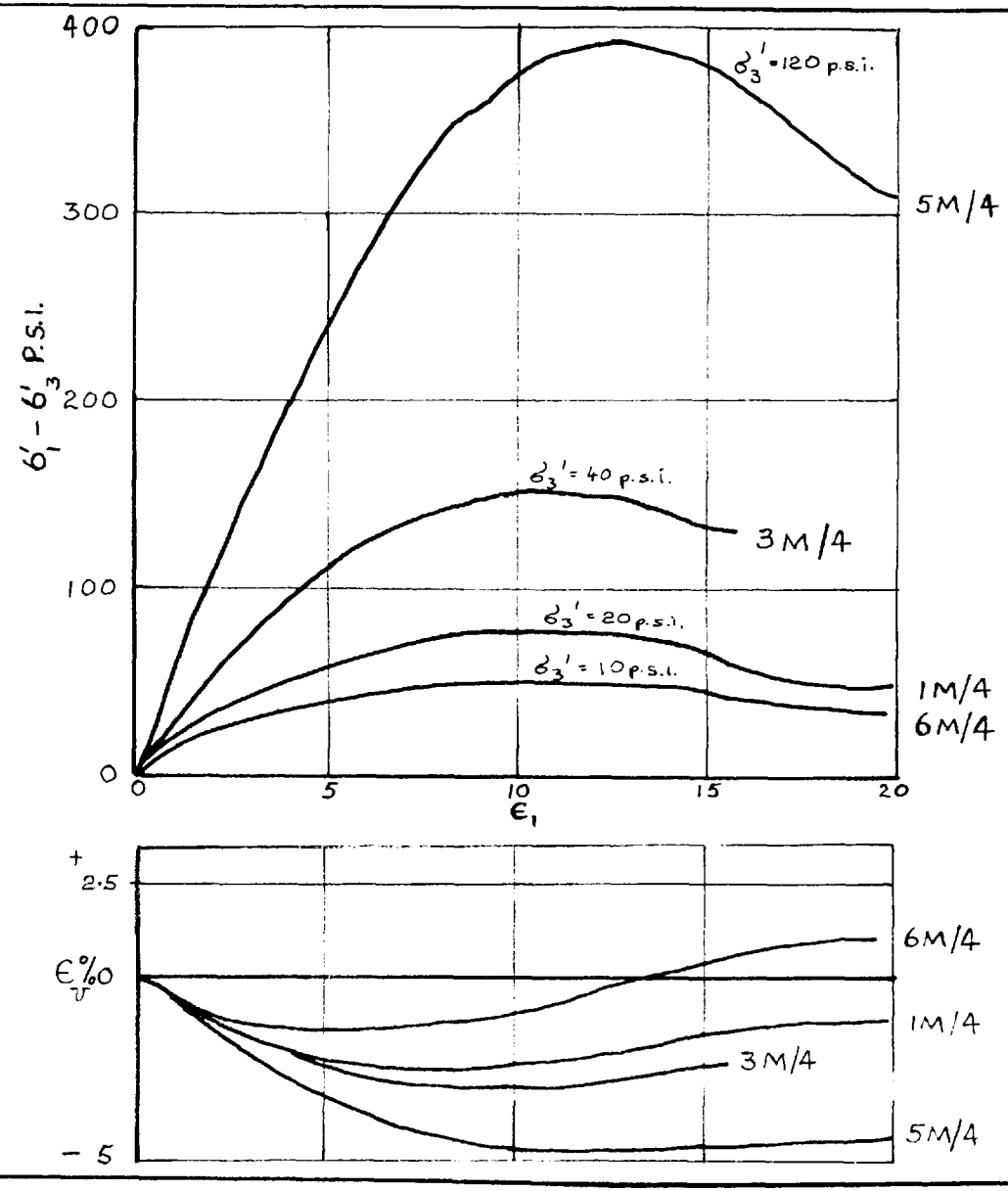


FIG. 7:3:4



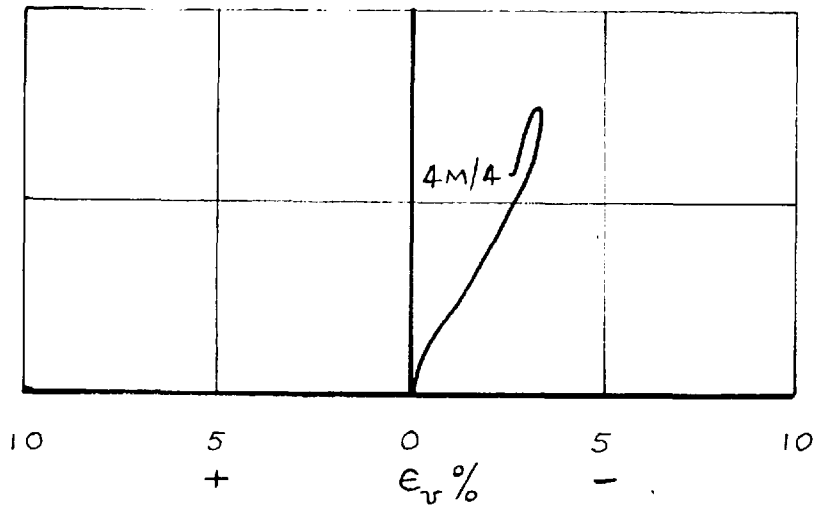


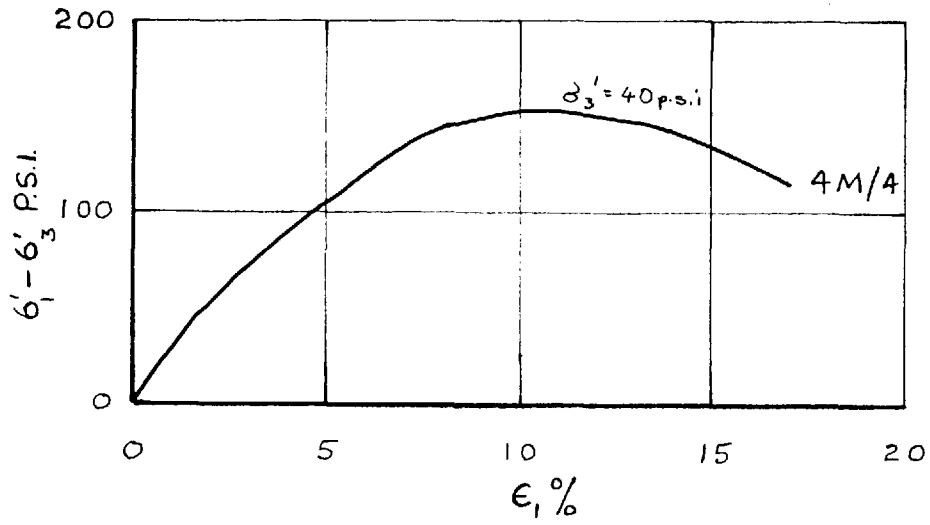
SILURIAN CLEAVED MUDSTONE

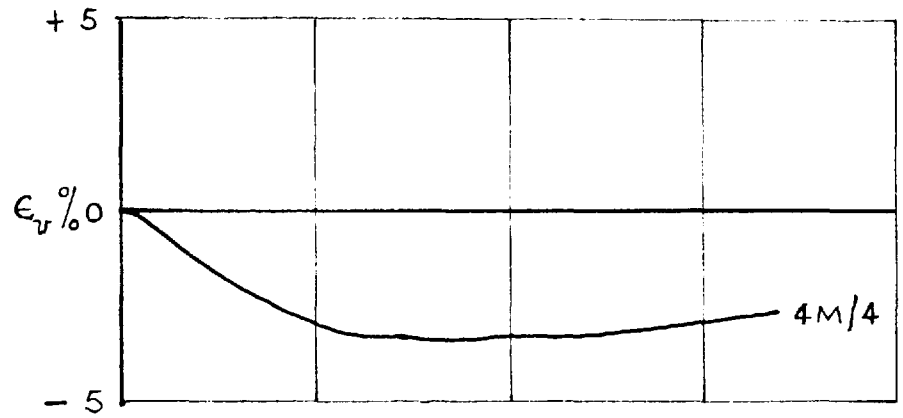
ROCKFILL

GRADING: F.

FIG. 7:3:5a.



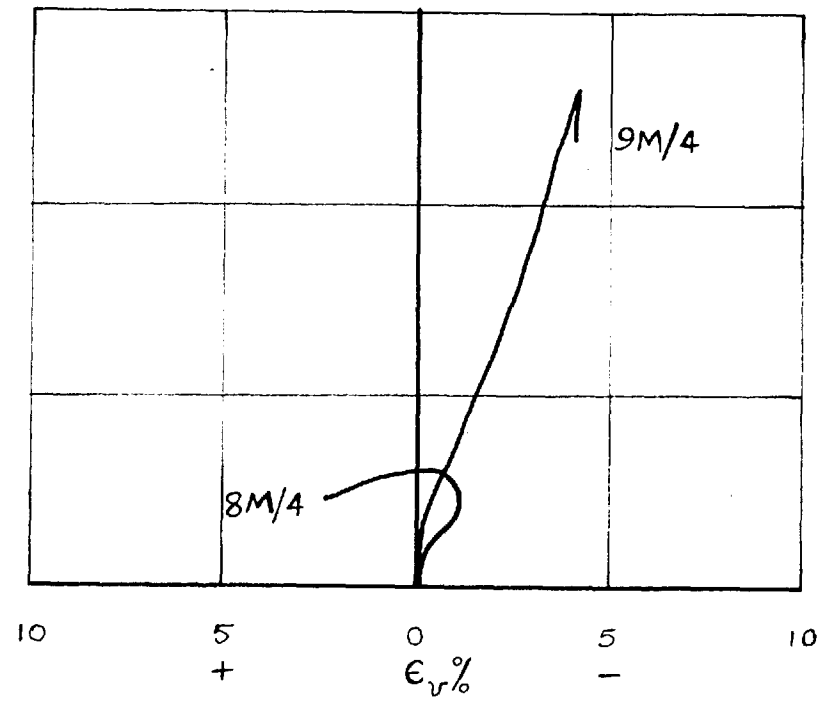


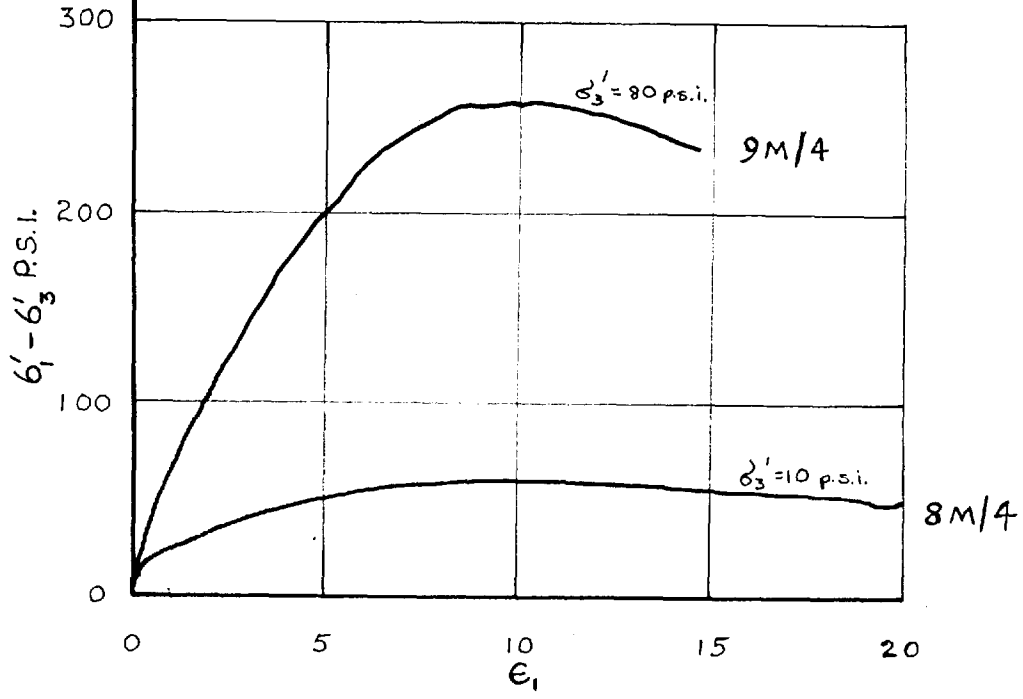


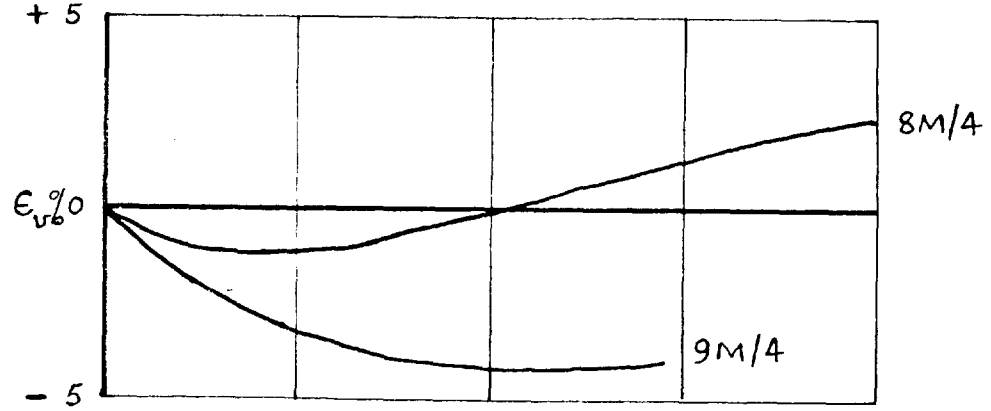
SILURIAN CLEAVED MUDSTONE

ROCKFILL.
GRADING F.

FIG. 7:3:56





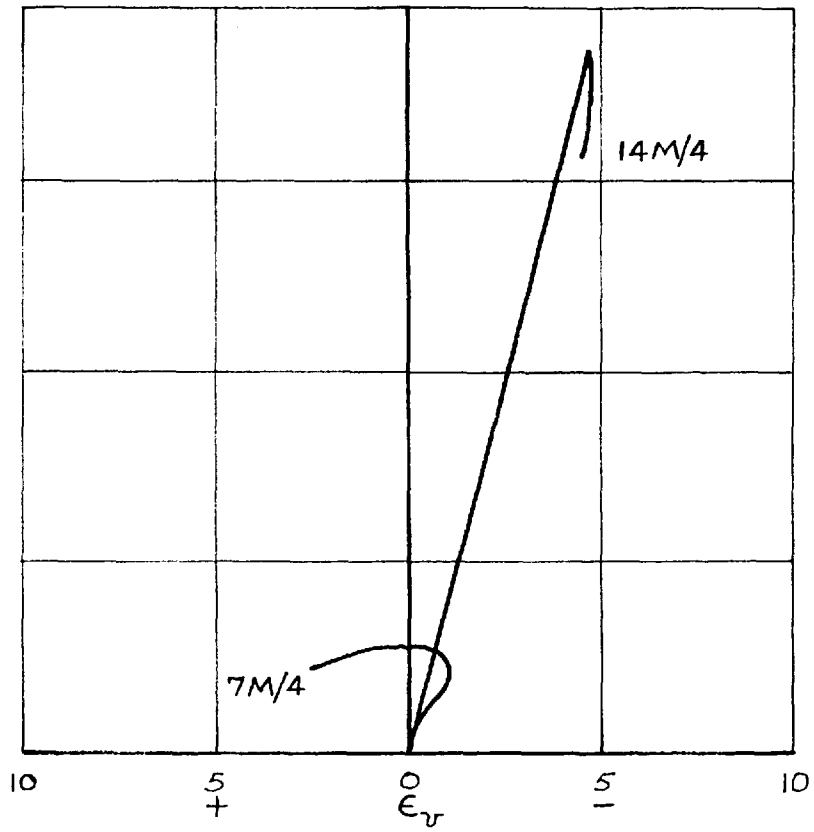


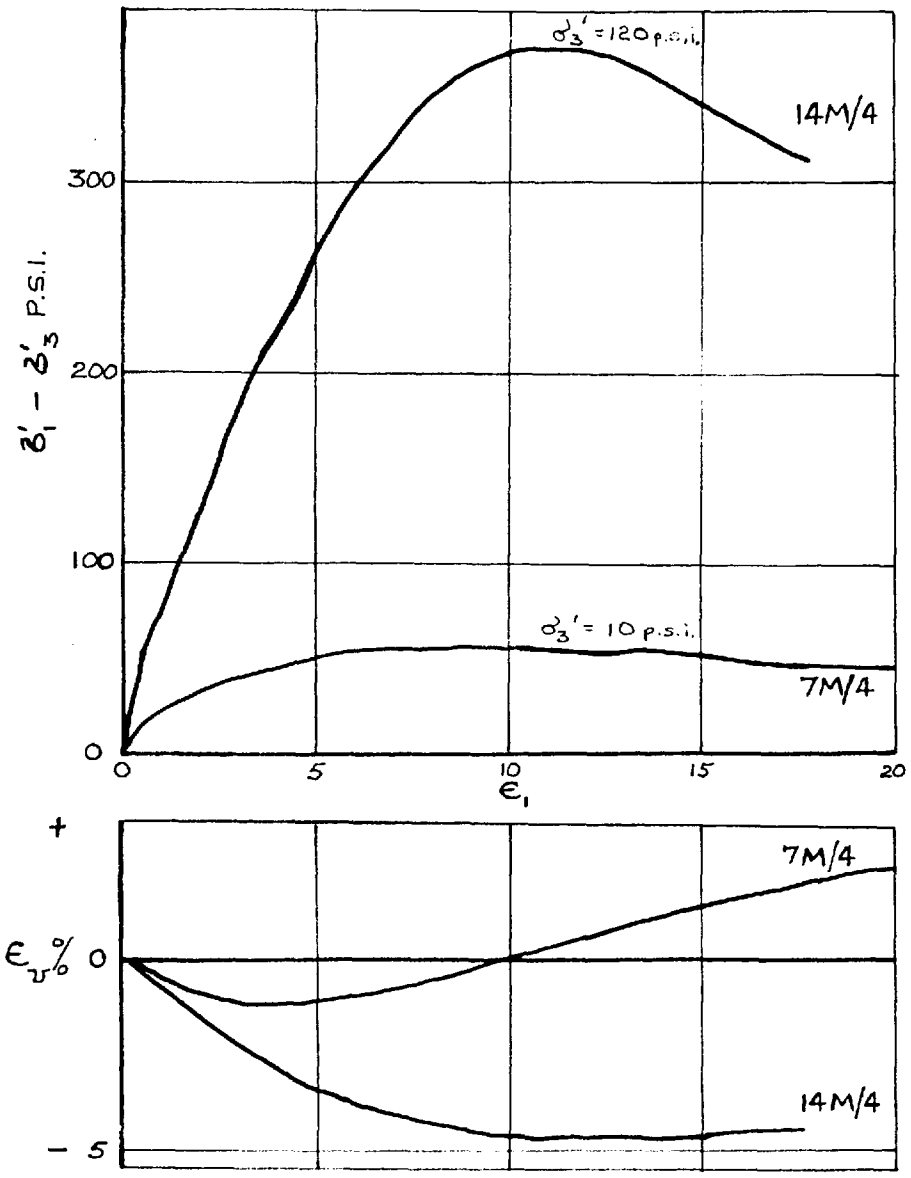
SILURIAN CLEAVED MUDSTONE

ROCKFILL

GRADING: C.

FIG. 7:3:5a



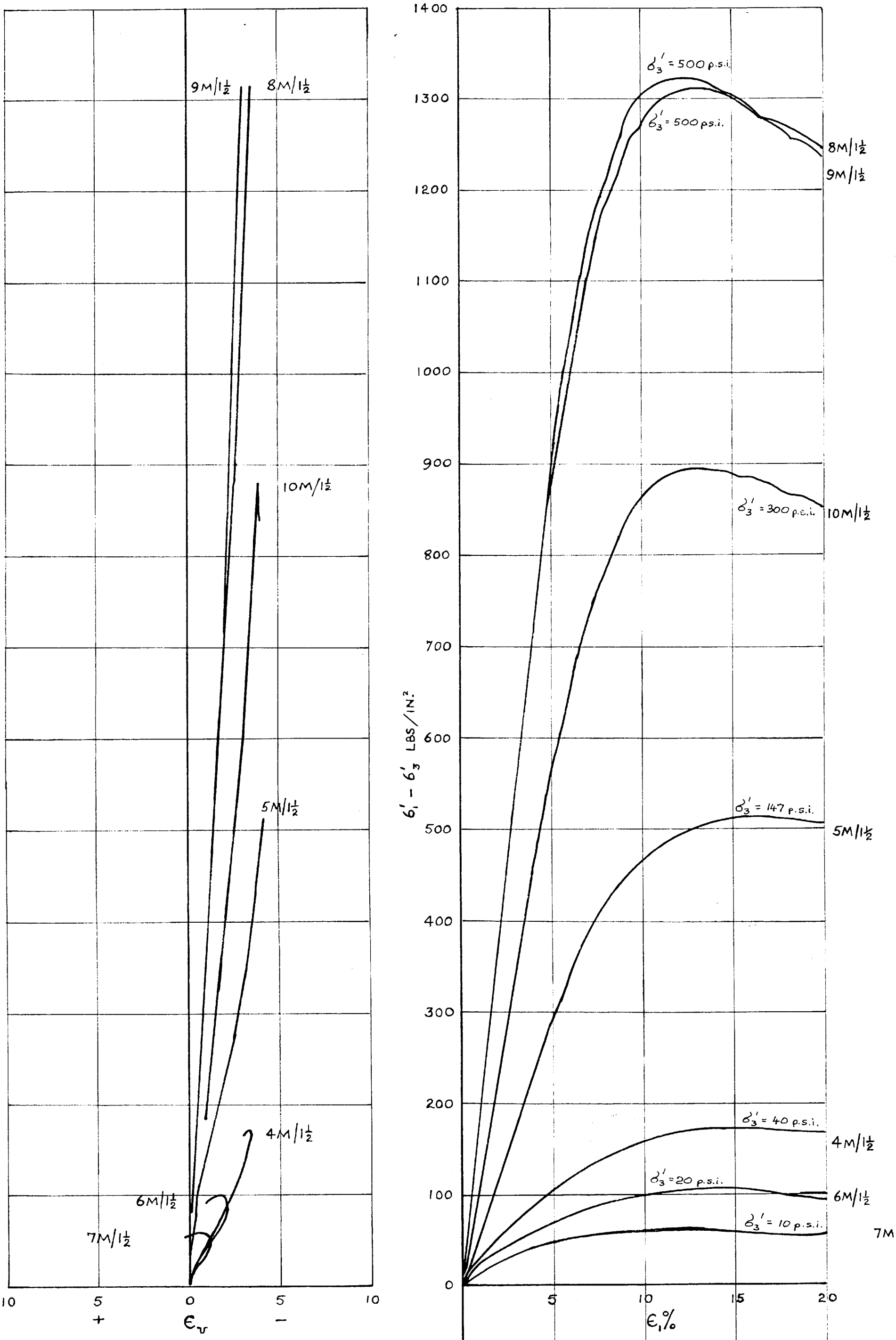


SILURIAN CLEAVED MUDSTONE

ROCKFILL

GRADING : D.

FIG. 7:3:5a

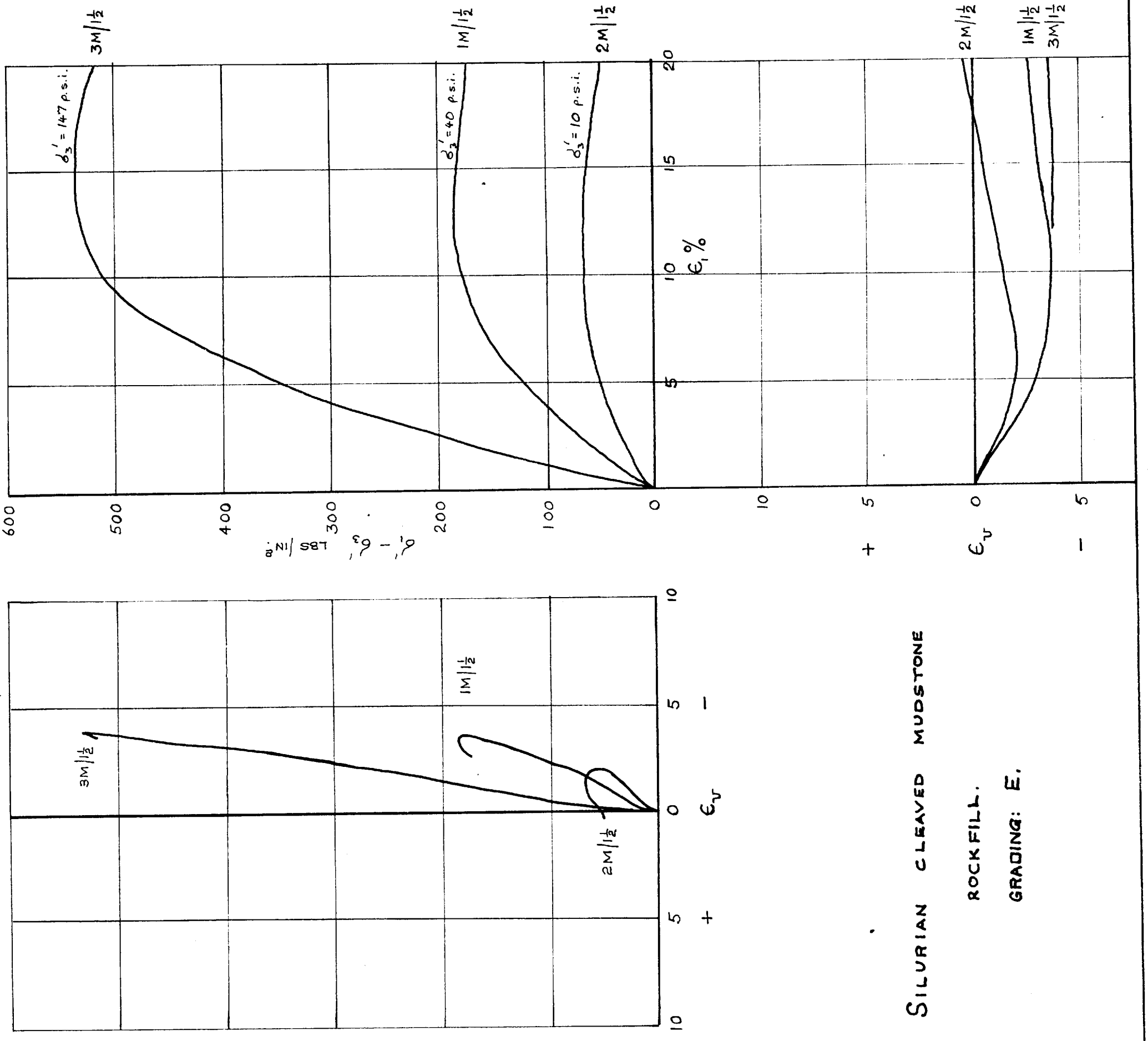


SILURIAN CLEAVED MUDSTONE

ROCKFILL.

GRADING: F.

FIG. 7:3:6a.

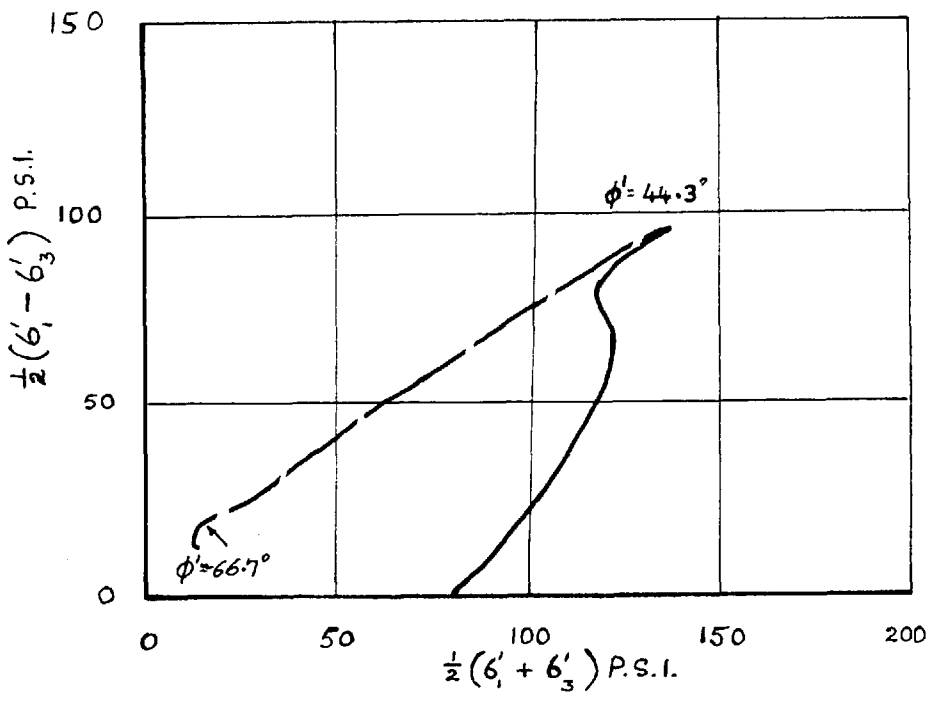


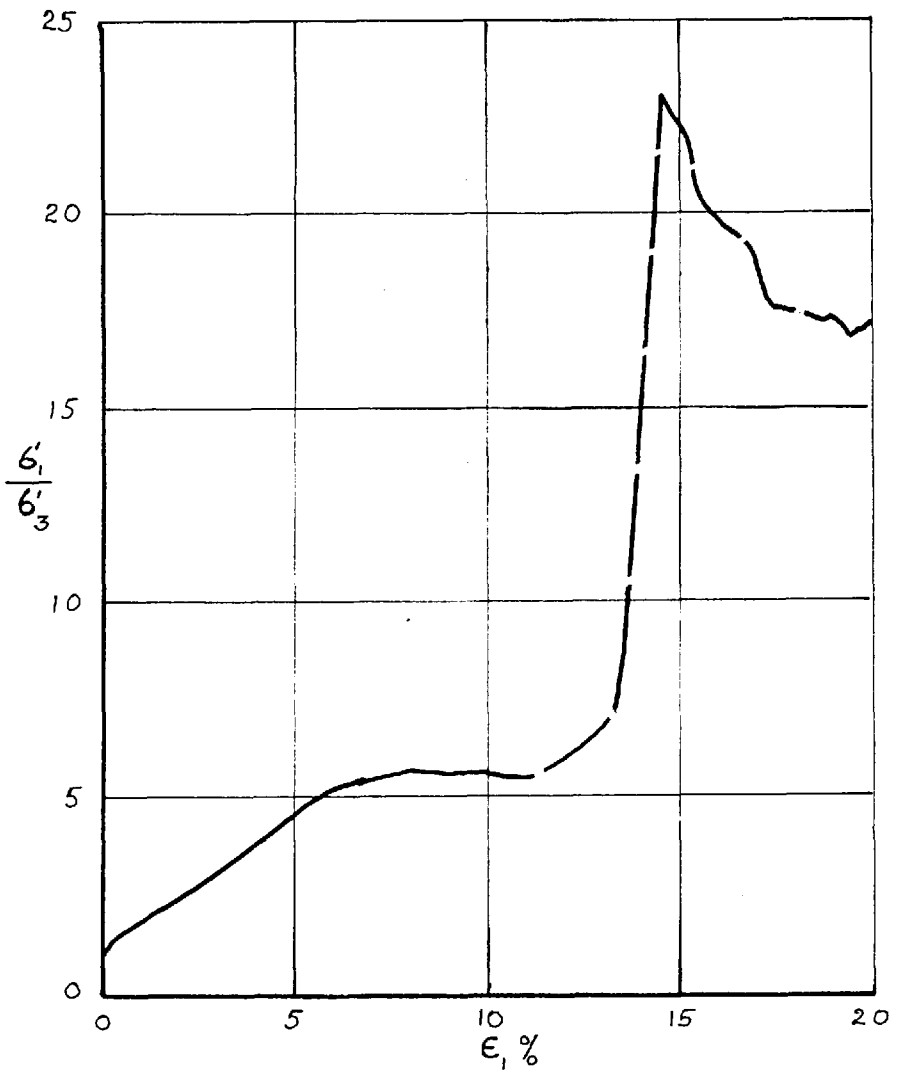
SILURIAN CLEAVED MUDSTONE

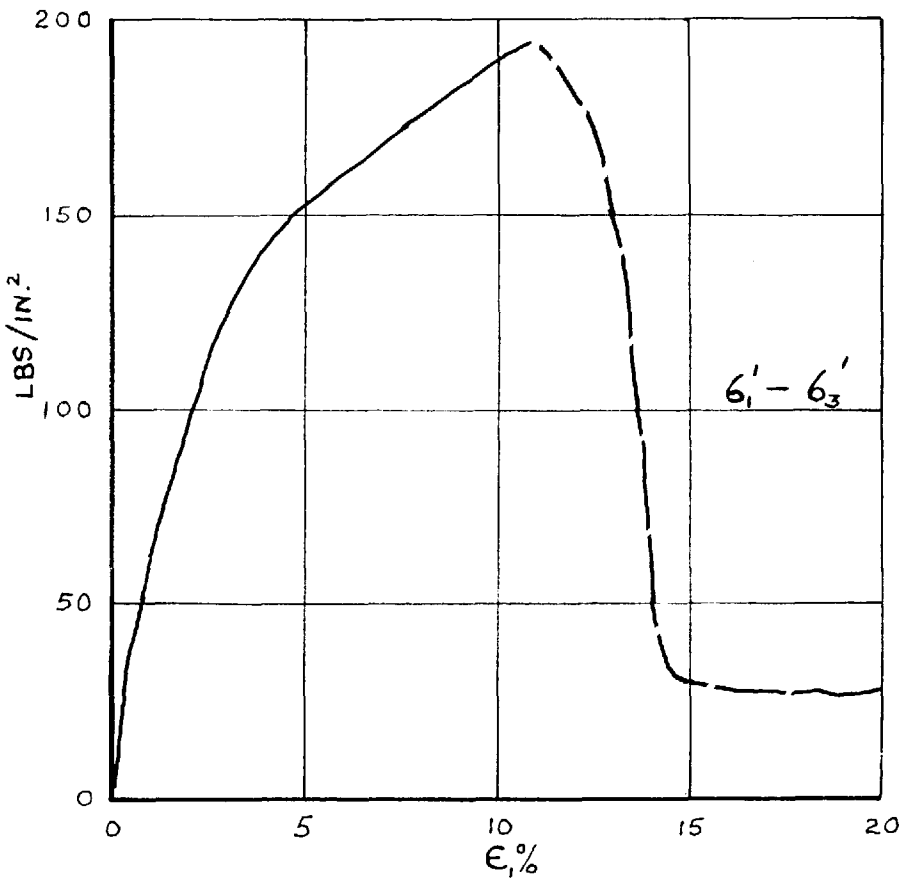
ROCKFILL.

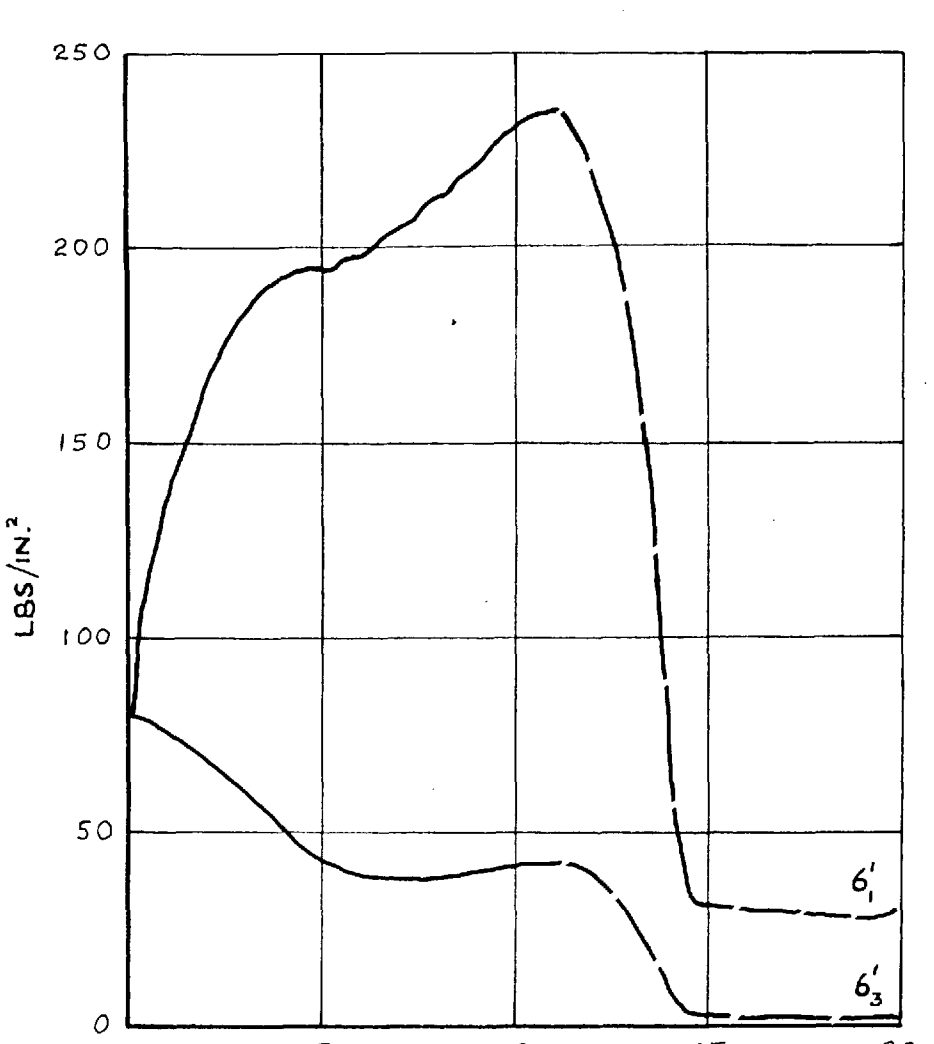
GRADING: E.

FIG. 7:3:6







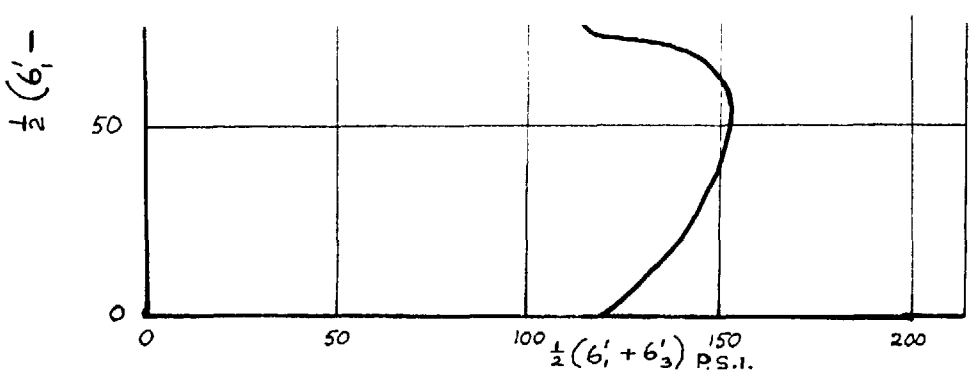


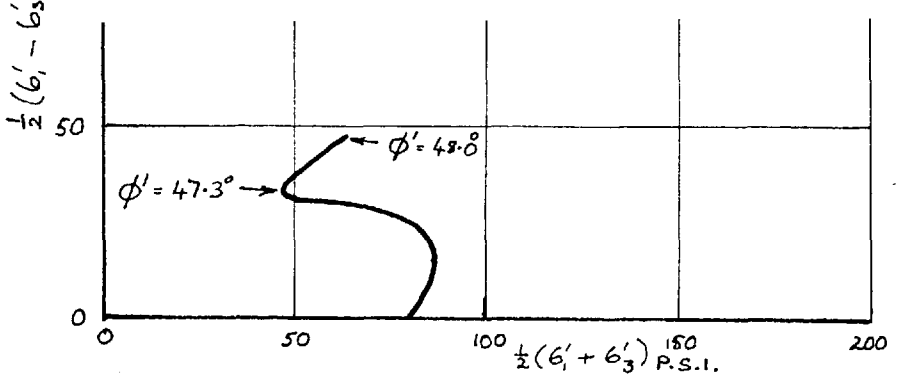
γ_d = 133·1 LBS/FT.³

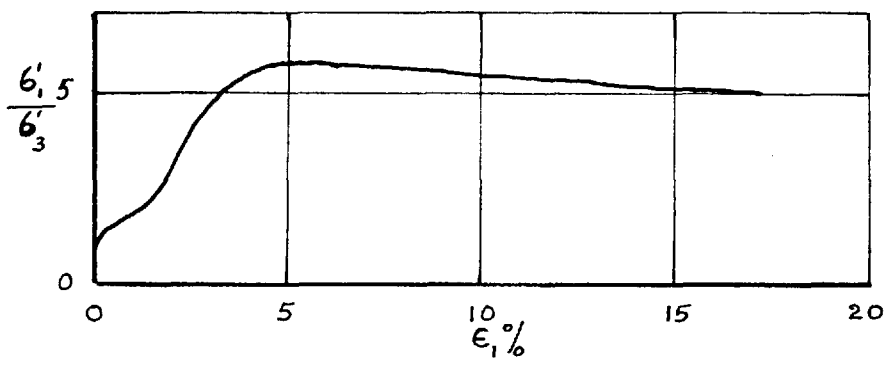
R_d = 83·5%

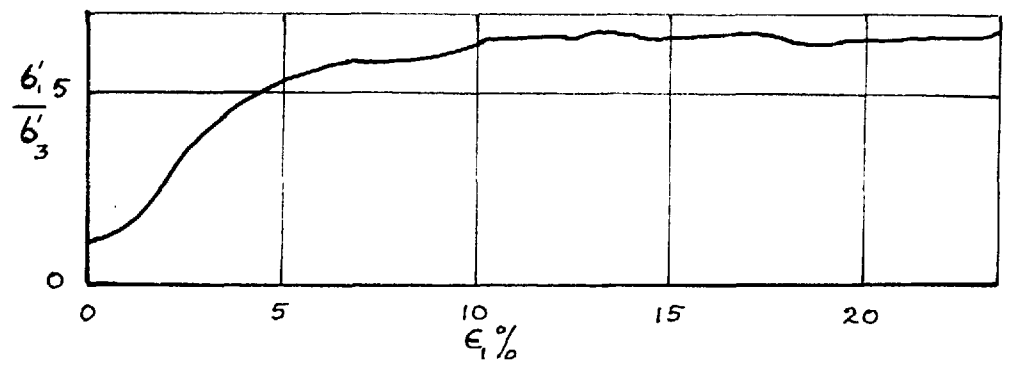
SILURIAN CLEAVED MUDSTONE SAMPLE No. 30

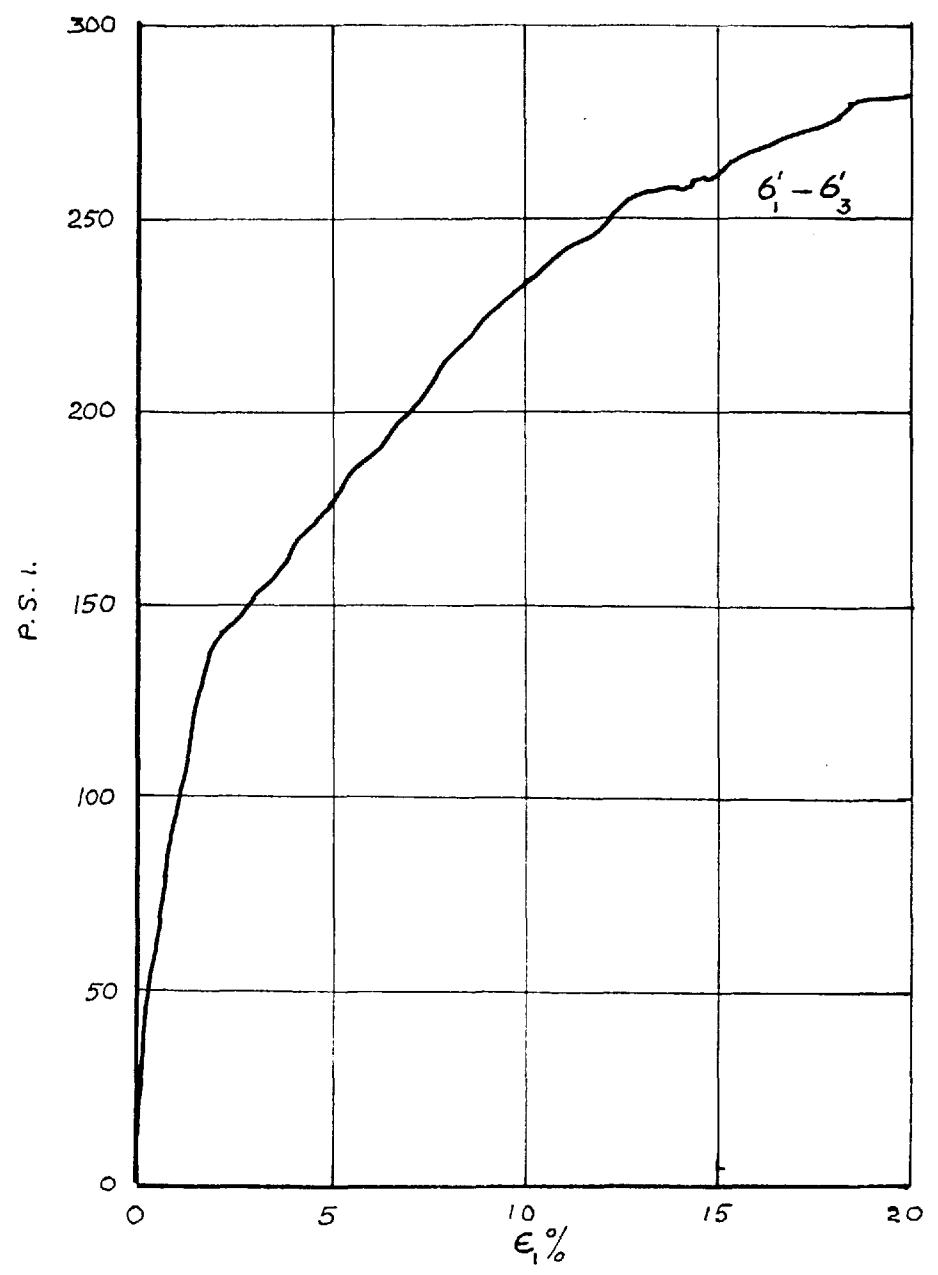
FIG. 7:3:7a

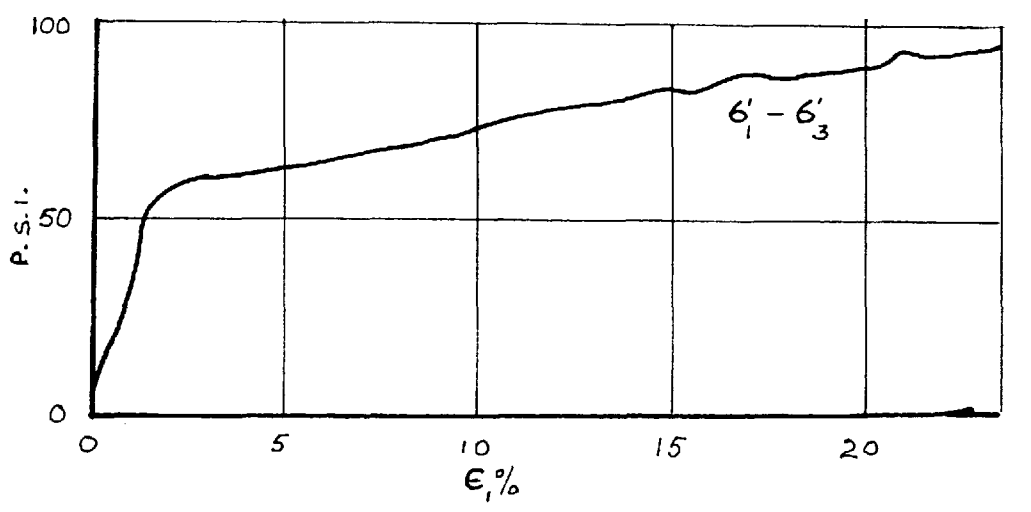


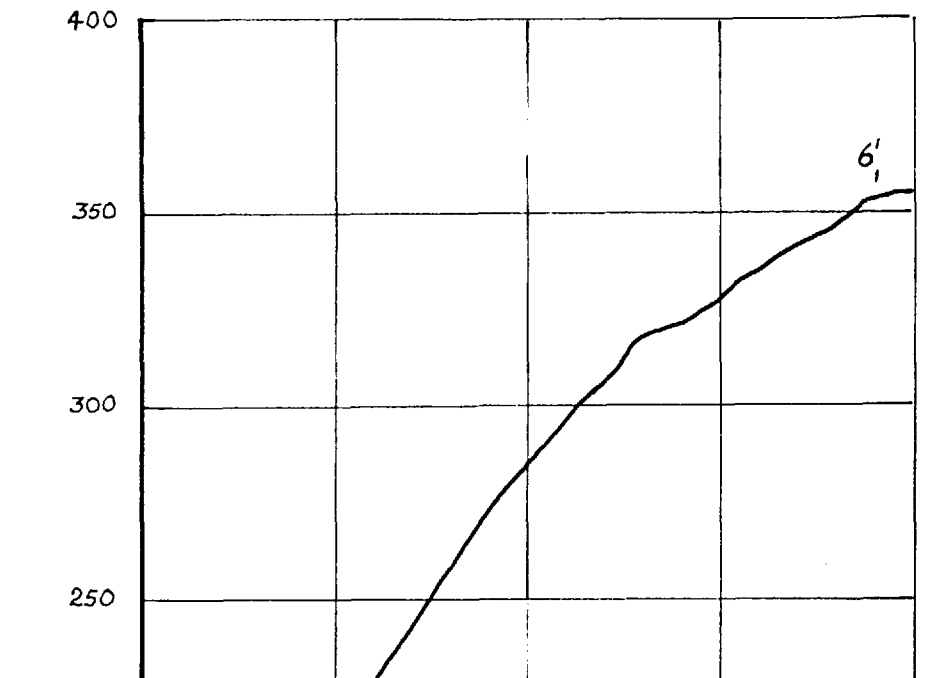


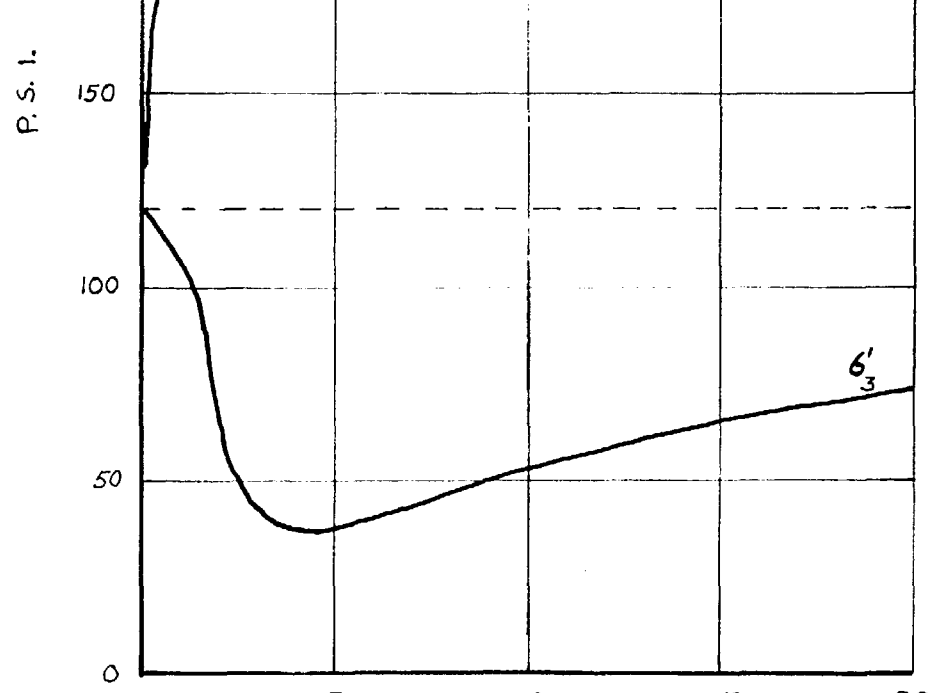


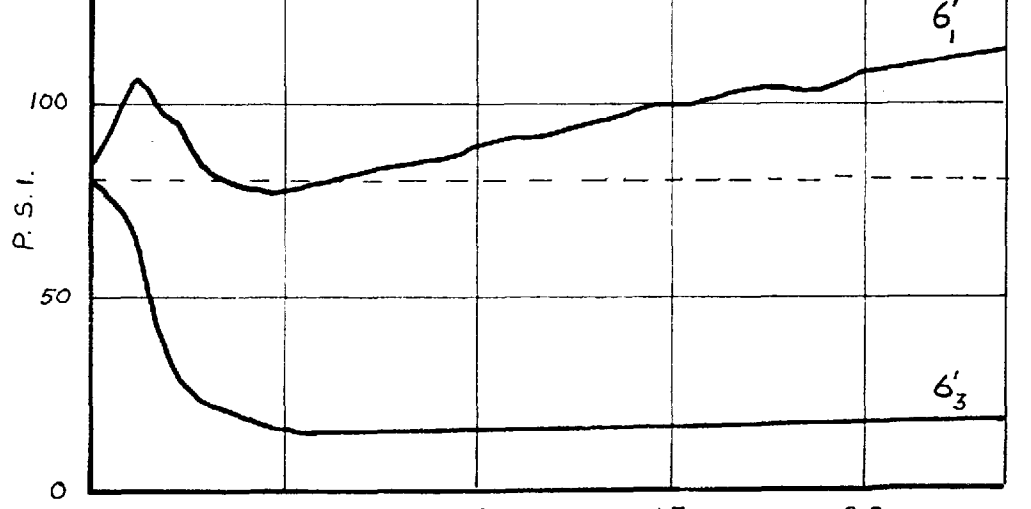












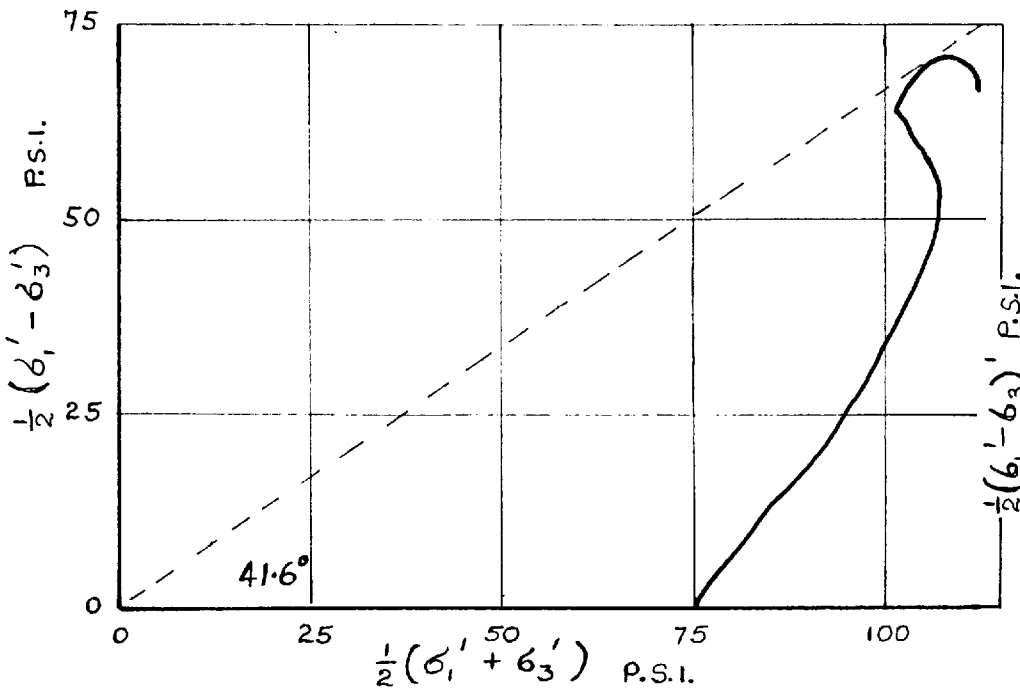
SAMPLE 31 γ_d = 141·5 LBS/FT.^{3} R_d = 97·5%

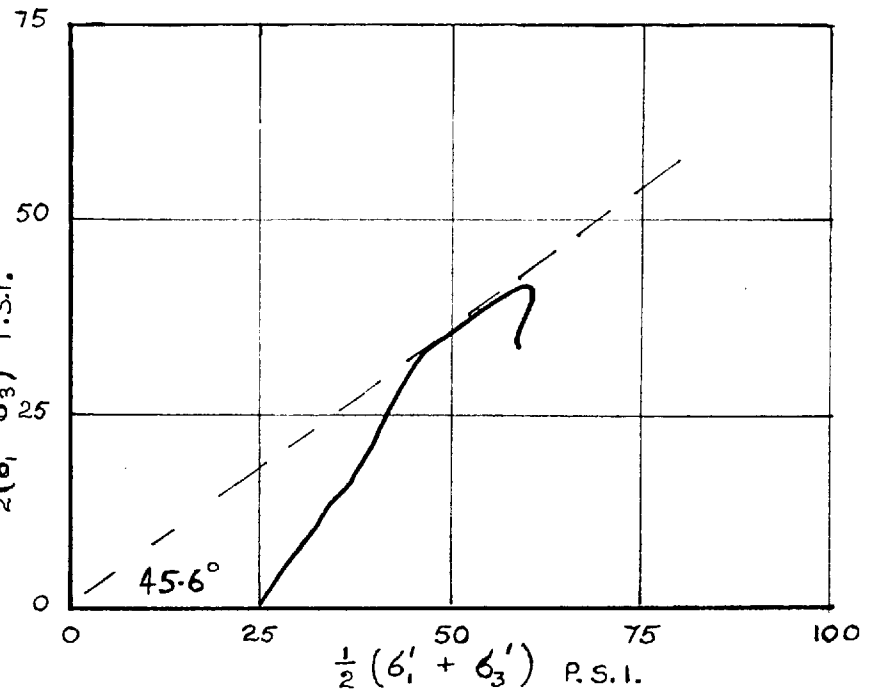
SAMPLE 32 γ_d = 108 LBS/FT.^{3} R_d = 27·0%

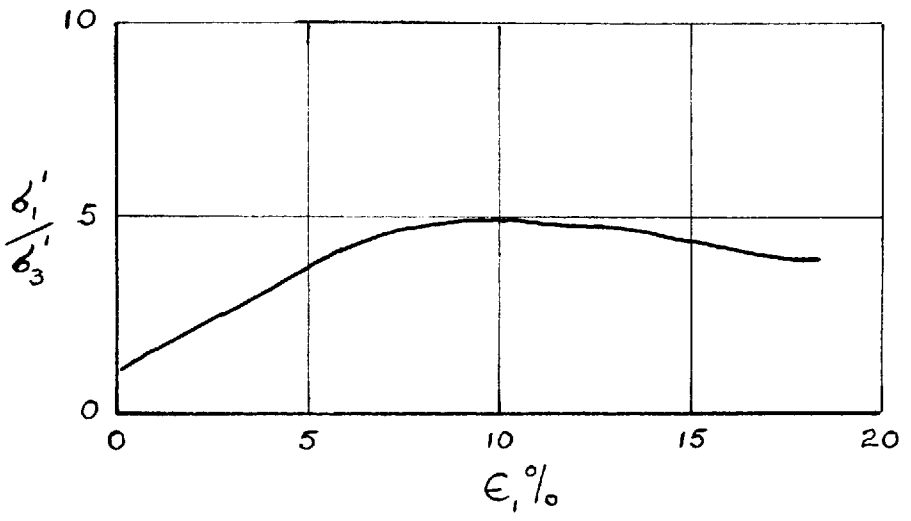
SILURIAN CLEAVED MUDSTONE.

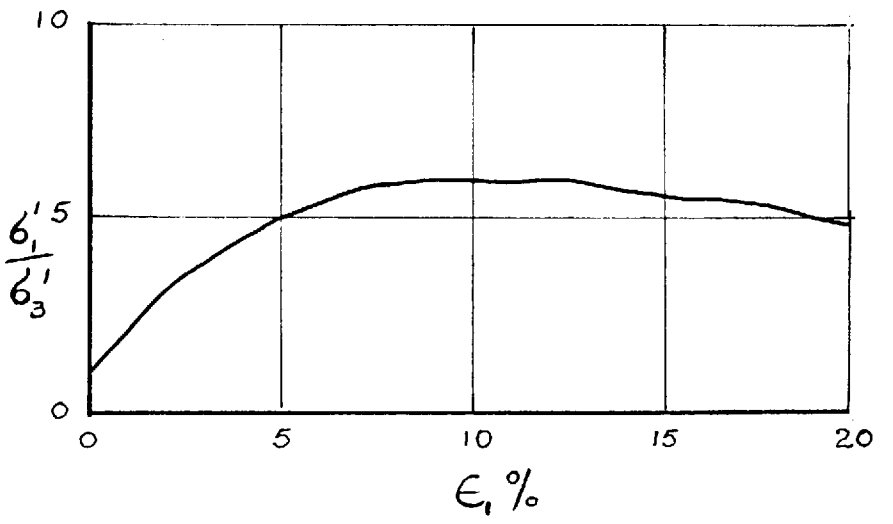
FIG. 7:3:76

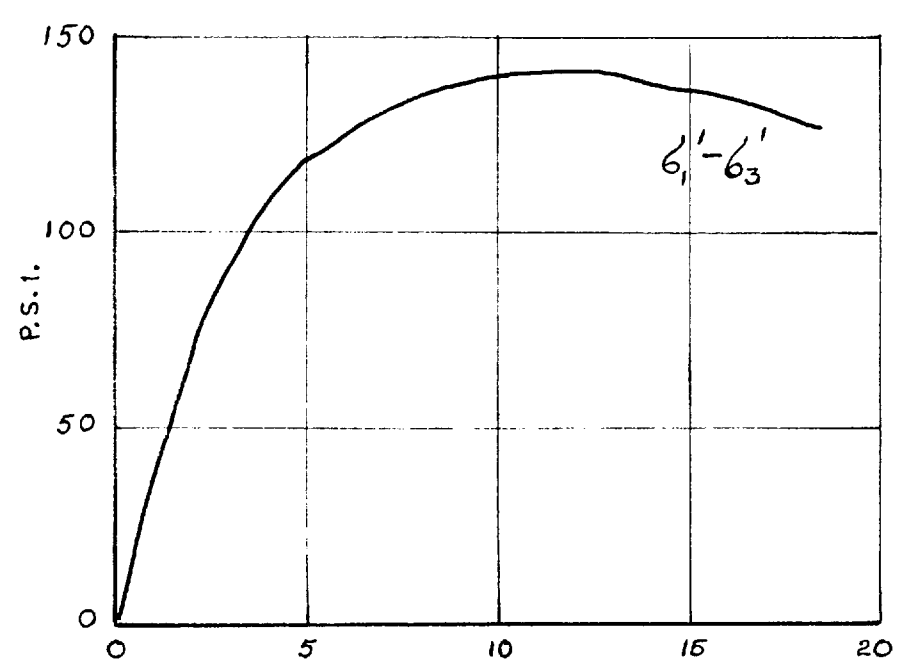
206

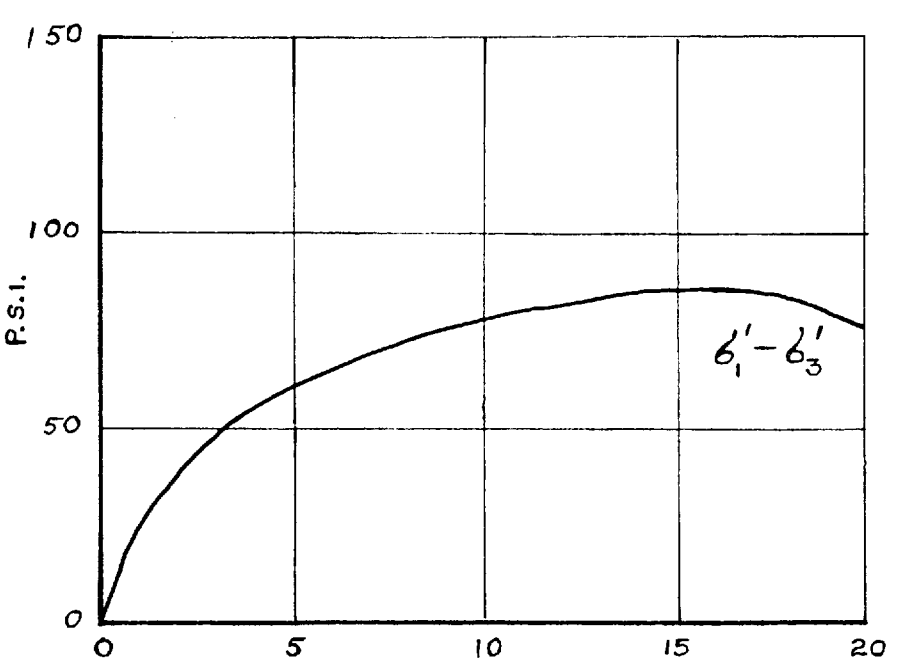


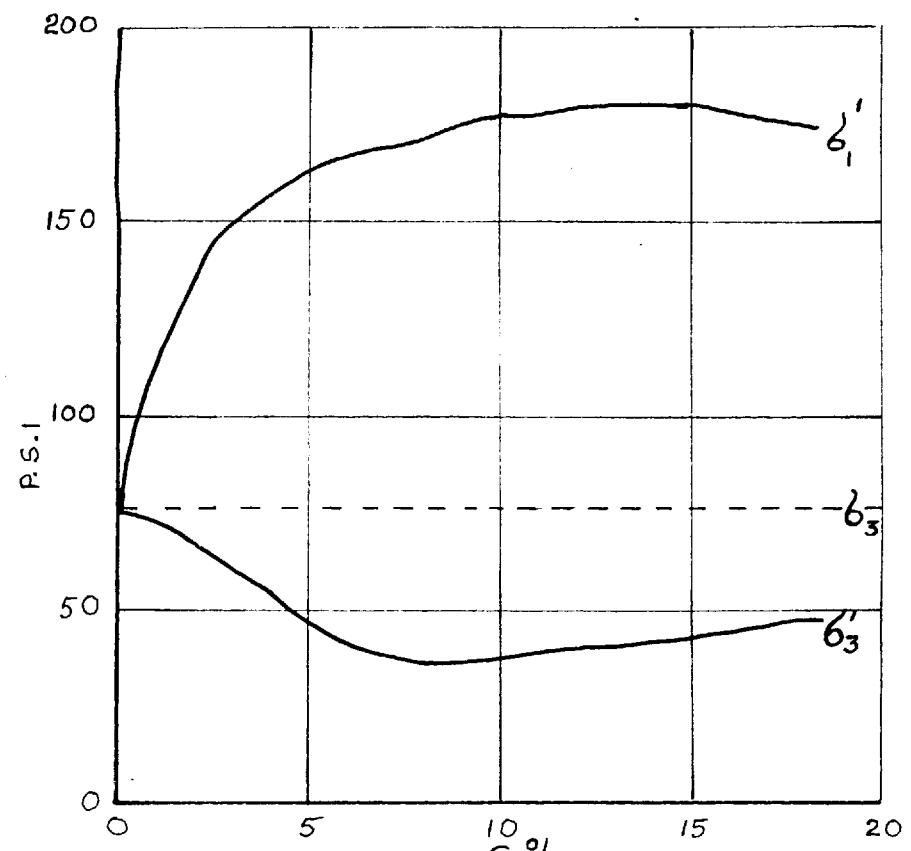


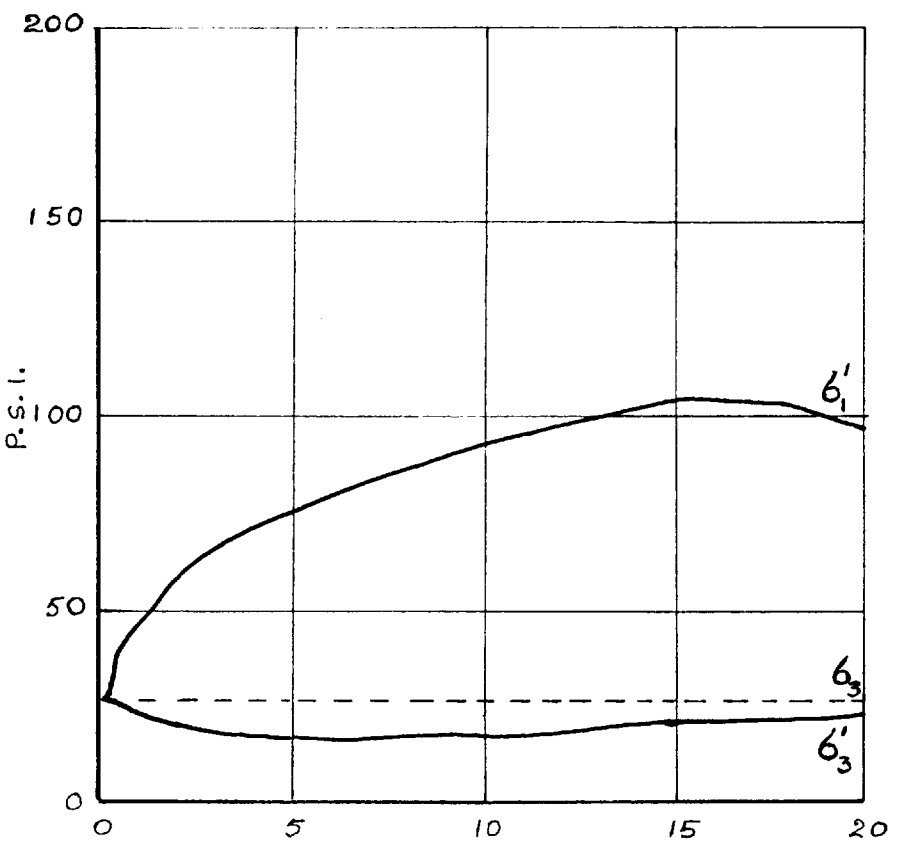


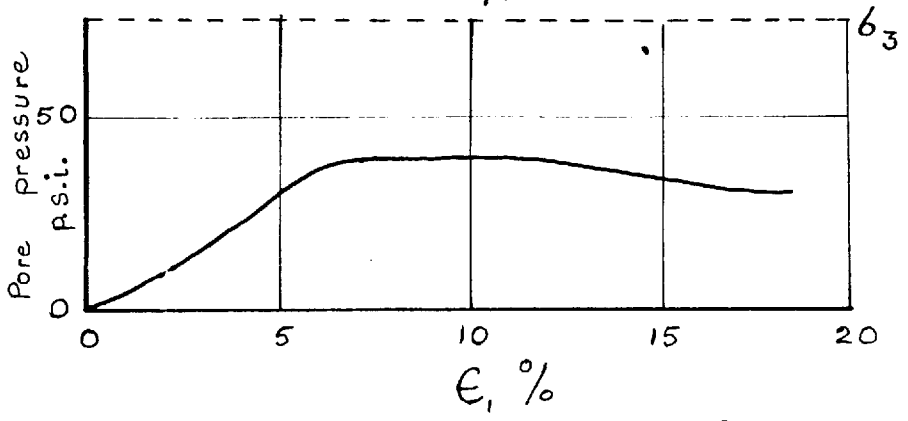


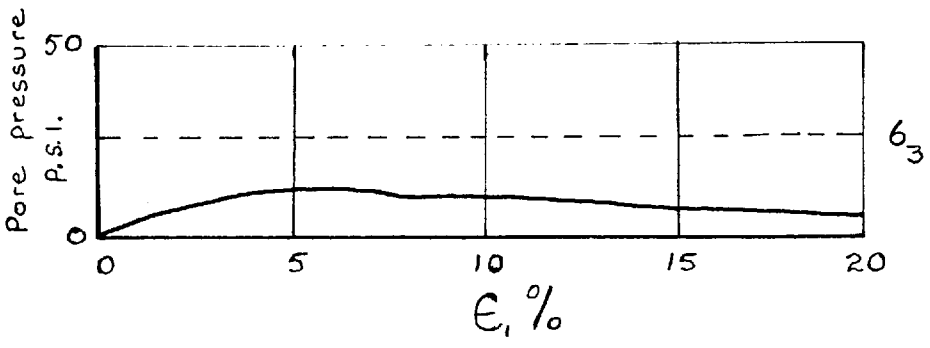










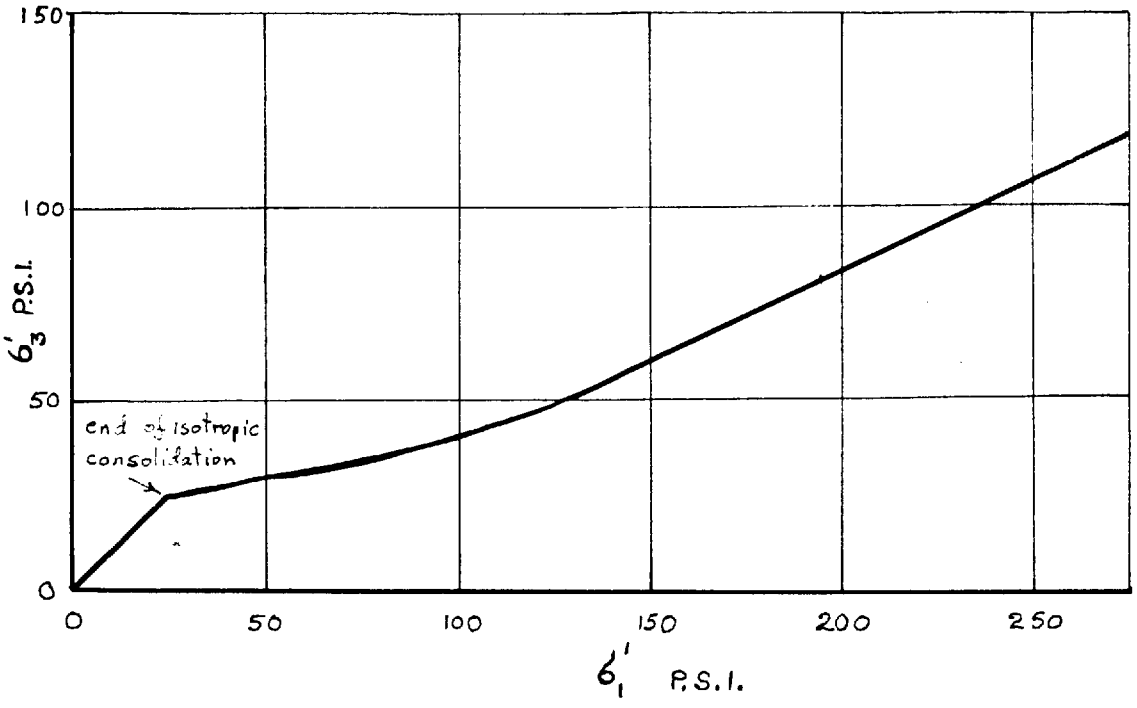


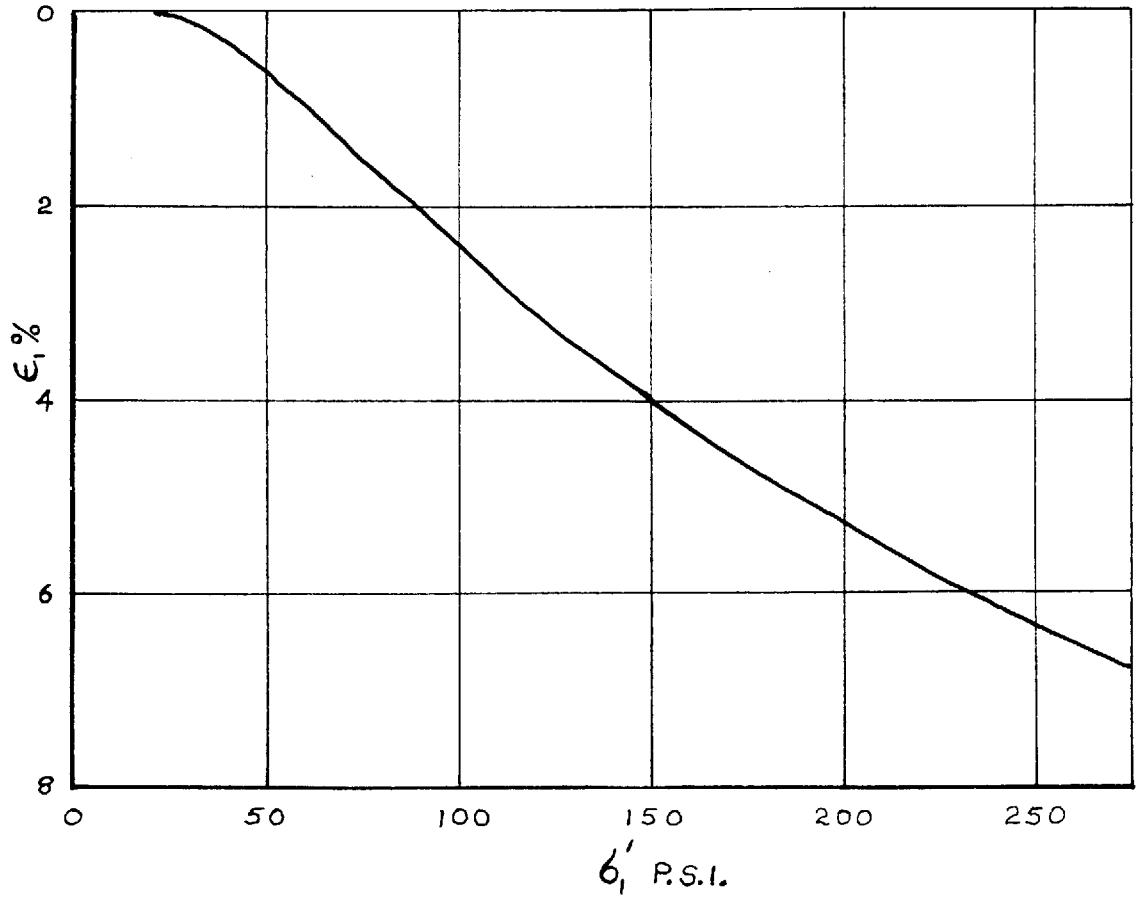
GRADING: D σ_3 = 75 LBS/IN.^{2}
γ_D : 126·2 LBS/FT.^{3} (AFTER CONSOLIDATION)
R_d : 64·0 %

GRADING: D. σ_3 = 25 LBS/IN.^{2}
γ_D : 128 LBS/FT.^{3} (AFTER CONSOLIDATION)
R_d : 68·0 %

SILURIAN CLEAVED MUDSTONE 4" DIA. SAMPLES.

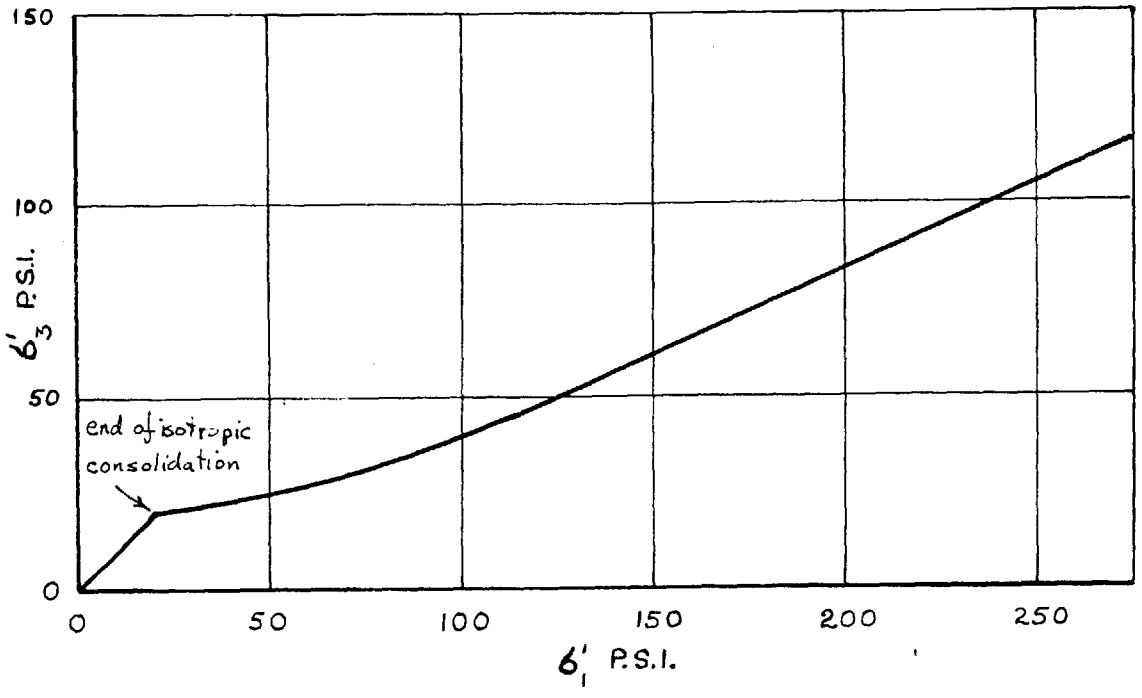
FIG. 7:3:7c

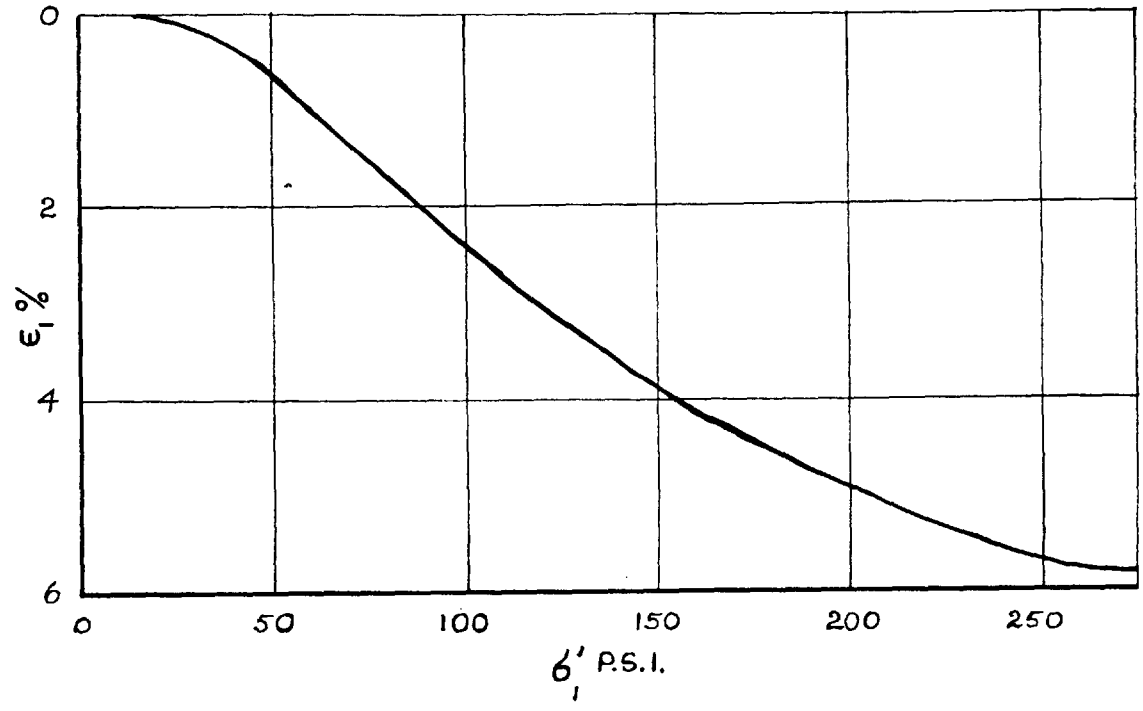




SILURIAN CLEAVED MUDSTONE SAMPLE No. 14M/12
K_o CONSOLIDATION STAGE.

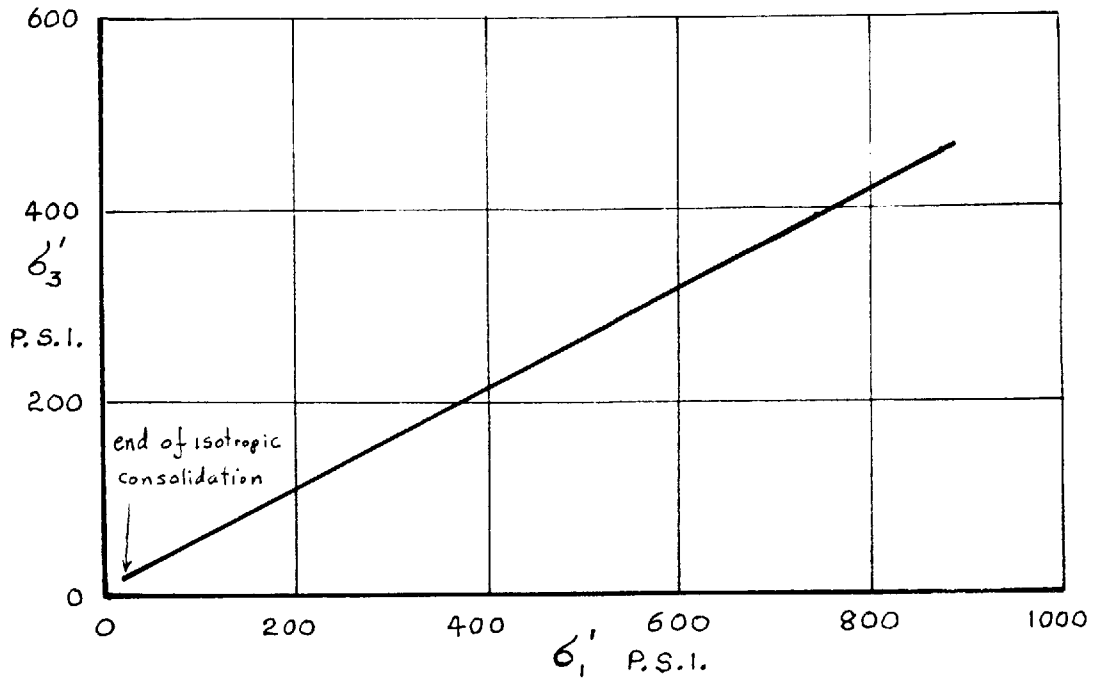
FIG. 7:4:10a

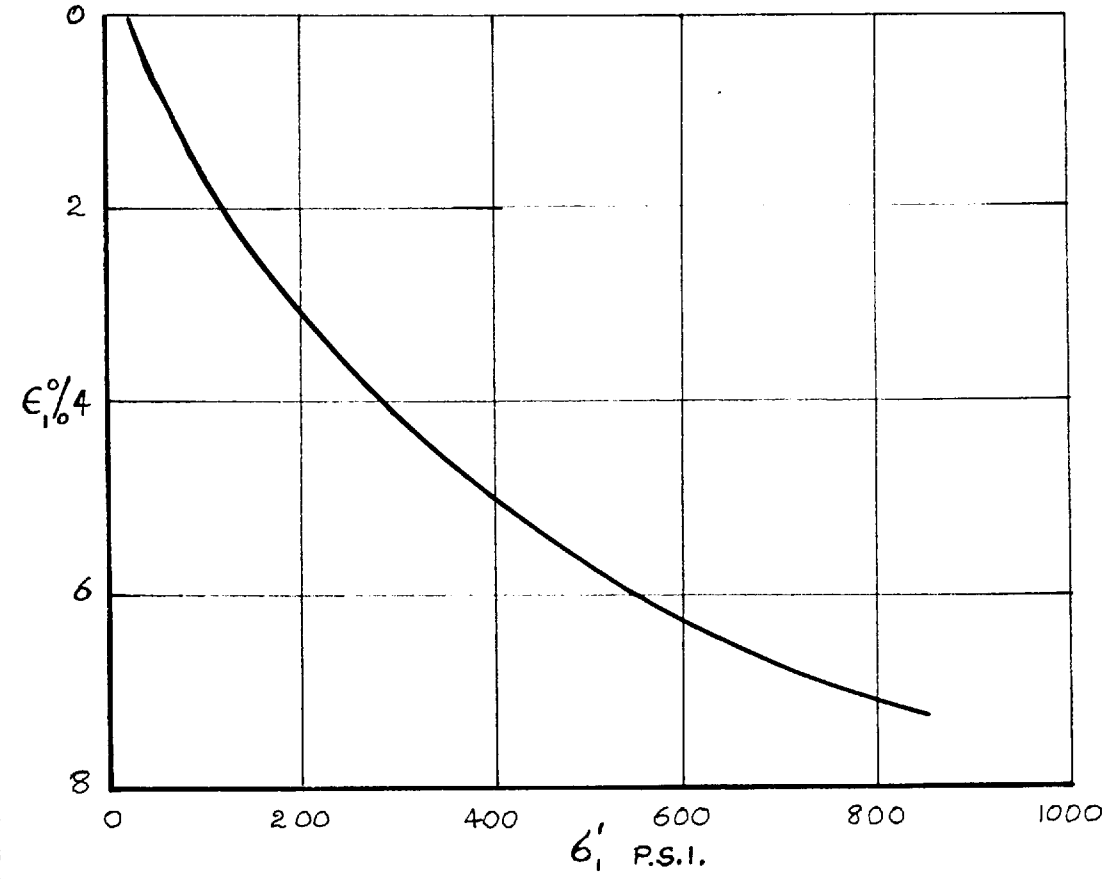




SILURIAN CLEAVED MUDSTONE SAMPLE 15M/12
K_o CONSOLIDATION STAGE.

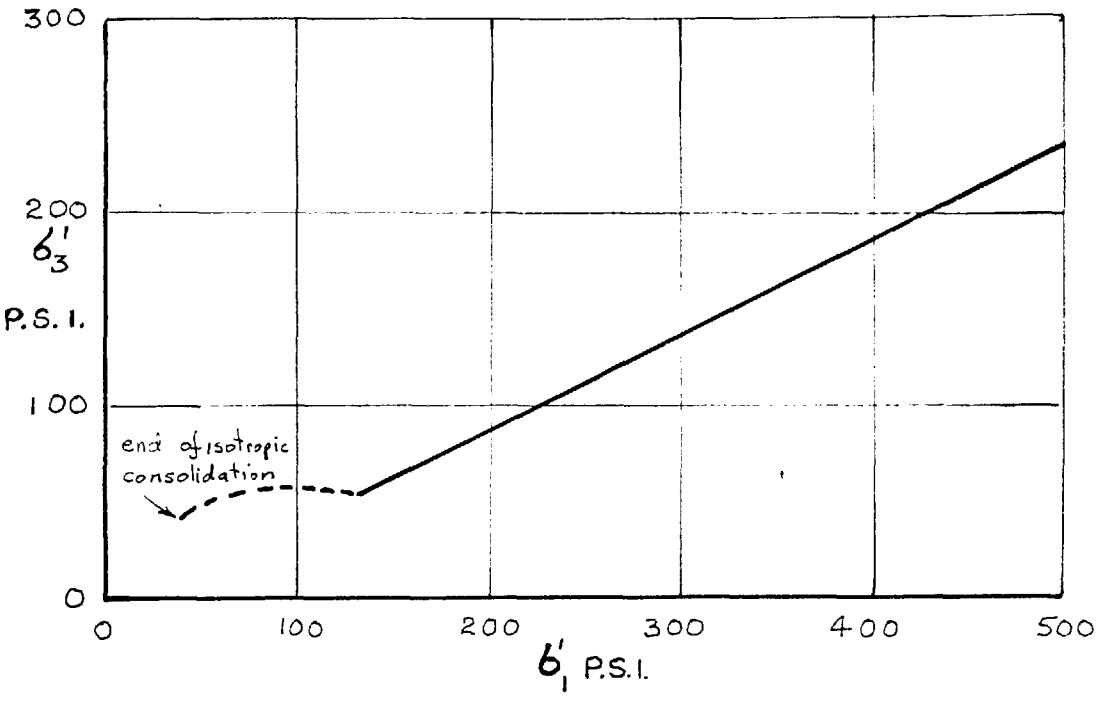
FIG. 7:4:106

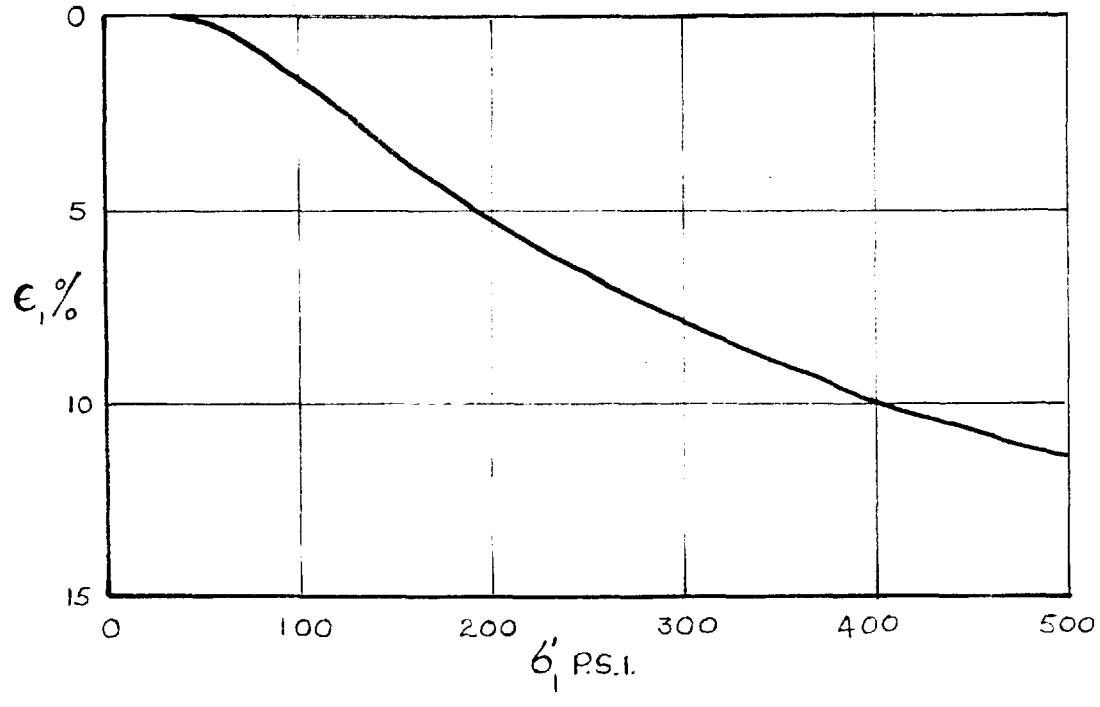




SILURIAN CLEAVED MUDSTONE SAMPLE No. 16M/12
K_o CONSOLIDATION STAGE.

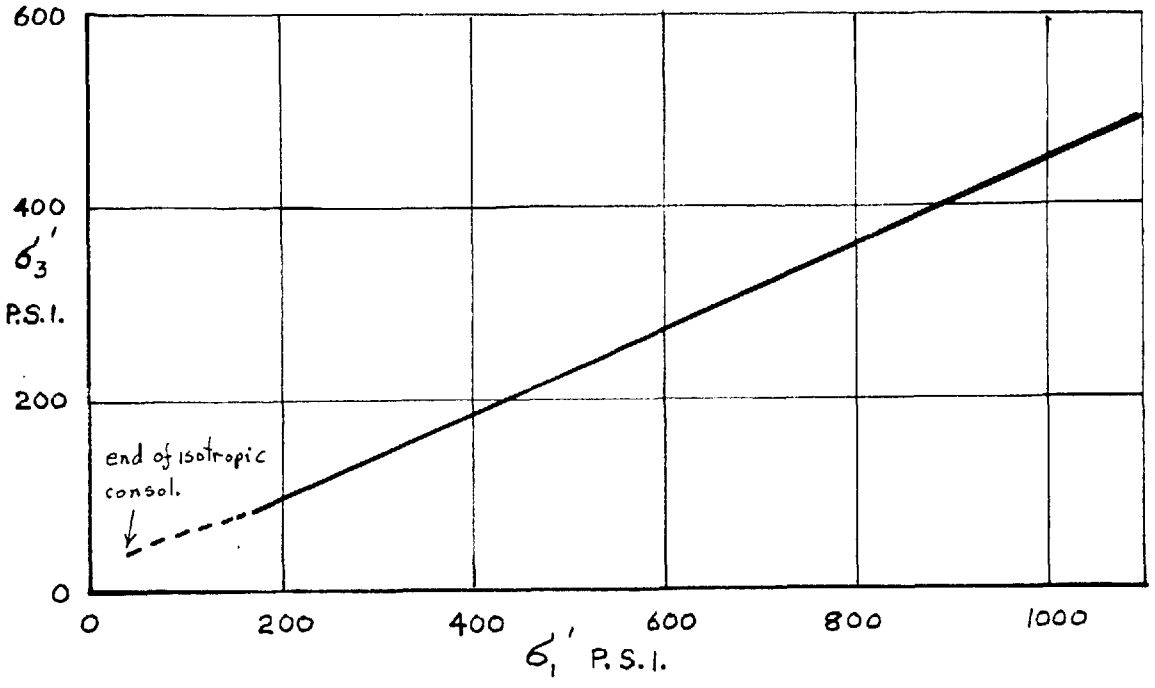
FIG. 7:4:10c

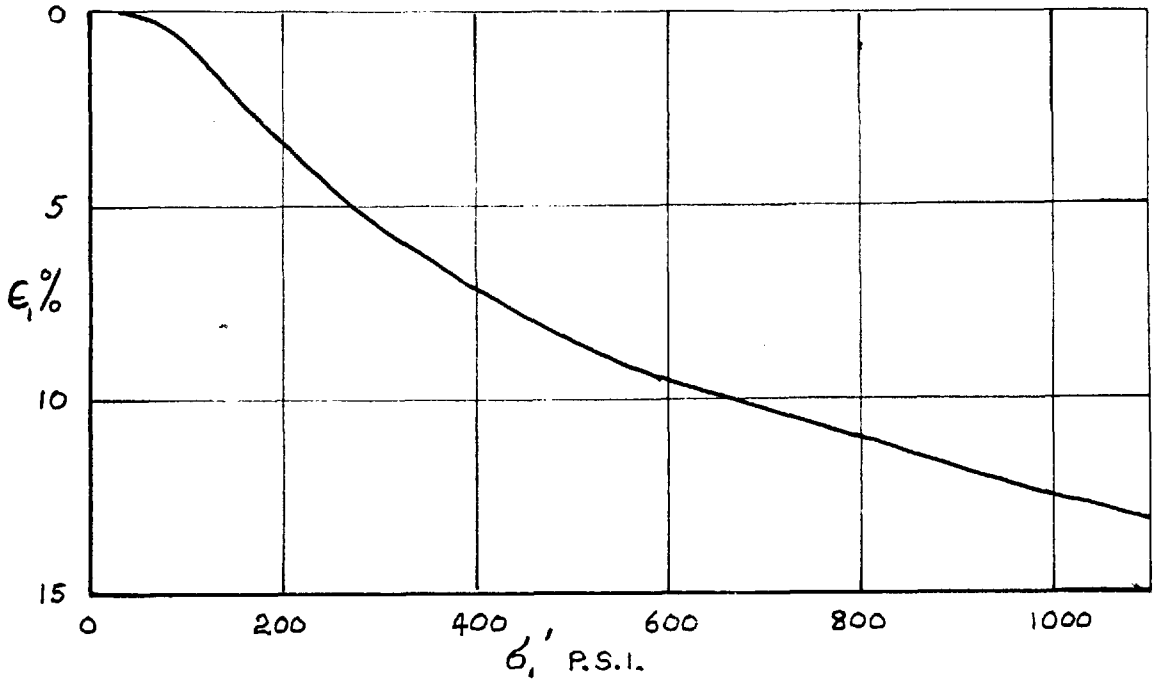




SILURIAN CLEAVED MUDSTONE SAMPLE No. 20M/12
K_o CONSOLIDATION STAGE.

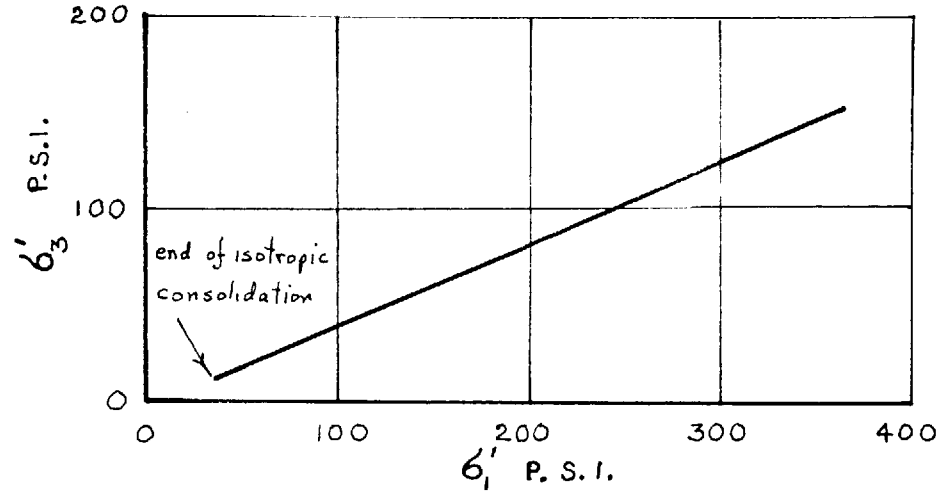
FIG. 7:4:10d

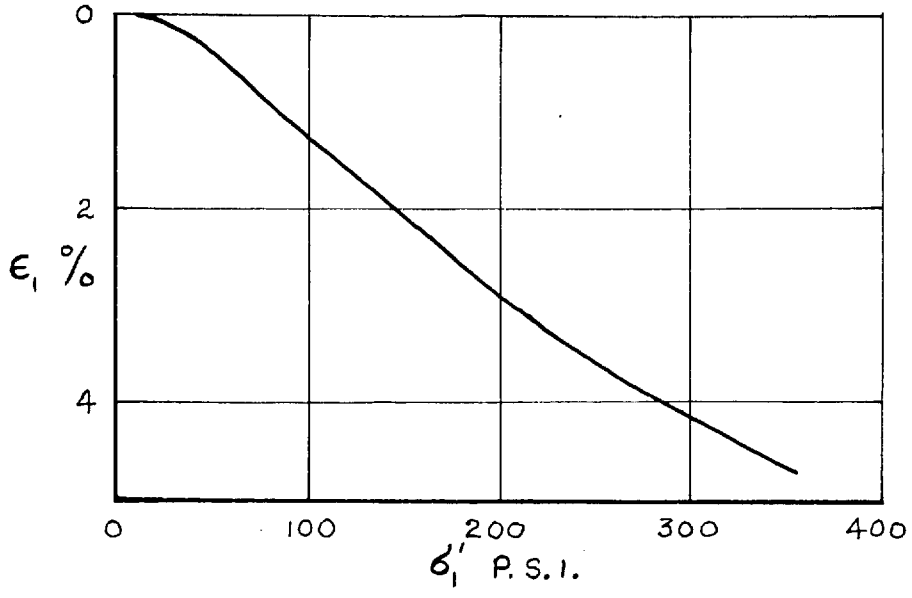


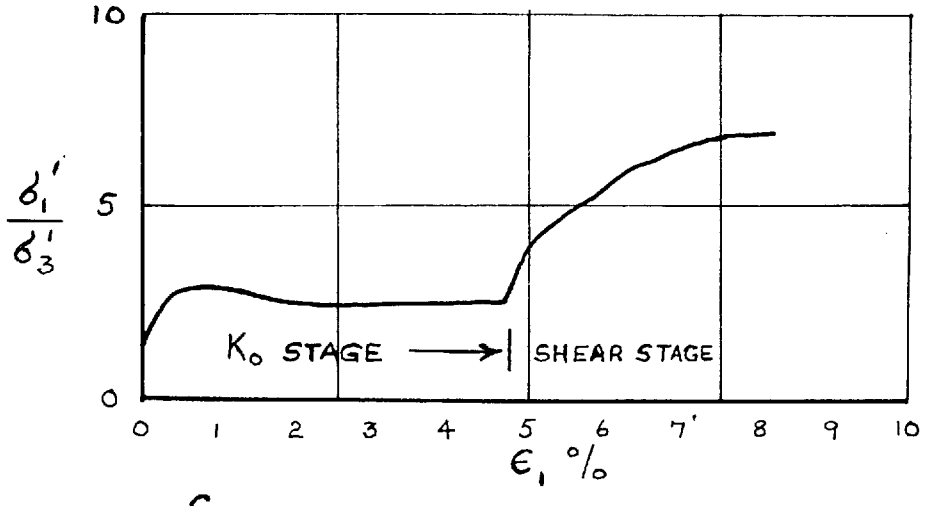


SILURIAN CLEAVED MUDSTONE
SAMPLE No. 21 M/12.
K_0 CONSOLIDATION STAGE.

FIG. 7: 4:10e

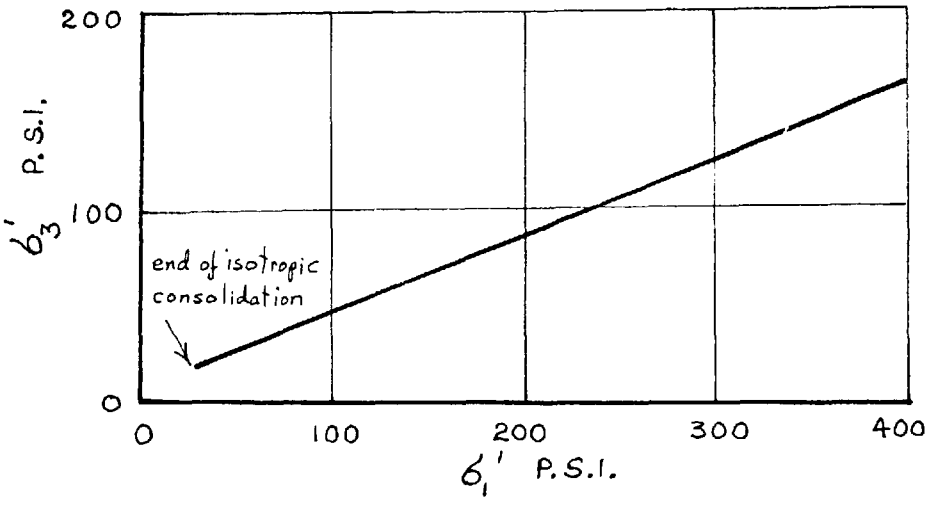


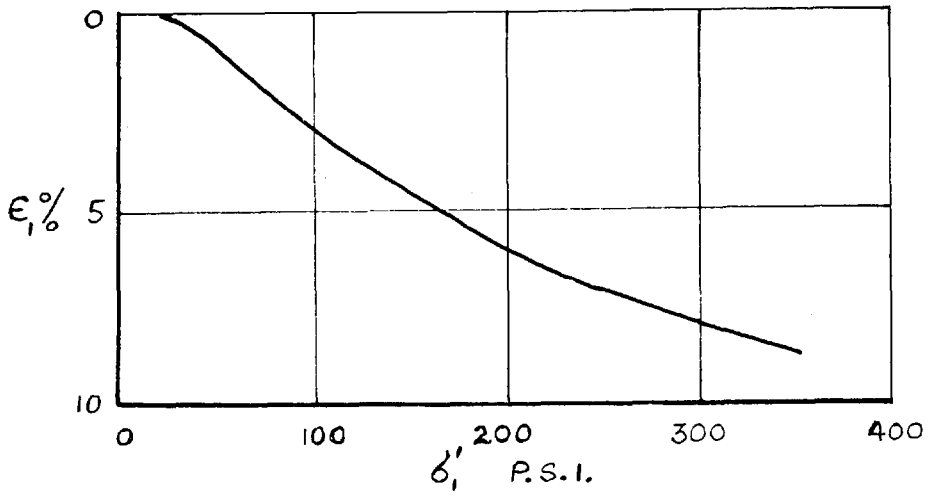


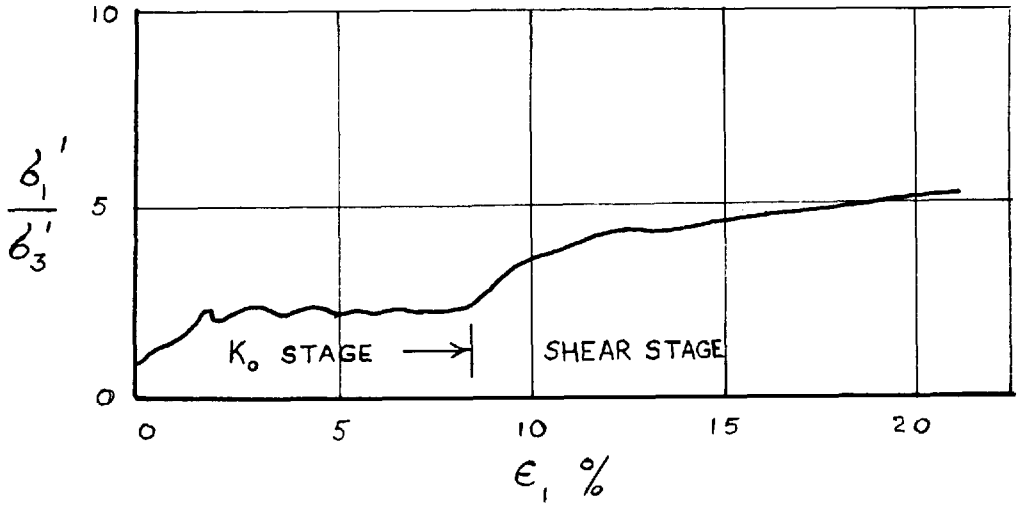


SILURIAN CLEAVED MUDSTONE
SAMPLE No. 26M/12.

FIG. 7: 4: 10f







SILURIAN CLEAVED MUDSTONE
SAMPLE No. 28M/12.

FIG. 7:4:10

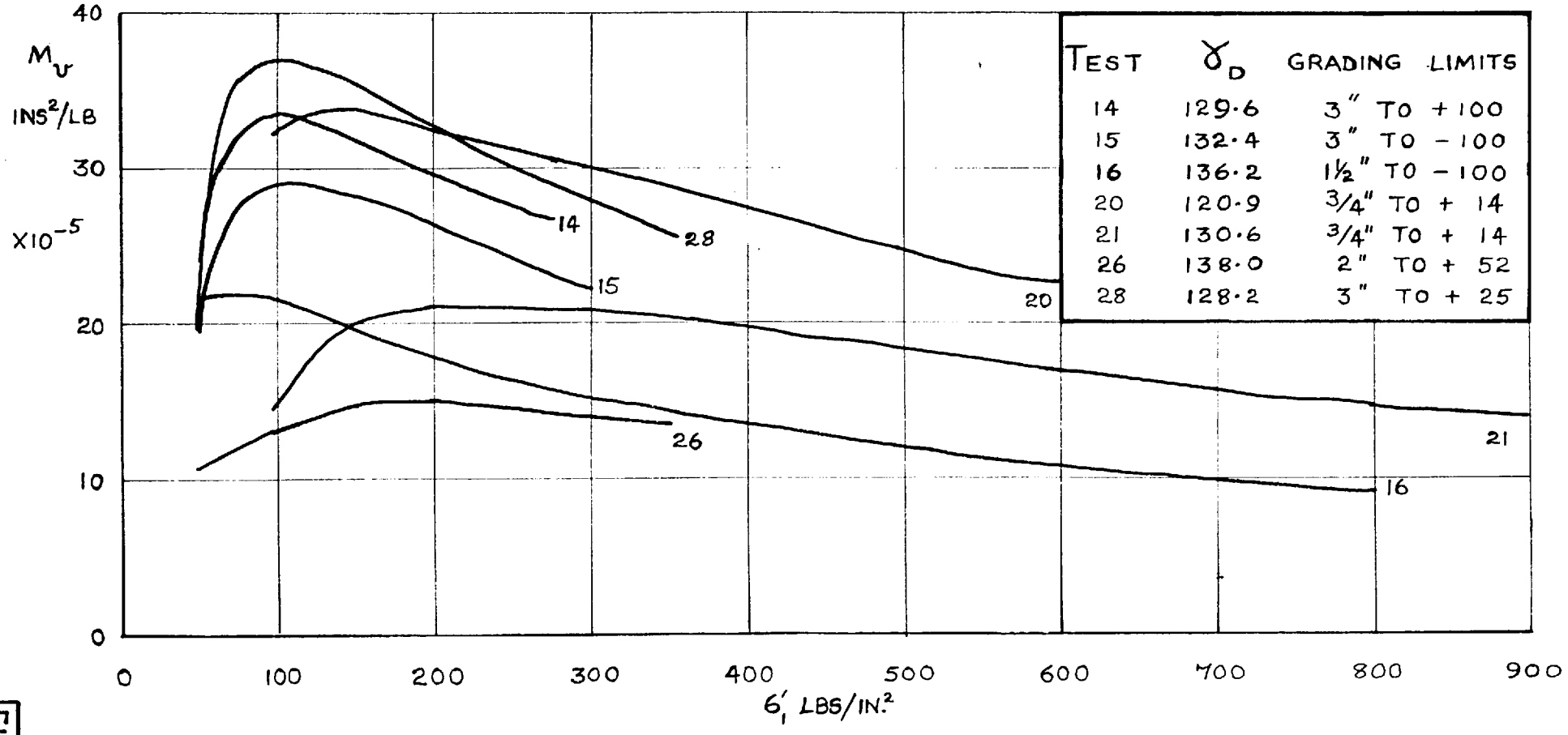


FIG. 7:4:104

SILURIAN CLEAVED MUDSTONE

SECANT VALUES OF m_v.

Test No.	1M/12	2M/12	3M/12	4M/12	5M/12	7M/12	8M/12	9M/12	10M/12	11M/12	12M/12	13M/12	14M/12	15M/12	16M/12	17M/12	19M/12	20M/12	21M/12	22M/12	23M/12	25M/12	26M/12	27M/12	28M/12	29M/12	30M/12	31M/12	32M/12
Type of test.	DS	DS	DS	DS	DS	DS	DS	DS	DSO	DS	DS	DS	K_oDS	K_o	K_o	DS	DSO	K_oDS	K_oDS	DSO	DSO	DS σ_3' dec	K_o δ_1'/δ_3' inc σ_3'=	DS	K_o O δ_1'/δ_3' inc σ_3'=	Int & Ext loadcells	CU	CU	CU
Nominal σ_3' (P.S.I.)	40	80	20	10	100	135	80	100	80	100	60	60	135			60	40	306	500	80	100		147	147	143	80	80	120	80
Axial strain rate % per hour.	4·1	4·0	4·0	4·1	4·1	4·2	8·2	8·5	9·1	0·28	8·85	8·85	9·3			8·9	8·7	10·0	10·3	2·6	8·9			8·8		8·0	8·0	8·0	8·0
ϕ_f'	44·5	43·0	48·1	50·5	40·3	39·9	43·5	42·0	43·1	39·4			39·8			45·5	42·6	35·8	34·2	38·8	37·6	47·0	48·3	41·0	42·2			44·8	47·3
Tan ϕ_f'	0·983	0·933	1·115	1·213	0·848	0·836	0·949	0·900	0·936	0·821			0·833			1·018	0·920	0·721	0·680	0·804	0·770	1·072	1·122	0·869	0·907			0·993	1·09
$\frac{1}{2}(\sigma_1'-\sigma_3')_f$ (P.S.I.)	95·5	173·5	60·2	34·6	185·2	243·2	178·5	205·0	172·2	172·8			244·0			153·0	86·0	431·5	644	136·9	158·3	123·6	95·9	282·6	103·8			92·7	40·7
$\frac{1}{2}(\sigma_1'+\sigma_3')_f$ (P.S.I.)	136·6	254·5	81·0	44·9	286·2	379·0	259·4	306·2	252·2	273·1			380·0			215·0	127·0	738·1	1145	218·4	259·5	168·9	128·5	430·9	154·5			131·5	55·5
σ_{1f}' (P.S.I.)	232·2	427·7	141·3	79·5	471·3	622·3	437·9	511·2	424·4	445·9			623·2			368·1	213·1	1169·6	1789	355·2	417·8	292·5	224·4	713·5	258·2			224·1	96·1
σ_{3f}' (P.S.I.)	41·1	80·8	20·8	10·3	101·0	135·8	80·9	101·2	80·0	100·3			136·3			62·0	41·0	306·6	500·5	81·5	101·2	45·3	32·6	148·3	50·7			38·8	14·8
$(d\epsilon_v/d\epsilon_1)_f$	-0·105	-0·077	-0·233	-0·256	-0·037	-0·041	-0·029	-0·044	+0·055	0			0			-0·10	0	+0·033	+0·070	+0·016	+0·100	0	-0·235	0	0				
γ_d (lbs/ft³)	128·0	140·0	141·8	132·8	133·5	141·0	138·0	136·7	113·0	131·4	114·6	115·1	129·6	132·4	136·2	132·3	126·8	120·9	130·6	125·1	125·8	146·2	138·0	141·4	128·2	134·4	133·1	141·4	108·0
R_d %	74·0	95·0	98·0	82·5	84·0	96·5	91·8	89·2		76·0			77·1	82·0	88·5	81·6	71·0			68·0						85·5	83·1	97·1	27·0
n %	25·8	18·9	17·9	23·0	28·6	18·3	20·1	20·7	34·5	23·8	33·6	33·3	24·8	23·3	21·1	23·3	26·6	30·0	24·3	27·5	27·2	15·3	20·1	18·2	25·7	22·2	22·8	18·2	37·4
Effective stress when measuring	12·0	12·0	12·0	2·5	4·6	0	0	0	12·0	6·0	6·0	6·0	6·0	6·0	6·0	6·0	4·8	2·1	6·6	4·7	9·0	14·0	1·0	1·0	13·7	1·0	1·7	1·0	1·0
ϵ_{1f} %	21·8	14·0	10·0	11·7	17·7	12·9	14·4	19·5	22·2	12·0			21·0			17·54	26·0	28·3	24·65	23·6	23·9	4·4	8·2	13·2	21·0			5·7	13·7
ϵ_{vf} %	-6·1	-1·9	-1·0	+0·1	-5·3	-3·6	-4·5	-4·4	-10·1	-3·2			-11·0			-5·58	-8·19	-18·3	-16·5	-3·8	-8·6	0	-1·7	-3·5	-9·6				
Membranes	1/8" R.F.	1/8" R.F.	1/8" R.F.	1/16" R.F.	1/8" R.F.	1/8" R.F.	1/8"+1/16" R.F.	1/8"+1/16" R.F.	1/8"+1/16" N.R.	1/8" N.R.	1/8" N.R.	1/8"+1/16" N.R.	1/8"+1/16" R.F.	1/8"+1/16" R.F.	1/8"+1/16" R.F.	1/8"+1/16" R.F.	1/8"+1/16" R.F.	1/8"+1/16" N.R.	1/8"+1/16" N.R.	1/8" R.F. 1/16" N.R.	1/8"+1/16" R.F.	1/8"+1/16" N.R.	3/16" R.F	3/16" R.F	3/16" R.F	3/16" R.F.	3/16" R.F.	3/16" R.F	3/16" R.F.
k before test cms/sec.									$3·46 \times 10^{-4}$	$9·75 \times 10^{-7}$		$3·7 \times 10^{-4}$				$3·06 \times 10^{-3}$	$1·2 \times 10^{-2}$	$2·2 \times 10^{-2}$	$4·6 \times 10^{-3}$	$1·8 \times 10^{-5}$	$1·7 \times 10^{-1}$	$1·9 \times 10^{-4}$		$3·0 \times 10^{-3}$	$3·3 \times 10^{-1}$			$8·5 \times 10^{-4}$	1·91
mean stress for above $\frac{1}{3}(\sigma_1'+2\sigma_3')$ (P.S.I.)									80	100		60				60	40	40	40	80	50	60		60	20			120	80
k after test. cms/sec.									$2·69 \times 10^{-4}$							$3·01 \times 10^{-4}$	$9·3 \times 10^{-4}$		$2·8 \times 10^{-5}$	$6·5 \times 10^{-7}$		$3·9 \times 10^{-5}$		$4·6 \times 10^{-4}$	$9·5 \times 10^{-4}$			$4·2 \times 10^{-4}$	$3·8 \times 10^{-2}$
mean stress for above $\frac{1}{3}(\sigma_1'+2\sigma_3')$ (P.S.I.)																													
γ_d at failure. (lbs/ft³)	140·1		144·3	133·3	151·1	150·8	150·1	150·5	133·8	142·4			146·7			145·4	149·0	150·3	152·8	138·8	148·0	146·2	140·0	150·2	146				
Grading.	A*		A*	A*	A*	A*	A*	A*	↑	↑	↑	↑	↑	↑	↑	↑	↑	↑	↑	↑	↑	↑	↑	↑	↑	↑	↑	↑	↑
Type of failure.	B/S		B/S	B/S			B/S	B/S	B/S	B/SS			B/SS				B/S	B	B	B/S	S	B	B	B	S	B/S		B	B/S
									30°								32°			60°	64°						2	3	3

TRIAXIAL TESTS ON 12" DIAMETER SAMPLES OF SILURIAN CLEAVED MUDSTONE.

* Approximately

↑ See Table. 5:6:1.

2 See Fig: 7:3:7a.

3 See Fig: 7:3:7b.

TABLE. 7A

Test No.	1M/4	3M/4	4M/4	5M/4	6M/4	7M/4	8M/4	9M/4	13M/4	14M/4	15M/4	16M/4	17M/4	18M/4	19M/4	20M/4	21M/4
Type of test.	DS	DS	DS	DS	DS	DS	DS	DS	DS	DS	DS	DS	DS	DS	DS	DS	DS
Nominal σ_3' (P.S.I.)	20	40	40	120	10	10	10	80	120	120	10	10	10	120		10	10
Axial strain rate % per hr.	8 Drainage both ends	2.5	0.4	2.5	2.0	5.0	8.0	8.0	8.0	8.0	8.0	8.0	2.5	2.5 Drainage both ends		2.0 Drainage both ends	0.168 Drainage both ends
ϕ_f'	41.0°	40.9°	40.9°	38.3°	44.6°	46.2°	48.5°	38.2°	37.4°	37.4°	43.7°	45.5°	43.0°	39.0°		46.6°	46.6°
Tan ϕ_f'	0.869	0.866	0.866	0.787	0.986	1.043	1.130	0.787	0.765	0.765	0.956	1.018	0.933	0.810		1.058	1.058
$\frac{1}{2}(\sigma_1'-\sigma_3')_f$ (P.S.I.)	38.3	76.0	76.0	195.5	24.3	27.2	30.9	129.5	186.0	186.0	23.2	25.8	22.1	204.2		27.8	27.8
$\frac{1}{2}(\sigma_1'+\sigma_3')_f$ (P.S.I.)	58.3	116.0	116.0	315.5	34.3	37.2	40.9	209.5	306.0	306.0	33.3	35.8	32.1	324.3		37.7	37.7
σ_{1f}' (P.S.I.)	96.5	192.0	192.0	511.0	58.6	64.3	71.7	339.0	492.0	492.0	56.5	61.6	54.2	528.5		65.5	65.5
σ_{3f}' (P.S.I.)	20.0	40.0	40.0	120.0	10.0	10.0	10.0	80.0	120.0	120.0	10.0	10	10	120		10	10
$(d\epsilon_v/d\epsilon_1)_f$	-0.123	0	-0.038	0	-0.230	-0.260	-0.30	+0.035	+0.031	+0.048	-0.177	-0.087	-0.160	-0.031		-0.25	-0.33
γ_d (lbs/ft^3)	130.0	129.8	128.9	129.0	128.2	133.3	132.3	132.6	128.4	130.7	125.6	124.8	127.0	127.5		132.5	132.8
R_d %	84.0	83.5	81.5	81.6	80.0	80.0	83.0	83.5	69.0	74.0	62.5	68.0	77.5	78.5		88.5	89.0
n %	24.7	24.6	25.3	25.3	25.7	28.8	23.4	23.2	25.6	24.3	27.3	27.6	26.4	26.1		23.2	23.1
Effective stress σ_3' when measuring (P.S.I.)	1.2	1.2	1.2	1.2	1.2	1.2	1.2	1.2	1.2	1.2	1.2	1.2	1.2	1.2		1.2	1.2
ϵ_{1f} %	10.7	10.4	10.5	12.43	10.1	8.68	9.93	10.1	12.7	10.70	10.07	10.69	9.52	14.10		8.33	7.79
ϵ_{vf} %	-2.33	-2.97	-3.37	-4.74	-0.88	-0.29	-0.24	-4.17	-5.34	-4.69	-1.77	-2.46	-1.72	-4.80		-0.26	-0.25
Membranes.	0.025"	2 x 0.025"	2x 0.025"	2x 0.085"	0.030"	2x 0.030"	2x 0.030"	2x 0.080"	0.055" 0.020"	0.055" 0.020"	0.055"	0.055"	0.055"	0.055"		2x 0.025"	2x 0.025"
k before test cms/sec.	7.5×10^{-6}	2.4×10^{-6}	2.0×10^{-6}			3.9×10^{-4}	2.8×10^{-3}	4.4×10^{-4}						3.5×10^{-5}			
mean stress for above $\frac{1}{3}(\sigma_1'+2\sigma_3')$ (P.S.I.)	20	40	40			10	10	80						30			
k after test. cms/sec.	6.1×10^{-7}	1.4×10^{-6}	2.9×10^{-6}	3.2×10^{-7}	4.4×10^{-5}	1.6×10^{-4}	2.1×10^{-3}	1.6×10^{-4}						7.3×10^{-8}		1.2×10^{-5}	4.6×10^{-6}
mean stress for above $\frac{1}{3}(\sigma_1'+2\sigma_3')$ (P.S.I.)	35	82	68	222	20	23	25	155						244		32	21
γ_d at failure (lbs/ft^3)	134.5	137.1	137.2	144.0	130.5	134.8	134.5	146.0	144.3	143.9	129.7	130.0	131.5	145.1		133.8	134.0
Grading.	F	F	F	F	F	D	C	C	D	D	D	C	F	F		F	F
Type of failure.	B/S	B/S	B/S	B/S	B/S	B/S	B/S	B/S	B	B/S	B/S	B/S	B/S	B		B/S	B/S

Note: ϕ_f' corrected for membrane effects.

TRIAXIAL TESTS ON 4" DIAMETER SAMPLES OF SILURIAN CLEAVED MUDSTONE

TABLE. 7B

Test No.	1M | 1½	2M | 1½	3M | 1½	4M | 1½	5M | 1½	6M | 1½	7M | 1½	8M | 1½	9M | 1½	10M | 1½	11M | 1½	12M | 1½	13M | 1½	14M | 1½	15M | 1½
Type of test.	DS	DS	DS	DS	DS	DS	DS	DS	DS	DS	DS	DS	DS	DS	DS
Nominal σ_3' (P.S.I.)	40	10	147	40	147	20	10	500	500	300	10	10	147	147	10
Axial strain rate % per hour	8.0	8.0	8.0	8.0	8.0	8.0	8.0	8.0	2.5	8.0	8.0	8.0	8.0	8.0	2.0 drainage both ends
ϕ_f'	44.1	48.9	40.1	42.7	39.4	45.2	47.2	34.6	34.7	36.7	47.1	46.0	38.7	38.6	45.5
Tan ϕ_f'	0.969	1.146	0.842	0.923	0.821	1.007	1.080	0.690	0.692	0.745	1.076	1.036	0.801	0.798	1.018
$\frac{1}{2}(\sigma_1'-\sigma_3')_f$ (P.S.I.)	92.5	32.5	267.5	85.9	256	50.6	29.4	656	661	447	29.1	27.1	246	246	26.3
$\frac{1}{2}(\sigma_1'+\sigma_3')_f$ (P.S.I.)	132.5	42.5	414.5	125.9	403	70.6	39.4	1156	1161	747	39.2	37.1	393	393	36.2
$\sigma_1'_f$ (P.S.I.)	225.0	74.9	682	211.8	659	121.1	68.8	1812	1821	1194	68.3	64.2	639	639	62.5
$\sigma_3'_f$ (P.S.I.)	40.0	10.0	147	40	147	20	10	500	500	300	10	10	147	147	10
$(d\epsilon_v/d\epsilon_1)_f$	-0.125	-0.182	0	-0.063	-0.010	-0.096	-0.204	0	0	+0.031	-0.188	-0.185	0	0	-0.155
γ_d (lbs/ft^3)	127.8	127.8	132.6	127.0	131.0	132.2	127.4	128.0	129.0	129.2	124.8	126.1	130.5	128.0	129.5
R_d %	76.5	76.5	86.0	77.5	85.5	88.0	78.5	80.0	82.0	82.5	70.0	76.0	85.0	77.0	2
n %	25.9	25.9	23.1	26.5	24.1	23.4	26.1	25.8	25.2	25.1	27.7	26.9	24.4	25.8	25.0
Effective stress when measuring	0.6	0.6	0.6	0.8	0.6	0.6	1.0	1.0	1.0	1.0	1.2	1.2	1.2	1.2	1.2
ϵ_{1f} %	12.76	12.54	15.0	15.4	16.0	14.0	13.25	12.25	12.25	12.40	11.30	11.49	14.89	17.35	8.31
ϵ_{vf} %	-3.43	-1.08	-3.72	-3.33	-4.17	-1.65	-0.10	-3.45	-3.25	-3.40	-0.58	-1.20	-3.94	-5.04	-0.85
Membranes	0.025"	0.025"	0.025"	0.025"	0.025"	0.025"	0.025"	0.025"	0.025"	0.025"	0.020"	0.020"	0.020"	0.020"	0.025"
k before test cms/sec.	9.13 x10^{-6}	1.83 x10^{-5}	1.0 x10^{-6}	4.56 x10^{-6}	5.0 x10^{-7}	1.02 x10^{-6}	3.74 x10^{-6}	6.5 x10^{-6}							
mean stress for above $\frac{1}{3}(\sigma_1'+2\sigma_3')$ (P.S.I.)	40	10	147	40	147	20	3	1.0							
k after test cms/sec	2.05 x10^{-6}	2.06 x10^{-5}	1.77 x10^{-7}	1.37 x10^{-6}	1.19 x10^{-7}	5.6 x10^{-7}	3.14 x10^{-6}	5.7 x10^{-8}							2.6 x10^{-6}
mean stress for above $\frac{1}{3}(\sigma_1'+2\sigma_3')$ (P.S.I.)	96.6	26.5	313	93	306	50	26.6								33
γ_d at failure (lbs/ft^3)	141.3	132.0	151.0	137.0	146.8	137.8	127.8	143.1		144.0					132.4
Grading	E	E	E	F	F	F	F	F	F	F	E	F	F	E	G
Type of failure	B/S	B/S	B	B	B	B/S	B	B	B		B/S	B/S	B	B	B

Note: Values of ϕ_f' corrected for membrane effects.

TRIAXIAL TESTS ON 1½" DIAMETER SAMPLES OF SILURIAN CLEAVED MUDSTONE.

TABLE. 7C

CHAPTER 8

The Results of Tests on Granitic Gneiss

(8:1) Compaction and Sample Density.

The gradings which were tested are given in Fig.5:6:2. The shape of the grading curve below the 100 B.S.sieve was not measured.

The 12" diameter samples of granitic gneiss were compacted in the same way as the large samples of silurian cleaved mudstone.

The dry densities achieved with gradings H and J were similar and quite consistent. The values were lower than for the mudstone but this had particles of a higher specific gravity and different shape as well as a grading containing more fines.

In was particularly difficult to produce a homogeneous sample with this material because of segregation. As with the mudstone the problem was overcome to a certain extent, by adding fine material after the coarse. The voids between coarse particles were so large that one could hear finer material working its way down the sample without compaction. As a result the lower portions of the samples always had lower porosities than the upper portions. This was sometimes evident from the failure deformations.

The tops of the samples were always very short of fines and the junction between the top cap and the sample had to be made up with small uniform material at the circumference to prevent subsequent rupture of the membranes.

During compaction a certain amount of particle breakdown took place. This was most noticeable in samples of grading H but, to a lesser extent, with grading J. It was expected that there would be little by comparison with the mudstone because the particles were stronger and the shapes more resistant to fracture. There was, though, a similar amount of particle fracture and this was probably due to two causes. Firstly, the grading was deficient in fines so the particles probably did not bed so well. Secondly, the material was tunnel spoil and hence had been subjected to intense shock on excavation. The micro fissuring, due to blasting and stress release, was therefore, part of the cause. The mudstone was also excavated by blasting but this material was so weak on cleavage planes that most breakdown resulting frm micro fissuring during blasting probably occurred during mechanical handling.

The granite had a gneissose structure and there were some weak planes caused by bands of mica.

As discussed in Section 7:1 higher densities were produced in the triaxial apparatus than in the oedometers.

The sample densities after compaction are given in Tables 8A, 8B and 8C.

The densely compacted 4" and 1½" diameter samples had approximately

equal densities which were about 10 lbs/ft. less than for 12" diameter samples.

With the granitic gneiss the problem of particles orientating, in such a way as to present a plane of weakness, did not arise.

(8:2) Isotropic Consolidation

All the volume changes measured during isotropic consolidation had an inherent error due to membrane penetration. The extent of this with the granitic gneiss was somewhat greater than with the silurian cleaved mudstone (Section 7:2) because of the fewer fines in the grading. However the resulting errors will be in the order of 2%.

The fines of the granitic gneiss did not form an adhesive paste as the silurian cleaved mudstone did. The samples could therefore be saturated very conveniently prior to consolidation whilst supported by the sample compaction mould.

Samples IIV/12 and 5V/12 show a greater apparent volume strain, for a given stress for the sample with the greater maximum particle size as also do samples 10V/4 and 21V/4 (Fig.7:2:2) and 2V/1½ and 4V/1½ (Fig.8:2:2)

This one would expect for two reasons. Firstly, the contact forces are 4 times as great when the maximum particle size is doubled. Secondly, the volume change due to membrane penetration would be larger with the coarser grading.

During the consolidation of gradings containing 3" material there was considerable audible evidence of particle fracture. It may well be that the greater volume strain of the coarser material is due to reorientation of the packing because a greater proportion of inherently weaker particles shearing through rather than just yielding at contacts.

Certainly after a shear test there was ample evidence of particles throughout the sample being sheared through.

The volume strains in the smaller samples were greater than those in larger samples having the same ratio of maximum particle size to sample diameter and at a given stress. This may have been partly due to the differences in porosity and the differences in membrane penetration because softer membranes were used on the smaller samples.

Loose material, of course showed in each sample size, a greater volume change than dense material for a given stress increment.

In general there was a large initial volume strain per unit stress increase and the curve then flattened out with increase in stress. This increase in stiffness was to be expected because of the increasing density of the packing and the lesser effects of membrane penetration.

Sample 5V/12 was initially consolidated in the dry state. During subsequent saturation at constant effective stress a further volume change of 12.5% occurred. This phenomena is discussed in Section 7:2

Sample IV/12 was also consolidated initially in the dry state. On subsequent saturation a dilation of 80% of the previous volume change occurred. This is unexplained and is thought to be an apparatus error as no evidence of dilation was ever found in any other samples.

(8:3) Shear strength

The relationship between the rate of dilatancy at failure and the angle of internal friction and the minor principal effective stress and ϕ_f' are plotted in Figs.8:3B and 8 :3A respectively.

(8:3:1) Shear strength of 12" diameter samples (drained shear tests).

A series of shear tests was performed on gradings H and J. The maximum confining pressure for grading H was limited to 150 p.s.i. because of membrane failures. The capacity of the loadframe limited the maximum confining pressure to 450 p.s.i. with grading J.

Dense samples of each grading had very high angles of internal friction those tested at low confining pressures showed a great tendancy to dilate (Figs.8:3:1a and b). This is in direct contrast to the mudstone which showed little dilation even when dense and subjected to low stresses.

The angles of internal friction for tests on grading H, at an assumed relative density of 90% varied from 58° to 43° at minor principal effective stresses of 10 p.s.i and 160 p.s.i respectively.

Grading J showed a lower strength than grading H at low stresses but a higher strength at high stresses. The angle of internal friction varied from 56° to 40° at minor principal effective stresses of 10 p.s.i and 450 p.s.i.

Over this range of stresses an almost linear relationship was obtained on a semi-log plot (Fig.8:3A)

Sample 12V/12 had a very low initial density, 107.8 lbs/ft. and it was sheared at a minor principal effective stress of 10 p.s.i. The stress strain curve is plotted in Fig.8:3:1c. The maximum angle of internal friction was some 10° above that suggested by the rate of dilatancy at failure. The sample deformation was so excessive that part of it was pressed against the inside of the cell, thus giving rise to peculiar volume change characteristics and an erroneous value of ϕ_f' . If the peak strength occurred at about 13% of axial strain the value of ϕ_f' was 47.0° which was 2.4° above that suggested by the rate of dilatancy at failure.

(8:3:2) Shear strength of 12" diameter samples subjected to anisotropic consolidation

Two shear tests were performed on samples of grading J after anisotropic consolidation. Failure was effected by increasing the stress ratio by raising the pore pressure.

Sample 18V/12 was compacted to 84.5% relative density. Failure by reducing the stresses gave an angle of internal friction of 54.9° which was about the mean for samples of grading J at 90% relative density.

Sample 19V/12 was compacted to 83.5% relative density. Failure by reducing the stresses gave an angle of internal friction of 48.5° which was 2.2° below the mean for drained shear tests on grading J.

With the former sample the rate of dilatancy at failure was similar to that obtained by causing failure by increasing the stresses in a drained shear test with the same ratio of maximum particle size to sample diameter. With the latter sample the rate of dilatancy at failure coincided more closely with that for normal samples with the ratio $D_d = 16$.

A slightly greater angle of internal friction would be expected from a sample failed by reducing stresses. The effect on the angle of internal friction of an anisotropic consolidation cannot be determined from these tests. Variations of up to 1° can be expected when testing essentially similar rockfill samples. Although sample 19V/12 had an angle of internal friction somewhat lower than expected no definite conclusion can be reached about the shear strength from this test.

(8:3:3) Shear strength of 4" diameter samples (drained shear tests)

(See Table 8B and Figs: 8:3:3a and b)

Samples 4" diameter with grading K, also $D/_d = 4$, compacted to a relative density of 9?% showed lower angles of internal friction than 12" diameter samples of grading H.

At confining pressures of 10 p.s.i. and 80 p.s.i the angles of internal friction were 7° and 4.2° respectively below those for 12" diameter samples. This suggests that there is a particle size effect which is a maximum at low pressures and slowly reduces. It may be that the shear strength is mainly dependant on two characteristics of the particles, namely, their shape and ultimate strength in shear. Effects due to the former predominate at low pressures and the effects due to particle strength at the higher pressures. This is suggested because of the reduced dilatancy and the large breakdown of particles at high stresses. Smaller particles should possess a higher unit shear strength than large particles and hence give higher shear strengths at very high stresses. Smaller particles also tended to have more rounded edges and

this was especially noticeable during sieve analysis of some of the larger material used in 4" diameter samples. Sieving for a prolonged period rounded off the jagged edges of the material retained on the $\frac{1}{2}$" B.S. sieve. This "rounding off" must have occurred with all the materials as the finer material was processed so many more times with initial bulk sieving.

The major part of the material used in 4" diameter samples had been used before in tests on 12" diameter samples. It had, therefore, been subjected to a considerable degree of processing.

In general all the rates of dilatancy at failure, for any given angle of internal friction, fell on one of three lines depending on the ratio of particle size to sample diameter (Fig.8:3B). The 4" diameter samples of grading K which were tested at low pressures, tended to give rather high dilatancy rates for a given value of ϕ'. This would suggest that the particles were somewhat more rounded.

The results of tests on grading L were contrary to those of all the other samples tested. The angles of internal friction obtained from tests on grading K were higher at high pressures than those on the finer grading L. At low stresses the angles of internal friction were similar and varied by about 1° at a minor principal effective stress of 100 p.s.i.

The relationship between the rate of dilatancy at failure and the angle of internal friction was the same for 4" and 12" diameter samples with $D/_d = 6$.

On a plot of ϕ_f against σ_3' at failure (Fig.8:3A), these tests gave parallel lines with the finer material in 4" diameter samples having a ϕ' value about 5.5° below the coarser material in the 12" diameter samples.

(8:3:4) Shear strength of $1\frac{1}{2}$" diameter samples (drained shear tests)

(See Table 8C and Figs. 8:3:4a and b)

The $1\frac{1}{2}$" diameter samples showed a greater shear strength than the 4" diameter samples but a lower strength than the 12" diameter samples having the same ratio of particle size to sample diameter.

The angles of internal friction, for samples of grading M, varied from 52.8° to 44.6° at minor principal effective stresses of 10 p.s.i. and 80 p.s.i. respectively. The finer grading, grading O, showed higher stresses In this case the angle of internal friction varied from 53° to 39.3° at minor principal effective stresses of 10 p.s.i. and 450 p.s.i. The angle of internal friction at the higher stress is only $\frac{1}{2}^{\circ}$ below that of grading J at similar relative density (Fig.8:3A). At low stresses the difference is about 3°. If it is assumed that piston friction accounts for between zero and 3° of the peak value of ϕ_f' there is little difference

between the results of the tests on $1\frac{1}{2}$" diameter and 12" diameter samples, the greatest variation being about 2° over the entire range of minor principal effective stresses from 10 p.s.i. to 450 p.s.i.

Differences in the angles of internal friction obtained with various gradings of silurian cleaved mudstone are discussed in Section 7:3:6.

It appears that a maximum particle size of $\frac{1}{4}$ the sample diameter is too great for the gradings of granitic gneiss and silurian cleaved mudstone tested. For representative behaviour of the soil sample a ratio as low as 1/16 is required. Nearly all the tests were performed using a ratio of $\frac{1}{4}$ or $\frac{1}{8}$.

Gradings which had $D/_d$ ratios of 16 in $1\frac{1}{2}$" diameter samples and 16 or greater in 4" diameter samples gave very similar angles of internal friction when allowance was made for the various relative densities, and there seemed to be a unique line on the plot of ϕ_f' against $(d\epsilon_v/d\epsilon_1)$ for $D/_d$ ratios above 16 (Fig.8:3?)

It would appear that the plot of the angle of internal friction against the rate of volume change at failure describes the fundamental behaviour of various materials and different gradings of the same material. At a given density the dilatancy decreases with increase of pressure. At a given pressure the dilatancy increases with increase in density. The two effects combine to give a unique plot for geometrically similar gradings with the same $D/_d$ ratio in various sizes of sample.

In Fig.7:3C the rate of dilatancy at failure is plotted against the minor principal effective stress. It will be seen that at low pressures dense sand demonstrates a high dilatancy until the behaviour approximates to that of loose sand at very high stresses. The Möhr envelope also tend to converge at high stresses, which suggests that the curvature for dense materials is due to the dilatancy. The dilatancy is governed by the particle strength in comparison with the applied stresses. At very high stresses particle breakdown occurs thus reducing dilatancy and giving initially dense material a behaviour similar to that of loose material.

It will be seen that the silurian cleaved mudstone behaves very much as a loose sand in all sizes of samples and all gradings. This is not surprising considering the large breakdown of particles during shear.

The samples of granitic gneiss with the greater D/d ratio plot towards the dense sand limit. The lower $D/_d$ ratios plot further towards the loose sand. This is consistant with the above because the contact forces are greater in the material with the greater maximum particle size and more breakdown occurs.

The shear strength of the various sizes of samples is further discussed in Section 7:3:6

The angle of internal friction is less dependant on the initial sample density at high pressures than at low pressures.

The Möhr failure circles for the gradings tested are given in Figs.8:3C, 8:3D and 8:3E.

The slope of the Möhr envelope for tests on gradingsof H and J in 12" diameter samples varied from about 60°, at low stresses, to 35° at a normal effective stress of 850 p.s.i.

The Möhr failure envelope for the $1\frac{1}{2}$" diameter samples was very similar at high stresses, to that for the 12" diameter samples.

The Möhr failure envelope for the 4" diameter samples was, in general, the equivalent of 3° of 4° below that for the 12" diameter samples.

(8:3:5) Shear strength of samples sheared under undrained condition

Two 12" diameter samples of grading J were consolidated isotropically and then sheared under undrained conditions.

Sample 16V/12 was compacted to a dense state, R_d = 85.0%. There was only a very small build up of pore water pressure and a large deviator stress was quickly built up. The stress path showed no tendancy to turn back on itself (Fig.8:3:5a), and a high angle of internal friction was mobilised at high effective stresses, thus giving a considerable shear strength. The value of ϕ'_f obtained (46°) was somewhat higher than the ϕ'_f corresponding to zero rate of dilatancy for drained samples (41°). In the undrained tests an average condition of no volume change was maintained. The end sections of the samples may have consolidated and the central portions dilated and thus a higher value of ϕ' was mobilised.

Sample 17V/12 was tested at the same minor principal total stress but at a relative density of only 30%. In this case a large pore pressure built up as the sample consolidated and although a high angle of internal friction was mobilised, the effective stresses and hence the shear strength were only about one quarter those of the dense sample.

Two further tests, on 4" diameter samples and using gradings with the same D/d ratio, were carried out by Dr.B.Bros. Both samples were medium dense. The first sample was consolidated to 75 p.s.i. A small pore water pressure built up and the sample showed an angle of internal friction of 41.8° which gave a high shear strength because of the high effective stresses. This value of ϕ'_f was about 5° below that of the denser large sample and coincided with the value of ϕ'_f rate of dilatancy for samples subjected to drained tests.

The second sample was consolidated to 25 p.s.i. and again a high angle of internal friction was recorded, along with high effective stresses (Fig.8:3:5b). The angle of internal friction was somewhat higher

than that corresponding to zero rate of dilatancy for samples subjected to drained tests.

It would appear, therefore, that saturated granular material, subjected to seismic shock, should be well compacted and the specified relative density may be based on the undrained behaviour.

(8:4) Deformation

Some factors affecting deformation are set out in Section 7:4.

(8:4:1) Deformation of 12" diameter samples (drained shear tests)

The axial strain at failure of 12" diameter dense samples of grading H varied from about 3% to 13% with minor principal effective stresses of 10 p.s.i and 150 p.s.i. respectively. (Fig.8:3:1a) Sample 12V/12, which was very loose, had a somewhat greater axial failure strain.

At low confining pressures there was a great tendancy for dense samples to dilate almost immediately that a deviator stress was applied. Sample 11V/12 was sheared at a confining pressure of 150 p.s.i. and showed little tendancy to dilate.

The axial strains at failure of 12" diameter dense samples, of grading J, varied from 3% to 16% with minor principal effective stresses of 10 p.s.i. and 450 p.s.i. respectively (Fig.8:3:1b).

Samples subjected to low stresses dilated strongly whereas those which were sheared at confining stresses above 300 p.s.i. consolidated throughout test.

The axial failure strains are very comparable with those of dense sand tested at similar confining pressures. The volume strains of the granitic gneiss however, are somewhat greater. This is not surprising though because of the fewer interparticle contacts and the vastly greater interparticle forces in the rockfill. It may be noted that the values of ϕ'_f for the rockfill are substantially higher too.

For similar initial densities the axial and volumetric strains were slightly smaller with the finer grading.

About half of the samples failed by bulging. In some cases bulging occurred in the top half or two thirds only and was a sign of a non homogeneous sample. Those samples tested at high pressures subsequently failed along a shear plane. This may be the reason for the premature peaks recorded with samples 7V/12 and 9V/12.

Sample 12V/12, which was very loose, also failed by shearing along a plane.

(8:4:2) Deformation of 12" diameter samples subjected to anisotropic consolidation

Sample 13V/12 was compacted to a dense state, using grading H, and then consolidated anisotropically. A linear relationship was obtained between axial strain and deviator stress. Samples 18V/12 and 19V/12, with the finer grading J, also showed a linear relationship between axial strain and deviator stress though the axial strain required for a given deviator stress was somewhat less (Fig.8:3:2).

At the end of the K_o stages in samples 18V/12 and 19V/12 failure was induced by increasing the pore water pressure. There was an immediate reduction in volume strain and a great dilation in each case. Eventually, the failure in each case was by very slight bulging.

The linear relation between ϵ_1 and deviator stress may be compared with that for the silurian cleaved mudstone where a definite stiffening of the sample occurred with increase in stress.

It may be that the fines in the granitic gneiss samples play little part in the strength or deformation at low strains because there are so few of them that they do not fill the voids. As a result there is only compression of the contacts between the large particles and the deformation of the particles themselves.

(8:4:3) Deformation of 4" diameter samples (drained shear tests)

All the gradings of granitic gneiss were so permeable that fully drained conditions existed at an axial strain rate of 8% per hour, even with grading Q. All the samples were therefore tested at this rate of strain.

The axial strains at failure incresed with increase in minor principal effective stress. At a confining pressure of 10 p.s.i. the axial failure strains of samples compacted to about 90% relative density and and of gradings K,L,N and P varied between 4% and 5%. At a confining pressure of 80 p.s.i. the axial strains at failure increased and varied between 7% and 8%.

Loose samples had considerably greater failure strains. Some dense samples, as IIV/4, also had large axial strains to failure. This was probably due to the sample construction. If the majority of fine material migrated to the base failure occurred almost wholly in the upper portion, which deformed considerably.

This variation in porosity thoughout samples probably accounts for a lot of the scatter in the test results.

With most gradings which are short of fines there will be different porosities operative at different stresses. Comparisons need to be made with the structural porosities rather than the actual porosities.

Initially, the fine material sits in the voids and contributes nothing to the strength of the grading. Only after deformation and breakdown of the skeleton occur do the voids fill up allowing the finer material to play its part in resisting further deformation. At low stresses, therefore, the finer material may not contribute anything to the strength of the grading.

In general the shape of the stress -strain curves was very similar for 4" and 12" diameter samples. The stress-strain curves were not flat topped after the peak deviator stress had been attained and at low confining pressures the peak load dropped off quite rapidly.

All of the 4" diameter samples failed initially by bulging followed by the formation of a shear plane. In general, the shear plane was more of a shear zone about 3" thick inthe 12" diameter samples and proportionally smaller in the smaller samples.

(8:4:4) Deformation of 1½" diameter samples (drained shear tests).

(See Figs.8:3:4a,b and c).

Drained shear tests were carried out on 1½" diameter samples, using gradings M,O,P and Q (Fig.5:6:2).

Again the axial strains at failure were of the same order of magnitude as those in 4" diameter and 12" diameter samples.

Sample 7V/1½, of grading O, was sheared at a minor principal effective stress of 300 p.s.i. The deviator stress fell off rapidly after peak and this was accompanied by a dilation.

Sample 8V/1½ of grading O, was sheared at a minor principle effective stress of 450 p.s.i. The stress-strain curve,like that of the 12"diameter sample, which was sheared at the same stress, was flat topped after the peak. A very slight dilation was shown by the small sample.

The 1½" diameter samples, which were sheared at low pressures,failed by bulging and subsequently along a shear plane except for the two samples of grading Q, which failed by bulging (Fig.8:3:4c).

The two samples, which were sheared at confining pressures above 300 p.s.i. failed by bulging.

(8:4:5) Axial deformation of samples sheared under undrained conditions

(See Figs.8:3:5a and b).

Two undrained shear tests were performed on 12" diameter samples of grading J (Fig.8:3:5a). Grading J was used rather than grading H to minimise the effects of membrane penetration on achieving an undrained condition because of variations in the pore water pressure.

Sample 16V/12 was compacted to a dense state and reached its peak stress ratio at a smaller axial strain than 17V/12, which was loosely

compacted.

A further two tests were carried out on 4" diameter samples of grading L. The first test was consolidated to 75 p.s.i. and the second to 25 p.s.i Both reached their peak stress ratios at about the same axial strain though the effective stresses were twice as high in the first sample. (Fig.8:3:5b)

The axial strain at failure of sample 16V/12 was slightly less than that of the 4" diameter sample at the equivalent pressure. The larger sample though was at a slightly greater relative density.

Considering the differences in the relative densities and consolidation pressures of the 4" and 12" diameter samples the behaviours were very similar.

The stress strain and volume strain curves were remarkably smooth considering the type of material being tested.

This is discussed in Section 9:4:1.

(8:4:6) Volumetric strain and deviator stress

An approximately linear relationship was found between volumetric strain and deviator stress, from the origin and almost to the peak deviator stress, for all the samples of granitic gneiss which were tested.

12" diameter samples of grading H and 4" diameter samples of grading K ($D/_d$ = 4 in each case) followed the same path, until peak deviator stress in each sample size between volumetric strain and deviator stress irrespective of the value of the minor principal effective stress (Fig.8: 3:1a and Fig. 8:3:3a).

The volume strain-deviator stress curves for the K_o tests during anisotropic consolidation were also straight lines (Fig.8:3:2). This is in contrast , to the results obtained with K_o tests on silurian cleaved mudstone (Fig.7:3:4).

The sample membranes probably had a more adverse effect on the volume changes of the granitic gneiss simples because of the smaller proportion of fine material available to fill the voids.

The effect of membrane penetration is to apply too great an axial strain and hence an excessively high major principal effective stress. Because of this too small a value of K_o is recorded in the initial stages of the K_o tests.

(8:4:7) Creep.

A certain amount of creep was noticed with granitic gneiss samples during isotropic consolidation and after completion of the shear stage. In general, the same remarks apply for the granitic gneiss as for the silurian cleaved mudstone (Section 7:4:9).

The initial consolidation was somewhat faster with the granite than with the silurian cleaved mudstone.

(8:4:8) One dimensional compressibility

Three K_o tests were carried out to determine the value of K_o and m_v.

Sample 13V/12 was made up using grad.H. Aslight effect, due to over-consolidation, was noticed during the initial stages of anisotropic s consolidation. This effect is partly due to the sample compaction and partly to excessive membrane penetration (Fig.8:4:8a).

Samples 18V/12 and 19V/12 (Fig 8:4:8b and c) were made up, using grading J. A very nearly linear relation was found between the axial strain and the major principal effective stress for each sample. The axial strain for a given stress was approximately the same for both samples, which had very similar densities, and was about 60% that of sample 13V/12 with the coarser grading and slightly lower density.

The value of K_o varied from just under 0.2 at the beginning of loading to just over 0.3 at major principal effective stresses above about 200p.s.i. It was thought that this low initial value was due to errors in maintaining a condition of zero lateral yield because of the volume changes due to membrane penetration. As both the coarse and the fine gradings demonstrate this property though at similar stresses there may well be another effect due to compaction.

The secant values of m_v for samples 18V/12 and 19V/12, were similar and fairly constant over the limited range of stresses at which they were tested.

Sample 13V/12, with a coarser grading, was somewhat more compressible and showed a pronounced effect due to overconsolidation in the initial stages (Fig.8:4:8d).

The samples of granitic gneiss were less compressible than those of the silurian cleaved mudstone with comparable particle sizes and relative densities (Fig.7:4:10h).

The average value of K_o for the mudstone (0.45) was somewhat higher than that for the granite (0.33). The K_o remained sensibly constant at higher stresses and ϕ'_f decreased with increasing stress. The simple relation $K_o = 1 - \sin \phi'$, did not therefore, hold at all stress levels. However, if the value of ϕ' at constant volume (41°) is substituted in the above equation there is a close agreement with the measured value of K_o.

(8:4:9) Particle breakdown

The general comments on the particle breakdown of the silurian cleaved mudstone set out in Section 7:4:11 also apply to the granitic gneiss.

The extent of the breakdown of the granitic gneiss particles during bulk sieve analysis was not as great as that for the mudstone. There was a noticeable rounding of the edges of granitic gneiss particles which were subjected to prolonged sieving on 12" diameter sieves.

The breakdown of particles under a particular stress system on first wetting and which was demonstrated by the volume change on saturation at constant stress was not as great with the granite as with the silurian cleaved mudstone.

On wetting the surface of the material the strength is reduced. The contact points collapse so that a greater area, commensurate with the new strength, transmits the load. On subsequent drying there is a return to the original strength but no expansion at the contact because the collapse was due to fracture rather than elasticity. Therefore, as long as the packing and particle contacts remain unchanged there is no further deformation on subsequent wetting. However, if the material is dried and the packing of the particles reconstituted there will again be further deformation on wetting.

There was no tendancy for the fine material to adhere to larger particles or to ball when sieved in the dry state.

Absolute comparison of particle breakdown in the various gradings and sample sizes and under various stress conditions were particularly difficult. In general, though, the breakdown increased according to the factors listed at the end of Section 7:4:11.

The particle breakdown at high stresses was very considerable and can be judged from the photographs in Plate 6:1:1B.

The increase in breakdown with stress for 12" diameter samples of grading H is shown in Table 8:4:9a. The increase in the percentage of material passing each sieve is given for samples 3V/12 and 11V/12.

B.S.Sieve	Initial grading % passing.	Increase in weight of material passing each sieve (%)	
		Confining pressure 10 p.s.i.	Confining pressure 150 p.s.i.
3"	100	0	•
1½"	53.6	9.6	17.6
¾"	27.1	7.7	16.5
⅜"	14.1	5.2	13.2
3/16"	8.4	4.0	10.4
No.7	6.1	2.8	7.5
No.14	4.8	2.1	5.7
No.25	3.4	1.7	4.1
No.52	2.2	1.2	2.8
No.100	1.4	0.8	1.5
		Σ = 35.1 mean = 3.5	79.3 7.9

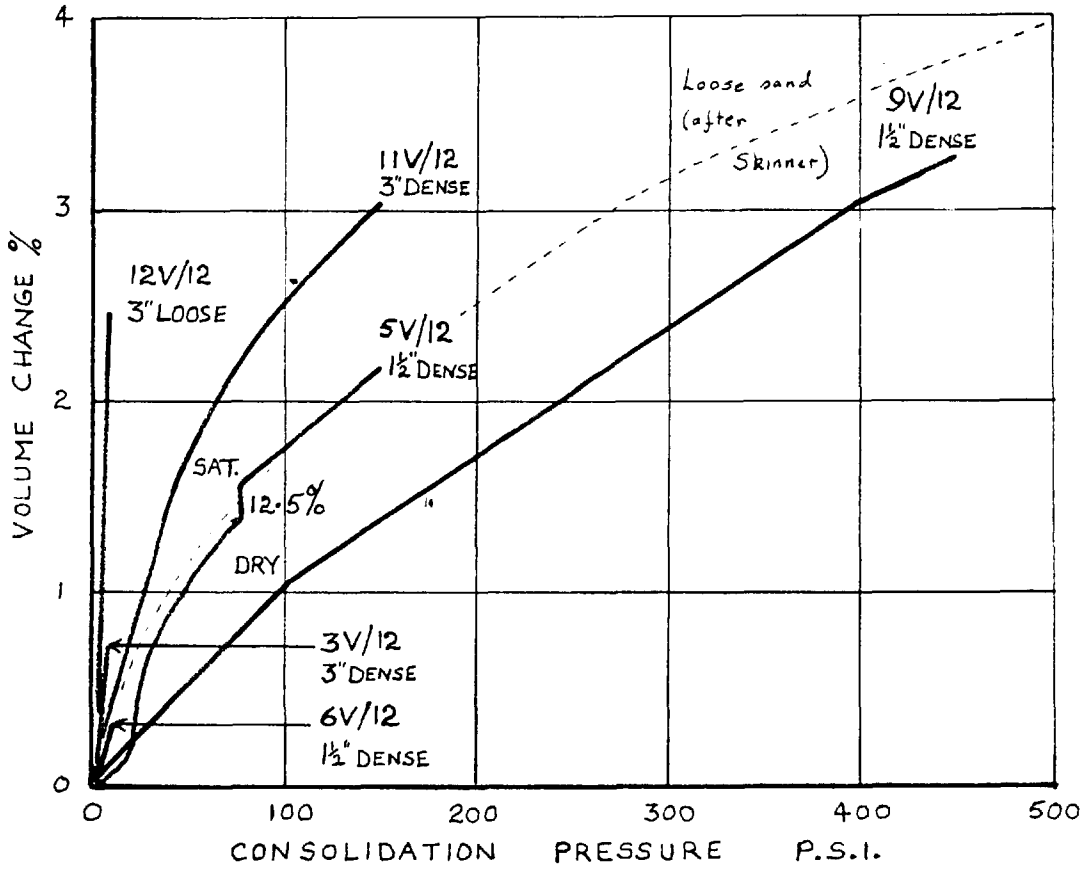
Table 8:4:9a.

The increase in breakdown with stress for the 12" diameter samples of grading J is shown in Table 8:4:9b.

B.S.Sieve	Initial grading % passing	Increase in weight of material passing each sieve (%)		
		= 10 p.s.i.	= 150 p.s.i.	= 450 p.s.i
1½"	100	•	0	•
¾"	53.6	5.8	13.8	21.0
⅜"	27.1	5.1	14.7	23.2
3/16"	14.1	4.2	12.7	20.9
No.7	8.4	3.2	10.3	18.7
No.14	6.1	2.3	7.8	14.5
No.25	4.8	1.5	5.4	10.5
No.52	3.4	1.1	3.7	7.2
No.100	2.2	0.7	2.4	4.9
		Σ = 23.9 mean = 2.7	70.8 7.9	120.9 13.4

Table 8:4:9b.

The sample permeabilities recorded in Tables 8A, 8B and 8C serve only as a general guide and the higher values probably reflect the permeability of the apparatus.

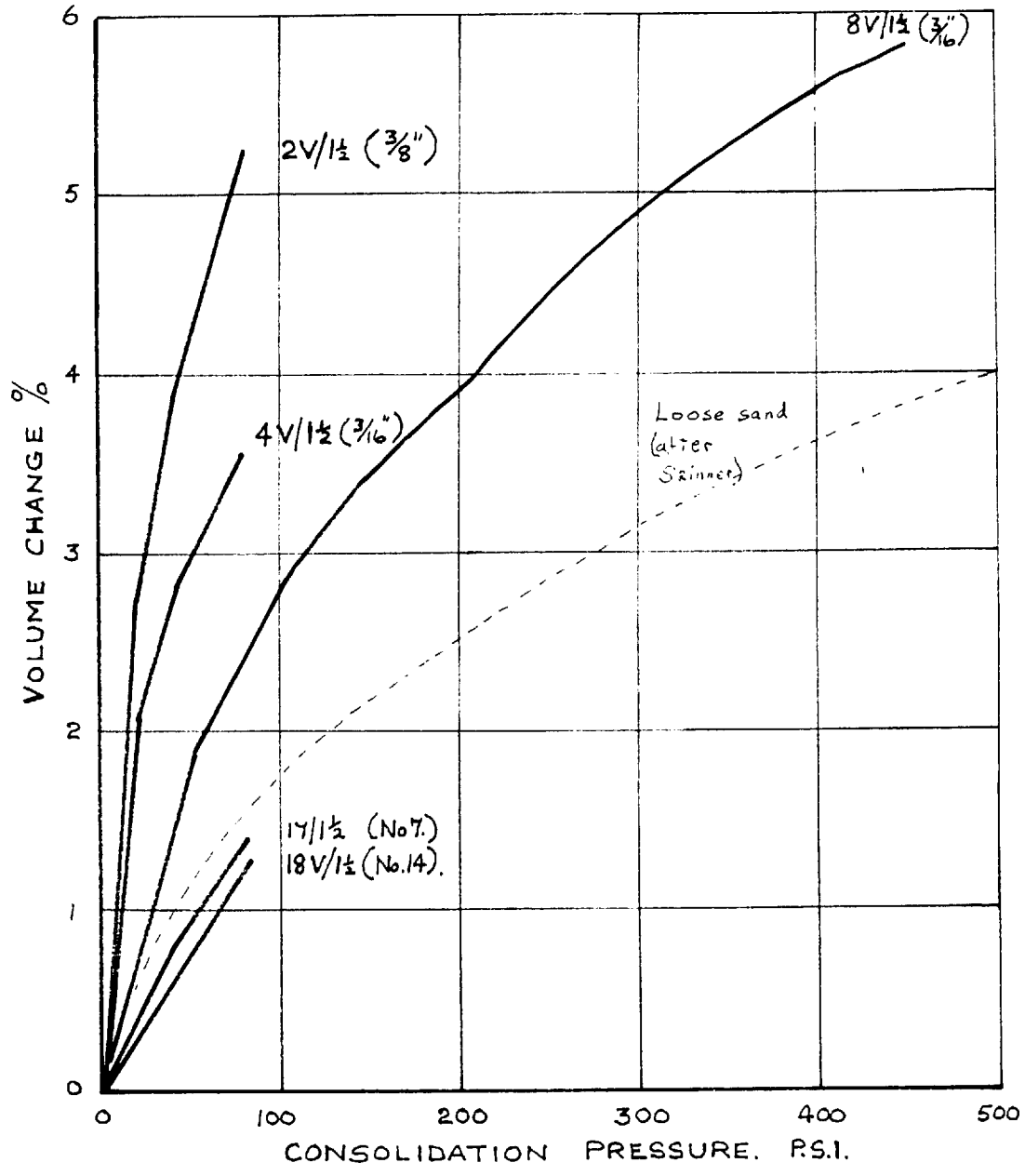


VOLUME CHANGES DURING ISOTROPIC CONSOLIDATION

GRANITIC GNEISS 12" DIA. SAMPLES.

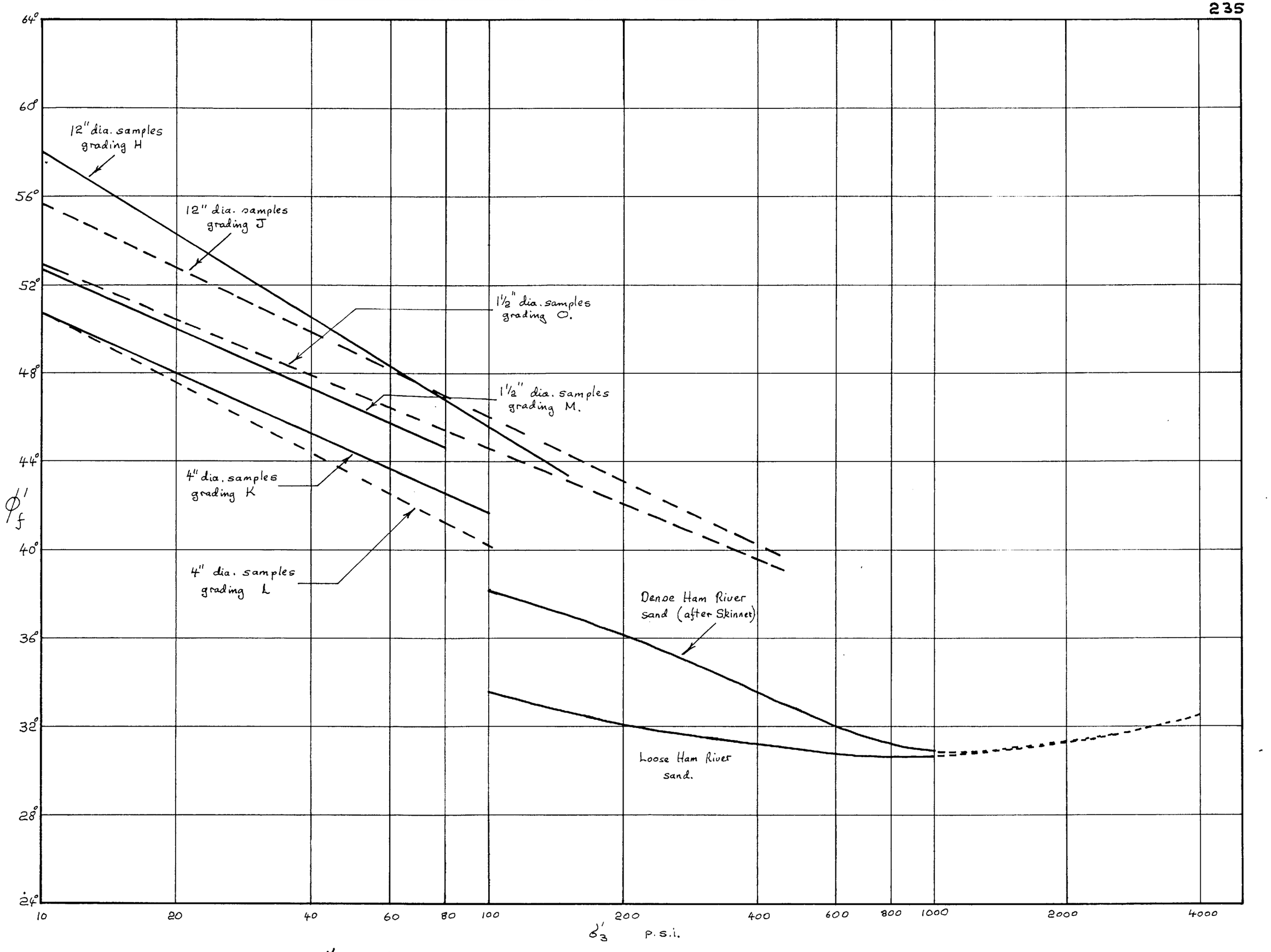
SATURATED.

FIG. 8:2:1



VOLUME CHANGES DURING ISOTROPIC CONSOLIDATION
GRANITIC GNEISS 1½" DIA. SAMPLES.
(SATURATED).

FIG. 8:2:2



THE RELATION BETWEEN ϕ'_f AND σ'_3 FOR GRANITIC GNEISS SAMPLES AT INITIAL R_d = 90%

FIG. 8:3A

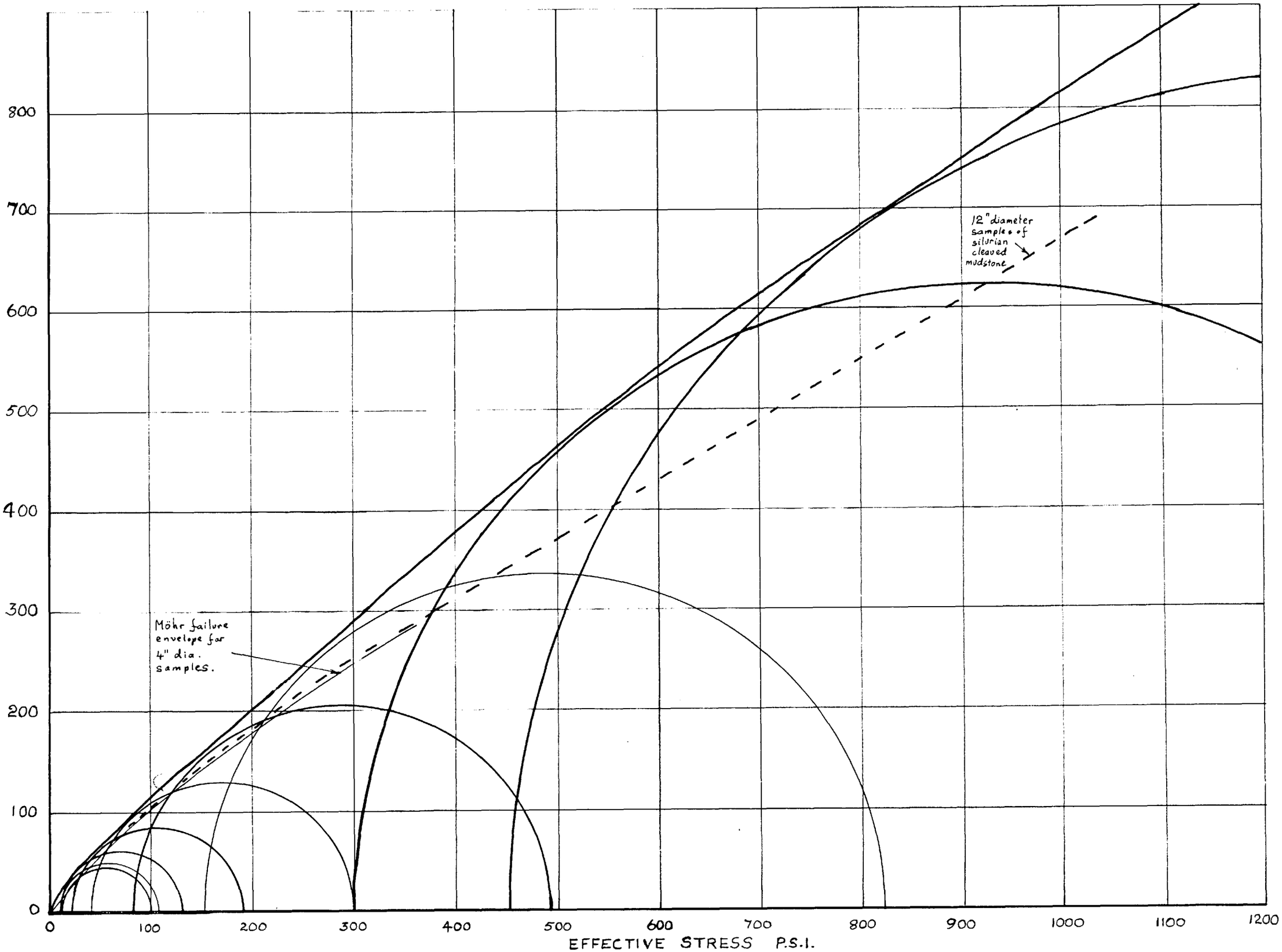
□ (max value 12v/12)

□ (1st peak 12v/12)

THE RELATION BETWEEN ϕ'_f AND $(d\epsilon_v/d\epsilon_1)_f$ FOR GRANITIC GNEISS.

Symbol.	Sample dia.	Grading.	D/d.
⊡	12"	H	4
△	12"	J	8
⊙	4"	K	4
+	4"	L	8
■	4"	N	16
▲	4"	P	÷40
X	1½"	M	4
▽	1½"	O	8
⋈	1½"	P	16
⊕	1½"	Q	32

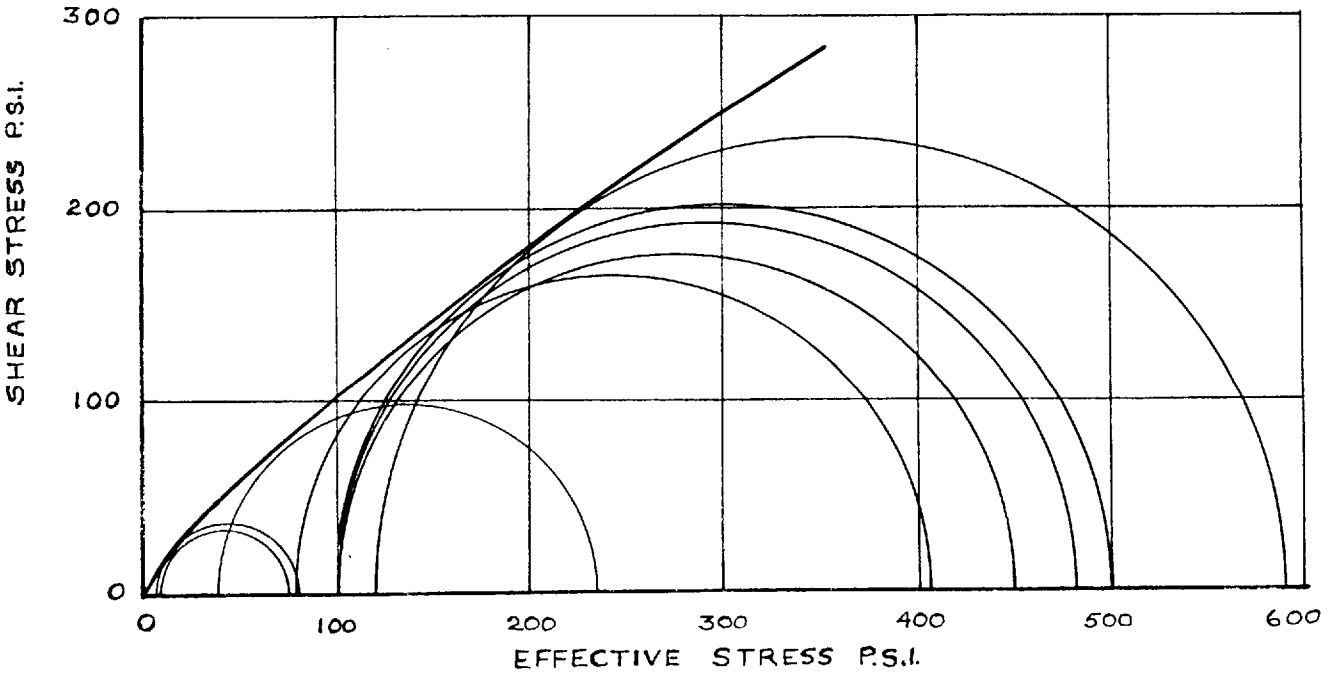
FIG. 8:38



MÖHR FAILURE CIRCLES

GRANITIC GNEISS 12" DIA. SAMPLES.

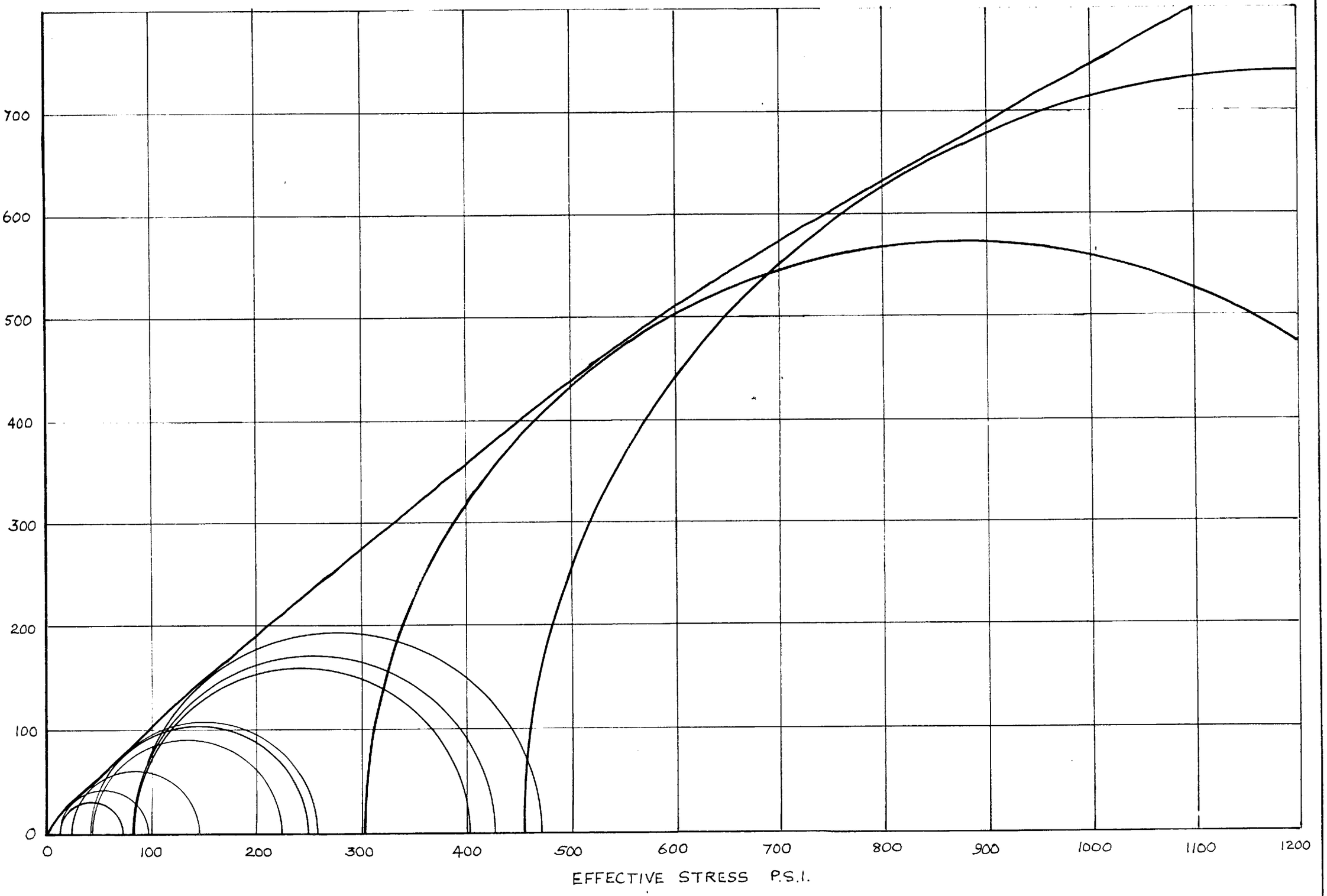
FIG. 8:3C



MÖHR FAILURE CIRCLES

GRANITIC GNEISS 4" DIA. SAMPLES.

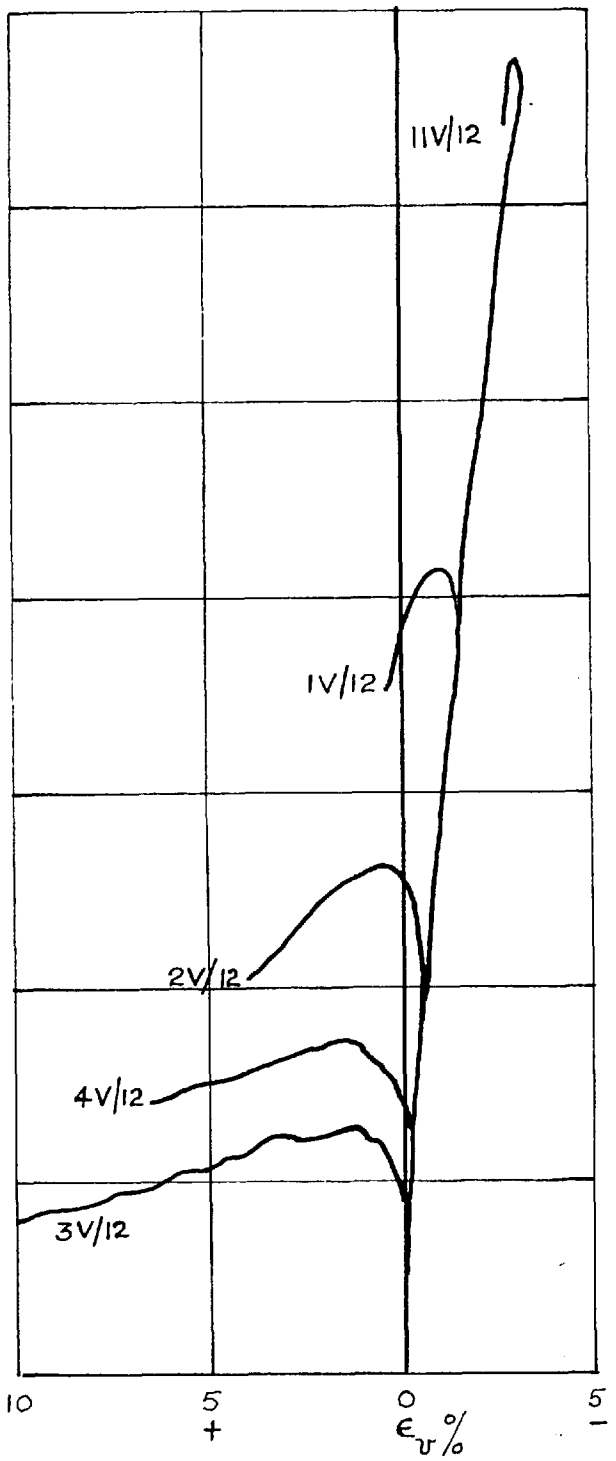
FIG. 8:3D

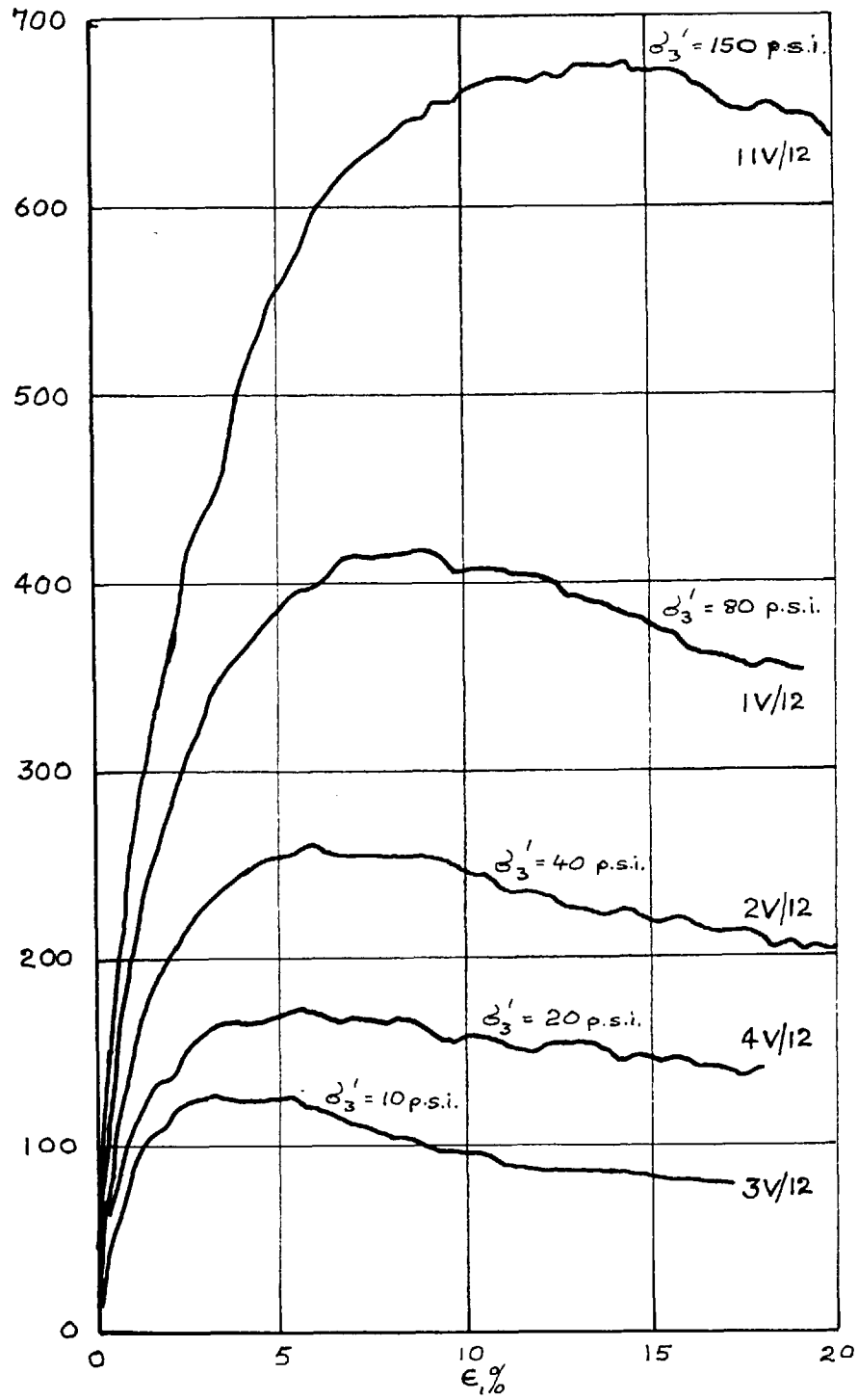


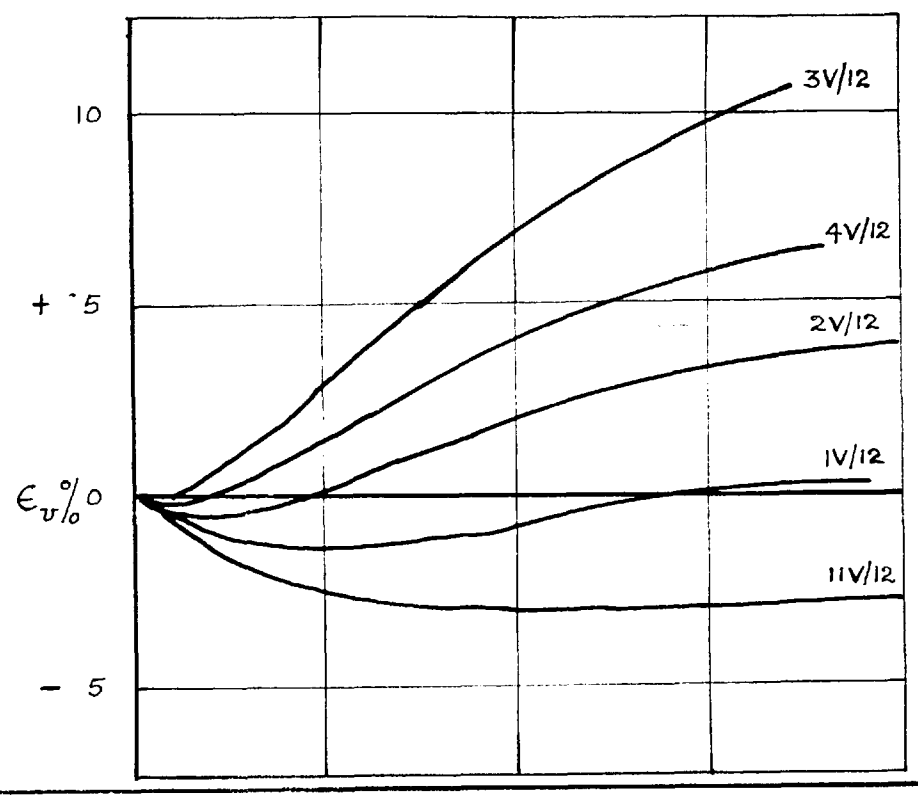
MÖHR FAILURE CIRCLES

GRANITIC GNEISS 1½" DIA. SAMPLES.

FIG. 8:3E





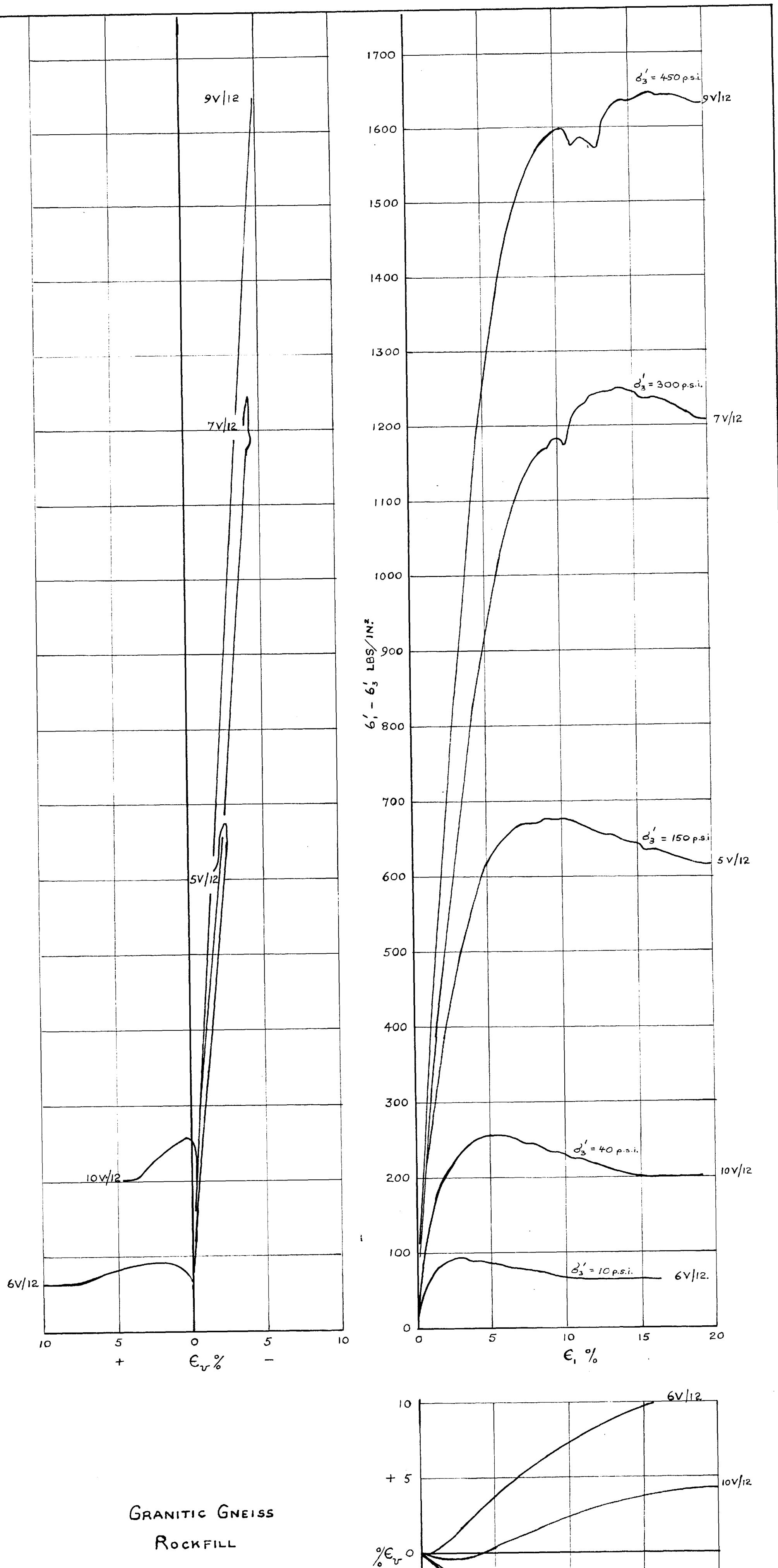


GRANITIC GNEISS

ROCKFILL

GRADING : H

FIG. 8:3:12

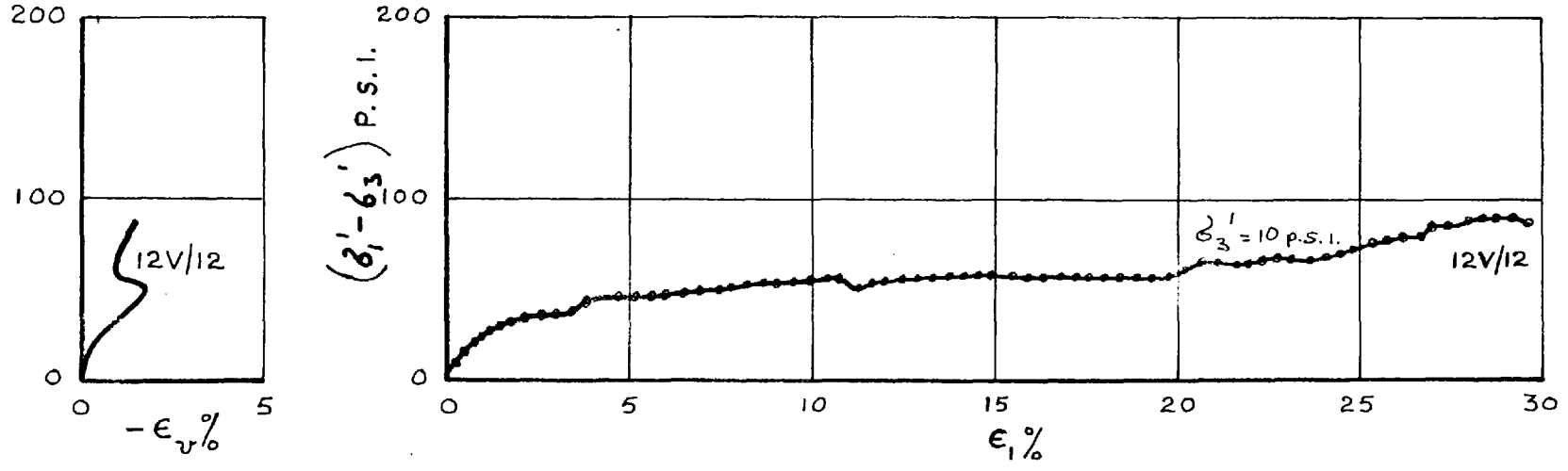


GRANITIC GNEISS

ROCKFILL

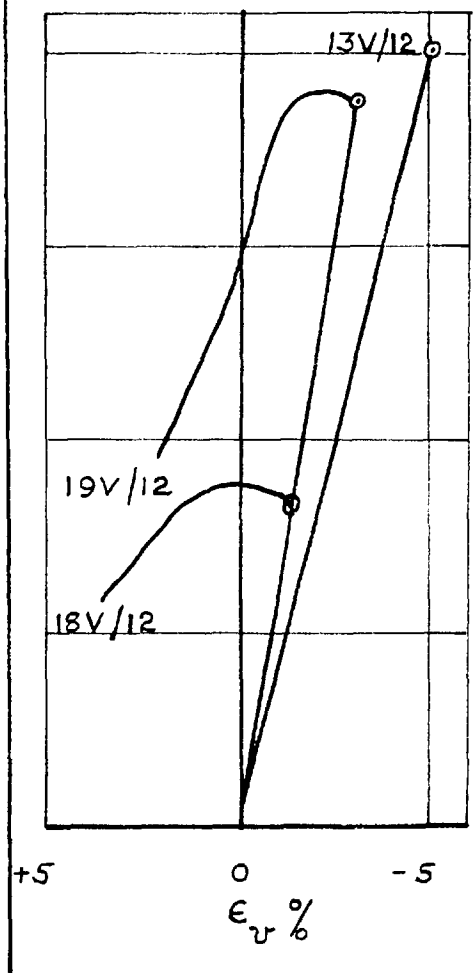
GRADING J

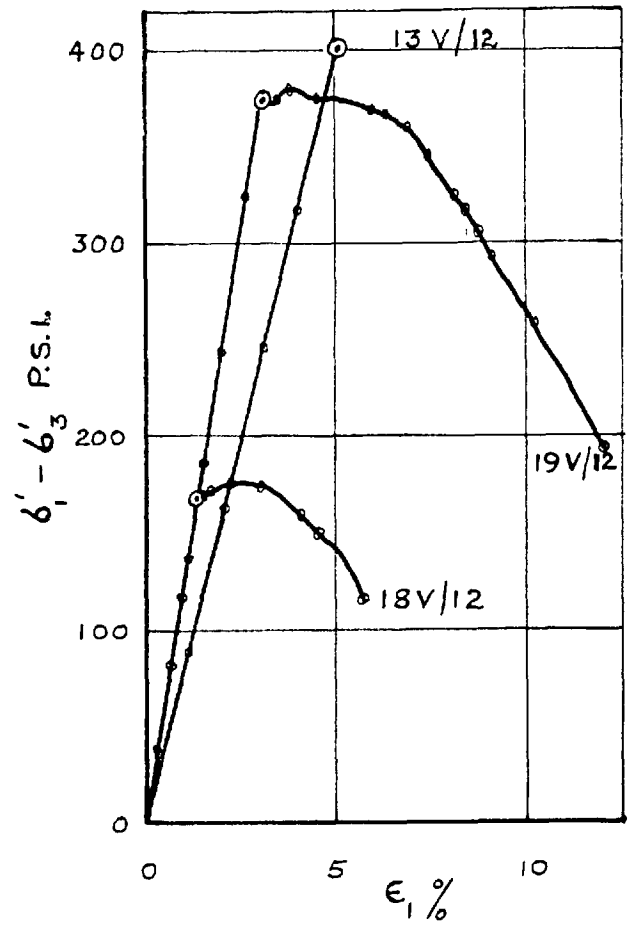
FIG. 8:3:14



GRANITIC GNEISS ROCKFILL. GRADING H.

FIG. 8:3:1c





GRANITIC GNEISS

K_o - TESTS.

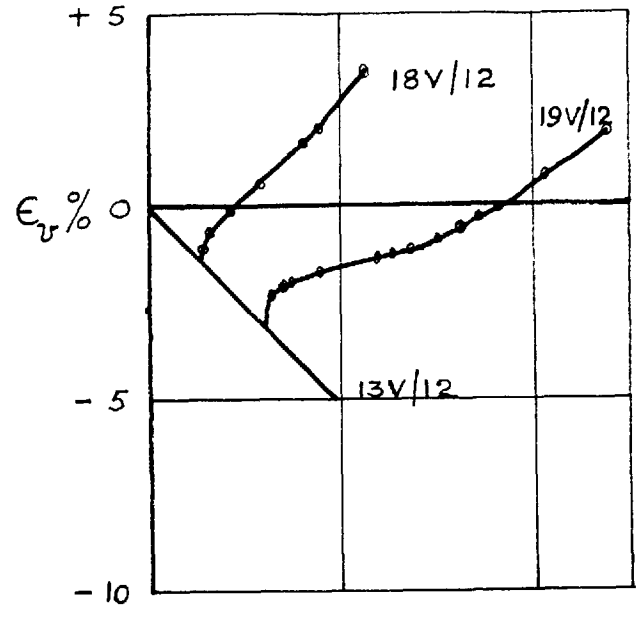
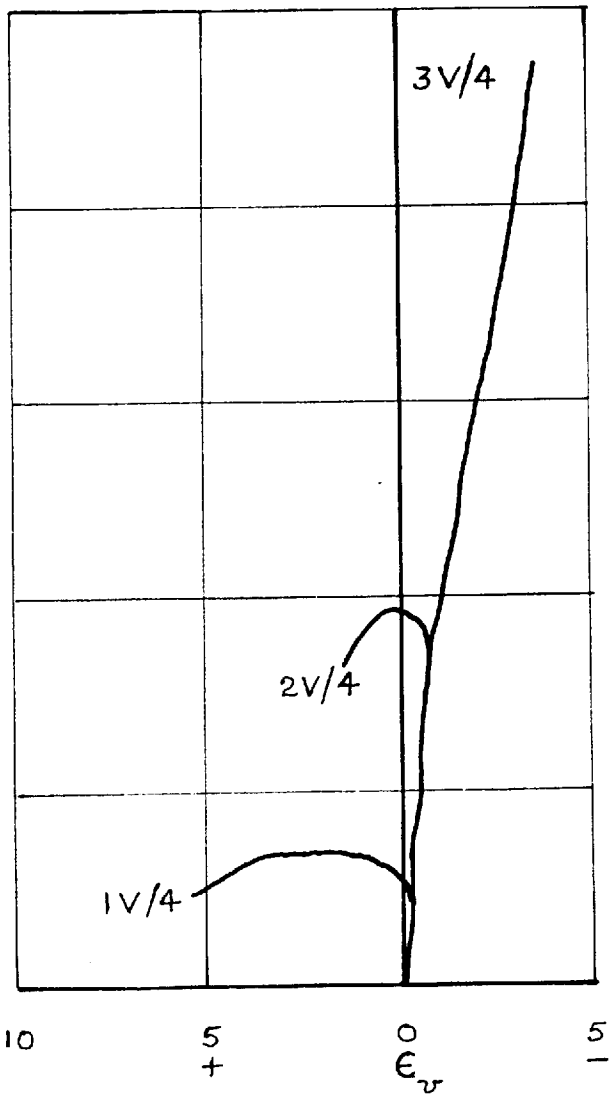
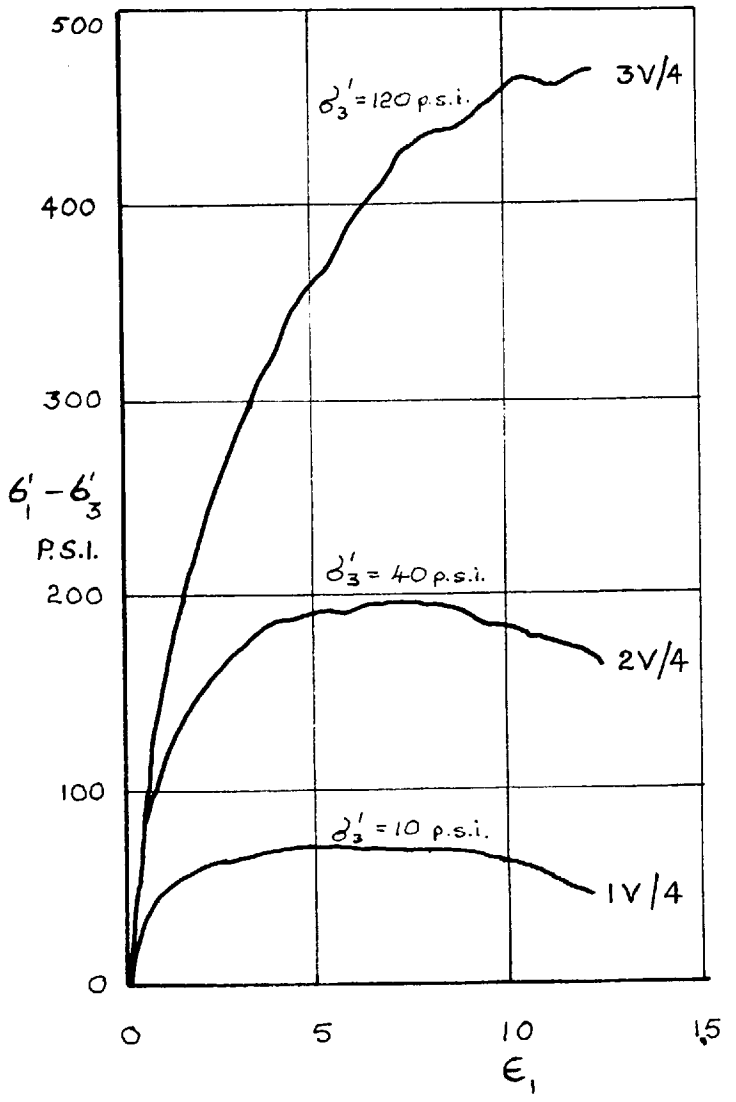


FIG. 8:3:2





GRANITIC GNEISS ROCKFILL
GRADING: K.

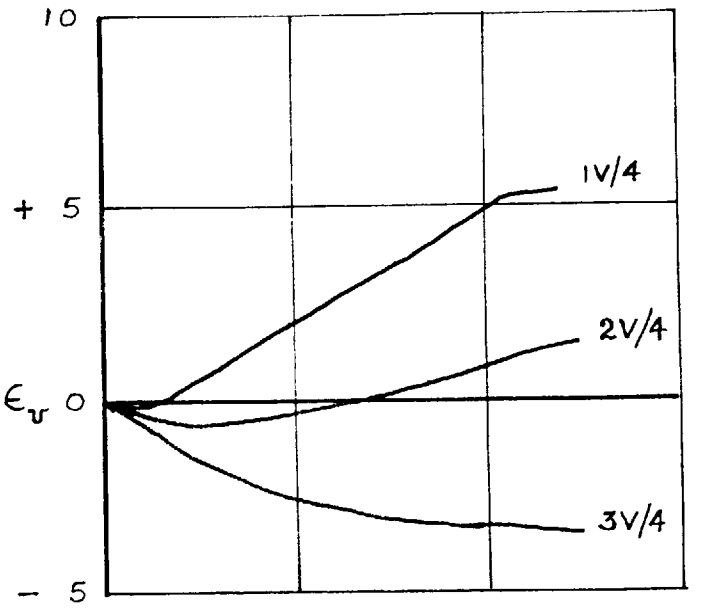
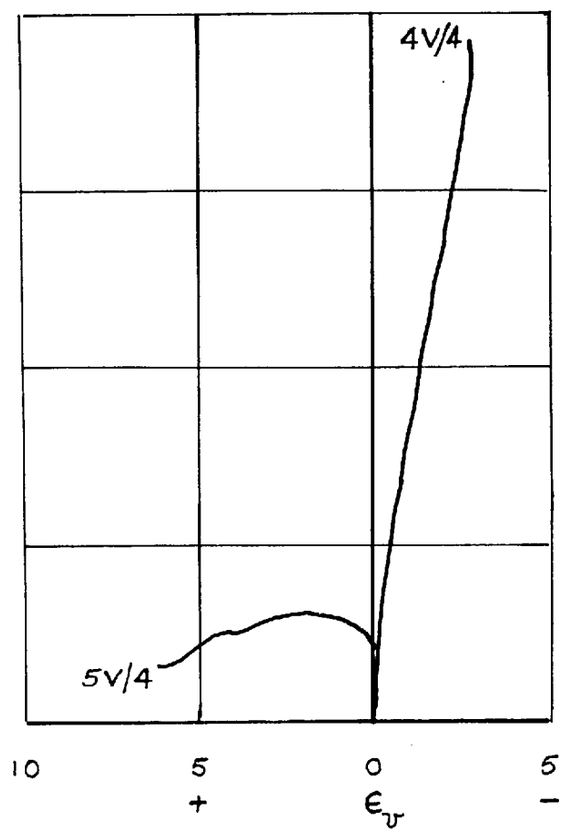
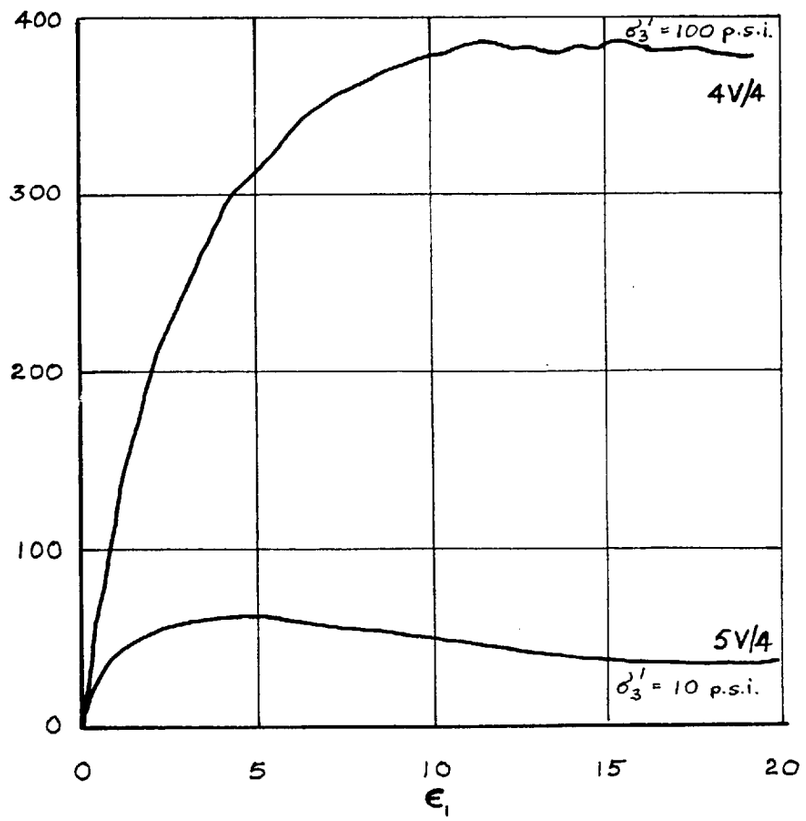
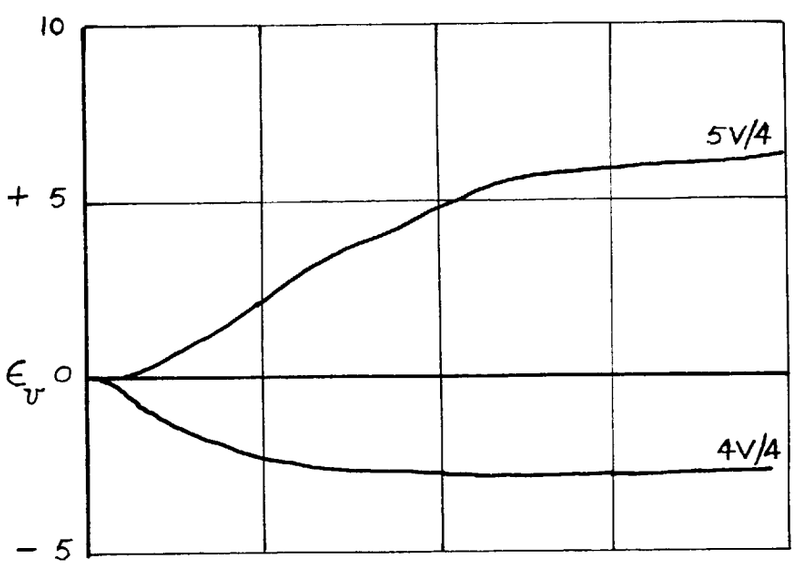


FIG. 8:3:3a.

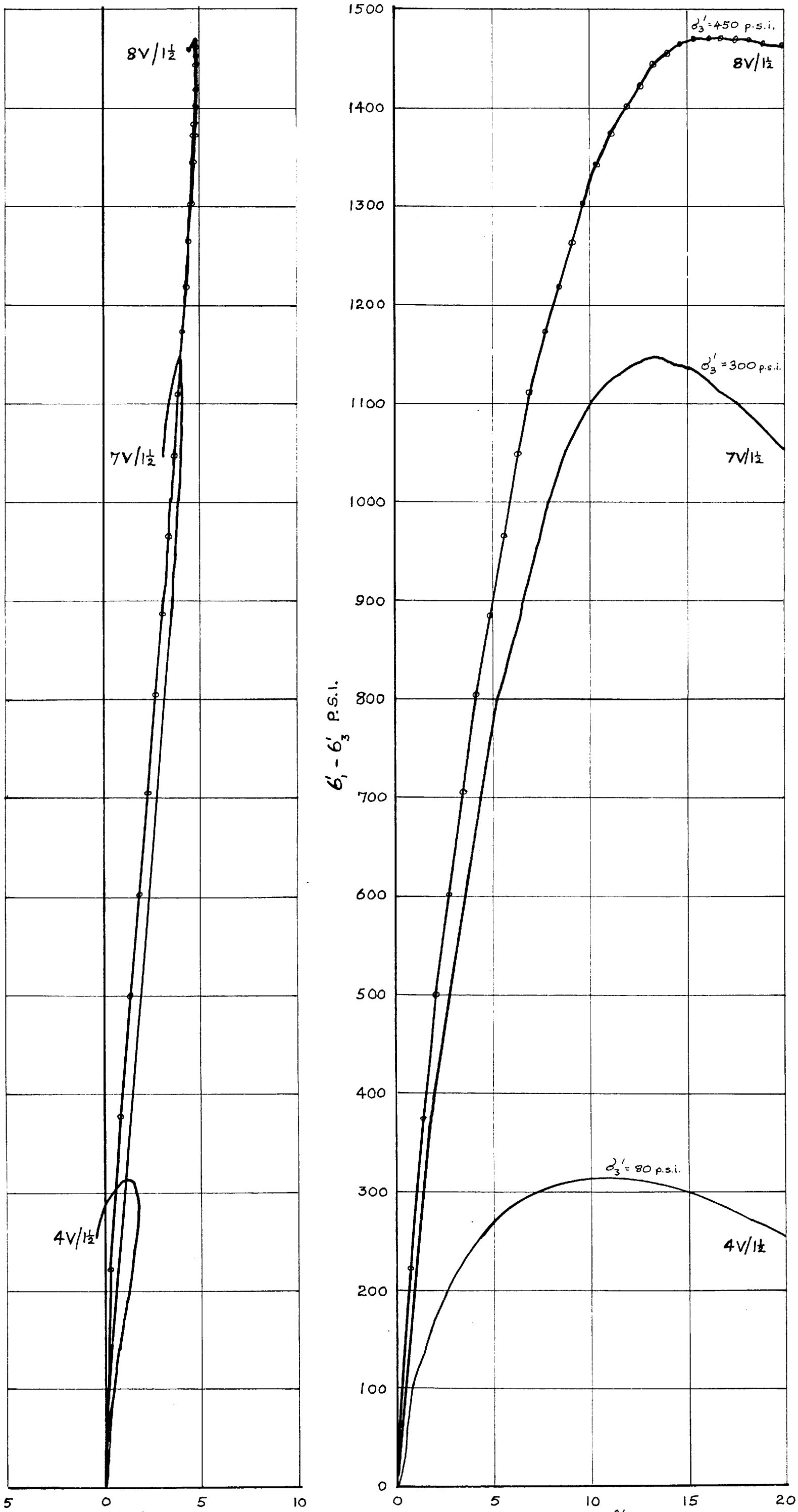






GRANITIC GNEISS ROCKFILL
GRADING: L.

FIG. 8:3:36.



GRANITIC GNEISS ROCKFILL
GRADING: O.

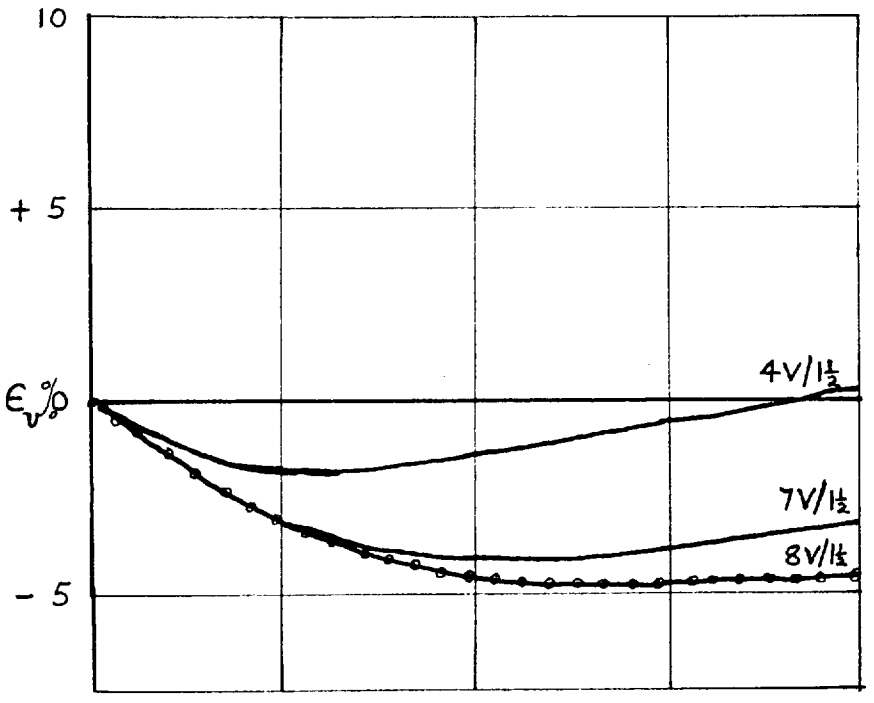
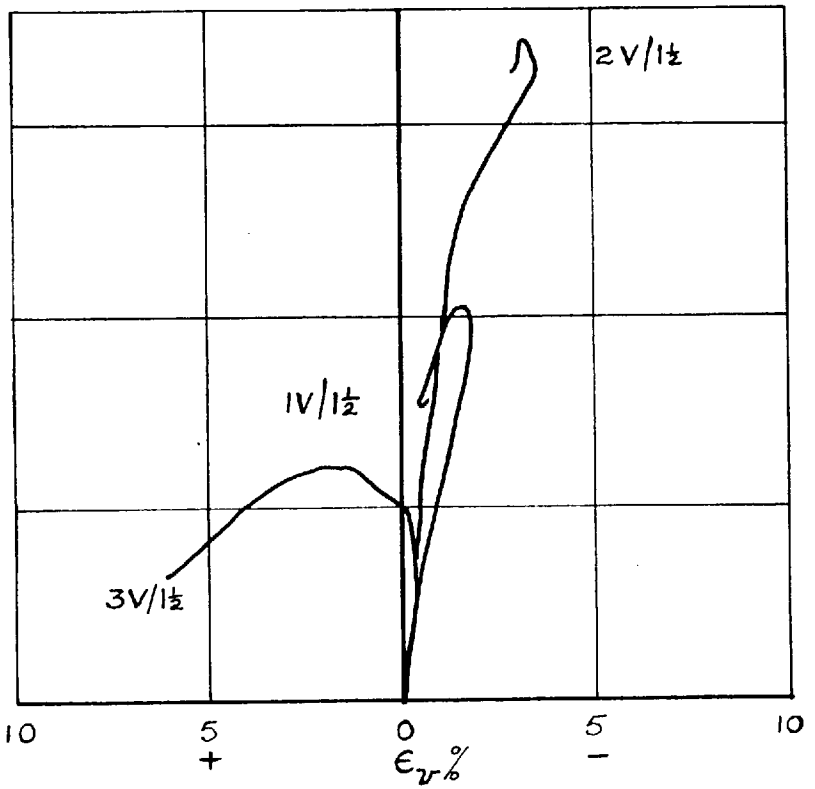
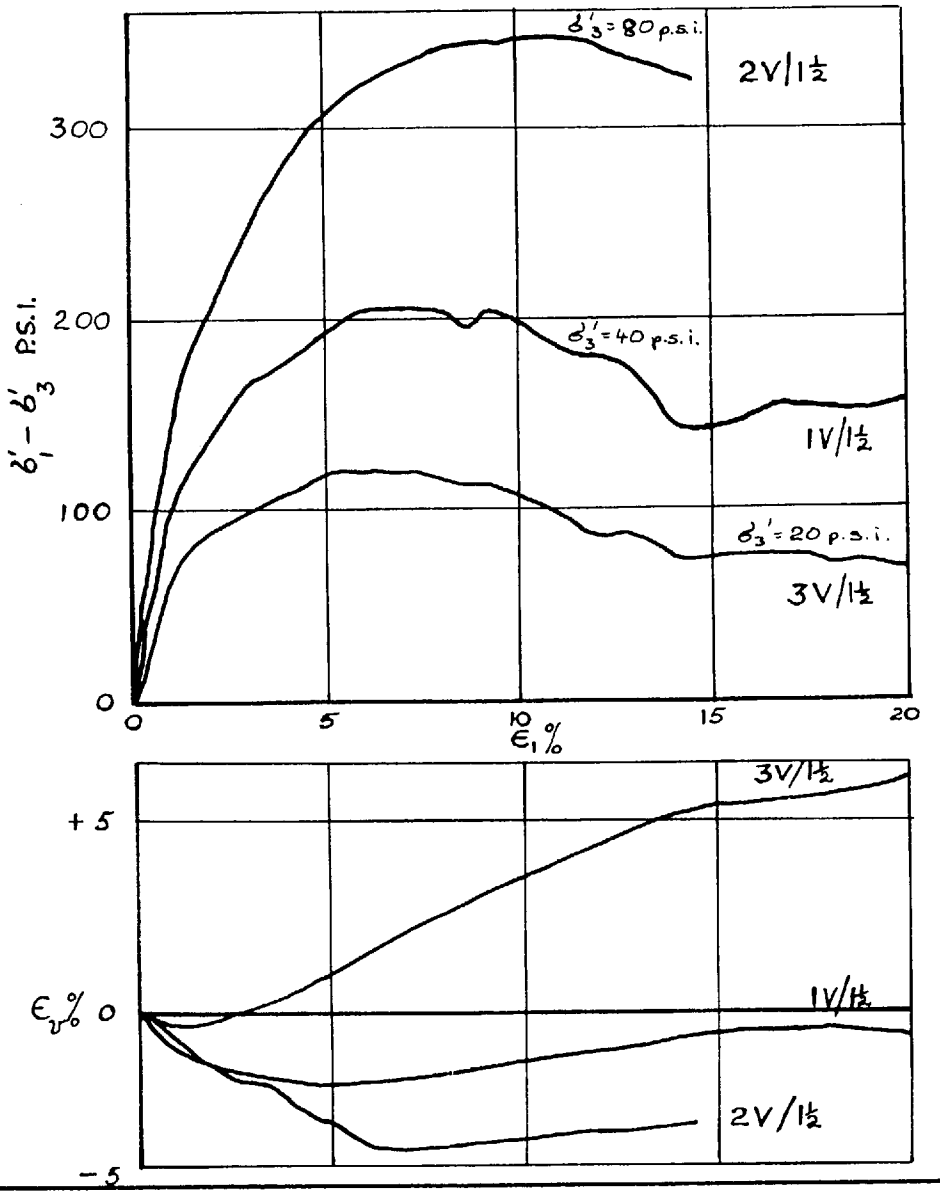


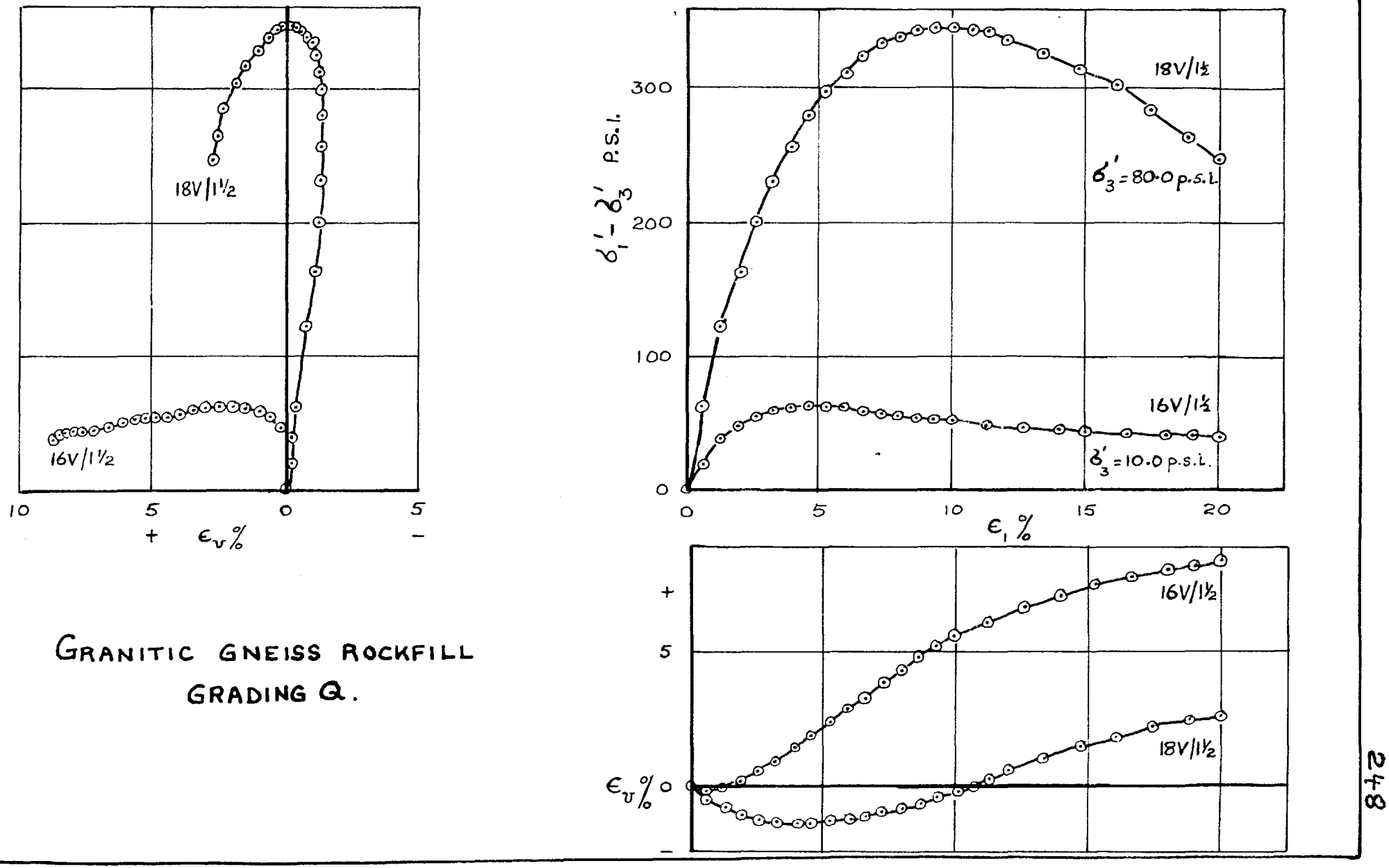
FIG. 8:3:4a.





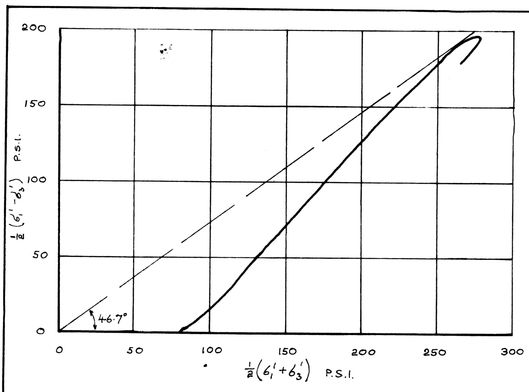
GRANITIC GNEISS ROCKFILL
GRADING M.

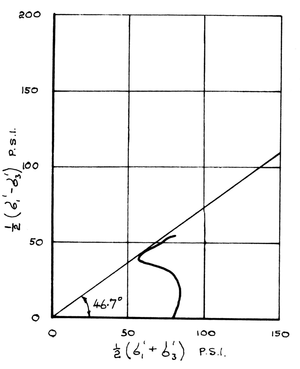
FIG. 8:3:47

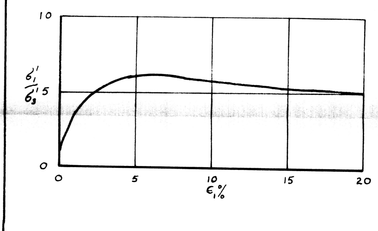


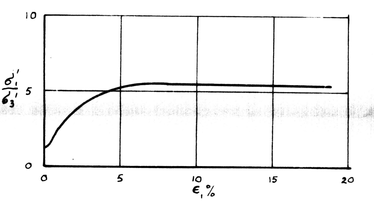
GRANITIC GNEISS ROCKFILL
GRADING Q.

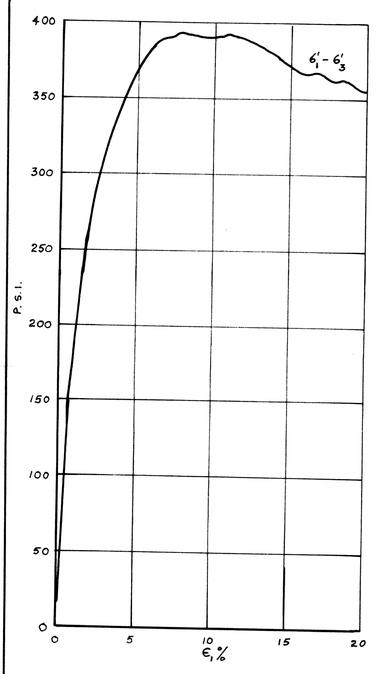
FIG: 8:3:4c

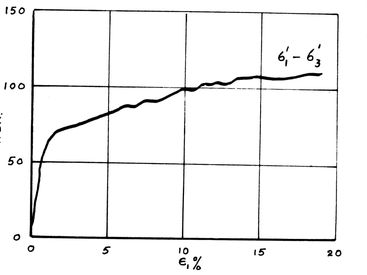


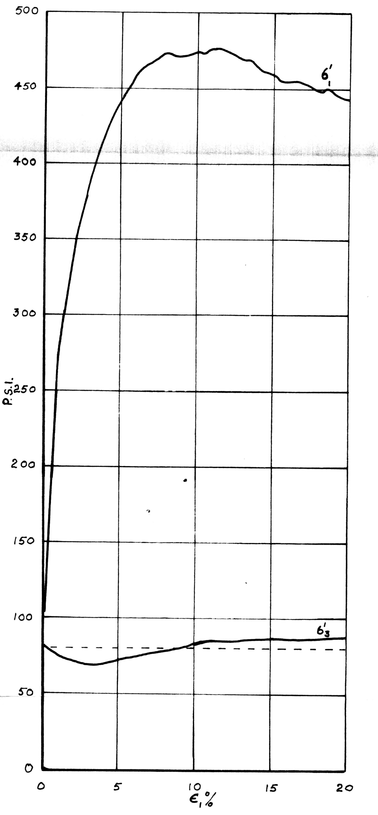


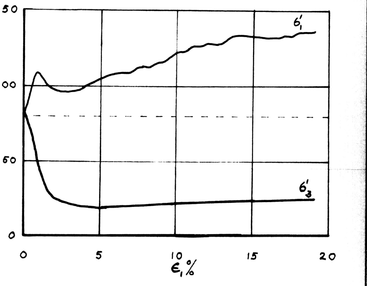


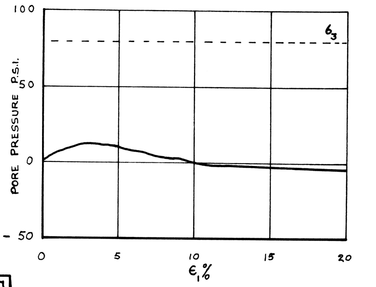


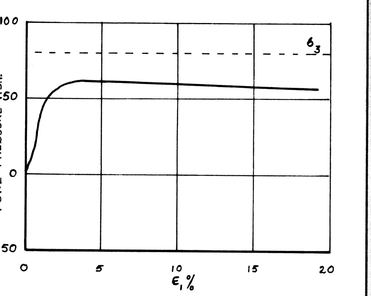










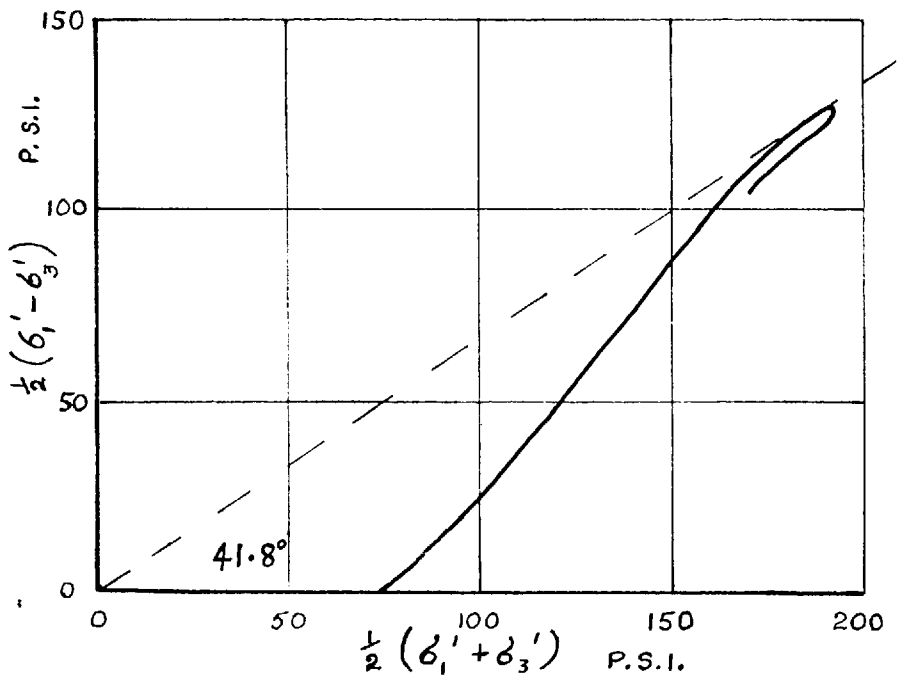


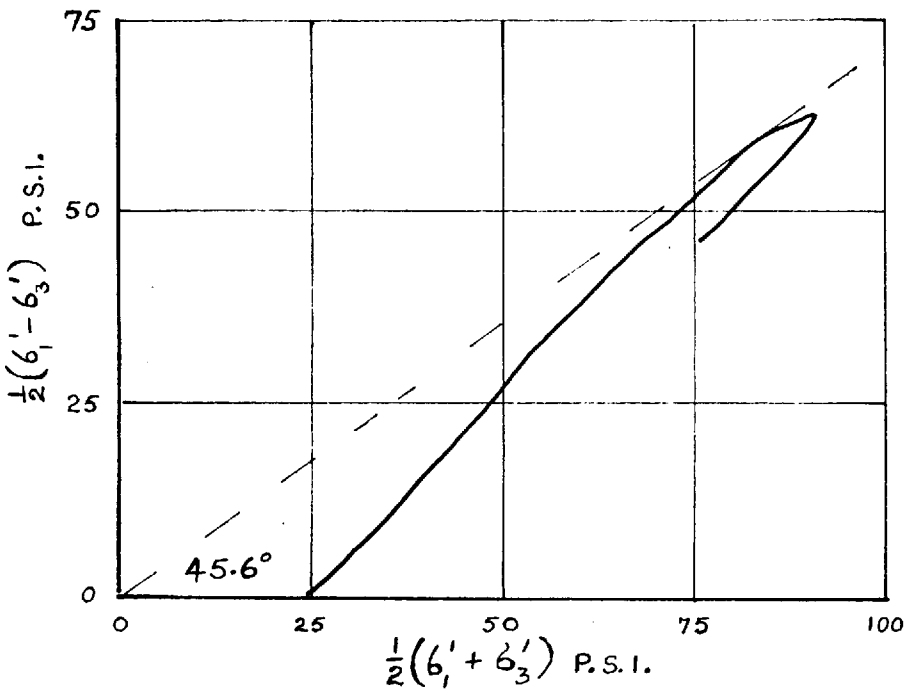
SAMPLE 16V/12 γ_d = 128·5 LBS/FT.^{3}
R_d = 85·0 %

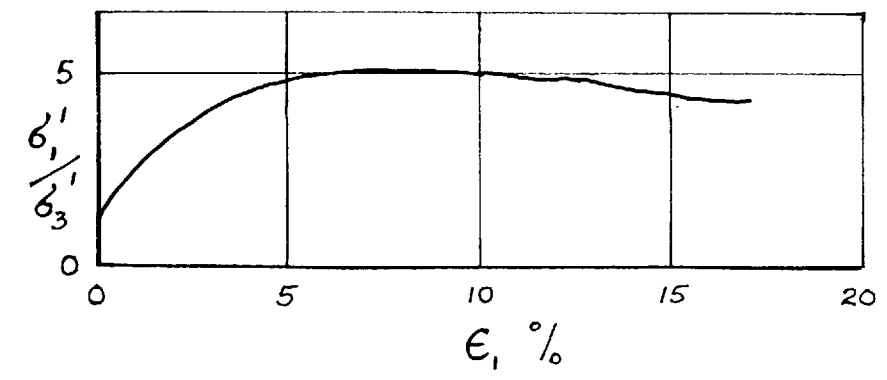
SAMPLE 17V/12 γ_d = 104·1 LBS/FT.^{3}
R_d = 30·0 %

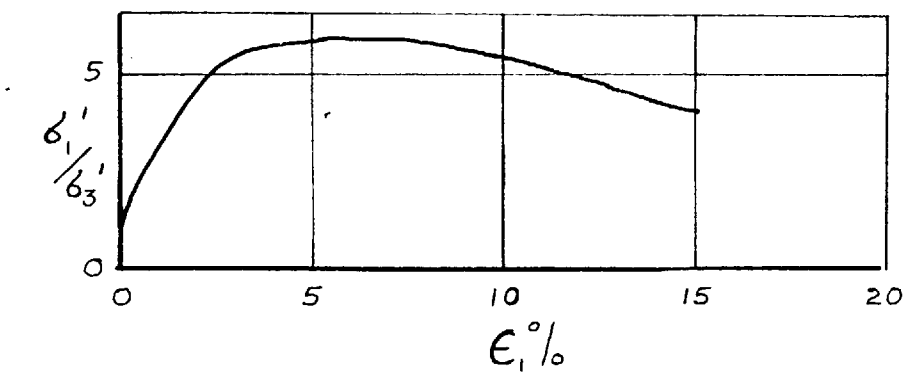
GRANITIC GNEISS ROCKFILL.

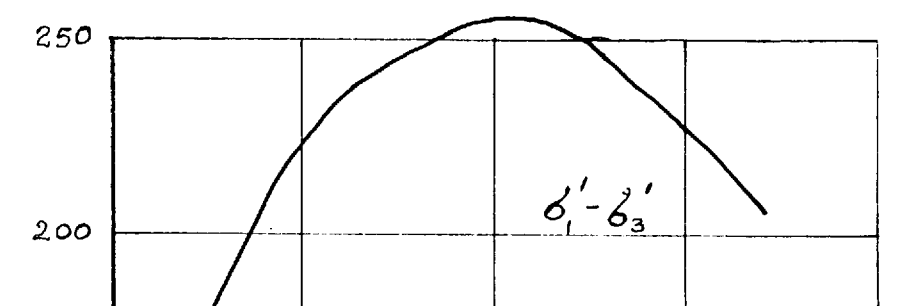
FIG. 8:3:Sa.

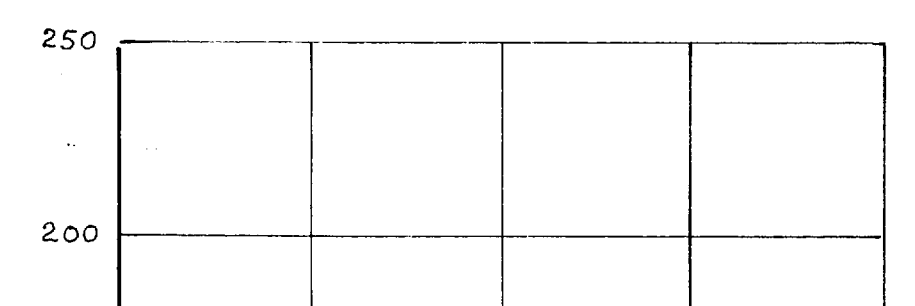


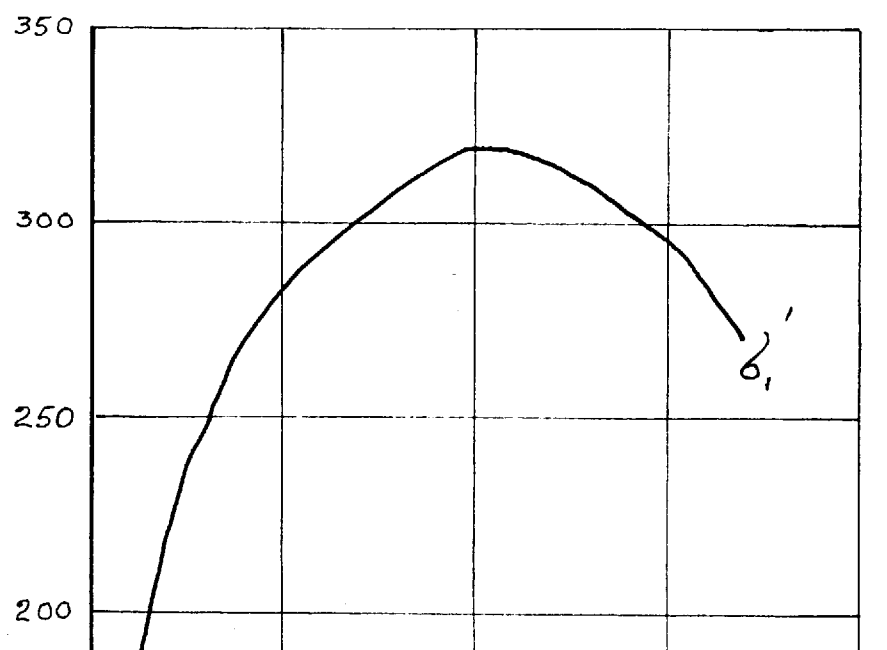


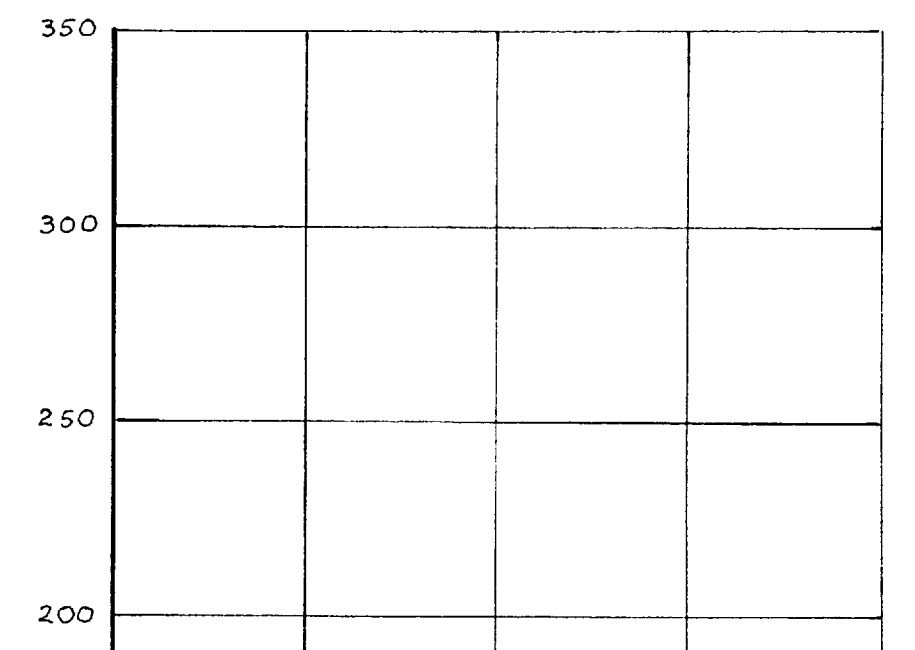


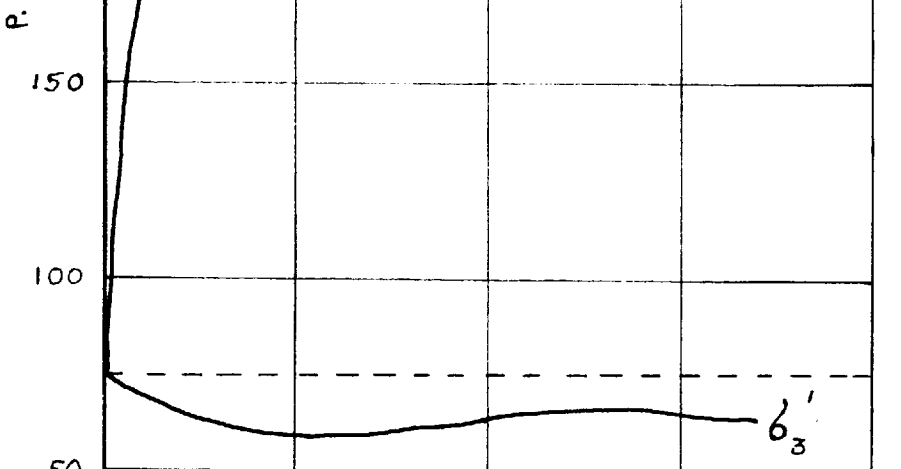




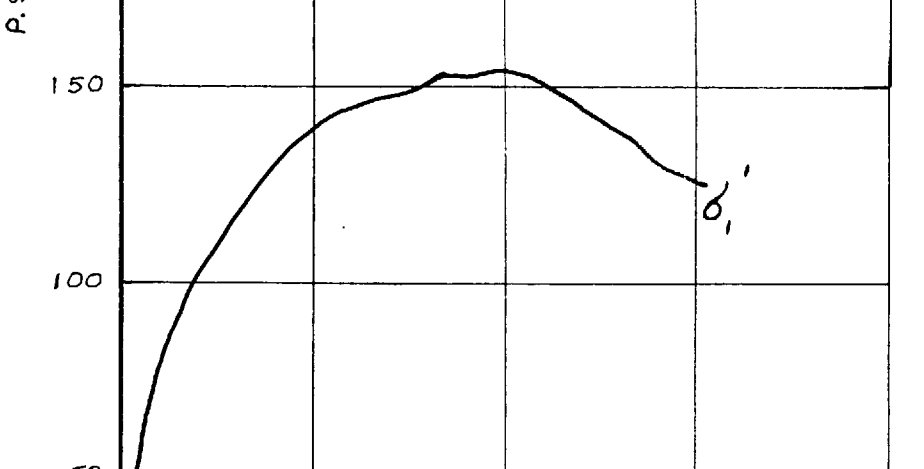








GRADING : L
γ_D : 117·0 LBS/FT.^{3} (AFTER CONSOLIDATION)
R_d : 73·0 %

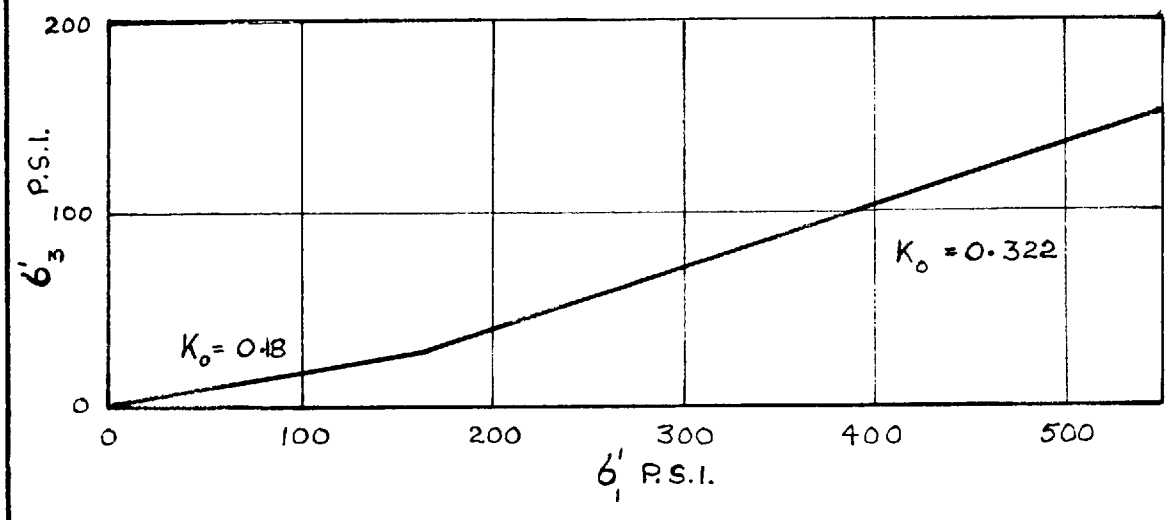


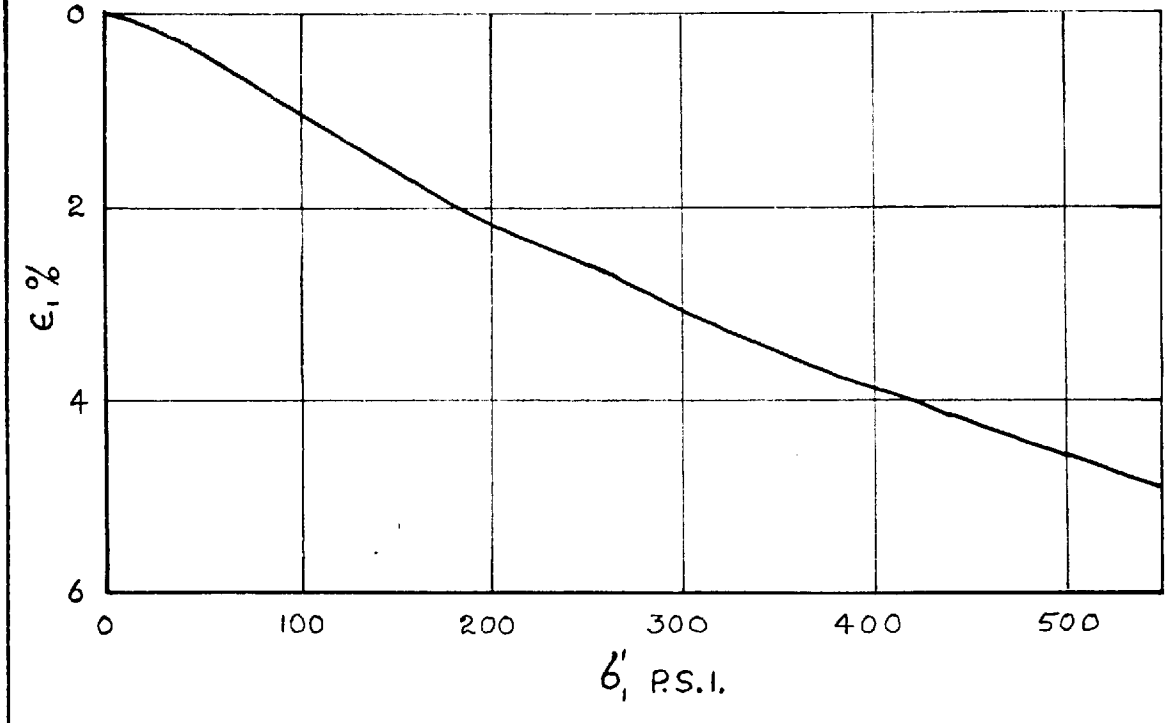
GRADING : L
γ_D : 113·6 LBS/FT.^{3} (AFTER CONSOLIDATION)
R_d : 64·0 %

FIG. 8 : 3 : 56.

GRANITIC GNEISS 4" DIA. SAMPLES.

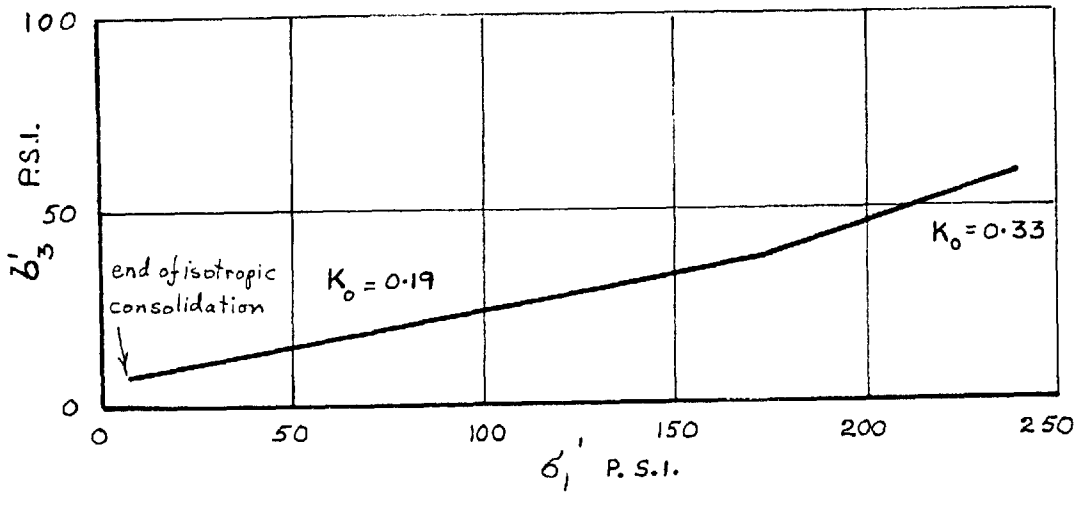
250

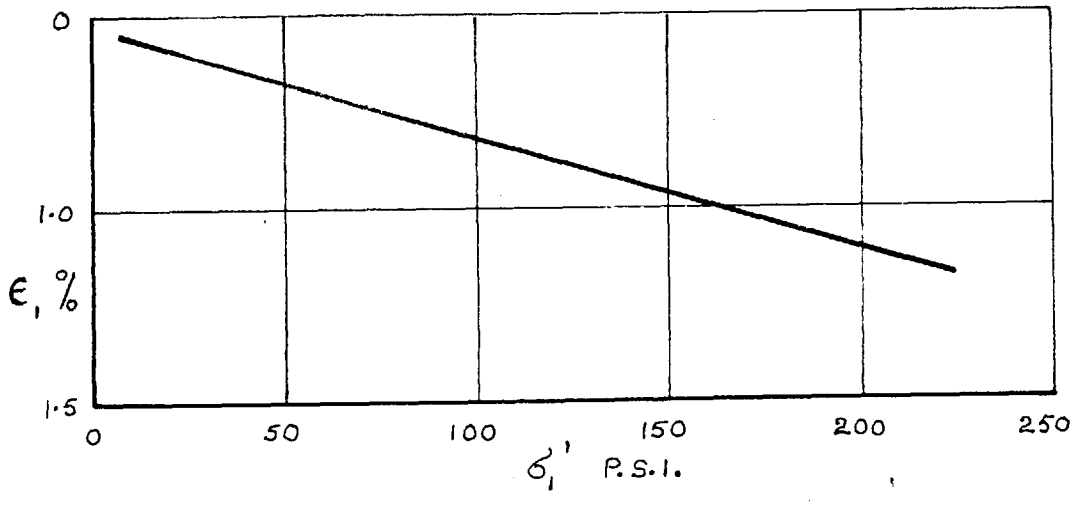


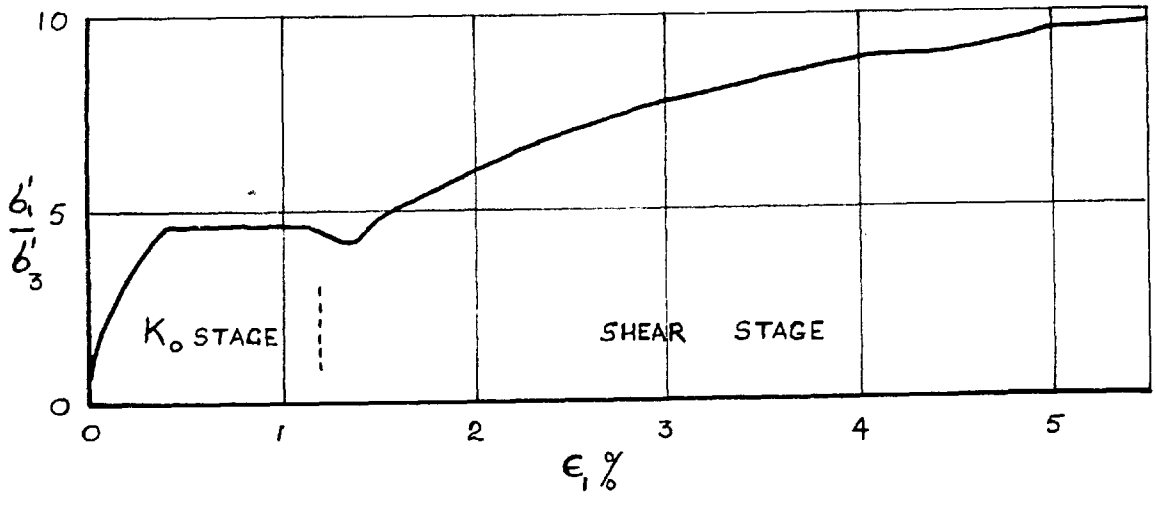


GRANITIC GNEISS SAMPLE No. 13V|12
K_0 CONSOLIDATION.

FIG. 8:4:8a

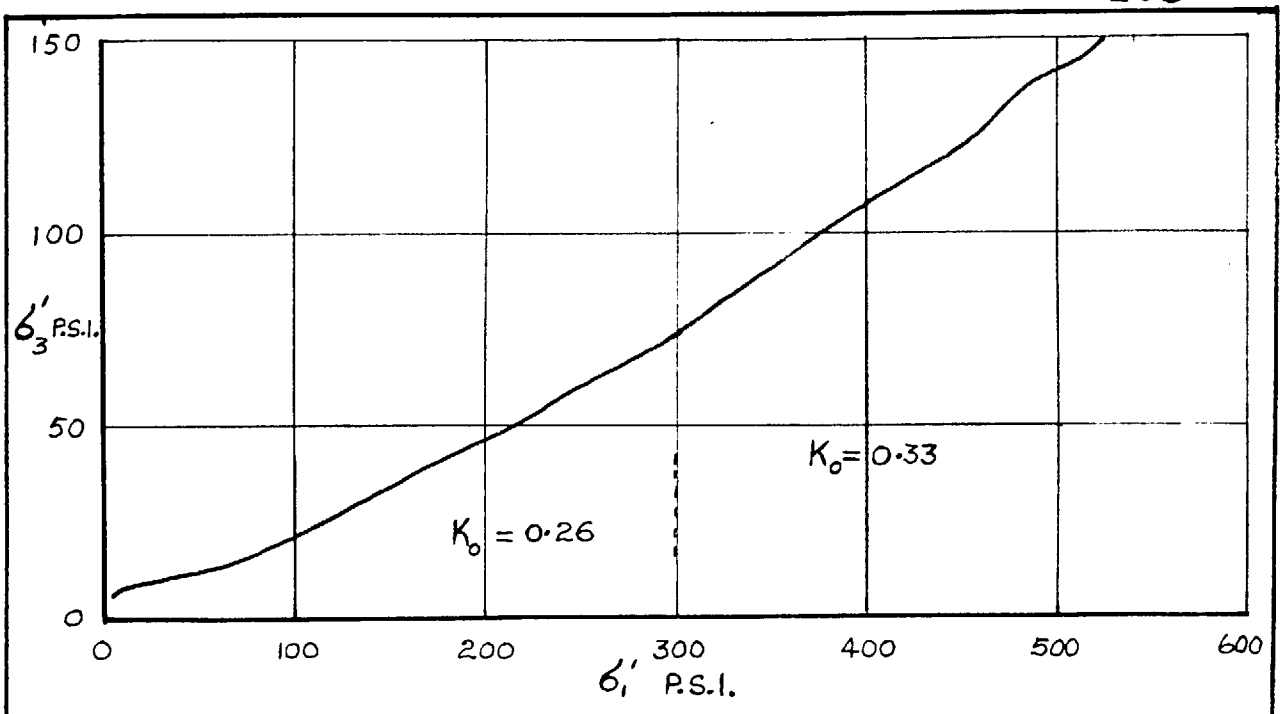


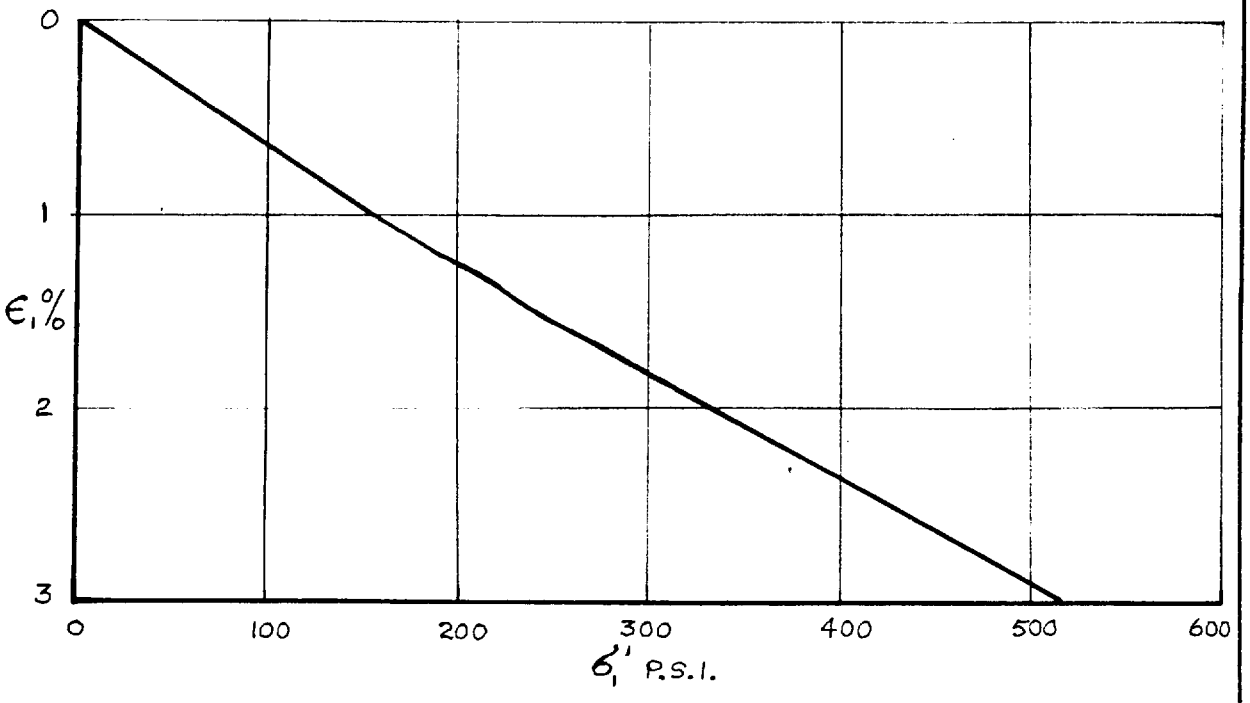


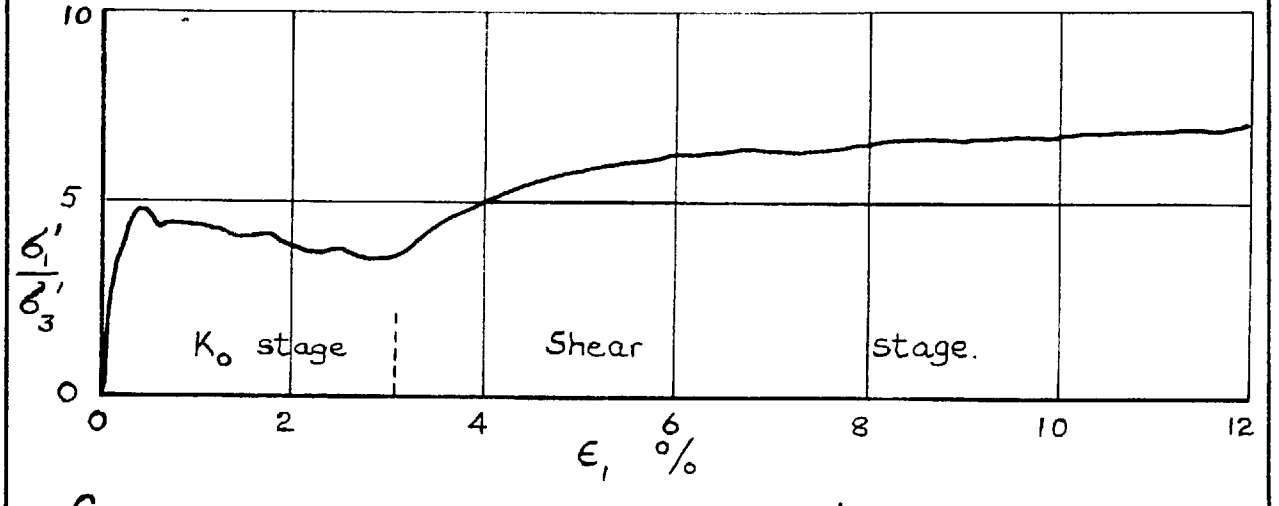


GRANITIC GNEISS SAMPLE No. 18V|12.

FIG. 8:4:86







GRANITIC GNEISS SAMPLE No. 19V/12.

FIG. 8:4:8c

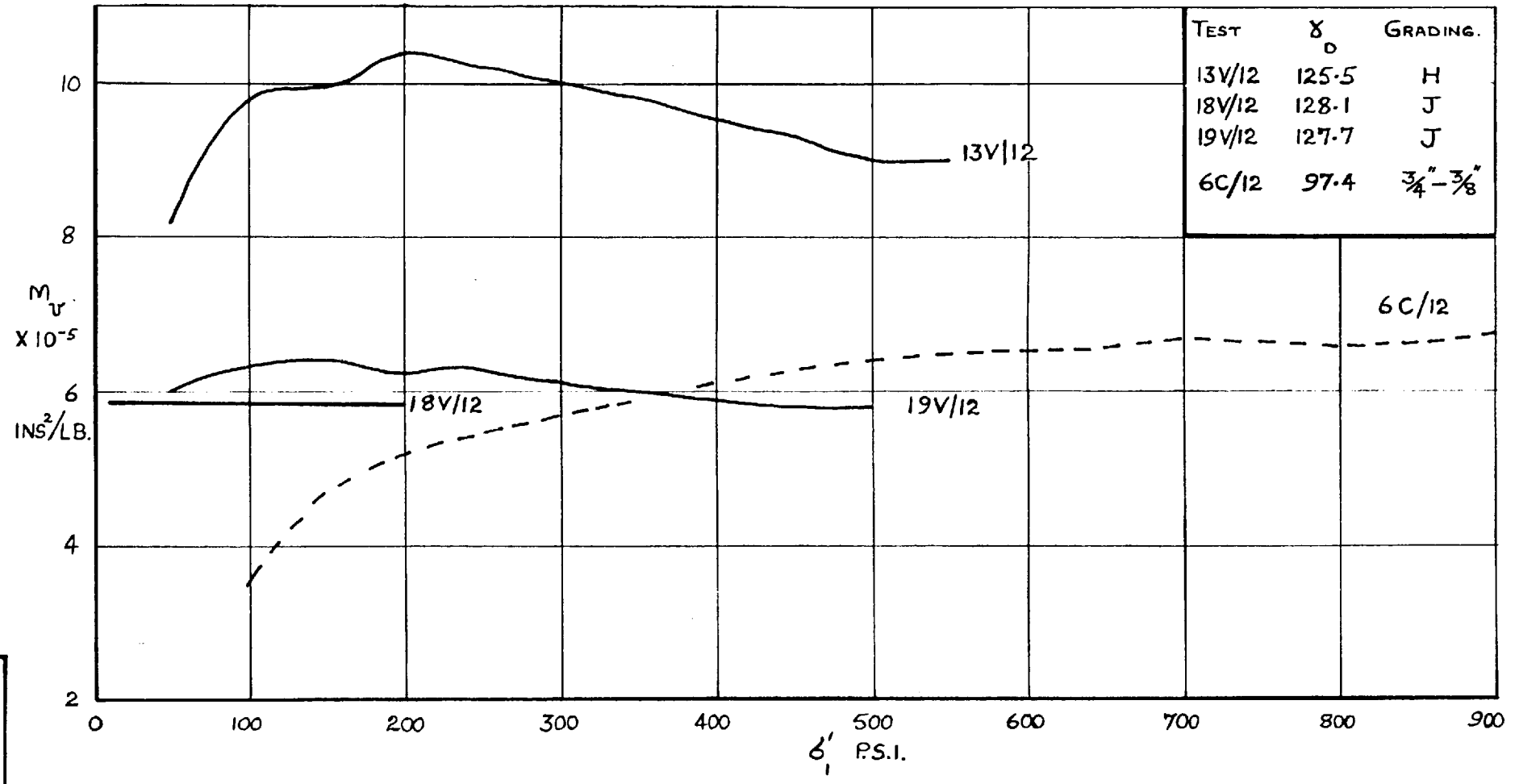


FIG. 8:4:84

SECANT VALUES OF m_v FOR GRANITIC GNEISS AND CHERT.

Test No.	1V|12	2V|12	3V|12	4V|12	5V|12	6V|12	7V|12	8V|12	9V|12	10V|12	11V|12	12V|12	13V|12	14V|12	15V|12	16V|12	17V|12	18V|12	19V|12
Type of test.	DS	DS	DS	DS	DS	DS	DS	DS	DS	DS	DS	DS	K_o	DS	—	CU	CU	σ_1'/σ_3' inc	σ_1'/σ_3' inc
Nominal σ_3' (P.S.I.)	80	40	10	20	150	10	300	500	450	40	150	10		80		σ_3=80	σ_3=80	σ_3=52	σ_3=151
Axial strain rate % per hour.	8.0	8.0	8.0	8.0	8.0	8.0	8.0		8.0	8.0	8.0	8.0		8.0					
ϕ_f'	46.0°	49.6°	60.0°	54.5°	43.7°	56.0°	42.5°		40.5°	49.4°	43.6°	54.6°		45.8°		46.0°	44.0°	54.9°	48.5°
Tan ϕ_f'	1.036	1.175	1.732	1.402	0.956	1.483	0.885		0.834	1.168	0.953	1.407		1.029		1.036	0.966	1.423	1.130
$\frac{1}{2}(\sigma_1'-\sigma_3')_f$ (P.S.I.)	207.2	130.7	63.5	85.6	337.5	46.6	624.5		829	127.2	337.8	43.9		202.3		189.6	47.4	58.6	96.9
$\frac{1}{2}(\sigma_1'+\sigma_3')_f$ (P.S.I.)	288.1	171.7	73.4	105.2	487.5	56.2	924.5		1279	168	489.5	53.9		282.3		263.5	68.2	71.8	129.3
$\sigma_1'_f$ (P.S.I.)	495.2	302.4	136.9	190.9	825.0	102.8	1549		2108	295.3	827.3	107.8		484.5		453.1	115.5	130.3	226.2
$\sigma_3'_f$ (P.S.I.)	80.9	41.0	9.9	19.6	150.0	9.6	300		450	40.8	151.6	10.0		80.8		73.8	20.8	13.2	32.4
$(d\epsilon_v/d\epsilon_1)_f$	-0.170	-0.354	-0.780	-0.620	-0.0667	-1.11	-0.0183		0	-0.40	-0.0116	-0.116		-0.116					
γ_d (lbs/ft^3)	129.8	128.1	137.1	130.5	131.1	130.8	130.8		130.5	132.2	128.8	107.8	125.5	127.1		128.5	104.1	128.1	127.7
R_d %	89.0	86.0	100.0	90.0	90.0	89.0	89.0		89.0	92.0	87.0	45.0		84.0		85.0	30.0	84.5	83.5
n %	21.4	22.4	16.9	21.0	20.5	20.8	20.8		21.0	19.8	22.0	34.8		23.0		22.2	36.9	22.4	22.7
Effective stress when measuring (P.S.I.)	9.0	5.0	1.0	1.0	2.7	1.0	1.0		1.0	1.0	1.0	1.0		1.2		1.0	1.0	1.2	1.0
$\epsilon_{1\,f}$ %	8.47	5.96	3.25	5.68	8.85	2.93	14.03		16.34	5.37	13.17	29.18		8.05		5.72	9.00	5.61	11.97
$\epsilon_{v\,f}$ %	-1.09	+0.48	+1.35	+1.67	-2.48	+1.72	-4.33		-4.83	+0.49	-3.09	-1.57		-1.34				+3.46	+2.01
Membranes	3/16" R.F.	3/16" R.F.	1/8" R.F.	1/8" R.F.	3/16" R.F.	1/8" R.F.	1/4" R.F.		1/4" R.F.	1/8" R.F.	1/4" R.F	1/8" R.F.	3/16" R.F.	3/16" R.F.	3/16" R.F.	3/16" R.F.	3/16" R.F.	3/16" R.F.	3/16" R.F.
k before test cms/sec.	8.0 x 10^{-3}	3.9 x 10^{-3}		2.6 x 10^{-3}															
mean stress for above $\frac{1}{3}(\sigma_1'+2\sigma_3')$ (P.S.I.)	80	40																	
k after test cms/sec.	8.8 x 10^{-3}	2.8 x 10^{-3}																	
mean stress for above $\frac{1}{3}(\sigma_1'+2\sigma_3')$ (P.S.I.)																			
γ_d at failure (lbs/ft^3)	133.1	128.3	136.4	129.5	134.3	127.2	139.8		139.8	129.3	135.8	111.6		132.0		130.6	111.0	124.1	125.1
Grading.	H	H	H	H	J	J	J	J	J	J	H	H	H	H		J	J	J	J
Type of failure.	B	B	B top 2/3	B at top	B	top B slight S	B/S	B	B/S	B	B	B/S		B		B top 2/3	B	slight B	slight B
														*		1	1	1	1

* Result by external loadcell See also Fig.

1 Failure defined as max $\frac{\sigma_1'}{\sigma_3'}$

TRIAXIAL TESTS ON 12" DIAMETER SAMPLES OF GRANITIC GNEISS

TABLE. 8A

Test No.	1V/4	2V/4	3V/4	4V/4	5V/4	6V/4	7V/4	8V/4	10V/4	11V/4	12V/4	13V/4	14V/4	15V/4	17V/4	18V/4	19V/4	20V/4	21V/4	22V/4	23V/4	24V/4	25V/4	26V/4
Type of test.	DS	DS	DS	DS	DS	DS	DS	DS	DS	DS	DS	DS	DS	DS	DS	DS	DS	DS	DS	DS	DS	DS	DS	DS
Nominal σ_3' (P.S.I.)	10	40	120	100	10	10	100	100	80	80	10	80	10	10	80	40	10	40	80	10	10	40	10	80
Axial strain rate % per hr.	8	8	8	8	8	8	8	8	8	8	8	8	8	8	8	8	8	8	8	8	8	8	8	8
ϕ_f'	50.9°	45.1°	41.5°	41.1°	47.8°	47.4°	39.4°	41.9°	42.3°	44.5°	50.8°	42.8°	51.8°	52.0°	41.4°	41.6°	43.0°	41.2°	39.4°	45.2°	48.5°	43.3°	50.0°	40.2°
Tan ϕ_f'	1.230	1.003	0.885	0.874	1.102	1.088	0.822	0.898	0.911	0.984	1.227	0.927	1.270	1.280	0.883	0.889	0.934	0.876	0.822	1.008	1.130	0.944	1.192	0.845
$\frac{1}{2}(\sigma_1'-\sigma_3')_f$ (P.S.I.)	35.6	98.0	234.5	191.0	29.8	29.0	174.0	200	164.5	188.9	35.8	169.8	38.0	38.8	157.0	80.1	22.5	77.8	139.3	25.5	31.0	87.8	34.4	146.0
$\frac{1}{2}(\sigma_1'+\sigma_3')_f$ (P.S.I.)	45.6	138.0	354.5	291.0	39.8	39.0	274.0	300	244.5	268.9	45.8	249.3	48.0	48.8	237.0	120.2	32.5	117.8	219.2	35.5	41.0	127.9	44.4	226.0
$\sigma_1'_f$ (P.S.I.)	81.1	236.0	589.0	482.0	69.5	68.0	448.0	500	409	457.9	81.5	418.5	86.0	87.6	394.0	200.3	55.0	195.6	358.5	61.0	72.0	215.7	78.8	372.0
$\sigma_3'_f$ (P.S.I.)	10.0	40.0	120.0	100.0	10.0	10.0	100.0	100	80	80	10.0	80.0	10.0	10.0	80.0	40.0	10.0	40.0	80	10.0	10.0	40.0	10.0	80.0
$(d\epsilon_v/d\epsilon_1)_f$	-0.558	-0.225	0	0	-0.684	-0.50	+0.097	0	-0.061	-0.089	-0.55	0	-0.76	-0.76	0	0	-0.252	-0.064	0	-0.55	-0.91	-0.23	-1.00	-0.111
γ_d (lbs/ft^3)	121.6	122.1	118.5	116.0	116.0	112.5	113.8	118.9	121.2	120.1	116.0	117.0	122.2	124.0	112.7	107.2	103.5	108.0	111.2	110.2	116.9	114.1	118.0	109.6
R_d %	91.0	92.5	84.0	70.5	70.5	61.0	64.5	84.5	90.5	88.0	78.0	80.2	92.5	96.5	69.2	53.5	33.0	47.5	56.5	53.0	70.5	65.5	73.5	51.0
n %	26.4	26.0	28.3	29.8	29.8	31.9	31.2	28.1	26.6	27.3	29.8	29.2	25.9	25.0	31.8	35.1	37.3	34.6	32.6	33.3	29.3	30.9	28.6	33.7
Effective stress (P.S.I.) when measuring.	1.2	1.2	1.2	1.2	1.2	1.2	1.2	1.2	1.2	1.2	1.2	1.2	1.2	1.2	1.2	1.2	1.2	1.2	1.2	1.2	1.2	1.2	1.2	1.2
ϵ_{1f} %	4.35	6.84	12.28	11.51	4.96	6.85	8.23	10.44	6.84	11.03	6.70	8.76	4.02	4.98	17.12	9.32	8.07	9.97	9.29	6.23	4.00	6.75	4.39	10.19
ϵ_{vf} %	+1.55	+0.03	-3.53	-2.96	+2.45	+1.76	-3.72	-2.66	-1.61	-2.19	+2.14	-2.27	+1.59	+2.69	-3.84	-2.81	+0.17	-2.39	-2.95	+1.39	+2.20	-0.39	+2.77	-2.48
Membranes.	0.050"	0.050"	0.050"	0.050"	0.050"	0.050"	0.050"	0.050"	0.050"	0.050"	0.050"	0.050"	0.050"	0.050"	0.010" 0.050"	0.010" 0.050"	0.060"	0.050"	0.050"	0.050"	0.050"	0.050"	0.050"	0.050"
k before test cms/sec.	5.8×10^{-3}	5.8×10^{-3}	5.6×10^{-3}	5.6×10^{-3}	5.8×10^{-3}														3.2×10^{-3}	7.8×10^{-3}	5.5×10^{-3}		1.6×10^{-3}	
mean stress for above $\frac{1}{3}(\sigma_1'+2\sigma_3')$ (P.S.I.)	10	40	120	100	10														80	10	10		10	
k after test cms/sec.	4.3×10^{-3}	4.3×10^{-3}		3.7×10^{-3}	3.2×10^{-3}														2.5×10^{-3}	4.8×10^{-3}	3.8×10^{-3}		2.2×10^{-3}	1.1×10^{-3}
mean stress for above $\frac{1}{3}(\sigma_1'+2\sigma_3')$ (P.S.I.)	26	91		214															157	19	19		16	139
γ_d at failure (lbs/ft^3)	121.8	126.0	128.2	123.5	114.7	111.9	122.8	127.7	128.6	128.5	116.1	125.0	120.8	122.8	124.5	116.3	105.5	115.5	117.0	109.4	114.8	117.2	115.0	115.4
Grading.	K	K	K	L	L	L	L	K	K	K	K	K	K	K	K	K	L	L	N	N	N	L	P	P
Type of failure.	B/S	B/S	B/S	B/S	B/S	B/S	B/S	B/S	B/S	B/S	B/S	B/S	B/S	B/S	B/S	B/S	B/S	B/S	B/S	B/S	B/S	B/S	B/S	B/S
			*					*					*						↑		2.	2.	2.	

Note: ϕ_f' corrected for membrane effects.

* Definite peak not attained

↑ Direction of shear plane changed during test.

2. Samples subjected to heavy compaction.

TRIAXIAL TESTS ON 4" DIAMETER SAMPLES OF GRANITIC GNEISS.

TABLE. 8B

Test No.	1V | 1½	2V | 1½	3V | 1½	4V | 1½	5V | 1½	7V | 1½	8V | 1½	9V | 1½	10V | 1½	11V | 1½	12V | 1½	13V | 1½	14V | 1½	15V | 1½	16V | 1½	17V | 1½	18V | 1½
Type of test.	DS	DS	DS	DS	DS	DS	DS	DS	DS	DS	DS	DS	DS	DS	DS	DS	DS
Nominal σ_3' (P.S.I.)	40	80	20	80	40	300	450	40	10	10	40	10	80	10	10	80	80
Axial strain rate % per hour.	8	8	8	8	8	4	2·5	8	8	8	8	8	8	8	8	8	8
ϕ_f'	46·0°	43·2°	48·4°	41·4°	46·5°	41·0°	38·4°	43·8°	47·8°	52·7°	43·4°	49·9°	44·8°	51·8°	48·3°	43·4°	43·0°
Tan ϕ_f'	1·037	0·940	1·127	0·883	1·053	0·870	0·794	0·960	1·102	1·311	0·946	1·188	0·995	1·270	1·122	0·946	0·934
$\frac{1}{2}(\sigma_1'-\sigma_3')_f$ (P.S.I.)	102·8	172·2	60·5	157	106·5	573	735	90·6	30·0	46·2	89·0	33·9	193·0	38·6	31·2	176·5	172·7
$\frac{1}{2}(\sigma_1'+\sigma_3')_f$ (P.S.I.)	142·8	251·8	80·5	237	146·5	873	11 86	130·6	40·0	56·3	129·1	43·9	273·0	48·5	41·2	256·5	252·8
$\sigma_{1\,f}'$ (P.S.I.)	245·5	423·5	140·9	394	253	1445	1921	221·6	69·9	92·5	218·1	77·8	466·0	87·1	72·4	433·0	425·5
$\sigma_{3\,f}'$ (P.S.I.)	40·0	79	20	80	40	300	450	40	10	10	40	10	80	10	10	80	80
$(d\epsilon_v/d\epsilon_1)_f$	-0·095	-0·092	-0·54	-0·152	-0·346	-0·10	-0·06	-0·138	-0·352	-1·12	-0·344	-0·71	-0·27	-1·03	-0·75	-0·306	-0·815
γ_d (lbs/ft^3)	116·4	117·0	116·8	114·1	116·9	118·2	116·2	110·9	106·9	122·0	111·8	113·1	123·8	122·6	117·1	116·8	115·2
R_d %	71·5	73·2	72·5	64	73	74	68·5	56	44	86	58	61	89·5	84	71	70	66·5
n %	29·5	29·2	29·3	30·9	29·2	28·4	29·6	32·9	35·3	26·1	32·3	31·5	25·0	25·8	29·1	29·3	30·3
Effective stress when measuring (P.S.I.)	1·0	1·0	1·0	1·0	1·0	1·0	1·0	1·2	1·2	1·2	1·2	1·2	1·2	1·2	1·2	1·2	1·2
$\epsilon_{1\,f}$ %	7·33	10·2	5·33	9·48	7·33	13·2	16·8	10·77	3·85	3·48	9·65	4·56	7·75	4·57	4·67	8·47	10·07
$\epsilon_{v\,f}$ %	-1·67	-3·34	+1·80	-1·48	+0·61	-3·97	-4·71	-0·77	+0·22	+2·22	+0·80	+1·52	-0·74	+2·58	+1·95	-0·60	-0·22
Membranes	0·025"	0·025"	0·025"	0·025"	0·025"	2 x 0·025"	2 x 0·025"	0·035"	0·010"	0·010" 0·005"	0·010"	0·025"	0·025"	0·025"	0·025"	0·025"	0·025"
k before test cms/sec.	1·7 x 10^{-3}	2·7 x 10^{-3}	2·3 x 10^{-3}	1·3 x 10^{-3}	2·2 x 10^{-3}	6·8 x 10^{-7}	7·3 x 10^{-5}					9·2 x 10^{-4}	6·7 x 10^{-4}	1·6 x 10^{-4}	1·7 x 10^{-4}	5·8 x 10^{-3}	2·1 x 10^{-4}
mean stress for above $\frac{1}{3}(\sigma_1'+2\sigma_3')$ (P.S.I.)	40	80	20	80	40	300	450					10	80	10	10	80	80
k after test cms/sec	1·3 x 10^{-3}	–	1·5 x 10^{-3}	7·0 x 10^{-4}	1·2 x 10^{-3}	2·2 x 10^{-7}	1·8 x 10^{-5}					6·9 x 10^{-4}	5·3 x 10^{-4}	1·7 x 10^{-4}	2·1 x 10^{-4}	3·8 x 10^{-3}	1·4 x 10^{-4}
mean stress for above $\frac{1}{3}(\sigma_1'+2\sigma_3')$ (P.S.I.)	89	–	42	161	81	621	912					26	194	20	23	159	155
γ_d at failure (lbs/ft^3)	122·4	128·8	1172	118·9	120·0	129·0	129·6	118·0	108·8	120·2	113·0	112·6	129·0	119·4	115·0	118·8	117·0
Grading	M	M	M	O	M	O	O	M	M	M	O	O	M	P	Q	P	Q
Type of failure	B/S	B/S	B/S	B/S	B/S	B	B	B/S	B/S	B/S	B/S	B/S	B/S	B/S	B	B/S	B
					Rot. bush not used									top ⅔			

Note: ϕ_f' corrected for membrane effects.

TRIAXIAL TESTS ON 1½" DIAMETER SAMPLES OF GRANITIC GNEISS

TABLE. 8 C

CHAPTER 9

The Results of the Tests on Chert

The type of fracture which occurred with the chert precluded the possibility of using the fine material to produce scaled gradings. As a result, only two uniform gradings were tested, $1\frac{1}{2}$" - $\frac{3}{4}$" and $\frac{3}{4}$" - $\frac{3}{8}$" using 12" diameter samples.

(9:1) Compaction and Sample Density

The usual method of compaction, using a Kango Hammer, was abandoned and a hand tamping tool was used to compact wetted material.

Similar densities were achieved with both sizes of chert. The densities were very low but this was to be expected from a coarse material of single size particles. Insufficient material was available to determine the density limits but the densities achieved were probably towards the maximum (Table 9A).

No particle breakdown was apparent during compaction.

(9:2) Isotropic Consolidation

The volume changes during isotropic consolidation may have a large error due to membrane penetration because of the large single size material tested. Membranes $\frac{1}{8}$" thick were used to contain the samples of the finer grading and 3/16" thick to contain the coarser grading.

The volume strains of the coarser material were twice those of the finer material for any given pressure. However, a volume strain of 4% is only equivalent to an average membrane displacement of 1/10". It is quite possible that the volume strain of 4% shown by sample 11C/12 (Fig.9:2) was in fact largely attributable to the membrane penetration between the particles. It is felt, therefore, that the volume strains measured during isotropic consolidation were not representative of the behaviour of the material but rather a measure of membrane penetration.

(9:3) Shear Strength

The contact forces between the chert particles were probably much greater than those of the silurian cleaved mudstone or the granitic gneiss for a given maximum particle size and applied effective stress because of the uniformity of the material.

There was a very large increase in deviator stress for a very small axial strain and particle fracture was audible at all stress levels though more particularly as the peak stress was approached and passed.

The material showed a powerful tendancy to dilate and the relationship between the angle of internal friction and the rate of dilatancy at failure was almost identical to that of the granitic gneiss (Fig.8:3B). It will be noticed that again this plot showed two separate behaviours for the two ratios of particle size to sample diameter. There did not, though, appear to be any difference in the angles of internal friction between the two gradings. Samples 40/12 gave a high angle of internal friction and had an inconsistent rate of volume change.

The mean angles of internal friction for both gradings were identical, varying between 50.0° and 40.5° at minor principal effective stresses of 10 p.s.i. and 80 p.s.i.

Bishop (1948) carried out a series of tests on Chesil Bank pebbles, having a grading between $1\frac{1}{2}$" and $\frac{3}{4}$" in a 1 foot square shear box. In the dense state and at low stresses they showed an angle of internal friction of about 46° (Section 3:5 and Fig.3:5:1).

The Chesil Bank pebbles had a lower angle of internal friction than the chert and this was probably because they were rounded whereas the chert was rather tuberous and interlocked somewhat more. The pebbles were also tested in a shear box which might give slightly lower values than the triaxial because of the boundary conditions.

The well graded Heathrow, Thames Valley gravel demonstrated a similar angle of internal friction (50° at a porosity of 26% and a normal stress of 2 tons/ft.^{2}) to the chert at low stresses. This may well be because of the increased number of particle contacts and hence smaller inter-particle forces and increased dilatancy.

The stress-strain curves for the tests on chert are plotted in Figs. 9:3A and 9:3B. The saw tooth nature of the deviator-stress axial strain curve is the result of particle fracture. It appeared, especially with the coarser grading, that, at times, the full deviator load was being transmitted in one particular plane by only a few particles (probably less than 45) some of which would suddenly break. The load cell measuring the deviator load was a very stiff element, and the resulting deformation of the sample was not taken up by a relaxation of the testing machine either, and so a large reduction in deviator stress occurred for a few seconds. The reaction time of the electronic circuit was too low to be able to pick up the minimum value to which the deviator stress dropped. The resulting volume change did not appear to effect the constant cell pressure.

The rate of dilatancy at failure for a given minor principal effective stress is plotted in Fig.9:3. Both the gradings of chert behave more as a loose sand at high stresses and a dense sand at low stresses and this is probably because of the uniform grading and the resultant particle breakdown.

(p:4) Deformation

Some of the factors on which deformation depends are set out in Section 7:4.

The axial strains at failure, for the finer grading, varied between about 5% and 12% at minor principal stresses of 10 p.s.i. and 80 p.s.i. respectively. Very similar results were obtained for the coarser grading (Table 9A and Figs.9:3A and 9:3B)

Except for sample 11C/12 all the samples dilated during shear at minor principal effective stresses between 10 p.s.i. and 80 p.s.i.

(9:4:1) Volumetric strain and deviator stress

There was a fairly linear relationship between the volumetric strain and the deviator stress up to about 75% of the peak deviator stress. As with the coarser gradings of granitic gneiss all the samples followed a similar path up to about 75% of their peak deviator stress irrespective of the minor principal effective stress (Figs.9:3A and 9:3B)

The large dilation which occurs after the peak deviator stress is most apparent on this plot.

(9:4:2) Creep

During isotropic consolidation the volume change, on application of an increase in stress, was almost instantaneous and no creep was noticed.

However, at the end of the shear stage the deviator load quickly reduced when the applied axial deformation was stopped. At this stage though the material was no longer solely rounded, tuberous bodies because of the particle breakdown (Section 9:4:4).

(9:4:3) One dimensional compressibility

One K_o test was carried out to determine the values of K_o and m_v. The $1\frac{3}{4}$" - $\frac{3}{8}$" grading was used to minimise membrane penetration.

An almost linear relationship was found between axial strain and the major principal effective stress.

The secant value of m_v is plotted for various major principal effective stresses in Fig.8:4:8d. There was an increase in compressibility up to a value of σ_1' = 400 p.s.i. This initial curvature was demonstrated by virtually all the samples subjected to anisotorpic consolidation and it was thought to be due to the effects of compaction. This initial hump in the curves (Figs.7:4:10h and 8:4:8d) was especially evident on the samples of uniform gradings and those containing 3" particles.

The secant value of m_v remained relatively constant from σ_1' = 400 p.s.i. to σ_1' = 900 p.s.i.

The value of K_o obtained increased with pressure but it is probable that the initial variations were due to membrane penetration and the value was 0.53. This value is somewhat higher than the average for mudstone (0.45) and granite (0.33). The simple relation, $K_o = 1 - \sin \phi'_c$, does not hold as ϕ' decreases with increasing stress. If ϕ at constant volume (40°) is substituted in the above equation a considerably lower value of K_o is predicted (0.36).

(9:4:4) Particle breakdown

The silurian cleaved mudstone and granitic gneiss particles tended to break into shapes similar to the original body and further fines were produced by the crushing of contacts.

The breakdown of the chert was of a different nature. The particles were smooth surfaced and tuberous and hence breakdown of the contacts did not occur. Instead, a large amount of strain energy was stored up in the particle until it burst into several concoidal bodies and numerous razor sharp splinters. As a result of this form of breakdown the material could not be scaled.

The sudden bursting of the particles was responsible for the saw toothed character of the latter parts of the stress-strain curves.

The breakdown of the $1\frac{1}{2}$" - $\frac{3}{4}$" grading, with stress, is shown in Table 9:4:4a.

B.S. Sieve	Initial grading % passing	Increase in weight of material passing each sieve %			
		σ'_3=10p.s.i.	σ'_3=20p.s.i.	σ'_3=40p.s.i.	σ'_3=80p.s.i.
$1\frac{1}{2}$"	100.0	0	0	0	0
$\frac{3}{4}$"	0	7.2	12.4	20.1	26.5
$\frac{3}{8}$"		1.1	1.7	3.9	7.5
3/16"		0.6	0.7	1.7	3.2
No.7			0.4	0.9	1.7
No.14				0.6	1.0
		Σ = 8.9	15.2	27.2	39.9
		mean = 1.49	2.53	4.53	6.65

Table 9:4:4a

The breakdown of the $\frac{3}{4}$" - $\frac{3}{8}$" grading with stress is shown in Table 9:4:4b.

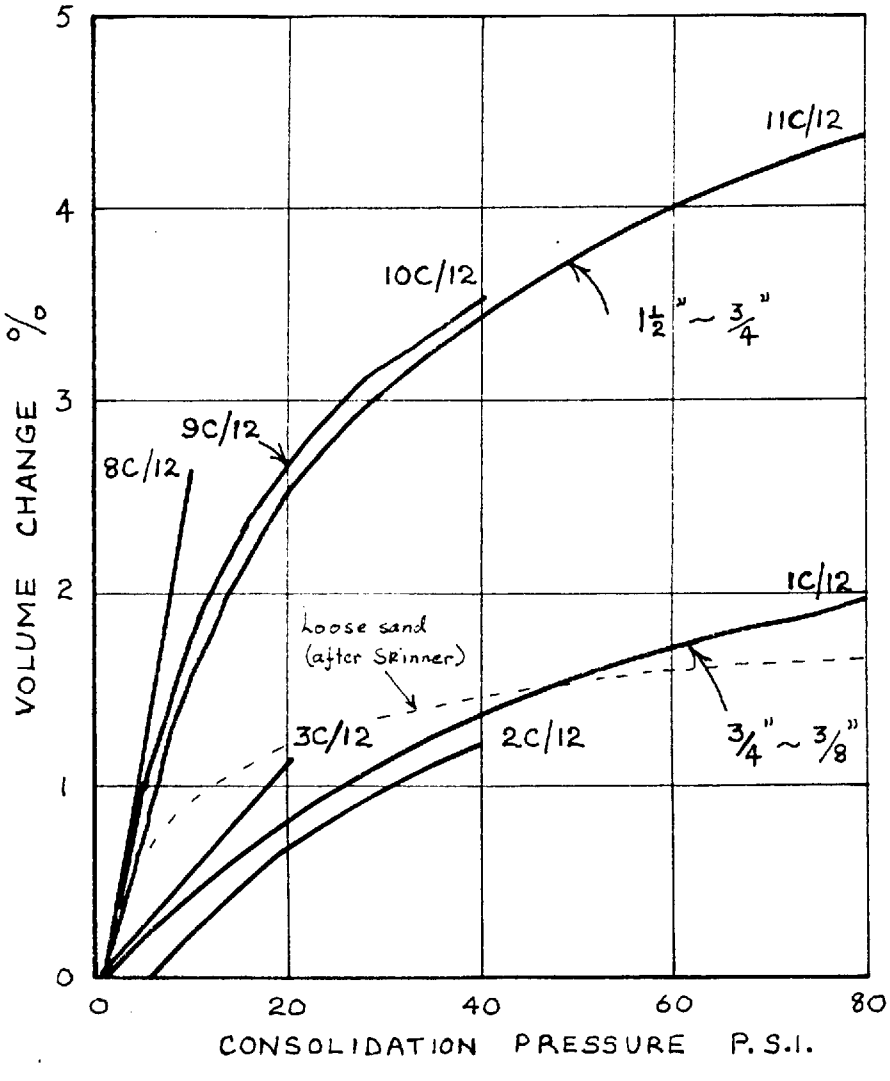
B.S.Sieve	Initial grading % passing	Increase in weight of material passing each sieve %		
		σ_3'=10p.s.i.	σ_3'=80p.s.i.	K_o to σ_3'=450p.s.i σ_1'=997p.s.i
¾"	100.0	0	0	0
⅜"	15.0	1.7	9.5	18.6
3/16"	2.0	-0.8	2.6	6.3
No.7		0.5	2.1	3.3
No.14		0.3	1.0	1.7
No.25			0.5	0.9
No.52			0.3	0.5
No.100			0.1	0.3
		Σ = 1.7	16.1	31.6
		mean = 0.21	2.01	3.95

Table 9:4:4b

About three times the amount of breakdown occurred in the coarser grading at equivalent stresses.

The general factors affecting particle breakdown are set out at the end of Section 7:4:11.

The permeabilities of the samples were so high that they could not be measured with the apparatus available at that time.

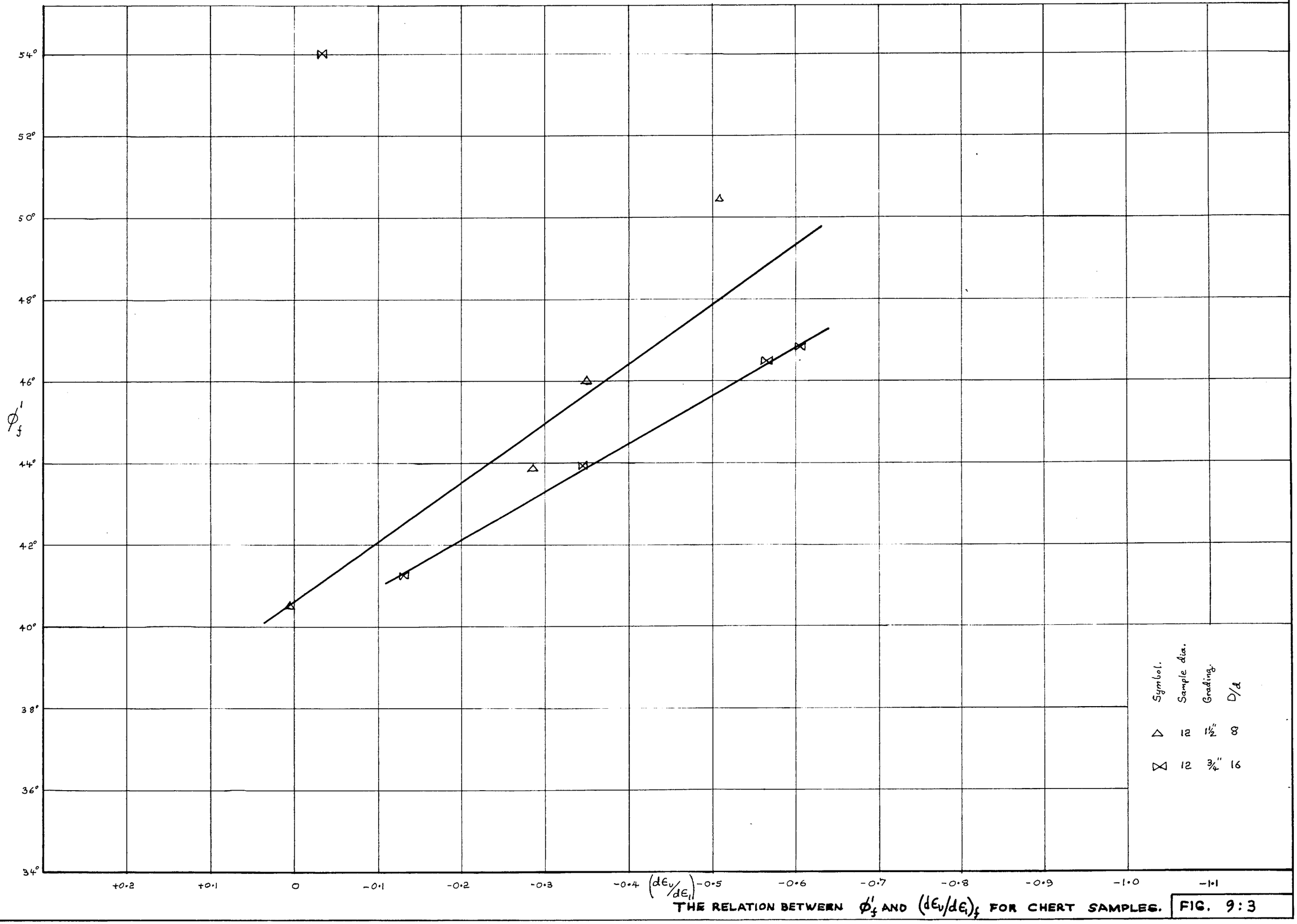


VOLUME CHANGES DURING ISOTROPIC CONSOLIDATION

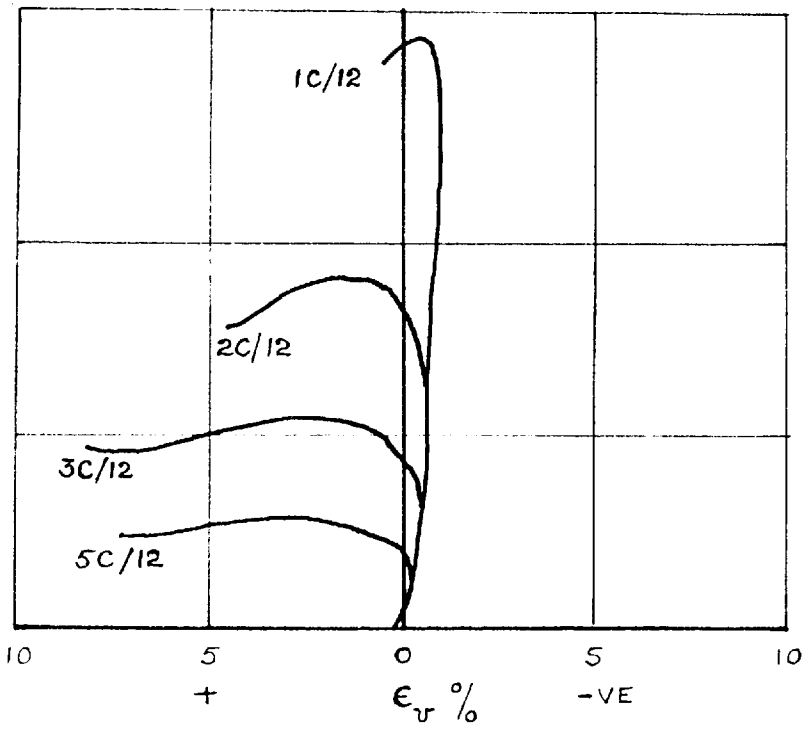
CHERT 12" DIA. SAMPLES.

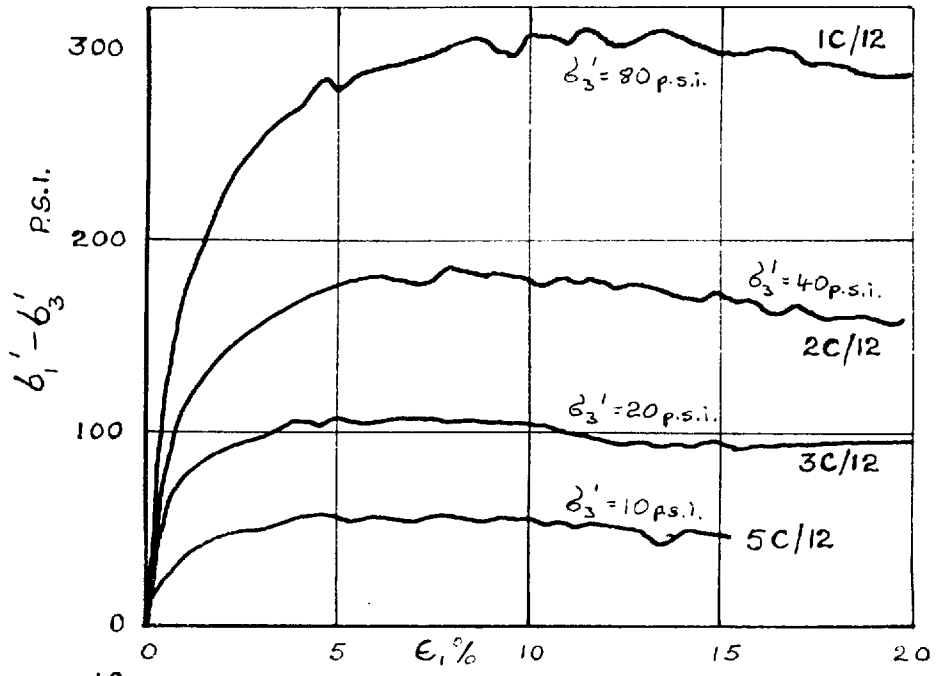
(SATURATED)

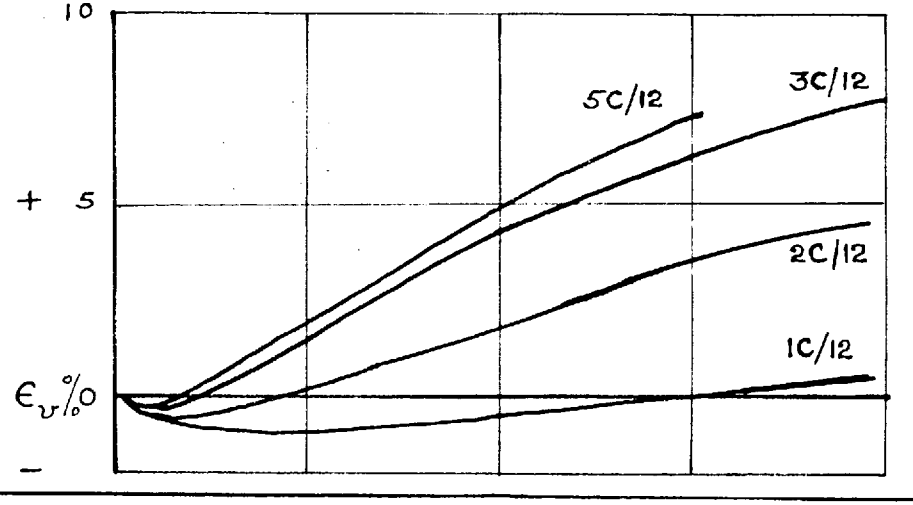
FIG. 9:2



THE RELATION BETWEEN ϕ'_f AND $(d\epsilon_v/d\epsilon_1)_f$ FOR CHERT SAMPLES. FIG. 9:3



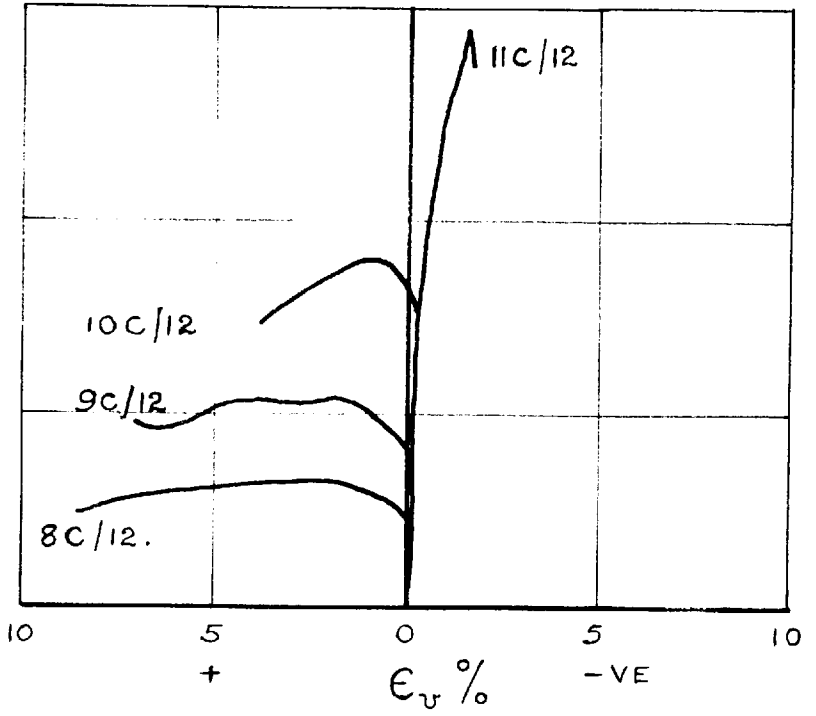


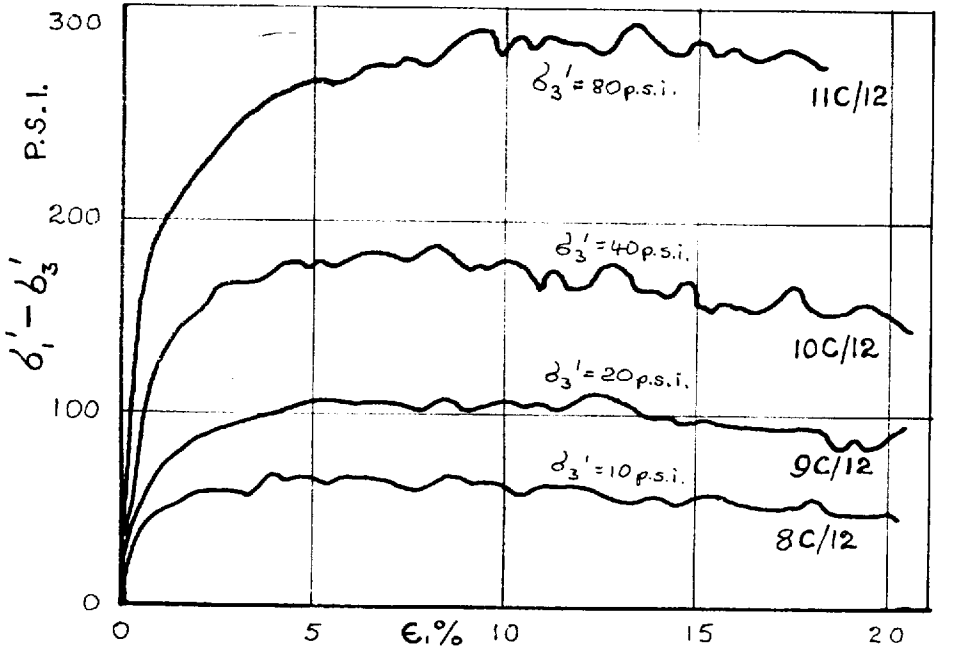


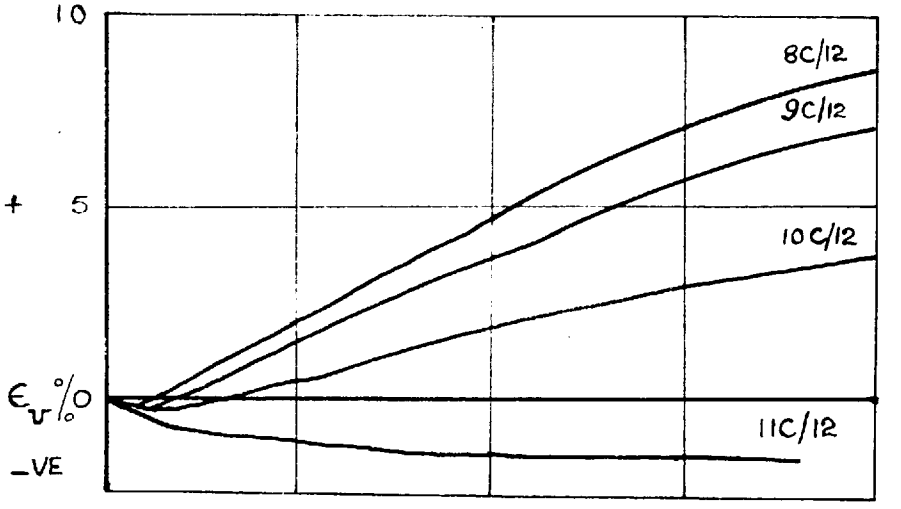
CHERT

$\frac{3}{4}$" ~ $\frac{3}{8}$"

FIG. 9:3A



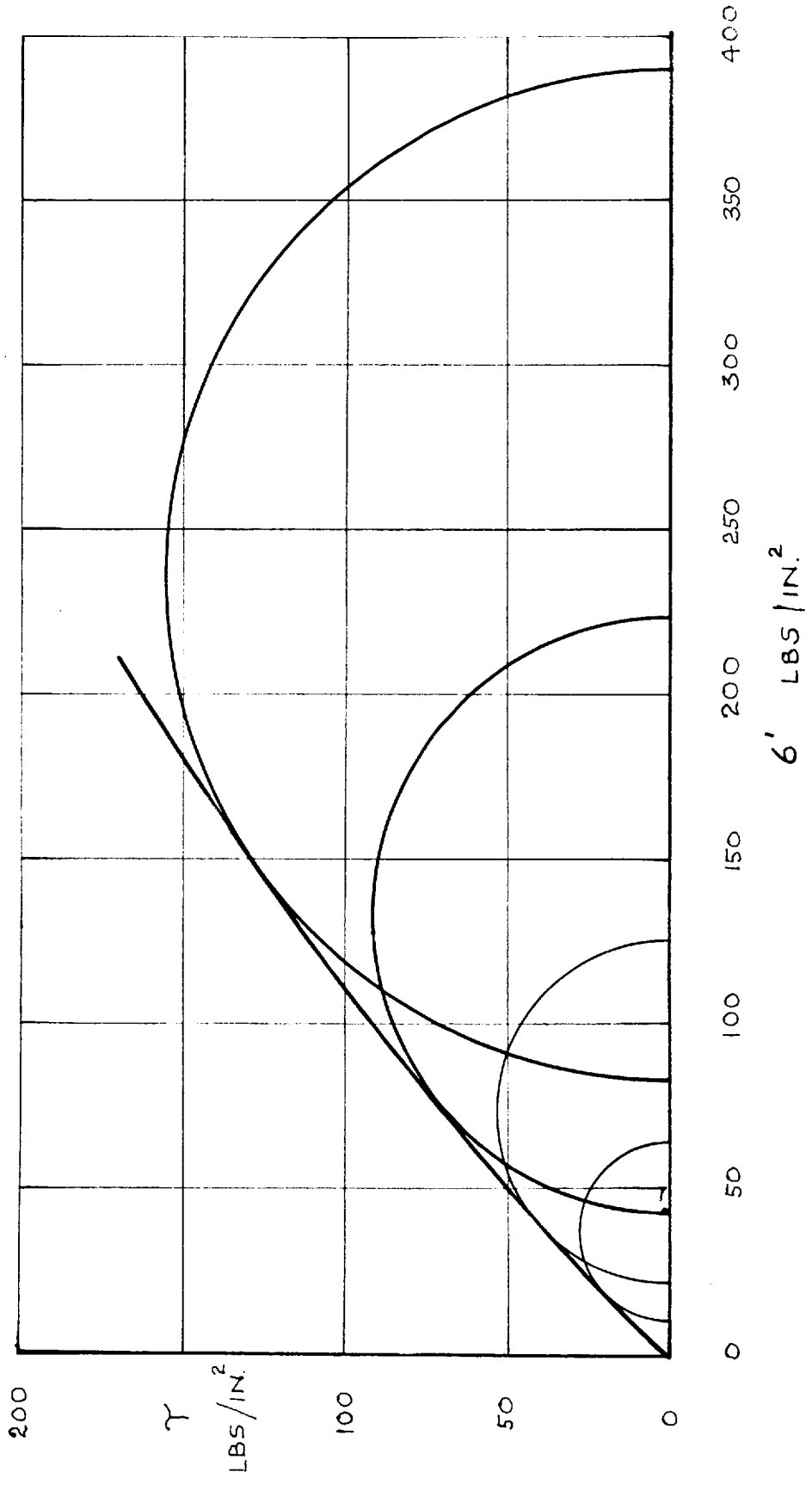




CHERT

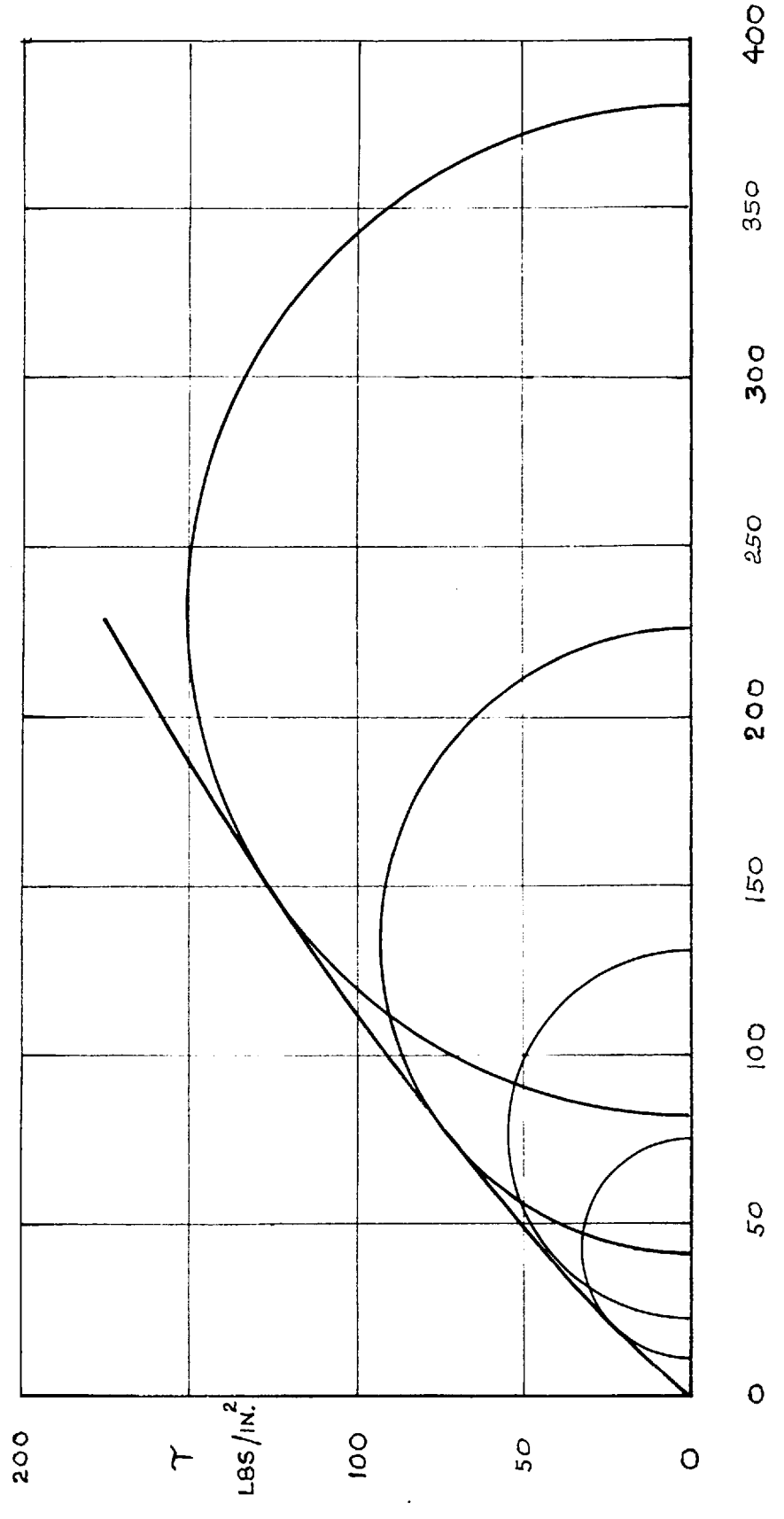
$1\frac{1}{2}$" ~ 3/4".

FIG. 9:38



MÖHR FAILURE CIRCLES
CHERT 3/4"-3/8".

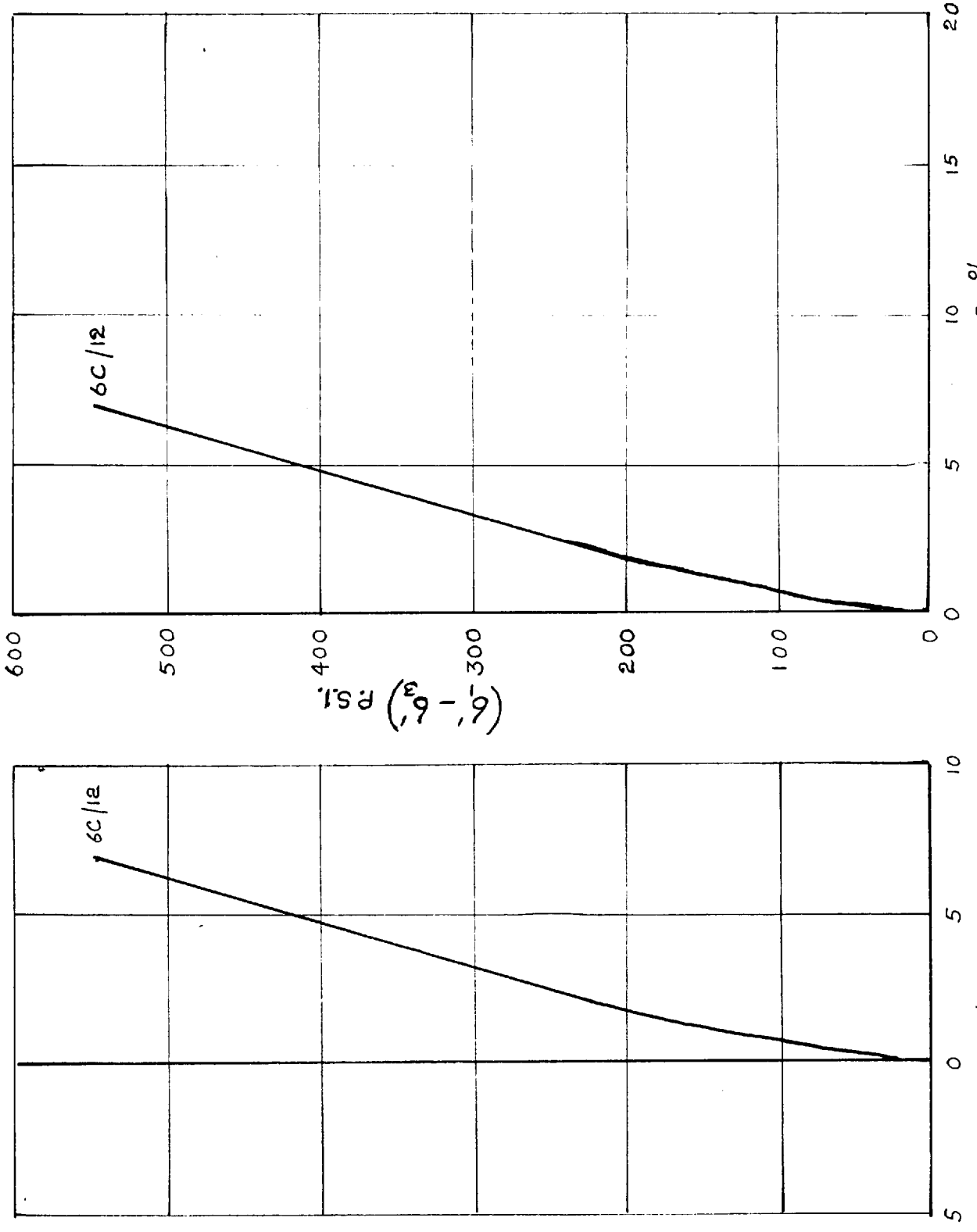
FIG. 9:3C

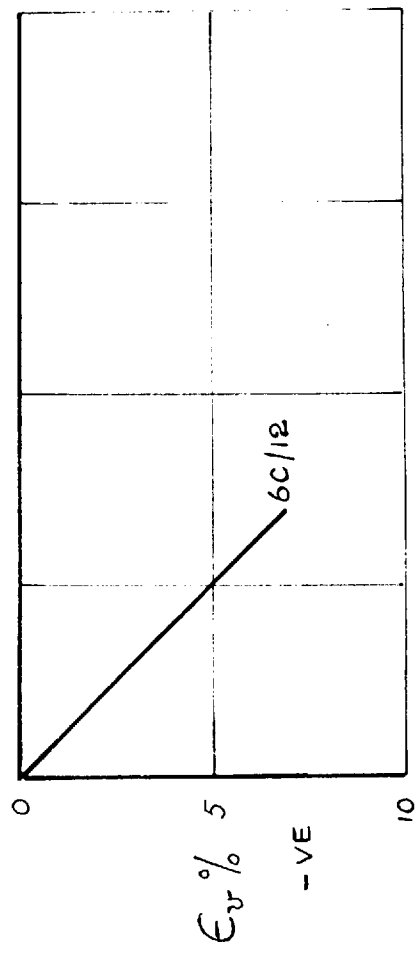


MÖHR FAILURE CIRCLES

CHERT 1½" - ¾".

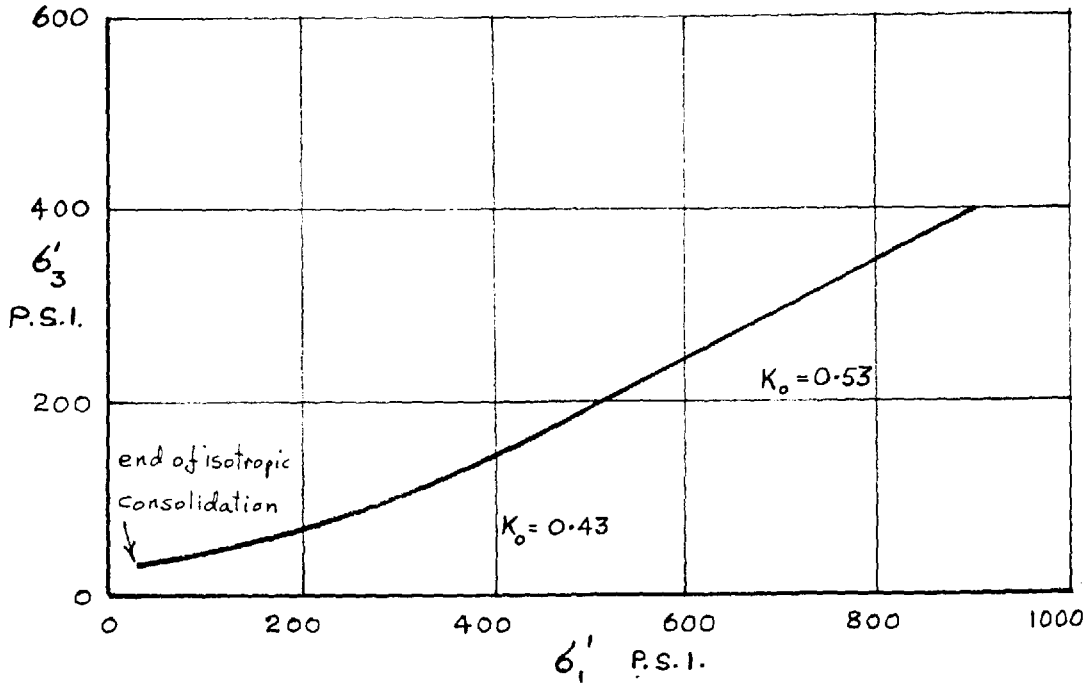
FIG. 9:3D

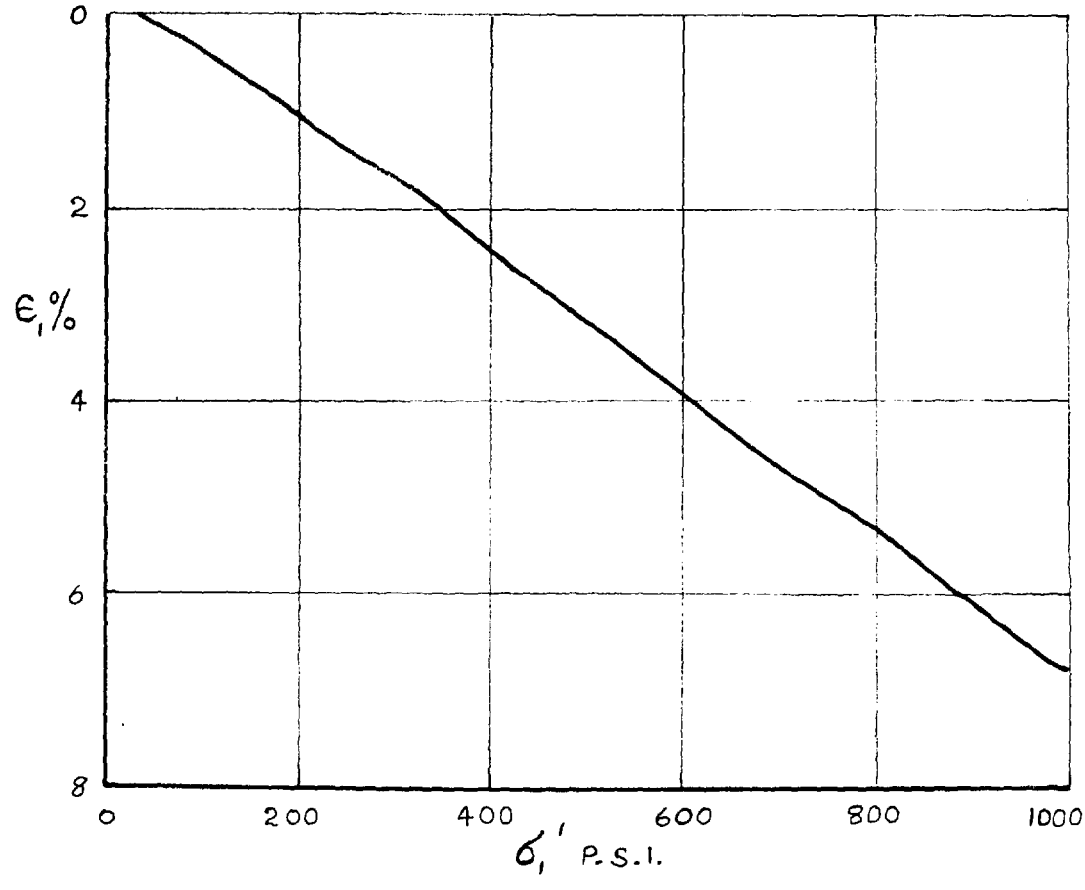




CHERT
3/4" – 3/8"
K_o TEST.

FIG. 9:4:3A





K_o TEST ON 3/4" - 3/8" CHERT.

FIG.

Test No.	1C/12	2C/12	3C/12	4C/12	5C/12	6C/12	7C/12	8C/12	9C/12	10C/12	11C/12
Type of test.	DS	DS	DS	DS	DS	K_o	K_o	DS	DS	DS	DS
Nominal σ_3' (P.S.I.)	80	40	20	10	10			10	20	40	80
Axial strain rate % per hour.	9.03	8.88	8.65	8.82	9.12			8.77	8.67	8.88	8.81
ϕ_f'	41.0°	43.9°	46.5°	54.0°	46.8°			50.5°	46.0°	43.8°	40.5°
Tan ϕ_f'	0.869	0.962	1.054	1.376	1.065			1.213	1.036	0.959	0.854
$\frac{1}{2}(\sigma_1'-\sigma_3')_f$ (P.S.I.)	154.6	92.1	53.7	48.3	27.1			32.9	54.9	92.0	150.0
$\frac{1}{2}(\sigma_1'+\sigma_3')_f$ (P.S.I.)	235.5	133.0	74.1	59.8	37.2			42.6	76.3	133.0	231.0
$\sigma_1'_f$ (P.S.I.)	390.1	225.1	127.8	108.1	64.3			75.5	131.2	224.9	381.1
$\sigma_3'_f$ (P.S.I.)	80.9	40.9	20.4	11.5	10.1			9.7	21.4	41.0	81.0
$(d\epsilon_v/d\epsilon_1)_f$	-0.133	-0.342	-0.565	-0.034	-0.605			-0.508	-0.350	-0.285	+0.005
γ_d lbs/ft^3	98.2	95.7	97.3	94.5	94.8	97.4		93.7	97.6	98.5	99.0
R_d %											
n %											
Effective stress when measuring P.S.I.	6.25	6.16	1.2	1.2	6.1			1.0	1.0	1.0	1.0
ϵ_{1f} %	11.43	7.81	7.16	19.75	5.33			3.84	12.68	8.22	13.35
ϵ_{vf} %	-0.32	+1.16	+2.84	+2.05	+2.22			+1.47	+4.81	+1.27	-1.58
Membranes	1/8" R.F.	1/8" R.F.	1/8" R.F.	1/8" R.F.	1/8" R.F.	3/16" R.F.		3/16" R.F.	3/16" R.F.	3/16" R.F.	3/16" R.F.
k before test (cms/sec)											
mean stress for above $\frac{1}{3}(\sigma_1'+2\sigma_3')$ (P.S.I.)											
k after test (cms/sec).											
mean stress for above $\frac{1}{3}(\sigma_1'+2\sigma_3')$ (P.S.I.)											
γ_d at failure (lbs/ft^3)	100.3	95.8	95.4	93.4	92.8			94.9	95.8	100.9	105.4
Grading.	3/4"-3/8"	3/4"-3/8"	3/4"-3/8"	3/4"-3/8"	3/4"-3/8"	3/4"-3/8"		1½"-3/4"	1½"-3/4"	1½"-3/4"	1½"-3/4"
Type of failure.	B	B						B/S	B	B	B
Remarks.											

TRIAXIAL TESTS ON 12" DIAMETER SAMPLES OF CHERT.

TABLE. 9A

CHAPTER 10

CONCLUSIONS

(10:1) Consolidation

The primary object of the research programme was not to study consolidation. Membrane penetration played a noticeable part in those stages of the tests in which σ'_3 was varying.

The apparent volume changes during isotropic consolidation of dense samples of silurian cleaved mudstone, granitic gneiss and chert were as large as or greater than those of loose sand (Figs.7:2:1, 7:2:3, 8:2:1 and 8:2:2). Loose sand showed a greater volume change for a given mean effective stress ($\frac{1}{3}(\sigma'_1 + \sigma'_2 + \sigma'_3)$) when subjected to shear stresses (from test data given by Skinner and Bishop 1966). The granitic gneiss also showed a greater volume change, for a given mean effective stress, under anisotropic stress conditions but this effect was not so apparent with the silurian cleaved mudstone. As expected, denser material underwent a smaller volume change for a given applied effective stress.

If a rockfill, no matter how dense, is compacted and consolidated in the dry state it will undergo, whilst subject to constant effective stress, further consolidation on first wetting. With the mudstone this was very substantial, varying between 49% and 211% of the previous apparent volume change in the dry state. (Fig.7:2:1). This phenomenon was less marked with the granitic gneiss, 30% being about the maximum and this figure was confirmed by tests in oedometers (Pigeon 1969). The minimum average moisture content required to prevent this sudden collapse on wetting was about 5% (this moisture content may well vary for other materials) for the mudstone (Howkins 1966). It is, therefore, necessary to keep a rockfill embankment wet during construction in order to minimise post construction settlement.

(10:2) Shear Strength

There is a very marked curvature of the Möhr failure envelope for densely compacted rockfill. For the silurian cleaved mudstone ϕ'_f reduced from about 50° to 34° for values of σ'_3 from 10 p.s.i. to 500 p.s.i. respectively. For granitic gneiss ϕ'_f reduced from about 60° to 40° over a similar stress range (Figs.7:3A, 8:3A). This demonstrates the importance of testing representative material at the relevant effective stresses.

The angle of internal friction depends on the effective stresses and the particle shape and strength. Materials obtained by blasting are generally angular and irregular. At low stresses, therefore, many quarried

materials demonstrate high angles of internal friction because of their irregular shape. At high stresses the contacts fracture and there is a reduction in dilatancy, which is then mainly governed by the particle strength and overall shape. Densely compacted, uniform gradings of rockfill at high stresses, and / or weak material, have dilatancy characteristics similar to those of loose sand (Fig.7:30).

For practical purposes there seems to be little significant variation of shear strength with sample size if geometrically similar gradings are used (Figs.10:2:1, 10:2:2).

Horne (Skinner 1969)* derived a theoretical relationship between ϕ_{cv} and $\phi\mu$ for triaxial conditions on the assumptions that the particles did not roll or crush. This relationship is plotted (Fig.10:2:3) with the results of the triaxial tests on rockfill and data obtained by Skinner from shear box tests on spherical materials. The theoretical relationship did not describe the behaviour of the spherical materials or the rockfill although this is inconsistent in the latter case because of the particle breakdown. The difference in the value of ϕ_{cv} for the spherical material and the rockfill clearly demonstrates the effect of the particle shape on the angle of internal friction.

The angle of friction between the particle surfaces does not seem to play a dominant part in determining the angle of internal friction. A very similar value of ϕ_{cv} was obtained for each material (chert 40°, mudstone 41° and granite 41°) although $\phi\mu$ varied from 11.5° to 36°. Basalt and metavolcanic rock also gave a value of ϕ_{cv} of 41° (Fig.10:2:4). Other tests on rhyolite obtained by ripping and blasting again gave a value of ϕ_{cv} of 41° (private communication). ϕ_{cv} for Ham River sand is about 33° and for steel balls (in the shear box) 22° (after Skinner 1969)

The plot of ϕ'_f against the rate of dilatancy at failure suggested that the ratio of sample diameter to particle size should be equal to, or greater than, 16 for samples tested under triaxial conditions for the same dilatancy although ϕ_{cv} is relatively insensitive to the $D/_d$ ratio.

On a plot of ϕ'_f versus porosity for all the granitic gneiss samples the effect of the ratio of sample diameter to particle size was not evident. This plot also demonstrated that ϕ'_f was more sensitive to the initial porosity at low stessses (Fig.10:2:5). A similar plot for samples of silurian cleaved mudstone sheared at a minor principal effective stress of 10 p.s.i. is given in Fig.10:2:6.

The angle of internal friction for a given material and effective stress is dependant on its initial relative density (Fig.10:2:5).

Tests on small scale samples showed that the angle of internal friction was about 4° lower for saturated than for dry granitic gneiss.

*To be published in Geotechnique March 1969.

The difference was only about 1° or 2° for the mudstone (Pigeon 1969).

The samples which were failed by increasing the stress ratio whilst reducing the mean effective stress had an angle of internal friction 1° to 2° higher than those failed by increasing σ_1'. Fraser (1957) noticed a similar effect when shearing sand; in this case the increase was 2° to 3°.

The stress path to failure of a rockfill, under undrained conditions is very dependant on the initial relative density. For greatest stability under undrained transient loading a material which wishes to dilate is to be preferred. This is best achieved by a well graded material with strong particles and which is compacted initially to maximum relative density.

The silurian cleaved mudstone was friable compared with the granite and chert and yet it demonstrated an angle of internal friction only 3° to 4° below the high values for the granite and 1° or 2° above those of the chert within the stress range shown in Fig.10:2.

The Möhr failure envelopes for various materials are compared in Fig.10:2:7.

(10:3) Deformation

As with sand loose material has an axial failure strain greater than dense material at a given effective stress.

The axial failure strain increases with increase in effective stress (Figs.10:3:1 and 10:3:2).

Loose material tends to consolidate during shear, even at low stresses.

At low stresses dense samples of chert and granitic gneiss showed a large dilatancy. The silurian cleaved mudstone did not show a great dilatancy even at low stresses. At high stresses all the materials tended to behave more as loose sand.

The volume strain of the mudstone for a given stress increment was greater when it was saturated than when it was dry (Fig.7:2:1).

The secant value of the coefficient of one dimensional compressibility decreases with increase in stress after an initial hump which is due to the effects of compaction (Figs.7:4:10h and 8:4:8d).

Material which was failed by increasing the stress ratio whilst reducing the mean effective stress had an axial strain to failure about $\frac{1}{3}$ to $\frac{1}{2}$ of that failed by increasing stresses.

After the peak deviator stress has been reached in drained tests on dense samples there is often a reduction in shear strength with increase in deformation. This should be borne in mind when determining the shear strength along a shear surface as highly stressed material reaches peak strength at greater strains and due allowance should be made to avoid the possibility of progressive failure.

Geometrically similar gradings in various sizes of sample have comparable axial and volumetric strain characteristics.

Within the working range of stress there is a linear relationship between volumetric strain and deviator stress (See stress-strain curves).

Rockfill creeps under load for an indeterminate period of time. Field evidence is given by the crest settlements of dams, some of which are still deforming 50 years after construction (Kjaernsli 1962). At a given time, after the initial immediate settlement, the rate of creep seemed to be independent of effective stress at the Venemo Dam (Kjaernsli 1962) although laboratory evidence by Lovenbury (1969) suggests that this may not be precisely true.

(10:4) Particle Breakdown

Particle breakdown increases with increase in maximum particle size uniformity of grading, mean effective stres and stress ratio and the angularity of the particles (Lee and Farhoomand). It is inferred that an increase in breakdown also occurs with a decrease in particle strength and on wetting and with increase in strain.

The mudstone had flat, platey, friable particles, the granite irregular, angular, hard particles and the chert smooth, tuberous, hard particles. For a given stress system the breakdown recorded was of the same order of magnitude for each material. A direct comparison though is misleading because the chert had a uniform grading and the mudstone contained a greater proportion of fines than the granite.

Other materials, however, under the same stress system may break down by varying amounts. It is thus important to determine whether materials for filters, which are usually made up of uniform gradings, will satisfy the filter requirements and remain pervious when they and adjacent materials are subject to effective stress.

The fine fractions of the silurian cleaved mudstone formed an impermeable paste. Some other materials may perform likewise and it is important to determine the permeability after breakdown under various stress ratios and effective stresses if the material is to be subjected to rapid draw down. A material which forms an impermeable paste is also unsuitable for filters.

A saturated material with a grading and/or particle strength such that it is prone to considerable breakdown, will tend to produce high pore pressures and a low shear strength under undrained loading and may be expected to behave in a similar manner under seismic loading.

(10:5) Sample size

There are distinct practical advantages to be gained by testing small size material because membrane failures are less likely and errors due to membrane penetration, when σ_3' is varying, are reduced. The handling, processing and testing are generally easier and cheaper although one instance was recorded where the cost of hand picking fine particles to achieve similar particle shapes in the large and small fractions of a grading outweighed the cost of large scale testing.

Three very different materials were tested in this research programme, platey friable mudstone, angular, hard granite and smooth, tuberous chert. For practical purposes the shear strength of each material was independent of particle size for geometrically similar gradings.

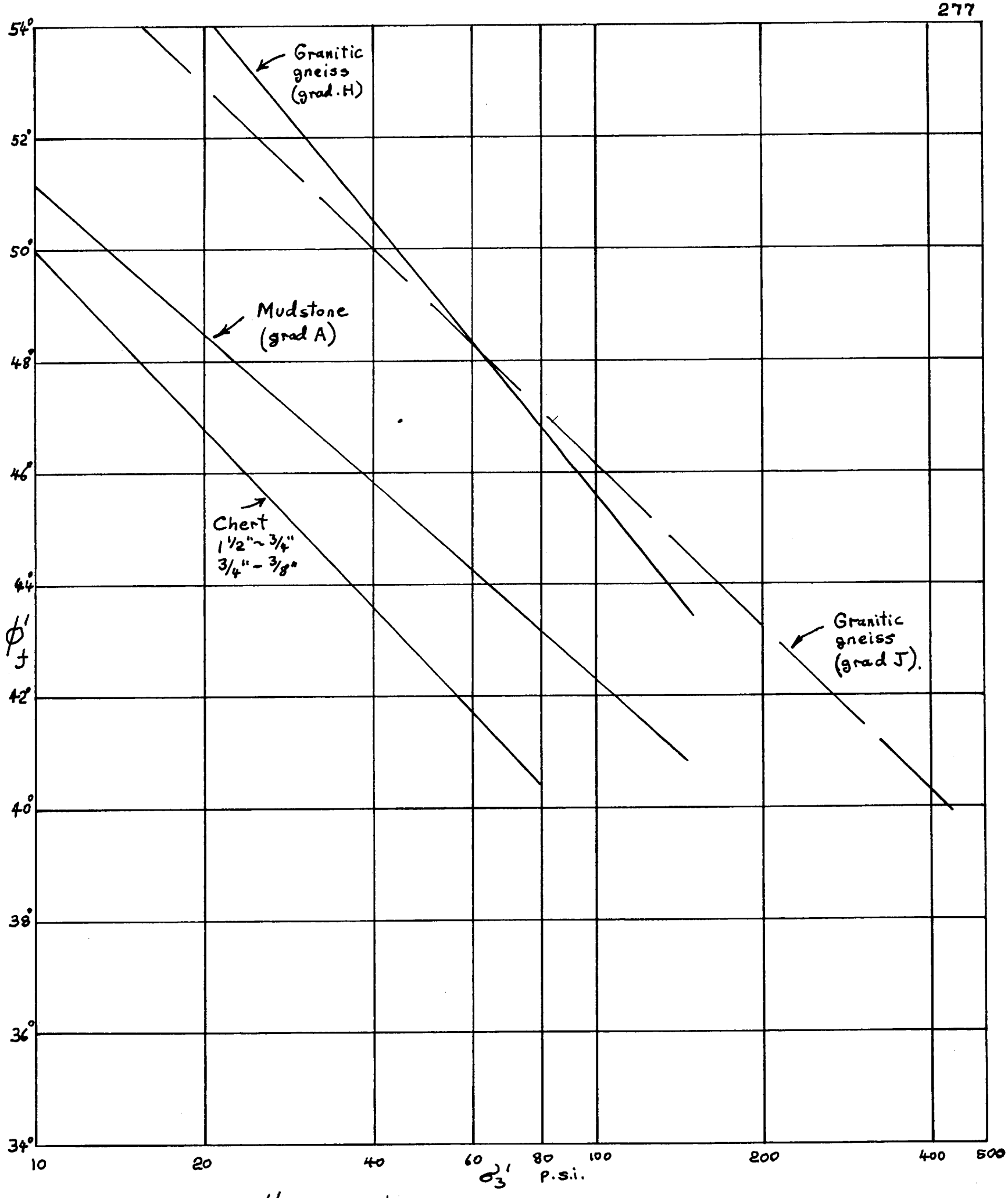
It appears that representative behaviour of a material is obtained, in a geometrically scaled model grading of the original, if it fractures during excavation in such a way that the particles of the resultant grading have similar shapes and unit strengths.

(10:6) Recommendations for future research

Future studies might profitably be undertaken to determine the effects of variations in grading on the shear strength and dilatancy of a material.

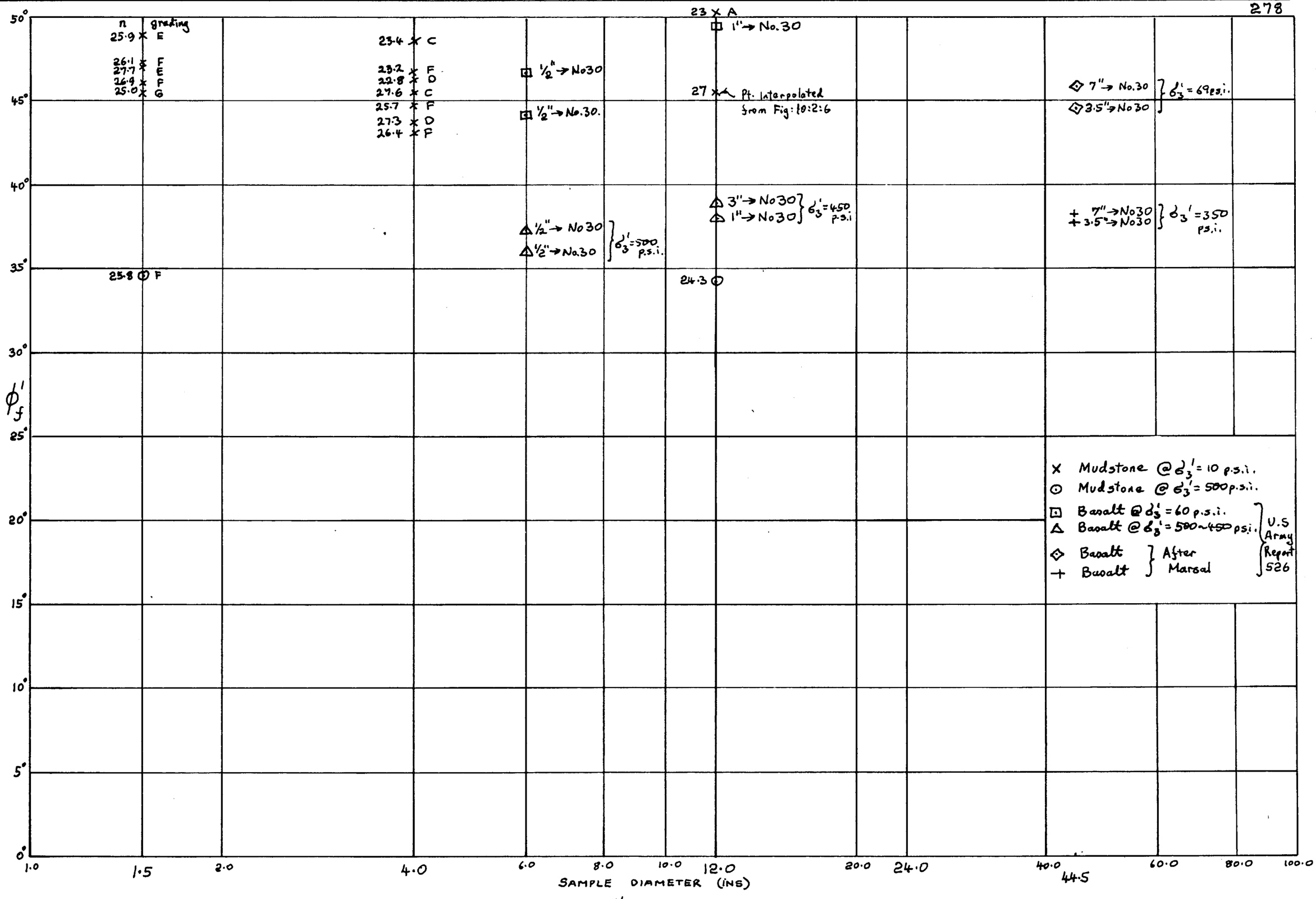
Different materials should also be tested, using a common grading, to determine the variation of shear strength with particle shape and strength and the breakdown of the materials might then be compared.

A programme should be initiated to correlate the results of the research which has been published to date and also an attempt should be made to extract the details of unpublished work for the benefit of other engineers.



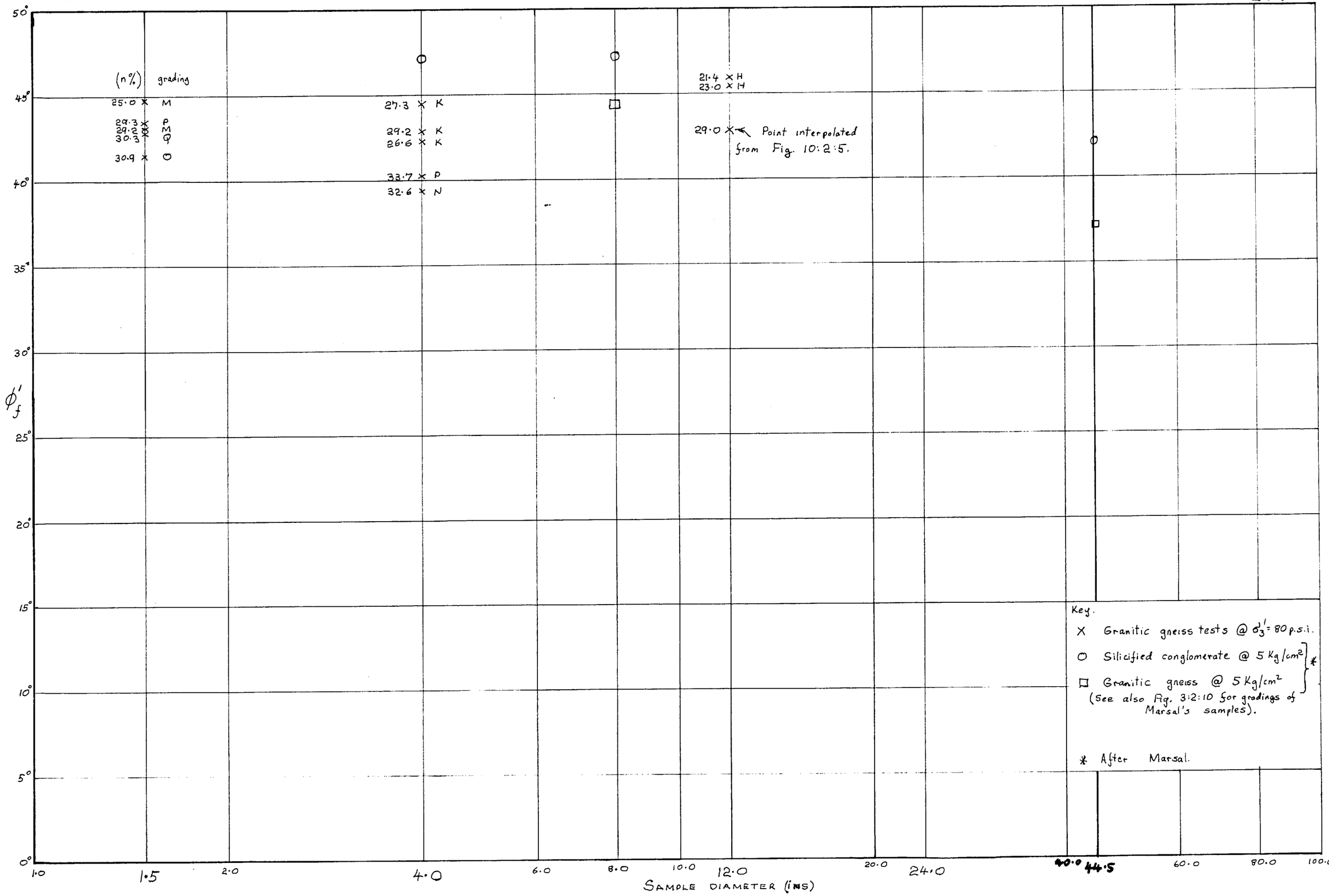
THE RELATION BETWEEN ϕ'_f AND σ'_3 FOR DENSE SAMPLES OF SILURIAN CLEAVED MUDSTONE, GRANITIC GNEISS AND CHERT.

FIG. 10:2.



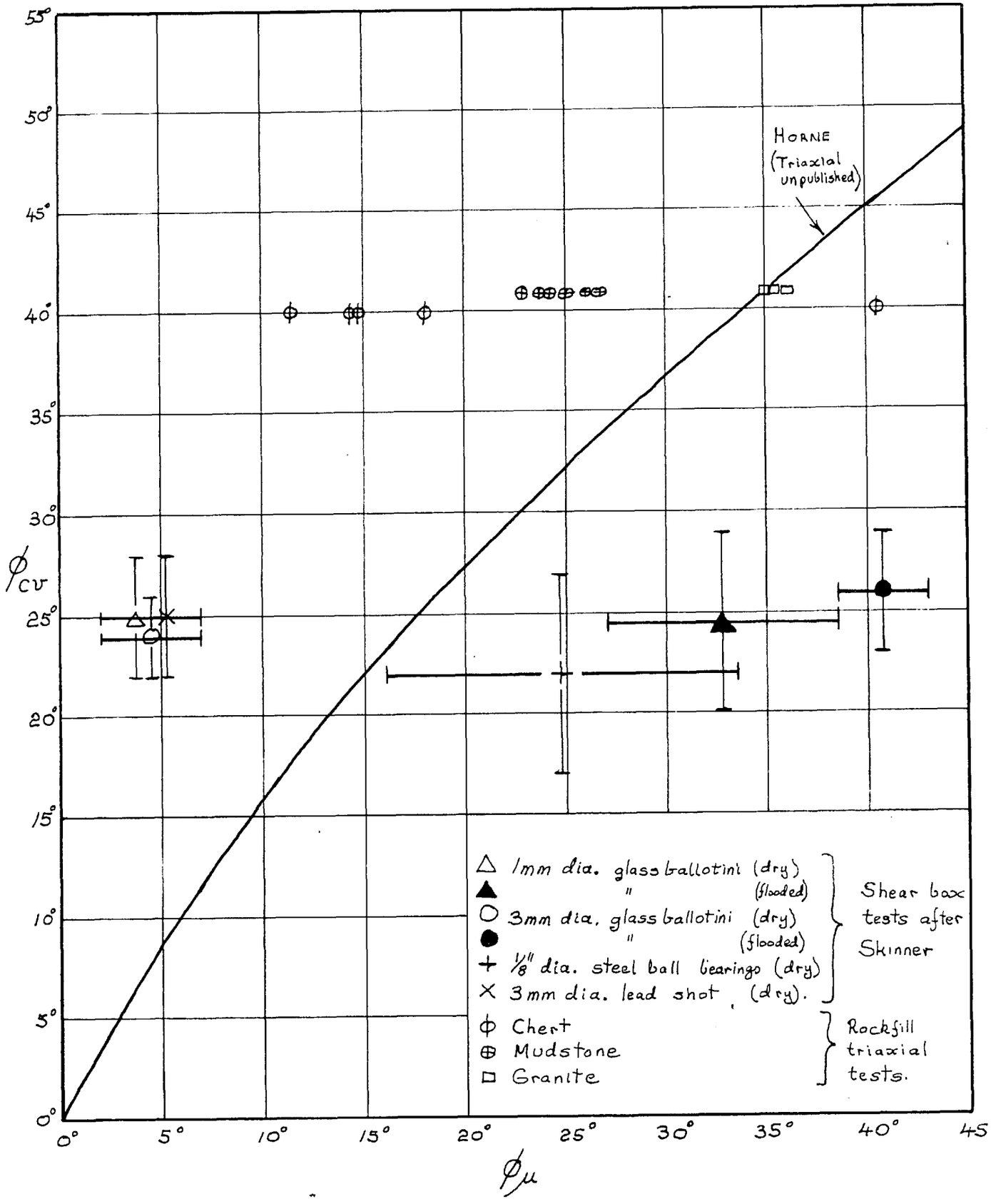
THE RELATION BETWEEN SAMPLE DIAMETER AND ϕ_f' FOR SAMPLES OF SILURIAN CLEAVED MUDSTONE

FIG. 10:2:1.



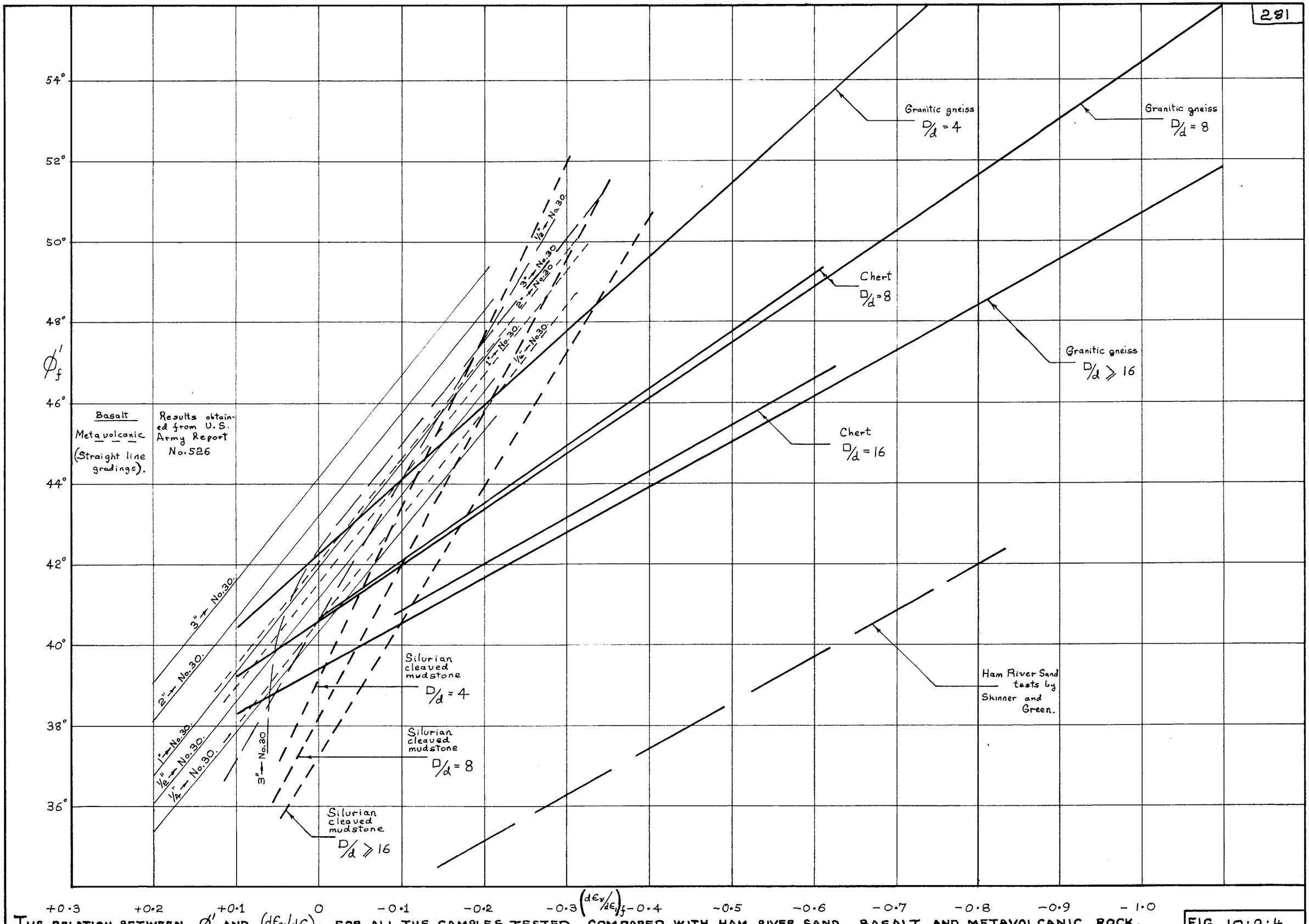
THE RELATION BETWEEN SAMPLE DIAMETER AND ϕ'_f FOR SAMPLES OF GRANITIC GNEISS.

FIG. 10:2:2



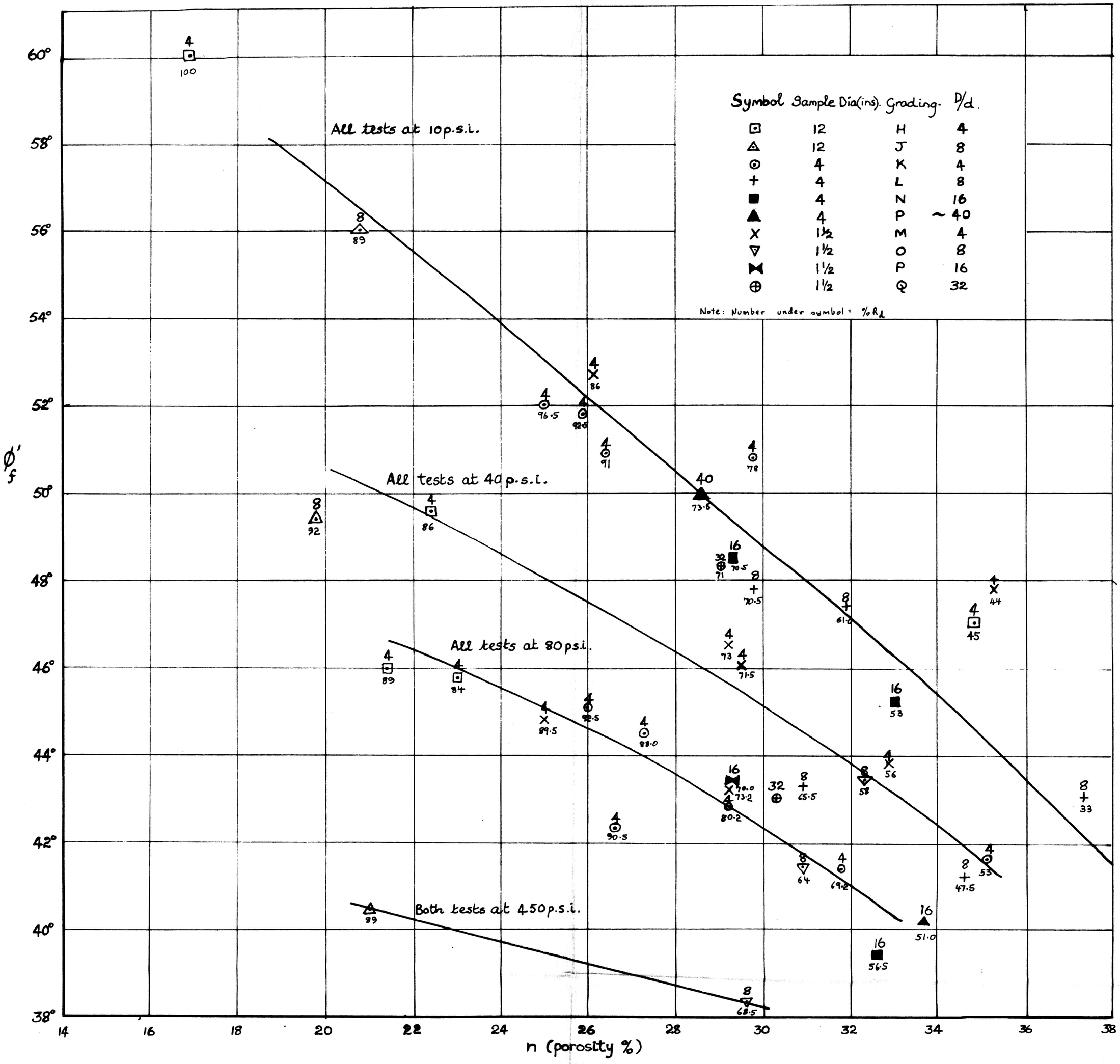
THE RELATION BETWEEN ϕ_{cv} AND ϕ_μ.

FIG. 10:2:3.



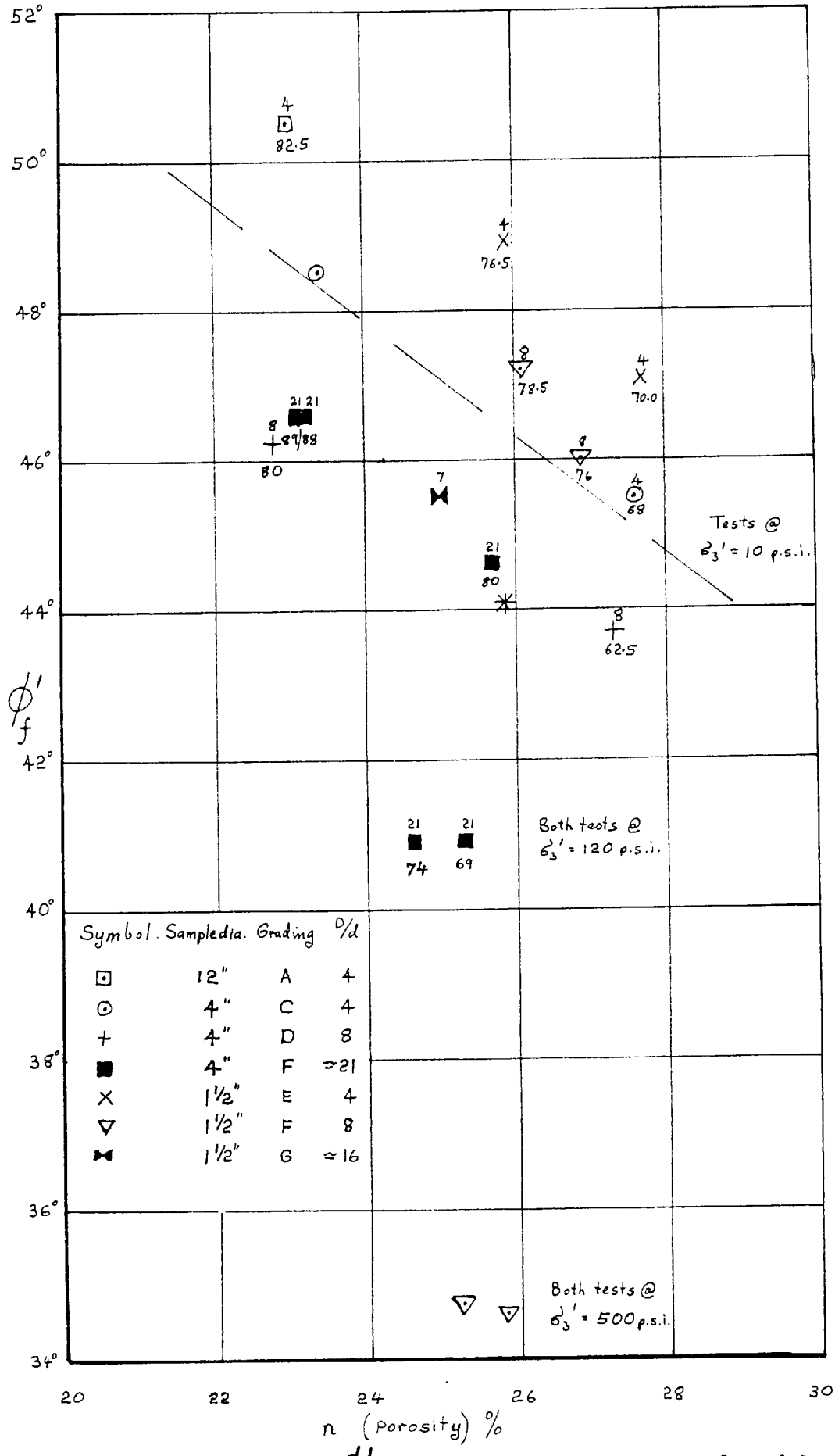
THE RELATION BETWEEN ϕ'_f AND $(d\epsilon_v/d\epsilon_1)_f$ FOR ALL THE SAMPLES TESTED COMPARED WITH HAM RIVER SAND, BASALT AND METAVOLCANIC ROCK.

FIG. 10:2:4



THE RELATION BETWEEN ϕ'_f AND n FOR SAMPLES OF GRANITIC GNEISS.

FIG: 10: 2:5



THE RELATION BETWEEN ϕ'_f AND n FOR SAMPLES OF SILURIAN CLEAVED MUDSTONE

FIG. 10:2:6

Key

① Dense granitic gneiss 12" dia. samples.
② Dense mudstone 12" dia. samples.
③ Dense uniform chert 12" dia. samples.
④ Pinzandaran gravel.*
⑤ Angular silicified conglomerate.*
⑥ Diorite.* *(Marsal)
⑦ Ham River sand. (Bishop et al.).
⑧ Silty, sandy gravel. (Hall et al.).
⑨ Avonmouth clay. (Smotrych).
⑩ London clay. (Bishop et al.).

60° 50° 40° 30° 20° 10°

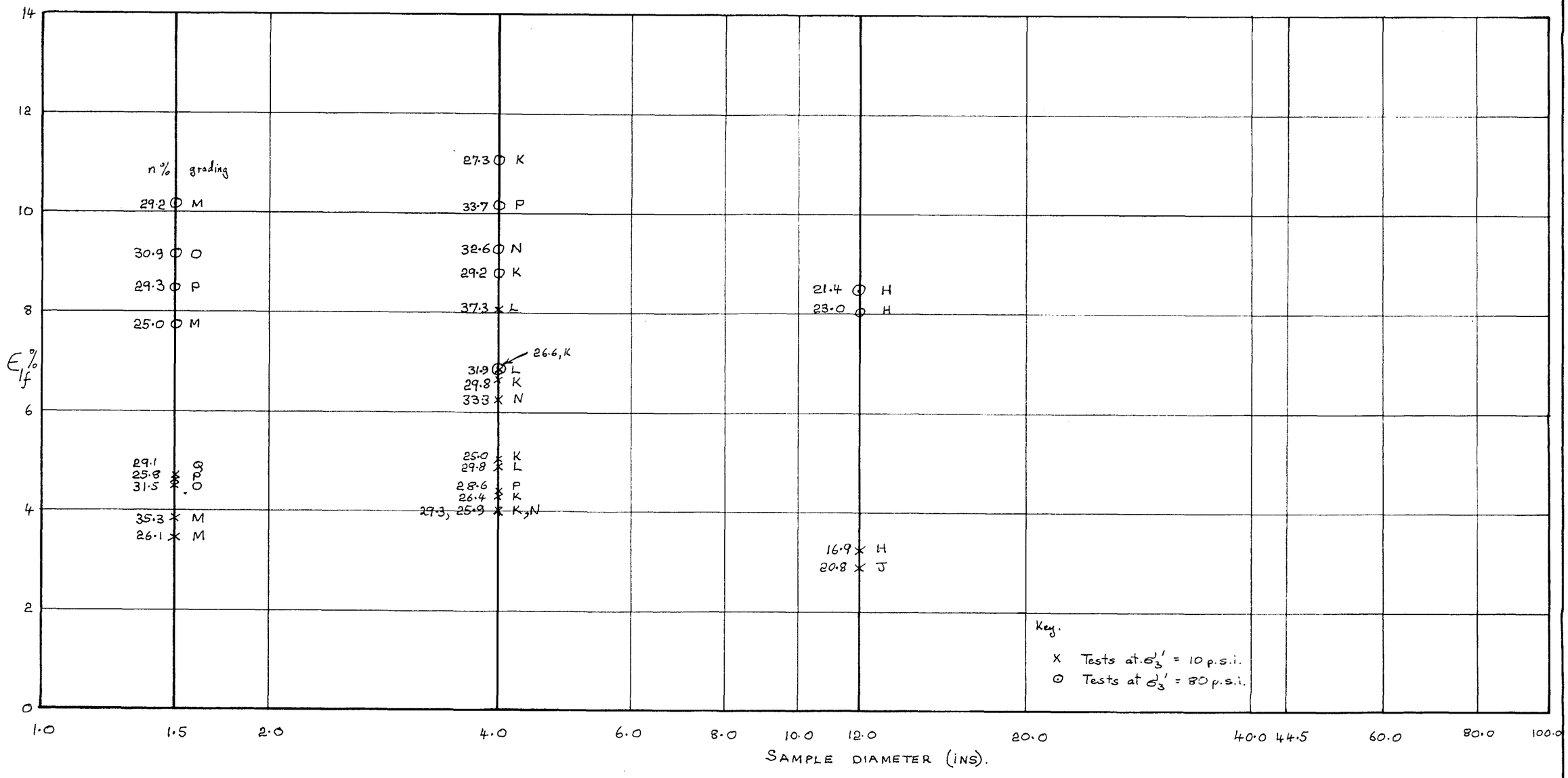
τ P.S.i.

0 100 200 300 400 500 600 700 800 900 1000 1100 1200 1300 1400 1500

σ P.S.i.

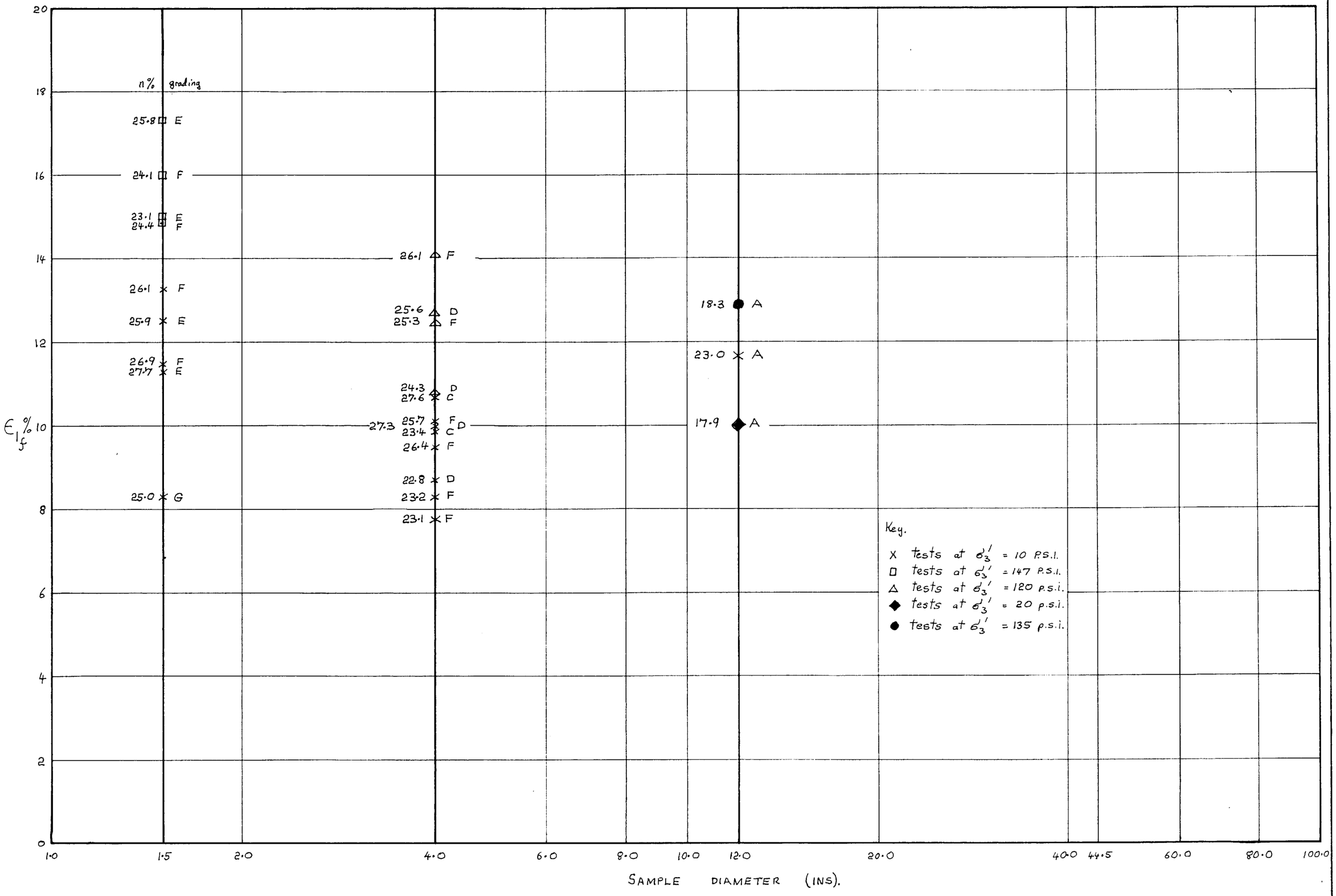
THE MÖHR FAILURE ENVELOPES OF SILURIAN CLEAVED MUDSTONE, GRANITIC GNEISS AND CHERT COMPARED WITH DIORITE, ANGULAR SILICIFIED CONGLOMERATE, PINZANDARAN GRAVEL, SANDY GRAVEL, HAM RIVER SAND, AVONMOUTH AND LONDON CLAYS.

FIG. 10:2:7



FAILURE STRAINS OF GRANITIC GNEISS SAMPLES

FIG. 10:3:1



FAILURE STRAINS OF SILURIAN CLEAVED MUDSTONE SAMPLES

FIG. 10: 3: 2

ACKNOWLEDGEMENTS

The research work reported in this thesis was carried out in the Soil Mechanics Laboratory of the Civil Engineering Department of Imperial College.

The author was particularly fortunate in being supervised by Professor A.W.Bishop whose contributions to Soil Mechanics and the engineering of earth dams are universally acknowledged.

Some of the data in this thesis is published with the kind permission of the Construction Industries Research and Information Association, The Director of The Royal Aircraft Establishment, Farnborough and Binnie and Partners, Consulting Civil Engineers.

Generous financial assistance for the construction and operation of the large triaxial apparatus was forthcoming from the Construction Industries Research and Information Association, The Science Research Council and Binnie and Partners.

The author was supported throughout the work, at first by a Science Research Council Studentship and later by a Research Assistantship from the Construction Industries Research and Information Association.

Thanks are also due to the Director of the Cement and Concrete Association for the loan of apparatus and facilities and also to the Director of the Norwegian Geotechnical Institute for kindly arranging the shipment of granitic gneiss from the Venemo Dam site.

The author is indebted to B.Stimpson and J.A.Franklin for the mineralogical analysis of the granitic gneiss.

Note: References marked with an asterisk are referred to in the text.

*Agarwal, K.B.1967. The influence of size and orientation of sample on the undrained strength of London Clay. Ph.D.Thesis. University of London.

Aisenstein,B.1965. Some observations on Deconsolidation of Limey Rocks on Steep Slopes. Proc.6th I.C.S.M.F.E. Vol.2 p.439. Montreal 1965.

Atkinson,G.H. 1967. Mangla (Construction). P.I.C.E. Nov.1967 pp 343 - 576. (Discussion Sept.1968.)

Balla,A. 1957. Stress conditions in the triaxial test. Proc.4th I.C.S.M.F.E. London 1957. Vol.I pp 140 - 143.

Barden, L. and McDermott, J.W. 1965. Use of free ends in triaxial testing of clays. Proc.Am.Soc.Civ.Engrs. 91 SM 6. 1 - 23.

Barocio, A.J. 1965. Infiernillo. Water Power, p 198 May 1965; p 217 June 1965; and p 280 July 1965.

*Baumann,P. 1941. Design and construction of San Gabriel Dam No.I A.S.C.E. Proc.Vol67 pp 1199 - 1238. 1941 and A.S.C.E. Trans.Vol. 107 pp 1595 - 1651. 1942.

*Baumann,P. 1958 Rockfill Dams: Cogswell and San Gabriel dams. Proc.A.S.C.E. Journal of Power Div.June 1958. Paper 1687.

Bernaix,J. 1966. Discussion: Properties of rocks and rock masses. Proc.1st. Int.Congress of Rock Mechanics.Vol.3 pp 279. Lisbon 1966.

*Bernaix,J. 1967. Un appareil de cisaillement pour échantillons de sols de grandes dimensions. Discussion. Proc. Geot. Conf. Vol.2 p 212, Oslo 1967.

Bernaix,J. 1967. La mesure de la résistance des roches. Proc.Geot. Conf. Vol.1 p 245. Oslo 1967.

Bernell,L. 1957 The properties of moraines. Proc.4th I.C.E.S.M.F.E. 1957.

Bernell,L. and Nilsson, R. 1957. Electrical Analogy Equipment for Solving Non-stationary Two - dimensional Flow Problems. Proc.4th I.C.S.M.F.E. 1957

Binnie, G.M. 1967 The effect of discontinuities in clay bedrock on the design of dams in the Mangla project. 9th I.C.O.L.D. Istanbul 1967.

Binnie,G.M. 1967. Mangla. P.I.C.E. Nov. 1967 pp 343 - 576. (Discussion Sept.1968).

*Bishop,A.W. 1948. A large shear box for testing sands and gravels. Proc.2nd. I.C.S.M.F.E. Vol.1 pp 207 - 211. 1948.

Bishop,A.W. 1952 Stability of earth dams. Ph.D. Thesis. University of London.

Bishop,A.W. and Gamal Eldin, A.K. 1953. The effect of stress history on the relation between ϕ and porosity in sand. Proc. 3rd. I.C.S.M.F.E. Vol.1. p.100. Zurich,1953.

*Bishop,A.W.1954. Correspondence on 'Shear characteristics of a saturated silt measured in triaxial compression' by A.D.M.Penman. Geotechnique 4. pp 43 - 45.

Bishop,A.W. 1954 The use of pore pressure coefficients in practice. Geotechnique 4. pp 148 - 152.

Bishop,A.W. 1955 The use of the slip circle in the stability analysis of slopes. Geotechnique, 5. pp 7 - 17.

Bishop,A.W. 1957 Some factors controlling the pore pressures set up during the construction of earth dams. Proc.4th. Int.Conf.S.M.F.E.2: pp 294-300.

Bishop,A.W. and Bjerrum,L. 1960. The relevance of the triaxial test to the solution of stability problems. Proc.Research.Conf. on Shear Strength of Cohesive Soils. p.437.

*Bishop,A.W. and Henkel,D.J. 1962. The measurement of soil properties in the triaxial test. Edward Arnold,London. 2nd ed.

Bishop,A.W. and Vaughan,P.R. 1962. Selset Reservoir: design and performance of the embankment. Proc.I.C.E. Vol.21. pp 305 - 346. 1962.

Bishop,A.W. and Kennard,M.F. and Vaughan, P.R. 1964. Developments in the measurement and interpretation of pore pressure in earth dams. Proc.8th. I.C.O.L.D. Edinburgh 1964.

*Bishop,A.W. 1965. Panel Discussion. Proc.6th. I.C.S.M.F.E. Vol.3, p.306. Montreal 1965.

*Bishop,A.W. 1966. The strength of soils as engineering materials. 6th. Rankine Lecture. Geotechnique Vol.16. P.91. 1966.

*Bishop,A.W. 1966. Soils and Soft Rocks as Engineering Materials. Inaugural Lecture. Imperial College.

Bishop,A.W. and Little, A.L. 1967. The influence of the size and orientation of the sample on the apparent strength of the London Clay at Maldon, Essex. Proc.Geot. Conf. Oslo. Vol.1

Bjerrum,L. and Jørstad,F. 1968. Stability of Rock Slopes in Norway. N.G.I. Publication No. 79

Blanc,G.J. 1963 The Derbandi Khan Dam. Water Power p.447 November 1963.

*Blight,G.E. 1963. Discussion: Pore pressures during triaxial compression. Laboratory Shear Testing of Soils. A.S.T.M. S.T.P. 361. P.199.

Bohn,M. and Hamon,M. 1967. The Djatiluhur Project. Water Power, p.305 Aug.1967.

*Bowden,F.P. and Tabor,D. 1956. Friction and Lubrication. Methuen,1967.

*Borowicka,H. 1963. Vienna method of shear testing. Laboratory shear testing of soils. A.S.T.M. S.T.P. 361. p 306.

*Brauns,J. and Leussink,H. 1967. Discussion: Large scale testing of rock-fill materials. A.S.C.E. Vol.93 No.S.M. 6 Nov.1967.p 383.

Breth,H. 1967. The dynamics of a landslide produced by filling a reservoir. 9th I.C.O.L.D. Q 32, 1967. p 37.

Broili,L. 1967. New Knowledge on the geomorphology of the Vaiont slide slip surfaces. Rock Mechanics and Eng. Geology. Vol.5 No.1, 1967.

Broms,B.B. and Jamal, A.K. 1965. Analysis of the triaxial test - cohesion-less soils. Proc.6th. Int. Conf. Soil Mech. I.184-188.

*Broscoe,A.J. 1967. Discussion: Compressibility of granular soil. Proc. Canadian Geotechnical Journal. Vol.4 No.1, Feb.1967.

*Brown,W.F.1965. The acoustic method of detecting crack propogation in metals. National Aeronautics and Space Administration.

Bukovansky,M. 1966. Three types of field shear tests on soft rocks. Proc. 1st. Congress of Rock Mechanics. Vol.1 p 343. Lisbon 1966.

Burgess,J.S. and Hicks,P.H. 1966. Riprap Protection for Slopes Subject to Wave Attack. CIRIA, May 1966.

*Burminster,D.M.1948. Importance and Practical Use of Relative Density in Soil Mechanics. Proc. Am. Soc. for Testing and Materials. Vol.48 pp 1249 - 1268, 1948.

*Burminster,D.M. 1964. Environmental factors in soil compaction. Compaction of Soils. Am.Soc.for Testing and Materials. S.T.P.377. p.47.

*Caquot,A. 1934. Equilibre des Massifs a Frattement Interne. Stabilite des Terres Pulverents et Coherentes. Paris: Gauthier Villars.

Caquot,A. La pressions dans les silos. Proc.4th. I.C.S.M.F.E. Vol.II, p.191.

Carlyle,W.J. 1965. Shek Pik Dam. Proc.I.C.E. March 1965 p 557 paper 6841.

Casagrande,A. 1961 Control of seepage through foundations and abutments of dams. Geotechnique Vol.II No.3. p 161.

Chauvin,J.M. 1961. The Cheffix Dam on the Oued - Bon - Namoussa. Travaux. Paris. English Version. May 1961 p 225.

Claydon,J.B. 1965. The Peace River Project. Water Power. p 339 Sept.1965.

Cooke, J.B. 1968. Rockfill Dams: Wishon and Courtright concrete face dams. Proc. A.S.C.E. Journal of Power Div.Aug. 1958. paper 1746.

*Cornforth,D.H. 1961. Plane strain failure characteristics of a saturated sand. Ph.D. Thesis. University of London.

*Cornforth,D.H. 1964. Some experiments on the influence of strain conditions on the strength of sand. Geotechnique Vol.XIV.1964.

*Coyne,A. 1958. Bigger and Better Dams. The French Contribution. Engineering News Record Sept.11th. 1958. p42.

Coyne,A. 1959. New Dam Techniques. Proc. I.C.E. Nov.1959. p. 285.

Creager,W.P., Justin,J.D. and Hinds, J. 1957. Engineering for Dams. J.Wiley, 1957.

Davis,C.V. 1958. Rockfill Dams: The Derbendi Khan Dam. Proc.A.S.C.E. Journal Power Div.Aug.1958 paper 1741.

Duffaut,M. et al. 1961. Resistance des barrages au glissement au contact betonrocher et sur une reprise de betonnage. 7th. I.C.O.L.D. Rome 1961.

Dunnicliff,C.J. 1968. Instrumentation of the Plover Cove Dam. Geotechnique 18 pp 283 - 300.

*Dvorak,A. and Peter,P. 1961. Field tests on soils and rocks. 5th. I.C.S M.F.E. Paris 1961. Vol.1, p 453.

Engelen,G.B. 1967. Landslides in the metamorphic northern border of the Dolomites (N.Italy). Eng.Geology. Vol.2 No.3 Dec.1967.

Erb.D.K. 1963. Symposium on Soil Exploration. A.S.T.M. S.T.P. 351 pp 3 - 16. 1963.

Evans, I. and Pomeroy,C.D. 1958. The strength of cubes of coal in uniaxial compression. Mechanical properties of non-metallic brittle materials. pp 5 - 28. Butterworth, London.

Evdokimov,P.D. 1958. Investigation of Foundation Strength and Shearing Resistance of Hydraulic Structures on Soft Soils and Rocks. 6th. I.C.O.L.D. New York 1958.

Feil,L.G. 1949. Unusual Design Problems - Harlan County Dam. Trans. Am.Soc.of Civ.Engs.Vol.114, p 321.

Fentzloff,H.E. 1967. A fundamental approach to tidal power. Water Power p 318. Aug.1967.

Fernandes,L.H.G. et al. 1958. Rockfill Dams: The Paradela concrete face dam. Proc.A.S.C.E. Journal of Power Div.Aug.1958. Paper 1747.

Fookes,P.G. 1965. Orientation of fissures in stiff,overconsolidated clay of the Siwalik system.Geotechnique Vol.15 pp 195-206. June 1965.

*Fraser,A.M. 1957. The influence of stress ratio on compressibility and pore pressure coefficients in compacted soils. Ph.D. Thesis. University of London.

*Frederick,M.R. 1962. The Significance of Particle Shape in Sand Behaviour, Ph.D. Thesis, University of Birmingham.

Fukuoka,M. 1957. Testing of gravelly soils with large scale apparatus. Proc.4th I.C.S.M.F.E. Vol.1 p 153. London 1957.

*Fumagalli,E. 1966. Stability of arch dam rock abutments. Proc.Ist.Int. Congress on Rock Mechanics. Vol.11 p 503.Lisbon 1966.

Fumagalli,E. 1968. Discussion: Problems in design and construction of earth and rockfill dams. A.S.C.E. Vol.94 S.M.2 March 1968 p 584.

Furon,R. 1963. The Problem of Water; A World Study. Trans.by Paul Barnes 1967 Faber and Faber Ltd.

Gamal Eldin, A.K. 1951. Some fundamental factors controlling the shear strength of sands. Ph.D. Thesis. University of London. 1951.

*Gibson,R.E. and Henkel,D.J. 1954. Influence of duration of tests at constant rate of strain on measured drained strength. Geotechnique. Vol.4. No.1. pp 6-15.

Gibson,R.E. 1963. An analysis of system flexibility and its effect on time lag in pore water pressure measurements. Geotechnique 13:1:1 1963.

Gibson,R.E. and Shefford,G.C. 1968. The efficiency of horizontal drainage layers for accelerating consolidation of clay embankments. Geotechnique 18 pp 327 - 335.

*Gilb,B. 1963. Discussion: Observations on settlements of fill.Proc. European Conf. on S.M.F.E. Vol.2 p 83.Wiesbaden 1963.

Gilb,B. 1965. A contribution to modern soil testing. Schweizerische Bauzeitung Vol.83. No.23. June 1965. p 413 6pp.10 ff.

Gilb,B.1965. Soil Mechanics Problems in the design of the Muttmark Dam. Schweizerische Bauzeitung Vol.83 No.11. March 1956 p 169, 10 pp 16 ff.

Golze,A.R. 1967. Power from Oroville. Water Power p 91. March 1967.

Golze,A.R. 1967. California leads the way in requiring safe dams. Water Power p 373 Sept.1967.

Gordon,B.B. and Hammond,W.D. and Miller,R.K. 1964. Effect of rock content on compaction characteristics of clayey gravel. Compaction of Soils. Am.Soc.for Testing and Materials. S.T.P. 377,1964.

Gordon,J.E. 1968. The new science of strong materials or Why you don't fall thro' the floor. Pelican 1968.

Growdon,J.P. 1958. Rockfill Dams: Nantahala sloping core dam. Proc.A.S.C.E. Journal of Power Div.Aug.1958 paper 1742.

Growdon,J.P. 1958. Rockfill Dams: Dams with Sloping Earth Cores. Rockfill Dams: Performance of Seven Sloping Core Dams. Proc. A.S.C.E. Journal of Power Div.Aug.1958. Papers 1743, 1744.

Habib,P. 1953. Influence of the variation of the average principal stress upon shearing strength of soils. 3rd.I.C.S.M. F.E. Switzerland 1953 Vol.1 pp 131-136.

Haefeli,R. 1965. Creep and Progressive failure in Snow,Soil,Rock and Ice. Proc.6th I.C.S.M.F.E. Vol.3 pp 134-148. 1965.

Haefeli,R. 1966. Discussion: Properties of rocks and rock masses.Proc. Ist Int.Conf.of Rock Mechanics.Lisbon 1966.Vol.3 p 272.

*Hall,E.B.and Gordon,B.B. 1964. Triaxial testing with large scale high pressure equipment S.T.P. 361. Amer.Soc.for Testing and Materials 1964.

Hanna, and Kennedy, Design of Dams. McGrow Hill 1938.

Harr,M.E. Groundwater and Seepage. McGrow Hill.

Hathaway,C.A. 1958. 'Dams - their effect on some ancient civilisations'. A.S.C.E. Civil Eng.Jan.1958 pp 58-63.

Haythornthwaite, R.M. 1960. Mechanics of the triaxial test for soils.Proc. Am.Soc.Civ.Engrs.86.S.M.5 pp 35062.

Hellstrom,B.1952. The oldest dam in the world. La Hoiulls Blanche,May - June 1952. pp 424-430.

*Henkel,D.J. and Gilbert,G.D. 1952. The effect of the rubber membrane on the measured triaxial compression strength of clay samples. Geotechnique Vol.3. pp 20-29.

Henkel,D.J. 1964. Stability of the foundations of Monar Dam. Proc.8th I.C.O.L.D.Q. 28 p 425 Edinburgh 1964.

Hilf,J.W. Estimating construction pore pressures in rolled earth dams. Proc.3rd I.C.O.L.D.

*Hillis,S.F. and Skermer,N.A. 1968. Discussion: Large scale testing of rockfill materials. A.S.C.E. Vol.94. No.S.M.I. Jan. 1968. p 326.

*Hirschfeld,R.C. and Poulos,S.J. 1963. High pressure triaxial tests on a compacted sand and an undisturbed silt. Laboratory shear testing of soils A.S.T.M. S.T.P. 361.

*Holestöl,K., Kjaernsli,B., and Torblaa,I. 1965. Compression of Tunnel Spoil at Venemo Dam. Proc.6th I.C.S.M.F.E. Montreal, Vol.2 p 490.

*Holubec,I. 1967. Discussion: Compressibility of granular soil. Proc. Canadian Geotechnical Journal.Vol.4 No.1 Feb.1967.

*Horn,H.M. and Deere,D.U. 1962. Frictional characteristics of minerals. Geotechnique. Vol.12 p 319. 1962.

Hoskins,A.D. 1956. Protective systems for seepage control in earth dams. Proc.2nd.Australia-NewZealand C.S.M.F.E.Vol.1.p 150.1956.

Hoskins,et al. 1968. A medium scale direct friction equipment. Int.journal of Rock Mechanics and Mining Science.Vol.5 pt.2.1968.

*Howkins,W. 1966. The compressibility of a coarse grained aggregate.M.Sc. Thesis. Imperial College,University of London. 1966.

Howkins,W. 1966. Internal Report Binnie and Partners. Report on 9" diameter oedometer tests on rockfill,carried out at Imperial College.

Hsu,S.J.C. and Ussami,A. 1967. The design and construction of Jupia earth embankments, Brazil. Proc.3rd Pan Am.C.S.M.F.E. Venezuela 1967. Vol.2 pp 77-97.

*Huber,W.G.1958. Rockfill Dams: Kenney and Cheakamus dams. Proc. A.S.C.E.Journal of Power div.Paper 1671.June,1958.

Huder,J. and Fetz,L.B. 1967. Shear strength and density of talus material used in the Gotschenenalp Dam.Proc.Geotechnical Conf. Oslo 1967. Vol.1 pp 205-207.

Hugon,A. and Costes,A. 1959. Le boulonnage des roches en souterrain. Eyrolles-Paris.

Hutchinson,J.N. 1967. Discussion: Proc.Geotechnical Conf. Oslo.Vol.2 p 214, 1967.

Idel,K.H. 1960. Die Scherfestigkeit rolliger Erdstoffe. Veroffenlichungen des Instituts für Bodenmechanik und Grundbau der Technischen Hochschule Fridericiana in Karlsruhe.Nr.2.

*Insley,A.E. and Hillis,S.F. 1963. Discussion: Hall and Gordon, Triaxial Testing with Large Scale High Pressure Equipment. A.S.T.M. S.T.P. 361, 1964.

*Insley,A.E. and Hillis, S.F. 1965. Triaxial shear characteristics of a Compacted Glacial Till under unusually high confining pressures. Proc. 6th. I.C.S.M.F.E. Montreal 1965. Vol.1 p 244.

*Insley,A.E. 1967. Discussion: Compressibility of granular soil. Proc. Canadian Geotechnical Journ l. Vol.4.No.1. Feb.1967.

Jaeger,C. 1968. Discontinuous creep of masses. Water Power.p 197. May 1968.

*Janbu,N. 1963. Soil compressibility as determined by oedometer and triaxial tests. Proc. European Conf. on S.M.F.E. Wiesbaden 1963. Vol.1 p 19.

Januskevicius,C.K. and Vey,E. 1965. Stresses and strains in triaxial specimens.Am.Soc.of Testing and Materials.S.T.P. 392.

Johnson,W.E. 1968. Large Dams in the U.S.A. Water Power.p445.Nov.1968.

Jones,M.P. and Fleming,M.G. 1965. Identification of Mineral Grains. Elsevier Publishing Co.Amsterdam.

Jørstad,F. 1968. Waves Generated by Landslides in Norwegian Fijords and Lakes. N.G.I. publication No.79.

Kallstenius,T. and Bergau,W. 1956. Investigations of soil pressure measuring by means of cells. Royal Swedish Geotechnical Institute Proc.No.12. Stockholm,1956.

*Kany,M. and Becker,H. 1967. Determination of the shear strength of a coarse grained rockfill by means of a large scale test. Proc. Geotechnical Conf. Oslo 1967.Vol.1 pp 209-213.

Kenney,T.C. 1967. Stability of the Vaiont Valley slope. Rock Mechanics and Engineering Geology.Vol.5 No.1,1967.

Kirkpatrick,W.M. and Belshaw,D.J. 1968. On the interpretation of the triaxial test. Geotechnique 18. pp 336-350.

Kjaernsli,B. 1962. Deformasjoner av fyllingsdammer.N.G.I.Pub.No.48. Oslo 1962

Kjaernsli,B. 1962. The Venemo Asphalt - Faced Rockfill Dam.N.G.I. Pub. No.69. Oslo 1966.

*Kjaernsli,B. and Sands,E. 1963. Compressibility of some coarse grained materials. Proc.European Conf. on S.M.F.E. Wiesbaden 1963. Vol.1, p 245.

Kjaernsli,B. 1968. General procedure in Investigation, Design and Control during Construction of Earth and Rockfill dams in Norway. N.G.I. Pub. No.80, 1968.

Kjellman, W. 1936. Report on an apparatus for consumate investigation of mechanical properties of soils. Proc. 1st.I.C.S.M.F.E. Vol.2 pp 16-20. 1936.

*Kjellman,W. and Jakobson,B.1955. Some relations between stress and strain in coarse grained,cohesionless materials. Royal Swedish Geotechnical Inst.Proc. No.9 Stockholm 1955.

Koenig,H.W. and Idel,K.H. 1964. Settlement measurements on a 52m.high rockfill dam with bituminous surface membrane.Proc. 8th I.C.O.L.D. Edinburgh,IV: 671

*Kolbuszewski,J. 1948. Research on packing and density of sands. Ph.D. University of London.

*Kolbuszewski,J.J. 1948. An experimental study of the maximum and minimum porosities of sands. Proc.2nd.Int.C.S.M.F.E. Vol.1 pp 158-165.

Kolbuszewski,J.J. 1963. The significance of particle shape and size on the mechanical behaviour of granular materials,Proc. European Conf.on S.M.F.E. Wiesbaden 1963. Vol.1 p 253.

*Krsmanovic,D. 1967.Discussion: Proc.Geotechnical Conf.Vol.2 p.205.Oslo.1967.

Krumhein,W.C. and Sloss,L.L. 1963. Stratigraphy and Sedimentation.W.H. Freeman and Co.Ltd. London.

*Ladanyi,B. 1967. Discussion: Compressibility of granular soil. Proc. Canadian Geotechnical Journal Vol.4 No.1 Feb.1967.

Lambe,T.W. 1963. An earth dam for the storage of fuel oil. Proc.2nd. Pan Am.Conf.of Soil Mechanics.Vol.2 p 257.Brazil 1963.

Lancaster -Jones,P. FF.1966. Methods of improving the properties of rock masses. Suramea Rock Mechanics Conf.1966.

Lane K.S. 1961. Field Slope Charts for Stability Studies.5th.I.C.S.M.F. E. Vol.2 p 651. Paris 1961.

La Rochelle,P. 1967. Membrane,Drain and Area Corrections in Triaxial Tests on Soil Samples failing along a single plane. Proc. 3rd. Pan Am.C.S.M.F.E.' Venezuela.

Laufer,H. 1961. Investigations for the earth core of Gepatsch Dam.Q.27 7th.I.C.O.L.D. Rome 1961

Laufer,H. 1964. The Gepatsch Dam in the Kauner Valley.Q.31.8th I.C.O.L.D. 1964.

Laufer,H. 1967. Uplift responsible for slope movements during the filling of Gepatsch reservoir.9th I.C.O.L.D. 1967. p 669.Q.32.

Laugher and Hargan. Handbook of fastening and joining of metal parts. McGraw Hill 1956.

Lauterbach,R. 1967. Friction under high normal pressures. Wear.Vol.10 No.6 pp 469 - 482. 1967.

*Lee,K.L.and Farhoomand,I. 1967. Compressibility and crushing of granular soil in anisotropic triaxial compression. Canadian Geotechnical Journal Vol.4 No.1 Feb.1967.

Leliavsky,S. 1965. Design of Dams for Percolation and Erosion. Chapman and Hall.

*Leonard,G.K. et al. 1958. Rockfill Dams: Performance of TVA central core dams. Proc.A.S.C.E.Journal of Power Div.Aug.1958, Paper 1736.

*Leslie,D.D. 1963. Large scale triaxial tests on gravelly soils. Proc.2nd Pan Am.Conf.S.M.F.E.Vol.1 p 181.Brazil 1963.

Leussink,H. and Wittke,W. 1963. Difference in triaxial and plain strain shear strength.Lab.shear testing of soils.A.S.T.M. S.T.P 361 p 77.

*Leussink,H. Effect of specimen size on the shear strength of granular materials. Panel discussion. 6th. Int.Conf. S.M.F.E. Vol.3 p316.

Lewis,J.G.1953. The sloping core principle for earth and rockfill dams. Ph.D. University of London. 1953.

*Lewis,J.G. 1956. Shear strength of rockfill. Proc,2nd. Australia -New Zealand C.S.M.F.E. Vol.I, 1956.

Lewis,W.A. 1957. A study of some of the factors likely to affect the performance of impact compactors on soil. Proc.4th. I.C.S.M.F.E. 1957.

Li,C.Y. and Oscar,M.V. 1967. Building earth dams in an area of residual soil in Columbia, S.America. Proc.3rd.Pan Am.C.S.M.F.E. Venezuela 1967. Vol.2 pp65-76.

Little,A.L. 1958. Compaction and Pore Water Pressure Measurement on some recent Earth Dams. Proc.6th.I.C.O.L.D. Q.22. R.42.

Little,A.L. 1968. Mangla Instrumentation. Water Power,July 1968.

Lloyd,H.E. et al. 1958. Rockfill Dams: Cherry Valley Central Core Dam. Proc.A.S.C.E. Jour. Power Div.Aug.1958. Paper 1733.

Lovell,S.M. 1965. Lancashire - Yorkshire Motorway (W.R.Section) Rock Excavation and Specification Trials, 2 Vols.

*Lowe,J. 1964. Shear strength of coarse embankment dam materials. R.II Q.31. Vol.3 p745 8th I.C.O.L.D.Edinburgh 1964.

Lueder,D.R. 1959. Aerial photographic interpretation, Principles and Applications. McGraw Hill 1959.

Luthra,S.D. 1956. Effect of subsoil stratification on seepage flow pattern. Irrigation and Power. April 1956.

Mackintosh,I.B. 1963. Wheel Excavator at Abiquiu Dam. Water Power Dec. 1963. p 510.

Mackintosh,I.B. 1964. American advances in earth dam construction. Water Power May 1964. p218.

Mackintosh,I.B. 1964. High rockfill dams in Russia. Water Power.July 1964. p315.

Mackintosh, I.B. 1965. Volta River Project - Akosombo Dam. Water Power May 1965. p175.

Mainfort,R.C. and Lawton,W.L. 1953. Laboratory compaction tests of coarse graded paving and embankment materials. Highway Research Board, Washington. Proc.Vol.32. pp555-566.

*Marsal,R.J. 1963. Contact forces in Soils and Rockfill Materials. 2nd. Pan Am. Conf.on Soil Mechanics.Vol.2 p67.Brazil 1963.

*Marsal,R.J. 1963. Triaxial apparatus for testing rockfill samples. Proc.2nd.Pan Am.Conf.on Soil Mechanics.Vol.2 pp99 Brazil 1963.

*Marsal,R.J. 1963. General Report: Earth and Rockfill Dams Proc.2nd. Pan Am.Conf.S.M.F.E. Vol.2 p485.Brazil 1963.

*Marsal,R.J. 1965. Stochastic Processes in the Grain Skeleton of Soils. 6th I.C.S.M.F.E. Montreal 1965. Vol.1. p303.

*Marsal,R.J.1967 Discussion:
6th. I.C.S.M.F.E. Vol.3 p310. Montreal 1965.

*Marsal,R.J. 1965. Research on the behaviour of granular materials and rockfill samples. Report: Comision Federal de Electricidad. Mexico 1965.

*Marsal,R.J. 1966. Large scale triaxial testing of granular materials. Conf. pre-print No.303. Paper presented to the A.S.C.E. Structural Eng.Conf. Miami, Jan.31st - Feb.4th.1966.

*Marsal,R.J. 1967. Grain forces in non-cohesive soils. Proc.3rd Pan Am. C.S.M.F.E. Venezuela 1967. Vol.I pp 227-248.

*Marsal,R.J. Large scale testing of rockfill materials. Proc.Am.Soc. Civil Engrs.Soil Mech. and Foundations Div.March 1967.

*Marsal,R.J. 1968. Discussion: Large scale testing of rockfill materials. A.S.C.E. Vol.94 No.SM4 July 1968. p1042.

Matyas,E.L. 1967 Air and water permeability of compacted soils. Permeability and Capillarity of Soils A.S.T.M. S.T.P. 417. Am.Soc.Testing Materials. 1967. p160.

Maurer, 1965. Shear failure of rock under compression.Soc.Pet.Eng. Journal Vol.5. No.2 1965.

Mehra,S.R. Ed.1966. Handbook on Landslide Analysis and Correction.Central Road Research Institute New Delhi,India.

Mencl,M.V. 1961. Discussion of General Report on Techniques of Field Measurement and Sampling. 5th.I.C.S.M.F.E. 1961.Vol.3 p165.

*Menzenbach,E. 1958.The use of penetrometers in site investigations.D.I.C. Imperial College.

Merrett,A.J. and Sykes,A. 1965. The Finance and analysis of capital projects. Longmans 1965.

Miller,R.K. 1964. Discussion: Research on vibratory maximum density test for cohesionless soils by H.C.Pettibone and J. Hardin. S.T.P. 377 Am.Soc.for testing and Materials. Philadelphia Pa. 1964.

Mitchell,J.K. and Younger,J.S. 1967. Abnormalities in hydraulic flow through fine grained soils. Permeability and Capillarity of Soils. A.S.T.M. S.T.P. 417 AM. Soc. Testing Mat.1967 p106.

Mitzukoshi,T. 1967. A geological investigation on the stability of reservoir banks.Q.32.9th.I.C.O.L.D. 1967.

Moss,A.J. Origin shaping and significance of quartz sand grains.

Muller,L. 1964. The rock slide in the Vaiont Valley. Rock Mechanics and Engineering Geology. Vol.2 p148. 1964.

Mundal,T. 1958. Rockfill Dams: Brownlee sloping core dam.Proc.A.S.C.E. Jour. Power Div.Paper 1734. Aug.1958.

Muskelishvili,N.I. Some basic problems of the Mathematical Theory of Elasticity.

Neuhauser, 1967. Placing of shell zones of Gepatsch Dam in winter. Q.35 9th. I.C.O.L.D. Istanbul. 1967.

*Nichiporovitch,A.A. and Rasskazov,L.N. 1967. Shear strength of coarse fragmental materials. Proc.Geotechnical Conf.Oslo 1967. Vol.1. pp225-229.

Niederhoff,A.E. 1939. Field tests on a shale foundation. Proc.Am.Soc.Civ. Engs.Vol.65. p1239. 1939.

Nonveiller,E. and Anagnosti,P. 1961. Stresses and Deformations in Cores of Rockfill Dams. 5th. I.C.S.M.F.E. Paris. Vol.II p673.

Obert,L. and Duvall,W.I. 1967. Rock mechanics and the design of structures in rock. Wiley,1967.

*Oberti,G. 1968. Discussion: Problems in design and construction of earth and rockfill dams. A.S.C.E. Vol.94.S.M.2 p583. March 1968.

O'Neill, A.L. and Nutting,R.G. 1964. Materials Exploration and Field Testing at Oroville Dam. S.T.P. 351. Am.Soc.for Testing and Materials. 1964.

Patel,V.J. 1964. Mechanics of Inclined filters in earth dams. Journal of S.M.F. Div. A.S.C.E. March 1964.

Patterson,F.W. et al. Rockfill Dams: The Bersimis sloping core dams. Proc.A.S.C.E. Journal Power Div. paper 1740.Aug.1958.

*Petley,D.J. 1966. The Shear Strength of Soils at Large Strains.Ph.D. Thesis. University of London.

*Pettibone,H.C. and Hardin,J. 1964. Research on vibratory maximum density test for cohesionless soils. Compaction of Soils,Am. Soc. for Testing and Materials Special Tech.Pub.No.377.

*Pettijohn,F.J. 1957. Sedimentary Rocks. Harper and Bros. New York.

Poorooshasb,H.B. and Roscoe,K.H. 1961. The correlation of the results of shear tests with varying degrees of dilation. Proc. 5th. Int.Conf.Soil Mechanics.Vol.1 pp 297-304.

Procter,R.R. 1933. Fundamental Principles of Soil Compaction.
a) Eng. News Record. p245 Aug.31st 1933
b) " " " p286 Sept.7th 1933
c) " " " p348 Sept.21st 1933
d) " " " p372 Sept.28th 1933

*Queiroz,L.A. 1963 Aspectos do Controle de Construcao da Barrogem de Furras. Proc. 2nd.Pan Am.Conf.S.M.F.E. Vol.1 p457. Brazil 1963.

Rabcewicz,L. 1964 The New Austrian Tunnelling Method. (Part 1). Water Power. Nov.1964. p453; Dec.1964 p511; Jan1965 p.19.

Raikes,R. 1967. Water, Weather and Prehistory. John Baker 1967.

*Rehbinder,P. and Lichtman,V. 1957. Effect of surface active media on strains and rupture in solids. Proc.2nd Int.Conf. of Surface Activity. Vol.III p.563.

Reinius, E. 1955. The Stability of the Slopes of Earth Dams. Geotechnique 5 pp181-189.

Richey,J.E. 1963. Granite. Water Power June,July,August,Sept. Nov.,Dec.1963.

Ripley,C.F. and Lee, K.L. 1961. Sliding friction tests on sedimentary rock specimens. 7th. I.C.O.L.D. Rome 1961. Communication No.8.

Roberts,C.M. 1958. The Quoich rockfill dam. Proc. 6th. I.C.O.L.D. Q.22. Vol. III p101.

Rocha,M. et al. 1955. Deformability of foundation rocks. Proc.5th I.C.O.L.D. 1955.

Rocha,M. et al. 1958. Portuguese experience of the compaction control of earth dams. 6th. I.C.O.L.D. New York. 1958.Q.22 Vol. III p.185.

Rolt,L.T.C. 1957 Isambard Kingdom Brunel. Longmans 1957.

Romero,S.U. 1966. Insitu direct shear test with saturation of the rock and interpretation of the great shear tests in nature. Proc. 1st.Int.Congress of Rock Mechanics.Vol.1 p353. Lisbon 1966.

Rosa,S.A. , Tartakocsky, D.M., Remiznikov,V.K. and Lobasov,P.D. The building of earth structures by dumping of clayey soils into water. Proc. 4th. Int. C.S.M.F.E. Vol.2.p368.

Rose,H.E. 1957. An analysis of the internal dynamics of the ball mill on the basis of probability theory. Trans.Inst.Chem. Eng.1957 Vol.35 p.87.
A study of vibration milling from considerations of dynamical similarity. As above p98.

*Rowe,P.W. 1962. The Stress Dilatancy Relation for Static Equilibrium of an Assembly of Particles in Contact. Proc.Royal Soc., Series A. London Vol.269,No.1339.Oct.9th,1962. pp 500 - 527.

*Rowe,P.W. 1963. Discussion: Hirschfeld and Pavlos,Triaxial testing with large scale high pressure equipment. Laboratory shear testing of soils. A.S.T.M. S.T.P. 361. p.340.

Rwoe,P.W. 1964. The calculation of the consolidation rates of laminated,varved or layered clays,with particular reference to sand drains. Geotechnique:Vol.14.No.4 pp321-340.

Rowe,P.W. 1968. The influence of geological features of clay deposits on the design and performance of sand drains. Supplement to: P.I.C.E. April 1968, Paper 7058 S.

Ruiz,M.D. 1966. A large scale field test on rock. Proc. 1st.Int.Congress of Rock Mechanics. Vol.1 p257. Lisbon 1966.

Salas, J.A.J. 1964. Some recent rock mechanics testing in Spain. R 53.Q.28 8th I.C.O.L.D. Edinburgh.1964.

Samside,A.F. 1955. Stresses in the downstream part of an earth or rockfill dam. Geotechnique. 5:2:200.

*Sande,A. 1966. The Tunhovd Dam: a new earth and rockfill dam incorporating an old concrete dam. N.G.I. Pub.No.68.1966.

Sandover,J.A. 1966. Construction of loose tip coffer dams. Water Power. p273. July 1966.

Sandover,J.A. and Tallis,J.A. 1966. Hydraulic stability of loose tip cofferdams. Water Power p.315. Aug.1966.

Sarkaria,G.S. and Dworsky,B.H. 1968. Model studies of an armoured rockfill overflow dam. Water Power. p455.Nov.1968.

Schmid,W.E. 1967. Field determination of permeability by the infiltration test. Permeability and Capillarity of Soils. A.S.T.M. S.T.P. 417, Am.Soc.Testing Materials.1967. p142.

Schmidt,L.A. 1958. Rockfill dams: Performance and maintenance of Dix River Dam. Proc.A.S.C.E. Journal of Power Div.June 1958. Paper 1683.

Schnitter,G. and Weber,E. 1964. The Vaiont Catastrophe. Wasser und Energiewirtschaft. Vol.56. No.2/3 Feb.-Mar 1964.p61.

*Schnitter,N.J. 1967. A short history of dam engineering. Water Power p.142.April 1967.

Schober, 1967. Behaviour of Gepatsch.Dam Q.34. 9th.I.C.O.L.D. Istanbul 1967.

*Schultze,E. 1957. Large scale shear tests. 4th. I.C.S.M.F.E. Vol. 1.1953

Scott,P.A. 1958. Observations on an experimental clay embankment to assist the design of the impermeable layer of a large rockfill dam. 6th. I.C.O.L.D. New York. Q.22.Vol.3. p237.

Searle,A.B. 1923. Sands and crushed rocks. Frowde and Stoughton,London.

Serafim,J.L. and Lopes,J.J.B. 1961. Insitu shear tests and triaxial tests of foundation rocks for concrete dams. Proc. 5th. I.C.S.M.F.E. Paris 1961. Vol.1 p533.

Serata,S. 1968. Application of continuum mechanics to the design of deep potash mines in Canada.Int.Jour.Rock Mech.Mining Science. Vol.5.No.4. 1968. p293.

Sharpe,C.F.S.1938. Landslides and Related Phenomena.Pageant Press Inc.New York.p137.

Sherard,J.L. et al 1963. Earth and Earth Rock Dams,Engineering Problems of Design and Construction. John Wiley 1963.

*Shockley,W.G. and Aglvin,R.G. 1960. Non uniform conditions in triaxial test specimens. A.S.C.E. Research Conf.on Shear Strength of Cohesive Soils. Boulder June 1960. p347.

Siraskar,K.A. and Patel,V.J. 1965. Equivalent permeability of anisotropic layered soils. Water Power. Oct.1965.

Skempton,A.W. 1954. The pore pressure coefficients A and B. Geotechnique 4. pp143 - 147.

Skempton,A.W. and Bishop,A.W. 1955. The gain in stability due to pore pressure dissipation in a soft clay foundation.Proc. 5th. I.C.O.L.D. Paris 1955.Vol.I. pp613 - 636.

Skempton,A.W.1964. The Long Term Stability of Clay Slopes. Geotechnique Vol.14. pp 77-102.June 1964.Rankine Lecture.

Skempton,A.W. 1966. Some Observations in Tectonic Shear Zones. 1st.Int. Congress on Rock Mechanics. Vol.1. p329.Lisbon 1966.

Skempton,A.W. 1966. Discussion: Properties of rocks and rock masses.1st. Int. Congress on Rock Mechanics.Vol.3 p277.Lisbon 1966.

Smalley,I.J. 1967. Variation of cohesion as to fineness of mineral powders and the development of cohesion during grinding. Mineral processing and extractive metallurgy.Vol.76.1967.

Smith,H.G. 1919. Minerals and the microscope. Thomas Murphy.1919.

Snethlage,J.B. et al. 1958. Rockfill dams: Review and Statistics.Proc. A.S.C.E. Journal of Power Div.Aug.1958.paper 1739.

Sokolovski,V.V. 1965. Statics of Granular Media. Pergamon Press Oxford 1965.

*Sowers,F.G. and Gore,C.E. 1961. Large scale preconstruction tests of embankment materials for an earth-rockfill dam. Proc. 5th. I.C.S.M.F.E. Vol.2 p717 Paris 1961.

Sowers,G.F.; Williams,R.C. and Wallace,T.S. 1965. Compressibility of broken rock and the settlement of rockfills. Proc.6th I.C.S.M.F.E. Montreal Vol.2 pp561-565.

Sowers,G.F. 1962. Earth and Rockfill Dam Engineering. Asia Publishing Hse. 1962.

Steele,I.C. et al. 1958. Rockfill dams: Salt Springs and Lower Bear River concrete face dams. Proc.A.S.C.E. Journal of Power Div. Aug.1958 Paper 1737.

*Steinfeld,K. 1952. Uber den raumlichen Erdwiderstand. Dissertation TH Hanover.

Subhash,C. 1962. Flownet for dams on stratified foundation. Irrigation and Power Oct.1962.

Sudman,G.F. 1958. Rockfill dams: Kajakat central core dam.Afghanistan. Proc.A.S.C.E. Journal Power Div.Aug.1958.paper 1735.

Sutherlane,H.B. and Neale,D.F. 1968. Determination of the shape factor of sands. Proc.3rd.Budapest Conf.on S.M.F.E.Oct.15th - 18th. 1968.

*Terzaghi,K. and Peck,R.B. 1948. Soil Mechanics in Engineering Practice. Wiley New York.

Thorfinnson,S.T. 1954. A large scale field test on a bantonite seam. Proc.A.Soc.Civil Engrs.Separate 549. 1954.

*Timoshenko,S. and Goodier,J.N. 1951. Theory of Elasticity. McGraw Hill. New York.

Trollope,D.H. and Brown,E.T. 1965. Pressure distributions in some discontinua. Water Power, p310.Aug.1965.

Tschebotarioff,G.P. 1952. Soil Mechanics,Foundations and Earth Structures. pp 249 - 252.

Uriel,S. 1964. La geotechnica aplicada a las grandes presas. Large dams in modern Spain,Revista de Obras Publicas.April 1964.

Varlet,H. 1965. Barrages - Reservoirs,Vols I and 2. Edition Eyrolles,Paris.

Varlet,H. 1968. Barrages - Reservoirs,Vol. 3 " " "

Vargas,M. 1965. Residual clay dams in the state of Sao Paulo,Brazil. Proc.6th I.C.S.M.F.E. Vol.2 p439.Montreal 1965.

Varnes,D.J. 1958. Landslide types and processes. In: E.B.Eckel (Ed.) Landslides and Engineering Practices.N.A.S. - N.R.C. Publ. 544. Highway Res.Board Special Report 29.pp20-47.

*Vesic,A. and Barksdale,D. 1963. Discussion: Test methods and new equipment. Laboratory shear testing of soils. A.S.T.M. S.T.P. 361.Ottawa 1963.

Warlam,A.A. 1960. Recent progress in Triaxial apparatus design. Am. Soc.Civil Eng.Research Conf.on Shear Strength of Cohesive Soils, Boulder,Colorado,June 1960,p859.

*Weber,J. 1966. Recherches Concernant les Contraintes Intergranulaires dans les Milieux Pulverulents. Bulletin de Liason des Laboratories Routiers. Ponts et Chaussees,July-Aug.1966.

Westenberger,F. 1967. Settlement and displacement measurements on dams. Die Wasserwirtschaft.Vol.5 No.2 p96. Feb.1967.

Weyermann,W.J. 1958. Rockfill Dams: The Paradela Dam - Foundation Treatment. Proc.A.S.C.E. Journal of Power Div.Aug. 1958. paper 1748.

Wilkins,J.K. 1956. Flow of water through rockfill and its application to the design of dams. Proc.2nd Australia-NewZealand C.S.M.F.E. Jan.1956. pp 141-149.

Wilkins,J.K. 1963 The stability of overtopped rockfill dams. Proc.4th. Aust. - New Zealand Conf. on S.M. and F.E. 1963. Adelaide. Vol.1 p.1

Wilson,E.M. 1966. A multi purpose barrage on the Bristol Channel. Water Power p.135. April 1966.

*Winnitoy,W.E. 1964. Ultimate densities and strength considerations of base and subgrade soils. Compaction of soils.Am.Soc. for testing and materials. S.T.P. 377.

*Wittke,W. 1963. Discussion: Borowicka: Vienna Method of Shear Testing. Laboratory Shear testing of Soils.A.S.T.M. S.T.P. 361. p 314.

Wood,A.M.M. 1955. Folkestone Warren Landslip Investigations. 1948 - 1950
" " " Remedial Measures.1948-1950. Proc.I.C.E. April 1955.

Yakovlav,N.N. 1967. Earth and Rockfill Dams in Russia. Irrigation and Power. Vol.24,No.3 p241. 16 pp 19 ff 3 tt. July 1967.

Yeates,J.A. 1966. The settlement of Rockfill Dams. M.Sc.Thesis. Imperial College.

Yung,E.H. 1967. A Critical Survey of Cracking in Earth and Earth Rock Dams. M.Sc. Thesis. Imperial College.

*Zeller,J. and Wullimann,R. 1957. The shear strenght of shell materials. for the Goeschenenalp Dam. Switzerland.Proc.4th I.C.S.M.F.E. Vol.2 p399. London 1957.

Zeller,J. and Zeindler,H. 1957. Test fills with coarse shell materials for the Goeschenenalp Dam. Proc.4th.I.C.S.M.F.E. Vol.2 p405. 1957.

Zienkiewicz,O.C. 1965. Problems of Rock Mechanics. The Engineer.p293. Feb.12th 1965.

Zienkiewicz,O.C. 1966. The cable method of insitu testing. Ist.Int. Congress of Rock Mechanics Vol.1 p667. Lisbon 1966.

Zimmerley and Gross. 1929. Crushing resistance of minerals. R.I.2948. U.S.Dept.of Interior.Bureau of Mines.1929.

Additional References

* (1) inzenyrske stavby Vol.15 No.9 September 1967.

* (2) Anderson,D., Paton,T.A.L., Blackburn,C.L. 1960. Zambezi Hydro-Electric Development at Kariba. 1st stage.Proc.I.C.E. September 1960. pp39 - 60.

* (3) Aldeadavila Dam. Ed.Water Power. Jan/Feb. 1964.

* (4) Technical News Item. The Journal of The Institution of Engineers, Australia Vol.39 No.12 Dec.1967.

* (5) U.S.Army Engineer Division Laboratory,South Pacific. Shear Strength of Rockfill, Engineering Study 526,1967.

* (6) The Tokke Hydro-Electric Scheme, Water Power. Feb.1965. March'65 April 1965.

* (7) U.S.B.R. Earth Manual, Washington, 1963.

(8) Piave-Boite-Mae-Vaiont Hydro-Electric Scheme. Societa Adriatica di Elettricita, Venice, 1963.

* (9) Waterways Experiment Station, Vicksburgh, 1950. Triaxial tests on sands. Reid Bedford Bend, Mississippi River. Report No. 5 - 3.